Characterization of aerosols and their sources in East-Mediterranean sites under industrial influence

Marc Fadel

Thèse de Doctorat

Mention : Chimie
Spécialité : Chimie théorique, physique, analytique

présentée à ***l'Ecole Doctorale en Sciences Technologie et Santé (ED 585)***
de l'Université du Littoral Côte d'Opale
et
à l'Ecole doctorale de Sciences, d'Ingénierie et de Technologie (EDSIT)
de l'Université Saint-Joseph de Beyrouth

par

Marc Fadel

pour obtenir le grade de Docteur de l'Université du Littoral Côte d'Opale et de l'Université Saint-Joseph de Beyrouth

Caractérisation des aérosols et de leurs sources dans des sites Est Méditerranéens sous influence industrielle

Characterization of aerosols and their sources in East-Mediterranean sites under industrial influence

Soutenue le 10 décembre 2021, après avis des rapporteurs, devant le jury d'examen :

M^me^ Marie Abboud, Pr., Université Saint-Joseph de Beyrouth, Liban	**Président**
M. Jean-François Doussin, Pr., Université Paris-Est Créteil, France	**Rapporteur**
M. Ignacio Fernández-Olmo, Pr., Universidad de Cantabria, Espagne	**Rapporteur**
M^me^ Agnès Borbon, Dr., Université Clermont Auvergne, France	**Examinateur**
M. Imad El Haddad, Dr., Paul Scherrer Institute, Suisse	**Examinateur**
M. Dominique Courcot, Pr., Université du Littoral Côte d'Opale, France	**Directeur de thèse**
M. Charbel Afif, Dr., Université Saint-Joseph de Beyrouth, Liban	**Directeur de thèse**
M. Frédéric Ledoux, Pr., Université du Littoral Côte d'Opale, France	**Co-encadrant**
M. Jean Sciare, Pr., The Cyprus Institute, Chypre	**Membre invité**
M^me^ Elise Noujeim, Dr., Conseil National de la Recherche Scientifique, Liban	**Membre invité**

Acknowledgments

1166 days since the beginning… 1166 Thank-you' s!

I would like to begin by thanking the members of the jury, Pr. Marie Abboud, Pr. Jean-François Doussin and Pr. Ignacio Fernádez-Olmo for accepting to evaluate this thesis and all the work that was put into it. I would also like to thank my committee members Dr. Agnès Borbon and Dr. Imad El Haddad for their vital comments and valuable suggestions during our annual meetings.

I would like to acknowledge "Université du Littoral Cote d'Opale" and the National Council for Scientific Research of Lebanon (CNRS-L) for granting me a doctoral fellowship. I would also like to thank the Research Council and the Faculty of Sciences at Saint Joseph University in Lebanon as well as the "Unité de Chimie Environnementale et Interactions sur le vivant" (UCEIV unit) for financially supporting this project. This work was also produced within the framework of the EMME-CARE project. My appreciation also goes to Pr. Richard Maroun, dean of the Faculty of Sciences at USJ and Pr. Stéphane Siffert, director of UCEIV at ULCO.

I would like to express my utmost and deepest gratitude to my supervisors Dr. Charbel Afif, Pr. Dominique Courcot, and Pr. Frédéric Ledoux for your help and guidance throughout these three years, for your continuous support, for our scientific discussions, and for your profound belief in my abilities. This work would have not been possible without your help, dedication, and meticulous work methods. Your insightful feedbacks pushed me to sharpen my critical thinking skills and elevated the quality of my work. I would personally like to thank the three of you as I feel blessed to have had the opportunity to work with you all. Dr. Afif, we have been working together for six years now, and without your help and guidance, I would not be where I am today. Thank you for all the knowledge you have passed onto me and I will remain forever grateful to all of the opportunities you offered me. I will never forget all of our 1 a.m. meetings that ultimately led to be the most productive. Pr. Courcot, words cannot describe my gratitude and appreciation. Despite everything you have been through, you gave me consistent support, encouragement, and guidance during my thesis. Thank you for all of the academic and personal help that you continuously provided for me during these years. You were like my godfather in France. Pr. Ledoux, I cannot thank you enough for your availability whenever I needed you despite all of your responsibilities. Thank you for all of the technical methods that helped shape this research, your accuracy in the bench work, all our valuable scientific as well as personal

discussions. I appreciate all your helpful suggestions, indispensable advices, and encouragement.

I would like to thank Dr. Adib Kfoury for all of his help in the sampling at Fiaa site. I also wish to thank the Centre Commun de Mesures, especially Dorothée Dewaele for her help in the ICP-AES analysis. I express my sincere acknowledgment to Marianne Seigneur for her help in the water-soluble ions analysis and to Amaury Kasprowiak who also offered important assistance during this analysis. As for organic analysis, I would like to thank Mariana Farhat for her help in the organic species analysis. Additionally, I acknowledge Pr. Gilles Roussel and Dr. Gilles Delmaire from the LISIC laboratory at ULCO for the application of the multiple linear regression method.

I address many thanks to my team CTEA at ULCO including Dr. Yann Landkocz, Dr. Anthony Verdin, and Dr. Sylvain Billet for their support. Thank you for my current and old PhD colleagues: Margaux, Stéphanie, Nour, Mia and Salimata. I will never forget all of our daily moments at the office, our laughs, our no-singing competitions, and of course our hard-working moments. As for my days at USJ, I am grateful for Mariana, Helga, Hilda and Nansi for all of our shared moments. I would like to thank my laboratory colleagues for all of our events, fun we shared and their support: Tarek, Rebecca, Murielle, Lilian, Maribelle, Sara, Pedro, Michel, Miriam, Bastien, Nancy, Tracy, Abir, Hadi, Layal, Ghidaa, Khaoula, Hamed, Bouthayna, and Layla.

I am extremely grateful for my childhood friends Rony, Roland A.K, Cindy, Roland B., Georges. I in addition to my university friends that I made throughout the years: Joe, Marc, Paola, and Joanne. You stood next to me from the beginning, pushed me to be the best and believed in me and in my strengths. I would also like to thank Sr Caroline, Tamara, Laura, Johnny, Elie C, Miriam T, Georges R., Stephany S., Louna, Carine, Ghiwa, Maria, Hala, Betty, Anthony, Tony Saadé, Georges S, Nisrine, Rami, Charbel N., Toni S., Lara, and Fawzi. I greatly value your friendship and appreciate your support!

A special thought goes to my partner, Lamia Nakhlé. It is an exquisite feeling to have worked alongside you in our PhD adventure. Thank you for all of your support, for your understanding, for taking care of me, and being such a great work partner until the early morning hours. Your continuous encouragement pushed me to always be better. Words cannot express how grateful I am for having you in my life.

*This thesis is dedicated to **my family**.*

The ones who never left my side, the ones that supported me in every single step of this work.

My words fail to express my appreciation, gratitude, and love
to my parents Imad and Thérèse
and my brothers Patrick and Freddy.

I am forever indebted to them for giving me the opportunities that have made me who I am today.

Thank you for all of your encouragements and prayers.

Publications and scientific activities

The work presented in this manuscript was valued in the form of publications and oral or poster communications. The list is presented below:

1. **Publications**

- Fadel M., Ledoux F., Farhat M., Kfoury A., Courcot D., Afif C. (2021). "$PM_{2.5}$ characterization of primary and secondary organic aerosols in two urban-industrial areas in the East Mediterranean." Journal of Environmental Sciences 101: 98-116. https://doi.org/10.1016/j.jes.2020.07.030

- Fadel M., Ledoux F., Afif C., Courcot D. "Human health risk assessment for PAHs, phthalates, metals, PCDD/F, and DL-PCBs in $PM_{2.5}$ and for NMVOCs in two East-Mediterranean urban sites under industrial influence". Atmospheric pollution research, under review.

- Fadel M., Ledoux F., Seigneur M., Oikonomou K., Sciare J., Courcot D., Afif C. "Chemical characterization of $PM_{2.5}$ sources from different anthropogenic activities: cooking, wood burning, and diesel generators.", Environmental research, under review.

- Fadel M., Courcot D., Seigneur M., Kfoury A., Oikonomou K., Sciare J., Ledoux F, Afif C. " $PM_{2.5}$ chemical characterization and sources identification in two sites in the East Mediterranean" in preparation.

- Fadel M., Courcot D., Delmaire G., Roussel G., Afif C., Ledoux F. "Temporal variations, relationship with chemical composition and source apportionment of oxidative potential of $PM_{2.5}$ in two East Mediterranean sites", in preparation

2. International presentations and posters

- Presentation

- Fadel M., Afif C., Seigneur M., Kfoury A., Oikonomou K., Sciare J., Ledoux F., Courcot D. $PM_{2.5}$ in two urban industrial sites in the East Mediterranean: chemical characterization and health risk assessment for metals**,** Chemistry of the Whole Environment Research (online), Royal Society of Chemistry, United Kingdom, 25 June 2021.

- Posters

- Fadel M., Ledoux F., Farhat M., Kfoury A., Oikonomou K., Sciare J., Courcot D., Afif C. Speciation of the $PM_{2.5}$ carbonaceous fraction in two urban industrial areas in the East Mediterranean, European Aerosol Conference (online), Birmingham, United Kingdom, August 30- September 3, 2021.

- Fadel M., Ledoux F., Afif C., Courcot D. Human health risk assessment for PAHs, phthalates, metals, PCDD/F, DL-PCBs in $PM_{2.5}$ in two East-Mediterranean urban sites under industrial influence, European Aerosol Conference (online), Birmingham, United Kingdom, August 30- September 3, 2021.

3. National presentations

- Participation in the "Hauts de France" regional selection for the competition "Ma thèse en 180 secondes", March 11, 2021- Villeneuve d'Ascq, France.

- Participation in the competition "Une image en 180 secondes", *journée des doctorants du pôle « Mutations Technologiques et Environnementales »*, July 1st 2021- Calais, France (first prize winner).

4. Summer school

- Participation in the summer school school on air quality organized by "Réseau de recherche Qualité de l'air en Ile de France" between July 4 and 9 2021, in Bouray sur Juine, France.

Table of contents

List of tables

List of figures

List of abbreviations

$(NH_4)_2SO_4$	ammonium sulfate
1,2,3,4,6,7,8 HpCDD	1,2,3,4,6,7,8-heptachlorinated dibenzo-p-dioxin
1,2,3,4,6,7,8 HpCDF	1,2,3,4,6,7,8-heptachlorinated dibenzofuran
1,2,3,4,7,8 HxCDD	1,2,3,4,7,8-hexachlorinated dibenzo-p-dioxin
1,2,3,4,7,8 HxCDF	1,2,3,4,7,8 hexachlorinated dibenzofuran
1,2,3,4,7,8,9 HpCDF	1,2,3,4,7,8,9-heptachlorinated dibenzofuran
1,2,3,6,7,8 HxCDD	1,2,3,6,7,8-hexachlorinated dibenzo-p-dioxin
1,2,3,6,7,8 HxCDF	1,2,3,6,7,8 hexachlorinated dibenzofuran
1,2,3,7,8 PeCDD	1,2,3,7,8-pentachlorinated dibenzo-p-dioxin
1,2,3,7,8 PeCDF	1,2,3,7,8 pentachlorinated dibenzofuran
1,2,3,7,8,9 HxCDD	1,2,3,7,8,9-hexachlorinated dibenzo-p-dioxin
1,2,3,7,8,9 HxCDF	1,2,3,7,8,9 hexachlorinated dibenzofuran
1,4-NQ	1,4-naphthoquinone
2,3,4,6,7,8 HxCDF	2,3,4,6,7,8 hexachlorinated dibenzofuran
2,3,4,7,8 PeCDF	2,3,4,7,8 pentachlorinated dibenzofuran
2,3,7,8 TCDF	2,3,7,8 tetrachlorinated dibenzofuran
2,3,7,8-TCDD	2,3,7,8-tetrachlorodibenzo-p-dioxin
2-MGA	2-methylglyceric acid
2-MT1	2-methylthreitol
2-MT2	2-methylerythritol
A1	3-hydroxyglutaric acid
A2	3-acetylglutaric acid
A3	3-isopropylglutaric acid
A4	3-methyl-1,2,3-butanetricarboxylic acid
AA	Ascorbic Acid
ABS	dermal adsorption factor
Ace	acenaphthene
Acy	acenaphthylene
ADD	average daily dose
ADI	Acceptable daily intake
AF	dermal adherence factor
Al	aluminum
Anth	anthracene
As	arsenic
Asc	ascorbate
AT	Average timing
ATSDR	U.S Agency for Toxic substances and Disease registry
B[a]An	benz[a]anthracene
B[a]P	benzo[a]pyrene
$B[a]P_{eq}$	b[a]P equivalent
B[b]Fl	benzo[b]fluoranthene
B[ghi]Pe	benzo[g,h,i]perylene
B[k]Fl	benzo[k]fluoranthene
Ba	barium
BEAS-2B	human non-tumorigenic lung epithelial cell line
BG	Beef Grilling
Bi	bismuth
BSOA	Biogenic Secondary Organic Aerosols
BW	Body Weight
C_{19}	nonadecane

C_{20}	heneicosane
C_{21}	eicosane
C_{22}	docosane
C_{23}	tricosane
C_{24}	tetracosane
C_{25}	pentacosane
C_{26}	hexacosane
C_{27}	heptacosane
C_{28}	octacosane
C_{29}	nonacosane
C_{30}	triacontane
C_{31}	hentriacontane
Ca	calcium
Ca^{2+}	ionic calcium
$CaCO_3$	calcium carbonate
CCR	Cumulative Cancer Risk
Cd	cadmium
Ce	cerium
CG	Chicken Grilling
Chr	chrysene
Cl^-	chloride
C_{max}	carbon number of the alkane having the maximum concentration
CMB	Chemical Mass Balance
CO	carbon monoxide
Co	cobalt
CO_2	carbon dioxide
CO_3^{2-}	carbonate ions
COPD	Chronic Obstructive Pulmonary Disease
CPI	Carbon Preference Index
CR	Cancer Risk
Cr	chromium
Cr(VI)	chromium (VI)
CRAES	Chinese Research Academy of Environmental Sciences
CSF	cancer slope factor
CSPSS	China Source Profile Shared Service
Cu	copper
D.L.	Detection Limit
DA	docosanoic acid
Da_e	equivalent aerodynamic diameter
DDA	dodecanoic acid
DEHP	bis(2-ethylhexylphthalate)
DG	Diesel Generator
DiB[a,h]An	dibenz[a,h]anthracene
DIBP	diisobutylphthalate
diC2	oxalic acid
diC6	adipic acid
diC9	azelaic acid
DISP	displacement analysis method
DL-PCBs	dioxin-like polychlorobiphenyls
DNA	desoxyribonucleic acid
DnBP	dibutylphthalate
DTNB	5,5-dithiobis-2-nitrobenzoic acid

DTT	dithiothreitol
E.F	Enrichment Factor
EA	eicosanoic acid
EC	Elemental Carbon
EC_i	exposure concentration in air
ED	Exposure duration
EF	Exposure frequency
ELV	Emission Limit Values
EMME	East Mediterranean Middle East
ESR	Electro Spin Resonance
ET	Exposure time
FA	Fiaa region
FAO	Food and agriculture organization
Fe	iron
Fla	fluoranthene
Flu	fluorene
GCA	General Cooking activities
GC-MS	Gas chromatography – mass spectrometry
GEMM	Global Exposure Mortality Model
GSH	glutathione
H1	trisnorneohopane
H2	17α(H)-trisnorhopane
H_2O	water
H_2O_2	hydrogen peroxide
H_2S	hydrogen sulfide
H_2SO_4	sulfuric acid
H3	17α(H)-21β(H)-norhopane
H4	17α(H)-21β(H)-hopane
H5	17α(H)-21β(H)-22S-homohopane
H6	17α(H)-21β(H)-22R-homohopane
HCl	hydrochloric acid
$HClO_4$	perchloric acid
HDA	hexadecanoic acid
HDV	Heavy Duty Vehicles
HF	hydrofluoric acid
HFO	Heavy Fuel Oil
HI	Hazard Index
HNO_3	nitric acid
$HO^{\cdot}$	hydroxyl radical
HQ	Hazard Quotient
HRGC/HRMS	High-Resolution Gas Chromatography -High-Resolution Mass Spectrometer
HULIS	humic-like substances
IARC	International Agency for Research on Cancer
IC	Ionic Chromatography
ICP-AES	Inductively Coupled Plasma-Atomic Emission Spectrometry
ICP-MS	Inductively Coupled Plasma-Mass spectrometry
IM	maximum individual mean
InPy	indeno[1,2,3-c,d]pyrene
IPCS	International Programme on Chemical Safety
IR_{ing}	soil intake rate
IR_{inh}	inhalation intake rate
IS	maximum individual standard deviation

IUR	inhalation unit risk
K	potassium
K^+	ionic potassium
$Kp_{2.5}$	partitioning coefficient
La	lanthanum
LADD	lifetime average daily dose
LCR	Lifetime Cancer Risk
MENA	Middle East and North Africa Region
Mg	magnesium
Mg^{2+}	ionic magnesium
MI	Myocardial Infracts
MLR	Multiple linear regression
Mn	manganese
MoE	Ministry of Environment
MRL	Minimal Risk Level
MW	Molecular Weight
Na^+	ionic sodium
NAAQS	National Ambient Air Quality Standards
NAD	Nicotinamide Adenine Dinucleotide
NADP	Nicotinamide Adenine Dinucleotide Phosphate
NaOH	sodium hydroxide
Nb	niobium
NH_3	ammonia
NH_4^+	ammonium
NH_4HSO_4	ammonium bisulfate
NH_4NO_3	ammonium nitrate
Ni	nickel
NMVOC	non-methanic volatile organic compounds
NO	nitrogen monoxide
NO_2	nitrogen dioxide
NO_3^-	nitrate
NO_x	nitrogen oxides
O_2^-	superoxide anion
O_3	ozone
OA	oleic acid
OC	Organic Carbon
OCDD	octachlorinated dibenzo-p-dioxin
OCDF	octachlorinated dibenzofuran
ODA	octadecanoic acid
OH	hydroxide
OM	Organic Matter
OP	Oxidative Potential
$OP\text{-}AA_m$	Mass-normalized OP-AA
$OP\text{-}AA_v$	Volume-normalized OP-AA
$OP\text{-}DTT_m$	Mass-normalized OP-DTT
$OP\text{-}DTT_v$	Volume-normalized OP-DTT
P	phosphorus
PA	pinic acid
PAHs	Polycyclic Aromatic Hydrocarbons
Pb	lead
PBS	phosphate buffer
PCA	Principal component analysis

PCB 105	2,3,3',4,4'-pentachlorobiphenyl
PCB 114	2,3,4,4',5-pentachlorobiphenyl
PCB 118	2,3',4,4',5-pentachlorobiphenyl
PCB 123	2,3',4,4',5'-pentachlorobiphenyl
PCB 126	3,3',4,4',5-pentachlorobiphenyl
PCB 156	2,3,3',4,4',5-hexachlorobiphenyl
PCB 157	2,3,3',4,4',5'-hexachlorobiphenyl
PCB 167	2,3',4,4',5,5'-hexachlorobiphenyl
PCB 169	3,3',4,4',5,5'-hexachlorobiphenyl
PCB 189	2,3,3',4,4',5,5'-heptachlorobiphenyl
PCB 77	3,3′,4,4′-tetrachlorobiphenyl
PCB 81	3,4,4',5-tetrachlorobiphenyl
PCDD	polychlorinated dibenzodioxins
PCDF	polychlorinated dibenzofurans
Ph	phenanthrene
PhA	phthalic acid
PM	particulate matter
$PM_{0.1}$	ultrafine particulate matter (aerodynamic diameter less than 0.1 µm)
$PM_{2.5}$	fine particulate matter (aerodynamic diameter less than 2.5 µm)
PM_{10}	particulate matter having an aerodynamic diameter less than 10 µm
PMF	Positive Matrix Factorization
POA	Primary Organic Aerosols
PTFE	Polytetrafluoroethylene
Pyr	pyrene
Q	Objective function
QA/QC	Quality assurance / Quality control
Rb	rubidium
RF	Response Factor
RfC	Reference concentration
RfD	Reference dose
ROS	Reactive Oxygen Species
RSD	Relative Standard Deviation
S/N	Signal-to-noise
SA	Exposed skin surface area
Sb	antimony
Sc	scandium
SD	Standard Deviation
SDG	Sustainable Development Goals
Se	selenium
SIA	Secondary Inorganic Aerosols
SLF	Simulated Lung Fluid
Sn	tin
SNA	sulfate nitrate ammonium
SO_2	sulfur dioxide
SO_4^{2-}	sulfate
SOA	Secondary Organic Aerosols
Sr	strontium
SVOCs	semi-volatile organic compounds
TA	tetracosanoic acid
TC	Total carbon
TDA	tetradecanoic acid
TEF	toxic equivalent factor

TEQ	toxic equivalent
THI	total hazard index
TI	Tolerable Intake
Ti	titanium
Tl	thallium
TNB	5-mercapto-2-nitrobenzoic acid
TSP	Total Suspended Particles
UNDP	United Nations Development Programme
UNMIX	Model for environmental model analysis
USAID	U.S. Agency for International Development
USEPA	United States Environmental Protection Agency
V	vanadium
VOCs	Volatile Organic Compounds
Wax%	Wax ratio
WB	Wood burning
WHO	World Health Organization
WSI	Water-soluble ions
WSOC	water-soluble organic carbon
ZK	Zouk Mikael region
Zn	zinc
βC	β-caryophyllinic acid

General Introduction

Rapid industrialization has led to an important economic prosperity and an increase in the living standards. This evolution was also accompanied by a deterioration of the environmental balance and a start of the drastic decrease in air quality (Fowler et al., 2020). The invention of steam power, the improvement of iron making techniques, the transformation in the textile industry, the use of coal and its products to replace wood, the combustion of fuel oil and many other major modifications have considerably changed due to this episode. The consumption of fossil fuels worldwide was amplified since the industrial revolution in the XXth century and contributed to the increase of sulfur and carbon emissions (Dentener et al., 2006). The effects of air pollution on human health have returned as a top priority at the end of the XXth and at the beginning of the XXIst century as new epidemiological evidence emerged (Fowler et al., 2020).

According to WHO, outdoor air pollution was responsible for about 4.2 million premature deaths worldwide in 2016 (WHO, 2016). In 2013, the International Agency for Research on Cancer (IARC) has classified outdoor air pollution and in particular particulate matter (PM) as Group 1 "carcinogenic to humans". PM, defined as a complex mixture of particles and droplets, are nowadays considered as one of the most challenging issues in the environmental field. This is mainly because of its effect on human health (respiratory illness, lung cancer, heart diseases, etc.) (Mark Goldberg, 2008; Anderson et al., 2012; Thurston et al., 2017; Cochard et al., 2020) and its contribution to the radiative forcing that may vary depending on the aerosols' composition (Lelieveld et al., 2012; 2015; Krishna et al., 2019). This phenomenon is considered as an important basis for understanding and predicting global climate changes (Bellouin et al., 2020).

With the increasing impact of the atmospheric particles on human health, the studies shifted from focusing on pollutants such as SO_2 and NO_2 to working on particles especially the fine and ultrafine ones (with an aerodynamic diameter less than 2.5 and 0.1 µm, respectively) (Riffault et al., 2015; Xing et al., 2016; Schraufnagel, 2020). The penetration and the interaction of airborne particles with the human respiratory tract is controlled by the size and the shape of the particle as well as its composition (Schwartz and Neas, 2000; Bell et al., 2009). Atmospheric particles represent a complex mixture of inorganic (elements, water-soluble ions, etc.), organic (polycyclic aromatic hydrocarbons, alkanes, hopanes, etc.), and biological fractions (pollen, spores, etc.). The composition of these particles varies strongly and depends on the sources of emissions that can be either natural or anthropogenic (Yu and Park, 2021). Natural sources of PM include sea-salts, desert dusts, wildfires, etc. As for anthropogenic emissions, they include biomass burning, fuel combustion, industrial processes, vehicular emissions, agricultural

operations, etc. Additionally, PM can be of primary origins, directly emitted from the source or of secondary origins, produced in the atmosphere mainly via oxidation processes.

The East Mediterranean region faces elevated concentrations of PM resulting from transported pollution mixed with anthropogenic emissions from traffic, industrial, and residential emissions, and natural emissions from Saharan and African deserts (ESCWA, 2009; im and Kanakidou, 2012). Additionally, the region is greatly affected by climate change, which has a warming rate (3.5-7°C) far above the global average of 1.5°C (Lelieveld et al., 2012; WWF, 2021). In 2018 and early 2019, earthquakes, flash floods, droughts, storms, and extreme temperatures hit most of the countries in the region (WHO, 2019). These high temperatures and the increase in the number of heatwaves will contribute to higher photochemical air pollution and leading to even higher concentrations of pollutants in the atmosphere (Lelieveld et al., 2014). Furthermore, WHO assessment in the region concluded that several countries still do not have adequate regulation for monitoring air pollution (WHO, 2021). Therefore, it seems convenient to determine the sources of pollution in the region and evaluate their health impact in order to develop efficient control strategies and implement adequate air quality policies. However, an important step to source identification and health risk evaluation is constituted by a chemical characterization of the atmospheric particles.

One of the countries in the region that is the most affected by outdoor air pollution is Lebanon (MoE, 2017), located on the eastern shore of the Mediterranean Sea. With a population in the last few years exceeding six million, Lebanon faces extensive urbanization with heavy road traffic, installation of private diesel generators with no law enforcement on stack emissions, open burning of waste, along with different types of industries (Waked et al., 2012). The national inventory of 2010 of Lebanon highlights the influence of the industrial sources and the power plants as major PM emitters of different pollutants in the atmosphere (Waked et al., 2012). Additionally, Lebanon is affected by long range transport of desert dust from Saharan and Arabian deserts (Waked et al., 2013; Borgie et al., 2016).

The studies regarding the air quality in the East Mediterranean region is still scarce with major works focusing on Megacities such as Istanbul and Egypt. Some studies were also conducted in Cyprus, Greece, and Lebanon. Most of the studies in Lebanon focused on urban areas especially the capital Beirut. As for industrial areas, some work was performed in the North of Lebanon and one exploratory study in Zouk Mikael region that encompasses the biggest power plant in Lebanon. Additionally, there were no studies in Lebanon and only one study in the East

Mediterranean that evaluates the health risks attributed to the exposure to atmospheric particles or its constituents.

In this context, this work is particularly focused on the study of $PM_{2.5}$ and volatile organic compounds (VOCs) in two urban sites in the East Mediterranean under industrial influence, namely Zouk Mikael and Fiaa, Chekka in Lebanon. Zouk Mikael encompasses the biggest power plant which runs on Heavy Fuel Oil (HFO). As for Fiaa, which is in Chekka region, might be under the influence of different locally established chemical industries such as cement plants, their corresponding quarries and a sulfuric acid and phosphate fertilizer industry.

In this thesis work, $PM_{2.5}$ samples and VOCs were collected from December 2018 to October 2019 in these two sites in Lebanon. Then, a detailed study of VOCs and an exhaustive chemical characterization of $PM_{2.5}$ was conducted. This characterization included the analysis of the carbonaceous matter, water-soluble ions, trace and major elements, and organic compounds. A selection of organic and inorganic compounds was used for applying a source receptor model, namely the Positive Matrix Factorization (PMF) in order to identify $PM_{2.5}$ sources and quantify their contribution. The sources identification was based on the database from the literature but also from the chemical characterization of $PM_{2.5}$ samples collected at near field for local sources profiles in Lebanon as part of this thesis. Additionally, the health risk evaluation due to the exposure to air pollution was presented by two different approaches. The first one is based on the health risk assessment approach for the evaluation of carcinogenic and non-carcinogenic risks due to the exposure to VOCs and classes of compounds in $PM_{2.5}$. The second approach is based on the measurement of the oxidative potential using two acellular assays: Dithiothreitol (DTT) and Ascorbic acid (AA) assays.

Therefore, this thesis report is divided into four chapters.

- The first chapter presents a literature review on atmospheric particles, their emission sources, their health impact as well as receptor modeling approaches. The chapter also focuses on the previous conducted studies on air quality and health impacts in the East Mediterranean region and most specifically the situation of Lebanon. Consequently, the hypothesis and scientific questions were established, and the applied methodology in this thesis work was presented.

- The second chapter presents the sampling sites, the material and methods used for sampling, the analysis of the different $PM_{2.5}$ fractions (organic, water-soluble ions;

major and trace elements, carbonaceous fraction), and the assessment of the $PM_{2.5}$ oxidative potential.

- The third chapter presents the chemical characterization and sources identification of $PM_{2.5}$. The results and discussions in this chapter were presented in the form of three articles. The first one presents some $PM_{2.5}$ chemical source profiles, the second one focuses on the primary and secondary organic fraction, and the third one presents the characterization of water-soluble ions, carbonaceous fraction, and elements with the source apportionment performed by the Positive Matrix Factorization (PMF).

- The fourth chapter will be dealing with the health risk evaluation due to the exposure to $PM_{2.5}$ and VOCs and the results will be presented in two articles. The first article will highlight the health risk evaluation for VOCs and different classes of $PM_{2.5}$ compounds regarding the cancer and non-cancer risk. The second article will present the results of the oxidative potential of $PM_{2.5}$.

The results presented in the different chapters will be of utmost importance in order to assess which of the sources identified at both sites is affecting air quality the most and how to mitigate the effects. The manuscript ends with a general conclusion, recommendations, and perspectives of the study.

References:

Anderson, J.O., Thundiyil, J.G., Stolbach, A., 2012. Clearing the air: a review of the effects of particulate matter air pollution on human health. J Med Toxicol 8, 166-175, 10.1007/s13181-011-0203-1.

Bell, M.L., Ebisu, K., Peng, R.D., Samet, J.M., Dominici, F., 2009. Hospital admissions and chemical composition of fine particle air pollution. American Journal of Respiratory and Critical Care Medicine

Bellouin, N., Davies, W., Shine, K.P., Quaas, J., Mülmenstädt, J., Forster, P.M., Smith, C., Lee, L., Regayre, L., Brasseur, G., Sudarchikova, N., Bouarar, I., Boucher, O., Myhre, G., 2020. Radiative forcing of climate change from the Copernicus reanalysis of atmospheric composition. Earth Syst. Sci. Data 12, 1649-1677, 10.5194/essd-12-1649-2020.

Borgie, M., Ledoux, F., Dagher, Z., Verdin, A., Cazier, F., Courcot, L., Shirali, P., Greige-Gerges, H., Courcot, D., 2016. Chemical characteristics of $PM_{2.5–0.3}$ and $PM_{0.3}$ and

consequence of a dust storm episode at an urban site in Lebanon. Atmos Res 180, 274-286, https://doi.org/10.1016/j.atmosres.2016.06.001.

Cochard, M., Ledoux, F., Landkocz, Y., 2020. Atmospheric fine particulate matter and epithelial mesenchymal transition in pulmonary cells: state of the art and critical review of the in vitro studies. Journal of Toxicology and Environmental Health, Part B, Critical reviews 23, 293-318, https://doi.org/10.1080/10937404.2020.1816238.

Dentener, F., Kinne, S., Bond, T., Boucher, O., Cofala, J., Generoso, S., Ginoux, P., Gong, S., Hoelzemann, J.J., Ito, A., Marelli, L., Penner, J.E., Putaud, J.P., Textor, C., Schulz, M., van der Werf, G.R., Wilson, J., 2006. Emissions of primary aerosol and precursor gases in the years 2000 and 1750 prescribed data-sets for AeroCom. Atmos. Chem. Phys. 6, 4321-4344, 10.5194/acp-6-4321-2006.

ESCWA, 2009. Air quality and atmospheric pollution in the Arab region.

Fowler, D., Brimblecombe, P., Burrows, J., Heal, M.R., Grennfelt, P., Stevenson, D.S., Jowett, A., Nemitz, E., Coyle, M., Liu, X., Chang, Y., Fuller, G.W., Sutton, M.A., Klimont, Z., Unsworth, M.H., Vieno, M., 2020. A chronology of global air quality. Philosophical Transactions of the Royal Society A: Mathematical, Physical and Engineering Sciences 378, 20190314, doi:10.1098/rsta.2019.0314.

im, u., Kanakidou, M., 2012. Impacts of East Mediterranean megacity emissions on air quality. Atmos. Chem. Phys. 12, 6335-6355, 10.5194/acp-12-6335-2012.

Krishna, R.K., Panicker, A.S., Yusuf, A.M., Ullah, B.G., 2019. On the Contribution of Particulate Matter (PM2.5) to Direct Radiative Forcing over Two Urban Environments in India. Aerosol and Air Quality Research 19, 399-410, 10.4209/aaqr.2018.04.0128.

Lelieveld, J., Evans, J.S., Fnais, M., Giannadaki, D., Pozzer, A., 2015. The contribution of outdoor air pollution sources to premature mortality on a global scale. Nature 525, 367-371, 10.1038/nature15371.

Lelieveld, J., Hadjinicolaou, P., Kostopoulou, E., Chenoweth, J., El Maayar, M., Giannakopoulos, C., Hannides, C., Lange, M.A., Tanarhte, M., Tyrlis, E., Xoplaki, E., 2012. Climate change and impacts in the Eastern Mediterranean and the Middle East. Climatic Change 114, 667-687, 10.1007/s10584-012-0418-4.

Lelieveld, J., Hadjinicolaou, P., Kostopoulou, E., Giannakopoulos, C., Pozzer, A., Tanarhte, M., Tyrlis, E., 2014. Model projected heat extremes and air pollution in the eastern Mediterranean and Middle East in the twenty-first century. Regional Environmental Change 14, 1937-1949, http://dx.doi.org/10.1007/s10113-013-0444-4.

Mark Goldberg, 2008. A systematic review of the relation between long-term exposure to ambient air pollution and chronic diseases. Rev. Environ. Health 23, 243-298, https://doi.org/10.1515/REVEH.2008.23.4.243.

MoE, 2017. Lebanon's National Strategy for Air Quality Management for 2030. http://www.databank.com.lb/docs/MoE-(2017)-National-Air-Quality-Management-Strategy-EN.pdf.

Riffault, V., Arndt, J., Marris, H., Mbengue, S., Setyan, A., Alleman, L.Y., Deboudt, K., Flament, P., Augustin, P., Delbarre, H., Wenger, J., 2015. Fine and ultrafine particles in the vicinity of industrial activities: A Review. Crit Rev Environ Sci Technol 45, 2305-2356, 10.1080/10643389.2015.1025636.

Schraufnagel, D.E., 2020. The health effects of ultrafine particles. Exp. Mol. Med. 52, 311-317, 10.1038/s12276-020-0403-3.

Schwartz, J., Neas, L., 2000. Fine particles are more strongly associated than coarse particles with acute respiratory health effects in school children.

Thurston, G.D., Kipen, H., Annesi-Maesano, I., Balmes, J., Brook, R.D., Cromar, K., De Matteis, S., Forastiere, F., Forsberg, B., Frampton, M.W., Grigg, J., Heederik, D., Kelly, F.J., Kuenzli, N., Laumbach, R., Peters, A., Rajagopalan, S.T., Rich, D., Ritz, B., Samet, J.M., Sandstrom, T., Sigsgaard, T., Sunyer, J., Brunekreef, B., 2017. A joint ERS/ATS policy statement: what constitutes an adverse health effect of air pollution? An analytical framework. European Respiratory Journal 49, 1600419, 10.1183/13993003.00419-2016.

Waked, A., Afif, C., Brioude, J., Formenti, P., Chevaillier, S., Haddad, I.E., Doussin, J.-F., Borbon, A., Seigneur, C., 2013. Composition and source apportionment of organic aerosol in Beirut, Lebanon, during winter 2012. Aerosol Sci. Technol. 47, 1258-1266, 10.1080/02786826.2013.831975.

Waked, A., Afif, C., Seigneur, C., 2012. An atmospheric emission inventory of anthropogenic and biogenic sources for Lebanon. Atmos Environ 50, 88-96, https://doi.org/10.1016/j.atmosenv.2011.12.058.

WHO, 2016. Ambient air pollution : a global assessment of exposure and burden of disease. Switzerland, Geneva. https://apps.who.int/iris/bitstream/10665/250141/1/9789241511353-eng.pdf.

WHO, 2019. Climate change in the Eastern Mediterranean Region: priorities in enhancement of health systems preparedness Weekly Epidemiological Record 94, xviii-xxi

WHO; 2021.Addressing the impact of air pollution on health in the Eastern Mediterranean Region. World Health Organization, Regional office for the Eastern Mediterranean. http://www.emro.who.int/about-who/rc61/impact-air-pollution.html. Consulted on 14/10/2021

WWF, 2021. “The climate change effect in the Mediterranean. Six stories from an overheating sea” WWF Mediterraean Marine Initiative, Rome, Italy.

Xing, Y.-F., Xu, Y.-H., Shi, M.-H., Lian, Y.-X., 2016. The impact of $PM_{2.5}$ on the human respiratory system. J Thorac Dis 8, E69-E74, 10.3978/j.issn.2072-1439.2016.01.19.

Yu, G.H., Park, S., 2021. Chemical characterization and source apportionment of $PM_{2.5}$ at an urban site in Gwangju, Korea. Atmos. Pollut. Res. 12, 101092, https://doi.org/10.1016/j.apr.2021.101092.

CHAPTER I

Literature and background studies

There's so much pollution in the air now that if it weren't for our lungs there'd be no place to put it all...

Robert Orben

1 Definition of air pollution

The World Health Organization defined air pollution as contamination of indoor or outdoor environments by any chemical, physical, or biological agent that modifies the characteristic of the atmosphere (WHO, 2021a). Seinfeld and Pandis (2006) added that these agents are considered toxic at a certain concentration or exposure duration that are above the natural levels with the potential to produce an adverse effect on human health. These air pollutants are considered a mixture of solid particles and gases according to United States Environmental Protection Agency (USEPA, 2021).

In 2015, the United Nations have published the Sustainable Development Goals (SDGs). The aim of these SDGs is to reduce the number of deaths and illness from hazardous chemicals in air, water, and soil pollution by 2030 **(Fig. I-1)**. SDG 11 entitled "sustainable cities and communities" focuses on the reduction of the adverse per capita environmental impact of cities, by paying attention to air quality and waste management. The indicator used to evaluate this goal is the annual mean levels of $PM_{2.5}$ in cities. If these goals were reached, countries might also reduce the burden of disease from cardiovascular problems such as strokes, heart diseases and pulmonary problems such as chronic and acute respiratory diseases (WHO, 2016).

Fig. I-1: 17 Sustainable Development Goals published by the United Nations

2 Sources of atmospheric pollution

Atmospheric pollutants can originate from natural (geogenic and biogenic-related) or anthropogenic (human-related) sources **(Fig. I-2)**. On one hand, natural sources mainly encompass soil dust, sea-salt, volcanic eruptions, wildfires, and biogenic particles **(Table I-1)**. On the other hand, anthropogenic sources are due to human activities which include industrial and manufacturing emissions, power generation services, transportation, fuel burning for cooking, heating and producing, agriculture and incinerations, etc. **(Table I-1)**.

Table I-1: Summary of natural and anthropogenic sources of emissions

Natural sources	
Crustal Source "Soil dust"	Soil dust, known as mineral dust, is naturally generated by strong winds and enter into the atmosphere. The major elements found in terrestrial dust are Al, Si, Fe, Ca, Mg, K and Ti. The aerosolization of the soil particles mainly depend on wind speed, physical properties of the soils and their surface conditions (Usher et al., 2003).
Marine Source "sea-salt"	Sea-salt or sea spray, is generated mainly by the "bubbling" phenomenon: salt water droplets are made by wave movements, emitted and dried up into the atmosphere to give solid salts having a very close chemical composition to that of sea water: Cl^-, Na, ss-SO_4^{2-}, Mg, Ca and K. However, the composition can be modified in the atmosphere due to chemical reactions with gaseous reactants and may lead to changes in the concentration ratios between the elements, mainly chloride deficit, and will be called aged sea-salt (Tang et al., 1997).
Volcanic eruptions	A distinction is made between silicate aerosols that mainly contain heavy metals and sulphate aerosols resulting from the transformation of sulfuric volcanic gas in contact with the vapors hat cool and condense (Zelenski et al., 2020). Gaseous emissions include SO_2, CO_2, H_2O, H_2S, etc.
Wildfires	Wildfires over a large area are manifested by forest and savannah fires. The composition of fumes emitted from these wildfires varies but they are mainly formed of primary particles along with gases that are capable of forming secondary aerosols by gas-particle conversion. The composition of the smokes mainly depends on the type of burned plant (Alves et al., 2010).
Biogenic particles	These aerosols can be directly emitted into the atmosphere as pollen, spores, animal or plant fragments, bacteria, algae, protozoa or viruses (Després et al., 2012). In addition to that, they can be emitted by numerous oxidation reactions of gaseous hydrocarbons emitted from plants (terpenoids like isoprene and α-pinene) and will be categorized as Secondary Organic Aerosols (SOA).
Anthropogenic sources	
Transport sector	Main emissions come from the combustion of fossil fuels (emission of organic and elementary carbon), tire friction, wear of brake pads and resuspension (emission of particles that contain metals: lead, zinc, copper, aluminum, mineral ions and carbon compounds) in a lesser amount than EC and OC (El Haddad et al., 2009).

Biomass Burning	Anthropogenic forest fires (intentional burning of lands and areas) and human activities (heating or cooking) are the origins of biomass burning (Koppmann et al., 2005). The composition of smoke from forest fires is mainly formed of primary particles to which are added gases which can lead to the formation of secondary compounds. The type and quantity of emissions from the biomass burning vary depending on the moisture content, type of wood, ambient temperature and wind speed (Chantara et al., 2019).
Industrial emissions	The emissions related to industrial activities depend largely on the type of industry, the manufacturing process, the type of fuel used for energy production, and the technology implemented. For example, V and Ni are tracers for oil combustion, As, Co, and Cr for coal combustion (Riffault et al., 2015).

These pollutants can also be of primary origins (emitted directly from the source) or of secondary origins formed by physical transformation or chemical processes in the atmosphere (Seinfeld and Pandis, 2016). Additionally, these pollutants are generally divided into 2 categories: gases and particles.

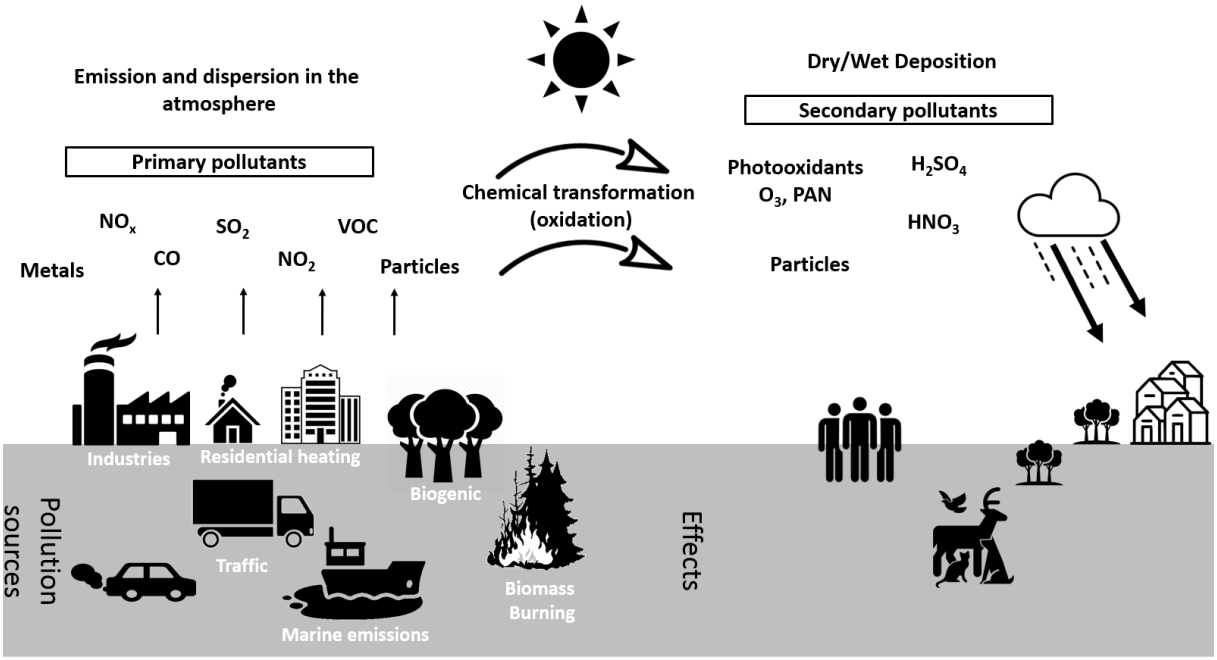

Fig. I-2: Sources of primary and secondary (natural and anthropogenic) atmospheric pollutants.

3 Gaseous pollutants

Gases pollutants include CO, NO_x, SO_2, NH_3, O_3, and volatile organic compounds that will be briefly presented in this paragraph.

3.1 Nitrogen oxides

Nitrogen oxides NO_x include mainly NO and NO_2 and are among the most important molecules in atmospheric chemistry. They are emitted mainly from combustion activities such as fuel burning for automobiles and power plants (Rai et al., 2011). NO_x is rapidly oxidized in the atmosphere. They are considered as precursors of a large number of atmospheric pollutants such as O_3, HNO_3, organic nitrates, etc. The fraction of NO in NOx for combustion sources is generally very high (>90%) while NO_2 fraction is generally small (<10%). Once emitted, a part of NO is oxidized into NO_2 in the atmosphere.

3.2 Carbon monoxide

CO is primarily emitted from incomplete combustion processes, including the combustion of fossil fuels derived from motor vehicle emissions, industrial heating and processing (Jaffe, 1968). It is an organic carbonaceous compound that has a low chemical reactivity and an important toxicity that is function of the CO concentration (discomfort starting 200 ppm) and the exposure duration (Harvey and Hutton, 1999). It is a colorless, odorless, and tasteless gas.

3.3 Sulfur dioxide

Sulfur dioxide (SO_2) is a primary pollutant that is mainly emitted from the combustion of sulfur-containing fuel such as coal, oil, or diesel in power plants, maritime traffic, and other industrial facilities. Sulfur dioxide is oxidized in the atmosphere to form sulfate in the form of sulfuric acid (H_2SO_4) and reacts quickly with ammonia to form non-volatile ammonium sulfate $(NH_4)_2SO_4$ (Fine et al., 2008).

3.4 Ammonia

Ammonia (NH_3) is the reduced form of nitrogen in the atmosphere. It is the most abundant alkaline gas in the atmosphere which is mainly emitted by agricultural activities (Behera et al., 2013). It contributes to the formation of ammonium sulfate and ammonium nitrate salts in the particulate phase by reacting with acidic species such as SO_2 and NO_x (Wang et al., 2015).

3.5 Ozone

Ozone (O_3) is present in two atmospheric layers: the stratosphere and the troposphere. It is considered a beneficial gas in the stratosphere because it is naturally present, and it forms a layer protecting the population living at the surface of the Earth from low wavelength solar radiations (Staehelin et al., 2001). However, tropospheric ozone or ground level ozone is considered dangerous because it is a main component of the photochemical smog which is toxic to human health. Ground-level ozone is a secondary pollutant resulting mainly from photochemical atmospheric reactions of NO_x, VOCs in the presence of light (Rai et al., 2011).

3.6 Volatile and Semi-volatile organic compounds

By definition, any organic compound that has a vapor pressure of 10 Pa or more at 20°C, or a corresponding volatility under the particular condition of use is called a Volatile Organic Compound (VOC) (Olsen and Nielsen, 2001). VOC possess high volatility, mobility, and strong resistance to degradation allowing them to be transported over long distance. They can be emitted either from natural sources such as trees and vegetations or anthropogenic sources (domestic and industrial processes) (Pandey and Yadav, 2018). VOCs include compounds as alkanes, alkenes, alkynes, aldehydes, and aromatic compounds, etc.

Semi volatile organic compounds (SVOCs) as defined by the USEPA Terminology Reference System represent compounds that volatilize relatively slowly at standard temperature and pressure. They have lower vapor pressure than VOCs that is in the range of 10^{-9} to 10 Pa (Xu and Zhang, 2011). They include a wide range of organic compounds such as polycyclic aromatic hydrocarbons (PAHs), polychlorinated biphenyls (PCBs), and some phthalates (He and Balasubramanian, 2010; Kondo et al., 2018).

4 Atmospheric particles

4.1 Definition

Particulate matter or PM represents a complex mixture of solid and liquid droplets, which in a carrier gas or gas mixture is called “aerosols”. Aerosols emitted directly from the pollution source are called primary aerosols while when formed in the atmosphere by physical transformation or chemical processes (gas-to-particle conversion or evolution of primary particles), they are named secondary aerosols (Seinfeld and Pandis, 2016).

4.2 Size of particles

The size of atmospheric particles ranges from few tens of Angstroms to several hundred of micrometers (Seinfeld and Pandis, 2016). Due to the difference in their morphology, an equivalent aerodynamic diameter "Da_e" is used to facilitate the comparison between the different types of particles. It represents the diameter of a unit density sphere (ρ= 1 g/cm^3) having the same terminal velocity as the particles. Based on this definition, an ultrafine particle has a diameter that is less than 0.1 µm and is also called $PM_{0.1}$. Additionally, particles with a diameter that is equal to or less than 2.5 µm are referred to as $PM_{2.5}$ and called fine particles. PM_{10} corresponds to particles with a Da_e that is equal or less than 10 µm including ultrafine, fine and a fraction of coarse particles (having a Da_e between 2.5 and 10 µm) (Seigneur, 2019).

4.3 Mechanism of particle formation

Another classification of atmospheric particles takes into account the different formation mechanisms that can affect the size distribution of particles. From these mechanisms, three processes are considered to control particle dynamics: nucleation, condensation, and coagulation. The nucleation is defined as the process of formation of a new particle from gaseous phase. The condensation is the mechanism where gas molecules condense into particles. This process increases the diameter of the particles but preserve their number. The coagulation is the mechanism of combination between particles. Many factors can influence the coagulation rate between particles such as their concentrations, composition, speed of movement and their specific surface area. It is a process where the diameter of particles increases while their number decreases.

According to these processes, Whitby (1978) defined three modes in the particle size distribution **(Fig. I-3):**

- The nucleation mode is part of the ultrafine fraction of the PM. It corresponds to particles formed from molecules in the gas phase and grown by condensing with other gaseous molecules or coagulating with other nucleated particles. Seinfeld and Pandis (2006) separated the nucleation mode from the Aitken mode. The Aitken mode contains particles having a diameter between 20 and 100 nm while the nucleation mode consists of particles with a diameter less than 20 nm.
- The accumulation mode results from fine particle emissions and from dynamic processes such as condensation and coagulation of nucleation and Aitken particles

- The coarse mode consists of particles mostly emitted from mechanical processes such as abrasion and wind erosion.

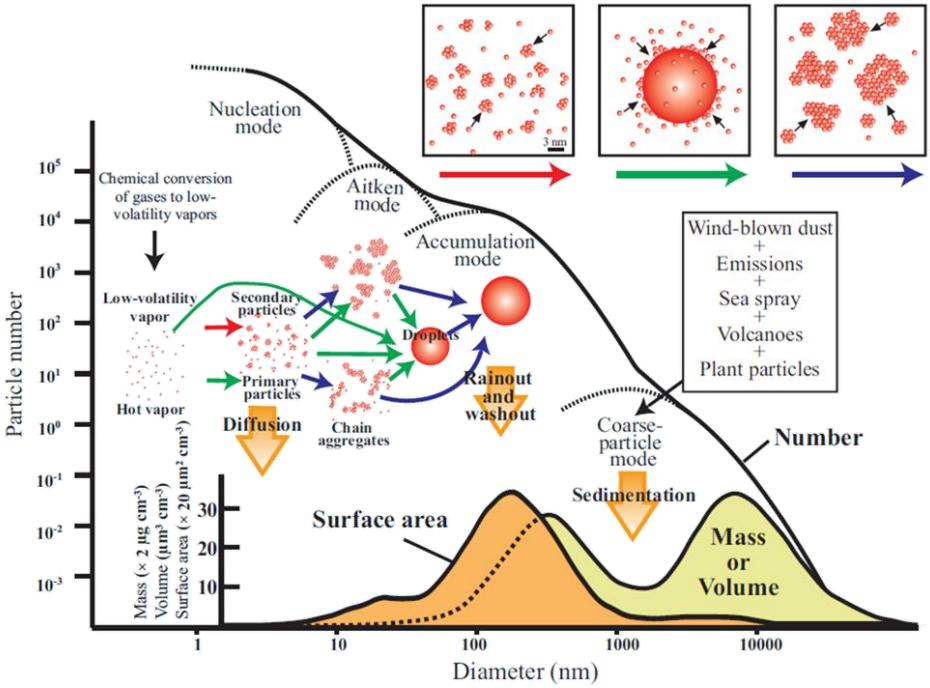

Fig. I-3: Schematic of the size distribution of particles along their formation mechanisms (Buseck and Adachi, 2007) adapted from Whitby (1978)

4.4 Composition of particles

Other than size differences, particles can have different chemical composition depending on several parameters including the emission sources and they may contain a large number of inorganic and organic species.

4.4.1 Carbonaceous fraction

Carbonaceous aerosol is divided into two fractions according to their chemical properties: organic and elemental carbon. Elemental carbon (EC) can only be emitted by primary sources, specifically combustion and burning processes. Due to its high chemical inertness, EC has become a very effective tracer of anthropogenic emissions, namely fossil fuel combustion originating from road transport in urban areas (Pio et al., 2011). This fraction of carbon is the most abundant light-absorbing aerosol species in the atmosphere and it volatilizes above a temperature of 550°C (Bond and Bergstrom, 2006; Seinfeld and Pandis, 2016). Organic carbon (OC) can be emitted directly into the atmosphere by combustion or biomass processes (Primary Organic Carbon, POC). Additionally, for the compounds with low vapor pressure, OC is formed

by gas-phase oxidation of VOCs and will be called Secondary Organic Carbon (SOC) (Sharma et al., 2018). The OC gathers a set of organic compounds present in the particulate phase such as polycyclic aromatic compounds (PAHs), alkanes, dioxins (PCDD), furans (PCDF), polychlorinated biphenyl (PCB), sugars, phthalates, hopanes, carboxylic acids and sugar alcohols (El Haddad et al., 2011a).

The natural contributors to the carbonaceous matter originate from biological sources (vegetation and micro-organisms) while the main contributor to the anthropogenic fraction is the combustion source because it emits both OC and EC but it is the type of fuel used and the combustion process that may change the OC/EC ratio. For example, an OC/EC ratio between 1 and 4.2 indicates a diesel and gasoline motor vehicle emission, while a ratio of 2.5-10 indicates coal combustion, while the biomass burning is characterized by a ratio of 3.8-13.2 and the cooking emissions by a ratio 32.9-81.6 (Qi et al., 2018).

However, to quantify the organic matter concentration (OM), organic carbon should be multiplied by a factor representing the ration OM/OC to account for the unmeasured H,O,N and S in the organic compounds (Chow et al., 2015). This ratio varies between 1.2 and 2.1 depending on the quantity of oxygenated aerosol in the PM (Turpin and Lim, 2001; Sciare et al., 2005).

4.4.2 Inorganic fraction

Water-soluble ions

Water soluble ions in atmospheric aerosols are generally composed of anions such as: chloride Cl, nitrate NO_3^-, sulfate SO_4^{2-}, fluoride F^-, phosphate PO_4^{3-} and cations such as: sodium Na^+, calcium Ca^{2+}, potassium K^+, ammonium NH_4^+ and magnesium Mg^{2+}. These compounds are either emitted directly from natural (marine or crustal) or anthropogenic (fertilizers, raw materials rich in salts, etc.) sources or produced in the atmosphere by the oxidation of the precursor gas, namely nitrogen oxides NO_x, sulfur dioxide SO_2 and ammonia NH_3 to give NO_3^-, SO_4^{2-} and NH_4^+. These three ions form together the Secondary Inorganic Aerosol (SIA). These precursor gases can be emitted from local sources but can also be due to long-range transport. The SIA compounds mainly occur as ammonium sulfate $(NH_4)_2SO_4$, ammonium bisulfate (NH_4HSO_4) and ammonium nitrate (NH_4NO_3).

SIA play a major role in determining some important physical properties of the particles such as hygroscopicity and acidity and may affect the optical properties and the Earth's radiation balance (Agarwal et al., 2020).

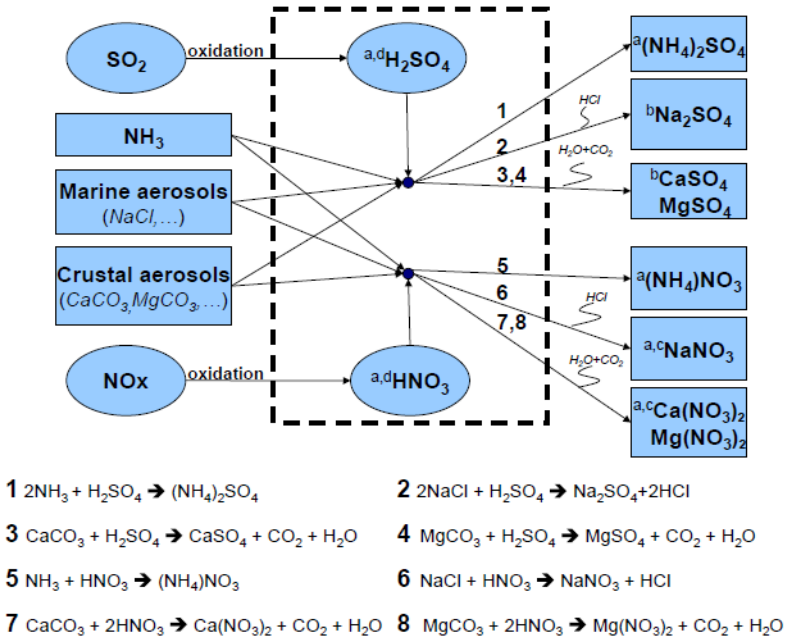

Fig. I-4: Formation of different nitrates and sulfates chemical species from precursor compounds taken from (Arruti et al., 2011)

Fig. I-4 represents the possible formation reactions of sulfates and nitrates in the atmosphere (Arruti et al., 2011). Generally, secondary sulfate is generated by the oxidation of sulfur dioxide SO_2 while nitrate is formed by the oxidation of nitrogen oxides. These two compounds are originally formed as sulfuric acid H_2SO_4 and nitric acid HNO_3 and are then neutralized by NH_3 forming ammonium salts.

Major and trace elements

In airborne particulate matter, elements can be emitted by different natural or anthropogenic sources **(Fig. I-5)**. However, some elemental ratios are specific to a source. The major elements found in PM are Fe, Ca, Al, Mg, K and Na while the others (ex. Ag, As, Cd, Cr, Cu, La, Mn, Ni, Ti, P, Pb, Rb, Sb, Se, Sc, V, Zn, Co, Mo, Mn) are considered as trace elements due to their low concentrations in PM. These elements can play a major role in the aerosol toxicity by the fact that they are either adsorbed or condensed on the surface of the particles. Transition metals are generally emitted through anthropogenic activities. As, Cd, Cu, Mn, Ni, Zn, V, Pb and Hg are emitted from high temperature human activities counting fuel combustion, vehicular emissions, steel smelters and are mainly accumulated in the fine fraction of PM (Riffault et al., 2015).

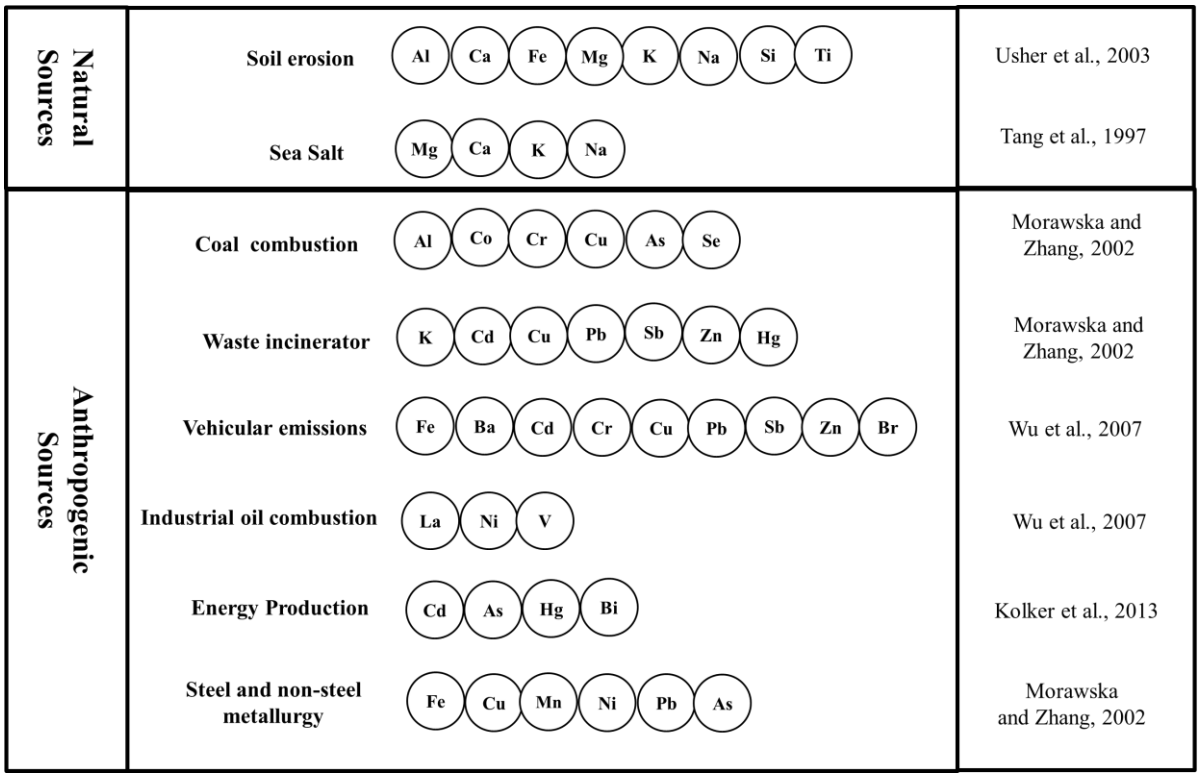

Fig. I-5: Elements emitted from different natural and anthropogenic activities

In addition to that, elements like Al, Ca, Fe, Mg, K, Na, Si and Ti are caused mainly by the natural crustal source and might be also emitted by other types of sources (industrial, ceramic and glass manufacturing, etc.).

4.4.3 Organic fraction

Primary organic aerosols

- Alkanes

Alkanes or paraffins are acyclic saturated hydrocarbons that do not contain any functional groups. These compounds are extremely unreactive and have a chemical formula of C_nH_{2n+2}. They can have either anthropogenic origins such as tire debris, brake lining dust, vehicular and industrial emissions or a biogenic source such as leaf abrasion products, garden soil and biomass burning (Yadav et al., 2013). The alkanes present in the atmosphere have in general a number of carbons between 12 and 40 (Alves, 2008). Generally, the light n-alkanes (MW<324 g/mol) are found to be in the gas phase while heavy n-alkanes are primarily in the particulate phase (Xie et al., 2014).

- Polycyclic Aromatic Hydrocarbons

PAHs refer to compounds formed by two or more benzene rings that are environmentally persistent with various structures and toxicity (Abdel-Shafy and Mansour, 2016). These compounds are generally partitioned between the gas and the particulate phase depending on the atmospheric temperature. PAHs with two or three aromatic rings are also called "light molecular weight PAHs" and are mostly in the gaseous phase while "high molecular weight PAHs" are formed of 5 or 6 aromatic rings and are present mostly in the particulate phase. The four-rings PAHs partitioning between the gaseous and the particulate phase is very sensitive to temperature (Srogi, 2007).

The toxicity, mutagenicity and/or carcinogenic properties of the PAHs have made 16 of them listed as priority pollutants (Hussar et al., 2012): naphthalene, acenaphthylene, acenaphthene, fluorene, phenanthrene, anthracene, fluoranthene, pyrene, chrysene, benz[a]anthracene, benzo[b]fluoranthene, benzo[k]fluoranthene, benzo[a]pyrene, indeno[1,2,3-c,d]pyrene, dibenz[a,h]anthracene and benzo[g,h,i] perylene.

The main source of emission of PAHs in the atmosphere is the combustion of fossil and non-fossil fuel. The anthropogenic sources attached to PAH emissions are engine exhaust, natural gas combustion, residential heating, incineration, smokes, and industrial processes. Forest fires and volcanic eruptions are considered as natural sources of these compounds (Mastral et al., 2003).

- Hopanes

Hopanes correspond to a class of pentacyclic saturated hydrocarbons. These compounds are not present in gasoline and diesel fuel because they belong to the higher boiling fraction of crude petroleum. They are mainly found in lubricating oil and can be used as molecular markers for vehicular emissions in the atmosphere (Yousef et al., 2001). These compounds are generally found in the particulate phase but are more volatile during the hot season (Ruehl et al., 2011).

- Phthalates

Phthalates are a group of man-made chemical compounds, esters of phthalic acid, used as plasticizers in industrial final products and building materials to give flexibility and elasticity to the material (Lu et al., 2018) . They are bonded to the material by weak intramolecular forces not in a chemical way leading sometimes to their detachment and their release into the atmosphere (Pei et al., 2013; Lu et al., 2018). These compounds fit the definition of SVOCs since they are present in both gas and particulate phases. The fraction associated with the

particulate phase of these compounds increase with the molecular weights of the phthalates (Weschler et al., 2008). Studies have shown that phthalates might be disruptors of the endocrine system in humans (Ji et al., 2014) and might also affect the reproductive systems and children's intelligence (Lu et al., 2018).

- Saturated and unsaturated fatty acids

Generally, this class of compounds is the most abundant in the organic fraction and is mostly observed in the particulate phase (Rogge et al., 1991). The main components are tetradecanoic, hexadecenoic and octadecanoic acids as saturated fatty acids and oleic acid as unsaturated fatty acid. These compounds are mainly emitted from cooking activities in urban areas but can be also found in oceanic biological and marine aerosols (Waked et al., 2014).

- Anhydrosugars and sugar alcohols

Anhydrosugars are sugar derivatives from the parent sugar such as cellulose and amylose by a mechanism of pyrolysis. The major compounds present in the atmosphere are levoglucosan, mannosan and galactosan and are predominantly emitted by anthropogenic activities (agricultural waste, residential wood heating, forest fires, etc.). The most abundant one is levoglucosan known to be the product of pyrolysis of cellulose and is considered as an organic marker for biomass burning emissions (Simoneit, 1999; Theodosi et al., 2018). It is mainly found in the particulate phase (Latif et al., 2012).

In addition to that, sugar alcohols such as sorbitol, arabitol, mannitol and primary saccharides (fructose, sucrose, glucose) are considered as molecular markers for the primary biogenic organic aerosols. These products are emitted by plants, spores and bacteria (Medeiros et al., 2006; Bauer et al., 2008; Samaké et al., 2019b).

- Dioxins, furans, and polychlorobiphenyls

The term "dioxins or dioxin-like substances" generally define a family of chlorinated compounds with similar chemical structures and biological activities but different toxicities. This term includes three important types of compounds:

- The polychlorinated dibenzo-p-dioxins (PCDDs) family that includes over 75 compounds
- The polychlorinated dibenzofurans (PCDFs) containing 135 compounds
- The polychlorinated biphenyls (PCBs) containing 209 individual compounds

These compounds are semi-volatile persistent organic pollutants that can be transported far from their emission sources (Koukoulakis et al., 2020). PCDDs and PCDFs are generally emitted by vehicular emissions and industrial processes especially industries producing compounds such as chlorophenols and phenoxy herbicides, chlorine bleaching of paper pulp and smelting (Cortés et al., 2014). Additionally, these compounds are emitted from high temperature processes such as waste incineration and sintering in iron and steel industries (Anderson and Fisher, 2002). PCBs are not natural substances but were manufactured for use as dielectric fluids, in larger-scale electrical products such as transformers and capacitors, in heat transfer and hydraulic systems and in industrial oils and lubricants (WHO, 2010).

From these 3 families, several compounds have toxicological effects and can have a significant dioxin-like-toxicity. These agents have the ability to bind to the aryl hydrocarbon receptor or known as Ah receptor. This protein is well known for its role in mediating toxicity and regulating enzymes and other proteins. It was originally characterized as a regulator of xenobiotic metabolism but in the presence of dioxin-like compounds, it also mediates a variety of biological responses leading to hepatocellular damage, thymic involution, immune suppression, and/or tumor promotion. (Stevens et al., 2009).

Secondary organic aerosols

- Mechanism of formation

The secondary organic aerosols (SOA) refer mainly to aerosols that have undergone oxidation reaction between VOCs and atmospheric oxidants such as ozone O_3, hydroxyl radicals OH and nitrate radicals NO_3 (Atkinson, 2008).

These reactions contribute to the generation of other VOCs with lower volatility until produced species have a sufficient low vapor pressure in order to condense and lead to the formation of the SOA. **Fig. I-6** shows a simplified reaction mechanism starting with VOCs that are initially attacked by the oxidants ($OH/O_3/NO_3$) with different action mechanisms to produce an alkyl radical. This radical rapidly form RO_2 radicals, which have an essential role in the production of lower-volatility products such as peroxynitrates, organic nitrates, hyperoxides, alcohols, carbonyls and alkoxy radicals.

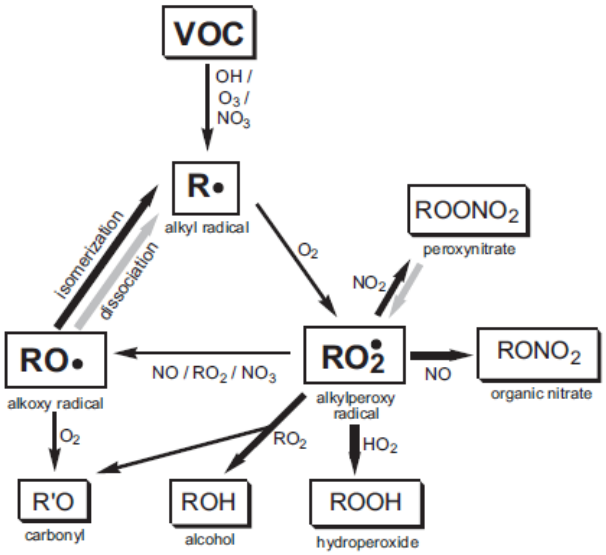

Fig. I-6: SOA formation cycle (Kroll and Seinfeld, 2008)

The SOA formation yields along with the SOA composition depend on the precursor concentrations, meteorological conditions, and NO_x concentrations (Atkinson and Arey, 2003). Alkoxy radicals can react with oxygen to form a carbonyl, or dissociate to form a carbonyl and an alkyl radical or isomerize by 1,5-hydrogen shift to produce alkyl radicals (Kroll and Seinfeld, 2008) .

- SOA precursors

Secondary organic aerosols are formed from both anthropogenic and biogenic gaseous precursors. The major anthropogenic precursors encompasses aromatic compounds, alkanes, fatty acids, PAHs, and phthalates and are mainly emitted by mobile and industrial sources (Alves and Pio, 2005). On the other hand, biogenic precursors involve isoprene, monoterpene, and sesquiterpene compounds that are largely emitted by terrestrial ecosystems and vegetations (Hallquist et al., 2009). Even though the anthropogenic precursors dominate in urban areas, it is well established that biogenic VOCs account for 75-90% of the total VOC emissions on a worldwide basis (Lamarque et al., 2010).

Monoterpenes are considered as the major biogenic compounds involved in the SOA formation, constituting more than 80% of conifers' VOC emissions (Alves and Pio, 2005). The most abundant monoterpene in the troposphere is the α-pinene with the biggest literature and studies conducted evaluating the SOA formation from its oxidation initiated with OH and O_3 (McVay et al., 2016). The oxidation chemistry of α-pinene relies on a complex dependency on NO_x

concentrations, also several oxidation conditions such as as the initial concentration of the precursor and the oxidant along with meteorological conditions (temperature and humidity) (Zhang et al., 2015; Shrivastava et al., 2017). The main oxidation products of α-pinene are pinic and pinonic acids as well as different higher generation oxidation products **(Fig. I-7).**

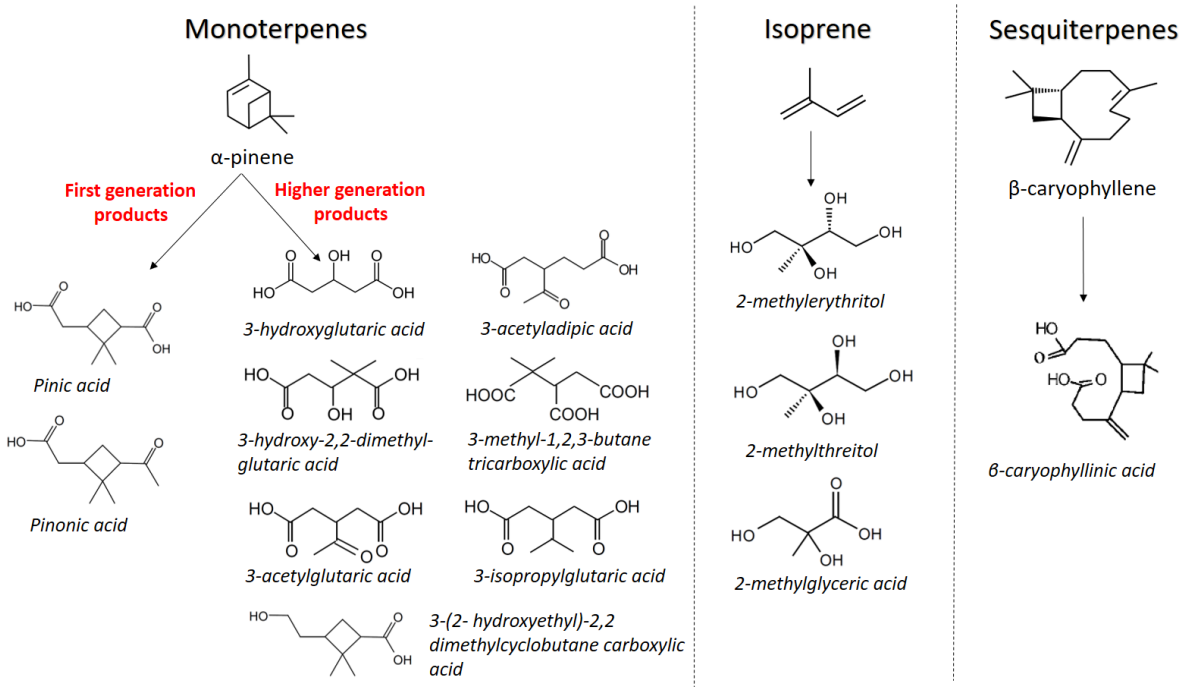

Fig. I-7: Biogenic VOCs and their oxidation products

Isoprene is a highly reactive compound due to its double bond and is oxidized in the atmosphere by the different oxidants (OH, O_3, NO_3). For years, it has been accepted that isoprene does not contribute to the SOA formation due to its high volatility (Carlton et al., 2009). Conversely, this topic has been reexamined and several field and laboratory studies showed that isoprene can contribue to the SOA formation (Carlton et al., 2009). The main oxidation products of isoprene are the 2-methyltetrols (2-methylthreitol and 2-merthylerythritol) and the 2-methylglyceric acid **(Fig. I-7).** The formation of these compounds depends on several parameters such as the aerosol acidity and the NO_x conditions. The acidity increases the concentration of the isoprene derived SOA, while high-NO_x conditions favors the 2-methyltetrol formation and low-NO_x conditions favors the formation of 2-methylglyceric acid (Hallquist et al., 2009).

Sesquiterpenes are becoming target analytes due to their reactivity and molecular mass making them more efficient SOA precursors compared to other biogenic VOCs (Jaoui et al., 2013). The

most abundant species in the sesquiterpenes emitted from plants is the β-caryophyllene. The photooxidation product of β-caryophyllene is the β-caryophyllinic acid that was first identified in simulation chambers and then in ambient air (Jaoui et al., 2007).

4.5 Types of sources

There are generally two types of emission sources:

- **Point sources:** They are stationary, identifiable sources of pollution where pollutants are released into the atmosphere using an exhaust pipe (stack, pipe, ditch, or factory smokestack) (Hill, 2020). For example, emissions from steel mills, oil refineries, coal preparation plants, etc. (Johannisson and Hiete, 2020)
- **Non-point sources:** They are generally referred to as "diffuse sources", representing inputs and impacts occurring on a wide area and cannot be attributed to a point source (Johannisson and Hiete, 2020).

4.6 Dispersion and elimination of atmospheric particles

Atmospheric dispersion is considered as an important process that governs the levels of air pollution. During this process, air pollutants are diluted owing to mixing into the air as a result of turbulence. However, the dominance of anticyclones increases the pressure of the atmosphere and by that decreasing the dispersion of the pollutants leading to the formation of pollution episodes (Seinfeld and Pandis, 2016). One of the important meteorological parameters for transport and dispersion is the wind. It has been found that PM mass is correlated with wind direction to have a significant but local effect on air pollution levels (Kim et al., 2015), however higher wind speeds are accompanied with a dilution of pollutants and ensure the transport of pollutants over long distances (Triantafyllou and Kassomenos, 2002). Additionally, the atmospheric stability is another factor explaining the dispersion and is generated by the vertical temperature gradient resulting of the heating and cooling of the Earth's surface. The greater the atmospheric stability, the greater the suppression of the turbulence and the smaller the exchange between atmospheric layers at different levels of the atmosphere (Camuffo, 2002). This will lead the pollutants to be trapped in one layer and only travel in it.

The atmospheric boundary layer is defined as the lowest part of the troposphere and directly influenced by the earth's surface. The variations of the boundary layer is important because it dictates the dispersion of the pollutants since most of them are either emitted or formed in this layer (Hu, 2015). The boundary layer depth varies greatly over lands. During the day, the

boundary layer is in a stability regime where the tubulence tends to mix heat, moisture, and pollutants in an uniform way in the mixed layer **(Fig. I- 8)** with a stable layer on its top called entrainment layer because entrainment into the mixed layer occurs (Allaerts, 2016). After sunset, turbulence decays in the formely mixed layer and will be divided into two portions: the residual layer and the stable boundary layer. In the residual layer, the state variables and the concentration of the pollutants remain invariant. The stable boundary layer is characterized with by statically stable air with weaker turbulence (Hu, 2015). Plumes from anthropogenic emissions are generally vertically dispersed when released in the mixed layer. Those released in the stable boundary layer are mostly horizontaly dispersed and those relased in the residual layer spread in a conelike shape.

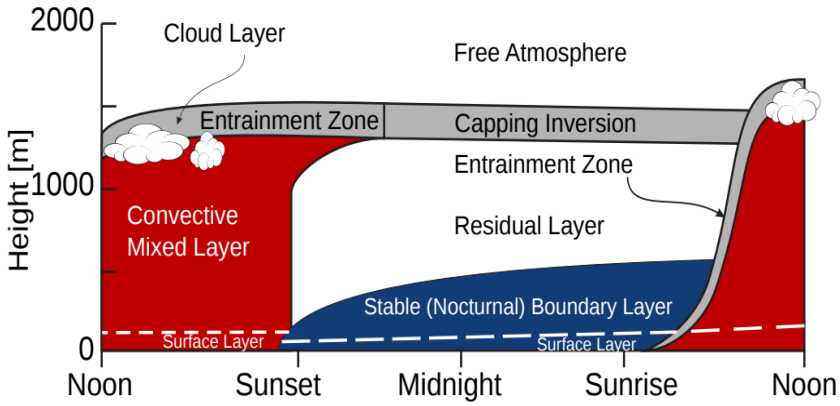

Fig. I- 8: Boundary layer structures during a diurnal cycle over land presented by Allaerts (2016) and adapted from Stull (1988)

Finally, rainfall is generally associated with unstable atmosphere, allowing a good dispersion of air pollutants.

Atmospheric particles are eliminated from the atmosphere by two main processes: the dry deposition and the wet deposition. The dry deposition represents the direct transfer of species in the gaseous or particulate phase to the Earth's surface without precipitation (Seinfeld and Pandis, 2016). The main mechanisms remain the sedimentation, impactation and Brownian diffusion. On the other hand, when atmospheric species are transferred to the surface in aqueous form (rain, snow or fog), we denote the phenomenom as wet deposition. These processes depend mainly on weather conditions and on the size of the particles.

5 Exploratory methods

In order to gain a preliminary picture of the most relevant sources and their contributions to PM, exploratory methods using simple mathematical calculations, relationships, and assumptions can be applied (Belis et al., 2014). In the following, methods involving different organic families and elements are presented.

5.1 Organic molecular markers

Organic molecular markers are quantifiable compounds that are generally emitted by a specific source or a class of sources. Ideally, each molecular marker corresponds to a unique emission source (Dutton et al., 2009). Due to this property, these compounds are important to use in source apportionment analysis (Robinson et al., 2006a).

The literature specified different molecular markers for several emission sources. Simoneit (2002) showed that levoglucosan, methoxyphenols, and syringol are markers for biomass burning while hopanes and steranes are tracers for vehicular emissions (Cass, 1998). Furthermore, cooking emissions are characterized by the abundance of cholesterol, and fatty acids specifically hexadecanoic and octadecanoic acids (Schauer et al., 1999; Robinson et al., 2006b). Molecular markers for diesel engine exhausts are mainly dicarboxylic acids (C_2- C_{10}) and n-alkanes (C_{20}-C_{21}) (Rogge et al., 1993). However, gasoline emissions are mainly characterized by C_{24} and C_{25} (Rogge et al., 1993). Regarding primary biogenic emissions for vegetation detritus, C_{27}-C_{34} n-alkanes are dominant specifically odd carbon number alkanes (C_{27}, C_{29}, C_{31}, C_{33}) along with sugar alcohols (Simoneit and Mazurek, 1982; Samaké et al., 2019a).

5.2 Diagnostic ratios and indexes

In order to try assigning emission sources to different classes of compounds such as alkanes and PAHs, statistical diagnostic methods based on the concentration of the species, are used in a semi-quantitative and qualitative way.

5.2.1 For n-alkanes

The alkanes profile pattern is the representation of the concentration of each paraffin in terms of carbon number. The alkane that has the highest concentration is referred to as "C_{max}" which is an indication of an emission source. C_{max} corresponding to eicosane and heneicosane (C_{20} - C_{21}) is mainly be assigned to diesel emissions while tetracosane and pentacosane (C_{24} – C_{25})

indicate gasoline or vehicular emissions (Rogge et al., 1993; Mikuška et al., 2015). Moreover, the primary biogenic emissions that are mainly due to vegetative detritus are marked by a C_{max} of nonacosane (C_{29}) and hentriacontane C_{31} (Li et al., 2006).

Second, the Wax n-alkane ratio is generally used to determine the distribution of the residual wax n-alkanes, when the petroleum n-alkanes are subtracted (Simoneit et al., 1991). Wax C_n is calculated by subtracting the odd average concentration C_n of the next higher C_{n+1} and lower C_{n-1} even carbon. The negative values of Wax C_n are taken as zero.

$$\text{Wax } C_n = C_n - \frac{1}{2}(C_{n-1} + C_{n+1})$$

$$\text{WNA\%} = \frac{\sum \text{Wax } C_n}{\sum A} \times 100$$

The wax ratio (Wax%) corresponds to the sum of Wax C_n by the total concentration of all n-alkanes in the sample.

Finally, the carbon preference index (CPI) is a measure of odd to even alkane predominance calculated using the following equations (Bray and Evans, 1961; Cooper and Bray, 1963):

$$\text{Overall CPI}_{19-32} = \frac{\sum \text{odd } C_{19} - C_{31}}{\sum \text{even } C_{20} - C_{32}}$$

$$\text{High CPI}_{25-32} = \frac{\sum \text{odd } C_{25} - C_{31}}{\sum \text{even } C_{26} - C_{32}}$$

An overall CPI value close to 1 indicates a petrogenic source, while a value between 2 and 5 mainly suggests biomass burning and a CPI value higher than 6 is characteristic of biogenic emissions (Simoneit, 2002). A value less than 1.5 for the High CPI indicates an anthropogenic source while a value higher than 3 indicates a natural one. An intermediate value explains a combination of natural and anthropogenic source.

5.2.2 For PAHs

PAHs diagnostic ratios have been used to identify the source of particle-containing PAHs. They can help to determine the different emission sources as well the different fuel types used in the combustion processes (Riffault et al., 2015). This methodology is based on the hypothesis that the PAHs concentration ratios remain constant between the emission source and the measuring site. This is particularly true for isomers having similar photochemical properties considered to be affected in a similar manner by the different reactions occurring in the atmosphere as

mentioned by Borgie et al. (2016) and references within. According to Tobiszewski and Namieśnik (2012), the confirmation of results while using this method should be based on more than one diagnostic ratio. In addition to that, the idea of having contradictory results is sometimes explainable since light PAHs might be emitted from more sources than the heavy ones. That is why results should be supported by different molecular markers. **Table I-2** summarizes some diagnostic ratios used in the literature for source identification.

Table I-2: Literature overview for different PAHs diagnostic ratios

Ratio	Values	Reference
Anth/(Phe+Anth)	>0.1 pyrogenic <0.1 petrogenic	(Tobiszewski and Namieśnik, 2012)
B[a]An/(B[a]An+Chr)	0.2-0.35 coal combustion >0.35 vehicular emissions <0.2 petrogenic	(Tobiszewski and Namieśnik, 2012)
B[a]P/(B[a]P+Chr)	0.33 urban environment 0.49 gasoline 0.73 diesel	(Guo, 2003) (Khalili et al., 1995)
Fla/(Fla+Pyr)	<0.2 petrogenic 0.4-0.5 fossil fuel combustion >0.5 coal and biomass burning	(Tobiszewski and Namieśnik, 2012)
InPy/(InPy+B[ghi]Pe)	0.18 cars 0.37 diesel 0.56 coal 0.62 Biomass burning 0.35-0.7 Diesel emissions	(Ravindra et al., 2008)
	0.82 residential heating appliance chimneys 0.90-0.96 cement plants 0.96 diesel emissions from taxis and buses	(Manoli et al., 2004) (Cecinato et al., 2014)
	0.2-0.5 gasoline source 0.35-0.7 diesel source >0.5 wood and coal combustion	(Riffault et al., 2015)

5.2.3 For metals

The enrichment factors are calculated to differentiate natural (marine or crustal) and anthropogenic sources of metals in the samples. It was first developed in the seventies by Dams and De Jonge (1976) and Lawson and Winchester (1979) and is calculated as follows:

$$EF = \frac{\frac{[X]_{aerosol}}{[Ref]_{aerosol}}}{\frac{[X]_{crustal}}{[Ref]_{crustal}}}$$

While [X] is the concentration of the metal in the sample (or the average concentration for the whole sampling period), and [Ref] is the concentration of the reference metal. The reference metal should be a stable element in soil, characterized by an absence of vertical mobility and/or degradation phenomena, and not anthropogenically altered (Ackermann, 2008). Typical elements used are Al, Ti, Fe, Mn, and Rb (Barbieri, 2016; rodriguez-espinosa et al., 2017).

An enrichment factor close to 1 means that the metal source is natural and is not affected by different emissions of other sources while a factor bigger than 10 implicates an anthropogenic source (Hlavay et al., 1996).

In addition to that, elemental ratios between metals can be used as tracers for the identification of different emission sources. **Table I-3** presents examples of elemental ratios used for industrial, urban, and natural sources.

5.3 Source profiles

5.3.1 Definition

By definition, a chemical source profile corresponds to the composition of PM particles derived from a specific pollution source generally expressed by the ratio between the mass of the species and the total PM mass.

The profiles are generally formed of a certain number of elements, ionic species and/or compounds that can be considered as specific markers to the emission source (Pernigotti et al., 2016). These profiles are essential because they are used as input data for some receptor models such as Chemical Mass Balance (CMB) or used as a comparison tool with the output data of multivariate analysis such as Positive Matrix Factorization (PMF). Additionally, these chemical fingerprints are used to interpret ambient measurement data and are important in establishing emission inventories for air quality modeling (Simon et al., 2010).

Several parameters can influence the source profiles and might change the weight fractions of the chemical species such as the sampling method, the type of fuel and its sulfur content for combustion emissions, the biofuel categories for biomass burning, the type and culture for cooking sources (Bi et al., 2019). These variations are examined using uncertainty analysis and cluster analysis and generally result in large variations between profiles for the same source.

Table I-3: Examples of elemental ratios used for industrial, urban, and natural sources.

Sources	PM size	Location (City)	Cu/Sb	Zn/Pb	Pb/Cd	V/Ni	Fe/Ca	Na/Mg	Reference
Industrial Source									
Fuel-oil combustion and petrochemical emissions	PM_{10}	Dunkirk, France				0.3-1.4			(Mbengue et al., 2014)
Steel Smelters	PM_{10}	Dunkirk, France		1.7-3.7	22-67				(Mbengue et al., 2014)
Petrochemical activities	PM_{10}	Dunkirk, France				2.37±0.91			(Tran et al., 2012)
The use of dolomite and coal in steel industry	PM_{10}	Dunkirk, France						2.2±0.7	(Tran et al., 2012)
Waste incineration combustion of residual oil	TSP	Gothenburg, Sweden	1.3±0.4						(Sternbeck et al., 2002)
Combustion of residual oil		Beskydy mountains (Czech Republic)				1.5-1.9			(Swietlicki and Krejci, 1996)
Steel Smelters	PM_{10} $PM_{2.5}$ $PM_{2.5-10}$	Genoa, Italy					4 5.6 3.12		(Prati et al., 2000)
Refinery – petrochemical activities	$PM_{2.5}$	Saby - Scandinavia				0.52-1.85			(Foltescu et al., 1996)
Refineries and petrochemical industries	$PM_{2.5}$	Marseille, France				1.3±0.2			(El Haddad et al., 2011b)
Heavy Fuel Oil (HFO) combustion with ship engines	$PM_{2.5}$	-				2.3±0.5			(Agrawal et al., 2008)
HFO / shipping traffic	$PM_{2.5}$	Dunkirk, France				1.6			(Ledoux et al., 2017)
Glassmaking activity	$PM_{2.5}$	Dunkirk, France			36				(Ledoux et al., 2017)
Shipping emissions	$PM_{2.5}$	Thessaloniki, Greece				2.7			(Saraga et al., 2019)

Urban-traffic source									
Major road		London, United Kingdom	7.9				3.1		(Gietl et al., 2010)
Soil erosion and urban road dust	PM_{10}	Dunkirk, France					<1		(Mbengue et al., 2014)
Traffic emissions	PM_{10}	Dunkirk, France	5.4-8.1						(Mbengue et al., 2014)
Urban traffic	PM_{10}	Dunkirk, France	5.5						(Alleman et al., 2010)
Urban traffic	PM_{10}	Dunkirk, France	6.6±1.0						(Tran et al., 2012)
Brake wear particles	TSP (similar in PM_{10} and $PM_{2.5}$)	Gothenburg, Sweden	4.6±2.3						(Sternbeck et al., 2002)
Brake linings	PM_{10} $PM_{2.5}$	Palermo, Italy	4.9 2.5						(Dongarrà et al., 2008)
Traffic	$PM_{2.5-10}$ $PM_{2.5}$	Genoa, Italy		1.1 1					(Prati et al., 2000)
Natural sources									
Marine Source	PM_{10}	Dunkirk, France						9.0-11.4	(Mbengue et al., 2014)
Marine Source	$PM_{2.5}$	Dunkirk, France						8.1	(Ledoux et al., 2017)
Marine Source	PM_{10}	Dunkirk, France						8.4	(Alleman et al., 2010)
Vegetation		Palermo, Italy	14-16						(Dongarrà et al., 2008)
Continental crust			125	4.17	173.47	2.43	1.16	2.17	(M. McLennan, 2001)

5.3.2 Available database for source profiles

Source profiles of PM have been developed all over the world especially in the USA, Europe, and East Asia. The American database SPECIATE was established by the EPA in 1988 and introduced as an online version since 1993 (Simon et al., 2010). The speciation profile provides the chemical composition of an emission source in weight percent of PM or VOC gas. The newest version updated in June 2020 (SPECIATE 5.1) contains 6,746 profiles of PM, gas, and others and gathers 2,814 unique species. 33% of the PM profiles are dust profiles (mainly road and industrial dust), while 62% are for combustion processes (biomass burning, cooking, industrial and residential combustion, mobile emissions, electric generation, etc.). Based on the objective to fill the gap in the availability of input data for source apportionment in European sites, SPECIEUROPE is an European database developed by the European Commission's Joint Research Centre (Pernigotti et al., 2016). This initiative was based on the scarcity of local source profiles in the continent that represented a challenge for receptor modeling. This database contains to date (October 2021) 287 PM and TSP profiles mainly including profiles for traffic (66), industrial emissions (109), biomass and other combustion sources (82). Finally, researchers from the Chinese research academy of environmental sciences (CRAES) developed in 2017 a new database of emission source profiles for PM called China Source Profile Shared Service (CSPSS 1.0). This database gathers profiles of coal-fired boilers, industrial emissions, fugitive dust, vehicular exhaust emissions, biomass burning, and cooking (Liu et al., 2017).

5.3.3 Overview on profiles for different pollution sources

This paragraph will present profiles for different pollution sources found in the literature along with their organic and inorganic marker species.

Cooking activities

The literature often presents different contributions of compounds to PM for cooking activities. These variations depend on the used raw material and additives, recipes, the type of oil used, and fat content especially for meat. Above all, the cooking method such as steaming, boiling, frying, broiling, grilling, or roasting can play a major role in the variation of PM composition (Zhang et al., 2017). However, organic cooking markers remain the same: oleic acid, palmitoleic acids and cholesterol as unsaturated fatty acids, hexadecanoic (palmitic) and octadecanoic (stearic) acids as saturated fatty acids (Robinson et al., 2006b). It has been found that higher fat contents in cooking ingredients will result in a higher relative contribution of fatty acids when compared to a low-fat content ingredient (Rogge et al., 1991).

In addition to that, Zhao et al. (2007) found that n-alkanes (especially C_{29} and C_{31}) can be emitted from cooking processes with high CPI values and also dicarboxylic acids as the oxidation products of dialdehydes that are formed during the oxidation process of unsaturated lipids in food. Chrysene is generally known to be the main PAH emitted compound specifically during meat or seed oils cooking. Different PAH diagnostic ratios have been found for the different types of cooking methods (Wei See et al., 2006; See and Balasubramanian, 2008; Zhang et al., 2017; Vicente et al., 2018). PAH emissions are important during charcoal cooking from the pyrolysis of carbohydrates, fats, and proteins or by the incomplete combustion of charcoal used as heating source for cooking (Cheng et al., 2019).

Biomass burning

The composition of particles emitted during biomass burning can vary depending on the moisture content and the type of wood that is used for combustion. The most abundant species are organic and elemental carbon followed by potassium and chloride (Sun et al., 2019). Additionnaly, an important organic species found in woodsmoke particles is levoglucosan that is formed during the pyrolysis of cellulose present in wood (Oros and Simoneit, 2001; Chantara et al., 2019). This source can also generate plentful n-alkanes especially odd high molecular weight ones as C_{27}, C_{29}, C_{31}, and C_{33} (de Oliveira Alves et al., 2011; Kang et al., 2018). As for PAHs, 4 rings aromatic group were the dominant with high levels of fluoranthene and pyrene. Elemental species are also found in biomass PM such as Na, Al, Si, S, Pb, and Mg, Ca, Fe, Cu, Zn to a lesser extent (Sun et al., 2019).

Diesel backup generators

Diesel generators are widely used in the world in temporary projects or as stand-by power in developed countries at power sensitive facilities or even as continuous backup power in developing countries due to power supply instability (Klimont et al., 2016). The largest proportion of PM from diesel generators are for OC and EC. The dominant elements are Fe, Ca, Zn, Mg, Al and Cr (Sothea and Kim Oanh, 2019). As for PAHs emissions, they depend on many factors such as engine size, operation of control device, operation conditions and fuel quality. The most abudant PAHs are usually pyrene, fluoranthene and chrysene. The profiles for diesel powered engines are also dominated by C_{20}-C_{21} alkanes (Rogge et al., 1993).

Road traffic emissions

The PM generated by road traffic is well studied in the literature in near-freeway and tunnel studies mainly in order to draw up a chemical source profile. This profile is characterized by

high EC concentrations relative to OC with a contribution of carbonaceous fraction that might go up to 70% of the total PM mass (El Haddad et al., 2009). In addition, many elemental species are found in road samples such as Cr, Fe, Cu, Zn, Zr, Mo, Sn, Sb, Ba and Pb (Wåhlin et al., 2006). As for the alkanes, the vehicle exhaust emissions are characterized by a low molecular weight ranging from C_{19} to C_{25} with no odd-to-even preference (Rogge et al., 1993). Additionally, hopanes and steranes were found that are derived from fuel oil and automotive lubricating oils (Yousef et al., 2001). By these findings, we can understand that the PM produced during vehicle driving can be divided into exhaust and non-exhaust emissions. Exhaust emissions generally include exhaust pipe and crankcase emissions mainly emitting carbonaceous matter (EC, OC) and organic compounds such as PAHs and n-alkanes (Charron et al., 2019; Guo et al., 2021). On the other hand, non-exhaust emissions mainly include brake and tire wears, road wear, and lubricating oils (Guo et al., 2021). Metals such as Ba, Cu, Sb, Fe, and Zn and hopanes are usually emitted by non-exhaust vehicular source (Charron et al., 2019).

Open burning of waste

The open burning is considered as an uncontrolled combustion phenomenon where the combustion products are directly emitted into the atmosphere without passing through a stack, duct or chimney (Estrellan and Iino, 2010). This pollution source can be observed in agricultural fields from crops burning and in the combustion of domestic waste. This source is generally known as the largest emitter of PCDD/Fs and DL-PCBs in the United States (Wang et al., 2020). The profiles of open burning of waste are generally composed of OC, EC, K^+, NH_4^+, Na^+, and Cl^- (Wang et al., 2020) that can differ from the controlled incineration profiles since the combustion process is different but also depending on the composition of waste (Yang et al., 2016).

Industrial emissions

Studies of fine particulate matter in the vicinity of industrial areas generally present a variable and complex chemical composition depending on several parameters such as the type of fuel used for combustion and the production process. Carbonaceous fine aerosols emitted from industrial activities show high concentrations of organic compounds such as polycyclic aromatic compounds (PAHs) emitted by different sources such as combustion processes, metal production, waste incineration, etc. (Riffault et al., 2015). Additionally, transition metals are largely emitted from industrial processes such as As, Cd, Cr, Cu, Hg, Mn, Ni, Pb, N, and Zn (Riffault et al., 2015).

- Emissions from cement plants

Different cement production processes are available: dry, semi-dry, semi-wet, and wet and might change the composition of the emitted PM (Yatkin and Bayram, 2008). The particles emitted from cement plants show high levels of Ca followed by Fe, K, Na, and Cl (Yatkin and Bayram, 2008). The variations in the profile mainly depend on the production process and the composition of the end-product (Samara et al., 2003).

- Heavy fuel oil combustion

The residual fuel oil or heavy fuel oil (HFO) is considered as the lowest grade fuel and is largely used for combustion processes in power plants and in marine diesel engines to generate steam for heating, electricity, and movement (Becagli et al., 2012). The different combustion designs (combustion conditions) result in changes in PM mass emissions and chemical composition (USEPA, 2002). The most significant elements from HFO combustion are V and Ni used as markers of this source. Additionnaly, SO_4^{2-} might contribute significantly to the ambient total PM mass originating from the oxidation of SO_2 emitted during the fuel combustion and depending on its sulfur content and the atmospheric conditions (Frey et al., 2014).

6 Quantitative methods – Source apportionment

6.1 Definition

Source apportionment is the practice of deriving information on different sources of pollution and their contribution to ambient air pollution levels (Belis et al., 2019). These models aim to reconstruct the impact of emissions from different sources of atmospheric pollutants but remain complex due to the high number of variables within (Viana et al., 2008). This apportionment can be determined and quantified by different approaches such as exploratory methods, emission inventories, source-oriented models and receptor-oriented models **(Fig. I-9).** The source-oriented models grid the source apportionment over a given domain or area using air quality models having as input data the emission inventories and meteorological fields as well as air concentrations at the boundaries of the area (Belis et al., 2019).

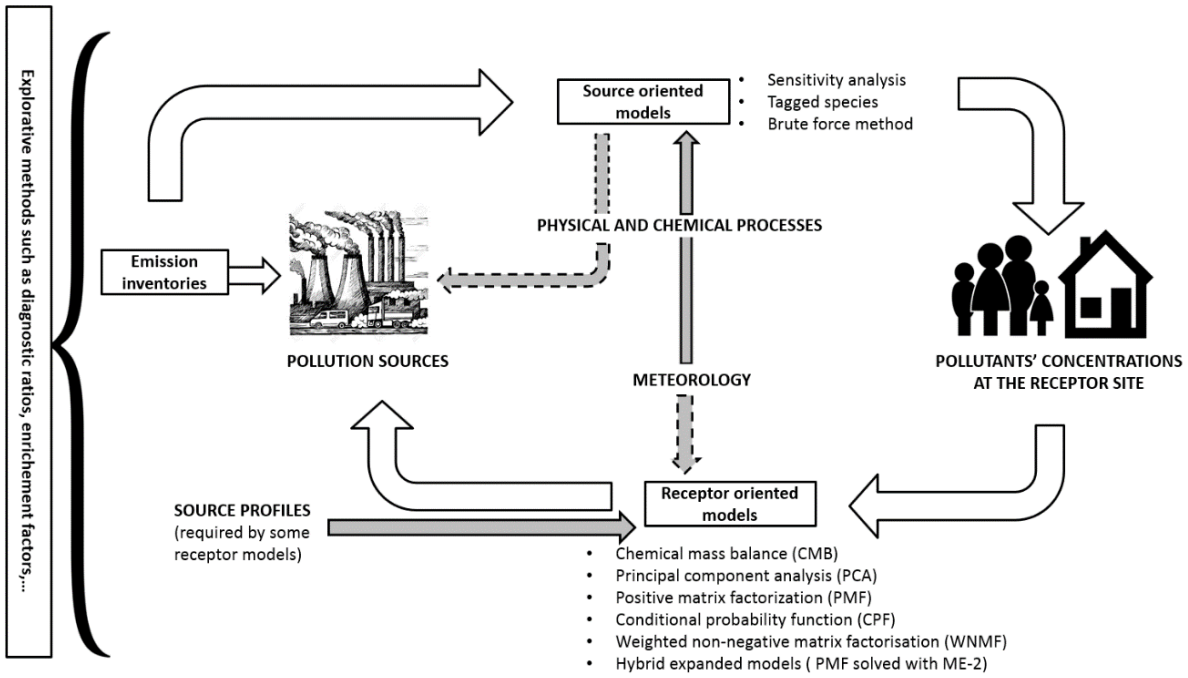

Fig. I-9: Representation of the different methods for source identification (adapted from Belis et al. (2019))

6.2 Receptor oriented models

The receptor-oriented models are mathematical approaches generally based on the assumption of the mass conservation between the emission source and the reception site.

Receptor models identify sources by solving the following mass balance equation:

$$x_{ij} = \sum_{k=1}^{p} g_{ik} \times f_{kj} + e_{ij}$$

Where:

x_{ij}: the concentration of the i^{th} species in the j^{th} sample

g_{ik}: the contribution of k^{th} source to i^{th} sample

f_{kj}: the concentration of the i^{th} species in the k^{th} source

e_{ij}: the residual

The concentrations used in the models are the ones measured at the sampling site. In general, these models do not depend on emission inventories, but certain receptor models require source profiles such as Chemical Mass Balance (CMB).

To apply the receptor models, it requires quantitative data on air pollution concentrations, an important knowledge in atmospheric processes, and a good usage of computational tools (Belis et al., 2019). In addition to that, exploratory methods can be used to obtain a preliminary idea of the most relevant sources especially when there is a lack of information regarding the sampling site.

The application of these models require a sufficient number of samples in order to obtain a robust solution. Furthermore, the minimum number of samples required for each model was presented (Henry et al., 1984):

$$\frac{D}{V} = N - (\frac{V}{2} - 1.5)$$

Where D is the degrees of freedom, V is the number of variables, N is the number of samples. In filter-based systems, the most common configuration is the collection of 24-hours samples. This configuration seems the most logic due to the presence of reference gravimetric methods for the determination of the particulate mass. Therefore, a 24-hour period covers a day to night cycle, and it is important to collect enough PM mass for analysis.

The chemical species that should be chosen to be included in the analysis and later for the models depend on different criteria:

- The objective of the study
- The site characteristics such as its topography
- The expected sources of emissions

The basic approach for airborne particulate matter is to choose a set of compounds that represent not only most of the particulate mass (major ions, carbonaceous fractions, and elements) but also other markers whose concentrations or ratios can indicate a specific source. Especially for the organic matter, the presence of molecular markers can help to identify additional sources (ex., hopanes for vehicular emissions, levoglucosan for biomass burning, etc.).

However, compounds that are considered unsuitable as source tracers can be excluded from the receptor models because they tend to result in meaningless factors (Belis et al., 2014). In

addition to that, redundant species such as Sulphur (S) and sulphate; Total carbon (TC) and OC/EC should be avoided to prevent double mass counting.

The selection of the receptor modeling approach depends mainly on the degree of knowledge required about the source of pollution before applying the model.

Fig. I-10 shows the different statistical models and approaches used for receptor modeling and classified depending on the pollution source knowledge criteria. The two extremes are the chemical mass balance (CMB) where the knowledge of source profiles is essential and the multivariate models such as positive matrix factorization (PMF) where little knowledge of pollution sources is required prior to receptor modelling (Viana et al., 2008).

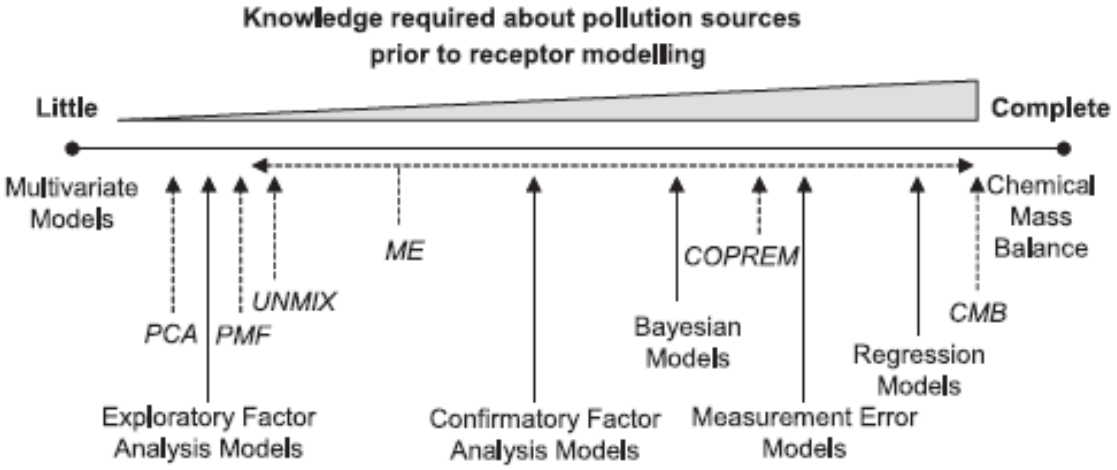

Fig. I-10: The different receptor modeling approaches based on the knowledge required about the pollution source (Viana et al., 2008)

6.2.1 Chemical Mass Balance (CMB)

CMB is a multiple regression model using the chemical and physical characteristics of the gases and particles at both the sources and the receptor sites in order to quantify the contribution of the sources. It represents by that a solution to linear equations expressing each receptor chemical concentrations as a linear sum of products of source profile abundances and source contributions (Friedlander, 1973; Cooper and Watson, 1980; Gordon, 1980; Watson, 1984; Watson et al., 1984; Watson et al., 1990; Hidy and Venkataraman, 1996). The input data of this

model are the source profile abundances and the receptor concentrations with their corresponding uncertainties (Watson et al., 1997). That is why a prior knowledge on the emission sources at the sampling site is crucial for CMB application. One characteristic of this model is that secondary aerosols should not be included as components of emission source profiles but as single chemical compounds. This can be a limitation of the model due to the absence of mixture of these compounds with other tracer elements (Viana et al., 2008).

6.2.2 Positive Matrix Factorization (PMF)

The aim of the PMF model system, like any receptor model, is to identify a number of factors, the species profile of each source, and the amount of mass contributing by each factor to each sample (Belis et al., 2019).

It is a weighted least square fit, with weights based on the known standard uncertainties of the element concentrations in the data matrix. This model was developed by (Paatero and Tapper, 1994) and the model can be written as follows:

$$X = G \times F + E$$

Where X is the known (n × m) matrix of the m measured species in n samples

G is the (n × p) matrix of the p source contribution on the sample for n samples

F is the (p × m) matrix that corresponds to the source compositions (source profile)

E is the residual matrix which is the difference between the measured X and the value of G ×F obtained by the model.

The results are obtained using the constraint that no sample can have a significant negative source contribution. The input data in this model is the known concentration of each species in each sample and the corresponding uncertainty to weight individual points. The obtained factor profiles as output data should be interpreted by the user in order to identify the source types by comparing to the source profiles to the ones found in the literature.

6.2.3 Challenges in the source apportionment usage

In the last few decades, action plans and pollution reduction strategies are being elaborated and/or evaluated in order to contribute to the improvement of air quality all over the globe. Consequently, knowledge about the main emission sources is needed based on established and quantitative data. This information started to become clearer once the usage of receptor models

started in the 1960s in the United States, Europe and several developed countries (Hopke et al., 2006). Nowadays, this study area is relatively mature regarding the used methods and the ability to adapt new measurement technologies in order to extract the maximum information from the collected data (Hopke, 2016). However, the lack of knowledge of the chemical composition for the emission sources is a major challenge for source apportionment application. All the efforts were focused on the development of source apportionment (SA) methods, but no efforts were made in developing countries to develop source profiles for stationary sources, or local profiles for important emission sources. The challenge also remains in the choice of the most suitable SA model to be used. In addition to that, profiles similarity between sources specifically industrial ones might limit the sensibility of the receptor model techniques causing a collinearity effect (Galvão et al., 2020).

Consequently, based on the points mentioned above, it is mandatory to choose specific organic and inorganic markers along with different exploratory methods and knowledge on local source profiles in order to have reliable results in the source apportionment application.

7 Health impact of atmospheric pollutants

Rapid industrialization has led to an important economic prosperity and an increase in the living standards. However, this episode was also accompanied by a deterioration of the environmental balance and a start of the drastic decrease in the air quality (Fowler et al., 2020). Nowadays, and according to the World Health Organization, 99% of the world's population live in areas where air quality levels exceed the WHO limits (WHO, 2021b).

7.1 Human exposure pathways

Exposure to chemicals can happen via three major routes:

- The skin or the dermal absorption
- The lungs or the inhalation pathway
- The mouth or the oral ingestion route

However, the physical and chemical properties of the substance will dictate the manner in which it enters the human body. Generally, vapor phase and fine particulate matter are likely to enter the body via the respiratory system while non-respirable PM will enter via the oral route. As for the dermal route, the skin absorbs most physical forms but especially liquids and solid materials (Asante-Duah, 2019).

The human skin is the outer covering of the body serving as a protective layer that obstructs the entry of substances in general and harmful agents and chemicals as well into the organism. It is mainly divided into a non-vascular epidermis layer, which corresponds to the outer layer and a vascularized dermis layer **(Fig. I-11)**. Chemicals enter the skin through hair follicles, sebaceous glands, sweat glands, and cuts.

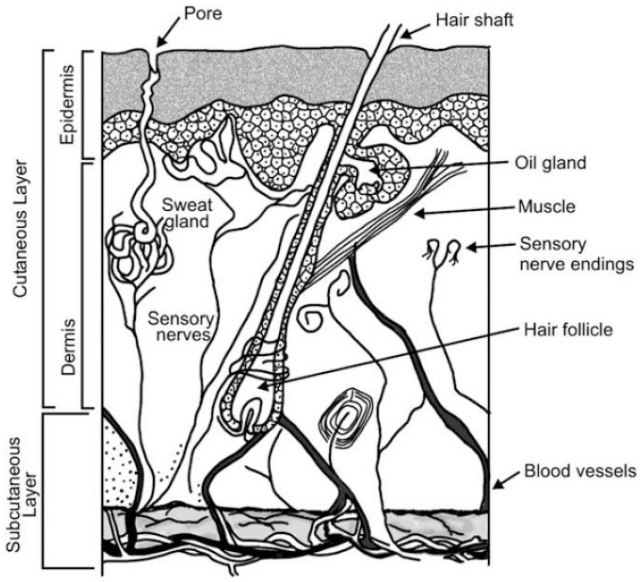

Fig. I-11: Layers of the skin (Asante-Duah, 2019)

When toxicants become localized in the epidermis, local toxicity is likely the result due to the fact the epidermis is avascular. However, the most common route of a toxicant via the skin is a passive diffusion through the epidermis into the dermis where the toxicant might enter a blood vessel. The distribution of absorbed chemical substances to different organs is subsequently done by the vascular system.

The human respiratory system is a group of organs and body parts including the mouth, nose, trachea, and the lungs **(Fig. I-12)**. Once inhaled, toxicants and chemicals are either exhaled or deposited in the respiratory tract. For example, particle deposition in the respiratory tract is governed by its size, shape, and density. Large particles (diameter > 10 µm) are retained in the oro-pharyngeal region due to impaction. Coarse particles (with diameter between 2.5 and 10 µm) are deposited in the tracheobronchial region while fine and ultrafine particles are deposited in the alveoli and small conducting airways due to gravitational sedimentation (Thakur et al., 2020). Upon contact with respiratory organs, chemicals may cause different health effects from simple irritation to severe tissue destruction.

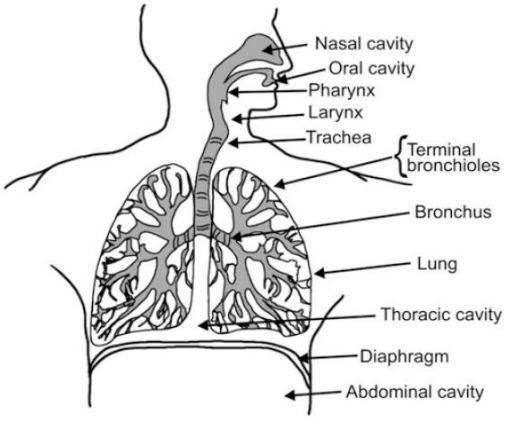

Fig. I-12: The respiratory system (Asante-Duah, 2019)

The lungs are considered as the organ where inhaled air encounters a huge contact surface of tissue allowing exchange with gas in the blood. The rate of the absorption will vary depending on the chemical's concentration, its solubility in tissue fluids, the amount of blood circulation, and the depth of respiration. Absorbed substances circulate in the blood and are distributed to different body organs. Health effects can occur in the organs that are sensitive to the toxicants.

The human gastro-intestinal tract includes the mouth, pharynx, esophagus, stomach, small intestines, large intestine, rectum and anus **(Fig. I-13)**. The absorption in the vascular system is the most important in the small intestine compared to other organs in the gastrointestinal tract. As for the kidneys, they contribute to a large share of the work required to eliminate toxic substances from the human body by separating these substances from the blood and eliminating them by urine (Asante-Duah, 2019).

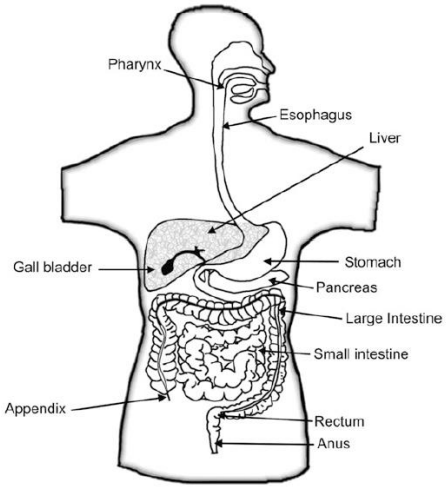

Fig. I-13: The digestive system (Asante-Duah, 2019)

7.2 Impact of air pollution on human health

A recent study conducted by Lelieveld et al. (2019) that combines the Global Exposure Mortality Model (GEMM) presented by Burnett et al. (2018) and the global air pollution exposure data, showed that the attributable excess mortality rate is about 8.8 million per year that is approximately twice the global premature mortality rate estimated before at 4.5 million people a year. According to WHO, the most vulnerable to air pollution are susceptible groups with pre-existing diseases respiratory or cardiovascular diseases as well as elderly people and children. Generally, PM emitted from various anthropogenic sources might produce short term effects ranging from simple discomfort as eyes irritation to serious pulmonary, cardiovascular, and dermal effects (Zaheer et al., 2018).

Several studies suggested that long-term exposure to high levels of PM is directly linked to different cardiovascular problems with an increase in the mortality rate in the most polluted cities compared to the least ones (Anderson et al., 2012; Chen and Hoek, 2020). Epidemiological, biomedical, and clinical studies indicate that long-term exposure to PM will increase the chance of having strokes, myocardial infracts (MI), vascular dysfunction, hypertension, heart insufficiency, and heart failure (Du et al., 2016; Lelieveld and Münzel, 2020; Manisalidis et al., 2020). As for the respiratory system, short-term exposure to PM is closely correlated to cough, shortness of breath, asthma, Chronic Obstructive Pulmonary Disease (COPD), and high rates of hospitalization. Additionally, long-term exposure to air pollution can be related to chronic asthma, pulmonary insufficiency, and might even promote lung cancer (Xing et al., 2016; Manisalidis et al., 2020).

Chen and Hoek (2020) presents a systematic review of evidence of association between long term exposure to $PM_{2.5}$ in relation to all cause and cause specific mortality using cohort and case control studies from Europe and United States mainly. A clear evidence of association was highlighted between $PM_{2.5}$ and mortality from all causes, cardiovascular and respiratory diseases, and lung cancer. The combined risk ratio for $PM_{2.5}$ and natural-cause mortality was 1.08 per 10 $\mu g/m^3$. Yu et al. (2020) showed that even at low $PM_{2.5}$ concentrations (ranging between 1.6 and 9 $\mu g/m^3$), long-term exposure to $PM_{2.5}$ was associated with cardiovascular and respiratory mortality. This study combined 242,320 death cases from Queenlands (Australia) between 1998 and 2013 and showed that for every 1 $\mu g/m^3$ increase in annual $PM_{2.5}$, there is a 2.02% increase in total mortality. Additionally, Wei et al. (2020) showed that in Massachusetts (United States of America), each 1 $\mu g/m^3$ increase in long and short-term $PM_{2.5}$ exposure was associated with 35.4 and 3.04 excess deaths per 10 million person-days, respectively. Johnson

et al. (2021) explained that maternal exposure to fine and ultrafine PM directly and indirectly yields adverse birth outcomes and impacts on the child's respiratory system, immune system, brain development, and cardiometabolic health. Finally, Lelieveld et al. (2020) highlighted that air pollution shortens the life expectancy of Europeans by 2 years. Around 120 people per 100,000 population die prematurely from the effects of air pollution at a global scale.

These health outcomes have an important economic impact on the world's countries. At the global level and by 2060, it is projected that the number of lost working days will increase from 1.2 billion to 3.7 billion affecting labor productivity (OECD, 2016).

7.3 Health risk assessment strategies

According to USEPA (1989c); (1991c), the 4 steps for the risk assessment process are as follows:

- **The hazard identification**: What health problems are caused by the pollutant? It is the process of determining whether the exposure to a stressor (chemical) can cause the increase in the incidence of specific adverse health effects.
- **The dose-response assessment**: What are the health problems at different exposures? It describes how the likelihood and severity of adverse health effects are related to the amount and condition of exposure to an agent.
- **The exposure assessment:** How much of the pollutant are people exposed to during a specific time period? How many people are exposed? It is the process of measuring or estimating the magnitude, frequency, and duration of human exposure to an agent in the environment.
- **The risk characterization:** What is the extra risk of health problems in the exposed population? It conveys the risk assessor's judgment as to the nature and presence or absence of risks, along with information about how the risk was assessed, where assumptions and uncertainties still exist, and where policy choices need to be made.

Following these steps, the cancer and the non-cancer risk assessment are evaluated.

7.3.1 IARC compound classification

The International Agency for Research on Cancer (IARC) created an index to evaluate the strength of the available evidence that an element or a species can cause cancer in general. This assessment can be based on three proofs:

- cancer in humans (strong/limited evidence of carcinogenicity in humans)

- cancer in experimental animals (sufficient evidence of carcinogenicity in animals)
- mechanistic evidence (strong evidence that the agent exhibits key characteristics of carcinogens)

However, substances in the same group can differ vastly regarding their carcinogenic effects. According to the IARC report, the elements are divided into 4 groups (IARC, 2019):

Group 1: Carcinogenic to humans: this category applies whenever there is sufficient evidence of carcinogenicity in humans (or sufficient evidence in animals and strong evidence that the agent exhibits key characteristics of carcinogens). It includes over 120 species **(Fig. I-14)** such as substances from smoking, exposure to solar radiations, alcoholic beverages, and processed meats.

Group 2A: Probably carcinogenic to humans: This category applies in these 2 cases:

- Limited evidence of carcinogenicity in humans and strong evidence that the agent exhibits key characteristics of carcinogens
- Sufficient evident of carcinogenicity in experimental animals and strong evidence that the agent exhibits key characteristics of carcinogens

It includes more than 82 species coming from emissions from high temperature frying, steroids, exposures working in hair dressing, red meat **(Fig. I-14)**.

Plus, this category might be applied in case of strong evidence that the agent belongs to class or family of compounds from which one agent or more members have been classified in Group 1 or Group 2A based on mechanistic considerations.

Group 2B: Possibly carcinogenic to humans: This category applies whenever one of the current evaluations have been made:

- limited evidence of carcinogenicity in humans
- Sufficient evidence of carcinogenicity in animals
- Strong evidence that the agent exhibits key characteristics of carcinogens

It includes over 311 species such as emissions from coffee, gasoline, gasoline engine exhaust, welding fumes, pickled vegetables, etc.

Group 3: Not classifiable as to its carcinogenicity to humans: For all agents that do not fall in any other groups (tea, static magnet fields, fluorescent lighting, polyethene)

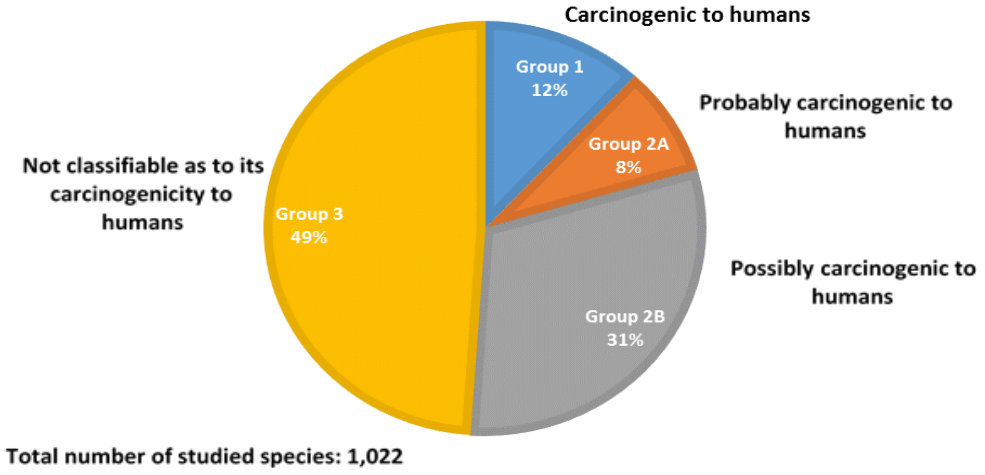

Fig. I-14: Distribution of compounds according to the IARC classification (IARC, 2021)

Among the compounds evaluated by the IARC and for which monographs exist (1,022 species), 12% were considered as carcinogenic to humans such as benzo[a]pyrene, 1,3-butadiene, benzene, polychlorinated biphenyls, 2,3,7,8-tetrachlorodibenzo-p-dioxin, 2,3,7,8-tetrachlorodibenzofuran, nickel, chromium (VI), arsenic, and cadmium. Styrene and dibenzo[a,h]anthracene are considered group 2A compounds.

7.3.2 Non-cancer risk assessment

Historically, it has been assumed that some molecular events can evoke mutagenic changes in a cell that leads to damage multiplication and carcinogenicity (Haber et al., 2012). This phenomenon is considered as a non-threshold effect because response generation is probable at all exposure levels. The non-carcinogenic effect is assumed to have a certain threshold or a certain value or level below which no response is generated. This is mainly due to adaptive protective mechanisms in the cells against toxic effects (Haber et al., 2012).

The safe subthreshold doses are used for the non-cancer risk assessment evaluation and are defined by a number of health agencies worldwide such as Reference Dose (RfD) or Reference Concentration (RfC) by the USEPA (1994), acceptable daily intake (ADI) by WHO (Lu, 1988), Tolerable Intake (TI) by the international programme on chemical safety (IPCS, 1994), and minimal Risk Level (MRL) by the U.S Agency for Toxic substances and Disease registry (ATSDR) (Pohl and Abadin, 1995).

According to USEPA (1989b), the calculated hazard for a non-carcinogenic health effect is not probability but a measured ratio of the magnitude of a receptor's potential exposure usually

called the average daily dose to a standard exposure level such as RfC or RfD. This ratio is also called "Hazard quotient" (HQ) and is calculated for a specific species in a specified exposure pathway (inhalation, oral ingestion, or dermal absorption). Generally, the more the value of HQ for a certain pollutant approaches or exceeds the value of 1 (one), the higher is the level of concern. Furthermore, a receptor might be exposed to different chemicals associated with non-cancer effects. A hazard index (HI) was defined as the sum of the hazard quotients generating a total hazard for a specific exposure pathway. Finally, a total hazard index gathers the hazard indexes of the different exposure pathways.

7.3.3 Cancer risk assessment

According to the USEPA (1991a), there is no exposure that have "zero risk" while evaluating cancer risk. Even a very low concentration of exposure to a cancer-causing pollutant can increase the risk of cancer assuming a linear correlation between dose and response.

The cancer risk evaluation is based on carcinogenic chemicals where risk estimates are assigned to a probability that an individual will develop a cancer over a lifetime as a result of an exposure to a carcinogenic chemical. So, the cancer risk associated with a chemical in a specific exposure pathway will be the product of a lifetime average daily dose by a carcinogenic slope factor (USEPA, 1989a). The total cancer risk for a specific exposure pathway is calculated as the sum of the different risks associated with the carcinogenic chemicals. Finally, the total cancer risk corresponds to the risk evaluated for the different exposure pathways. USEPA (1991b) considers risk level of 10^{-6} as the threshold limit. Higher values are considered dangerous and more concern should be given regarding these chemicals.

7.4 Assessment of the $PM_{2.5}$ oxidative potential

7.4.1 $PM_{2.5}$ and cellular oxidative stress

It has been established that the major effect of particulate matter on the pulmonary system is the exacerbation of inflammation with different mechanisms, one of which is the generation of oxidative stress (Li et al., 2008). By definition, oxidative stress is defined as the excess production of reactive oxygen species (ROS) relative to antioxidant defense (Shankar and Mehendale, 2014). ROS are species having an unpaired electron in their valence shell and can react with other molecules close to their place of production. They consist of radical and non-radical oxygen species such as superoxide anion (O_2^-), hydrogen peroxide (H_2O_2), and hydroxyl radical ($HO^{\cdot}$). Cellular ROS are generated through exogenous cellular processes such as the

interactions with xenobiotic systems and through endogenous processes as the process of mitochondrial oxidative phosphorylation (Ray et al., 2012). Generally, ROS production in the cells is a highly regulated phenomenon due to many enzymes. In addition, against these ROS, we can also find non-enzymatic defense systems. This regulatory process is called the antioxidant system (Alkoussa et al., 2020). These species can play a beneficial role at low doses by interacting in physiological processes and a negative role by causing cellular damages through their ability to interact with several cellular components (Sies, 2018). It has been shown that the exposure of lung cells to $PM_{2.5}$ can generate ROS species from soluble transition metals such as Cu, Cr, Fe, and Zn and from organic compounds such as Polycyclic aromatic hydrocarbons (Akhtar et al., 2010). When ROS overwhelm the cellular antioxidant defense system, either by an overproduction of ROS or a decrease in the cellular antioxidant capacity, oxidative stress occurs. Oxidative stress arises then once the balance between ROS production and antioxidant response is no longer maintained, such after exposure to $PM_{2.5}$ or to stress.

At low levels of oxidative stress, antioxidant enzymes are activated to protect the lungs. If this response fails to provide enough protection against ROS production, an inflammatory response may be induced. However, at toxic levels, cell death occurs through apoptosis and necrosis (Akhtar et al., 2010).

To conclude, oxidative stress can cause biological effects induced by the increase of oxidative activity due to exposure to PM. Different factors can vary the ROS production such as the particulate size as well as the composition of the atmospheric particles (especially in transition metals and organic compounds).

7.4.2 Acellular oxidative potential measurement assays

Based on the idea that exposure to PM can induce oxidative stress, and in order to have an indicator to characterize exposure reflecting the oxidative capacity of PM, the oxidative potential is used. By definition, the oxidative potential measures the ability of PM to deplete certain antioxidant molecules in synthetic airway fluids (Crobeddu et al., 2017; Moufarrej et al., 2020). It has been used as an exposure metric to try to link atmospheric aerosols and health end points. Acellular assays have been developed to measure the oxidative potential (OP):

- Ascorbic acid (OP-AA) and glutathione (OP-GSH) assays measure the ability of PM to deplete antioxidants (Ascorbic acid AA and glutathione GSH), which are proportional to the ROS generation rate.

- Dithiothreitol assay (OP-DTT) assay measure the ability of PM to deplete a cellular reductant (Dithiothreitol DTT), which is proportional to the ROS generation rate.
- Electron Spin Resonance assay (OP-ESR) is applied to quantify the ability of PM to induce specific ROS such as hydroxyl radicals.

These acellular assays present the advantage of being practical, fast, at low price, and have a high data throughput when compared to cellular assays (Pietrogrande et al., 2019).

Among commonly used approaches, DTT and AA assays will be presented in this manuscript because they will be used in this study.

7.4.3 The ascorbic acid assay

Ascorbic acid is an important physiological antioxidant found in lung lining fluid and has a major role in preventing the oxidation of lipids and proteins (Mudway et al., 2005).

The AA assay uses Ascorbate (Asc) because it is the most abundant antioxidant found in lung fluids and therefore has an important role in oxidant production from ROS (Mudway et al., 2004). This assay simulates the mechanism of electron transfer from AA to oxygen based on the ability of redox-active species (Ayres et al., 2008). The response obtained from this assay is the ascorbate oxidation rate **(Fig. I-15).** According to Crobeddu et al. (2017), this assay is considered as the most likely to predict the biological effect driven by atmospheric particles and related to oxidative stress.

Literature showed that OP-AA has a significant correlation with soluble and total metals including Cu, Mn, Pb, Zn, and Fe (Bates et al., 2019). The AA assay has been shown to be most sensitive to transition metals, but quinone compounds might also react with AA (Fang et al., 2016).

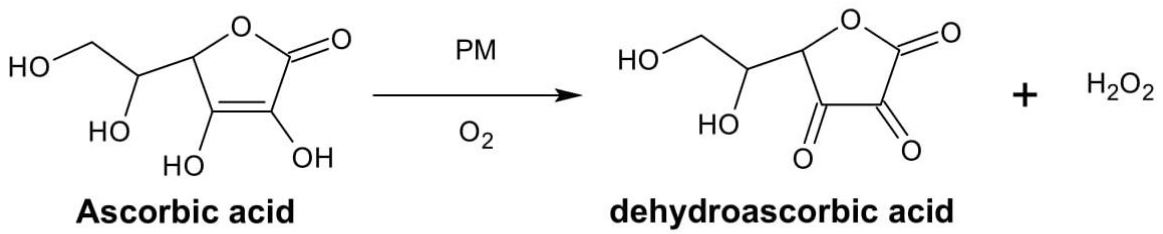

Fig. I-15: Chemical basis of the AA assay

7.4.4 The Dithiothreitol assay

The DTT simulates reductant species in cells like Nicotinamide adenine dinucleotide (NAD) or nicotinamide adenine dinucleotide phosphate (NADP). The DTT assay evaluates the ability of redox active species associated with PM to transfer electron from the dithiothreitol to the oxygen leading to the generation of superoxide anion that comproportionates to oxygen and H_2O_2 (**Fig. I-16)**. The PM components play a catalyst role by increasing the oxygen species reduction to ROS. The rate of the reaction is monitored by DTT consumption calculated indirectly by measuring the formation of 5-mercapto-2-nitrobenzoic acid (TNB). The latter is the product of the reaction between non-reacted DTT with 5,5-dithiobis-2-nitrobenzoic acid (DTNB) (**Fig. I-16)** that has a maximum absorption at 412 nm and that will be measured by spectrophotometer (Kumagai et al., 2002; Cho et al., 2005; Ayres et al., 2008).

Studies showed the DTT oxidative potential is generally correlated with transition metals such as copper and manganese, with organic carbon (OC) especially water-soluble organic carbon (WSOC), and organic species such as humic-like substances (HULIS) and oxidative forms of PAHs (quinones), which are known to be DTT active (Fang et al., 2016; Bates et al., 2019). This shows that photochemical aging plays an important role in determining particle-bound ROS and affects the capability of organic species to induce a response in OP.

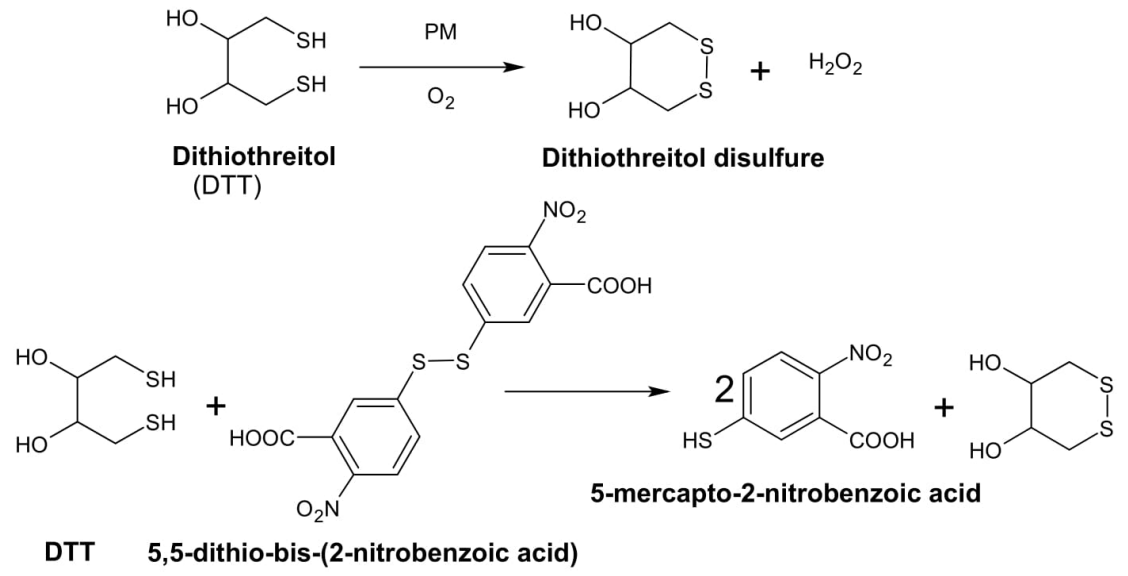

Fig. I-16: Chemical basis of the DTT assay

Based on this evidence of SOA influencing the values of OP specifically OP-DTT, chamber studies have been investigated (Verma et al., 2015; Tuet et al., 2017). It has been shown that

the identity of the precursor and its source as biogenic or anthropogenic is more influential than the reaction conditions in simulation chambers. This emphasizes on the importance of sources in the aerosol toxicity due to the oxidative potential. Tuet et al. (2017) demonstrated that naphthalene SOA generate the highest OP-DTT while oxidation products of isoprene might generate the lowest OP-DTT. Otherwise, in an urban atmosphere in low NO_x conditions, toluene and isoprene SOA contribute more to the OP than α-pinene (Jiang et al., 2016). Differences occur between the different simulation chamber studies, but anthropogenic and biogenic SOA seem to be critical to DTT oxidative potential.

8 Local context – Lebanon

8.1 General overview (demographic, topographic and geographic aspects)

The Mediterranean region is considered as a major investigation area for researchers in different scientific fields. It is a "test area" with the longest and the most intense human occupation in the world (Moatti and Thiébault, 2018). The area is considered as a hotspot for climate change and atmospheric forcing (Kim et al., 2019). Additionally, the region is an enclosed area favoring the entrapment of pollutants due to stagnant winds from Eastern Europe and intense solar radiations (Saliba et al., 2006). Also, its location at the intersection of air masses circulating among Asia, Europe, and Africa, enhances the aerosol transportation (Saliba et al., 2007).

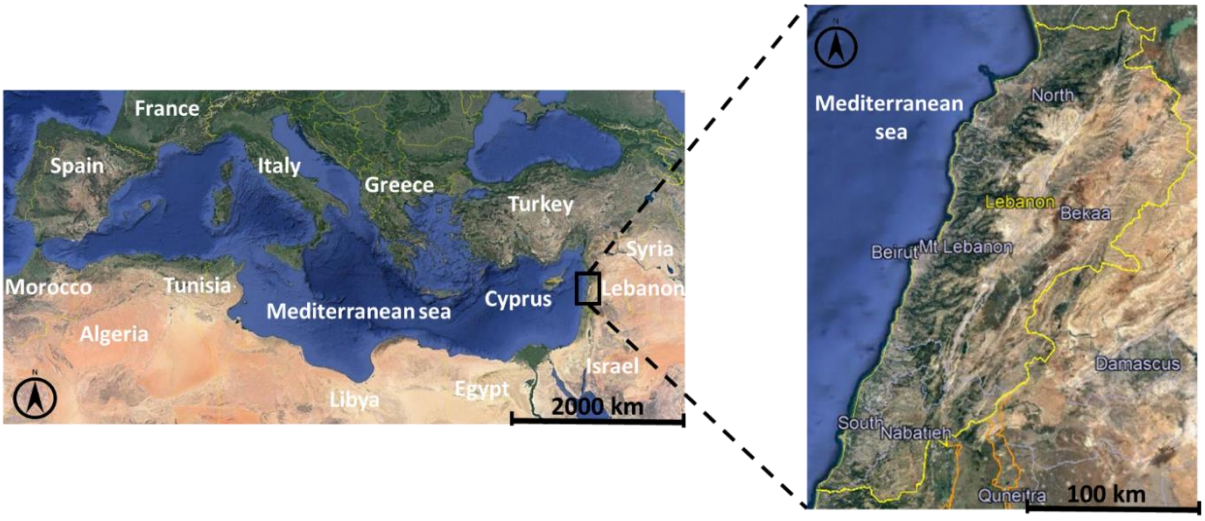

Fig. I-17: Geographical location of Lebanon in the Mediterranean region

Lebanon is located on the eastern shore of the Mediterranean Sea **(Fig. I-17).** It is the second smallest country in the Middle East and the East Mediterranean with a surface of 10,452 km^2.

It is characterized by a population of more than 6 million in the last few years, and a density of population of around 496 persons/km^2, including foreign workers (MoE/UNDP/GEF, 2016).

Lebanon is divided into 4 topographic areas **(Fig. I-18)**: the narrow coastal area, the Mount Lebanon chain with an average elevation of 2,200 m, the anti-Lebanon mountain chain subdivided into two massifs: Talaat Moussa (2,629 m) in the north and Jabal el Sheikh or the Mount Hermon (2,814 m) in the south, and the Bekaa valley between the two mountain chains.

Generally, the climate is typically Mediterranean with rainy winters and long warm summers with an average annual temperature of 15°C. The topographic features, along with the influence of the sea, and the Syrian desert create a variety of microclimates within the country with temperature differences and contrasting rainfall distributions (Frenken, 2009). The majority of the Lebanese population lives near the coast, in or around the capital Beirut. Around 85% of the population live in urban areas making the country highly urbanized (MoE/UNDP/GEF, 2011).

Fig. I-18: Physical regions of Lebanon. Source: USAID, 2016. Fact Sheet. Climate Change Risk Profile Lebanon (https://www.climatelinks.org/resources/climate-change-risk-profile-lebanon).

8.2 Anthropogenic and biogenic emissions in Lebanon

The main sources of air pollution in Lebanon are local especially in the winter season with primary compounds emissions and local formation of secondary aerosols (Waked et al., 2013a).

Episodically, the country is affected by long-range transport of dust from the Arabian and the Saharan deserts constituting the major source of mineral elements (Borgie et al., 2016). For the Arabian dust episodes, the storms cross different urban environments while Saharan dust crosses also the Mediterranean sea (Dada et al., 2013).

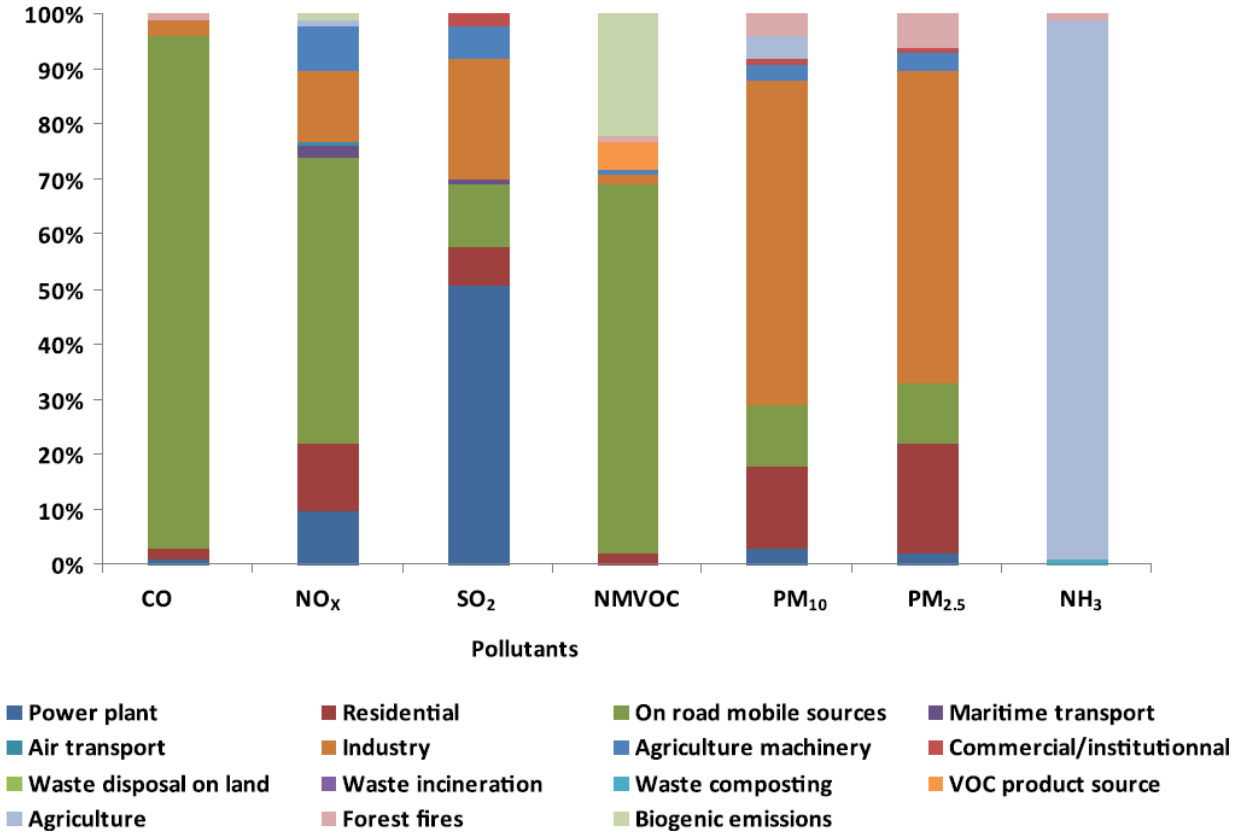

Fig. I-19: Emission contribution by source category in 2010 (Waked et al., 2012a)

The first temporally resolved and spatially distributed emission inventory gathering anthropogenic and biogenic sources was developed by Waked et al. (2012a) for the base year 2010 and provided quantitative information for research studies as well as input data for air quality models (Waked and Afif, 2012; Waked et al., 2012a; 2013b; Abdallah et al., 2016; 2018). The on-road transport sector emits 93% of national CO, 52% of NO_x emissions, and 67% of non-methanic volatile organic compounds (NMVOC) **(Fig. I-19)**. On the other hand, 73% of SO_2 emissions, 62% of PM_{10}, and 59% of $PM_{2.5}$ originate from power plants and industrial sources. The spatial distribution of the emissions shows that a large fraction of the on-road transport emissions is observed in the capital Beirut and its suburbs while other urban

areas such as Zouk Mikael, Chekka, Selaata, and Jiyeh are mostly touched by industrial and energy production emissions.

The road transport emissions are mainly due to traffic jams following the increase in the number of vehicles, the absence of public transportation systems, but also a vehicle fleet dominated by poorly maintained private cars, and inadequate road maintenance with poor road safety conditions (Waked and Afif, 2012; MoE/UNDP/GEF, 2016). These problems lead to a continuous stop and go driving pattern, an inefficient operation of combustion engines, and a high consumption of fuel resulting in high concentrations of pollutants emitted by this sector (CO, NO, NO_2, VOC, PM) affecting air quality and climate (Abdallah et al., 2020).

To date, there are no regulations governing passenger vehicle emissions. However, different legal texts can be found for the on-road transport sector:

- Law 150/1992 banned the import of passenger cars with a vehicle age of more than 8 years.
- Law 341/2001 and decree 7858/2002 banned the use of private and public cars with diesel engines, and the use of public buses of 16 to 24 passengers with diesel engines. Law 341/2001 also made catalytic converters a mandatory requirement in all vehicle categories for the first time and reinstated the mandatory vehicle inspection.
- Law 243/2012 reinstated the installation of catalytic converters in all gasoline vehicles.
- Another decree published in 2016 (decree 3054/2016) lowered the limit of sulfur content in automotive diesel to 10 ppm after being 350 ppm

Based on Waked's 2010 emission inventory, the main PM emitter is the industrial sector on a national level. Lebanon encompasses different industry types in all regions: food and beverages, metal production and non-metallic mineral products, chemical, furniture manufacturing, electrical machinery manufacturing, and the energy production industries (MoE/UNDP/GEF, 2016). The latter are unable to supply the electricity needed by the different sectors knowing that Lebanon comprises 7 thermal power plants, 3 of which operate on heavy fuel oil and 4 on gas diesel oil at present. To compensate theses shortages, backup private generators are used for power cut hours (minimum of 3 hours/day unevenly distributed between cities) with no law enforcement on the stack emissions and design.

The population growth hypothesis along with the refugees displacement lead to an important residential solid waste generation and saturation of landfills that resulted in waste accumulation

on the streets and in neighborhoods in 2017 (Abbas et al., 2019b). These episodes caused a substantial increase in open burning of waste in many parts of the country, and a creation of unlicensed landfills in inhabited areas. Additionally, it was estimated that the emissions in Lebanon increased of up to 20% between 2010 and 2014 due to the displacement of refugees due to the Syrian conflict (MoE/EU/UNDP, 2014). The major sectors contributing to this increase were the on-road transport sector, electricity production, and open burning of waste (MoE/EU/UNDP, 2014).

As for biogenic emissions, forests in Lebanon occupy around 13% of the total surface with an additional 10% covered by wooded land (FAO, 2005; MoE/UNDP/GEF, 2011). These areas are divided into broadleaf forests representing 57% of forests, 32% of coniferous forests and 11% of mixed forests. For the forested areas, oak forests are the most abundant, then pine, and finally juniper forests. Cedar and fir were far less abundant (MoE/UNDP/GEF, 2011, 2016). These areas are exposed to different threats such as quarries, urbanization, pests, and diseases but the most important danger is forest fires. The number of fires and their severity are increasing in Lebanon over the past 15 years and are mainly due to high temperatures, low humidity, heatwaves, and strong winds along with human activities and neglect.

8.3 Ambient air quality standards and emission limits in Lebanon

The World Health Organization guidelines are intended for worldwide use and have been developed to improve air quality in the considered areas (WHO, 2021b). In September 2021, WHO has published a new guideline after their last update in 2006 based on recent epidemiological, toxicological, and chemical characterization studies. Based on these guidelines, national standards should be made taking into account the economic, political, technological situations, and social factors that depend on the level of development and the national capability in air quality management.

The first regulations for ambient air quality in Lebanon were published by the Ministry of Environment (MoE) in 1996 (Decision 52/1 dated 12/09/1996) presenting the National Ambient Air Quality Standards (NAAQS) **(Table I-4)**. NAAQS were never updated and are considered nowadays outdated compared to the current air quality standards proposed by WHO and by the European Union. In addition to that, they do not define standards for $PM_{2.5}$ concentrations.

Table I-4: Air quality standards in Lebanon as found in the legislation of 1996, in Europe from the European Union legislation and from the World Health Organization

Pollutant	Duration of exposure	Lebanon (NAAQS)	EU	WHO 2006	WHO 2021
$PM_{2.5}$	24 hours	-	-	25 µg/m^3	15 µg/m^3
	1 year	-	25 µg/m^3	10 µg/m^3	5 µg/m^3
PM_{10}	24 hours	80 µg/m^3	50 µg/m^3	50 µg/m^3	45 µg/m^3
	1 year	-	40 µg/m^3	20 µg/m^3	15 µg/m^3
SO_2	10 minutes	-	-	500 µg/m^3	500 µg/m^3
	1 hour	350 µg/m^3	350 µg/m^3	-	-
	24 hours	120 µg/m^3	125 µg/m^3	20 µg/m^3	40 µg/m^3
	1 year	80 µg/m^3	-	-	-
NO_2	1 hour	200 µg/m^3	200 µg/m^3	200 µg/m^3	200 µg/m^3
	24 hours	150 µg/m^3	-	-	25 µg/m^3
	1 year	100 µg/m^3	40 µg/m^3	40 µg/m^3	10 µg/m^3
Lead (Pb)	1 year	1 µg/m^3	0.5 µg/m^3	0.5 µg/m^3	0.5 µg/m^3
CO	15 minutes			-	100 mg/m^3
	1 hour	30 mg/m^3	-	30 mg/m^3	35 mg/m^3
	8 hours	10 mg/m^3	10 mg/m^3	-	10 mg/m^3
	24 hours			10 mg/m^3	4 mg/m^3
Benzene	1 year	16.2 µg/m^3	5 µg/m^3	-	-
Ozone	1 hour	150 µg/m^3	-	-	-
	8 hours	100 µg/m^3	120 µg/m^3	100 µg/m^3	100 µg/m^3
Arsenic (As)	1 year	-	6 ng/m^3	-	-
Cadmium (Cd)	1 year	-	5 ng/m^3	5 ng/m^3	5 ng/m^3
Nickel (Ni)	1 year	-	20 ng/m^3	-	-
PAHs (equivalent B[a]P)	1 year	-	1 ng/m^3	-	-

The decision 52/1 also presented emission limit values (ELVs) that were amended by the decision 8/1 in 2001 and were specific to point sources in Lebanon covering stack emissions and effluent discharge for new and existing industrial establishments (MoE/UNDP/GEF, 2016). Law 78 published in 2018 on the Protection of air stipulates the adoption of the air quality WHO guidelines as legal national standards, but new updates values for air quality standards have not been officially adopted yet and the 1996 limits are still valid to present.

8.4 Economic impact of air pollution in Lebanon

In 2016, the World Bank in collaboration with the Institute for health Metrics and Evaluation at the University of Washington published a report on the cost of ambient and household air pollution worldwide (WorldBank, 2016). It has been found that the number of premature deaths in 2013 due to air pollution cost the global economy about $225 billion in lost labor income

(equivalent to $5.11 trillion in welfare losses). Losses were largely caused by outdoor air pollution from fine particulate matter ($PM_{2.5}$) in all the regions of the world. More specifically, in Lebanon, the total deaths from air pollution increased from 1,160 to 1,816 in the period between 1990 and 2013 according to this study. The total welfare losses due to the air pollution in 2013 were 4 times higher than the losses in 1990 ($683 million in 1990 vs $2,660 million in 2013).

Another study conducted by Greenpeace in the Middle East and North Africa Region (MENA) in 2020 revealed that air pollution resulting from fossil fuel combustion in the MENA region is responsible for approximately 4.5 million premature deaths each year, and costs the region $8 billion per day that is equivalent to 3.1% of the global gross domestic product (Farrow et al., 2020). From the countries of the MENA region, Lebanon has the highest estimated premature death rate (0.39) per 1000 people attributed to fossil fuels air pollution followed by Egypt (0.33) and Syria (0.28) **(Fig. I-20)**. The annual environmental cost in Lebanon reaches $1.4 billion (equivalent to 2% of the GDP) from fossil fuels air pollution (Farrow et al., 2020).

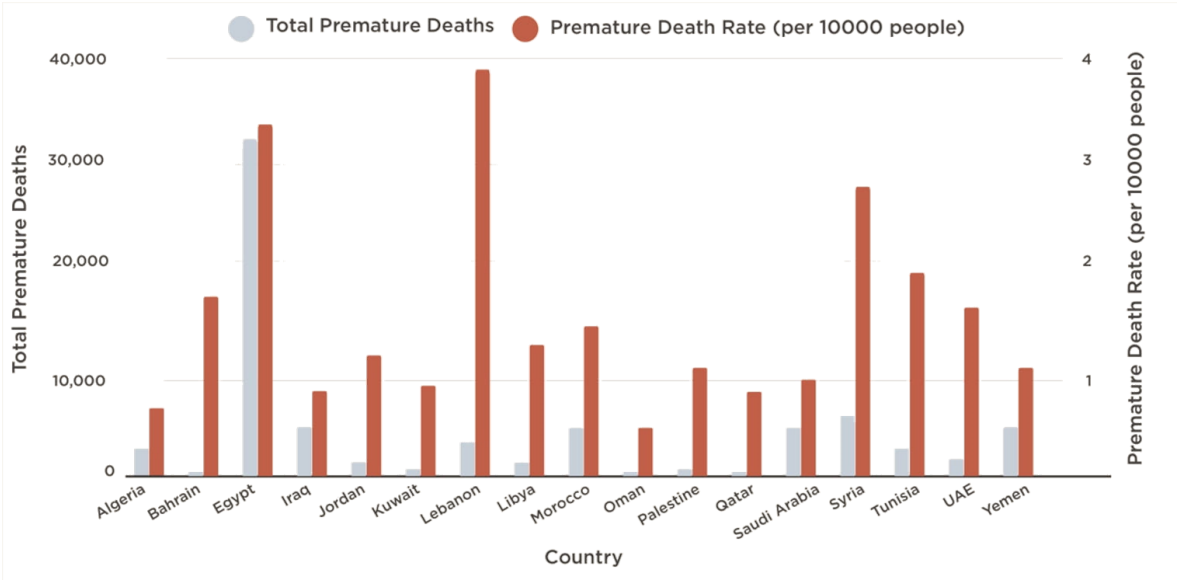

Fig. I-20: Total premature deaths and death rate attributed to air pollution from fossil fuel per country in the Middle East and North Africa Region (MENA) region (central estimates) (Farrow et al., 2020)

These studies show that the economic cost of air pollution is very high and underline the necessity to reduce emissions and transition to renewable energies and less polluting industries and on-road transport fleet.

8.5 PM studies in Lebanon

Different air pollution studies were conducted in Lebanon focusing either on the gas or the particulate phase. Atmospheric inorganic gases and VOCs were mainly measured in the capital Beirut and reported in different studies (Afif et al., 2008; Salameh et al., 2015; Salameh et al., 2016). These papers showed that long-range transport contributed to an important fraction of SO_2 emissions in the capital beside local sources such as the harbor and the coaching stations and NO_x are mainly emitted from traffic (Saliba et al., 2006; Afif et al., 2008; Afif et al., 2009).

Table I-5 shows the different studies of PM conducted in Lebanon from 2003 to date. Most of these studies encompasses short to medium term field campaigns in different locations in Lebanon and with different measurement technologies. The observed $PM_{2.5}$ values show exceedances compared to the new annual WHO value reported as 5 µg/m^3 and are mostly higher than the recommended concentration by the European Union of 25 µg/m^3. As for PM_{10}, the values are higher than the annual values recommended by WHO (15 µg/m^3) and EU (40 µg/m^3) but not all sites show exceedances compared to the Lebanese Air quality standard for PM_{10} of 80 µg/m^3.

Shaka' and Saliba (2004) showed that the fine fraction of PM holds higher concentrations of organic and inorganic species compared to other fractions. Long-range transport due to dusty events was also studied by Jaafar et al. (2014) and Borgie et al. (2016) emphasizing on the idea that the relative chemical composition of organic and inorganic constituents changes due to dust events with higher mass concentrations. Other studies focused on the organic fraction of PM in the suburbs of the capital. Waked et al. (2013a); (2014) showed high levoglucosan concentrations especially in winter and was associated to biomass burning for residential heating during the cold season while carboxylic acids were linked mainly to cooking emissions. On the contrary, high concentrations of the biogenic secondary aerosols (BSOA) and dicarboxylic acids were found in summer and this increase was justified by greater photochemical activity in summer. A tracer-based approach was also used to apportion OC to different source emissions during both seasons (biogenic SOC, fossil-fuel combustion and cooking activities were the most contributors to OC). Near-freeway study showed that PM levels are 1.3 to 2.6 times higher than a background site with high concentrations of hopanes, steranes, and PAHs (Daher et al., 2013). PAH levels are influenced by different combustion sources especially by diesel (buses, trucks, generator sets) and gasoline (private cars) emissions and are more concentrated in the $PM_{0.3}$ fraction compared to other fractions (Borgie et al., 2016; Badran et al., 2020).

Studies on PM conducted in Lebanese industrial areas generally focused on the inorganic composition. Yammine et al. (2010) showed that high levels of nitrates were found in Selaata region in the North of Lebanon due to gas-particle conversion of NO_2 emitted from heavy-duty machinery. Enrichment factors of different elements such as P, Ca, V, Ni, Cu, Zn, Cd, Pb, and Cr were indicative that these elements were emitted by anthropogenic sources in the area (dry milling of phosphate rocks, chemical reactions used for fertilizers production, and vehicular activities. Kfoury et al. (2009) focused on aerosol samples in Chekka region and found high levels of potassium in some samples that were linked to biomass combustion. The mass concentration of particles increased as the sites approached the industrial area (cement factories and quarries). Recently, Melki et al. (2017) showed higher phosphates, trace metals, and PAHs concentrations in a site under industrial influence (Zakroun) compared to a rural one (Kaftoun) in the North of Lebanon. According to the study, these compounds might be emitted from the cement factories and their quarries, the fertilizer industry, and from tire burning.

The Zouk Mikael region in Lebanon is considered as a residential area with important industrial activity with the presence of the biggest Heavy Fuel Oil (HFO) power plant in Lebanon. Only one exploratory study was conducted in the region by measuring the PAHs levels showing higher levels than two urban coastal areas (Baalbaki et al., 2018).

8.6 Health risk assessment studies in Lebanon

The study of the impact of polluted air on human health was tackled in different ways in Lebanon. First, several studies were made in order to correlate air pollution and health effects. Kobrossi et al. (2002) reported an increase in the frequency of respiratory problems among children living near cement and fertilizer industries in the North of Lebanon.

Second, epidemiological studies were done to associate outdoor air pollution to several health problems such as chronic obstructive pulmonary diseases, chronic bronchitis, cardiovascular diseases and lung cancer (Salameh et al., 2012; Waked et al., 2012b; Aoun et al., 2013; Nasser et al., 2015). Additionally, Al Noaimi et al. (2021) showed that maternal exposure to air pollution has been associated with higher birth defects in Lebanon based on 533 cases and 10,124 controls between June 2014 and June 2017.

Table I-5: PM studies in different sites in Lebanon listed from newest to oldest according to the sampling date

References	Site	Date of Sampling	Characteristic of the site	PM	Average concentration ($\mu g/m^3$)	Studied compounds
Abdallah et al. (2018)	All over Lebanon	Data from MoE AQMN		$PM_{2.5}$ PM_{10}	28.6 36.7	-
	Beirut	Data from MoE AQMN		$PM_{2.5}$ PM_{10}	28.8 37.9	-
Badran et al. (2020)	Sin el Fil (Suburb of Beirut)	January - March 2017	Huge road traffic Diesel powered generators Waste incineration	$PM_{2.5}$	54	PAHs Ions Elements PCDD/F PCB
Abbas et al. (2019a)	Old airport Avenue in South Beirut	November 2015-January 2016	Huge road traffic Large residential area Commercial centers	$PM_{2.5}$	48	PAHs PCDD/F PCB
Baalbaki et al. (2018)	AUB (background site)	January - March 2015 June - July 2015	Urban site	PM_{10}	-	PAHs
	Dora (urban-industrial area)		Industrial area with major traffic	PM_{10}	-	
	Zouk Mikael (industrial area)		Major Heavy fuel oil power plant	PM_{10}	-	
Melki et al. (2017)	Kaftoun (Rural site)	February - April 2014	Rural site	$PM_{2.5-0.3}$	10.7	n-alkanes PAHs Ions Elements Total carbon
	Zakroun (Industrial site)	February - April 2014	Site under industrial influence (cement industries + Quarries + Phosphate fertilizer industry)	$PM_{2.5-0.3}$	18.5	

Jaafar et al. (2014)	AUB (Background site)	Summer-Fall 2012 Comparison between dust and non-dust episodes	Green areas Pedestrian roads Sea	$PM_{2.5}$ PM_{10}	21-39 10-53	Ions Elements OC - EC
Daher et al. (2013)	AUB (Background site)	July - August 2012	Vegetation Pedestrian roads	$PM_{2.5}$ PM_{10}	22.6 38.4	n-alkanes PAHs Hopanes Dicarbox. acids Ions Elements
	Near freeway Jal el Dib (Traffic site)	July - August 2012	Highway	$PM_{2.5}$ PM_{10}	49.9 83.9	
Nakhlé et al. (2015)	Beirut (Urban site)	January - December 2012	Urban site	$PM_{2.5}$ PM_{10}	30.16 50.5	-
Waked et al. (2013)	Mansourieh (Suburban site)	February 2012	Pine forests Commercial residential site	$PM_{2.5}$	-	Fatty acids PAHs SOA Sugars OC - EC
Waked et al. (2014)	Mansourieh (Suburban site)	July 2011	Pine forests Commercial residential site	$PM_{2.5}$	-	Fatty acids PAHs SOA Sugars OC - EC
Borgie et al. (2016)	Sin el Fil (Suburb of Beirut)	May - September 2011	Vehicle traffic Industrial activities	$PM_{2.5}$	41	PAHs Ions Elements Total carbon
	Bejje (Rural site)	May - September 2011	Rural site	$PM_{2.5}$	22	
	AUB (Background site)	May 2009 - April 2010	Campus Park Pedestrian roads	$PM_{2.5}$ PM_{10}	20.2 54.7	Ions Elements

Massoud et al. (2011)	Grand Lycée Franco-Libanais (GLFL)	May 2009 - April 2010	Located between 2 major highways	$PM_{2.5}$ PM_{10}	20.3 60.7	
	Lycée Abdel Kader (LAK)	May 2009 - April 2010	Populated area	$PM_{2.5}$ PM_{10}	20.6 60.7	
Kfoury et al. (2009)	North Region	August - October 2008		TSP	-	Ions Elements
Yammine et al. (2010)	North region	April - June 2008		TSP	-	Ions Elements
	Haret Hreik (Urban site)	2006 - 2007	Post-war construction activity Inner city site	$PM_{2.5}$ PM_{10}	27.63 86.81	-
	AUB (Urban site)	2003 - 2004	Coastal site	PM_{10}	86.9	-
Kouyoumdjian and Saliba (2006)	Bliss (Urban site)	2003	Coastal site	$PM_{2.5}$ PM_{10}	40.95 71.34	- Ions
	Bourj Hammoud (Urban site)	February 2004 - January 2005	Highly populated area Commercial and industrial facilities Traffic Beirut Harbor	$PM_{2.5}$ $PM_{10-2.5}$ PM_{10}	31 53 84	
Saliba et al. (2007)	Bourj Hammoud (Urban site)	February 2004 - January 2005	Residential area Commercial Vehicular traffic	$PM_{2.5}$ $PM_{10-2.5}$	38.86 64.96	Elements
Shaka' and Saliba (2004)	AUB (Background site)	February - May 2003	Green area Traffic	$PM_{2.5}$ $PM_{10-2.5}$ PM_{10}	39.9 78.9 118.8	Ions Organic compounds

All of these studies were based on hospital case control studies for data collection and statistical analysis. A recent study also showed that the duration of exposure to traffic related air pollution was associated with a reduction in lung function and an increase in the severity of respiratory systems (Tayara et al., 2020).

Third, the first toxicological study in Lebanon was conducted by Borgie et al. (2015) that provided a comparative and comprehensive analysis of the chemical composition of atmospheric particles and their toxic effects on human lung cell line. The study showed that ultrafine particles can cause earlier alterations of mitochondrial metabolism and membrane integrity for lower particle concentrations. Additionally, exposure to ultrafine particles may lead to an increase in DNA damages. Melki et al. (2017) explained that proximity of industries to sampling sites or residential areas could increase PM genotoxicity and mutagenic potential. Other studies worked on different cell lines and studied the response variations depending on the size of particles and well as their composition (Abbas et al., 2019a; Badran et al., 2020).The results of these studies show that exposure of the organic extractable fraction of PM (especially $PM_{0.3}$) to BEAS-2B cells will lead to genotoxic events together with cell survival events, and possible harmful cell deregulation.

Finally, two health risk assessment studies based on the atmospheric composition were presented by Dhaini et al. (2017) for non-methane hydrocarbons (NMHCs) in Beirut area and by Baalbaki et al. (2016) for PM_{10} under the very near direct influence of an open waste burning site in Beirut. The latter study showed an increase in the short-term cancer risk from 1 to 20 cases per million during the waste combustion. The study conducted by Dhaini et al. (2017) showed an average cumulative cancer risk exceedance of 40 times in summer and 30 times in winter in Greater Beirut area compared to the USEPA standards with benzene as the main contributor followed by 1,3-butadiene emitted from traffic and combustion processes.

9 Hypothesis, objectives and methodologies

The East Mediterranean is considered as a hotspot of climate change. Model projections in the region show a strong warming of about 3.5°C to 7°C till the end of the century with an increase of heat wave days, stronger photochemical air pollution leading to higher concentration of pollutants in the atmosphere (Lelieveld et al., 2014). The major anthropogenic sources in the region are road traffic, urbanization, and industrial emissions (ESCWA, 2009). The region is also affected by natural sources such as dust storms from African and Arabian deserts. All of these sources contribute to high levels of PM that deteriorates the air quality leading to major

impacts on human health that were presented previously. The East Mediterranean region is the third region with the highest ambient and household air pollution attributable death rate (age-standardized) scoring 125 per 100,000 population according to WHO in 2016. These numbers will tend to rise with the increase of the PM concentrations due to climate change. However, in order to reduce the pollutants concentrations, it is essential to identify the sources that contribute the most to the mass of PM in different countries in order to improve the air quality in the region.

Literature regarding the air quality in the East Mediterranean is still scarce with studies focusing on Istanbul (Szigeti et al., 2013; Ozturk and Keles, 2016; Thera et al., 2019; Çapraz and Deniz, 2021) , Cyprus (Achilleos et al., 2016; Pikridas et al., 2018; Kafouris et al., 2020), Greece (Andreou et al., 2007; Vasilatou et al., 2017; Taghvaee et al., 2019), Egypt (Shaltout et al., 2018), and Lebanon. Looking at the different studies of air pollution in Lebanon, it appears that most of them were conducted in Greater Beirut area. Studies on PM were performed for a short period of time and focused either on the inorganic or organic composition and very few focused on both. As for industrial areas, some works were done in the North of Lebanon and one exploratory study in Zouk Mikael region. Air quality models of Abdallah et al. (2018) and Waked et al. (2013b) in Lebanon showed high pollutant concentrations over these regions. The overview of the natural and anthropogenic sources affecting the air quality in Lebanon and their impact show that a lot of work is needed to fully understand the atmospheric dynamics and the sources contributions to the air pollution especially in industrial areas.

Therefore, this study is particularly focused on the study of $PM_{2.5}$ in two urban-industrial areas in Lebanon, namely Fiaa, Chekka and Zouk Mikael. Chekka is characterized by the presence of cement plants along with their quarries and power plants while Zouk Mikael comprises the biggest power plant in Lebanon.

9.1 Objectives of this study

The main objectives of this work are:

- Study the chemical composition and the temporal variability of $PM_{2.5}$ (major and trace elements, water-soluble ions, organic compounds, and carbonaceous matter) and VOCs in the atmosphere in two urban sites under industrial influence
- Characterize the sources of pollution in the two areas in order to determine the contribution of the different pollution sources to the observed concentration of fine particles

- Evaluate the health risk associated with the human exposure to different classes of compounds in $PM_{2.5}$ and VOCs and evaluate the oxidative potential of $PM_{2.5}$

The available data and the results of this study will be an important database that can be used in the future to assess the performance of air quality modeling systems in these areas (emission inventories, chemistry transport model…) Therefore, this work will help in filling the gap of knowledge to better characterize the pollution sources in industrial areas and to better assess how air pollution is affecting the public health in Lebanon and in the region.

9.2 Scientific questions

A comprehensive list of scientific questions needs to be answered to reach these objectives:

- What is the concentration and chemical composition of $PM_{2.5}$ in these sites? (Chapter III)
- What are the main natural and anthropogenic sources of $PM_{2.5}$ affecting the sampling sites? (Chapter III)
- How can we assess the health impact of $PM_{2.5}$ and VOCs in the region and what are the most toxic sources to human health? (Chapter IV)

9.3 Methodology

In order to accomplish these objectives, the following methodology should be adopted **(Fig. I-21)**:

First, a one-year field campaign should be conducted for $PM_{2.5}$ and VOC in the two considered regions. to constitute a database which will be the basis of the study.

Second, a detailed study of the VOC compounds and an exhaustive characterization of $PM_{2.5}$ including the analysis of water-soluble ions, metals, carbonaceous fraction, and organic compounds should be performed. The data will then be treated, interpreted, and analyzed with time series. In addition to that, exploratory methods should be investigated to obtain a preliminary idea on the emission sources such as Carbon Preference Index (CPI) and Wax ratios for n-alkanes, diagnostic ratios for PAHs, OC/EC ratio, enrichment factors for metals, as well as the study of long-range transport of pollutants by evaluating backward trajectories.

Third, receptor modeling approaches should be applied to the database using PMF for the two areas in order to identify the pollution sources and quantify their contributions to the total PM.

The database should contain the concentrations of the compounds in each sample and their corresponding uncertainties. In order to assign the output factors of the models to the emission sources, source profiles are an essential tool. And based on the importance to determine local profiles, samples from different sources should be collected under different sampling conditions and analyzed for their chemical composition.

Fourth, the health risk should be evaluated using two techniques: the health risk associated with the exposure to the different classes of compounds (cancer and non-cancer risk) using their concentrations for the $PM_{2.5}$ and NMVOC and the assessment of the $PM_{2.5}$ oxidative potential. Finally, the relationship between the oxidative potential and the PM chemical composition should be studied and the contribution of the different sources to the overall $PM_{2.5}$ oxidative potential should be evaluated.

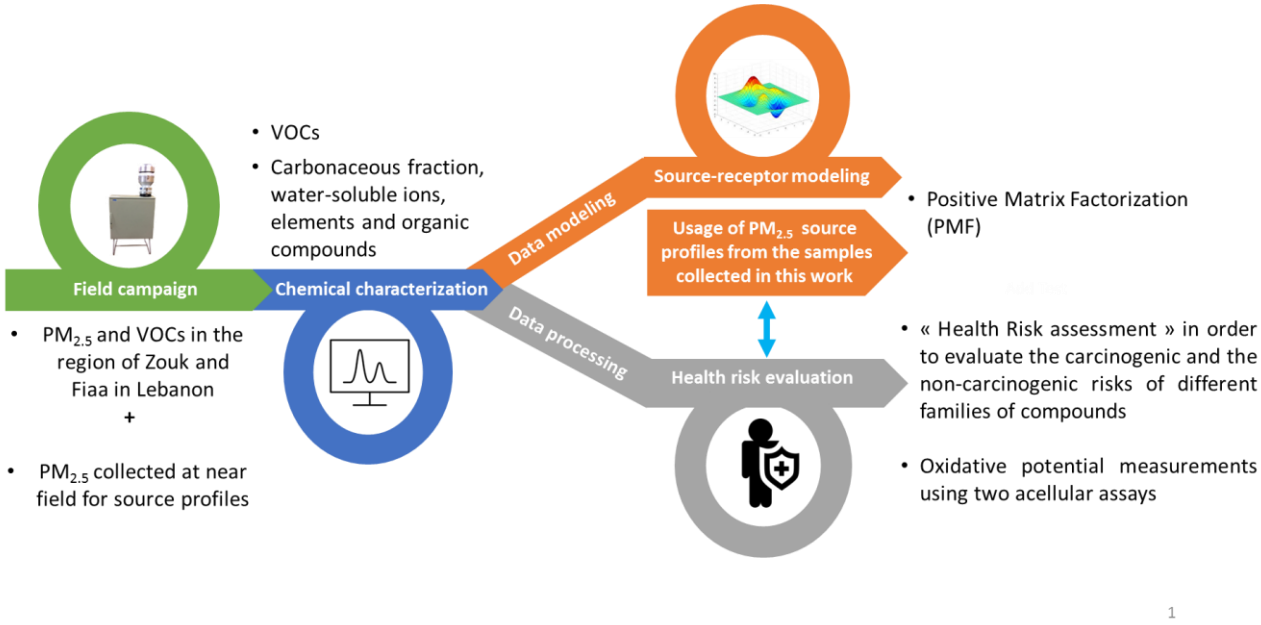

Fig. I-21: Scientific methodology adopted in this work

References:

Abbas, I., Badran, G., Verdin, A., Ledoux, F., Roumie, M., Lo Guidice, J.-M., Courcot, D., Garçon, G., 2019a. In vitro evaluation of organic extractable matter from ambient $PM_{2.5}$ using human bronchial epithelial BEAS-2B cells: Cytotoxicity, oxidative stress, pro-inflammatory response, genotoxicity, and cell cycle deregulation. Environ. Res. 171, 510-522, https://doi.org/10.1016/j.envres.2019.01.052.

Abbas, I., Chaaban, J., Al-Rabaa, A.-R., Shaar, A., Shaar, A., 2019b. Solid Waste Management in Lebanon: Challenges and Recommendations. Int J Environ Waste Manag

Abdallah, C., Afif, C., Masri, N., Öztürk, F., Dağkuş Keleş, M., Sartelet, K., 2018. A first annual assessment of air quality modeling over Lebanon using WRF/Polyphemus. Atmos. Pollut. Res. 9, https://doi.org/10.1016/j.apr.2018.01.003.

Abdallah, C., Afif, C., Sauvage, S., Borbon, A., Salameh, T., Kfoury, A., Leonardis, T., Karam, C., Formenti, P., Doussin, J.F., Locoge, N., Sartelet, K., 2020. Determination of gaseous and particulate emission factors from road transport in a Middle Eastern capital. Transp Res D Transp Envrion 83, 102361, https://doi.org/10.1016/j.trd.2020.102361.

Abdallah, C., Sartelet, K., Afif, C., 2016. Influence of boundary conditions and anthropogenic emission inventories on simulated O_3 and $PM_{2.5}$ concentrations over Lebanon. Atmos. Pollut. Res. 7, 10.1016/j.apr.2016.06.001.

Abdel-Shafy, H.I., Mansour, M.S.M., 2016. A review on polycyclic aromatic hydrocarbons: Source, environmental impact, effect on human health and remediation. Egyptian Journal of Petroleum 25, 107-123, https://doi.org/10.1016/j.ejpe.2015.03.011.

Achilleos, S., Wolfson, J.M., Ferguson, S.T., Kang, C.-M., Hadjimitsis, D.G., Hadjicharalambous, M., Achilleos, C., Christodoulou, A., Nisanzti, A., Papoutsa, C., Themistocleous, K., Athanasatos, S., Perdikou, S., Koutrakis, P., 2016. Spatial variability of fine and coarse particle composition and sources in Cyprus. Atmos Res 169, 255-270, https://doi.org/10.1016/j.atmosres.2015.10.005.

Ackermann, F., 2008. A procedure for correcting the grain size effect in heavy metal analyses of estuarine and coastal sediments. Environ Technol Lett 1, 10.1080/09593338009384008.

Afif, C., Chélala, C., Borbon, A., Abboud, M., Gerard, J., Farah, W., Jambert, C., Zaarour, R., Saliba, N., Perros, P., Rizk, T., 2008. SO_2 in Beirut: air quality implication and effects of local emissions and long-range transport. Air Qual Atmos Health 1, 167-178, 10.1007/s11869-008-0022-y.

Afif, C., Dutot, A.L., Jambert, C., Abboud, M., Adjizian-Gérard, J., Farah, W., Perros, P.E., Rizk, T., 2009. Statistical approach for the characterization of NO_2 concentrations in Beirut. Air Quality, Atmosphere & Health 2, 57-67, 10.1007/s11869-009-0034-2.

Agarwal, A., Satsangi, A., Lakhani, A., Kumari, K.M., 2020. Seasonal and spatial variability of secondary inorganic aerosols in $PM_{2.5}$ at Agra: Source apportionment through receptor models. Chemosphere 242, 125132, https://doi.org/10.1016/j.chemosphere.2019.125132.

Agrawal, H., Welch, W.A., Miller, J.W., Cocker, D.R., 2008. Emission measurements from a crude oil tanker at sea. Environ. Sci. Technol. 42, 7098-7103, 10.1021/es703102y.

Akhtar, U., McWhinney, R., Rastogi, N., Abbatt, J., Evans, G., Scott, J., 2010. Cytotoxic and proinflammatory effects of ambient and source-related particulate matter (PM) in relation to the production of reactive oxygen species (ROS) and cytokine adsorption by particles. Inhalation Toxicol. 22 Suppl 2, 37-47, 10.3109/08958378.2010.518377.

Al Noaimi, G., Yunis, K., El Asmar, K., Abu Salem, F.K., Afif, C., Ghandour, L.A., Hamandi, A., Dhaini, H.R., 2021. Prenatal exposure to criteria air pollutants and associations

with congenital anomalies: A Lebanese national study. Environ. Pollut. 281, 117022, 10.1016/j.envpol.2021.117022.

Alkoussa, S., Hulo, S., Courcot, D., Billet, S., Martin, P., 2020. Extracellular vesicles as actors in the air pollution related cardiopulmonary diseases. Crit. Rev. Toxicol. 50., https://doi.org/10.1080/10408444.2020.1763252.

Allaerts, D., 2016. Large-eddy simulation of wind farms in conventionally neutral and stable atmospheric boundary layers. in: Science, A.D.S.F.o.E. (Ed.).

Alleman, L., Lamaison, L., Esperanza, P., Robache, A., Galloo, J.-C., 2010. PM_{10} metal concentrations and source identification using positive matrix factorization and wind sectoring in a french industrial zone.

Alves, C., 2008. Characterisation of solvent extractable organic constituents in atmospheric particulate matter: An overview. An. Acad. Bras. Cienc. 80, 21-82, 10.1590/S0001-37652008000100003.

Alves, C.A., Gonçalves, C., Pio, C.A., Mirante, F., Caseiro, A., Tarelho, L., Freitas, M.C., Viegas, D.X., 2010. Smoke emissions from biomass burning in a Mediterranean shrubland. Atmos Environ 44, 3024-3033, https://doi.org/10.1016/j.atmosenv.2010.05.010.

Alves, C.A., Pio, C.A., 2005. Secondary organic compounds in atmospheric aerosols: speciation and formation mechanisms. jbchs Journal of the Brazilian Chemical Society 16, 1017-1029

Anderson, D.R., Fisher, R., 2002. Sources of dioxins in the United Kingdom: the steel industry and other sources. Chemosphere 46, 371-381, https://doi.org/10.1016/S0045-6535(01)00178-3.

Anderson, J.O., Thundiyil, J.G., Stolbach, A., 2012. Clearing the air: a review of the effects of particulate matter air pollution on human health. Journal of medical toxicology : official journal of the American College of Medical Toxicology 8, 166-175, 10.1007/s13181-011-0203-1.

Andreou, G., Alexiou, S., Loupa, G., Rapsomanikis, S., 2007. Identification, abundance and origin of aliphatic hydrocarbons in the fine atmospheric particulate matter of Athens, Greece. Water, Air, & Soil Pollution: Focus 8, 99-106, 10.1007/s11267-007-9142-x.

Aoun, J., Saleh, N., Waked, M., Salamé, J., Salameh, P., 2013. Lung cancer correlates in Lebanese adults: a pilot case--control study. J Epidemiol Glob Health 3, 235-244, 10.1016/j.jegh.2013.06.005.

Arruti, A., Fernández-Olmo, I., Irabien, A., 2011. Regional evaluation of particulate matter composition in an Atlantic coastal area (Cantabria region, northern Spain): Spatial variations in different urban and rural environments. Atmos Res 101, 280-293, https://doi.org/10.1016/j.atmosres.2011.03.001.

Asante-Duah, K., 2019. Public health risk assessment for human exposure to chemicals. SPRINGER.

Atkinson, R., 2008. Our present understanding of the gas-phase atmospheric degradation of VOCs. Springer Netherlands, Dordrecht, pp. 1-19.

Atkinson, R., Arey, J., 2003. Atmospheric degradation of volatile organic compounds. Chemical Reviews 103, 4605-4638, 10.1021/cr0206420.

Ayres, J.G., Borm, P., Cassee, F.R., Castranova, V., Donaldson, K., Ghio, A., Harrison, R.M., Hider, R., Kelly, F., Kooter, I.M., Marano, F., Maynard, R.L., Mudway, I., Nel, A., Sioutas, C., Smith, S., Baeza-Squiban, A., Cho, A., Duggan, S., Froines, J., 2008. Evaluating the Toxicity of Airborne Particulate Matter and Nanoparticles by Measuring Oxidative Stress Potential—A Workshop Report and Consensus Statement. Inhalation Toxicol. 20, 75-99, 10.1080/08958370701665517.

Baalbaki, R., el hage, R., Nassar, J., Gerard, J., Saliba, N., Zaarour, R., Abboud, M., Farah, W., Khalaf, L., Shihadeh, A., Saliba, N., 2016. Exposure to Atmospheric PMs, PAHs, PCDD/Fs and Metals near an Open Air Waste Burning Site in Beirut. Lebanese Science Journal 17, 10.22453/LSJ-017.2.091103.

Baalbaki, R., Nassar, J., Salloum, S., Shihadeh, A.L., Lakkis, I., Saliba, N.A., 2018. Comparison of atmospheric polycyclic aromatic hydrocarbon levels in three urban areas in Lebanon. Atmos Environ 179, 260-267, https://doi.org/10.1016/j.atmosenv.2018.02.028.

Badran, G., Ledoux, F., Verdin, A., Abbas, I., Roumie, M., Genevray, P., Landkocz, Y., Lo Guidice, J.-M., Garçon, G., Courcot, D., 2020. Toxicity of fine and quasi-ultrafine particles: Focus on the effects of organic extractable and non-extractable matter fractions. Chemosphere 243, 125440, https://doi.org/10.1016/j.chemosphere.2019.125440.

Barbieri, M., 2016. The Importance of Enrichment Factor (EF) and Geoaccumulation Index (Igeo) to Evaluate the Soil Contamination. Journal of Geology & Geophysics 5, 10.4172/2381-8719.1000237.

Bates, J.T., Fang, T., Verma, V., Zeng, L., Weber, R.J., Tolbert, P.E., Abrams, J.Y., Sarnat, S.E., Klein, M., Mulholland, J.A., Russell, A.G., 2019. Review of acellular assays of ambient particulate matter oxidative potential: methods and relationships with composition, sources, and health effects. Environ. Sci. Technol. 53, 4003-4019, 10.1021/acs.est.8b03430.

Bauer, H., Schüller, E., Weinke, G., Berger, A., Hitzenberger, R., Marr, I., Puxbaum, H., 2008. Significant contributions of fungal spores to the organic carbon and to the aerosol mass balance of the urban atmospheric aerosol. Atmos Environ 42, 5542-5549, 10.1016/j.atmosenv.2008.03.019.

Becagli, S., Sferlazzo, D.M., Pace, G., di Sarra, A., Bommarito, C., Calzolai, G., Ghedini, C., Lucarelli, F., Meloni, D., Monteleone, F., Severi, M., Traversi, R., Udisti, R., 2012. Evidence for heavy fuel oil combustion aerosols from chemical analyses at the island of Lampedusa: a possible large role of ships emissions in the Mediterranean. Atmos. Chem. Phys. 12, 3479-3492, https://doi.org/10.5194/acp-12-3479-2012.

Behera, S.N., Sharma, M., Aneja, V.P., Balasubramanian, R., 2013. Ammonia in the atmosphere: a review on emission sources, atmospheric chemistry and deposition on terrestrial bodies. Environ Sci Pollut Res Int 20, 8092-8131, 10.1007/s11356-013-2051-9.

Belis, C.A., Favez, O., Harrison, R.M., Larsen, B.R., Amato, F., El Haddad, I., Hopke, P.K., Nava, S., Paatero, P., Prévôt, A., Quass, U., Vecchi, R., Viana, M., European, C., Joint Research, C., Institute for, E., Sustainability, 2014. European guide on air pollution source apportionment with receptor models.

Belis, C.A., Favez, O., Mircea, M., Diapouli, E., Manousakas, M.I., Vratolis, S., Gilardoni, S., Paglione, M., Decesari, S., Mocnik, G., Mooibroek, D., Salvador, P., Takahama, S., Vecchi, R., Paatero, P., European, C., Joint Research, C., 2019. European guide on air pollution source apportionment with receptor models : revised version 2019.

Bi, X., Dai, Q., Wu, J., Zhang, Q., Zhang, W., Luo, R., Cheng, Y., Zhang, J., Wang, L., Yu, Z., Zhang, Y., Tian, Y., Feng, Y., 2019. Characteristics of the main primary source profiles of particulate matter across China from 1987 to 2017. Atmos. Chem. Phys. 19, 3223-3243, 10.5194/acp-19-3223-2019.

Bond, T.C., Bergstrom, R.W., 2006. Light Absorption by Carbonaceous Particles: An Investigative Review. Aerosol Sci. Technol. 40, 27-67, 10.1080/02786820500421521.

Borgie, M., Dagher, Z., Ledoux, F., Verdin, A., Cazier, F., Martin, P., Hachimi, A., Shirali, P., Greige-Gerges, H., Courcot, D., 2015. Comparison between ultrafine and fine particulate matter collected in Lebanon: Chemical characterization, in vitro cytotoxic effects and metabolizing enzymes gene expression in human bronchial epithelial cells. Environ. Pollut. 205, 250-260, https://doi.org/10.1016/j.envpol.2015.05.027.

Borgie, M., Ledoux, F., Dagher, Z., Verdin, A., Cazier, F., Courcot, L., Shirali, P., Greige-Gerges, H., Courcot, D., 2016. Chemical characteristics of $PM_{2.5–0.3}$ and $PM_{0.3}$ and consequence of a dust storm episode at an urban site in Lebanon. Atmos Res 180, 274-286, https://doi.org/10.1016/j.atmosres.2016.06.001.

Bray, E.E., Evans, E.D., 1961. Distribution of n-paraffins as a clue to recognition of source beds. Geochim. Cosmochim. Acta 22, 2-15, https://doi.org/10.1016/0016-7037(61)90069-2.

Burnett, R., Chen, H., Szyszkowicz, M., Fann, N., Hubbell, B., Pope, C., Apte, J., Brauer, M., Cohen, A., Weichenthal, S., Coggins, J., Di, Q., Brunekreef, B., Frostad, J., Lim, S., Kan, H., Walker, K., Thurston, G., Hayes, R., Spadaro, J., 2018. Global estimates of mortality associated with long-term exposure to outdoor fine particulate matter. Proceedings of the National Academy of Sciences 115, 201803222, 10.1073/pnas.1803222115.

Buseck, P., Adachi, K., 2007. Nanoparticles in the Atmosphere. ELEMENTS 4, 389-394, 10.2113/gselements.4.6.389.

Camuffo, D., 2002. Microclimate for cultural heritage. Elsevier, Amsterdam.

Çapraz, Ö., Deniz, A., 2021. Particulate matter (PM10 and PM2.5) concentrations during a Saharan dust episode in Istanbul. Air Quality, Atmosphere and Health 14, 109-116, 10.1007/s11869-020-00917-4.

Carlton, A.G., Wiedinmyer, C., Kroll, J.H., 2009. A review of Secondary Organic Aerosol (SOA) formation from isoprene. Atmos. Chem. Phys. 9, 4987-5005, 10.5194/acp-9-4987-2009.

Cass, G.R., 1998. Organic molecular tracers for particulate air pollution sources. TrAC Trends in Analytical Chemistry 17, 356-366, https://doi.org/10.1016/S0165-9936(98)00040-5.

Cecinato, A., Guerriero, E., Balducci, C., Muto, V., 2014. Use of the PAH fingerprints for identifying pollution sources. Urban Climate 10, 630-643, https://doi.org/10.1016/j.uclim.2014.04.004.

Chantara, S., Thepnuan, D., Wiriya, W., Prawan, S., Tsai, Y.I., 2019. Emissions of pollutant gases, fine particulate matters and their significant tracers from biomass burning in an open-system combustion chamber. Chemosphere 224, 407-416, https://doi.org/10.1016/j.chemosphere.2019.02.153.

Charron, A., Polo-Rehn, L., Besombes, J.L., Golly, B., Buisson, C., Chanut, H., Marchand, N., Guillaud, G., Jaffrezo, J.L., 2019. Identification and quantification of particulate tracers of exhaust and non-exhaust vehicle emissions. Atmos. Chem. Phys. 19, 5187-5207, 10.5194/acp-19-5187-2019.

Chen, J., Hoek, G., 2020. Long-term exposure to PM and all-cause and cause-specific mortality: A systematic review and meta-analysis. Environ Int 143, 105974, 10.1016/j.envint.2020.105974.

Cheng, J., Zhang, X., Ma, Y., Zhao, J., Tang, Z., 2019. Concentrations and distributions of polycyclic aromatic hydrocarbon in vegetables and animal-based foods before and after grilling: Implication for human exposure. Sci. Total Environ. 690, 965-972, https://doi.org/10.1016/j.scitotenv.2019.07.074.

Cho, A.K., Sioutas, C., Miguel, A.H., Kumagai, Y., Schmitz, D.A., Singh, M., Eiguren-Fernandez, A., Froines, J.R., 2005. Redox activity of airborne particulate matter at different sites in the Los Angeles Basin. Environ. Res. 99, 40-47, 10.1016/j.envres.2005.01.003.

Chow, J.C., Lowenthal, D.H., Chen, L.W.A., Wang, X., Watson, J.G., 2015. Mass reconstruction methods for $PM_{2.5}$: a review. Air quality, atmosphere, & health 8, 243-263, 10.1007/s11869-015-0338-3.

Cooper, J.A., Watson, J.G., 1980. Receptor oriented methods of air particulate source apportionment. Journal of the Air Pollution Control Association 30, 1116-1125, 10.1080/00022470.1980.10465157.

Cooper, J.E., Bray, E.E., 1963. A postulated role of fatty acids in petroleum formation. Geochim. Cosmochim. Acta 27, 1113-1127, https://doi.org/10.1016/0016-7037(63)90093-0.

Cortés, J., González, C.M., Morales, L., Abalos, M., Abad, E., Aristizábal, B.H., 2014. PCDD/PCDF and dl-PCB in the ambient air of a tropical Andean city: Passive and active sampling measurements near industrial and vehicular pollution sources. Sci. Total Environ. 491-492, 67-74, https://doi.org/10.1016/j.scitotenv.2014.01.113.

Crobeddu, B., Aragao-Santiago, L., Bui, L.-C., Boland, S., Baeza Squiban, A., 2017. Oxidative potential of particulate matter 2.5 as predictive indicator of cellular stress. Environ. Pollut. 230, 125-133, https://doi.org/10.1016/j.envpol.2017.06.051.

Dada, L., Mrad, R., Siffert, S., Saliba, N., 2013. Atmospheric markers of African and Arabian dust in an urban eastern Mediterranean environment, Beirut, Lebanon. J. Aerosol Sci. 66, 187–192, 10.1016/j.jaerosci.2013.09.002.

Daher, N., Saliba, N.A., Shihadeh, A.L., Jaafar, M., Baalbaki, R., Sioutas, C., 2013. Chemical composition of size-resolved particulate matter at near-freeway and urban background sites in the greater Beirut area. Atmos Environ 80, 96-106, 10.1016/j.atmosenv.2013.08.004.

Dams, R., De Jonge, J., 1976. Chemical composition of Swiss aerosols from the Jungfraujoch. Atmospheric Environment (1967) 10, 1079-1084, https://doi.org/10.1016/0004-6981(76)90117-7.

de Oliveira Alves, N., Matos Loureiro, A.L., dos Santos, F.C., Nascimento, K.H., Dallacort, R., de Castro Vasconcellos, P., de Souza Hacon, S., Artaxo, P., de Medeiros, S.R.B., 2011. Genotoxicity and composition of particulate matter from biomass burning in the eastern Brazilian Amazon region. Ecotoxicol. Environ. Saf. 74, 1427-1433, https://doi.org/10.1016/j.ecoenv.2011.04.007.

Després, V., Huffman, J.A., Burrows, S.M., Hoose, C., Safatov, A., Buryak, G., Fröhlich-Nowoisky, J., Elbert, W., Andreae, M., Pöschl, U., Jaenicke, R., 2012. Primary biological aerosol particles in the atmosphere: a review. Tellus B: Chemical and Physical Meteorology 64, 15598, 10.3402/tellusb.v64i0.15598.

Dhaini, H.R., Salameh, T., Waked, A., Sauvage, S., Borbon, A., Formenti, P., Doussin, J.-F., Locoge, N., Afif, C., 2017. Quantitative cancer risk assessment and local mortality burden for ambient air pollution in an eastern Mediterranean City. Environ Sci Pollut Res Int 24, 14151-14162, https://doi.org/10.1007/s11356-017-9000-y.

Dongarrà, G., Manno, E., Varrica, D., 2008. Possible markers of traffic-related emissions. Environmental Monitoring and Assessment 154, 117, 10.1007/s10661-008-0382-7.

Du, Y., Xu, X., Chu, M., Guo, Y., Wang, J., 2016. Air particulate matter and cardiovascular disease: the epidemiological, biomedical and clinical evidence. J Thorac Dis 8, E8-E19, 10.3978/j.issn.2072-1439.2015.11.37.

Dutton, S.J., Williams, D.E., Garcia, J.K., Vedal, S., Hannigan, M.P., 2009. PM2.5 characterization for time series studies: Organic molecular marker speciation methods and observations from daily measurements in Denver. Atmos Environ 43, 2018-2030, https://doi.org/10.1016/j.atmosenv.2009.01.003.

El Haddad, I., Marchand, N., Dron, J., Temime-Roussel, B., Quivet, E., Wortham, H., Jaffrezo, J.L., Baduel, C., Voisin, D., Besombes, J.L., Gille, G., 2009. Comprehensive primary particulate organic characterization of vehicular exhaust emissions in France. Atmos Environ 43, 6190-6198, https://doi.org/10.1016/j.atmosenv.2009.09.001.

El Haddad, I., Marchand, N., Wortham, H., Piot, C., Besombes, J.L., Cozic, J., Chauvel, C., Armengaud, A., Robin, D., Jaffrezo, J.L., 2011a. Primary sources of $PM_{2.5}$ organic aerosol in an industrial Mediterranean city, Marseille. Atmos. Chem. Phys. 11, 2039-2058, 10.5194/acp-11-2039-2011.

El Haddad, I., Marchand, N., Wortham, H., Piot, C., Besombes, J.L., Cozic, J., Chauvel, C., Armengaud, A., Robin, D., Jaffrezo, J.L., 2011b. Primary sources of $PM_{2.5}$ organic aerosol in an industrial Mediterranean city, Marseille. Atmos. Chem. Phys. 11, 2039-2058, 10.5194/acp-11-2039-2011.

ESCWA, 2009. Air Quality and Atmospheric Pollution In the Arab Region.

Estrellan, C.R., Iino, F., 2010. Toxic emissions from open burning. Chemosphere 80, 193-207, 10.1016/j.chemosphere.2010.03.057.

Fang, T., Verma, V., Bates, J.T., Abrams, J., Klein, M., Strickland, M.J., Sarnat, S.E., Chang, H.H., Mulholland, J.A., Tolbert, P.E., Russell, A.G., Weber, R.J., 2016. Oxidative potential of ambient water-soluble PM2.5 in the southeastern United States: contrasts in sources and health associations between ascorbic acid (AA) and dithiothreitol (DTT) assays. Atmos. Chem. Phys. 16, 3865-3879, 10.5194/acp-16-3865-2016.

FAO, 2005. National Forest and Tree Resources Assessment 2003-05 (TCP/LEB/2903). Working paper 95, Forest Resources Assessment, Forestry. Food and Agriculture Organization.

Farrow, A., Miller, K.A., Myllyvirta, L., 2020. Toxic air: The price of fossil fuels. Greenpeace Middle East and North Africa 35pp. .

Fine, P.M., Sioutas, C., Solomon, P.A., 2008. Secondary particulate matter in the United States: Insights from the particulate matter Supersites program and related studies. J. Air Waste Manage. Assoc. 58, 234-253, 10.3155/1047-3289.58.2.234.

Foltescu, V.L., Selin Lindgren, E., Isakson, J., Öblad, M., Tiede, R., Sommar, J., Pacyna, J.M., Toerseth, K., 1996. Airborne concentrations and deposition fluxes of major and trace species at marine stations in Southern Scandinavia. Atmospheric Environment 30, 3857-3872, https://doi.org/10.1016/1352-2310(96)00064-7.

Fowler, D., Brimblecombe, P., Burrows, J., Heal, M.R., Grennfelt, P., Stevenson, D.S., Jowett, A., Nemitz, E., Coyle, M., Liu, X., Chang, Y., Fuller, G.W., Sutton, M.A., Klimont, Z., Unsworth, M.H., Vieno, M., 2020. A chronology of global air quality. Philosophical Transactions of the Royal Society A: Mathematical, Physical and Engineering Sciences 378, 20190314, doi:10.1098/rsta.2019.0314.

Frenken, K., 2009. Irrigation in the middle East region in figures. FAO, Rome.

Frey, A.K., Saarnio, K., Lamberg, H., Mylläri, F., Karjalainen, P., Teinilä, K., Carbone, S., Tissari, J., Niemelä, V., Häyrinen, A., Rautiainen, J., Kytömäki, J., Artaxo, P., Virkkula, A., Pirjola, L., Rönkkö, T., Keskinen, J., Jokiniemi, J., Hillamo, R., 2014. Optical and chemical characterization of aerosols emitted from coal, heavy and light fuel oil, and small-scale wood combustion. Environ. Sci. Technol. 48, 827-836, 10.1021/es4028698.

Friedlander, S.K., 1973. Chemical element balances and identification of air pollution sources. Environ. Sci. Technol. 7, 235-240, 10.1021/es60075a005.

Galvão, E.S., Reis, N.C., Santos, J.M., 2020. The role of receptor models as tools for air quality management: a case study of an industrialized urban region. Environmental science and pollution research international 27, 35918-35929, 10.1007/s11356-020-07848-8.

Gietl, J.K., Lawrence, R., Thorpe, A.J., Harrison, R.M., 2010. Identification of brake wear particles and derivation of a quantitative tracer for brake dust at a major road. Atmos Environ 44, 141-146, https://doi.org/10.1016/j.atmosenv.2009.10.016.

Gordon, G.E., 1980. Receptor models. Environ. Sci. Technol. 14, 792-800, 10.1021/es60167a006.

Guo, D., Wei, H., Guo, Y., Wang, C., Yin, Z., 2021. Non-exhaust particulate matter emission from vehicles: A review. E3S Web of Conferences 268, 01015, 10.1051/e3sconf/202126801015.

Guo, H., 2003. Particle-associated polycyclic aromatic hydrocarbons in urban air of Hong Kong. Atmos Environ 37, 5307-5317, 10.1016/j.atmosenv.2003.09.011.

Haber, L.T., Strawson, J.E., Maier, A., Baskerville-Abraham, I.M., Parker;, A., Dourson, M.L., 2012. Noncancer risk assessment: principles and practice in environmental and occupational Settings. Patty's Toxicology, pp. 89-132.

Hallquist, M., Wenger, J.C., Baltensperger, U., Rudich, Y., Simpson, D., Claeys, M., Dommen, J., Donahue, N., George, C., Goldstein, A., Hamilton, J., Herrmann, H., Hoffmann, T., Iinuma, Y., Jang, M., Jenkin, M.E., Jimenez, J., Kiendler-Scharr, A., Maenhaut, W., McFiggans, G., Mentel, T.F., Monod, A., Prévôt, A.S.H., Seinfeld, J.H., Surratt, J.D., Szmigielski, R., Wildt, J., 2009. The formation, properties and impact of secondary organic aerosol: Current and emerging issues. Atmos. Chem. Phys. 9, 5155–5236, 10.5194/acpd-9-3555-2009.

Harvey, W.R., Hutton, P., 1999. Carbon monoxide: chemistry, role, toxicity and treatment. Current Anaesthesia & Critical Care 10, 158-163, https://doi.org/10.1016/S0953-7112(99)80008-8.

He, J., Balasubramanian, R., 2010. Semi-volatile organic compounds (SVOCs) in ambient air and rainwater in a tropical environment: Concentrations and temporal and seasonal trends. Chemosphere 78, 742-751, https://doi.org/10.1016/j.chemosphere.2009.10.042.

Henry, R.C., Lewis, C.W., Hopke, P.K., Williamson, H.J., 1984. Review of receptor model fundamentals. Atmos Environ 18, 1507-1515, https://doi.org/10.1016/0004-6981(84)90375-5.

Hidy, G.M., Venkataraman, C., 1996. The chemical mass balance method for estimating atmospheric particle sources in southern California. Chem. Eng. Commun. 151, 187-209, 10.1080/00986449608936548.

Hill, M.K., 2020. Understanding environmental pollution.

Hlavay, J., Polyák, K., Bódog, I., Molnár, Á., Mészáros, E., 1996. Distribution of trace elements in filter-collected aerosol samples. Fresenius. J. Anal. Chem. 354, 227-232, 10.1007/PL00012730.

Hopke, P.K., 2016. Review of receptor modeling methods for source apportionment. J. Air Waste Manage. Assoc. 66, 237-259, 10.1080/10962247.2016.1140693.

Hopke, P.K., Ito, K., Mar, T., Christensen, W.F., Eatough, D.J., Henry, R.C., Kim, E., Laden, F., Lall, R., Larson, T.V., Liu, H., Neas, L., Pinto, J., Stölzel, M., Suh, H., Paatero, P., Thurston, G.D., 2006. PM source apportionment and health effects: 1. Intercomparison of source apportionment results. Journal of Exposure Science & Environmental Epidemiology 16, 275-286, 10.1038/sj.jea.7500458.

Hu, X.M., 2015. Boundary layer (atmospheric) and air pollution | Air Pollution Meteorology. in: North, G.R., Pyle, J., Zhang, F. (Eds.). Encyclopedia of Atmospheric Sciences (Second Edition). Academic Press, Oxford, pp. 227-236.

Hussar, E., Richards, S., Lin, Z.-Q., Dixon, R.P., Johnson, K.A., 2012. Human Health Risk assessment of 16 priority Polycyclic Aromatic Hydrocarbons in soils of Chattanooga, Tennessee, USA. Water, Air, Soil Pollut. 223, 5535-5548, 10.1007/s11270-012-1265-7.

IARC, 2019. IARC Monographs on the identification of carcinogenic hazards to Humans. International Agency for research on cancer, World Health Organization.

IARC; 2021.IARC monographs on the identifcation of carcinogenic hazards to Humans. https://monographs.iarc.who.int/list-of-classifications/. Accessed on 11/10/2021

IPCS, 1994. Assessing human health risks of chemicals: derivation of guidance values for health-based exposure limits, International Programme for Chemical Safety, World Health Organization, Geneva, 170.

Jaafar, M., Baalbaki, R., Mrad, R., Daher, N., Shihadeh, A., Sioutas, C., Saliba, N.A., 2014. Dust episodes in Beirut and their effect on the chemical composition of coarse and fine particulate matter. Sci. Total Environ. 496, 75-83, https://doi.org/10.1016/j.scitotenv.2014.07.018.

Jaffe, L.S., 1968. Ambient carbon monoxide and its fate in the atmosphere. Journal of the Air Pollution Control Association 18, 534-540, 10.1080/00022470.1968.10469168.

Jaoui, M., Kleindienst, T., Docherty, K., Lewandowski, M., Offenberg, J., 2013. Secondary organic aerosol formation from the oxidation of a series of sesquiterpenes: α-cedrene, β-caryophyllene, α-humulene and α-farnesene with O_3, OH and NO_3 radicals. Environ. Chem. 10, 178, 10.1071/EN13025.

Jaoui, M., Lewandowski, M., Kleindienst, T.E., Offenberg, J.H., Edney, E.O., 2007. β-caryophyllinic acid: An atmospheric tracer forβ-caryophyllene secondary organic aerosol. Geophys. Res. Lett. 34, 10.1029/2006gl028827.

Ji, Y., Wang, F., Zhang, L., Shan, C., Bai, Z., Sun, Z., Liu, L., Shen, B., 2014. A comprehensive assessment of human exposure to phthalates from environmental media and food in Tianjin, China. J. Hazard. Mater. 279, 133-140, https://doi.org/10.1016/j.jhazmat.2014.06.055.

Jiang, H., Jang, M., Sabo-Attwood, T., Robinson, S.E., 2016. Oxidative potential of secondary organic aerosols produced from photooxidation of different hydrocarbons using outdoor chamber under ambient sunlight. Atmos Environ 131, 382-389, https://doi.org/10.1016/j.atmosenv.2016.02.016.

Johannisson, J., Hiete, M., 2020. A Structured Approach for the Mitigation of Natural Methane Emissions—Lessons Learned from Anthropogenic Emissions. C 6, 24

Johnson, N.M., Hoffmann, A.R., Behlen, J.C., Lau, C., Pendleton, D., Harvey, N., Shore, R., Li, Y., Chen, J., Tian, Y., Zhang, R., 2021. Air pollution and children's health—a review of adverse effects associated with prenatal exposure from fine to ultrafine particulate matter. Environmental Health and Preventive Medicine 26, 72, 10.1186/s12199-021-00995-5.

Kafouris, D., Koukkidou, A., Christou, E., Hadjigeorgiou, M., Yiannopoulos, S., 2020. Determination of polycyclic aromatic hydrocarbons in traditionally smoked meat products and charcoal grilled meat in Cyprus. Meat Science, 108088, https://doi.org/10.1016/j.meatsci.2020.108088.

Kang, M., Ren, L., Ren, H., Zhao, Y., Kawamura, K., Zhang, H., Wei, L., Sun, Y., Wang, Z., Fu, P., 2018. Primary biogenic and anthropogenic sources of organic aerosols in

Beijing, China: Insights from saccharides and n-alkanes. Environmental Pollution 243, 1579-1587, https://doi.org/10.1016/j.envpol.2018.09.118.

Kfoury, A., Ledoux, F., El Khoury, B., Nakat, H., Nouali, H., Cazier, F., Courcot, D., Abi-Aad, E., Aboukaïs, A., 2009. A study of the inorganic chemical composition of atmospheric particulate matter in the region of Chekka, North Lebanon. Lebanese Science Journal 10, 3-16

Khalili, N.R., Scheff, P.A., Holsen, T.M., 1995. PAH source fingerprints for coke ovens, diesel and, gasoline engines, highway tunnels, and wood combustion emissions. Atmos Environ 29, 533-542, https://doi.org/10.1016/1352-2310(94)00275-P.

Kim, G.-U., Seo, K.-H., Chen, D., 2019. Climate change over the Mediterranean and current destruction of marine ecosystem. Scientific Reports 9, 18813, 10.1038/s41598-019-55303-7.

Kim, K.H., Lee, S.-B., Woo, D., Bae, G.-N., 2015. Influence of wind direction and speed on the transport of particle-bound PAHs in a roadway environment. Atmos. Pollut. Res. 6, 1024-1034, https://doi.org/10.1016/j.apr.2015.05.007.

Klimont, Z., Kupiainen, K., Heyes, C., Purohit, P., Cofala, J., Rafaj, P., Borken-Kleefeld, J., Schoepp, W., 2016. Global anthropogenic emissions of particulate matter including black carbon. Atmospheric Chemistry and Physics Discussions 2016, 1-72, 10.5194/acp-2016-880.

Kobrossi, R., Nuwayhid, I., Sibai, A.M., El-Fadel, M., Khogali, M., 2002. Respiratory health effects of industrial air pollution on children in North Lebanon. Int J Environ Health Res 12, 205-220, https://doi.org/10.1080/09603/202/000000970.

Kondo, K., Kagi, N., Namiki, N., 2018. Study on the mechanism of SVOC adsorption onto airborne particles in indoor air. Japan Architectural Review 1, 10.1002/2475-8876.12052.

Koppmann, R., von Czapiewski, K., Reid, J.S., 2005. A review of biomass burning emissions, part I: gaseous emissions of carbon monoxide, methane, volatile organic compounds, and nitrogen containing compounds. Atmos. Chem. Phys. Discuss. 2005, 10455-10516, 10.5194/acpd-5-10455-2005.

Koukoulakis, K.G., Kanellopoulos, P.G., Chrysochou, E., Costopoulou, D., Vassiliadou, I., Leondiadis, L., Bakeas, E., 2020. Atmospheric Concentrations and Health Implications of PAHs, PCBs and PCDD/Fs in the Vicinity of a Heavily Industrialized Site in Greece. Applied Sciences 10, 9023, https://doi.org/10.3390/app10249023.

Kouyoumdjian, H., Saliba, N.A., 2006. Mass concentration and ion composition of coarse and fine particles in an urban area in Beirut: effect of calcium carbonate on the absorption of nitric and sulfuric acids and the depletion of chloride. Atmos. Chem. Phys. 6, 1865-1877, 10.5194/acp-6-1865-2006.

Kroll, J.H., Seinfeld, J.H., 2008. Chemistry of secondary organic aerosol: Formation and evolution of low-volatility organics in the atmosphere. Atmos Environ 42, 3593-3624, https://doi.org/10.1016/j.atmosenv.2008.01.003.

Kumagai, Y., Koide, S., Taguchi, K., Endo, A., Nakai, Y., Yoshikawa, T., Shimojo, N., 2002. Oxidation of proximal protein sulfhydryls by phenanthraquinone, a component of diesel exhaust particles. Chem. Res. Toxicol. 15, 483-489, 10.1021/tx0100993.

Lamarque, J.F., Bond, T.C., Eyring, V., Granier, C., Heil, A., Klimont, Z., Lee, D., Liousse, C., Mieville, A., Owen, B., Schultz, M.G., Shindell, D., Smith, S.J., Stehfest, E., Van Aardenne, J., Cooper, O.R., Kainuma, M., Mahowald, N., McConnell, J.R., Naik, V., Riahi, K., van Vuuren, D.P., 2010. Historical (1850–2000) gridded anthropogenic and biomass burning emissions of reactive gases and aerosols: methodology and application. Atmos. Chem. Phys. 10, 7017-7039, 10.5194/acp-10-7017-2010.

Latif, M.T., Mei, C., Hanif, N., Srithawirat, T., 2012. Levoglucosan as an indicator of biomass burning from selected tropical plants. EnvironmentAsia 5, 22-27, 10.14456/ea.2012.15.

Lawson, D.R., Winchester, J.W., 1979. Sulfur, potassium, and phosphorus associations in aerosols from South American tropical rain forests. Journal of Geophysical Research: Oceans 84, 3723-3727, https://doi.org/10.1029/JC084iC07p03723.

Ledoux, F., Kfoury, A., Delmaire, G., Roussel, G., El Zein, A., Courcot, D., 2017. Contributions of local and regional anthropogenic sources of metals in $PM_{2.5}$ at an urban site in northern France. Chemosphere 181, 713-724, https://doi.org/10.1016/j.chemosphere.2017.04.128.

Lelieveld, J., Hadjinicolaou, P., Kostopoulou, E., Giannakopoulos, C., Pozzer, A., Tanarhte, M., Tyrlis, E., 2014. Model projected heat extremes and air pollution in the eastern Mediterranean and Middle East in the twenty-first century. Regional Environmental Change 14, 1937-1949, http://dx.doi.org/10.1007/s10113-013-0444-4.

Lelieveld, J., Klingmüller, K., Pozzer, A., Pöschl, U., Fnais, M., Daiber, A., Münzel, T., 2019. Cardiovascular disease burden from ambient air pollution in Europe reassessed using novel hazard ratio functions. European Heart Journal 40, 1590-1596, 10.1093/eurheartj/ehz135.

Lelieveld, J., Münzel, T., 2020. Air pollution, the underestimated cardiovascular risk factor: The original manuscript published in EHJ from Jos Lelieveld and Thomas Münzel came in position 72 of the top 100 papers of the Altmetric Top 100 score for 2019. The Altmetric worldwide ranking was the result of tracking 62.5 million mentions of 2.7 million research outputs. The result highlights the popularity of the Lelieveld / Münzel article. European Heart Journal 41, 904-905, 10.1093/eurheartj/ehaa063.

Lelieveld, J., Pozzer, A., Pöschl, U., Fnais, M., Haines, A., Münzel, T., 2020. Loss of life expectancy from air pollution compared to other risk factors: a worldwide perspective. Cardiovasc. Res., 10.1093/cvr/cvaa025.

Li, M., McDow, S.R., Tollerud, D.J., Mazurek, M.A., 2006. Seasonal abundance of organic molecular markers in urban particulate matter from Philadelphia, PA. Atmos Environ 40, 2260-2273, https://doi.org/10.1016/j.atmosenv.2005.10.025.

Li, N., Xia, T., Nel, A.E., 2008. The role of oxidative stress in ambient particulate matter-induced lung diseases and its implications in the toxicity of engineered nanoparticles. Free Radical Biol. Med. 44, 1689-1699, 10.1016/j.freeradbiomed.2008.01.028.

Liu, Y., Zhang, W., Bai, Z., Yang, W., Zhao, X., Han, B., Wang, X., 2017. China Source Profile Shared Service (CSPSS): The Chinese $PM_{2.5}$ Database for Source Profiles. Aerosol and Air Quality Research 17, 1501-1514, 10.4209/aaqr.2016.10.0469.

Lu, F.C., 1988. Acceptable daily intake: inception, evolution, and application. Regulatory toxicology and pharmacology : RTP 8, 45-60, 10.1016/0273-2300(88)90006-2.

Lu, S., Kang, L., Liao, S., Ma, S., Zhou, L., Chen, D., Yu, Y., 2018. Phthalates in $PM_{2.5}$ from Shenzhen, China and human exposure assessment factored their bioaccessibility in lung. Chemosphere 202, 726-732, https://doi.org/10.1016/j.chemosphere.2018.03.155.

M. McLennan, S., 2001. Relationships between the trace element composition of sedimentary rocks and upper continental crust.

Manisalidis, I., Stavropoulou, E., Stavropoulos, A., Bezirtzoglou, E., 2020. Environmental and health impacts of air pollution: A Review. Front Public Health 8, 14, 10.3389/fpubh.2020.00014.

Manoli, E., Kouras, A., Samara, C., 2004. Profile Analysis of Ambient and Source Emitted Particle-Bound Polycyclic Aromatic Hydrocarbons from Three Sites in Northern Greece. Chemosphere 56, 867-878, 10.1016/j.chemosphere.2004.03.013.

Massoud, R., Shihadeh, A.L., Roumié, M., Youness, M., Gerard, J., Saliba, N., Zaarour, R., Abboud, M., Farah, W., Saliba, N.A., 2011. Intraurban variability of PM10 and PM2.5 in an Eastern Mediterranean city. Atmos Res 101, 893-901, 10.1016/j.atmosres.2011.05.019.

Mastral, A., Callén, M., Lopez, J., Murillo, R., Garcia, T., Navarro, M., 2003. Critical review on atmospheric PAH. Assessment of reported data in the Mediterranean basin. Fuel Process. Technol. 80, 183-193, 10.1016/S0378-3820(02)00249-7.

Mbengue, S., Alleman, L.Y., Flament, P., 2014. Size-distributed metallic elements in submicronic and ultrafine atmospheric particles from urban and industrial areas in northern France. Atmos Res 135-136, 35-47, 10.1016/j.atmosres.2013.08.010.

McVay, R., Zhang, X., Bernard, A., Valorso, R., Camredon, M., La, Y.S., Wennberg, P., Seinfeld, J., 2016. SOA formation from the photooxidation of α -pinene: systematic exploration of the simulation of chamber data. Atmospheric Chemistry and Physics 16, 10.5194/acp-16-2785-2016.

Medeiros, P.M., Conte, M.H., Weber, J.C., Simoneit, B.R.T., 2006. Sugars as source indicators of biogenic organic carbon in aerosols collected above the Howland Experimental Forest, Maine. Atmos Environ 40, 1694-1705, https://doi.org/10.1016/j.atmosenv.2005.11.001.

Melki, P.N., Ledoux, F., Aouad, S., Billet, S., El Khoury, B., Landkocz, Y., Abdel-Massih, R.M., Courcot, D., 2017. Physicochemical characteristics, mutagenicity and genotoxicity of airborne particles under industrial and rural influences in Northern Lebanon. Environ Sci Pollut Res Int 24, 18782-18797, https://doi.org/10.1007/s11356-017-9389-3.

Mikuška, P., Křůmal, K., Večeřa, Z., 2015. Characterization of organic compounds in the $PM_{2.5}$ aerosols in winter in an industrial urban area. Atmos Environ 105, 97-108, https://doi.org/10.1016/j.atmosenv.2015.01.028.

Moatti, J.-P., Thiébault, S.; 2018.The Mediterranean region under climate change : a scientific update.

MoE/EU/UNDP, 2014. Lebanon Environmental Assessment of the Syrian Conflict & Priority Interventions.

MoE/UNDP/GEF, 2011. Lebanon's Second National Communication Report to the UNFCCC. 228pp.Beirut, Lebanon.

MoE/UNDP/GEF, 2016. Lebanon's Third National Communication Report to the UNFCCC. 237pp. Beirut, Lebanon.

Moufarrej, L., Courcot, D., Ledoux, F., 2020. Assessment of the $PM_{2.5}$ oxidative potential in a coastal industrial city in Northern France: Relationships with chemical composition, local emissions and long range sources. Sci. Total Environ. 748, 141448, 10.1016/j.scitotenv.2020.141448.

Mudway, I.S., Duggan, S.T., Venkataraman, C., Habib, G., Kelly, F.J., Grigg, J., 2005. Combustion of dried animal dung as biofuel results in the generation of highly redox active fine particulates. Part Fibre Toxicol 2, 6, 10.1186/1743-8977-2-6.

Mudway, I.S., Stenfors, N., Duggan, S.T., Roxborough, H., Zielinski, H., Marklund, S.L., Blomberg, A., Frew, A.J., Sandström, T., Kelly, F.J., 2004. An in vitro and in vivo investigation of the effects of diesel exhaust on human airway lining fluid antioxidants. Arch. Biochem. Biophys. 423, 200-212, 10.1016/j.abb.2003.12.018.

Nakhlé, M.M., Farah, W., Ziadé, N., Abboud, M., Salameh, D., Annesi-Maesano, I., 2015. Short-term relationships between emergency hospital admissions for respiratory and cardiovascular diseases and fine particulate air pollution in Beirut, Lebanon. Environ. Monit. Assess. 187, 196, https://doi.org/10.1007/s10661-015-4409-6.

Nasser, Z., Salameh, P., Dakik, H., Elias, E., Abou Abbas, L., Levêque, A., 2015. Outdoor air pollution and cardiovascular diseases in Lebanon: a case-control study. J Environ Public Health 2015, 810846, https://doi.org/10.1155/2015/810846.

OECD, 2016. The economic consequences of outdoor air pollution.

Olsen, E., Nielsen, F., 2001. Predicting Vapour Pressures of Organic Compounds from Their Chemical Structure for Classification According to the VOCDirective and Risk Assessment in General. Molecules : A Journal of Synthetic Chemistry and Natural Product Chemistry 6, 370-389, 10.3390/60400370.

Oros, D.R., Simoneit, B.R., 2001. Identification and emission factors of molecular tracers in organic aerosols from biomass burning Part 2. Deciduous trees. Applied geochemistry : journal of the International Association of Geochemistry and Cosmochemistry. 16, 1545-1565

Ozturk, F., Keles, M., 2016. Wintertime chemical compositions of coarse and fine fractions of particulate matter in Bolu, Turkey. Environ Sci Pollut Res Int 23, 14157-14172, 10.1007/s11356-016-6584-6.

Paatero, P., Tapper, U., 1994. Positive matrix factorization: A non-negative factor model with optimal utilization of error estimates of data values. Environmetrics 5, 111-126, 10.1002/env.3170050203.

Pandey, P., Yadav, R., 2018. A Review on Volatile Organic Compounds (VOCs) as Environmental Pollutants: Fate and Distribution. International Journal of Plant and Environment 4, 10.18811/ijpen.v4i02.2.

Pei, X.Q., Song, M., Guo, M., Mo, F.F., Shen, X.Y., 2013. Concentration and risk assessment of phthalates present in indoor air from newly decorated apartments. Atmos Environ 68, 17-23, https://doi.org/10.1016/j.atmosenv.2012.11.039.

Pernigotti, D., Belis, C.A., Spanò, L., 2016. SPECIEUROPE: The European data base for PM source profiles. Atmos. Pollut. Res. 7, 307-314, 10.1016/j.apr.2015.10.007.

Pietrogrande, M., Russo, Zagatti, 2019. Review of PM oxidative potential measured with acellular assays in urban and rural sites across Italy. Atmosphere 10, 626, 10.3390/atmos10100626.

Pikridas, M., Vrekoussis, M., Sciare, J., Kleanthous, S., Vasiliadou, E., Kizas, C., Savvides, C., Mihalopoulos, N., 2018. Spatial and temporal (short and long-term) variability of submicron, fine and sub-10 μm particulate matter (PM_1, $PM_{2.5}$, PM_{10}) in Cyprus. Atmos Environ 191, 79-93, 10.1016/j.atmosenv.2018.07.048.

Pio, C., Cerqueira, M., Harrison, R.M., Nunes, T., Mirante, F., Alves, C., Oliveira, C., Sanchez de la Campa, A., Artíñano, B., Matos, M., 2011. OC/EC ratio observations in Europe: Re-thinking the approach for apportionment between primary and secondary organic carbon. Atmos Environ 45, 6121-6132, https://doi.org/10.1016/j.atmosenv.2011.08.045.

Pohl, H.R., Abadin, H.G., 1995. Utilizing uncertainty factors in minimal risk levels derivation. Regulatory toxicology and pharmacology : RTP 22, 180-188, 10.1006/rtph.1995.1083.

Prati, P., Zucchiatti, A., Lucarelli, F., Mandò, P.A., 2000. Source apportionment near a steel plant in Genoa (Italy) by continuous aerosol sampling and PIXE analysis. Atmospheric Environment 34, 3149-3157, https://doi.org/10.1016/S1352-2310(99)00421-5.

Qi, M., Jiang, L., Liu, Y., Xiong, Q., Sun, C., Li, X., Zhao, W., Yang, X., 2018. Analysis of the Characteristics and Sources of Carbonaceous Aerosols in $PM_{2.5}$ in the Beijing, Tianjin, and Langfang Region, China. International journal of environmental research and public health 15, 1483, 10.3390/ijerph15071483.

Rai, R., Rajput, M., Agrawal, M., Agrawal, S., 2011. Gaseous air pollutants: a review on current and future trends of emissions and impact on agriculture. J. Sci. Res. 55

Ravindra, K., Sokhi, R., Vangrieken, R., 2008. Atmospheric polycyclic aromatic hydrocarbons: Source attribution, emission factors and regulation. Atmos Environ 42, 2895-2921, 10.1016/j.atmosenv.2007.12.010.

Ray, P.D., Huang, B.-W., Tsuji, Y., 2012. Reactive oxygen species (ROS) homeostasis and redox regulation in cellular signaling. CLS Cellular Signalling 24, 981-990

Riffault, V., Arndt, J., Marris, H., Mbengue, S., Setyan, A., Alleman, L.Y., Deboudt, K., Flament, P., Augustin, P., Delbarre, H., Wenger, J., 2015. Fine and ultrafine particles in the vicinity of industrial activities: A Review. Crit Rev Environ Sci Technol 45, 2305-2356, 10.1080/10643389.2015.1025636.

Robinson, A.L., Subramanian, R., Donahue, N.M., Bernardo-Bricker, A., Rogge, W.F., 2006a. Source apportionment of molecular markers and organic aerosol--1. Polycyclic aromatic hydrocarbons and methodology for data visualization. Environ. Sci. Technol. 40, 7803-7810, 10.1021/es0510414.

Robinson, A.L., Subramanian, R., Donahue, N.M., Bernardo-Bricker, A., Rogge, W.F., 2006b. Source Apportionment of Molecular Markers and Organic Aerosol. 3. Food Cooking Emissions. Environ. Sci. Technol. 40, 7820-7827, 10.1021/es060781p.

rodriguez-espinosa, P., Flores, R., Mugica-Alvarez, V., Morales García, S., 2017. Sources of trace metals in PM_{10} from a petrochemical industrial complex in Northern Mexico. Air Quality, Atmosphere & Health 10, 10.1007/s11869-016-0409-0.

Rogge, W.F., Hildemann, L.M., Mazurek, M.A., Cass, G.R., Simoneit, B.R.T., 1991. Sources of fine organic aerosol. 1. Charbroilers and meat cooking operations. Environ. Sci. Technol. 25, 1112-1125, 10.1021/es00018a015.

Rogge, W.F., Hildemann, L.M., Mazurek, M.A., Cass, G.R., Simoneit, B.R.T., 1993. Sources of fine organic aerosol. 2. Noncatalyst and catalyst-equipped automobiles and heavy-duty diesel trucks. Environ. Sci. Technol. 27, 636-651, 10.1021/es00041a007.

Ruehl, C.R., Ham, W.A., Kleeman, M.J., 2011. Temperature-induced volatility of molecular markers in ambient airborne particulate matter. Atmos. Chem. Phys. 11, 67-76, 10.5194/acp-11-67-2011.

Salameh, P., Salame, J., Khayat, G., Akhdar, A., Ziadeh, C., Azizi, S., Khoury, F., Akiki, Z., Nasser, Z., Abou Abbass, L., Saadeh, D., Waked, M., 2012. Exposure to outdoor air pollution and chronic bronchitis in adults: a case-control study. Int J Occup Environ Med 3, 165-177

Salameh, T., Sauvage, S., Afif, C., Borbon, A., Léonardis, T., Brioude, J., Waked, A., Locoge, N., 2015. Exploring the seasonal NMHC distribution in an urban area of the Middle East during ECOCEM campaigns: Very high loadings dominated by local emissions and dynamics. Environ. Chem., 10.1071/EN14154.

Salameh, T., Sauvage, S., Afif, C., Borbon, A., Locoge, N., 2016. Source apportionment vs. emission inventories of non-methane hydrocarbons (NMHC) in an urban area of the Middle East: local and global perspectives. Atmos. Chem. Phys. 16, 3595-3607, 10.5194/acp-16-3595-2016.

Saliba, N.A., El Jam, F., El Tayar, G., Obeid, W., Roumie, M., 2010. Origin and variability of particulate matter (PM10 and PM2.5) mass concentrations over an Eastern Mediterranean city. Atmos Res 97, 106-114, https://doi.org/10.1016/j.atmosres.2010.03.011.

Saliba, N.A., Kouyoumdjian, H., Roumié, M., 2007. Effect of local and long-range transport emissions on the elemental composition of $PM_{10–2.5}$ and $PM_{2.5}$ in Beirut. Atmos Environ 41, 6497-6509, 10.1016/j.atmosenv.2007.04.032.

Saliba, N.A., Moussa, S., Salame, H., El-Fadel, M., 2006. Variation of selected air quality indicators over the city of Beirut, Lebanon: Assessment of emission sources. Atmos Environ 40, 3263-3268

Samaké, A., Jaffrezo, J.-L., Favez, O., Weber, S., Jacob, V., Canete, T., Albinet, A., Charron, A., Riffault, V., Perdrix, E., Waked, A., Golly, B., Salameh, D., Chevrier, F., Oliveira, D.M., Besombes, J.-L., Martins, J.M.F., Bonnaire, N., Conil, S., Guillaud, G., Mesbah, B., Rocq, B., Robic, P.-Y., Hulin, A., Le Meur, S., Descheemaecker, M., Chretien, E., Marchand, N., Uzu, G., 2019a. Arabitol, mannitol, and glucose as tracers of primary biogenic organic aerosol: the influence of environmental factors on ambient air concentrations and spatial distribution over France. Atmos. Chem. Phys. 19, 11013-11030, 10.5194/acp-19-11013-2019.

Samaké, A., Jaffrezo, J.L., Favez, O., Weber, S., Jacob, V., Canete, T., Albinet, A., Charron, A., Riffault, V., Perdrix, E., Waked, A., Golly, B., Salameh, D., Chevrier, F., Oliveira, D.M., Besombes, J.L., Martins, J.M.F., Bonnaire, N., Conil, S., Guillaud, G., Mesbah, B., Rocq, B., Robic, P.Y., Hulin, A., Le Meur, S., Descheemaecker, M., Chretien, E., Marchand, N., Uzu, G., 2019b. Arabitol, mannitol, and glucose as tracers of primary biogenic organic aerosol: the influence of environmental factors on ambient air concentrations and spatial distribution over France. Atmos. Chem. Phys. 19, 11013-11030, 10.5194/acp-19-11013-2019.

Samara, C., Kouimtzis, T., Tsitouridou, R., Kanias, G., Simeonov, V., 2003. Chemical mass balance source apportionment of PM10 in an industrialized urban area of Northern Greece. Atmos Environ 37, 41-54, https://doi.org/10.1016/S1352-2310(02)00772-0.

Saraga, D.E., Tolis, E.I., Maggos, T., Vasilakos, C., Bartzis, J.G., 2019. $PM_{2.5}$ source apportionment for the port city of Thessaloniki, Greece. Science of The Total Environment 650, 2337-2354, https://doi.org/10.1016/j.scitotenv.2018.09.250.

Schauer, J.J., Kleeman, M.J., Cass, G.R., Simoneit, B.R.T., 1999. Measurement of Emissions from Air Pollution Sources. 1. C_1 through C_{29} Organic Compounds from Meat Charbroiling. Environ. Sci. Technol. 33, 1566-1577, 10.1021/es980076j.

Sciare, J., Oikonomou, K., Cachier, H., Mihalopoulos, N., Andreae, M.O., Maenhaut, W., Sarda-Estève, R., 2005. Aerosol mass closure and reconstruction of the light scattering coefficient over the Eastern Mediterranean Sea during the MINOS campaign. Atmos. Chem. Phys. 5, 2253-2265, 10.5194/acp-5-2253-2005.

See, S.W., Balasubramanian, R., 2008. Chemical characteristics of fine particles emitted from different gas cooking methods. Atmos Environ 42, 8852-8862, https://doi.org/10.1016/j.atmosenv.2008.09.011.

Seigneur, C., 2019. Air pollution : concepts, theory, and applications.

Seinfeld, J.H., Pandis, S.N., 2006. Atmospherifc chemistry and physics : from air pollution to climatic change. John Wiley & Sons, Hobroken, N.J.

Seinfeld, J.H., Pandis, S.N., 2016. Atmospheric Chemistry and Physics: From Air Pollution to Climate Change, 3r. John Wiley & Sons.

Shaka', H., Saliba, N., 2004. Concentration measurements and chemical composition of PM10-2.5 and PM2.5 at a coastal site in Beirut, Lebanon. Atmos Environ 38, 523-531, 10.1016/j.atmosenv.2003.10.009.

Shaltout, A.A., Hassan, S.K., Karydas, A.G., Zaki, Z.I., Mostafa, N.Y., Kregsamer, P., Wobrauschek, P., Streli, C., 2018. Comparative elemental analysis of fine particulate matter (PM2.5) from industrial and residential areas in Greater Cairo-Egypt by means of a multi-

secondary target energy dispersive X-ray fluorescence spectrometer. Spectrochimica Acta Part B: Atomic Spectroscopy 145, 29-35, https://doi.org/10.1016/j.sab.2018.04.003.

Shankar, K., Mehendale, H.M., 2014. Oxidative Stress. in: Wexler, P. (Ed.). Encyclopedia of Toxicology (Third Edition). Academic Press, Oxford, pp. 735-737.

Sharma, N., Agarwal, A.K., Eastwood, P., Gupta, T., Singh, A.P., International Conference on "Sustainable, E., Environmental, C., 2018. Air pollution and control.

Shrivastava, M., Cappa, C.D., Fan, J., Goldstein, A.H., Guenther, A.B., Jimenez, J.L., Kuang, C., Laskin, A., Martin, S.T., Ng, N.L., Petaja, T., Pierce, J.R., Rasch, P.J., Roldin, P., Seinfeld, J.H., Shilling, J., Smith, J.N., Thornton, J.A., Volkamer, R., Wang, J., Worsnop, D.R., Zaveri, R.A., Zelenyuk, A., Zhang, Q., 2017. Recent advances in understanding secondary organic aerosol: Implications for global climate forcing. Reviews of Geophysics 55, 509-559, 10.1002/2016rg000540.

Sies, H., 2018. On the history of oxidative stress: Concept and some aspects of current development. Current Opinion in Toxicology 7, 122-126, https://doi.org/10.1016/j.cotox.2018.01.002.

Simon, H., Beck, L., Bhave, P.V., Divita, F., Hsu, Y., Luecken, D., Mobley, J.D., Pouliot, G.A., Reff, A., Sarwar, G., Strum, M., 2010. The development and uses of EPA's SPECIATE database. Atmos. Pollut. Res. 1, 196-206, 10.5094/apr.2010.026.

Simoneit, B.R.T., 1999. A review of biomarker compounds as source indicators and tracers for air pollution. Environ Sci Pollut Res 6, 159-169, 10.1007/BF02987621.

Simoneit, B.R.T., 2002. Biomass burning — a review of organic tracers for smoke from incomplete combustion. Appl. Geochem. 17, 129-162, https://doi.org/10.1016/S0883-2927(01)00061-0.

Simoneit, B.R.T., Mazurek, M.A., 1982. Organic matter of the troposphere—II.∗∗For Part I, see Simoneit et al. (1977). Natural background of biogenic lipid matter in aerosols over the rural western united states. Atmospheric Environment (1967) 16, 2139-2159, https://doi.org/10.1016/0004-6981(82)90284-0.

Simoneit, B.R.T., Sheng, G., Chen, X., Fu, J., Zhang, J., Xu, Y., 1991. Molecular marker study of extractable organic matter in aerosols from urban areas of China. Atmos Environ 25, 2111-2129, https://doi.org/10.1016/0960-1686(91)90088-O.

Sothea, K., Kim Oanh, N.T., 2019. Characterization of emissions from diesel backup generators in Cambodia. Atmos. Pollut. Res. 10, 345-354, https://doi.org/10.1016/j.apr.2018.09.001.

Srogi, K., 2007. Monitoring of environmental exposure to polycyclic aromatic hydrocarbons: a review. Environ. Chem. Lett. 5, 169-195, 10.1007/s10311-007-0095-0.

Staehelin, J., Harris, N.R.P., Appenzeller, C., Eberhard, J., 2001. Ozone trends: A review. Reviews of Geophysics 39, 231-290, https://doi.org/10.1029/1999RG000059.

Sternbeck, J., Sjödin, Å., Andréasson, K., 2002. Metal emissions from road traffic and the influence of resuspension—results from two tunnel studies. Atmos Environ 36, 4735-4744, https://doi.org/10.1016/S1352-2310(02)00561-7.

Stevens, E.A., Mezrich, J.D., Bradfield, C.A., 2009. The aryl hydrocarbon receptor: a perspective on potential roles in the immune system. Immunology 127, 299-311, 10.1111/j.1365-2567.2009.03054.x.

Stull, R.B., 1988. An Introduction to boundary layer meteorology. Springer.

Sun, J., Shen, Z., Zhang, Y., Zhang, Q., Lei, Y., Huang, Y., Niu, X., Xu, H., Cao, J., Ho, S.S.H., Li, X., 2019. Characterization of PM2.5 source profiles from typical biomass burning of maize straw, wheat straw, wood branch, and their processed products (briquette and charcoal) in China. Atmos Environ 205, 36-45, https://doi.org/10.1016/j.atmosenv.2019.02.038.

Swietlicki, E., Krejci, R., 1996. Source characterisation of the Central European atmospheric aerosol using multivariate statistical methods. Nuclear Instruments and Methods in Physics Research Section B: Beam Interactions with Materials and Atoms 109-110, 519-525, https://doi.org/10.1016/0168-583X(95)01220-6.

Szigeti, T., Mihucz, V.G., Óvári, M., Baysal, A., Atılgan, S., Akman, S., Záray, G., 2013. Chemical characterization of $PM_{2.5}$ fractions of urban aerosol collected in Budapest and Istanbul. Microchem. J. 107, 86-94, https://doi.org/10.1016/j.microc.2012.05.029.

Taghvaee, S., Sowlat, M.H., Diapouli, E., Manousakas, M.I., Vasilatou, V., Eleftheriadis, K., Sioutas, C., 2019. Source apportionment of the oxidative potential of fine ambient particulate matter (PM2.5) in Athens, Greece. Sci. Total Environ. 653, 1407-1416, https://doi.org/10.1016/j.scitotenv.2018.11.016.

Tang, I.N., Tridico, A.C., Fung, K.H., 1997. Thermodynamic and optical properties of sea salt aerosols. Journal of geophysical research, 0148-0227

Tayara, L., Charif, F., Diab, A.H., Toufaily, A., 2020. Effect of Traffic-Related Air Pollution on Lung Function in Taxi Drivers: A Cross Sectional Study. Int J Respir Pulm Med International Journal of Respiratory and Pulmonary Medicine 7

Thakur, A.K., Kaundle, B., Singh, I., 2020. Chapter 22 - Mucoadhesive drug delivery systems in respiratory diseases. in: Dua, K., Hansbro, P.M., Wadhwa, R., Haghi, M., Pont, L.G., Williams, K.A. (Eds.). Targeting chronic inflammatory lung diseases using advanced drug delivery systems. Academic Press, pp. 475-491.

Theodosi, C., Panagiotopoulos, C., Nouara, A., Zarmpas, P., Nicolaou, P., Violaki, K., Kanakidou, M., Sempéré, R., Mihalopoulos, N., 2018. Sugars in atmospheric aerosols over the Eastern Mediterranean. Progress in Oceanography 163, 70-81, https://doi.org/10.1016/j.pocean.2017.09.001.

Thera, B.T.P., Dominutti, P., Öztürk, F., Salameh, T., Sauvage, S., Afif, C., Çetin, B., Gaimoz, C., Keleş, M., Evan, S., Borbon, A., 2019. Composition and variability of gaseous organic pollution in the port megacity of Istanbul: source attribution, emission ratios, and inventory evaluation. Atmos. Chem. Phys. 19, 15131-15156, 10.5194/acp-19-15131-2019.

Tobiszewski, M., Namieśnik, J., 2012. PAH diagnostic ratios for the identification of pollution emission sources. Environ. Pollut. 162, 110-119, https://doi.org/10.1016/j.envpol.2011.10.025.

Tran, T., Alleman, L., Coddeville, P., Galloo, J.-C., 2012. Elemental characterization and source identification of size resolved atmospheric particles in French classrooms.

Triantafyllou, A.G., Kassomenos, P.A., 2002. Aspects of atmospheric flow and dispersion of air pollutants in a mountainous basin. Sci. Total Environ. 297, 85-103, 10.1016/s0048-9697(02)00090-6.

Tuet, W.Y., Chen, Y., Xu, L., Fok, S., Gao, D., Weber, R.J., Ng, N.L., 2017. Chemical oxidative potential of secondary organic aerosol (SOA) generated from the photooxidation of biogenic and anthropogenic volatile organic compounds. Atmos. Chem. Phys. 17, 839-853, 10.5194/acp-17-839-2017.

Turpin, B.J., Lim, H.-J., 2001. Species Contributions to $PM_{2.5}$ Mass Concentrations: Revisiting Common Assumptions for Estimating Organic Mass. Aerosol Sci. Technol. 35, 602-610, 10.1080/02786820119445.

USEPA, 1989a. Air Superfund National Technical Guidance Series. Volume IV: Procedures for Dispersion Modeling and Air Monitoring for Superfund Air Pathway Analysis. Interim Final. Office of Air Quality Planning and Standards. Research Triangle Park, NC. EPA/450/1-89/004.

USEPA, 1989b. General Quantitative Risk Assessment Guidelines for Noncancer Health Effects. External Review Draft. Risk Assessment Forum Technical Panel on Risk Assessment Guidelines for Noncancer Health Effects.

USEPA, 1989c. General Quantitative Risk Assessment Guidelines for Noncancer Health Effects. External Review Draft. Risk Assessment Forum Technical Panel on Risk Assessment Guidelines for Noncancer Health Effects, U.S. Environmental Protection Agency, Washington, DC.

USEPA, 1991a. Risk assessment for toxic air pollutants : a citizen's guide. U.S. Environmental Protection Agency, Air Risk Information Support Center, Research Triangle Park, NC.

USEPA, 1991b. Risk Assessment Guidance for Superfund: Volume I - Human Health Evaluation Manual (Part B, Development of Risk-based Preliminary Remediation Goals).

USEPA, 1991c. Risk Assessment Guidance for Superfund: Volume I - Human Health Evaluation Manual (Part B, Development of Risk-based Preliminary Remediation Goals) Publication 9285.7-01B. Office of Emergency and Remedial Response, Washington, DC. NTIS PB92-963333.

USEPA, 1994. Methods for derivation of inhalation reference concentrations and application of inhalation dosimetry. Environmental Criteria and Assessment Office, Office of Health and Environmental Assessment, Office of Research and Development, U.S. Environmental Protection Agency, Research Triangle Park, NC.

USEPA, 2002. Primary Particles Generated by the Combustion of Heavy Fuel Oil and Coal. Review of Research Results from EPA’s National Risk Management Research Laboratory.

USEPA; 2021.Particulate Matter (PM) Pollution. https://www.epa.gov/pm-pollution/particulate-matter-pm-basics. consulted on 11/10/2021

Usher, C.R., Michel, A.E., Grassian, V.H., 2003. Reactions on Mineral Dust. Chem. Rev. (Washington, DC, U. S.) 103, 4883-4940, 10.1021/cr020657y.

Vasilatou, V., Diapouli, E., Abatzoglou, D., Bakeas, E.B., Scoullos, M., Eleftheriadis, K., 2017. Characterization of $PM_{2.5}$ chemical composition at the Demokritos suburban station, in Athens Greece. The influence of Saharan dust. Environ Sci Pollut Res Int 24, 11836-11846, 10.1007/s11356-017-8684-3.

Verma, V., Fang, T., Xu, L., Peltier, R.E., Russell, A.G., Ng, N.L., Weber, R.J., 2015. Organic Aerosols Associated with the Generation of Reactive Oxygen Species (ROS) by Water-Soluble PM2.5. Environ. Sci. Technol. 49, 4646-4656, 10.1021/es505577w.

Viana, M., Kuhlbusch, T.A.J., Querol, X., Alastuey, A., Harrison, R.M., Hopke, P.K., Winiwarter, W., Vallius, M., Szidat, S., Prévôt, A.S.H., Hueglin, C., Bloemen, H., Wåhlin, P., Vecchi, R., Miranda, A.I., Kasper-Giebl, A., Maenhaut, W., Hitzenberger, R., 2008. Source apportionment of particulate matter in Europe: A review of methods and results. J. Aerosol Sci. 39, 827-849, 10.1016/j.jaerosci.2008.05.007.

Vicente, E.D., Vicente, A., Evtyugina, M., Carvalho, R., Tarelho, L.A.C., Oduber, F.I., Alves, C., 2018. Particulate and gaseous emissions from charcoal combustion in barbecue grills. Fuel Process. Technol. 176, 296-306, https://doi.org/10.1016/j.fuproc.2018.03.004.

Wåhlin, P., Berkowicz, R., Palmgren, F., 2006. Characterisation of traffic-generated particulate matter in Copenhagen. Atmos Environ 40, 2151-2159, https://doi.org/10.1016/j.atmosenv.2005.11.049.

Waked, A., Afif, C., 2012. Emissions of air pollutants from road transport in Lebanon and other countries in the Middle East region. Atmos Environ 61, 446-452, 10.1016/j.atmosenv.2012.07.064.

Waked, A., Afif, C., Brioude, J., Formenti, P., Chevaillier, S., Haddad, I.E., Doussin, J.-F., Borbon, A., Seigneur, C., 2013a. Composition and Source Apportionment of Organic Aerosol in Beirut, Lebanon, During Winter 2012. Aerosol Sci. Technol. 47, 1258-1266, 10.1080/02786826.2013.831975.

Waked, A., Afif, C., Formenti, P., Chevaillier, S., El-Haddad, I., Doussin, J.-F., Borbon, A., Seigneur, C., 2014. Characterization of organic tracer compounds in $PM_{2.5}$ at a semi-urban site in Beirut, Lebanon. Atmos Res 143, 85-94, 10.1016/j.atmosres.2014.02.006.

Waked, A., Afif, C., Seigneur, C., 2012a. An atmospheric emission inventory of anthropogenic and biogenic sources for Lebanon. Atmos Environ 50, 88-96, https://doi.org/10.1016/j.atmosenv.2011.12.058.

Waked, A., Seigneur, C., Couvidat, F., Kim, Y., Sartelet, K., Afif, C., Borbon, A., Formenti, P., Sauvage, S., 2013b. Modeling air pollution in Lebanon: evaluation at a suburban site in Beirut during summer. Atmos. Chem. Phys. 13, 5873-5886, 10.5194/acp-13-5873-2013.

Waked, M., Salame, J., Khayat, G., Salameh, P., 2012b. Correlates of COPD and chronic bronchitis in nonsmokers: data from a cross-sectional study. Int J Chron Obstruct Pulmon Dis 7, 577-585, 10.2147/COPD.S35044.

Wang, J., Niu, X., Sun, J., Zhang, Y., Zhang, T., Shen, Z., Zhang, Q., Xu, H., Li, X., Zhang, R., 2020. Source profiles of PM2.5 emitted from four typical open burning sources and

its cytotoxicity to vascular smooth muscle cells. Sci. Total Environ. 715, 136949, https://doi.org/10.1016/j.scitotenv.2020.136949.

Wang, S., Nan, J., Shi, C., Fu, Q., Gao, S., Wang, D., Cui, H., Saiz-Lopez, A., Zhou, B., 2015. Atmospheric ammonia and its impacts on regional air quality over the megacity of Shanghai, China. Scientific Reports 5, 15842, 10.1038/srep15842.

Watson, J., Robinson, N.F., Lewis, C.W., Coulter, C.T., Chow, J., Fujita, E.M., Lowenthal, D.H., Conner, T., Henry, R., Willis, R.D., 1997. Chemical mass balance receptor model version 8 (CMB) user's manual.

Watson, J.G., 1984. Overview of Receptor Model Principles. Journal of the Air Pollution Control Association 34, 619-623, 10.1080/00022470.1984.10465780.

Watson, J.G., Cooper, J.A., Huntzicker, J.J., 1984. The effective variance weighting for least squares calculations applied to the mass balance receptor model. Atmos Environ 18, 1347-1355

Watson, J.G., Robinson, N.F., Chow, J.C., Henry, R.C., Kim, B.M., Pace, T.G., Meyer, E.L., Nguyen, Q., 1990. The USEPA/DRI chemical mass balance receptor model, CMB 7.0. Environmental Software 5, 38-49, https://doi.org/10.1016/0266-9838(90)90015-X.

Wei See, S., Karthikeyan, S., Balasubramanian, R., 2006. Health risk assessment of occupational exposure to particulate-phase polycyclic aromatic hydrocarbons associated with Chinese, Malay and Indian cooking. J. Environ. Monit. 8, 369-376, 10.1039/B516173H.

Wei, Y., Wang, Y., Wu, X., Di, Q., Shi, L., Koutrakis, P., Zanobetti, A., Dominici, F., Schwartz, J.D., 2020. Causal effects of air pollution on mortality rate in massachusetts. American journal of epidemiology 189, 1316-1323, 10.1093/aje/kwaa098.

Weschler, C.J., Salthammer, T., Fromme, H., 2008. Partitioning of phthalates among the gas phase, airborne particles and settled dust in indoor environments. Atmos Environ 42, 1449-1460, https://doi.org/10.1016/j.atmosenv.2007.11.014.

Whitby, K.T., 1978. The physical characteristics of sulfur aerosols. Atmospheric Environment (1967) 12, 135-159, https://doi.org/10.1016/0004-6981(78)90196-8.

WHO, 2010. Exposure to dioxins and dioxin-like substabces: a major public health concern.

WHO, 2016. Ambient air pollution : a global assessment of exposure and burden of disease. Switzerland, Geneva. https://apps.who.int/iris/bitstream/10665/250141/1/9789241511353-eng.pdf.

WHO; 2021a.Air pollution - Overview. https://www.afro.who.int/health-topics/air-pollution. consulted on 11/10/2021

WHO, 2021b. WHO air quality guidelines. Particulate matter ($PM_{2.5}$ and PM_{10}), ozone, nitrogen dioxide, sulfur dioxide and carbon monoxide. Geneva: World Health Organization Switzerland. Licence: CC BY-NC-SA 3.0 IGO.

WorldBank, 2016. The cost of air pollution : strengthening the economic case for action. Institute for Health Metrics and Evaluation.; World Bank. Washington, DC. © World Bank. https://openknowledge.worldbank.org/handle/10986/25013 License: CC BY 3.0 IGO.".

Xie, M., Hannigan, M., Barsanti, K.C., 2014. Gas/particle partitioning of n-alkanes, PAHs and oxygenated PAHs in urban Denver. Atmos Environ 95, 355-362

Xing, Y.-F., Xu, Y.-H., Shi, M.-H., Lian, Y.-X., 2016. The impact of $PM_{2.5}$ on the human respiratory system. J Thorac Dis 8, E69-E74, 10.3978/j.issn.2072-1439.2016.01.19.

Xu, Y., Zhang, J., 2011. Understanding SVOCs. ASHRAE Journal 53(12):121-125

Yadav, S., Tandon, A., Attri, A.K., 2013. Monthly and seasonal variations in aerosol associated n-alkane profiles in relation to meteorological parameters in New Delhi, India. Aerosol Air Qual Res 13, 287-300, 10.4209/aaqr.2012.01.0004.

Yammine, P., Kfoury, A., El Beyrouthy, M., Nouali, H., El-Nakat, H., Ledoux, F., Cazier, F., Courcot, D., Aboukaïs, A., 2010. A preliminary evaluation of the inorganic chemical composition of atmospheric TSP in the Selaata region, North Lebanon. Lebanese Science Journal 11, 13-29

Yang, H.-H., Luo, S.-W., Lee, K.-T., Wu, J.-Y., Chang, C.W., Chu, P.F., 2016. Fine particulate speciation profile and emission factor of municipal solid waste incinerator established by dilution sampling method. J. Air Waste Manage. Assoc. 66, 807-814, 10.1080/10962247.2016.1184195.

Yatkin, S., Bayram, A., 2008. Determination of major natural and anthropogenic source profiles for particulate matter and trace elements in Izmir, Turkey. Chemosphere 71, 685-696, https://doi.org/10.1016/j.chemosphere.2007.10.070.

Yousef, N., Omar, M., Radzi, M., Bin Abas, M.R., Ketuly, K., Mohd Tahir, N., 2001. Heavy Molecularweight Organic Compounds in the Atmosphere: The Hopanes. 7

Yu, W., Guo, Y., Shi, L., Li, S., 2020. The association between long-term exposure to low-level $PM_{2.5}$ and mortality in the state of Queensland, Australia: A modelling study with the difference-in-differences approach. PLoS Med 17, e1003141-e1003141, 10.1371/journal.pmed.1003141.

Zaheer, J., Jeon, J., Lee, S.-B., Kim, J.S., 2018. Effect of Particulate Matter on Human Health, Prevention, and Imaging Using PET or SPECT. 29, 81, 10.14316/pmp.2018.29.3.81.

Zelenski, M., Kamenetsky, V.S., Taran, Y., Kovalskii, A.M., 2020. Mineralogy and Origin of Aerosol From an Arc Basaltic Eruption: Case Study of Tolbachik Volcano, Kamchatka. Geochemistry, Geophysics, Geosystems 21, e2019GC008802, https://doi.org/10.1029/2019GC008802.

Zhang, N., Han, B., He, F., Xu, J., Zhao, R., Zhang, Y., Bai, Z., 2017. Chemical characteristic of $PM_{2.5}$ emission and inhalational carcinogenic risk of domestic Chinese cooking. Environ. Pollut. 227, 24-30, https://doi.org/10.1016/j.envpol.2017.04.033.

Zhang, X., McVay, R.C., Huang, D.D., Dalleska, N.F., Aumont, B., Flagan, R.C., Seinfeld, J.H., 2015. Formation and evolution of molecular products in α-pinene secondary

organic aerosol. Proceedings of the National Academy of Sciences 112, 14168-14173, 10.1073/pnas.1517742112.

Zhao, Y., Hu, M., Slanina, S., Zhang, Y., 2007. Chemical Compositions of Fine Particulate Organic Matter Emitted from Chinese Cooking. Environ. Sci. Technol. 41, 99-105, 10.1021/es0614518.

CHAPTER II

Materials and methods

This thesis project aims to characterize atmospheric particles and VOCs in two urban sites under industrial influence in the East Mediterranean and then evaluate the health risk associated to the exposure to these species and sources. To do this, $PM_{2.5}$ samples and VOCs were collected in Zouk Mikael (ZK) and Fiaa (FA) regions in Lebanon for almost a year from December 2018 to October 2019. Additionally, samples were collected at near field for the characterization of $PM_{2.5}$ chemical profiles. Then, the $PM_{2.5}$ samples were analyzed for their carbonaceous fraction, organic compounds, water-soluble ions, and major and trace elements. The organic characterization included the analysis of PAHs, alkanes, phthalates, hopanes, dicarboxylic acids, biogenic SOA, levoglucosan, fatty acids, dioxins, furans, and dioxin-like polychlorbiphenyls. A selection of organic and inorganic tracer species was made in order to apply PMF on the database of both sites. Finally, the experimental work for the health risk evaluation will be based on the measurement of the oxidative potential using two acellular assays: dithiothreitol and ascorbic acid. In this chapter, we will present the sampling procedures, the different methods used for the characterization as well the analytical work conducted, the PMF application, and the measurement method of oxidative potential.

1 Site selection and sampling

1.1 Site description

In this paragraph, we will be presenting the sampling sites as well as their characteristics and potential sources in the surrounding areas.

1.1.1 Zouk Mikael site

The Zouk Mikael region (ZK) is located on the Keserwan coast. The area is characterized by a high residential density (4,200 inhabitants/km^2), but also commercial, industrial, cultural and tourism activities.

ZK has the biggest power plant in Lebanon of 1 $GW_{electrical}$ which runs on Heavy Fuel Oil (HFO). It encompasses 607 $MW_{electrical}$ of boilers with 2 common stacks releasing the emissions at 145 m in height, 198 $MW_{electrical}$ of reciprocating engines installed in 2017 with stack height of around 40 m, and a power barge with 11 reciprocating engines with a total capacity of 198 $MW_{electrical}$ installed in 2012 with a stack height of around 50 m **(Fig. II-1)**. The distance between the power plant and the nearest residential area in ZK is less than 200 m.

Fig. II-1: The Zouk power plant taken in 2015 by Dark Matters Entertainment

Moreover, due to the deficiency in the energy production in Lebanon, a high number of private generators with relatively short stacks with no law enforcement on emissions are installed in neighborhoods between buildings and in industries releasing soot and PM inside the city and between residential buildings.

Fig. II-2: The view from the sampling site at the residential region of Zouk Mikael facing the power plant

Furthermore, small industries for plastic production, woodworks, steel construction, aluminum extrusion, marble, and granite production, etc. exist in this area. The sampling site in the ZK region is at the top of a residential building (15 m above ground), 14 km northeast the capital Beirut and facing the power plant (33°57'57.07''N ; 35°37'09.46''E) **(Fig. II-2)**. The Zouk Mikael highway and the power plant are respectively 1.2 and 1.5 km away from the sampling site **(Fig. II-3).**

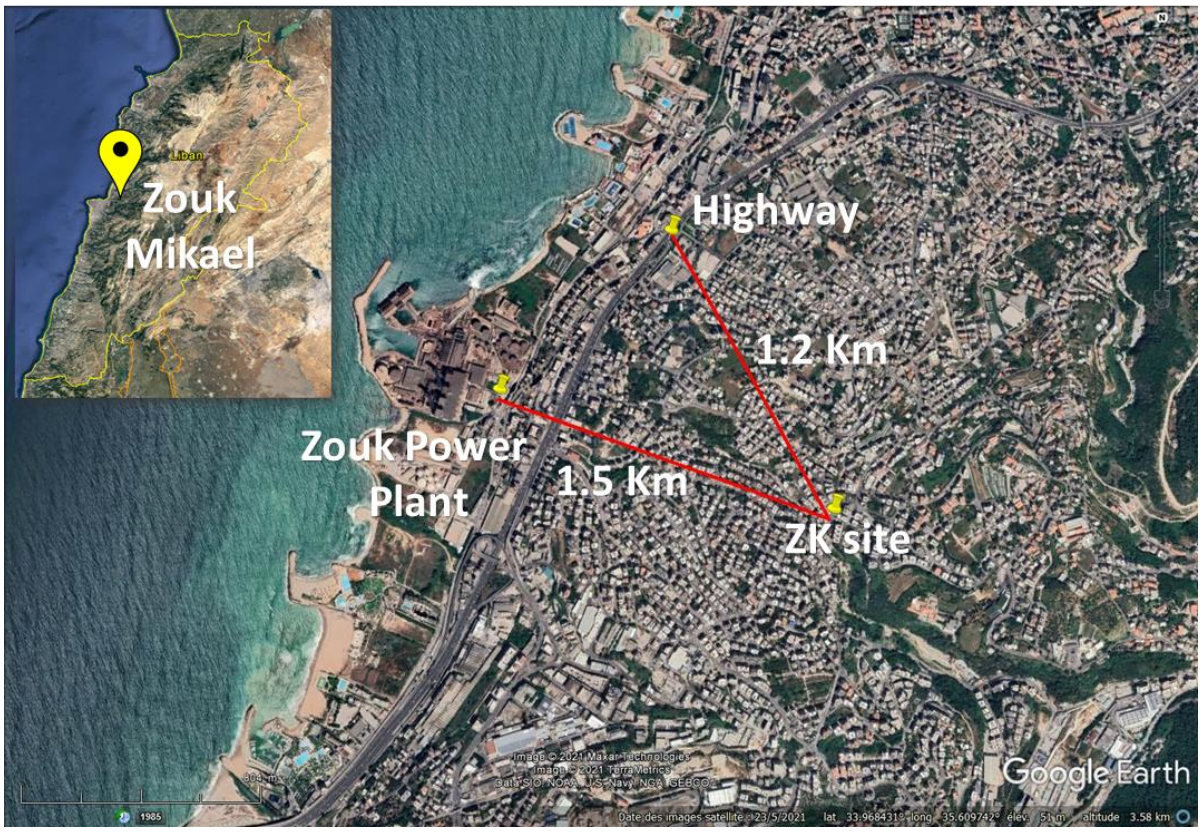

Fig. II-3: Location of the sampling site at Zouk Mikael (ZK)

1.1.2 Fiaa, Chekka site

Chekka region is considered as a division of North Lebanon governorate. Since 1932, the region encompasses the largest cement production facilities due to the local availability of raw materials and ease of marine shipping **(Fig. II-4)**.

Fig. II-4: Cement plants in Chekka region

The sampling site in Chekka area was in a small village named Fiaa (34°20’47.8’’N ; 35°47’14.0’’E) **(Fig. II-5)**. It is co-located with the ministry of environment (MoE) air quality monitoring station. Fiaa (FA) is far less populated than ZK (250 residents/km^2). It is also influenced by local private generators emissions, among other sources.

Fig. II-5: The view from the sampling site at Fiaa facing the chemical industries in Chekka and their quarries

The main potential sources encompass the operating cement industries along with their corresponding power plants and limestone quarries in the adjacent villages and their transportation system to the factories. In addition, the nearest highway is 4 km away from FA with moderate traffic **(Fig. II-6)**. The two cement plants are 5 and 7 km away from the sampling site **(Fig. II-6)**. The site is located 60 km north-north-east of Beirut and 10 km southwest of Tripoli.

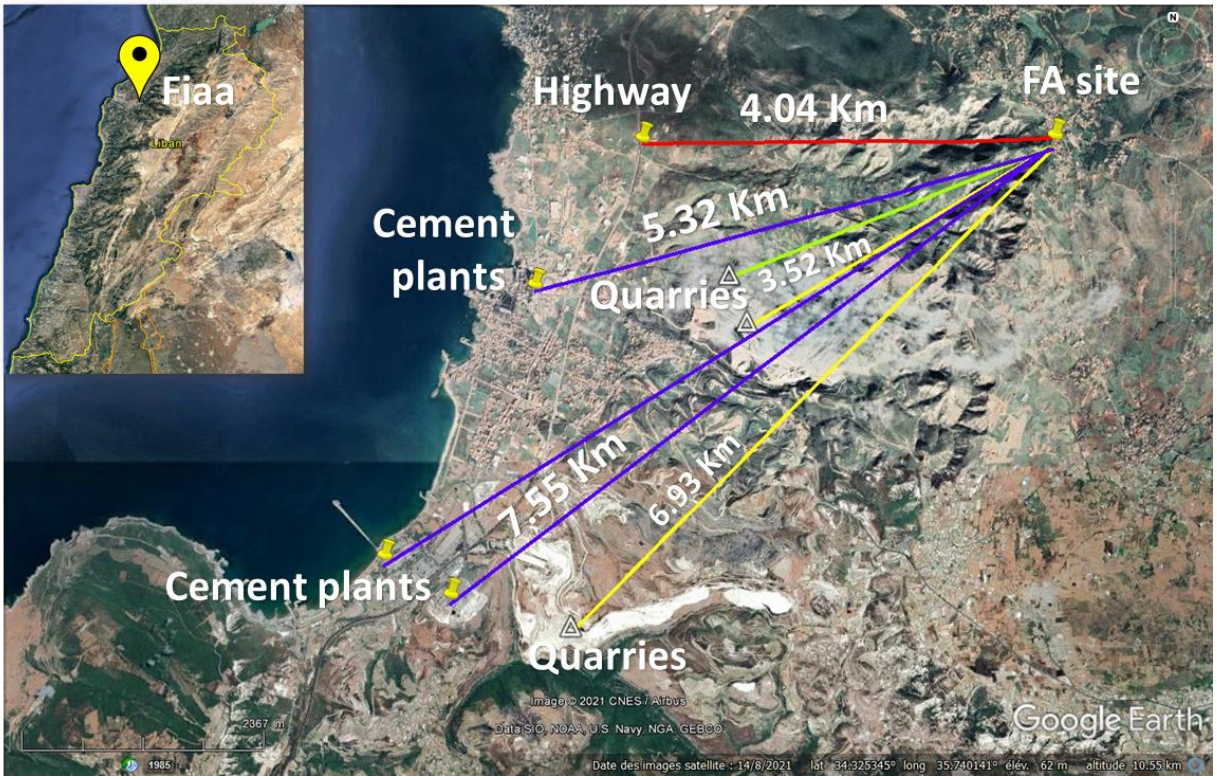

Fig. II-6: Location of the sampling site at Fiaa (FA)

1.2 Filter conditioning and weighing process

150 mm diameter quartz microfiber filters (Fiorini, France) were baked at 550°C for 12 hours before use to remove all the organic impurities. The determination of the $PM_{2.5}$ mass was done following the standard EN 12341:2014 (Standard gravimetric measurement method for the determination of the PM_{10} or $PM_{2.5}$ mass concentration of suspended particulate matter). Briefly, $PM_{2.5}$ filters were conditioned and weighted before and after sampling using an electronic balance (Mettler Toledo, AB204, United States of America) with a resolution of 100 µg. The temperature was controlled to 20 ± 0.5°C and the humidity to 50 ± 5% for 48 hours before any weighing of blank and loaded filters **(Fig. II-7)**. In order to ensure reliable results, QA/QC procedures were applied such as scale verification before every weighting with

calibration weights (Class E) from 1 mg to 5g. Additionally, control blank filters were added to the rest of the filters at each conditioning serving as tool to ensure repeatability of the conditions between the different conditioning sessions.

Fig. II-7: Conditioning of blank and sampled filters

1.3 Sampling strategy

1.3.1 $PM_{2.5}$ sampling

The sampling of fine particles ($PM_{2.5}$) was performed on a 24-hour basis every third day from 13th of December 2018 to 15th October 2019 at both sites **(Table II-1)**. The sampling was performed using high volume samplers (CAV-A/mb, MCV S.A., Spain) operating at 30 m^3/h, onto the 150 mm pure quartz microfibres filters conditioned and weighted before. After sampling, the filters (98 in Zouk and 95 in Fiaa) were sealed in aluminum foil and stored at -20°C until analysis. The collected filters were cut into quarters and one-eighths depending on the requirements of the chemical analyses. These parts of filters will be used for organic, ionic, major and trace metals, carbonaceous fractions, dioxins, furans, and dioxin-like compounds analyses. A field blank was also taken every month in every site. It is a filter properly conditioned and weighed that will be installed in the sampler but without launching the instrument. It will be removed after 24 hours like the PM filters.

Table II-1: Summary of the field campaigns at both sites

	Site 1: Zouk Mikael	Site 2: Fiaa, Chekka
Start date	December 15, 2018	December 13, 2018
End date	October 15, 2019	October 16, 2019
Instrumentation	High-volume sampler (CAV-A/mb, MCV S.A., Spain) operating at 30 m^3/h equipped with a $PM_{2.5}$ size selective inlet	
	Sampling duration: 24 hours Frequency: every third day	
	Passive tubes changed every 4 weeks to measure Non-Methane Volatile organic compounds (NMVOCs) and 1,3-butadiene	
Frequency of the visit at the site	2 consecutive days every 3 days (First day: installing the filter and start of sampling, Second day: end of sampling and collection of filters)	2 consecutive days every 3 days (First day: installing the filter and start of sampling, Second day: end of sampling and collection of filters)
Number of filters collected	98 filters 6 field blanks	95 filters 8 field blanks
Number of Radiello tubes	11	11
Number of Carbopack X tubes	9	9

1.3.2 NMVOCs and 1,3-butadiene sampling

NMVOCs sampling was performed on passive tubes (Radiello, code 130) during the campaign at both sites **(Fig. II-8)**. Eleven NMVOC tubes were collected over 4 weeks at both sites. The cartridges were kept at 4°C until the analysis. The passive tubes have a 5.8 mm diameter stainless steel net cylinder (100 mesh grid opening) packed with activated charcoal with particle size of 35-50 mesh (530 ± 30 mg).

NMVOCs are trapped by adsorption and recovered by extraction in carbon disulfide. The cartridge is drawn from the glass tube and put in the white diffusive body with a diffusive path length of 18 mm made of 1.7 mm microporous polyethylene with an average porosity of 25 ± 5 µm (Radiello, code 120). The passive tubes were put in a mountable polypropylene shelter for outdoor exposures.

As for the 1,3-butadiene, the compound was trapped using Carbopack X diffusion tubes from Gradko International (Winchester, England) over 4 weeks **(Fig. II-8)**. The passive tubes were stored in a dark place away from any heating source before exposure and always stored and handled in clean environments to avoid contaminations. Once the sampling is completed, tubes

were returned within 3 days to the company for the analysis. 9 tubes were collected for each site along with blanks.

Fig. II-8: NMVOCs and 1,3-butadiene diffusion tubes at the sampling site

1.3.3 $PM_{2.5}$ near-sources sampling

Given the lack of knowledge on the profiles of certain emission sources, it was found mandatory to obtain data on the PM composition of some local sources and to create a small source profile database in order to use them in source apportionment methods. Consequently, $PM_{2.5}$ samples were taken near local sources:

- 3 samples for wood combustion emissions
- 4 samples taken at the stack of a private diesel generator
- 1 sample for beef charcoal grilling
- 1 sample for chicken charcoal grilling
- 5 samples for cooking emissions at a university cafeteria

These profiles might differ from those in other regions (for example USA, Europe, etc.) due to local practices commonly observed in the East Mediterranean - Middle Eastern region. The operating conditions, under which the sampling for the different anthropogenic sources was conducted, were detailed in the sections below and were summarized in **Table II-2**. All the methods described below are representative of common practices in the East Mediterranean region.

Table II-2: Operating conditions under which the different anthropogenic samples were obtained

	Wood burning	**Diesel generator**	**Cooking**		
			Beef grilling	**Chicken grilling**	**Cooking activities**
Abbreviation	**WB**	**DG**	**BG**	**CG**	**GCA**
Main contents	Wood branches of broad-leaved trees (hardwood)	Volvo Penta TAD531GE diesel generator, 100 kVA, four cylinders at 1500 rpm	Small pieces of beef grilled on both sides	Large pieces of skinned chicken grilled on both sides	Burger grilling, french fries frying, use of vegetables, daily dishes served
Combustible	Biomass	Diesel fuel	Charcoal	Charcoal	Natural gas liquid (LPG)
Sampling method	High volume sampler for $PM_{2.5}$				
Filter used	Quartz filters – 150 mm diameter				
Number of samples	4	3	1	1	5
Sampling time	10-15 min	30 min	20 min	20 min	75 min

2 Analytical procedures

Different analytical methods and different punches of the sample **(Fig. II-9)** were used in order to fully characterize $PM_{2.5}$ samples and VOCs:

- Organic compounds were quantified using a quarter of the filter and analyzed by GC/MS (USJ, Lebanon)
- Water-soluble ions were analyzed by ionic chromatography using 3 filter punches of 19 mm diameter (ULCO, France)
- Major and trace elements were analyzed by ICP-AES and ICP-MS using a punch of 47 mm diameter (ULCO, France in collaboration with le "Centre Commun de Mesure" and "Institut Chevreul")
- Carbonaceous matter was quantified using a punch 1.5 cm^2 and analyzed by an OC/EC analyzer at the Cyprus Institute
- PCDD/Fs and DL-PCBs were quantified by grouping 2 punches of each filter and analyzed at MicroPolluants Technology SA (Saint Julien Les Metz, France) using HRGC/HRMS
- VOCs were quantified by GC/MS (USJ, Lebanon)
- 1,3-butadiene was analyzed by Gradko, Environmental
- Oxidative potential was analyzed using a punch of 19 mm diameter (ULCO, France)

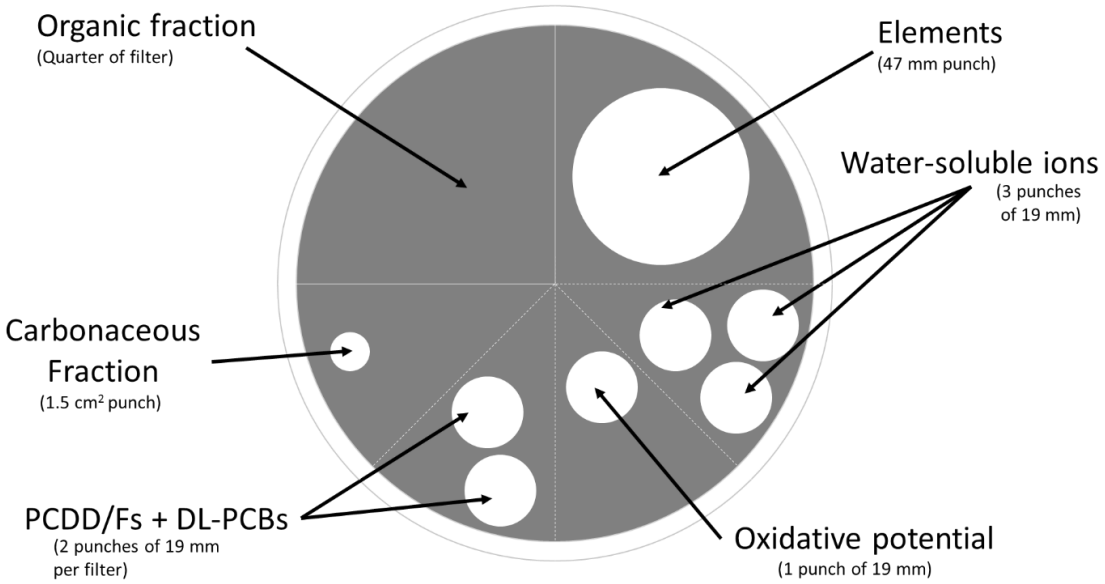

Fig. II-9: Filter fractions used for the different preparations and analyses done at USJ, ULCO, and other collaborating laboratories

2.1 Chemical characterization of $PM_{2.5}$

2.1.1 Organic compounds

The method used for the analysis of organic compound was found in (Waked et al., 2013; 2014; Fadel et al., 2021). In brief, a quarter of the filter was spiked with 50 µL of 2 internal standards, namely ketopinic acid and bornylacetate at a concentration of 0.2 g/L. The spiked filter was then extracted by sonication at 50°C for 30 min using a 30 mL of a mix acetone/dichloromethane (50:50/ v:v). The volume of the obtained solution was then reduced to 200 µL under a gentle flow of nitrogen gas. 50 µL of the extract was used to directly quantify non-polar compounds such as alkanes, PAHs, phthalates, hopanes while other 50 µL were derivatized in order to quantify polar compounds such as carboxylic acids, alcohols, and SOA.

The derivatization was performed with 50 µL of the extract mixed with 50 µL of N,O-bis(trimethylsilyl)-trifluoroacetamide (BSTFA) with 1% trimethylchlorosilane used as a silylation agent and 10 µL of pyridine used as a catalyst at 70°C for 2 hr. This step will convert the polar compounds into trimethylsilyl derivatives that are less polar and more volatile compounds. A 2 µL aliquot of the derivatized and the non-derivatized extracts were injected

into a gas chromatography coupled to a mass spectrometer (ISQ 7000 single quadrupole GC-MS system, Thermo Scientific, United States of America) in the split mode (split ratio 1/25).

The GC was equipped with an Agilent J&W HP-5ms Ultra inert capillary column ((5%-phenyl)-methylpolysiloxane, 95% dimethylpolysiloxane ,30 m x 0.25 mm x 0.25 μm, Agilent; United States of America). The column temperature program consisted of an injection at 65°C hold for 2 min, a ramp of temperature corresponding to 6°C/min up to 300°C followed by an isothermal hold step at 300°C for 20 min. The GC was interfaced to an ion trap MS with an external electron ionization (EI) source (220 ˚C, 70 eV).

The identification of the compounds was based on the comparison of the retention time and the mass spectrum of either the reference compound if an authentic standard was available in the laboratory (50 compounds) or the reference mass spectrum found in the literature **(Table II-3)**.

In the latter case, the quantification of the compounds was based on the response factor (RF) of a surrogate compound having a similar chemical structure. The different surrogate compounds used in this study are as follows:

- The RF of glyceric acid was used for 2-methylglyceric acid
- The RF of malic acid was assigned to 3-hydroxyglutaric acid, 3-acetylglutaric acid, 3-isopropylglutaric acid, and 3-methyl-1,2,3- butanetricarboxylic acid
- The RF of threitol was used for 2-methylthreitol and 2-methylerythritol
- The RF of pinic acid was used for β-caryophyllinic acid
- The RF of 17α(H)-21β(H)-hopane was used to quantify trisnorneohopane, 17 α(H)-trisnorhopane, 17 α(H)- 21 β(H)-norhopane, 17 α(H)-21 β(H)-22S, and 22R-homohopane

The quantification was done on the base ion fragments m/z extracted from the full scan mode (range 50-500 m/z) **(Fig. II-10)**. The same analytical procedures were applied for the field blank filters. The concentrations of the different organic compounds found in the samples were corrected by subtracting the average value obtained for the field blank filters.

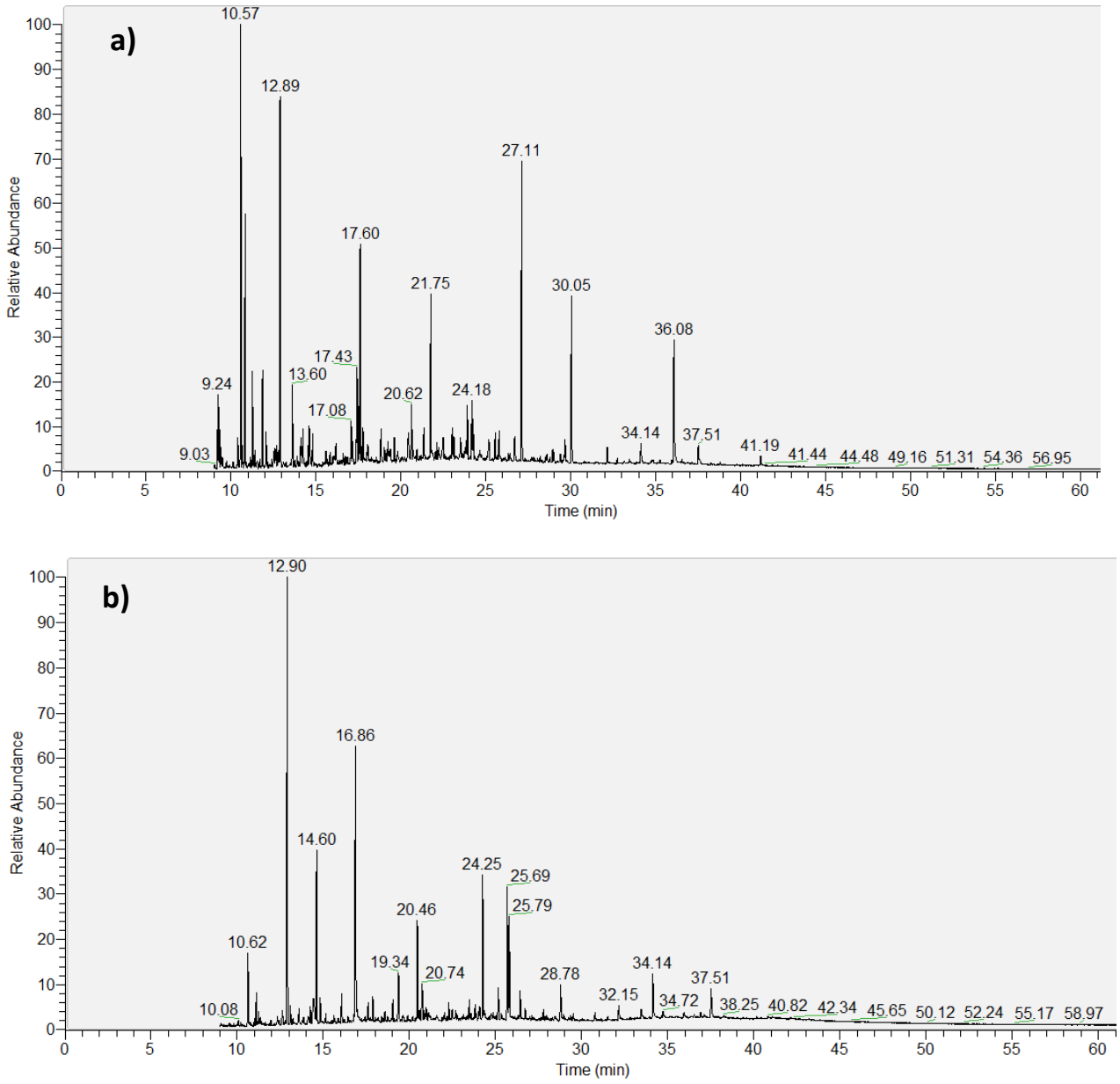

Fig. II-10: Chromatograms of a derivatized (a) and non-derivatized (b) sample in full scan mode (50-500 m/z)

The detection limit (D.L.) of the compounds corresponds to the average value of the blank filters plus 3 times the standard deviation calculated over 3 measurements. For non-polar compounds, DL values ranged between 0.0003 and 0.08 ng/m^3 while for polar compounds, D.L. ranged between 0.002 and 0.25 ng/m^3 (except for stearic acid with D.L. value of 2.3 ng/m^3).

Table II-3: List of the analyzed organic compounds

Compounds			
Alkanes	nonadecane	**Hopanes**	trisnorneohopane
	heneicosane		17α(H)-trisnorhopane
	heneicosane		17α(H)-21β(H)-norhopane
	docosane		17α(H)-21β(H)-hopane
	tricosane		17α(H)-21β(H)-22S-homohopane
	tetracosane		17α(H)-21β(H)-22R-homohopane
	pentacosane	**Fatty acids**	dodecanoic acid
	hexacosane		tetradecanoic acid
	heptacosane		hexadecanoic acid
	octacosane		octadecanoic acid
	nonacosane		eicosanoic acid
	triacontane		docosanoic acid
	hentriacontane		tetracosanoic acid
	dotriacontane		oleic acid
Polycyclic Aromatic Hydrocarbons (PAHs)	acenaphthylene	**Phthalates**	diisobutylphthalate
	acenaphthene		dibutylphthalate
	fluorene		bis(2-ethylhexylphthalate)
	anthracene	**Isoprene oxidation products**	2-methylglyceric acid
	phenanthrene		2-methylthreitol
	fluoranthene		2-methylerythritol
	pyrene	**α-pinene oxidation products**	Pinic acid
	benz[a]anthracene		3-hydroxyglutaric acid
	chrysene		3-acetylglutaric acid
	benzo[b]fluoranthene		3-isopropylglutaric acid
	benzo[k]fluoranthene		3-methyl-1,2,3-butanetricarboxylic acid
	benzo[a]pyrene	**β-caryophyllene oxidation product**	β-caryophyllinic acid
	dibenz[a,h]anthracene		
	benzo[g,h,i]perylene		
	indeno[1,2,3-c,d]pyrene	**Anhydrosugar**	levoglucosan
Dicarboxylic acids	oxalic acid		
	adipic acid		
	azelaic acid		
	phthalic acid		

Calibration curves were made for the different analytes using the corresponding internal standard. Six concentration levels for each analyte were employed with concentrations ranging between 0.02 and 0.0003 g/L (DRI, 2003). The determination coefficient R^2 of the calibration curves for compounds with authentic standards ranged between 0.93 - 0.99 except for tetracosanoic acid (R^2=0.90). Additionally, control points were inserted during the analysis to verify the stability of the RF and subsequently the full system.

Repeatability was evaluated by studying the variation in the response factor of 5 consecutive injections of the authentic standards (DRI, 2003). A good repeatability was observed between the results since the variations for all the studied compounds were less than 14%. Recoveries

were determined by spiking blank filters with known concentrations of the compounds. The values were estimated to be 80%, 82%, 92%, 90%, 85%, 82%, and 97% for alkanes, PAHs, fatty acids, phthalates, dicarboxylic acids, pinic acid, and hopanes respectively. For compounds with no authentic standard (i.e., some SOA markers), the recovery of the surrogate compound was determined to be 85% for glyceric acid and 95% for threitol.

2.1.2 Major and trace elements

In order to determine the elemental composition of $PM_{2.5}$, samples were analyzed by ICP-AES (Inductively coupled Plasma-Atomic Emission Spectroscopy) for major elements and ICP-MS (Inductively Coupled Plasma-Mass Spectrometry) for trace elements. The digestion of a 47 mm punch of the quartz filter was done by an acid mixture HNO_3/HF/$HClO_4$ (4/1/0.5, v/v/v) in a PTFE flask placed in DigiPREP MS system (SCP Science®) at 120°C overnight **(Fig. II-11)**.

Fig. II-11: Mineralization of samples in the DigiPREP system

This acid mixture, and in particular HF, ensure a total mineralization of the particles, even the most refractory elements. The acids were then evaporated at 170°C to the last drop, followed by the addition of few milliliters of ultrapure water. The obtained solution was then diluted to 15 mL by ultrapure water, acidified to 2% by HNO_3 and filtered on 0.45 µm cellulose acetate filter prior to analysis (Ledoux et al., 2006; Kfoury et al., 2016). The same procedure was followed for the field blank filters. Mg, Mn, Al, Ba, Ca, Fe, K, Ni, Pb, P, Sr, Ti, and Zn were quantified by Inductively Coupled Plasma-Atomic Emission Spectrometry (ICP-AES, iCAP 6000 series, Thermo Scientific, United Kingdom). The detection limits were calculated based on the analyzed acid mixture solutions. The chosen wavelengths, the range for the calibration curves and the atmospheric detection limits of the species were reported in **Table II-4**.

Table II-4: ICP-AES: Calibration curve ranges for the species, the wavelength chosen for quantification and the atmospheric detection limit

Major elements	Wavelength (nm)	Calibration curve range (ppb)	Atmospheric detection limit (ng/m^3)
Mg	280.3	50 - 20 000	0.03
Mn	260.6	5 - 2 000	0.01
Al	396.1	50 - 20 000	0.14
Ba	455.4	0.5 - 200	0.01
Ca	315.9	50 - 20 000	0.45
Fe	238.2	50 - 20 000	0.14
K	766.5	50 - 20 000	0.23
Ni	231.6	5 - 2 000	0.02
Pb	220.3	5 - 2 000	0.13
Sr	407.8	0.5 - 200	0.004
Ti	323.4	5 - 2 000	0.08
Zn	213.8	5 - 2 000	0.08
P	178.3	5 - 2 000	0.27

On the other hand, V, Cr, Co, Cu, As, Rb, Nb, Cd, Sn, Sc, Tl, Sb, La, Ce, and Bi were quantified by ICP-Mass Spectrometry (ICP-MS, Agilent 7900, United States of America). This technique follows the same introduction principle of the sample as the ICP-AES, but it differs in the detector that is a mass spectrometer in this case. In order to reduce interferences, the collision gas can be different for the species. However, in our case, we used helium as the collision gas and the quantification was based on the internal standard ^{185}Re. The isotope analyzed by ICP-MS as well as the calibration curve ranges, and the atmospheric detection limit were presented in **Table II-5**.

For both techniques, each sample is analyzed three times and the average value between the three replicates is considered. Consequently, the repeatability of the measurements was evaluated by calculating the relative standard deviation (RSD) between the replicates. For both ICP-AES and ICP-MS, RSD values for samples were less than 5%. The concentrations of the different elements found in the samples were corrected by subtracting the average value obtained for the field blank filters. Additionally, a control sample (with known concentrations) was included in the analysis list after every 10 analyzed samples in ICP-AES and after every 20 samples in ICP-MS. The analytical procedure from the preparation of the sample to the measurement was validated by considering the standard reference material: SRM 1648 "urban particulate matter" from the National Institute of Standards and Technology (NIST, USA).

Table II-5: ICP-MS: Calibration curve ranges for the species, the isotope chosen for quantification and the atmospheric detection limit

Trace elements	Isotope	Calibration curve range (ppb)	Atmospheric detection limit (ng/m^3)
Sc	^{45}Sc	0 - 100	0.002
V	^{51}V	0 - 100	0.001
Cr	^{52}Cr	0 - 100	0.01
Co	^{59}Co	0 - 100	0.0002
Cu	^{63}Cu	0 - 100	0.017
As	^{75}As	0 - 100	0.0003
Rb	^{85}Rb	0 - 100	0.002
Nb	^{93}Nb	0 - 100	0.002
Cd	^{111}Cd	0 - 100	0.0006
Sn	^{118}Sn	0 - 100	0.0005
Sb	^{121}Sb	0 - 100	0.0004
La	^{139}La	0 - 100	0.0003
Ce	^{140}Ce	0 - 100	0.0003
Tl	^{205}Tl	0 - 100	0.0007
Bi	^{209}Bi	0 - 100	0.0005

The recovery rates for the species found in the SRM 1648 sample are presented in **Table II-6.** Recovery rates were within the acceptable range with values varying between 89% and 103% with an exception for Cr (76%) and As (113%).

Table II-6: Recovery rates for the elements found in the NIST-SRM 1648 sample

Elements analyzed by ICP-AES	Recovery rate (%)	Elements analyzed by ICP-MS	Recovery rate (%)
Al	93%	Co	100%
Fe	99%	As	113%
Mn	96%	Cd	101%
Ni	92%	Cu	101%
Sr	103%	Cr	76%
Zn	89%	Sb	99%
Pb	97%	V	103%

2.1.3 Water-soluble ions

The concentrations of water-soluble ions (Cl^-, NO_3^-, SO_4^{2-}, Na^+, NH_4^+, K+, Ca^{2+} and Mg^{2+}) were determined by ion chromatography. 3 filter punches of 19 mm diameter each for every sample were placed in a beaker, covered with 3 to 4 milliliters of ultrapure water (MilliQ®,

Millipore; resistivity = 18.2 MΩ.cm), and closed with paraffin wax film **(Fig. II-12,a-b-c)**. The ions were ultrasonically extracted for 20 min and the obtained solution was collected using a syringe, then filtered through a Nylon membrane filter (Grosseron, France, 0.2 µm, 25 mm) previously rinsed three times with ultrapure water to remove insoluble matters **(Fig. II-12,d-e)**. The leachate containing the ions is placed in a polyethylene scintillation flask of 20 mL weighed before. The filters were submerged again with ultrapure water prior to 2 additional ultrasonic extractions and filtrations. The flask containing the accumulated filtrates for the 3 extractions was then stored at -20°C until analysis. The same protocol was applied for the field blank filters for blank corrections.

The samples were analyzed using ion chromatography (Dionex™ ICS-900, Thermo Scientific, United Kingdom). For the analysis of anions, the eluting solution is a mix of Na_2CO_3 and $NaHCO_3$ ($8x10^{-3}$ and $1x10^{-3}$ M respectively). It passes in the chromatographic column (Dionex™ IonPac™ AS14A) in a flowrate of 1 ml/min. An electrochemical suppressor is used to make possible the detection of the ions. The eluting solution for the cation analysis is methane sulfonic acid CH_3SO_3H at $18x10^{-3}$ M with an eluent flux in the column (Dionex™ IonPac™ CS12A) of 1 ml/min.

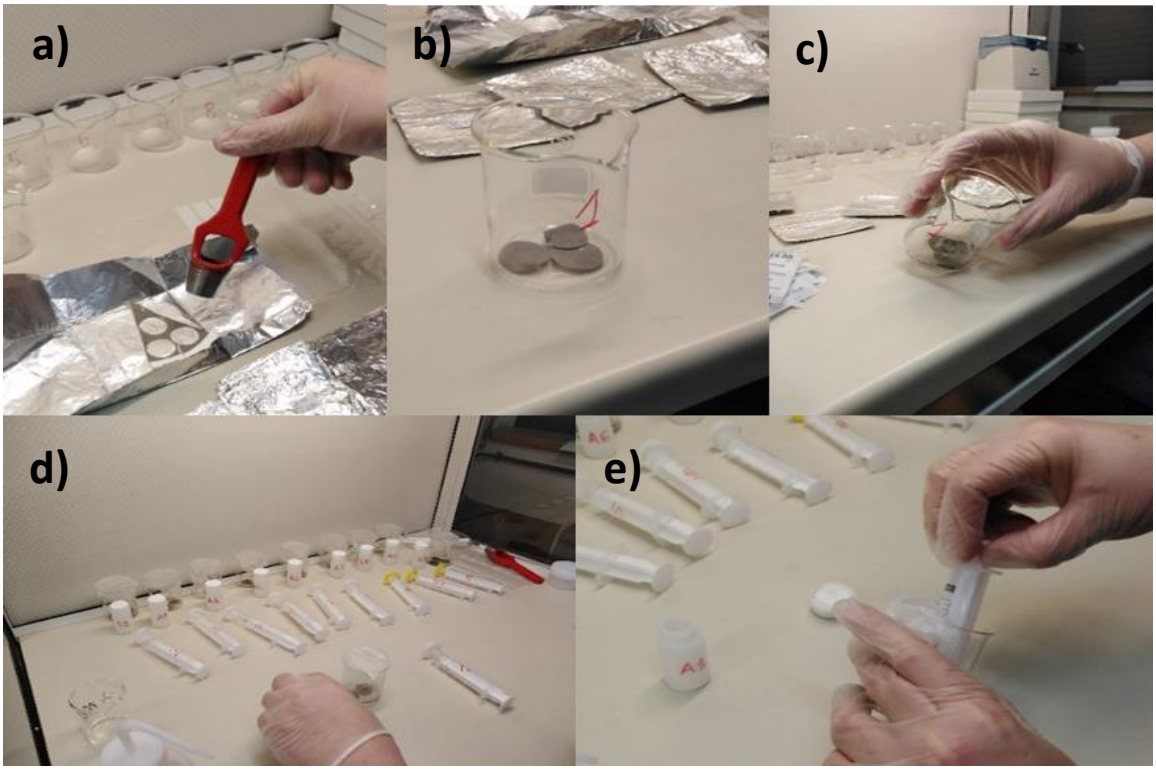

Fig. II-12: Pictures of the different steps of the water-soluble ions extraction: a,b) filter punching and preparation before extraction, c) covering punches in ultrapure water, d,e) collecting the leachate after extraction

Calibration curves were made from mix solutions at different concentrations with a range of 0.2 ppm to 25 ppm for both anions and cations. Cations standard solutions were prepared from the AN CUS 0131 reference material (analytika, spol) containing Ca, K, Li, Mg, Na and NH_4^+. Anion standards were prepared from a mix solution of bromide, chloride, fluoride, nitrate, nitrite, phosphate, and sulfate (IV-stock-59, inorganic ventures).

To ensure that the system is stable, a control sample (with known concentrations) was included in the analysis list after every 10 analyzed samples. The detection limits calculated for the studied elements are equal to three times the standard deviation value obtained from blank solution measurements and were presented in **Table II-7**.

Additionally, the anion-cation balance was used in order to examine the reliability of the analytical data and as a quality control check. According to **Fig. II-13,** the balance between cations and anions for the samples of both sites show a linear correlation with determination coefficients R^2 of 0.97 and 0.98 at ZK and FA, respectively.

Table II-7: Atmospheric detection limits (ng/m^3) of analyzed ions

Ion	Detection limit (ng/m^3)	Ion	Detection limit (ng/m^3)
Cl^-	0.39	**NH_4^+**	0.67
NO_3^-	0.22	**K^+**	0.25
SO_4^{2-}	0.78	**Ca^{2+}**	0.39
Na^+	0.17	**Mg^{2+}**	0.53

However, the slopes of the linear curves are higher than 1, i.e., 1.25 at ZK and 1.19 at FA, meaning that the anions could not neutralize all the cations. This anion deficit is mainly linked to unmeasured anion species such as MSA (methanesulfonic acid) and carbonate ions. This deficit is commonly observed in Lebanon since the Lebanese soils are rich in $CaCO_3$ (Verheye, 1973).

2.1.4 Carbonaceous fraction

The carbonaceous fraction (OC, EC, and TC) was analyzed at the Cyprus Institute. A punch of 1 cm^2 of the quartz filter was used to quantify organic and elemental carbon by a thermal optical transmission technique using a Sunset Laboratory OC/EC analyzer implementing the EUSAAR2 temperature protocol (Cavalli et al., 2010) with a transmittance optical correction for pyrolysis. Field blank filters were also analyzed in the same way and the concentrations of OC, EC, and TC were corrected by subtracting the average blank values.

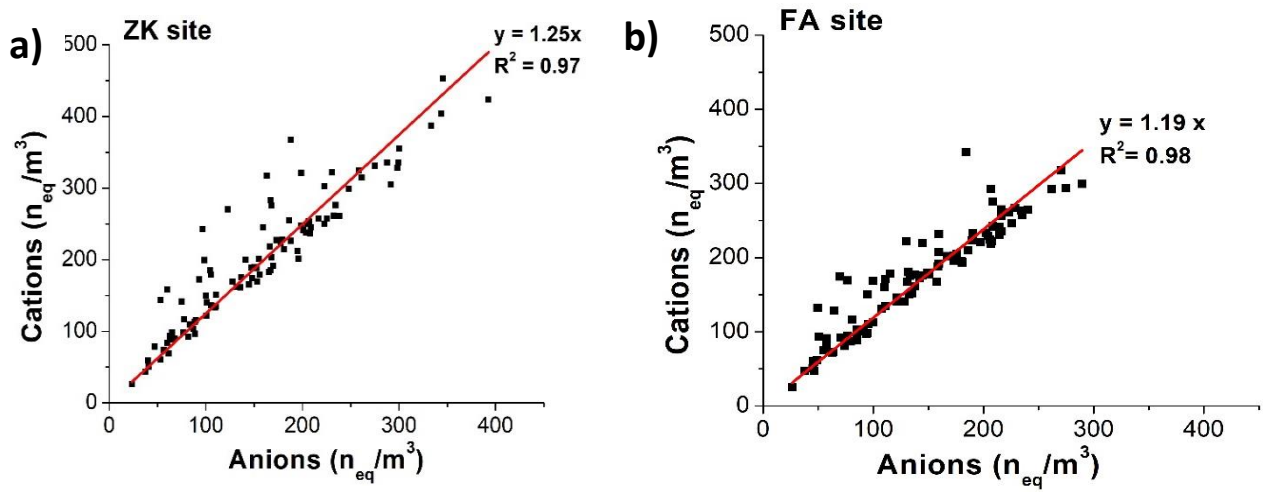

Fig. II-13: Ion balance evaluation between water soluble ions (expressed in nanoequivalents per liter) in $PM_{2.5}$ samples at ZK (a) and FA (b) sites considering all the measured anions and cations

2.1.5 PCDD/Fs and DL-PCBs

In order to ensure a sufficient mass for the analysis of these organic compounds, 2 punches (19 mm) of each filter were taken and the samples were regrouped. For every site, the samples were divided into 3 groups: 1 group with samples taken during the summer period, another for the winter period and the third for samples taken between the two previously mentioned periods. Dioxins, furans and dioxin-like polychlorobiphenyls were quantified by MicroPolluants Technology SA (Saint Julien Les Metz, France). The group of filters were soaked in 1 mL HCl (12N) and then left to dry overnight. Extraction markers (EN-1948 ES) were added, and filter pieces were extracted using toluene by Soxhlet for 24h. The concentration of the solution was done under a gentle flow of nitrogen gas up to 20 mL, purified on a silica column and eluted with hexane. The obtained eluate was concentrated to 20 mL, purified on an alumina column, and then PCBs were eluted with toluene and concentrated to 100 µL while PCDD/Fs were eluted with a mixture dichloromethane/hexane (60/40) and concentrated to 10 µL (Borgie et al., 2015). The extracts were then analyzed based on the US EPA method 1613 and 1688 respectively using a high-resolution gas chromatography coupled to a high-resolution mass spectrometer (HRGC/HRMS).

2.2 Quantification of NMVOCs

The chemical extraction of NMVOCs from the passive tubes was performed in the Radiello glass tube by adding 2 mL of CS_2 and 100 µL of 2-fluorotoluene used as internal standard for 30 min by stirring every 2 min before discarding the cartridge. The obtained solution was filtered using PTFE Whatman filters (0.2 µm) and then injected in the GC/MS (ISQ 7000, Thermo Scientific, United States of America) operating in the split mode (split ratio of 25).

The GC was equipped with a 100% dimethyl polysiloxane column (50 m x 0.2 mm x 0.5 µm, Supelco, United States of America). The column temperature program consisted of an injection at 35°C hold for 5 min, a ramp of temperature corresponding to 1°C/min up to 135°C followed by another ramp of temperature of 5˚C/min up to 250°C and finally an isothermal hold step at 250°C for 7 min. The GC was interfaced to an ion trap MS with an external electron ionization (EI) source (220 ˚C, 70 eV). The identification of the compounds was made by comparing their retention times and their mass spectrum (full scan mode, range 25-350 m/z) to the authentic standards. The concentrations of the compounds (in ng/m^3) were calculated using the equations provided by the manufacturer of Radiello diffusive passive sampler (Fondazione Salvatore Maugeri- IRCCS, Padova, Italy).

Field blanks were analyzed following the the same procedures as the sampling cartridges and the concentrations of the different species were corrected by subtracting the average concentrations of the field blanks. The regression coefficients R^2 for the calibration curves were in the range of 0.96 - 0.99 for the different compounds.

The targeted compounds were n-hexane, tetrachloroethene, benzene, cyclohexane, n-heptane, methylcyclohexane, toluene, ethylbenzene, and xylenes (m,p,o). The detection limit (D.L.) of the compounds corresponds to the average value of the blank filters plus 3 times the standard deviation calculated over 3 measurements. For these species, D.L. varied between 0.01 and 0.1 $\mu g/m^3$.

1,3-butadiene was analyzed at Gradko International (Winchester, England) using a Thermal Desorption GC-MS. The analysis performed in this laboratory is UKAS accredited, ensuring conformance with the requirements of ISO/IEC 17025. The detection limit of 1,3-butadiene was 0.05 $\mu g/m^3$.

2.3 Measurements of oxidative potential

Due to the absence of a standardized method for OP measurements and the large differences between the methods found in the literature (Bates et al., 2019), a compromise between the different parameters is necessary in order to obtain reliable results. The method presented in our study for the measurement of OP-AA and OP-DTT is found in Moufarrej et al. (2020).

2.3.1 Sample preparation and extraction

The leaching agent that was used for the PM extraction was the Gamble solution (pH = 7.4), considered as the most used simulated lung fluid (SLF) and represent the interstitial fluid in the deep lung. However, to avoid any significant influence of bioaccessibility of metals in the lungs, the Solid (S)/Liquid (L) ratio should be in the range of 1/500 - 1/50,000; avoiding by that any risk of saturation and competition between soluble compounds (Caboche et al., 2011).

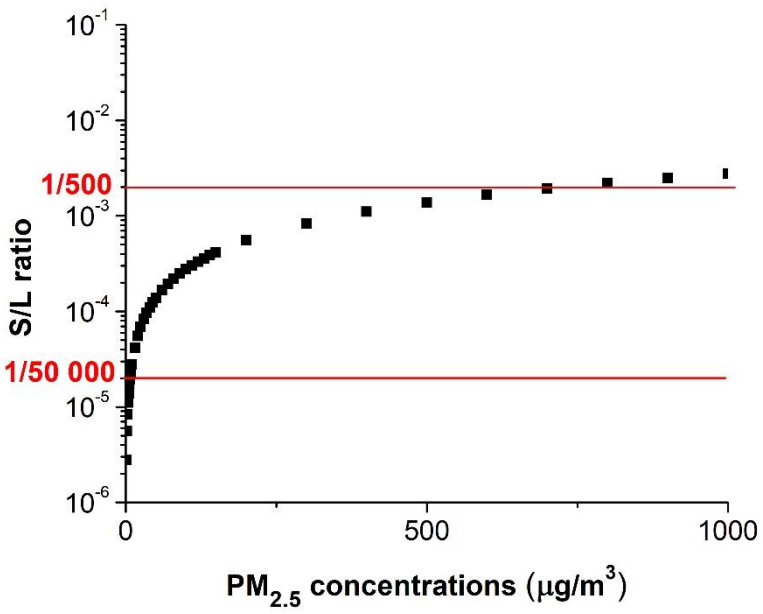

Fig. II-14: Plot showing the variations of the S/L ratio (using a filter punch of 19 mm of diameter and an extraction volume of 5 mL) when increasing atmospheric $PM_{2.5}$ concentrations

Accordingly, the fraction of the $PM_{2.5}$ filter and the volume of the extraction solution should be chosen. As shown in **Fig. II-14**, when considering a filter punch of 19 mm of diameter and an extraction volume of 5 mL per sample, the S/L ratio is considered acceptable for atmospheric $PM_{2.5}$ concentrations ranging between 8 and 700 µg/m^3. The latter range is considered acceptable for our measurements since the $PM_{2.5}$ concentrations at both sampling sites were within this range.

The Gamble solution was freshly prepared every day by adding in order the different components presented in **Table II-8** to avoid salt precipitations (Colombo et al., 2008). The pH of the solution was adjusted to 7.4 by either adding dropwise HCl 10% or NaOH 1M.

For the extraction, the 19 mm diameter filter punch was placed in a 15 mL glass tube with 5 mL of the gamble solution. The tubes were covered in aluminum foil and placed in a heated orbital shaker for 24 h at 37°C, at a speed of 250 oscillations/min. The obtained solutions were then filtered on 0.45 µm PTFE filters (VWR international, North America), and the filtrates were placed in flasks and stored at -20°C until analysis. Field blanks were also analyzed with the same protocol as the $PM_{2.5}$ samples.

Table II-8: Composition (in g/L) of the gamble solution as found in Colombo et al. (2008)

Reagents	Chemical formula	Concentration (g/L)
magnesium chloride	$MgCl_2$	0.095
sodium chloride	NaCl	6.019
potassium chloride	KCl	0.298
disodium hydrogen phosphate	Na_2HPO_4	0.126
sodium sulfate	Na_2SO_4	0.063
calcium chloride dihydrate	$CaCl_2$, $2H_2O$	0.368
sodium acetate	$C_2H_3O_2Na$	0.574
sodium hydrogen carbonate	$NaHCO_3$	2.604
sodium citrate dihydrate	$C_6H_5Na_3O_7$, $2H_2O$	0.097

2.3.2 Dithiothreitol OP test (OP-DTT)

The measurement of OP-DTT was carried out using a 96 well black plates with clear flat bottom (Coastar® 3631, Corning Incorporated Life Sciences, USA). As shown in **Fig. II-15**, 120 µL of the phosphate buffer (pH=7.4) solution and 40 µL of the extracted PM solution in gamble (or blank or 1,4-Naphtaquinone (1,4-NQ) taken as positive control) were added in each well. Then, after 10 min of incubation at 37°C under shaking, 25 µL of DTT (0.4 mM prepared in PBS) was added to start the oxidation reaction. At specific times (0, 5, 10, 20, 30, 45 and 60 minutes) after the reaction between PM extracts and DTT at 37°C, 15 µL of DTNB (1.5 mM prepared in PBS) were added to each well to convert the remaining DTT to TNB. 10 minutes after the last addition of DTNB, the absorbance of TNB was measured at 412 nm using a microplate reader spectrophotometer (Multiskan Go, Thermo Fisher Scientific, Finland), and converted to remaining DTT concentrations using the calibration curve.

The DTT depletion rate was calculated using the slope of the linear part of the curve representing the remaining DTT quantity versus time. Field blank filters were analyzed in the same way of the PM extracts. Samples were analyzed in triplicates and the average value is corrected by subtracting the average value of the field blank filters and the gamble solution. The relative standard deviation (RSD) between the triplicates was less than 10%.

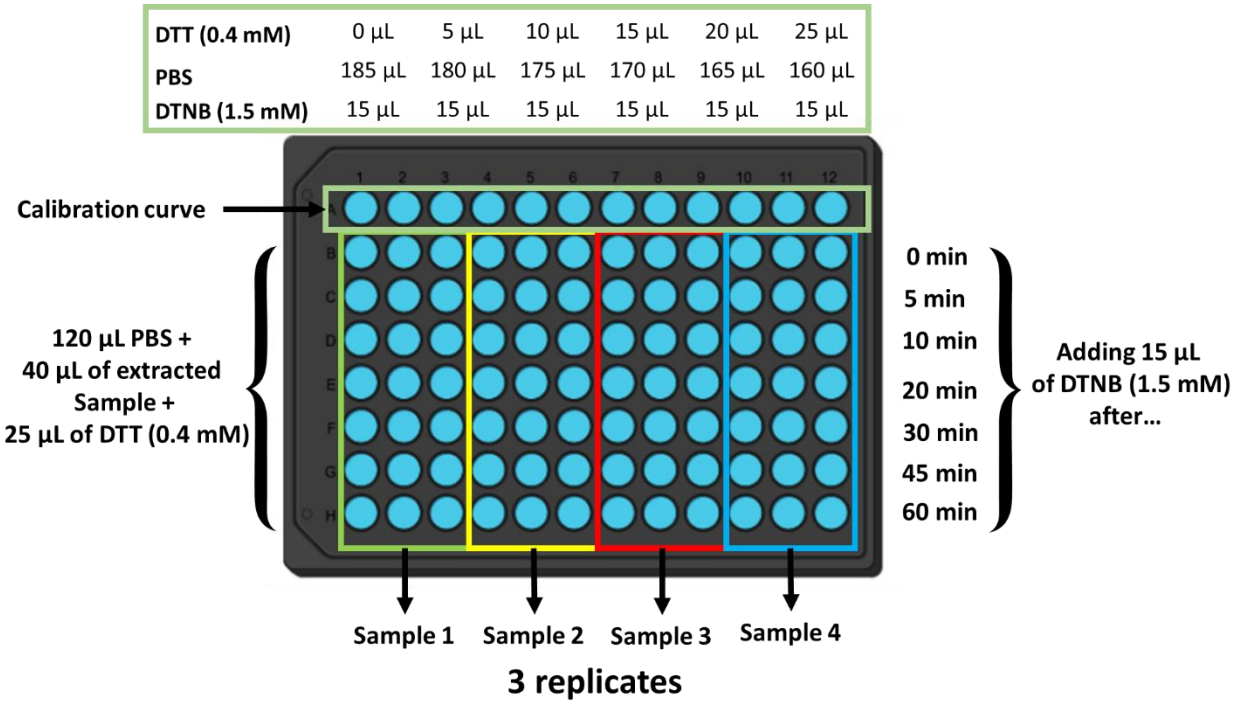

Fig. II-15: Schematic representation of an OP-DTT plate with the different reagents added to the different wells

2.3.3 Ascorbic acid OP test (OP-AA)

The measurement of OP-AA was done in 96 well plates with UV-transparent flat bottom (UV-Star® 655801, Greiner bio-one, Austria). In each well of the plate corresponding to a sample, 160 µL of the PM extracts (or 1,4-NQ taken as a positive control) were added and then the plate was incubated for 10 min at 37°C. Then, 40 µL of the ascorbic acid (AA) solution (with a concentration of 1mM prepared in ultrapure water) were added into the wells, before shaking the plate for 1 min **(Fig. II-16)**. The latter was directly placed in the microplate spectrophotometer (Multiskan Go, Thermo Fisher Scientific, Finland) at 37°C, and the absorbance was measured at 265 nm for 2 hours every 2 minutes with 30 seconds shaking before every measurement.

The values of OP-AA were determined as the slope of the linear part of the curve representing AA depletion versus time. Field blanks were analyzed in the same way as the extracts. Samples were analyzed in triplicates and the average value is corrected by subtracting the average value of the field blank filters and the gamble solution. The relative standard deviation (RSD) between the triplicates was less than 7%.

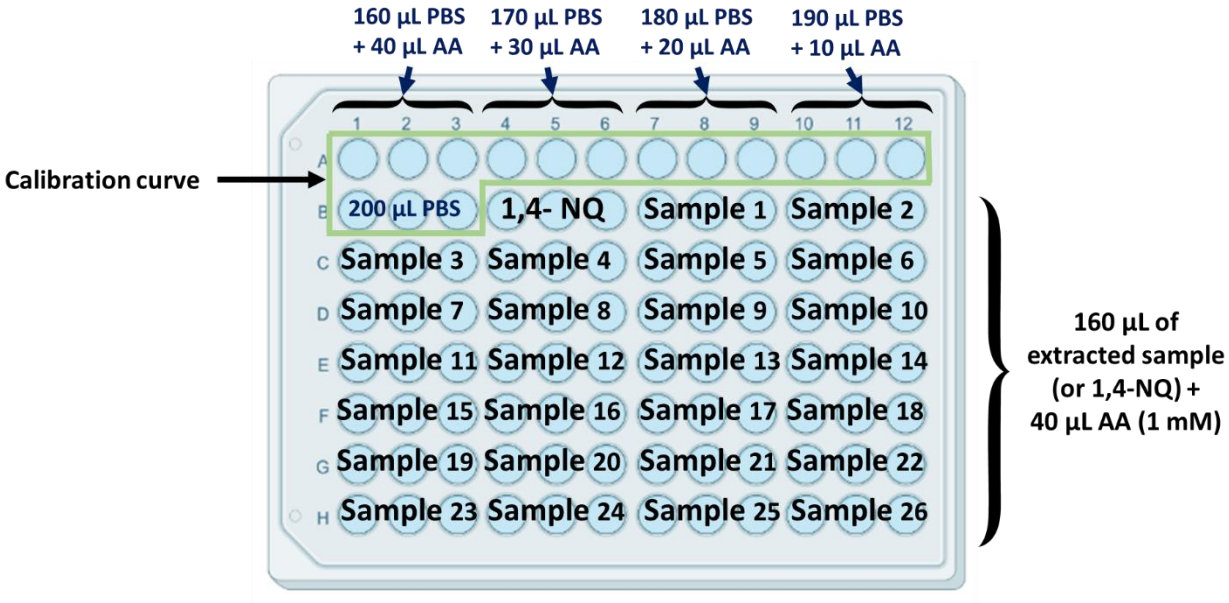

Fig. II-16: Schematic representation of an OP-AA plate with the different reagents added to the different wells

3 Application of PMF

As a receptor-based model, PMF has been widely used for source apportionment of various environmental pollutants. This model was chosen because little knowledge of pollution sources in the region is required prior to the receptor modeling. Additionally, it provides different uncertainty estimation methods to examine the robustness of the solution.

3.1 Input data

The EPA PMF 5.0 was used for the source apportionment application in our study. For the input data, two input files are required: the concentrations of the species and their corresponding uncertainties both expressed in ng/m^3. The species chosen for this application are mainly organic and inorganic tracers of different sources and were presented in **Table II-9**.

In the concentration matrix, values below the detection limit were replaced by D.L./2, while missing values were replaced by the geometric means of concentrations (Polissar et al., 1998). Uncertainty values were also calculated according to Polissar et al. (1998) by considering :

- the sum of the analytical uncertainty added to D.L./3 for determined values
- 5/6 D.L. for values below detection limit
- and 4 times the geometric mean of the measured concentrations for missing values

Table II-9: Organic and inorganic tracers used for the source apportionment by PMF

Fraction	Tracer	Source
Carbonaceous fraction	OC	Combustion sources
	EC	Combustion sources
Water-soluble ions	Na^+, Cl^-	Sea salt
	SO_4^{2-}, NO_3^- and NH_4^+	Secondary inorganic aerosols
Elements	Mg, Al, Fe, K, Ti	Desert dust
	Ca	Desert dust or cement industries
	Cu, Sb, Sn	Road dust
	V, Ni	HFO combustion
Organic compounds	levoglucosan	Biomass burning
	hexadecanoic acid (palmitic) octadecanoic acid (stearic)	Cooking emissions
	17α(H)-21β(H)-hopane	Vehicular emissions
	isoprene and α-pinene oxidation products	Biogenic SOA
	C_{20}, C_{21}	Diesel emissions
	C_{24}, C_{25}	Gasoline emissions
	C_{27}, C_{29}, C_{31}	Plant wax emissions

The evaluation of the input data is based on the Signal-to-noise (S/N) ratio that indicates whether the variability in the measurements is real or within the noise of the data. The calculations of this parameter is based on the following equations:

$$\left(\frac{S}{N}\right)_j = \frac{1}{n}\sum_{i=1}^{n} d_{ij}$$

$$d_{ij} = \left(\frac{x_{ij} - s_{ij}}{s_{ij}}\right) \; if \; x_{ij} > s_{ij}$$

$$d_{ij} = 0 \; if \; x_{ij} \leq s_{ij}$$

According to these equations, concentrations (x_{ij}) that are below uncertainty (s_{ij}) are determined to have no signal, and for concentrations above uncertainty, the difference between the

concentration and the uncertainty is used for the signal calculations. Upon the obtained values for the S/N, the user can classify the species into three categories: strong species with S/N > 2, weak species with 0.2 < S/N < 2, and bad species with S/N < 0.2. The weak categorization triples the uncertainty provided and the bad categorization excludes the species from the rest of the analysis.

3.2 Determination of the number of factors and the optimal solution

The objective function Q in PMF is considered as a critical parameter. PMF minimize it for better estimate factor contributions and profiles. Q is defined as follows :

$$Q = \sum_{i=1}^{n}\sum_{j=1}^{n}\left[\frac{x_{ij} - \sum_{k=1}^{p} g_{ik}f_{kj}}{u_{ij}}\right]^2 = \sum_{i=1}^{n}\sum_{j=1}^{m}\left(\frac{e_{ij}}{u_{ij}}\right)^2$$

Two versions of Q are present in the model: Q(true) and Q(robust)

- Q(true) represents the goodness-of-fit parameter calculated including all the data points
- Q(robust) represents the goodness-of-fit parameter calculated excluding the points that are not fitted by the model

The difference between Q(true) and Q(robust) corresponds to the measure of the impact of the points with high scaled residuals.

Since the number of factors in PMF is unknown, we start by the minimum number of factors (which is 2) and we start increasing this number. To select the appropriate number of factors, different mathematical diagnostic methods can be investigated such as the maximum individual mean (IM) and the maximum individual standard deviation (IS) that are calculated as follows (Lee et al., 1999):

$$IM = \max_{j=1\ldots m}\left(\frac{1}{n}\times\sum_{i=1}^{n} r_{ij}\right) \quad and \quad IS = \max_{j=1\ldots m}\left(\sqrt{\frac{1}{n-1}\times\sum_{i=1}^{n}\left(r_{ij} - \bar{r}_j\right)^2}\right)$$

$$r_{ij} = \frac{e_{ij}}{s_{ij}}$$

When the number of factors increases to a critical value, IM and IS will show a drastic drop. Graphical representations of IM and IS statistics along with the Q-value showed a constant decrease of their values when increasing the number of factors and a stabilization starting the 12-factor solution for both sites **(Fig. II-17)**. Additionally, the user should have a certain

understanding of the sources impacting the sampling site and the species characteristics in order to choose the most suitable number of factors.

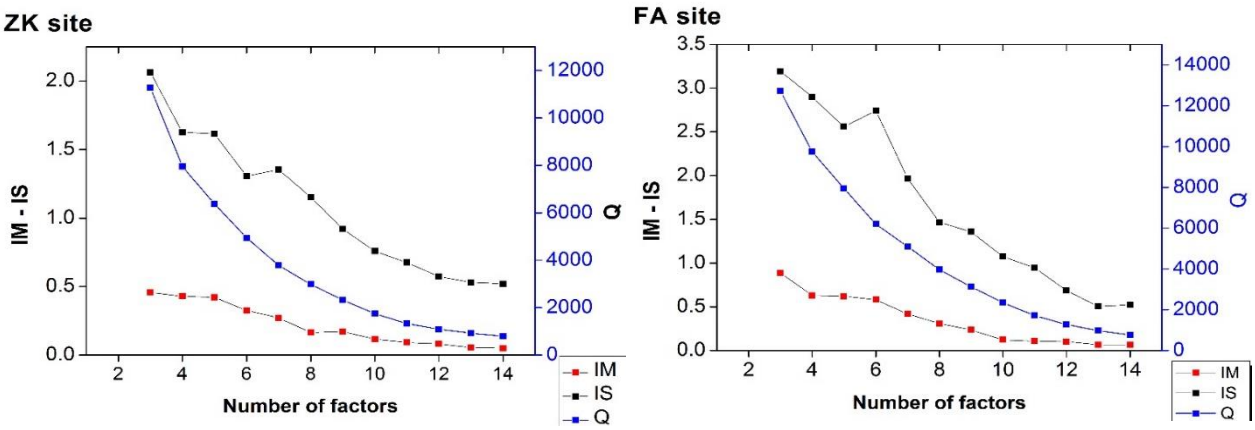

Fig. II-17: The diagnostic factor of PMF model showing IM, IS and Q-value or the different factor solutions for Zouk (ZK) and Fiaa (FA) sites

In order to obtain robust results in PMF, several points should be taken into consideration:

- Ensure that the residuals of all the species are generally normally distributed (with residuals varying between -3 and +3)
- Check that all the species are well modeled with high determination coefficients (R^2) between observed and predicted observations
- Examine the Q/Qexp values for the different species and ensure that this value is lower than 2. For each species, the Q/Qexp is the sum of the squares of the scaled residuals for that species divided by the overall $Q_{expected}$ divided by the number of strong species.
- Evaluate the Q(true)/Q(robust) ratio – optimal ratio : 1
- Evaluate F_{peak} results used to explore rotations of the solutions of a given number of factors

3.3 Stability of the model result

The variability in PMF solutions can be estimated using different methods that were applied on the results obtained at both sites **(Table II-10; Table II-11).** These methods are complementary since the bootstrap analysis focuses on the random errors while displacement analysis includes the effects of rotational ambiguity.

3.3.1 Bootstrap analysis on F matrix

This method shows the effects from random errors and include partially the effects of rotational ambiguity. It is used to find if there is a small set of observations that can largely influence the solution. The sets of bootstrap data are constructed by randomly selecting blocks of observations from the initial dataset. The length of each block depends on the dataset and is chosen in a way to keep the correlations that may be present in the general dataset.

Table II-10: Base error estimation summary for PMF results at ZK site

DISP diagnostics													
Error code	0												
Largest decrease	-0.025												
%dQ	-0.002302535												
Swaps	**1**	**2**	**3**	**4**	**5**	**6**	**7**	**8**	**9**	**10**	**11**	**12**	
	0	0	0	0	0	0	0	0	0	0	0	0	
Bootstrap Mapping													
	1	**2**	**3**	**4**	**5**	**6**	**7**	**8**	**9**	**10**	**11**	**12**	**Unmapped**
Boot Factor 1	99	0	0	0	0	0	1	0	0	0	0	0	0
Boot Factor 2	0	92	2	0	0	1	3	0	0	0	1	0	1
Boot Factor 3	0	0	100	0	0	0	0	0	0	0	0	0	0
Boot Factor 4	0	0	0	100	0	0	0	0	0	0	0	0	0
Boot Factor 5	0	0	0	0	100	0	0	0	0	0	0	0	0
Boot Factor 6	0	0	1	0	0	98	1	0	0	0	0	0	0
Boot Factor 7	0	0	1	0	0	0	98	1	0	0	0	0	0
Boot Factor 8	0	0	0	0	0	1	1	96	2	0	0	0	0
Boot Factor 9	0	0	0	0	0	0	0	0	100	0	0	0	0
Boot Factor 10	0	0	0	0	0	0	0	0	0	100	0	0	0
Boot Factor 11	0	0	0	0	0	0	0	0	0	0	100	0	0
Boot Factor 12	0	0	0	0	0	0	0	0	0	0	0	100	0

100 bootstrap runs with a correlation of 0.60 were performed for the two datasets. The subset number chosen was the one suggested by the model (Block size of 8 at ZK and 7 at FA). Mapping over 80% of the factors indicates that the BS uncertainties can be interpreted and the number of factors may be appropriate (USEPA, 2014). The bootstrap results at both sites show a high mapping rate with values exceeding 92% at ZK and 96% **(Table II-10; Table II-11)** at FA meaning that the bootstraps were mapped to the respective base case factor.

3.3.2 Displacement DISP on F matrix

This analysis method helps to understand in details the selected solution, including the sensitivity to small changes. This method includes the effects of rotational ambiguity but not the effects of random errors like the bootstrap analysis. Each value in the factor profile is at first

adjusted up and down and then all other values are computed to achieve a convergence to a minimum value of Q. Data uncertainty can directly impact DISP error estimates so intervals for down weighted species are likely to be large (USEPA, 2014). According to the PMF guide, if factor swaps occur, it means that there is a significant rotational ambiguity and that the solution is not sufficiently robust to be used.

Table II-11: Base error estimation summary for PMF results at FA site

DISP diagnostics													
Error code	0												
Largest Decrease	0												
%dQ	0												
Swaps	**1**	**2**	**3**	**4**	**5**	**6**	**7**	**8**	**9**	**10**	**11**	**12**	
	0	0	0	0	0	0	0	0	0	0	0	0	
Bootstrap Mapping													
	1	**2**	**3**	**4**	**5**	**6**	**7**	**8**	**9**	**10**	**11**	**12**	**Unmapped**
Boot Factor 1	100	0	0	0	0	0	1	0	0	0	0	0	0
Boot Factor 2	0	98	0	0	0	0	0	0	1	1	0	0	0
Boot Factor 3	0	0	100	0	0	0	0	0	0	0	0	0	0
Boot Factor 4	0	1	0	98	1	0	0	0	0	0	0	0	0
Boot Factor 5	0	0	0	0	99	0	0	1	0	0	0	0	0
Boot Factor 6	0	0	0	0	0	100	0	0	0	0	0	0	0
Boot Factor 7	0	0	0	0	0	0	100	0	0	0	0	0	0
Boot Factor 8	0	0	0	0	0	0	0	100	0	0	0	0	0
Boot Factor 9	0	0	0	0	0	0	0	0	100	0	0	0	0
Boot Factor 10	0	0	0	0	0	2	0	1	0	97	0	0	0
Boot Factor 11	0	0	0	0	0	0	0	0	0	0	100	0	0
Boot Factor 12	1	0	1	0	0	0	0	1	0	1	0	96	0

Additionally, if the decrease in the Q value is greater than 1%, this means that the true global minimum was not found (USEPA, 2014). The results of the DISP analysis for both sites show that there are no swaps between the factors and the decrease in the Q value is less than 1%. This means that there is no rotational ambiguity between the obtained factors at both sites and that we have found the true global minimum of Q value.

4 Personal contribution to the current works

As previously shown, different analytical techniques were used in order to fully characterize $PM_{2.5}$, NMVOCs, and to measure the oxidative potential. Additionally, computational work was required in order to run the PMF model and achieve exploitable results, and to link oxidative potential results to the sources contributions at both sites. **Table II-12** shows the

different works that were done by me from sample preparations to the data processing and those that were outsourced.

Table II-12: Personal contributions to the current work and analyses conducted

	Tasks	# of samples	Person in charge	Location
Sample preparation and gravimetric $PM_{2.5}$ analysis	$PM_{2.5}$ filter preparation for weighing and sampling	250	Marc Fadel	USJ - Lebanon
	$PM_{2.5}$ gravimetric analysis (weighing room preparation, conditioning, weighing, QA/QC)	250	Marc Fadel	USJ - Lebanon
Sampling	$PM_{2.5}$ sampling at ZK site	104	Marc Fadel	USJ - Lebanon
	$PM_{2.5}$ sampling at FA site	103	Marc Fadel with the help of Dr. Adib Kfoury (Univ. Balamand)	USJ - Lebanon
	$PM_{2.5}$ sampling for source profiling	16	Marc Fadel	USJ - Lebanon
	NMVOCs sampling at ZK	20	Marc Fadel	USJ - Lebanon
	NMVOCs sampling at FA	20	Marc Fadel	USJ - Lebanon
Organic compounds analysis	Sample preparation (cutting of filters, etc.)	250	Marc Fadel	USJ - Lebanon
	Extraction and derivatization	250	Marc Fadel	USJ - Lebanon
	Analysis by GC-MS	250	Marc Fadel	USJ - Lebanon
	Analysis of chromatograms	250	Marc Fadel with the help of Mariana Farhat	USJ - Lebanon
NHMCs analysis	Extraction	22	Marc Fadel	USJ - Lebanon
	Analysis by GC-MS	22	Marc Fadel	USJ - Lebanon
	Analysis of chromatograms	22	Marc Fadel	USJ - Lebanon
	Analysis of 1,3-butadiene	18	Gradko Environment	
Major and trace elements analysis	Sample preparation (cutting of filters, etc.)	250	Marc Fadel	ULCO - France
	Digestion, etc.	250	Marc Fadel	ULCO - France
	Analysis by ICP-AES	250	Marc Fadel with the help of Centre Commun de Mesure (CCM) at ULCO	ULCO - France
	Analysis by ICP-MS	250	Marc Fadel with the help of Institut Chevreul – Université de Lille	ULCO - France
Water-soluble ions analysis	Sample preparation (cutting of filters, etc.)	250	Marc Fadel	ULCO - France
	Extraction, etc.	250	Marc Fadel	ULCO - France
	Analysis by IC	250	Marianne Seigneur	ULCO - France
OC/EC analysis	Sample preparation (cutting of filters, etc.)	250	Marc Fadel	USJ - Lebanon
	Analysis of OC/EC	250	The Cyprus Institute	
PCDD/Fs and DL-PCBs analysis	Sample preparation (cutting of filters, etc.)		Marc Fadel	ULCO - France
	Analysis of group of filters	12	Micropolluants Technology SA	

PMF application	Zouk site	98	Marc Fadel	USJ - Lebanon ULCO - France
	FA site	95	Marc Fadel	USJ - Lebanon ULCO - France
OP analysis	Sample preparation (cutting of filters, etc.)	500	Marc Fadel	ULCO - France
	Extraction	500	Marc Fadel	ULCO - France
	OP-AA analysis	500	Marc Fadel	ULCO - France
	OP-DTT analysis	500	Marc Fadel	ULCO - France
	Applying multiple linear regression model on OP and PMF data		Pr. Gilles Roussel and Dr. Gilles Delmaire made the model	ULCO - France
	Results interpretation		Marc Fadel	USJ - Lebanon ULCO - France

References:

Bates, J.T., Fang, T., Verma, V., Zeng, L., Weber, R.J., Tolbert, P.E., Abrams, J.Y., Sarnat, S.E., Klein, M., Mulholland, J.A., Russell, A.G., 2019. Review of acellular assays of ambient particulate matter oxidative potential: methods and relationships with composition, sources, and health effects. Environ. Sci. Technol. 53, 4003-4019, 10.1021/acs.est.8b03430.

Borgie, M., Dagher, Z., Ledoux, F., Verdin, A., Cazier, F., Martin, P., Hachimi, A., Shirali, P., Greige-Gerges, H., Courcot, D., 2015. Comparison between ultrafine and fine particulate matter collected in Lebanon: Chemical characterization, in vitro cytotoxic effects and metabolizing enzymes gene expression in human bronchial epithelial cells. Environ. Pollut. 205, 250-260, https://doi.org/10.1016/j.envpol.2015.05.027.

Caboche, J., Perdrix, E., Malet, B., Laurent, Y.A., 2011. Development of an in vitro method to estimate lung bioaccessibility of metals from atmospheric particles. J. Environ. Monit. 13, 621-630, 10.1039/c0em00439a.

Cavalli, F., Viana, M., Yttri, K.E., Genberg, J., Putaud, J.P., 2010. Toward a standardised thermal-optical protocol for measuring atmospheric organic and elemental carbon: the EUSAAR protocol. Atmos. Meas. Tech. 3, 79-89, 10.5194/amt-3-79-2010.

Colombo, C., Monhemius, A.J., Plant, J.A., 2008. Platinum, palladium and rhodium release from vehicle exhaust catalysts and road dust exposed to simulated lung fluids. Ecotoxicol. Environ. Saf. 71, 722-730, https://doi.org/10.1016/j.ecoenv.2007.11.011.

DRI, 2003. Analysis of Semi-volatile Organic Compound by GC/MS. Desert Research Institute, DRI Standard Operating Procedure., 1–25

Fadel, M., Ledoux, F., Farhat, M., Kfoury, A., Courcot, D., Afif, C., 2021. $PM_{2.5}$ characterization of primary and secondary organic aerosols in two urban-industrial areas in the East Mediterranean. J Environ Sci 101, 98-116, https://doi.org/10.1016/j.jes.2020.07.030.

Kfoury, A., Ledoux, F., Roche, C., Delmaire, G., Roussel, G., Courcot, D., 2016. $PM_{2.5}$ source apportionment in a French urban coastal site under steelworks emission influences using constrained non-negative matrix factorization receptor model. J Environ Sci 40, 114-128, https://doi.org/10.1016/j.jes.2015.10.025.

Ledoux, F., Courcot, L., Courcot, D., Aboukaïs, A., Puskaric, E., 2006. A summer and winter apportionment of particulate matter at urban and rural areas in northern France. Atmos Res 82, 633-642, https://doi.org/10.1016/j.atmosres.2006.02.019.

Lee, E., Chan, C.K., Paatero, P., 1999. Application of positive matrix factorization in source apportionment of particulate pollutants in Hong Kong. Atmos Environ 33, 3201-3212, https://doi.org/10.1016/S1352-2310(99)00113-2.

Moufarrej, L., Courcot, D., Ledoux, F., 2020. Assessment of the $PM_{2.5}$ oxidative potential in a coastal industrial city in Northern France: Relationships with chemical composition, local emissions and long range sources. Sci. Total Environ. 748, 141448, 10.1016/j.scitotenv.2020.141448.

Polissar, A.V., Hopke, P.K., Paatero, P., Malm, W.C., Sisler, J.F., 1998. Atmospheric aerosol over Alaska: 2. Elemental composition and sources. Journal of Geophysical Research: Atmospheres 103, 19045-19057, https://doi.org/10.1029/98JD01212.

USEPA, 2014. EPA Positive Matrix Factorization (PMF) 5.0 Fundamentals and User Guide. EPA/600/R-14/108.U.S. Environmental Protection Agency Office of Research a nd Development Washington, DC 20460.

Verheye, W., 1973. Formation, classification and land evaluation of soils in mediterranean areas : with special reference to the southern Lebanon, Gent.

Waked, A., Afif, C., Brioude, J., Formenti, P., Chevaillier, S., Haddad, I.E., Doussin, J.-F., Borbon, A., Seigneur, C., 2013. Composition and source apportionment of organic aerosol in Beirut, Lebanon, during winter 2012. Aerosol Sci. Technol. 47, 1258-1266, 10.1080/02786826.2013.831975.

Waked, A., Afif, C., Formenti, P., Chevaillier, S., El-Haddad, I., Doussin, J.-F., Borbon, A., Seigneur, C., 2014. Characterization of organic tracer compounds in $PM_{2.5}$ at a semi-urban site in Beirut, Lebanon. Atmos Res 143, 85-94, 10.1016/j.atmosres.2014.02.006.

CHAPTER III

Chemical characterization and sources identification of $PM_{2.5}$

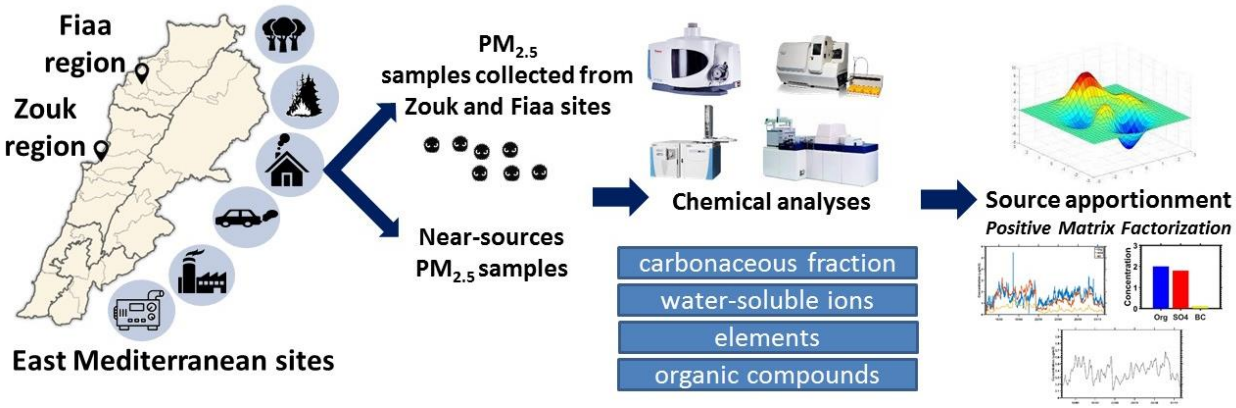

Introduction

To successfully understand the behavior and origins of the particulate matter in the air, one should characterize them chemically, among others, and identify/exhibit their sources in a quantitative way. This requires ambient measurements of particles, which will feed into source apportionment models that necessitate source profiles to identify the sources. The ambient measurements and the establishment of source profiles can be led concurrently, and at a later stage, their output will be used to run the source apportionment model and analyze its output.

One of the major challenges of source apportionment applications is the lack of knowledge on chemical composition for some emissions sources and the difficulty to find local source profiles to be used in order to have reliable results (Hopke et al., 2016). The East Mediterranean is one of the regions for which very few source profiles were established. This pushed us to focus on the chemical characterization of $PM_{2.5}$ emitted from typical anthropogenic sources since they differ from those observed in other regions (for example USA, Europe, etc.) following local practices commonly observed in the East Mediterranean - Middle Eastern region. The sources we investigated are charcoal grilling of beef and chicken, general cooking activities, wood burning and emissions from non-road diesel generators. The determination of the chemical characteristics of the $PM_{2.5}$ emitted from these sources including organic compounds, carbonaceous fraction, trace and major elements, and water-soluble ions were the subject of the first manuscript in this chapter entitled "chemical profiles of $PM_{2.5}$ emitted from various anthropogenic sources of the Eastern Mediterranean: cooking, wood burning, and diesel generators" and submitted to the journal "Environmental Research" (Impact factor 2021: 6.498).

On the other hand, the chemical composition of ambient $PM_{2.5}$ varies depending on the influence of local emission sources, chemical atmospheric processes, meteorological conditions, and the long-range transport of pollutants. Hence, an exhaustive chemical characterization of $PM_{2.5}$ appears to be mandatory to further evaluate the air quality on the sites under study, the atmospheric dynamics and at a later stage, the contribution of the sources. We started by studying the organic fraction of $PM_{2.5}$ since it is poorly studied in the East Mediterranean region. The few studies found focused on certain classes of compounds and were limited to a short sampling period with a limited number of samples. Additionally, several organic compounds are considered as tracers of different sources and can be used for source identification. Hence, it was essential to look into this fraction and quantify as many compounds

as possible in the $PM_{2.5}$ collected at Zouk (ZK) and Fiaa (FA) sites. The results of the organic characterization are presented in the second article of this chapter entitled "$PM_{2.5}$ characterization of primary and secondary organic aerosols in two urban-industrial areas in the East Mediterranean". This paper was published in the "Journal of Environmental Sciences" (Impact factor 2021: 5.565) and focuses on the speciation of more than 60 organic compounds among which alkanes, PAHs, hopanes, fatty acids, secondary biogenic aerosols, dicarboxylic acids, and phthalates. The secondary biogenic compounds include oxidation products of isoprene, α-pinene, and β-caryophyllene. Diagnostic ratios and molecular markers were considered to show contribution of the different anthropogenic and natural sources at both sites.

Following the analysis of the speciated organic fraction, the analysis of the carbonaceous matter (OC, EC), water-soluble ions, and major and trace elements in $PM_{2.5}$ was conducted by studying the temporal variations of the species, the concentrations ratios, and the enrichment factors to further understand the influence of the anthropogenic sources. Additionally, cluster analysis of air mass back-trajectories was applied to evaluate the impact of the long-range transport on air quality in the studied region. Finally, organic, and inorganic markers or species were chosen to be included in the PMF model to identify the sources with the help of the above-mentioned local source profiles that we established and to assess their contribution to $PM_{2.5}$ levels at both sites. All of these results were included in the third manuscript of this chapter entitled "$PM_{2.5}$ chemical characterization and sources identification in two sites in the East Mediterranean" to be submitted to "Science of the Total Environment" (impact factor 2021: 7.963).

By these manuscripts and articles, we would have tried to answer a part of the scientific questions presented at the end of chapter I and we would have constructed a better picture of the different natural and anthropogenic sources affecting the concentrations of $PM_{2.5}$ in the sites under study.

Article 1: Chemical profiles of $PM_{2.5}$ emitted from various anthropogenic sources of the Eastern Mediterranean: cooking, wood burning, and diesel generators

Marc Fadel[1,2], Frédéric Ledoux[2], Marianne Seigneur[2], Konstantina Oikonomou[3], Jean Sciare[3], Dominique Courcot[2], Charbel Afif [1,3,]*

[1]Emissions, Measurements, and Modeling of the Atmosphere (EMMA) Laboratory, CAR, Faculty of Sciences, Saint Joseph University, Beirut, Lebanon

[2]Unité de Chimie Environnementale et Interactions sur le Vivant, UCEIV UR4492, FR CNRS 3417, University of Littoral Côte d′Opale (ULCO), Dunkerque, France

[3]Climate and Atmosphere Research Center, The Cyprus Institute, Nicosia, Cyprus

*Corresponding author: charbel.afif@usj.edu.lb

Abstract

The chemical profiles of $PM_{2.5}$ emitted from a non-road diesel generator, wood burning and cooking activities including chicken and beef charcoal grilling and general cooking activities were determined. The characterization included the carbonaceous fraction (OC/EC), water-soluble ions, elements, and organic species comprising n-alkanes, polycyclic aromatic hydrocarbons, carboxylic acids, levoglucosan, dioxins, furans, and dioxin-like polychlorinated biphenyls. The main component in the $PM_{2.5}$ from the different sources was carbonaceous matter with a mass contribution of 64% for cooking activities, 72% for wood burning, 84% for beef grilling, 86% for diesel generator, and 97% for chicken grilling with different OC/EC concentration ratios. The analysis of organic compounds contents using diagnostic ratios and indexes showed differences between the sources and revealed specific source markers. The water-soluble ions had the highest contribution in the cooking activities profile with 22% and the least in the chicken grilling profile (1.5%). Additionally, 29 analyzed elements were identified, and their contribution varied with the sources (ranging from 2% to 14%). These findings could be used to differentiate these sources and could assist in the use of source apportionment methods.

Keywords: source profiles, $PM_{2.5}$, organic species, inorganic species, cooking, diesel generator, combustion.

Synopsis: This study presents different chemical composition profiles of sources commonly observed in the Mediterranean region that have not yet been fully chemically characterized.

Introduction

Source profiles or chemical fingerprints refer to the average relative chemical composition of the PM deriving from a pollution source, expressed as the mass ratio between each species to the total PM or the total identified mass (Pernigotti et al., 2016; Belis et al., 2019). These profiles are commonly used as input data for some receptor modeling approaches such as Chemical Mass Balance (CMB) where a priori knowledge of the composition of the emissions is crucial (Viana et al., 2008). They are also used to attribute output factors to specific sources in multivariate factor analysis methods such as Positive Matrix Factorization (PMF) (Bove et al., 2018). Additionally, source profiles contribute to the chemical speciation of emission inventories whether to estimate emissions of hazardous and toxic pollutants or in source oriented modeling for policy makers (Chow et al., 2004).

Several source profile databases have been created across the globe. Source profiles have been gathered since 1988 in the United States Environmental Protection Agency (USEPA) SPECIATE database (Simon et al., 2010). To date, the database contains more than 6,700 PM, gas and other profiles covering more than 2,800 unique species. Recently, a European database, SPECIEUROPE, was published in 2015 by the European Joint Research Centre consisting of more than 280 profiles and reaching 250 species (Pernigotti et al., 2016). In 2017, researchers from the Chinese Research Academy of Environmental Sciences (CRAES) developed a new database of emission source profiles for PM in Chinese environments (Liu et al., 2017). The China Source Profile Shared Service contains more than 500 profiles in its first version (CSPSS 1.0) (Liu et al., 2017). These databases were built following the shortage of local source profiles that represented a true challenge for receptor modeling studies in terms of source identification and comparability between studies (Pernigotti et al., 2016). Numerous source apportionment studies have been carried out using the American, European, and Chinese databases not only in their countries of development but also for most of the source apportionment studies in developing countries despite the divergence in national circumstances (Gupta et al., 2007; Chelani et al., 2008). Indeed, the chemical speciation of emissions from certain sources largely depend on parameters such as geological substrate, local practices, emission control technologies, as well as the fuel quality in the case of combustion sources and the combustion efficiency, etc. which leads to higher uncertainty in source apportionment studies (Colombi et

al., 2010; Salameh et al., 2014; Bove et al., 2018; Weber et al., 2019). Hopke (2016) stressed on the idea that no efforts were deployed to develop source profiles especially for stationary sources and for many others in developing countries. The main obstacle to achieve effective and accurate source apportionment remains in the lack of regional source profiles.

The Middle East is a vast region encompassing around 300 million inhabitants, different countries including some of the East Mediterranean. Most of these countries are considered as developing, with several cultures, traditions, and languages but mainly share common practices such as some cooking techniques, lack of law enforcement in many cases, etc. Different important sources of pollution can be of interest in the region among which cooking, power generation, and wood burning especially in the Eastern Mediterranean. The variety of products, seasoning, and cooking techniques make the gastronomical rituals different in the Middle East from other regions. It is well established that cooking plays a major role in the Middle Eastern culture, (Essid, 2012) especially during family gatherings on weekends, holidays, and special occasions with outdoor barbecue and several other cooking activities. Most of the literature studies related to emissions from cooking focused on Indian (Bano et al., 2018), Chinese (He et al., 2004; Zhang et al., 2017; Zhao et al., 2019), and fast food (Rogge et al., 1991) that have different cooking practices than the Middle East and focusing on certain species and classes of compounds. On the other hand, diesel generators are widely used in the world in temporary projects or as stand-by power in developed countries at power sensitive facilities or even as continuous backup power in developing countries due to power supply instability (Klimont et al., 2016). The literature mostly present $PM_{2.5}$ profiles for regulated diesel engines (Liang et al., 2005; Yilmaz and Davis, 2016) like Tier 1 to 4 in North America, Stage 1 and above in Europe, etc. However, many countries especially developing ones do not always effectively enforce the law when it comes to stack emissions (Waked et al., 2012), do not have regulations on the import of regulated engines, and mostly allow the installation of the generators in heavily populated areas without any pollution abatement. Another combustion source commonly known in the region due to forest fires but also used for cooking, residential heating, and outdoor activities such as camping is the wood burning. The emission characterization of these sources in the region is still limited (Alves et al., 2010; Kostenidou et al., 2013) and more focus should be given due to their impacts on air quality.

The objective of this paper is to determine, for the first time in the Middle Eastern region, $PM_{2.5}$ chemical source profiles for different anthropogenic sources such as cooking, wood burning, and emissions from unregulated non-road diesel generator. While most of $PM_{2.5}$ chemical

profiles found in the literature focus on specific chemical fractions or species, this study presents for the first time, to the best of our knowledge, a full chemical characterization including carbonaceous fraction, ionic, elemental, and organic species. The organic speciation includes n-alkanes, Polycyclic Aromatic Hydrocarbons (PAHs), carboxylic acids, levoglucosan, dioxins (PCDD), furans (PCDF), and dioxin-like polychlorinated biphenyls (DL-PCBs). PCDD/Fs and DL-PCBs are presented for the first time in general cooking activities. Furthermore, source markers, diagnostic ratios, and indexes are presented in order to be used in source identification. All of these results will be compared to available database in order to conclude whether the differences are significant. Additionally, these results will provide valuable information for source apportionment applications, speciated emission inventories, as well as for health impact assessment studies.

1 Experimental

1.1 Sample collection

$PM_{2.5}$ samples were collected onto 150 mm pure quartz microfibres filters (Fiorini, France) using a high-volume sampler (CAV-A/mb, MCV S.A., Spain) operating at 30 m^3/h in different locations in Lebanon. Filters were pre-heated for 12 hours at 550°C before sampling to decrease the level of organic impurities. The collected filters were sealed in aluminum foil and stored at -20°C until analysis. It is worth noting that for combustion sources, the sampling was made at a sufficient distance from the combustion process to let the plume cool down and to collect the condensed fraction in the particulate phase.

1.2 Experimental design

The operating conditions, under which the sampling for the different anthropogenic sources was conducted, were detailed in the sections below and were summarized in **Table III- 1**. All the methods described below are representative of common practices in the East Mediterranean region.

1.2.1 Wood burning (WB)

The wood combustion (open fire) experiment was conducted outdoor away from trees and other plant materials. Dry wood branches of hardwood broad-leaved trees were added into the firepit in the shape of a pyramid, ignited using a lighter and burned with free air supply. The sampler was placed directly in the smoke plume and 3 filters (sample label: WB) were exposed during

the flaming combustion phase. Throughout the sampling, new pieces of wood were added to keep the fire going. The sampling duration varied between 10 and 15 minutes for each sample.

Table III- 1: Operating conditions under which the different anthropogenic samples were obtained

	Wood burning	**Diesel generator**	**Cooking**		
			Beef grilling	**Chicken grilling**	**Cooking activities**
Abbreviations	**WB**	**DG**	**BG**	**CG**	**GCA**
Main contents	Wood branches of broad-leaved trees (hardwood)	Volvo Penta TAD531GE diesel generator, 100 kVA, four cylinders at 1500 rpm	Small pieces of beef grilled on both sides	Large pieces of skinned chicken grilled on both sides	Burger grilling, french fries frying, use of vegetables, daily dishes served
Combustible	Biomass	Diesel fuel	Charcoal	Charcoal	Natural gas liquid (LPG)
Sampling method	High volume sampler for $PM_{2.5}$				
Filter used	Quartz filters – 150 mm diameter				
Number of samples	4	3	1	1	5
Sampling time	10-15 min	30 min	20 min	20 min	75 min

1.2.2 Diesel private generator (DG)

The generator, with an engine capacity of 100 kVA, is placed in the basement of a residential building. This type is representative of the most used category (below 250 kVA) of diesel generators producing electricity for households. The fuel type used is automotive diesel oil. The generator has an extended exhaust pipe of about 18 m to release emissions above the rooftop level. The sampler was placed at the same level as the top of the stack in order to collect the particulate sample with minimal influence by ambient PM. No sample was taken during the cold-start phase (the first 20 min of the engine operation). Four diesel generator samples (DG) were collected under the same operating conditions for 30 min each.

1.2.3 Cooking

In order to have exhaustive cooking source chemical profiles, 7 samples were collected from different cooking experiments: 2 for charcoal grilling and 5 for general cooking activities.

1.2.3.1 Beef and chicken charcoaled experiments

The Mediterranean region is known for its tradition of charcoal grilling especially during weekends and holidays. The most commonly observed charcoal-grilled food in the region are mainly beef and chicken. The charcoal is made of oak wood. It was piled in a pyramid shape in the grill to help increase the contact between the charcoal and make the fire spread. A fire starter cube was inserted into the pyramid and lighted. After 20 min, the coal was covered in ash. It was then laid evenly in the grill and was ready to use. Two $PM_{2.5}$ samples were taken during this procedure: the first one was sampled during beef grilling (BG) and the second one for chicken (CG). The sampling duration was 20 min for each sample. First, the meat (BG) was cooked over charcoal for 20 min and turned several times during the total cooking time. The distance between the meat and the charcoal was approximately 10 cm. The sampler was placed directly in the grill smoke plume. Then, the chicken (CG) was grilled.

1.2.3.2 General Cooking activities (GCA)

The sampling was carried out in a university kitchen cafeteria during the peak hour of work for 5 consecutive days. The cooking equipment mainly consists of gas deep frying machines, free standing griddles, and steam tables for the daily dishes. The main cooking technique is gas-grilling activity to make burgers or sandwiches (meat, chicken, etc.), and frying of French fries, etc. The frying oils used are Canola and Soybean seed. There was no major outdoor ventilation leading to the assumption that the $PM_{2.5}$ mass collected was mainly due to the cooking activities. The sampler was placed next to the steam tables, deep-frying machine, and grill and 5 samples (GCA) were taken for 75 min each.

1.3 Chemical analysis

1.3.1 Carbonaceous fraction

The organic carbon (OC) and the elemental carbon (EC) were quantified on a punch of the quartz filter (1 cm^2) by a thermal optical transmission technique. It consists of a Sunset Laboratory OC/EC analyzer implementing the EUSAAR2 protocol (Cavalli et al., 2010) with a transmittance optical correction for pyrolysis.

1.3.2 Organic compounds

The organic compounds were quantified by gas chromatography (ISQ 7000, Thermo Scientific, United States of America) coupled to a mass spectrometer (GC-MS) following the method described in previous studies (Waked et al., 2013; 2014; Fadel et al., 2021). In brief, one quarter

of each filter was extracted with acetone and dichloromethane (1:1, v/v) by sonication for 30 min at 50℃ after spiking it with two internal standards (bornylacetate and ketopinic acid). The extracts were concentrated to 200 µL under a gentle flow of nitrogen gas. An aliquot of the sample is injected directly in the GC-MS to quantify non-polar compounds such as n-alkanes and PAHs while another aliquot was derivatized before injection to identify levoglucosan and carboxylic acids.

1.3.3 Elements

Elements were analyzed by inductively coupled plasma (More detailed information on the analysis are available in previous publications (Ledoux et al., 2006a; Kfoury et al., 2016). In brief, for each sample, a 47 mm punch of the quartz filter was digested by an acid mixture of 4 mL nitric acid (HNO_3), 1 mL of hydrofluoric acid (HF), and 0.5 mL of perchloric acid ($HClO_4$) in a PTFE flask at 120℃ overnight. Then, the acid evaporation was made at 170℃ to the last drop followed by the addition of few milliliters of ultrapure water. The obtained solution was then diluted to 15 mL by ultrapure water, acidified to 2% by HNO_3 and filtered on 0.45 µm cellulose acetate filter prior to analysis. Mg, Mn, Al, Na, Ba, Ca, Fe, K, Ni, P, Pb, S, Sr, Ti, and Zn were quantified by Inductively Coupled Plasma-Atomic Emission Spectrometry (ICP-AES, iCAP 6000 series, Thermo Scientific, United Kingdom). V, Cr, Co, Cu, As, Rb, Nb, Ag, Cd, Sn, Sb, La, Ce, and Bi were quantified by ICP-Mass Spectrometry (ICP-MS, Agilent 7900, United States of America).

1.3.4 Water-soluble ions

The protocol for water-soluble analysis was detailed elsewhere (Ledoux et al., 2006b; Kfoury et al., 2016). Briefly, three filter punches of 19 mm diameter each for every sample were ultrasonically extracted by few milliliters of ultrapure water for 20 min. The obtained solution is collected using a syringe, then filtered through a 0.45 µm porosity cellulose acetate membrane previously rinsed with ultrapure water. The leachate containing the ions was placed in a polyethylene flask of 20 mL. The filters were submerged with ultrapure water prior to 2 additional ultrasonic extractions and filtrations and then stored at -20℃ until analysis. The samples were analyzed by liquid ion chromatography (Dionex™ ICS-900, Thermo Scientific, United Kingdom) for the quantification of Cl^-, SO_4^{2-}, NO_3^-, Ca^{2+}, Mg^{2+}, K^+, Na^+, and NH_4^+.

1.3.5 Dioxins, furans and dioxin-like polychlorobiphenyls

Dioxins, furans and dioxin-like polychlorobiphenyls were quantified by MicroPolluants Technology SA (Saint Julien Les Metz, France). The PCDD/PCDF and DL-PCB analysis method was based on the US EPA method 1613 and 1688 respectively using a high-resolution gas chromatography coupled to a high-resolution mass spectrometer (HRGC/HRMS). Detailed information are found in Borgie et al. (2015).

2 Results and discussions

The chemical relative abundance of the different species in the carbonaceous, ionic, and elemental fractions were calculated by dividing their mass by the sum of the analyzed species. They were presented in **(Fig. III-1)**, and in details in **Appendix A -Table S1** and **Appendix A - Figure S1.** The organic species were reported to the OC mass and were given in **Appendix A - Table S2**.

2.1 Carbonaceous fraction

In the different chemical profiles of $PM_{2.5}$, OC was the main component, ranging from 54% for WB to 97% for CG **(Fig. III-1)**. EC ranged from 0.2% for CG to 23% for DG which presents the second most abundant share in WB and DG profiles.

High differences in the distribution of the carbonaceous fraction (OC+EC) occur between charcoal and general cooking activities profiles. GCA releases less carbonaceous matter (64%) compared to BG (84%) and CG (97%). These differences were mainly attributed to the cooking process and ingredients (Abdullahi et al., 2013). Many studies have compared cooking styles and reported different chemical profiles for the emitted particulate matter.

The OC/EC ratio is an essential tool to differentiate combustion sources. This study determined a value of 3.4 for wood burning, comparable to the findings reported by Sun et al. (2019) for wood branches (2.69). As for cooking profiles, the highest ratio was found for CG (622), followed by BG (45) and GCA (18). This large difference between CG and BG could be attributed to the difference in fat content between the two types of food. Foods containing high percentage of fat usually generate higher OC emission rates than those with a lower fat percentage (Abdullahi et al., 2013).

The ratio for GCA was close to the value of 19.3 reported for samples collected form the exhaust stacks of a university canteen in Portugal (Alves et al., 2014). The lowest ratio was found for

the diesel generator (2.9), slightly higher than 2.61 reported by Sothea and Kim Oanh (2019) for a 92 kW backup generator in Cambodia. For comparison, values of 0.37 were reported for tunnel studies (diesel and gasoline vehicles), 2.2-6.2 for urban areas, and 0.64 for diesel trucks (El Haddad et al., 2009; Waked et al., 2014).

2.2 Organic compounds

2.2.1 N-alkanes

C_{13}-C_{32} homologue series are presented for the different profiles in **(Fig. III-2)**. Total C_{13}-C_{32} average contribution to OC were 14%, 1%, 1%, 0.9%, and 0.4% for DG, BG, WB, GCA, and CG, respectively. The high contribution of n-alkanes in the DG profile is mainly due to the composition of the diesel fuel that comprises a large fraction of n-alkanes (Liang et al., 2005).

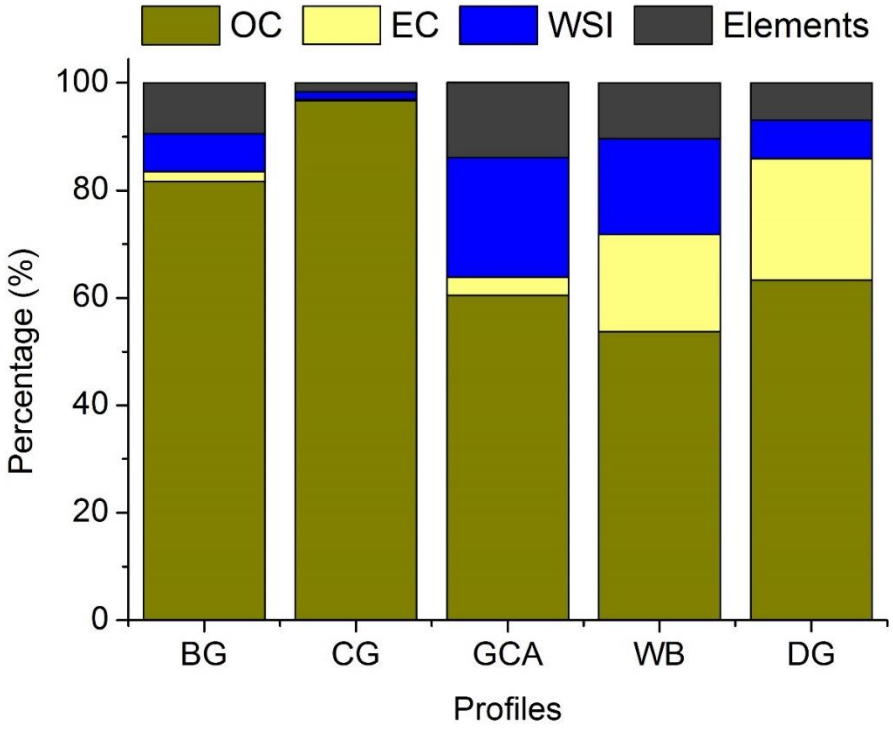

Fig. III-1: Percentage of OC, EC, water-soluble ions (WSI), and elements in $PM_{2.5}$ emitted from the different sources (BG: beef grilling, CG: chicken grilling, GCA: general cooking activities, WB: wood burning, DG: diesel generator).

Different methods can be used to characterize the alkanes profiles (Fadel et al., 2021). Briefly, the overall carbon preference index (Overall CPI) for C_{13}-C_{31} is a measure of odd to even carbon predominance with a value close to 1 for petrogenic sources, 2 to 5 for biomass and coal burning and values higher than 6 for biogenic emissions. The wax ratio (Wax%) can be used to assess

the contribution of wax n-alkanes from plants. The n-alkanes distribution pattern can be used to identify alkanes with the highest concentrations. For wood burning, the profile pattern shows a predominance of high molecular weight n-alkanes especially C_{27}, C_{29}, and C_{31} with a maximum at C_{29} **(Fig. III-2)**. This pattern is considered as a plant epicuticular wax signature leading to a high Wax% of 58%. C_{27}, C_{29}, and C_{31} are considered as n-alkanes tracers for biomass burning (Simoneit, 2002). The CPI value for WB (CPI=4) is in the range reported for biomass activities of 2 to 5 (Simoneit, 2002). A distinctive pattern was observed for DG where the n-alkane homologues partitioning exhibited a smooth hump-like distribution with the highest contribution for C_{20}-C_{21} **(Fig. III-2).** A similar profile was observed for diesel powered engines (Rogge et al., 1993).

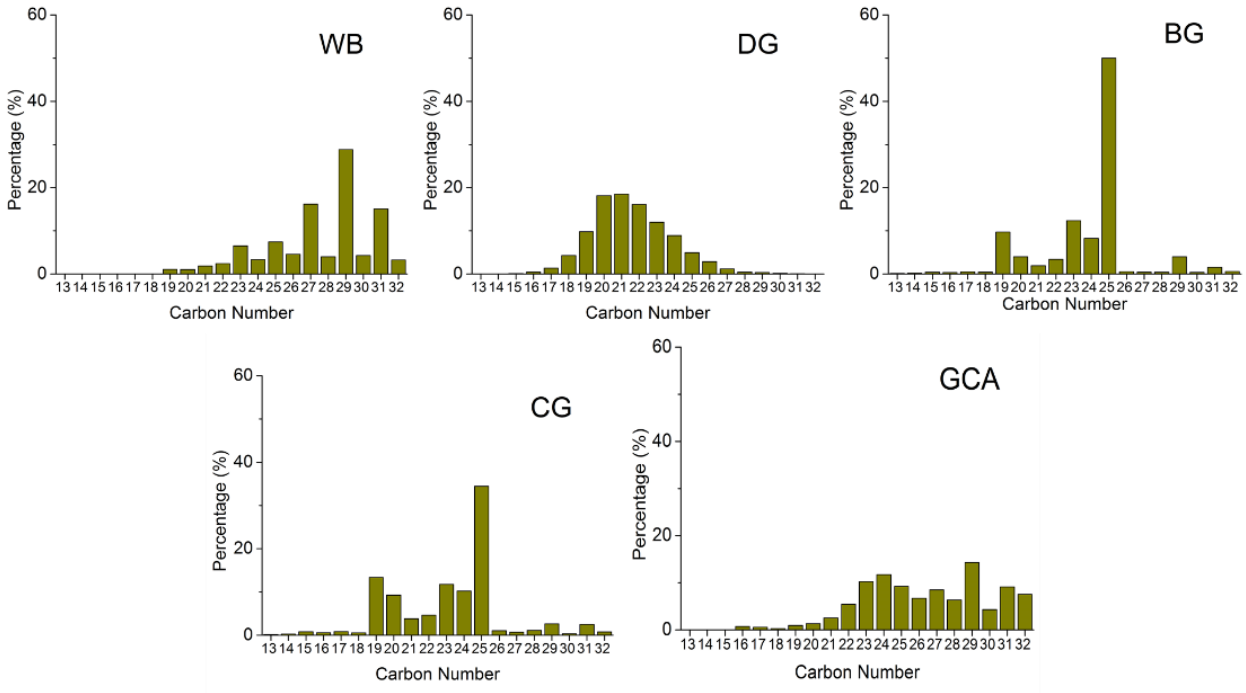

Fig. III-2: N-alkanes profile patterns associated with $PM_{2.5}$ for the different sources (WB: wood burning, BG: beef grilling, CG: chicken grilling, DG: diesel generator, GCA: general cooking activities).

A CPI value (0.9) close to unity usually attributed for petrogenic sources and a very negligible Wax% characterizes the diesel emissions from non-road generators.

For charcoal cooking (BG and CG), the profiles are much alike with a maximum contribution for C_{25}. This observation can lead to the assumption that the n-alkanes are not predominantly

emitted from the food itself but from the charcoal combustion. This hypothesis can be supported by CPI values of 2.5 and 4.5 for CG and BG respectively that are in the range of coal combustion. However, a different pattern was observed for GCA. The CPI value for this GCA profile (1.3) and the Wax% (22%) were relatively low compared to various Chinese cooking restaurants with calculated CPI and Wax% in the ranges of 2.3-4.6 and 40-64%, respectively (He et al., 2004; Zhao et al., 2007a). These differences may be attributed to the different cooking methods and frying techniques without forgetting the large consumption of vegetables in the Chinese cooking causing higher CPI and Wax% ratios (Zhao et al., 2007b).

2.2.2 Polycyclic Aromatic Hydrocarbons

The relative concentration profiles of the different PAHs are presented in **Appendix A- Table S2** with the share (in mg/g of OC) of each one. Additionally, the distribution of these species with aromatic ring number was also shown in **(Fig. III-3)** to further characterize them in the profiles.

The wood burning experiment emitted 10 times more PAHs normalized to OC than the other sources (4.55 mg/g for WB against 0.72 for BG, 0.47 for CG, 0.21 for GCA, and 0.53 for DG). The higher PAHs share for WB compared to CG and BG can be attributed to the more complete combustion of charcoal compared to wood. Furthermore, the volatilization and the pyrolysis of the volatile matter during the production of charcoal, and its low water content could also reduce the aromatic compounds formation (Oanh et al., 1999; Shen et al., 2011).

Low PAHs shares were observed for the different cooking profiles. McDonald et al. (2003) suggested that the PAHs emitted during grilling activities were formed from the interaction between the lipidic material in food and the cooking appliance since the temperature reached on the surface of food was relatively low to form PAHs (maximum PAHs production occurs at 750 °C) and PAHs compounds were absent in the food chemical analysis. Furthermore, the abundance of 4-rings PAHs in BG and CG profiles might be related to the coal combustion. According to Vicente et al. (2018), fly ashes from charcoal combustion are rich in 4-rings PAHs with fluoranthene and pyrene as the most abundant aromatics whereas raw charcoal is mainly rich in 3-rings PAHs. As for GCA, several studies showed that 6-rings PAHs were rarely generated during cooking processes especially during deep frying activities because high temperatures can decompose high molecular weight PAHs (Zhao et al., 2019; Sun et al., 2020). The most abundant PAHs for GCA were B[b]Fl, Pyr, and Chr.

Like BG, CG, and GCA, 4-rings PAHs predominated the total detected $PM_{2.5}$-bound PAHs emitted from WB with Fla, Pyr, B[a]An as the most abundant compounds. This distribution pattern along with the dominant PAHs were consistent with the data reported for the combustion of different types of biomass fuels (maize straw, wheat straw, and wood branches) (Sun et al., 2019). Pyrene was the most abundant PAH in the diesel generator profile, accounting for more than 50% of the sum of PAHs and highly contributing to the 4-rings category that is the most abundant.

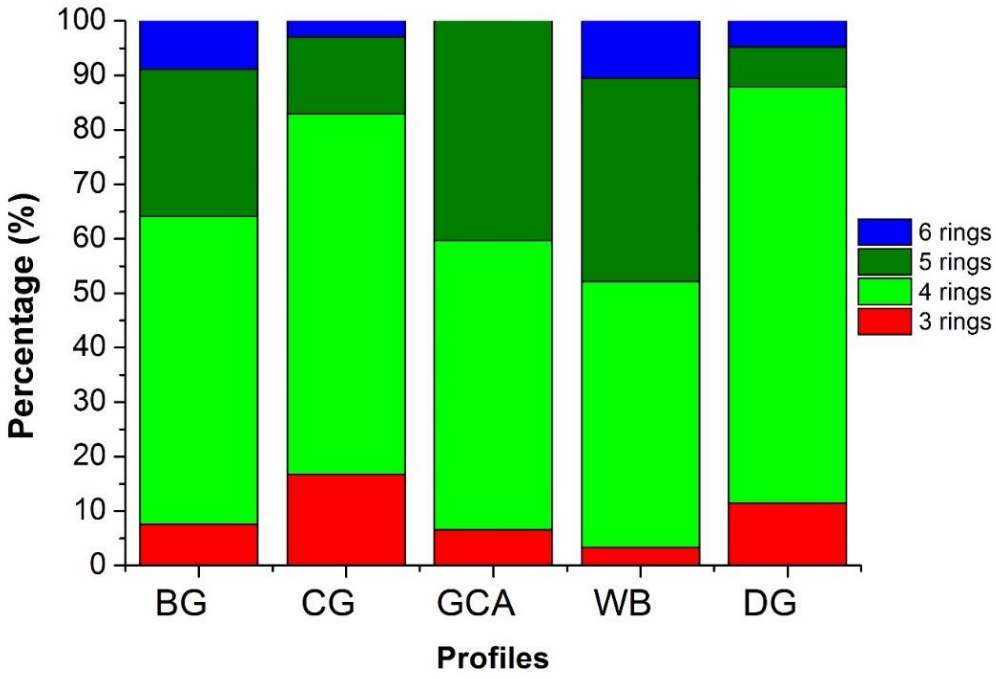

Fig. III-3: Distribution of PAHs for the different sources (BG: beef grilling, CG: chicken grilling, GCA: general cooking activities, WB: wood burning, DG: diesel generator) according to the number of aromatic rings in mass percentages.

PAHs diagnostic ratios were usually used for source apportionment in different environmental samples (Tobiszewski and Namieśnik, 2012). For every ratio, the species used should have similar reactivity in the atmosphere: Fla and Pyr (Molecular Weight =202 g/mol), B[a]An and Chr (MW = 228 g/mol), InPy and B[ghi]Pe (MW= 278 g/mol), and Anth and Phe (MW= 178 g/mol). These ratios could serve as markers for the different profiles presented in this paper and were reported in **Table III-2**.

The values obtained for wood burning (0.49 for Fla/(Fla+Pyr), 0.57 for B[a]An/(B[a]An+Chr), 0.45 for InPy/(InPy+B[ghi]Pe), and 0.7 for Anth/(Anth+Phe)) are mostly in the ranges of ratios reported in other studies for biomass burning (Tobiszewski and Namieśnik, 2012; Vicente et al., 2012; Gong et al., 2019) **(Table III-2**).

As for grilling activities, the similarity in the ratios and the closeness to the values reported in the literature imply that these PAHs are mainly emitted from the charcoal combustion in the barbecue grills (Vicente et al., 2018; Gong et al., 2019). For GCA, Fla/(Fla+Pyr) and B[a]An/(B[a]An+Chr) ratio values are close to those reported for deep-frying activities and Chinese gas cooking (Wei See et al., 2006; See and Balasubramanian, 2008). A particular attention was given to the ratios determined for diesel generators emissions. The values present in the literature describe mostly diesel emissions from on-road vehicles (Ravindra et al., 2008; Shi et al., 2014; Riffault et al., 2015; Gong et al., 2019). Although many similarities exist, the modes of operation are different. Non-road diesel generators run at a certain rpm (revolutions per minute) and voltage and the amperage they produce can vary with the load while on-road diesel vehicles operate in transient conditions (Liang et al., 2005; Shah et al., 2006). These differences in the operation mode can potentially result in different emission characteristics and different diagnostic ratios for PAHs. On the other hand, Liang et al. (2005) studied the organic composition of diesel particulate matter from a non-road diesel generator and showed Fla/(Fla+Pyr) and B[a]An/(B[a]An+Chr) ratio values (0.28 and 0.5, respectively) close to the values obtained in this study (0.24 and 0.41, respectively) while values for InPy/(InPy+B[ghi]Pe) and Anth/(Anth+Phe) were different **(Table III-2**).

2.2.3 Carboxylic acids

According to **Appendix A- Table S2,** carboxylic acids were the most abundant organic species in the chemical profiles of cooking activities. The highest contribution was observed for GCA explaining 36% of the OC mass followed by BG with 25% and CG with 14%. During high temperature treatment of food, several chemical processes occur such as sugar degradation, pyrolysis of proteins and amino-acids, and the degradation of fats. These mechanisms lead to the production of free fatty acids, glycerol, and glycerides (Abdullahi et al., 2013). Additionally, the use of oils in cafeteria cooking operations such as deep frying will increase fatty acids emissions being the major constituents of triglycerides in seed oils (Schauer et al., 2002; Zhao et al., 2007a). From the saturated fatty acids presented in this paper, the most abundant are palmitic (C_{16}) and stearic (C_{18}) acids accounting for more than 80% of the total mass of fatty

acids in the three cooking profiles. These compounds are usually used as organic markers for cooking activities in different source apportionment studies (Abdullahi et al., 2013). Carboxylic acids were also found in biomass burning events and contribute to 9% of the OC mass. The highest concentration was observed for palmitic acid (C_{16}) accounting for 33% of the sum of carboxylic acids. These findings were in accordance with the results obtained from wildfires organic speciation in central Portugal (Vicente et al., 2012) and with the combustion of hardwoods (Oros and Simoneit, 2001). Long-chain fatty acids are mainly considered as basic units of plant fats, oils, and phospholipids while short-chain species (C<16) are reported as minor species of fungi and insects. As for the diesel generator, carboxylic acids contribute to almost 10% of the OC mass. Liang et al. (2005) determined the abundance of fatty acids in the engine oil and the diesel particulate matter and found a strong similarity, bringing the conclusion that fatty acids in diesel particles are not emitted from the combustion process itself but from the evaporation of engine oil.

2.2.4 Levoglucosan

Levoglucosan or 1,6-anhydro-β-D-glucopyranose originates from the pyrolysis of cellulose and hemicellulose at high temperature (Giannoni et al., 2012). It is considered as an organic molecular marker for biomass burning due to its stability and its relatively high share in biomass smoke (Chantara et al., 2019). This compound is the most abundant organic species in the WB profile accounting for 30% of the OC mass. Levoglucosan/OC ratio is commonly used to differentiate softwood and hardwood combustion. The value obtained in our study of 0.3 is in the range of hardwood combustion (0.25-0.4) reported by Fine et al. (2004) compared to lower ratios for softwood ranging between 0.1 and 0.23.

2.2.5 Dioxins, furans, and DL-PCBs

Appendix A - Table S3 shows congeners contribution to OC of PCDD/Fs and DL-PCBs for each source. The BG and CG were combined in one factor and will be presented as "charcoal grilling". 1,2,3,4,6,7,8 HpCDD was identified in all emissions and was the only PCDD detected in GCA, while OCDD contributed the most to the other profiles (73% of PCDD in WB, 76% in DG, and 70% in charcoal grilling, i.e., BG and CG). The DG emissions are 4, 3, and 1.5 more concentrated in PCDD than GCA, charcoal grilling, and WB, respectively. However, charcoal grilling showed the highest value when calculating the 2,3,7,8-TCDD equivalent (calculated by summing the multiplication results of each congener by its corresponding toxic equivalent

factor (WHO-TEF) (Van den Berg et al., 2006). As for furans, 6 species out of 10 were identified in the grilling sample mainly HxCDF and HpCDF.

The highest concentrations were recorded for PCDF emitted from the diesel generator with also the highest 2,3,7,8-TCDD equivalent. The PCDD/PCDF ratio is generally used to identify emission sources. It was calculated for the different profiles and values are presented in **(Table III-2**).

A lower ratio value for DG was shown in this study (1.16) compared to literature values (3.07-5.73) (Rey et al., 2014). This variance might be assigned to the difference in the generator size and the type of diesel fuel used for the experiment. The wood burning exhibited a higher ratio (3.27) compared to the value reported for rice straw burning (1.1) (Chang et al., 2014) meaning that combustion of wood emits a higher proportion of PCDD compared to PCDF than rice straw.

Table III-2: Experimental source diagnostics ratios and comparison with the literature (in brackets) when available

	Wood burning	Diesel generator	Cooking		
			Beef grilling	Chicken grilling	General cooking activities
OC/EC ratio	3.4	2.9	45	621	18
n-alkanes diagnostic indexes					
Overall CPI	4.00	0.94	4.48	2.53	1.34
Wax%	57.5%	1.4%	64.7%	46.1%	22.1%
PAHs diagnostic ratios					
Fla/(Fla+Pyr)	0.49 (0.2-0.7)[a]	0.24 (0.28)[b]	0.51 (0.47)[a]	0.56 (0.47)[a]	0.47 (0.53)[c]
B[a]An/(B[a]An+Chr)	0.57 (>0.37) [e]	0.41 (0.5)[b]	0.46 (0.47)[a]	0.43 (0.47)[a]	0.44 (0.28; 0.4)[c,f]
InPy/(InPy+B[ghi]Pe)	0.45 (>0.5)[d]	0.18 (0.68)[b]	0.56 (0.50)[a]	0.45 (0.50)[a]	-
Anth/(Anth+Phe)	0.70 (>0.1)[e]	0.85 (0.05)[b]	0.75 (>0.1)[e]	0.73 (>0.1)[e]	-
PCDD/PCDF ratio	3.27	1.16	1.95		2.44
Water-soluble ions ratios					
K^+/EC	0.36	0.01	1.32	3.61	0.12
K^+/OC	0.12	0.003	0.03	0.01	0.007
Cl^-/SO_4^{2-}	3.96	-	1.34	0.4	-

[a](Vicente et al., 2012), [b](Liang et al., 2005), [c](See and Balasubramanian, 2008), [d](Tobiszewski and Namieśnik, 2012), [e](Gong et al., 2019), [f](Wei See et al., 2006)

This ratio was also calculated for other sources present in the literature: it ranged between 0.26 and 0.33 in a road traffic environment (Rahman et al., 2014), between 0.33 and 0.46 in an industrial area (Bi et al., 2020), and 0.27-0.67 for solid waste incineration (Li et al., 2021). Charcoal combustion showed PCDD/PCDF ratio (1.95) lower than the one reported for the wood burning (3.27). A similar observation was made by Lee et al. (2005) showing higher PCDD/PCDF emission factor ratio for domestic biomass burning (4.7) compared to coal combustion (2.1). Up to our knowledge, there is no PCDD/F data reported for oil cooking activities. The ratio in our study showed that the oil cooking source emits 2.4 times more PCDD than PCDF. The most abundant DL-PCB was PCB 118 accounting for 46%, 51%, 52%, and 52% of the total PCB in charcoal grilling, WB, GCA, and DG respectively followed by PCB 105. The total TEQ value expressed in pg/g of OC was the highest for DG, followed by charcoal grilling, GCA, and WB.

2.3 Water-soluble ions (WSI) composition

Water-soluble ions have the highest share of $PM_{2.5}$ in the GCA profile (22%), then WB (18%), then DG and BG (7%), and finally CG (2%) **(Fig. III-2)**.

GCA profile showed more than 85% of the ionic mass for SO_4^{2-}, NO_3^-, and NH_4^+. This result was also observed by See and Balasubramanian (2008) for oil deep-frying activities. Although WSI contributed more to the total $PM_{2.5}$ mass in BG compared to CG, they have a similar distribution in ions with K^+, SO_4^{2-}, and Cl^- having the highest contribution and accounting for more than 70% of the total WSI mass. McDonald et al. (2003) also reported these ions as the most abundant in the fumes of meat charbroiling. The high amounts of K^+ and Cl^- in both charcoal and wood burning are mainly due to their abundance in the fluid of plants ; they volatilize during the combustion process and, after condensation or nucleation reaction (Alves et al., 2010), become in the particulate phase. In the three cooking profiles, Ca^{2+} ions could mainly be emitted from the cooking utensils and raw materials (Sun et al., 2020).

As for wood burning, K^+ and Cl^- have the highest share of WSI (74%) followed by SO_4^{2-} and Ca^{2+}. These ions account for nearly 92% of the total soluble ions in the profile. Our results are consistent with those reported for other biomass burning experiments (86-94%) (Chantara et al., 2019; Sun et al., 2019).

The main water-soluble ions in diesel particulate matter were Ca^{2+}, SO_4^{2-}, and NO_3^-. SO_4^{2-} only accounted for 27% of the total WSI mass which is lower than the 80% value reported by Sothea and Kim Oanh (2019) for a 25 kVA and a 110 kVA diesel backup generators. However, the

main difference between the two experiments remains in the diesel sulfur content. The diesel used by the latter study was assumed to have the same quality as the diesel oil used for transportation and thus a sulfur content of 0.2% (2,000 ppm). On the other hand, since 2017, Lebanon implemented stricter laws on the quality of the imported automotive diesel by decreasing the sulfur content to 10 ppm and allowing higher sulfur content diesel to be delivered only to the big industries (ex. cement plants, fertilizer industry, etc.) and power plants. Despite that law enforcement is not always guaranteed, the sulfur content in automotive diesel did not exceed the 200-300 ppm since 2014-2015. This difference in the fuel oil sulfur content might explain the chemical composition differences since it has been established that sulfate in diesel particulate matter is function of the engine operating mode and the fuel sulfur content (Saiyasitpanich et al., 2005).

Different diagnostic ratios including water-soluble ions are used to distinguish emission sources. For instance, K^+/EC and K^+/OC ratios can be used to distinguish biomass burning from fossil fuel combustion. The ratios calculated from this study can be used as marker values for the sources and are reported in **Table III-2**.

DG exhibited low K^+/EC and K^+/OC (0.01 and 0.003, respectively) compared to WB (0.36 and 0.12, respectively). These findings were also reported by Benetello et al. (2017) that assigned a range of K^+/EC and K^+/OC at the source of 0.025-0.09 and 0.01 for fuel burning, respectively and 0.21-0.46 and 0.1 for biomass burning, respectively. Additionally, the Cl^-/SO_4^{2-} ratio might be used to differentiate wood and coal combustion. In this study, higher values were observed for biomass burning (3.96) compared to coal combustion (0.4-1.34) and indicate that SO_4^{2-} is less emitted from WB compared to CG and BG.

2.4 Elemental composition

Twenty-nine analyzed elements in the profiles present different fractions of the total mass: the lowest total contribution of the considered elements was observed for CG which accounted to 1.6%, followed by DG (7%), then BG (9%), WB (10%), and GCA (14%) **(Appendix A - Figure S1).**

Ca is the most abundant element in the DG profile contributing to 56% of the sum of metals and is classified as the third most abundant species after OC and EC contributing to 3.5% of the total mass. Other metals such as Fe, Al, Mg, K, and Zn were also abundant in the profile sharing 25% of their sum. These results are consistent with the ones from the composition of particles emitted by a lab-designed engine (Mg, Na, Al, K, Ca, Fe, Zn) (Kerminen et al., 1997),

and in diesel PM composition reported by Yang et al. (1998) including Fe, Al, Ca, Na, Cr, Ba, Ni, Mg, and K. However, some differences exist between the three profiles that might be caused by the presence of organometallic additives in the diesel, the lubricating oil quality, and the operating conditions. For instance, elements such as Ca and Zn can be used as markers of total lubrication oil consumption and their contribution to the total mass of elements may vary depending on its quality (Sippula et al., 2014).

In the WB profile, K shares 50% of the mass of the 29 analyzed elements and is identified as a major metal in biomass burning since it is a major constituent of plants (Adam et al., 2021). The other abundant elements in descending order were Ca, Al, S, Na, Fe, and Mg. These findings were also observed during biomass burning events and in ash samples in a simulated open combustion chamber (Akbari et al., 2021). Fe is considered as an important component in vegetation and intervenes in physiological processes while Mg and Na play a major role in the metabolism and the structure of the plant respectively (Brownell, 1979; Alves, 2008). Other elements accumulated by trees were also present in WB such as Cu, Pb, Ti, Zn, and Mn.

Even though the total mass fraction of elements differs between BG, CG, and GCA, the most abundant elements observed are S, Ca, Na, K, Al, Mg, and Fe. They account for about 98% of the measured elements despite the cooking method used. Similar observations were made by See and Balasubramanian (2008) showing high content in Ca, Na, Fe, Mg, and Al for different cooking styles. This study showed sulfur as the dominant element for GCA in agreement with other residential cooking experiments (Wang et al., 2015; Zhao et al., 2019). This might be due to the addition of organic sulfur compounds such as ethyl mercaptan to liquid natural gas used for the detection of leak.

As for the other metals, Na is attributed to the salts and seasoning added to the food while Ca which has an important contribution in the three cooking profiles could be released from raw materials (Zhang et al., 2017). K showed a considerable abundance in BG and CG and is mainly associated with charcoal combustion (Zhao et al., 2019). Although their contribution is negligible to the total mass of the profile, trace elements are known to have harmful effects on the human health. The GCA profile shows the presence of Pb and Mn that could be emitted from cooking oil (peanut and canola oil) (Zhao et al., 2019). Other trace metals such as Cr, Ni, Cu along with Fe are released from the interaction between the heating source and the stainless steel wok used as cooking utensils in the different cooking profiles (Sun et al., 2020).

3 Conclusions

This study presented a full chemical characterization of 5 $PM_{2.5}$ sources in the East Mediterranean region: hardwood burning, diesel generator, beef and chicken charcoal grilling and general cooking activities. The markers of hardwood burning were OC, EC (with an OC/EC ratio of 3.4), potassium in its ionic and elemental form, and Cl^-, accounting for 90% of the sum of all species. Levoglucosan was the major contributor to organic compounds along with the predominance of high molecular weight n-alkanes, higher PAHs mass per gram of OC compared to the other profiles especially for Fla, Pyr, and B[a]An. The values of the characteristic PAHs ratios were 0.49 for Fla/(Fla+Pyr) and 0.57 for B[a]An/(B[a]An+Chr). The K^+/EC and K^+/OC ratios were used to differentiate wood from fuel combustion and were reported as 0.36 and 0.12 for WB, respectively. The Levoglucosan/OC ratio for the hardwood combustion was found 0.3 in this study.

The major contributors to DG profile were OC and EC accounting for more than 86% with an OC/EC ratio of 2.9, followed by SO_4^{2-}, NO_3^-, Ca, Ca^{2+}, and S. N-alkanes showed a high contribution to OC in this profile with a profile pattern maximizing at C_{20}-C_{21}, a CPI value close to unity (0.9) and very low wax percentage (1.4%). Pyr was the most abundant compound between PAHs. The PAHs ratios reported for the diesel combustion in our study were 0.24 for Fla/(Fla+Pyr), 0.41 for B[a]An/(B[a]An+Chr), and 0.18 for InPy/(InPy+B[ghi]Pe). The profile also recorded the highest relative share of PCDD/F and DL-PCBs compared to the other profiles. The K^+/EC and K^+/OC ratios were 0.01 and 0.003, respectively.

The three cooking profiles showed similarities with a high contribution of carboxylic acids, especially palmitic and stearic acids, high OC contribution and low EC share. The presence of food with different fat content and composition might increase the share of OC in the chemical profile. Chicken grilling profile recorded the highest OC contribution of 96% of the total sum of species with an OC/EC ratio of 622, followed by EC and Cl^- contributing to more than 1%. Beef grilling profile markers were OC, EC (with an OC/EC ratio of 45), Cl^-, K, NO_3^-, and SO_4^{2-}. For both profiles, C_{25} having the highest contribution to n-alkanes, CPI values between 2 and 5, and high abundance of 4-rings PAHs with Fla/(Fla+Pyr), B[a]An/(B[a]An+Chr), and InPy/(InPy+B[ghi]Pe) close to 0.5 were attributed to the charcoal combustion. The GCA profile presented an OC/EC ratio of 18, an important contribution of SO_4^{2-}, NO_3^-, and NH_4^+ (85%), and a high abundance of Al, Na, and Ca. The n-alkanes pattern maximized at C_{29}, and the major emitted PAHs were B[b]Fl, Pyr, and Chr.

This study is a first in the East Mediterranean and Middle East region presenting an exhaustive characterization of $PM_{2.5}$ from different sources. The results of this study will contribute to further broaden our knowledge of the PM sources in the region by expanding the database for the East Mediterranean - Middle Eastern region. The markers for the profiles along with the different ratios will be of utmost importance for future source apportionment and modeling studies. It might be also interesting to evaluate the impact of using these local profiles on the policy making in the region.

Funding sources

The authors would like to acknowledge the National Council for Scientific Research of Lebanon (CNRS-L) and University of Littoral Côte d'Opale (UCLO) for granting a doctoral fellowship to Marc Fadel. This project was also funded by the Research Council and the Faculty of Sciences at Saint Joseph University of Beirut – Lebanon. The "Unité de Chimie Environnementale et Interactions sur le Vivant" (UCEIV-UR4492) participates in the CLIMIBIO project, which is financially supported by the Hauts-de-France Region Council, the French Ministry of Higher Education and Research, and the European Regional Development Funds. This publication has been also produced within the framework of the EMME-CARE project, which has received funding from the European Union's Horizon 2020 Research and Innovation Programme (under grant agreement no. 856612) and the Cyprus Government.

Acknowledgments

The authors thank MicroPolluants Technologie S.A. (Saint Julien Les Metz, France) for dioxins, furans, and DL-PCBs analysis and Institut Chevreul - Université de Lille for the analysis of metals by ICP-MS. The authors would also like to thank Dorothée Dewaele (Centre Commun de Mesures, ULCO) for her help in the ICP-AES analysis, Amaury Kasprowiak for his help in the ionic chromatography analysis, and also Mariana Farhat for her help in the organic species analysis.

References:

Abdullahi, K.L., Delgado-Saborit, J.M., Harrison, R.M., 2013. Emissions and indoor concentrations of particulate matter and its specific chemical components from cooking: A review. Atmos Environ 71, 260-294, https://doi.org/10.1016/j.atmosenv.2013.01.061.

Adam, M.G., Tran, P.T.M., Bolan, N., Balasubramanian, R., 2021. Biomass burning-derived airborne particulate matter in Southeast Asia: A critical review. J. Hazard. Mater. 407, 124760, https://doi.org/10.1016/j.jhazmat.2020.124760.

Akbari, M.Z., Thepnuan, D., Wiriya, W., Janta, R., Pansompong, P., Hemwan, P., Charoenpanyanet, A., Chantara, S., 2021. Emission factors of metals bound with $PM_{2.5}$ and ashes from biomass burning simulated in an open-system combustion chamber for estimation of open burning emissions. Atmos. Pollut. Res. 12, 13-24, https://doi.org/10.1016/j.apr.2021.01.012.

Alves, C., 2008. Characterisation of solvent extractable organic constituents in atmospheric particulate matter: An overview. An. Acad. Bras. Cienc. 80, 21-82, 10.1590/S0001-37652008000100003.

Alves, C., Nunes, T., Moreira, R., Rocha, S., 2014. Carbonaceous particles emitted from cooking activities in Portugal.

Alves, C.A., Gonçalves, C., Pio, C.A., Mirante, F., Caseiro, A., Tarelho, L., Freitas, M.C., Viegas, D.X., 2010. Smoke emissions from biomass burning in a Mediterranean shrubland. Atmos Environ 44, 3024-3033, https://doi.org/10.1016/j.atmosenv.2010.05.010.

Bano, S., Pervez, S., Chow, J.C., Matawle, J.L., Watson, J.G., Sahu, R.K., Srivastava, A., Tiwari, S., Pervez, Y.F., Deb, M.K., 2018. Coarse particle ($PM_{10–2.5}$) source profiles for emissions from domestic cooking and industrial process in Central India. Sci. Total Environ. 627, 1137-1145, https://doi.org/10.1016/j.scitotenv.2018.01.289.

Belis, C.A., Favez, O., Mircea, M., Diapouli, E., Manousakas, M.I., Vratolis, S., Gilardoni, S., Paglione, M., Decesari, S., Mocnik, G., Mooibroek, D., Salvador, P., Takahama, S., Vecchi, R., Paatero, P., European, C., Joint Research, C., 2019. European guide on air pollution source apportionment with receptor models : revised version 2019.

Benetello, F., Squizzato, S., Hofer, A., Masiol, M., Khan, M.B., Piazzalunga, A., Fermo, P., Formenton, G.M., Rampazzo, G., Pavoni, B., 2017. Estimation of local and external contributions of biomass burning to $PM_{2.5}$ in an industrial zone included in a large urban settlement. Environ Sci Pollut Res Int 24, 2100-2115, 10.1007/s11356-016-7987-0.

Bi, C., Chen, Y., Zhao, Z., Li, Q., Zhou, Q., Ye, Z., Ge, X., 2020. Characteristics, sources and health risks of toxic species (PCDD/Fs, PAHs and heavy metals) in $PM_{2.5}$ during fall and winter in an industrial area. Chemosphere 238, 124620, https://doi.org/10.1016/j.chemosphere.2019.124620.

Borgie, M., Dagher, Z., Ledoux, F., Verdin, A., Cazier, F., Martin, P., Hachimi, A., Shirali, P., Greige-Gerges, H., Courcot, D., 2015. Comparison between ultrafine and fine particulate matter collected in Lebanon: Chemical characterization, in vitro cytotoxic effects and metabolizing enzymes gene expression in human bronchial epithelial cells. Environ. Pollut. 205, 250-260, https://doi.org/10.1016/j.envpol.2015.05.027.

Bove, M.C., Massabò, D., Prati, P., 2018. PMF5.0 vs. CMB8.2: An inter-comparison study based on the new European SPECIEUROPE database. Atmos Res 201, 181-188, https://doi.org/10.1016/j.atmosres.2017.10.021.

Brownell, P.F., 1979. Sodium as an essential micronutrient element for plants and its possible role in metabolism. Academic Press, London; New York.

Cavalli, F., Viana, M., Yttri, K.E., Genberg, J., Putaud, J.P., 2010. Toward a standardised thermal-optical protocol for measuring atmospheric organic and elemental carbon: the EUSAAR protocol. Atmos. Meas. Tech. 3, 79-89, 10.5194/amt-3-79-2010.

Chang, S.-S., Lee, W.-J., Holsen, T.M., Li, H.-W., Wang, L.-C., Chang-Chien, G.-P., 2014. Emissions of polychlorinated-p-dibenzo dioxin, dibenzofurans (PCDD/Fs) and polybrominated diphenyl ethers (PBDEs) from rice straw biomass burning. Atmos Environ 94, 573-581, https://doi.org/10.1016/j.atmosenv.2014.05.067.

Chantara, S., Thepnuan, D., Wiriya, W., Prawan, S., Tsai, Y.I., 2019. Emissions of pollutant gases, fine particulate matters and their significant tracers from biomass burning in an open-system combustion chamber. Chemosphere 224, 407-416, https://doi.org/10.1016/j.chemosphere.2019.02.153.

Chelani, A.B., Gajghate, D.G., Devotta, S., 2008. Source Apportionment of PM_{10} in Mumbai, India Using CMB Model. Bull. Environ. Contam. Toxicol. 81, 190-195, 10.1007/s00128-008-9453-2.

Chow, J.C., Watson, J.G., Kuhns, H., Etyemezian, V., Lowenthal, D.H., Crow, D., Kohl, S.D., Engelbrecht, J.P., Green, M.C., 2004. Source profiles for industrial, mobile, and area sources in the Big Bend Regional Aerosol Visibility and Observational study. Chemosphere 54, 185-208, https://doi.org/10.1016/j.chemosphere.2003.07.004.

Colombi, C., Gianelle, V., Belis, C., Larsen, B., 2010. Determination of local source profile for soil dust, brake dust and biomass burning sources. Chemical Engineering Transactions 22, 233-238, 10.3303/CET1022038.

El Haddad, I., Marchand, N., Dron, J., Temime-Roussel, B., Quivet, E., Wortham, H., Jaffrezo, J.L., Baduel, C., Voisin, D., Besombes, J.L., Gille, G., 2009. Comprehensive primary particulate organic characterization of vehicular exhaust emissions in France. Atmos Environ 43, 6190-6198, https://doi.org/10.1016/j.atmosenv.2009.09.001.

Essid, M.Y., 2012. Chapter 2. History of Mediterranean food. MediTERRA 2012 (english). Presses de Sciences Po, Paris, pp. 51-69.

Fadel, M., Ledoux, F., Farhat, M., Kfoury, A., Courcot, D., Afif, C., 2021. $PM_{2.5}$ characterization of primary and secondary organic aerosols in two urban-industrial areas in the East Mediterranean. J Environ Sci 101, 98-116, https://doi.org/10.1016/j.jes.2020.07.030.

Fine, P., Cass, G., Simoneit, B., 2004. Chemical characterization of fine particle emissions from the wood stove combustion of prevalent United States tree species. Environmental Engineering Science - ENVIRON ENG SCI 21, 705-721, 10.1089/ees.2004.21.705.

Giannoni, M., Martellini, T., Del Bubba, M., Gambaro, A., Zangrando, R., Chiari, M., Lepri, L., Cincinelli, A., 2012. The use of levoglucosan for tracing biomass burning in $PM_{2.5}$ samples in Tuscany (Italy). Environ. Pollut. 167, 7-15, https://doi.org/10.1016/j.envpol.2012.03.016.

Gong, X., Shen, Z., Zhang, Q., Zeng, Y., Sun, J., Ho, S.S.H., Lei, Y., Zhang, T., Xu, H., Cui, S., Huang, Y., Cao, J., 2019. Characterization of polycyclic aromatic hydrocarbon (PAHs)

source profiles in urban $PM_{2.5}$ fugitive dust: A large-scale study for 20 Chinese cites. Sci. Total Environ. 687, 188-197, https://doi.org/10.1016/j.scitotenv.2019.06.099.

Gupta, A.K., Karar, K., Srivastava, A., 2007. Chemical mass balance source apportionment of PM10 and TSP in residential and industrial sites of an urban region of Kolkata, India. J. Hazard. Mater. 142, 279-287, https://doi.org/10.1016/j.jhazmat.2006.08.013.

He, L.-Y., Hu, M., Huang, X.-F., Yu, B.-D., Zhang, Y.-H., Liu, D.-Q., 2004. Measurement of emissions of fine particulate organic matter from Chinese cooking. Atmos Environ 38, 6557-6564, https://doi.org/10.1016/j.atmosenv.2004.08.034.

Hopke, P.K., 2016. Review of receptor modeling methods for source apportionment. J. Air Waste Manage. Assoc. 66, 237-259, 10.1080/10962247.2016.1140693.

Kerminen, V.-M., Mäkelä, T.E., Ojanen, C.H., Hillamo, R.E., Vilhunen, J.K., Rantanen, L., Havers, N., von Bohlen, A., Klockow, D., 1997. Characterization of the Particulate Phase in the Exhaust from a Diesel Car. Environ. Sci. Technol. 31, 1883-1889, 10.1021/es960520n.

Kfoury, A., Ledoux, F., Roche, C., Delmaire, G., Roussel, G., Courcot, D., 2016. $PM_{2.5}$ source apportionment in a French urban coastal site under steelworks emission influences using constrained non-negative matrix factorization receptor model. J Environ Sci 40, 114-128, https://doi.org/10.1016/j.jes.2015.10.025.

Klimont, Z., Kupiainen, K., Heyes, C., Purohit, P., Cofala, J., Rafaj, P., Borken-Kleefeld, J., Schoepp, W., 2016. Global anthropogenic emissions of particulate matter including black carbon. Atmospheric Chemistry and Physics Discussions 2016, 1-72, 10.5194/acp-2016-880.

Kostenidou, E., Kaltsonoudis, C., Tsiflikiotou, M., Louvaris, E., Russell, L., Pandis, S., 2013. Burning of olive tree branches: A major organic aerosol source in the Mediterranean. Atmospheric Chemistry & Physics Discussions 13, 7223-7266, 10.5194/acpd-13-7223-2013.

Ledoux, F., Courcot, L., Courcot, D., Aboukaïs, A., Puskaric, E., 2006a. A summer and winter apportionment of particulate matter at urban and rural areas in northern France. Atmos Res 82, 633-642, https://doi.org/10.1016/j.atmosres.2006.02.019.

Ledoux, F., Laversin, H., Courcot, D., Courcot, L., Zhilinskaya, E.A., Puskaric, E., Aboukaïs, A., 2006b. Characterization of iron and manganese species in atmospheric aerosols from anthropogenic sources. Atmos Res 82, 622-632, https://doi.org/10.1016/j.atmosres.2006.02.018.

Lee, R.G.M., Coleman, P., Jones, J.L., Jones, K.C., Lohmann, R., 2005. Emission Factors and Importance of PCDD/Fs, PCBs, PCNs, PAHs and PM_{10} from the Domestic Burning of Coal and Wood in the U.K. Environ. Sci. Technol. 39, 1436-1447, 10.1021/es048745i.

Li, M., Zhou, Y., Wang, G., Zhu, G., Zhou, X., Gong, H., Sun, J., Wang, L., Jinsong, L., 2021. Evaluation of atmospheric sources of PCDD/Fs, PCBs and PBDEs around an MSWI plant using active and passive air samplers. Chemosphere 274, 129685, https://doi.org/10.1016/j.chemosphere.2021.129685.

Liang, F., Lu, M., Keener, T.C., Liu, Z., Khang, S.J., 2005. The organic composition of diesel particulate matter, diesel fuel and engine oil of a non-road diesel generator. J. Environ. Monit. 7, 983-988, 10.1039/b504728e.

Liu, Y., Zhang, W., Bai, Z., Yang, W., Zhao, X., Han, B., Wang, X., 2017. China Source Profile Shared Service (CSPSS): The Chinese $PM_{2.5}$ database for source profiles. Aerosol and Air Quality Research 17, 1501-1514, 10.4209/aaqr.2016.10.0469.

McDonald, J., Zielinska, B., Fujita, E., Sagebiel, J., Chow, J., Watson, J., 2003. Emissions from Charbroiling and Grilling of Chicken and Beef. J. Air Waste Manage. Assoc. 53, 185-194, 10.1080/10473289.2003.10466141.

Oanh, N.T.K., Reutergårdh, L.B., Dung, N.T., 1999. Emission of polycyclic aromatic hydrocarbons and particulate matter from domestic combustion of selected fuels. Environ. Sci. Technol. 33, 2703-2709, 10.1021/es980853f.

Oros, D.R., Simoneit, B.R., 2001. Identification and emission factors of molecular tracers in organic aerosols from biomass burning Part 2. Deciduous trees. Applied geochemistry : journal of the International Association of Geochemistry and Cosmochemistry. 16, 1545-1565

Pernigotti, D., Belis, C.A., Spanò, L., 2016. SPECIEUROPE: The European data base for PM source profiles. Atmos. Pollut. Res. 7, 307-314, 10.1016/j.apr.2015.10.007.

Rahman, M.M., Kim, K.-H., Brown, R.J.C., Bae, I.S., Park, C.G., 2014. PCDD and PCDF concentrations in a traffic tunnel environment. Sci. Total Environ. 493, 773-780, https://doi.org/10.1016/j.scitotenv.2014.06.073.

Ravindra, K., Sokhi, R., Vangrieken, R., 2008. Atmospheric polycyclic aromatic hydrocarbons: Source attribution, emission factors and regulation. Atmos Environ 42, 2895-2921, 10.1016/j.atmosenv.2007.12.010.

Rey, M.D., Font, R., Aracil, I., 2014. PCDD/F emissions from light-duty diesel vehicles operated under highway conditions and a diesel-engine based power generator. J. Hazard. Mater. 278, 116-123, https://doi.org/10.1016/j.jhazmat.2014.05.101.

Riffault, V., Arndt, J., Marris, H., Mbengue, S., Setyan, A., Alleman, L.Y., Deboudt, K., Flament, P., Augustin, P., Delbarre, H., Wenger, J., 2015. Fine and ultrafine particles in the vicinity of industrial activities: A Review. Crit Rev Environ Sci Technol 45, 2305-2356, 10.1080/10643389.2015.1025636.

Rogge, W.F., Hildemann, L.M., Mazurek, M.A., Cass, G.R., Simoneit, B.R.T., 1991. Sources of fine organic aerosol. 1. Charbroilers and meat cooking operations. Environ. Sci. Technol. 25, 1112-1125, 10.1021/es00018a015.

Rogge, W.F., Hildemann, L.M., Mazurek, M.A., Cass, G.R., Simoneit, B.R.T., 1993. Sources of fine organic aerosol. 2. Noncatalyst and catalyst-equipped automobiles and heavy-duty diesel trucks. Environ. Sci. Technol. 27, 636-651, 10.1021/es00041a007.

Saiyasitpanich, P., Lu, M., Keener, T.C., Liang, F., Khang, S.-J., 2005. The effect of diesel fuel sulfur content on particulate matter emissions for a nonroad diesel generator. J. Air Waste Manage. Assoc. 55, 993-998, 10.1080/10473289.2005.10464685.

Salameh, T., Afif, C., Sauvage, S., Borbon, A., Locoge, N., 2014. Speciation of non-methane hydrocarbons (NMHCs) from anthropogenic sources in Beirut, Lebanon. Environmental science and pollution research international 21, 10.1007/s11356-014-2978-5.

Schauer, J.J., Kleeman, M.J., Cass, G.R., Simoneit, B.R.T., 2002. Measurement of emissions from air pollution sources. 4. C1−C27 Organic Compounds from Cooking with Seed Oils. Environ. Sci. Technol. 36, 567-575, 10.1021/es002053m.

See, S.W., Balasubramanian, R., 2008. Chemical characteristics of fine particles emitted from different gas cooking methods. Atmos Environ 42, 8852-8862, https://doi.org/10.1016/j.atmosenv.2008.09.011.

Shah, S.D., Cocker Iii, D.R., Johnson, K.C., Lee, J.M., Soriano, B.L., Wayne Miller, J., 2006. Emissions of regulated pollutants from in-use diesel back-up generators. Atmos Environ 40, 4199-4209, https://doi.org/10.1016/j.atmosenv.2005.12.063.

Shen, G., Wang, W., Yang, Y., Ding, J., Xue, M., Min, Y., Zhu, C., Shen, H., Li, W., Wang, B., Wang, R., Wang, X., Tao, S., Russell, A.G., 2011. Emissions of PAHs from Indoor Crop Residue Burning in a Typical Rural Stove: Emission Factors, Size Distributions, and Gas−Particle Partitioning. Environ. Sci. Technol. 45, 1206-1212, 10.1021/es102151w.

Shi, G.-L., Liu, G.-R., Tian, Y.-Z., Zhou, X.-Y., Peng, X., Feng, Y.-C., 2014. Chemical characteristic and toxicity assessment of particle associated PAHs for the short-term anthropogenic activity event: During the Chinese New Year's Festival in 2013. Sci. Total Environ. 482-483, 8-14, https://doi.org/10.1016/j.scitotenv.2014.02.107.

Simon, H., Beck, L., Bhave, P.V., Divita, F., Hsu, Y., Luecken, D., Mobley, J.D., Pouliot, G.A., Reff, A., Sarwar, G., Strum, M., 2010. The development and uses of EPA's SPECIATE database. Atmos. Pollut. Res. 1, 196-206, 10.5094/apr.2010.026.

Simoneit, B.R.T., 2002. Biomass burning — a review of organic tracers for smoke from incomplete combustion. Appl. Geochem. 17, 129-162, https://doi.org/10.1016/S0883-2927(01)00061-0.

Sippula, O., Stengel, B., Sklorz, M., Streibel, T., Rabe, R., Orasche, J., Lintelmann, J., Michalke, B., Abbaszade, G., Radischat, C., Gröger, T., Schnelle-Kreis, J., Harndorf, H., Zimmermann, R., 2014. Particle emissions from a marine engine: chemical composition and aromatic emission profiles under various operating conditions. Environ. Sci. Technol. 48, 11721-11729, 10.1021/es502484z.

Sothea, K., Kim Oanh, N.T., 2019. Characterization of emissions from diesel backup generators in Cambodia. Atmos. Pollut. Res. 10, 345-354, https://doi.org/10.1016/j.apr.2018.09.001.

Sun, J., Shen, Z., Niu, X., Yu, J., Zhang, Y., Liu, S., Niu, X., Zhang, Y., Xu, H., Li, X., Cao, J., 2020. $PM_{2.5}$ source profiles from typical Chinese commercial cooking activities in northern China and its influences on bioreactivity of vascular smooth muscle cells (VSMCs). Atmos Environ 239, 117750, https://doi.org/10.1016/j.atmosenv.2020.117750.

Sun, J., Shen, Z., Zhang, Y., Zhang, Q., Lei, Y., Huang, Y., Niu, X., Xu, H., Cao, J., Ho, S.S.H., Li, X., 2019. Characterization of $PM_{2.5}$ source profiles from typical biomass burning of maize straw, wheat straw, wood branch, and their processed products (briquette and charcoal) in China. Atmos Environ 205, 36-45, https://doi.org/10.1016/j.atmosenv.2019.02.038.

Tobiszewski, M., Namieśnik, J., 2012. PAH diagnostic ratios for the identification of pollution emission sources. Environ. Pollut. 162, 110-119, https://doi.org/10.1016/j.envpol.2011.10.025.

Van den Berg, M., Birnbaum, L.S., Denison, M., De Vito, M., Farland, W., Feeley, M., Fiedler, H., Hakansson, H., Hanberg, A., Haws, L., Rose, M., Safe, S., Schrenk, D., Tohyama, C., Tritscher, A., Tuomisto, J., Tysklind, M., Walker, N., Peterson, R.E., 2006. The 2005 World Health Organization reevaluation of human and Mammalian toxic equivalency factors for dioxins and dioxin-like compounds. Toxicol. Sci. 93, 223-241, https://doi.org/10.1093/toxsci/kfl055.

Viana, M., Kuhlbusch, T.A.J., Querol, X., Alastuey, A., Harrison, R.M., Hopke, P.K., Winiwarter, W., Vallius, M., Szidat, S., Prévôt, A.S.H., Hueglin, C., Bloemen, H., Wåhlin, P., Vecchi, R., Miranda, A.I., Kasper-Giebl, A., Maenhaut, W., Hitzenberger, R., 2008. Source apportionment of particulate matter in Europe: A review of methods and results. J. Aerosol Sci. 39, 827-849, 10.1016/j.jaerosci.2008.05.007.

Vicente, A., Alves, C., Monteiro, C., Nunes, T., Mirante, F., Cerqueira, M., Calvo, A., Pio, C., 2012. Organic speciation of aerosols from wildfires in central Portugal during summer 2009. Atmos Environ 57, 186-196, https://doi.org/10.1016/j.atmosenv.2012.04.030.

Vicente, E.D., Vicente, A., Evtyugina, M., Carvalho, R., Tarelho, L.A.C., Oduber, F.I., Alves, C., 2018. Particulate and gaseous emissions from charcoal combustion in barbecue grills. Fuel Process. Technol. 176, 296-306, https://doi.org/10.1016/j.fuproc.2018.03.004.

Waked, A., Afif, C., Brioude, J., Formenti, P., Chevaillier, S., Haddad, I.E., Doussin, J.-F., Borbon, A., Seigneur, C., 2013. Composition and source apportionment of organic aerosol in Beirut, Lebanon, during winter 2012. Aerosol Sci. Technol. 47, 1258-1266, 10.1080/02786826.2013.831975.

Waked, A., Afif, C., Formenti, P., Chevaillier, S., El-Haddad, I., Doussin, J.-F., Borbon, A., Seigneur, C., 2014. Characterization of organic tracer compounds in $PM_{2.5}$ at a semi-urban site in Beirut, Lebanon. Atmos Res 143, 85-94, 10.1016/j.atmosres.2014.02.006.

Waked, A., Afif, C., Seigneur, C., 2012. An atmospheric emission inventory of anthropogenic and biogenic sources for Lebanon. Atmos Environ 50, 88-96, https://doi.org/10.1016/j.atmosenv.2011.12.058.

Wang, G., Cheng, S., Wei, W., Wen, W., Wang, X., Yao, S., 2015. Chemical Characteristics of Fine Particles Emitted from Different Chinese Cooking Styles. Aerosol and Air Quality Research 15, 2357-2366, 10.4209/aaqr.2015.02.0079.

Weber, S., Salameh, D., Albinet, A., Alleman, L., Waked, A., Besombes, J.-L., Jacob, V., Guillaud, G., Meshbah, B., Rocq, B., Hulin, A., Dominik-Sègue, M., Chrétien, E., Jaffrezo, J.-L., Favez, O., 2019. Comparison of PM_{10} Sources Profiles at 15 French Sites Using a Harmonized Constrained Positive Matrix Factorization Approach. Atmosphere 10, 10.3390/atmos10060310.

Wei See, S., Karthikeyan, S., Balasubramanian, R., 2006. Health risk assessment of occupational exposure to particulate-phase polycyclic aromatic hydrocarbons associated with Chinese, Malay and Indian cooking. J. Environ. Monit. 8, 369-376, 10.1039/B516173H.

Yang, H.-H., Lee, W.-J., Chen, S.-J., Lai, S.-O., 1998. PAH emission from various industrial stacks. J. Hazard. Mater. 60, 159-174, https://doi.org/10.1016/S0304-3894(98)00089-2.

Yilmaz, N., Davis, S.M., 2016. Polycyclic aromatic hydrocarbon (PAH) formation in a diesel engine fueled with diesel, biodiesel and biodiesel/n-butanol blends. Fuel 181, 729-740, https://doi.org/10.1016/j.fuel.2016.05.059.

Zhang, N., Han, B., He, F., Xu, J., Zhao, R., Zhang, Y., Bai, Z., 2017. Chemical characteristic of $PM_{2.5}$ emission and inhalational carcinogenic risk of domestic Chinese cooking. Environ. Pollut. 227, 24-30, https://doi.org/10.1016/j.envpol.2017.04.033.

Zhao, Y., Chen, C., Zhao, B., 2019. Emission characteristics of $PM_{2.5}$-bound chemicals from residential Chinese cooking. Building and Environment 149, 623-629, https://doi.org/10.1016/j.buildenv.2018.12.060.

Zhao, Y., Hu, M., Slanina, S., Zhang, Y., 2007a. Chemical compositions of fine particulate organic matter Emitted from Chinese Cooking. Environ. Sci. Technol. 41, 99-105, 10.1021/es0614518.

Zhao, Y., Hu, M., Slanina, S., Zhang, Y., 2007b. The molecular distribution of fine particulate organic matter emitted from Western-style fast food cooking. Atmos Environ 41, 8163-8171, https://doi.org/10.1016/j.atmosenv.2007.06.029.

Article 2: $PM_{2.5}$ characterization of primary and secondary organic aerosols in two urban-industrial areas in the East Mediterranean

Marc Fadel[1,2], Frédéric Ledoux[2], Mariana Farhat[1], Adib Kfoury[3], Dominique Courcot[2], Charbel Afif [1,4,]*

1. Emissions, Measurements, and Modeling of the Atmosphere (EMMA) Laboratory, CAR, Faculty of Sciences, Saint Joseph University, Beirut, Lebanon
2. Unité de Chimie Environnementale et Interactions sur le Vivant, UCEIV UR4492, FR CNRS 3417, University of Littoral Côte d′Opale (ULCO), Dunkerque, France
3. Department of Environmental Sciences, University of Balamand, Al Kourah, Lebanon
4. Climate and Atmosphere Research Center, The Cyprus Institute, Nicosia, Cyprus

*Corresponding author. charbel.afif@usj.edu.lb (Charbel Afif)

Published in Journal of Environmental Sciences: *Fadel, M., F. Ledoux, M. Farhat, A. Kfoury, D. Courcot and C. Afif (2021). "$PM_{2.5}$ characterization of primary and secondary organic aerosols in two urban-industrial areas in the East Mediterranean." Journal of Environmental Sciences 101: 98-116. https://doi.org/10.1016/j.jes.2020.07.030*

Abstract

Primary and secondary organic aerosols in $PM_{2.5}$ were investigated over a one-year campaign at Zouk Mikael and Fiaa, Lebanon. The n-alkanes concentrations were quite similar at both sites (26-29 ng/m^3) and mainly explained by anthropogenic emissions rather than natural ones. The concentrations of total Polycyclic Aromatic Hydrocarbons (PAHs) were nearly three times higher at Zouk Mikael (2.56 ng/m^3) compared to Fiaa (0.95 ng/m^3), especially for indeno[1,2,3-c,d]pyrene linked to the presence of the power plant. A characteristic indeno[1,2,3-c,d]pyrene/(indeno[1,2,3-c,d]pyrene + benzo[g,h,i]perylene) ratio in the range 0.8-1.0 was determined for heavy fuel oil combustion from the power plant. Fatty acids and hopanes were also investigated and were assigned to cooking activities and vehicular emissions, respectively. Phthalates were identified for the first time in Lebanon with high concentrations at Zouk and Fiaa (106.88 and 97.68 ng/m^3 respectively). Moreover, the biogenic secondary aerosols revealed higher concentrations in summer. The total terpene concentration varied between 131 ng/m^3 at Zouk Mikael in winter to 469 ng/m^3 at Fiaa in summer. Additionally, the concentrations of the dicarboxylic acids especially for adipic and phthalic acids were more

influenced by anthropogenic sources. The analysis of molecular markers and diagnostic ratios indicated that the sites were strongly affected by anthropogenic sources such as waste open burning, diesel private generators, cooking activities, road transport, power plant, and industrial emissions. Moreover, results showed different pattern during winter and summer seasons. Whereas higher concentrations of biogenic markers were clearly encountered during the summer period.

Keywords: $PM_{2.5}$, Secondary organic aerosols, PAHs, Phthalates, Lebanon, Urban-industrial sites.

Introduction

Atmospheric particulate matter (PM) which refers to a mixture of solid particles and liquid droplets suspended in air, is one of the most challenging issues in the environmental field nowadays due to its chemical complexity, its measurement, and its source apportionment leading to air quality management (Seinfeld and Pandis, 2016). Recent studies have shown that the premature mortality rate associated with exposure to ambient air pollution reached 8.8 million per year (Lelieveld et al., 2020) emphasizing on the seriousness of the human health hazards (Anderson et al., 2012; WHO, 2013; Zaheer et al., 2018). Due to their very small size, $PM_{2.5}$ which are particles having an equivalent aerodynamic diameter less than 2.5 µm, have drawn much attention. Not only they can penetrate deeply into the lungs, but also they can be retained inside and induce respiratory (Xing et al., 2016) and cardiovascular diseases (Du et al., 2016).

The organic aerosol (OA) can contribute up to 50% to the total $PM_{2.5}$ dry mass (De Gouw and Jimenez, 2009) which can be divided into Primary (POA) and Secondary (SOA) Organic Aerosols. Primary organic compounds can serve as molecular markers of a specific source of pollution such as hopanes for vehicular emissions (Rogge et al., 1996), fatty acids for cooking activities (Robinson et al., 2006), PAHs for fossil and non-fossil fuel combustion (Mastral et al., 2003). In addition, products of oxidation of different terpenes (α-pinene, isoprene and β-caryophyllene) have been used to characterize and quantify the biogenic SOA (Kleindienst et al., 2007).

Lebanon, a Middle Eastern Mediterranean country, with a population of more than 6 million in the last few years, faces some important pollution events. Episodically, the country is affected by long range transport of dust from deserts (Borgie et al., 2016), but the main sources of

pollution are local, especially in winter (Waked et al., 2013). Air quality in Lebanon is heavily affected by road transport emissions caused by the absence of the public transportation system. The road transport sector is the main source of CO, NO_x and Non-Methane Volatile Organic Compounds (NMVOC) (Waked and Afif, 2012; Salameh et al., 2015; Abdallah et al., 2020). Moreover, since the national electricity company is unable to provide electricity 24/7, private diesel generators fill the gap with no law enforcement on stack emissions (Waked et al., 2012). On the other hand, based on the 2010 national inventory, the main emitter of PM is the industries followed by others like the transport and the power generation sectors. Finally, the population growth hypothesis along with the refugees displacement has led to an important residential solid waste generation that caused , in 2017, a substantial increase in open burning of waste in many parts of the country (Abbas et al., 2019).

Main air pollution studies conducted in Lebanon focused on the capital Beirut (Afif et al., 2008; Daher et al., 2013; Salameh et al., 2015). Studies on PM conducted in Lebanon generally focused on the inorganic composition (Kfoury et al., 2009; Yammine et al., 2010; Jaafar et al., 2014), and fewer examined certain organic families such as PAHs in urban areas (Daher et al., 2013; Borgie et al., 2016; Badran et al., 2020). Furthermore, Baalbaki et al. (2018) studied the PAH concentrations in PM_{10} samples at a site in Zouk Mikael and showed higher values compared to two other urban sites in Beirut. Melki et al. (2017) presented the difference of PAHs and alkanes concentrations and corresponding ratios between a site under industrial influence and a rural one in the Northern region of Lebanon. All the studies done on the $PM_{2.5}$ concentration reported values exceeding the WHO daily guideline (25 $\mu g/m^3$) and sometimes double or triple this value during dust storm events (Jaafar et al., 2014). A more complete study of the detailed organic characterization in summer and winter has also been performed in a semi-urban area in Beirut (Waked et al., 2013; Waked et al., 2014) measuring for the first time SOA in Lebanon.

Although these studies bring valuable information on air quality, they are limited to certain classes of organic compounds, and a short sampling period of few days to few weeks with a limited number of samples. In this context, this paper will bring a first detailed study of the organic compounds in $PM_{2.5}$ collected over almost one-year period in Lebanon at a mixed industrial and heavy populated site in Zouk Mikael and an industrial-residential site in Chekka region, Fiaa. The present paper will focus on the composition and the seasonal variations of the POA including PAHs, alkanes, hopanes, carboxylic acids, and phthalates as well as the SOA including the oxidation products of α-pinene, isoprene and β-caryophyllene, and dicarboxylic

acids. Some of these compounds, notably phthalates are reported for the first time in Lebanon. In order to identify the possible PM sources in the sampling areas, diagnostic ratios for different classes of compounds were also used. This first one-year study in the East Mediterranean region will help in assessing the impact of the industrial emissions on the organic aerosol composition.

1 Experimental

1.1 Sampling sites

$PM_{2.5}$ was collected at two sites in Lebanon: Zouk Mikael (33°57'57.07''N 35°37'09.46''E) – Mount Lebanon district, 14 km north-east of the capital Beirut, at the rooftop of a residential building (15 m above ground level), and in Chekka region, specifically Fiaa village (34°20'47.8''N 35°47'14.0''E)- Koura district, 60 km north-north-east of Beirut and 10 km southwest of Tripoli **(Fig. III-4)**.

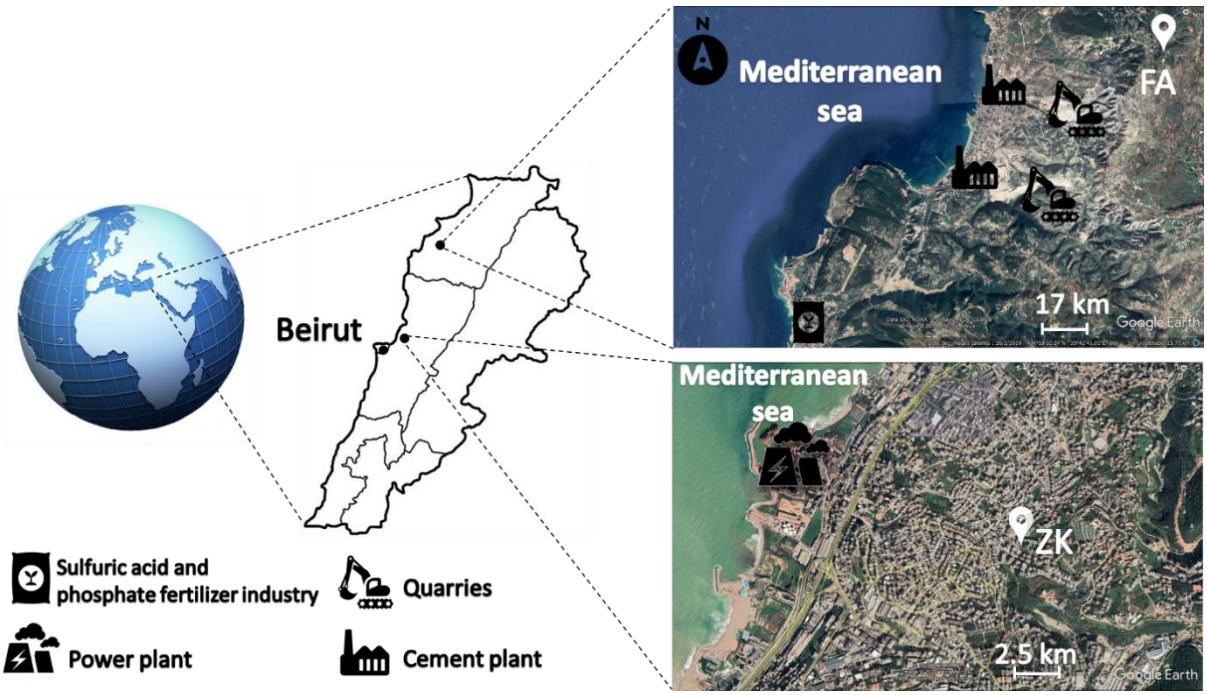

Fig. III-4: Location of the two sampling sites in Lebanon: Zouk Mikael (ZK) and Fiaa (FA) and the nearby industries (modified from Google Earth)

Zouk Mikael area (ZK) is characterized by a high residential density (4,200 inhabitants/km^2), but also commercial and industrial activities. ZK has the biggest power plant in Lebanon of 1 $GW_{electrical}$ which runs on Heavy Fuel Oil (HFO). It encompasses 607 $MW_{electrical}$ of boilers with

2 common stacks releasing the emissions at 145 m, 198 $MW_{electrical}$ of reciprocating engines installed in 2017 with stack heights of around 40 m, and a power barge with 11 reciprocating engines with a total capacity of 198 $MW_{electrical}$ installed in 2012 with a stack height of around 50 m. Moreover, a high number of private generators along with small industries for plastic production, woodworks, steel construction, aluminum extrusion, marble, and granite production, etc. exist in this area. The Zouk Mikael highway and the thermal power plant are respectively 1.2 and 1.5 km away from the sampling site.

Fiaa area (FA) is far less populated than ZK (250 residents/km^2). It is also influenced by private generators emissions. The main potential sources encompass chemical industries: two cement industries along with their corresponding quarries in Chekka, and a sulfuric acid and phosphate fertilizer industry few kilometers away **(Fig. III-4)**. In addition, the nearest highway is 4 km away from FA with moderate traffic. The two cement plants are 5 and 7 km away from the sampling site.

1.2 Sample collection

The sampling of fine particles ($PM_{2.5}$) was performed on 24-hour basis every three days from 13th of December 2018 to 15th of October 2019. $PM_{2.5}$ was sampled using high-volume samplers (CAV-A/mb, MCV S.A., Spain) operating at 30 m^3/h, onto 150 mm pure quartz microfibres filters (Fiorini, France). Filters were heated for 12 hours at 550°C before sampling to decrease the organic impurities content and kept at -20℃ till sampling. Over the sampling period, 98 samples in ZK and 95 samples in FA have been collected. Field blanks (at least one/month) were also considered at each site by placing a blank filter in sampling conditions but without pumping. The collected filters were sealed in aluminum foil and stored at -20°C until analysis. A wireless weather station (TFA-Dostmann 35.1112 OPUS) was installed at the ZK site to collect meteorological data. During the whole sampling period, 93% of the samples were collected under low windspeed (<2 m/s) indicating that the site was mainly under turbulent atmospheric conditions.

1.3 Organic compounds analysis

The method used for the organic compounds analysis was described elsewhere (Waked et al., 2013; 2014). In brief, a quarter of the filter was spiked with 50 µL of 2 internal standards (cis-ketopinic acid and bornylacetate) followed by an extraction by sonication for 30 min at 50°C using 30 mL of acetone/dichloromethane (50:50, V/V). After the extraction, the volume of the

samples was reduced to 200 µL under a constant flow of nitrogen gas. The obtained solution was used to directly quantify non-polar compounds such as alkanes, PAHs, hopanes and some phthalates while polar compounds such as fatty acids and SOA compounds were quantified after derivatization. Derivatization was achieved with 50 µL of the extract treated using N,O-bis(trimethylsilyl)-trifluoroacetamide (BSTFA) with 1% trimethylchlorosilane and 10 µL of pyridine as a catalyst at 70°C for 2 hr.

2 µL of the derivatized and the non-derivatized extracts were injected using a gas chromatography coupled to a mass spectrometer (GC/MS) in the split mode with a split ratio of 1/25. The GC consisted of an ISQ 7000 (Thermo Scientific, United States of America) equipped with an HP 5MS UI capillary column (30 m x 0.25 mm x 0.25 µm, Agilent; United States of America). The column temperature program consisted of an injection at 65°C hold for 2 min, a ramp of temperature corresponding to 6°C/min up to 300°C followed by an isothermal hold step at 300°C for 20 min. The GC was interfaced to an ion trap MS with an external electron ionization (EI) source (220°C, 70 eV).

1.4 Identification and quantification of organic compounds

For compounds for which an authentic standard was available in the laboratory (around 50 compounds), the identification was made by comparing the retention time and the mass spectrum associated to the reference compound (full scan mode, range 50-500 m/z). Additionally, this method permitted the identification of alkanes from C_{12} to C_{40}.

For other compounds, the identification was based on the retention time, and the reference mass spectrum from the literature (Claeys et al., 2004; Jaoui et al., 2007; El Haddad et al., 2011b). In this case, the quantification was done using the response factor (RF) of a surrogate compound. For α-pinene oxidation products: (i) the RF of malic acid was used for 3-hydroxyglutaric acid (A1), 3-acetylglutaric acid (A2), 3-isopropylglutaric acid (A3), and 3-methyl-1,2,3-butanetricarboxylic acid (A4); (ii) the RF of glyceric acid was assigned to 2-methylglyceric acid (2-MGA) ; (iii) the RF of threitol was used for 2-methylthreitol (MT1), 2-methylerythritol (MT2), and (iv) the RF of pinic acid was used for β-caryophyllinic acid (βC). For the hopane family, the RF of 17α(H)-21β(H)-hopane, an authentic standard, was used to quantify the concentrations of trisnorneohopane, 17α(H)-trisnorhopane, 17α(H)-21β(H)-norhopane, 17α(H)-21β(H)-22S, and 22R-homohopane.

The field blanks were analyzed following the same procedure as the sampling filters. The concentrations of the species in the $PM_{2.5}$ samples were corrected by subtracting the mean value obtained for the field blank filters.

The detection limit was evaluated for all the compounds and corresponds to the blank filter value plus 3 times the standard deviation calculated over 3 measurements. It ranged between 0.0003 and 0.08 ng/m^3 for non-derivatized compounds and between 0.002 and 0.25 ng/m^3 for derivatized compounds except for stearic acid with a higher detection limit (2.3 ng/m^3).

The coefficient of determination (R^2) of the calibration curves, determined several times during the analysis period, for compounds with authentic standards, ranged between 0.93 - 0.99 except for tetracosanoic acid (0.90). Repeatability was assessed by studying the variation in the RF of 5 consecutive injections of the authentic standards (DRI, 2003). The variations were less than 14%. The analytical uncertainty was calculated using the quantification limit of the compound, the repeatability, and the concentration of the compound. The total uncertainty including the analytical uncertainty and the uncertainty associated to the mass flow measurement of the sampler was in the range of 9% - 30% at 2σ.

Recoveries were determined by spiking blank filters by standard solutions. The values were estimated to be 80%, 82%, 92%, 90%, 85%, 82%, and 97% for alkanes, PAHs, fatty acids, phthalates, dicarboxylic acids, pinic acid, and hopanes respectively. For compounds with no authentic standard (i.e., some SOA markers), the recovery of the surrogate compound was determined to be 85% for glyceric acid and 95% for threitol.

1.5 Index and diagnostic ratios calculation

Statistical diagnostic methods were used in a quantitative and qualitative way in order to investigate the origin of the different organic species in the $PM_{2.5}$. The indexes for the n-alkanes were used to differentiate the anthropogenic and the biogenic origins. As for the PAHs, the ratios were used to separate pyrogenic and petrogenic sources with a focus on the type of combustion.

1.5.1 Ratios for the n-alkanes

Three methods were used to assess the contribution of the sources for the paraffins: the carbon number of the alkane having the maximum concentration (C_{max}), the carbon preference index (CPI), and the input of wax from plants (Wax ratio).

C_{max} is used in general to differentiate between two alkane sources: vegetation wax emissions for the high odd number of carbons, i.e. 27, 29, and 31, and anthropogenic source for the lower numbers (Andreou and Rapsomanikis, 2009).

The Carbon Preference Index (CPI) is a measure of odd to even alkanes predominance (Simoneit, 1999) and evaluates the contribution of the anthropogenic and the biogenic source. Two CPI parameters were adopted: the Overall CPI_{19-32} for all the alkanes and the High CPI_{25-32} for the biogenic n-alkanes and were calculated using equations Eq. 1 and Eq. 2 (Bray and Evans, 1961; Cooper and Bray, 1963).

$$\text{Overall CPI}_{19-32} = \frac{\sum \text{odd } C_{19} - C_{31}}{\sum \text{even } C_{20} - C_{32}} \qquad \text{(Eq. 1)}$$

$$\text{High CPI}_{25-32} = \frac{\sum \text{odd } C_{25} - C_{31}}{\sum \text{even } C_{26} - C_{32}} \qquad \text{(Eq. 2)}$$

An overall CPI value close to 1 indicates a petrogenic source, between 2 and 5 mainly biomass burning, while a value higher than 6 is characteristic of biogenic emissions (Simoneit, 2002). For the High CPI, a value less than 1.5 indicates an anthropogenic source while a value higher than 3 indicates a biogenic one (Melki et al., 2017). An intermediate value explains a mix of biogenic and anthropogenic sources.

The Wax ratio was used to determine the distribution of the residual wax n-alkanes when the petroleum n-alkanes are subtracted (Simoneit et al., 1991). First, Wax_{Cn} is calculated by subtracting the odd average concentration C_n of the next higher C_{n+1} and lower C_{n-1} even carbon. Then, the Wax ratio (Wax%) corresponding to the percentage of Wax related n-alkanes, is calculated by dividing the $\sum Wax_{Cn}$ (the sum of Wax_{Cn} for odd alkanes, with negative values of Wax_{Cn} taken as a Zero) by the total concentration of all the n-alkanes in the sample ($\sum A$).

$$Wax_{Cn} = C_n - \frac{1}{2}(C_{n-1} + C_{n+1}) \qquad \text{with n: odd number} \qquad \text{(Eq. 3)}$$

$$\text{Wax \%} = \frac{\sum Wax_{Cn}}{\sum A} \times 100 \qquad \text{(Eq. 4)}$$

1.5.2 PAHs diagnostic ratios

PAHs diagnostic ratios have been used to determine the source of particle-containing PAHs. They can help to determine the different emission sources as well the different fuel types used in the combustion processes (Riffault et al., 2015). This methodology is based on the hypothesis

that the PAH concentration ratios remain constant between the emission source and the measuring site. This is particularly true for isomers having similar photochemical properties considered to be affected in a similar manner by the different reactions occurring in the atmosphere (Borgie et al., 2016). Different ratios were calculated considering the concentrations of fluoranthene (Fla), pyrene (Pyr), indeno[1,2,3-c,d]pyrene (InPy), benzo[g,h,i]perylene (B[ghi]Pe), benz[a]anthracene (B[a]An), chrysene (Chr), and benzo[a]pyrene (B[a]P), and compared to the literature: Fla/(Fla+Pyr), InPy/(InPy+B[ghi]Pe), B[a]An/(B[a]An+Chr), and B[a]P/(B[a]P+Chr).

The ratio of sum of the non-alkylated compounds (fluorene, pyrene, benz[a]anthracene, chrysene, benzo[b]fluoranthene, benzo[k]fluoranthene, benzo[a]pyrene, indeno[1,2,3-c,d]pyrene and benzo[g,h,i]perylene), noted C_{PAH}, to the total concentration of the PAHs, noted T_{PAH}, evaluates the contribution of the compounds related to combustion processes (Ravindra et al., 2008). Finally, the Low Molecular Weight (LMW) PAHs to the High Molecular Weight (HMW) ratio, noted (3+4 rings)/ (5+6 rings) ratio, can be used as an indicator of the local or distant origin of PAH (Tan et al., 2011).

2 Results and discussions

This study was performed over almost a one-year period. We chose to discuss the average concentrations calculated for the overall period as well as the concentrations associated with the winter (December 2018 till March 2019) and the summer periods (June 2019 till September 2019) in order to assess seasonal trends. The corresponding concentrations for all studied compounds are given in **Table III-3**, **Table III-4** and **Table III-6**.

Chronological evolutions are included in the supplementary material to support interpretations **(Appendix B - Fig. S2, Fig. S3, Fig. S4)**.

2.1 Primary Organic Aerosols (POA)

Primary emissions from biogenic and anthropogenic sources include more than forty sources in urban areas (Rogge et al., 1996) such as road transport, road dust, tire wear, cooking operations, industrial boilers, fireplaces burning woods, plant leaf abrasion, etc.

2.1.1 n-alkanes

The yearly average of n-alkanes concentrations at both sites is quite similar with 26.70 ng/m^3 at ZK versus 29.12 ng/m^3 at FA **(Table III-3**). Nevertheless, the distribution of the n-alkanes

concentration over the year was different: at ZK site, the winter period concentration (31.63 ng/m^3) is much higher than the summer one (17.61 ng/m^3) whereas it is similar for both seasons at FA (25.76 vs 28.11 ng/m^3). The observed values are similar to those reported (23 ng/m^3) for a coastal urban-industrial site at Dunkirk, France (Landkocz et al., 2017) and much lower than those presented for an industrial site in Tianjin, China (136-314 ng/m^3) (Li et al., 2010). This difference gets more important with a big population in China and a site exposed to intensive coal burning emissions for industrial and domestic purposes. A clear seasonal pattern for the n-alkanes distribution ranging from C_{19} to C_{32} was observed at ZK and FA with higher concentrations of C_{21}-C_{27} during winter compared to summer especially for the ZK site **(Fig. III-5)**. This could be attributed to the higher contribution of the residential heating in the cold period. The larger difference observed for ZK reinforces this hypothesis since ZK is much more populated than FA.

In the summer period, the n-alkanes distribution profile shifts to the highest carbon number, ≥ C_{27}, ascribable to plant wax-derived alkanes (Rogge et al., 1993b). The concentrations of the high odd alkanes in FA are remarkably higher than those in ZK showing higher contribution of the natural source at FA. This can be explained by the fact that Chekka region, and Fiaa precisely are more densely surrounded by green lands and trees. In both sites in winter, C_{max} was at C_{25} indicating the prevalence of the anthropogenic sources (Simoneit, 1989). In summer, the most abundant n-alkanes are C_{29} and C_{31} at ZK and C_{27} and C_{29} at FA suggesting a higher relative contribution of biogenic aerosols during the hot season (Li et al., 2006).

The CPI values were calculated as described in section 1.5.1 for each $PM_{2.5}$ sample and presented in **(Fig. III-6)**. In the winter period, for both sites, the obtained High CPI values, below 1.5, indicate a quasi-exclusively anthropogenic origin for the n-alkanes. The Overall CPI close to 1 also indicates the contribution of a petrogenic source (petroleum residues). In the summer period, the High CPI shifted to values between 1.5 and 3 for most of the samples in ZK, indicating a mixed influence of natural and anthropogenic sources. Only few samples have the same tendency in FA site suggesting the higher impact of the anthropogenic sources during summer.

Table III-3: Atmospheric concentrations (in ng/m^3) of identified n-alkanes and hopanes during the entire sampling period (Total: Dec 2018- Nov 2019), winter (Dec 2018-March 2019), and summer (June 2019-September 2019) periods at Zouk (ZK) and Fiaa (FA) sites

Compounds	Average concentration (min-max) (ng/m^3)					
	ZK site			FA site		
	Total	Winter	Summer	Total	Winter	Summer
n-alkanes						
Nonadecane (C19)	0.42 (0.11-0.97)	0.44 (0.13-0.84)	0.34 (0.11-0.82)	0.15 (0.01-0.78)	0.19 (0.01-0.78)	0.11 (0.01-0.77)
Heicosane (C20)	0.45 (0.01-1.50)	0.53 (0.04-1.50)	0.26 (0.01-1.06)	0.33 (0.02-1.19)	0.40 (0.02-1.19)	0.23 (0.03-0.83)
Heneicosane (C21)	0.56 (0.04-2.42)	0.80 (0.13-2.42)	0.26 (0.04-0.74)	0.49 (0.04-1.94)	0.63 (0.04-1.94)	0.33 (0.09-1.07)
Docosane (C22)	1.03 (0.11-3.61)	1.56 (0.39-3.61)	0.50 (0.11-1.22)	0.80 (0.07-3.54)	1.04 (0.07-3.54)	0.56 (0.15-1.81)
Tricosane (C23)	1.84 (0.09-6.49)	2.67 (0.84-6.49)	0.94 (0.09-3.83)	1.55 (0.24-5.57)	1.81 (0.31-5.57)	1.10 (0.24-3.95)
Tetracosane (C24)	2.55 (0.10-12.7)	3.69 (1.07-12.7)	1.26 (0.10-2.99)	2.37 (0.79-7.42)	2.70 (0.79-7.42)	1.89 (0.82-5.86)
Pentacosane (C25)	2.99 (0.45-13.2)	3.80 (0.99-13.2)	1.62 (0.45-3.77)	3.23 (0.60-10.2)	3.28 (0.73-10.2)	2.79 (0.60-8.77)
Hexacosane (C26)	2.90 (0.44-15.1)	3.69 (0.78-15.1)	1.67 (0.44-4.23)	3.23 (0.47-12.1)	3.06 (0.75-9.76)	3.14 (0.47-12.1)
Heptacosane (C27)	3.25 (0.73-16.9)	3.77 (0.73-16.9)	2.16 (0.80-5.30)	4.10 (0.86-15.1)	3.03 (0.86-9.53)	4.43 (1.09-15.1)
Octacosane (C28)	2.16 (0.21-11.6)	2.60 (0.52-11.6)	1.44 (0.21-4.77)	2.96 (0.64-12.0)	2.46 (0.64-9.32)	3.19 (0.64-12.0)
Nonacosane (C29)	2.94 (0.51-25.8)	2.79 (0.55-9.79)	2.26 (0.51-4.74)	3.93 (0.73-15.4)	2.88 (0.79-10.7)	4.02 (0.73-12.8)
Triacontane (C30)	1.65 (0.92-6.59)	1.82 (0.40-6.59)	1.28 (0.22-4.17)	2.02 (0.23-8.46)	1.52 (0.23-5.95)	2.13 (0.42-8.46)
Hentriacontane (C31)	2.66 (0.02-18.5)	2.34 (0.40-7.74)	2.42 (0.02-5.91)	2.58 (0.17-9.96)	1.72 (0.17-6.41)	2.63 (0.33-9.96)
Dotriacontane (C32)	1.27 (0.15-5.18)	1.12 (0.17-3.40)	1.18 (0.15-3.35)	1.37 (0.02-6.85)	1.05 (0.02-4.82)	1.54 (0.34-6.85)
Total (∑A)	**26.70**	**31.63**	**17.61**	**29.12**	**25.76**	**28.11**
Hopanes						
Trisnorneohopane (H1)	0.28 (0.03-1.37)	0.32 (0.04-0.89)	0.30 (0.03-1.37)	-	-	-
17α(H)-trisnorhopane (H2)	0.37 (0.06-1.48)	0.46 (0.10-1.48)	0.33 (0.06-1.01)	-	-	-
17α(H)-21β(H)-norhopane (H3)	1.08 (0.24-3.51)	1.26 (0.29-3.51)	0.83 (0.34-2.19)	-	-	-
17α(H)-21β(H)-hopane (H4)	1.08 (0.28-3.39)	1.24 (0.33-3.39)	0.87 (0.28-1.94)	-	-	-
17α(H)-21β(H)-22S-homohopane (H5)	0.74 (0.13-3.19)	0.69 (0.13-1.55)	0.84 (0.20-3.19)	-	-	-
17α(H)-21β(H)-22R-homohopane (H6)	0.67 (0.10-3.74)	0.68 (0.11-3.74)	0.75 (0.18-2.27)	-	-	-
Total (∑Hop)	**4.22**	**4.66**	**3.91**	-	-	-

Table III-4: Atmospheric concentrations (in ng/m^3) of identified polycyclic aromatic hydrocarbons(PAHs), fatty acids, and phthalates during the entire sampling period (Total: Dec 2018- Nov 2019), winter (Dec 2018-March 2019), and summer (June 2019-September 2019) periods at Zouk (ZK) and Fiaa (FA) sites

Compounds	Average concentration (min-max) (ng/m^3)					
	ZK site			FA site		
	Total	Winter	Summer	Total	Winter	Summer
PAHs						
Acenaphthylene (Acy)[1]	0.02 (0.01-0.08)	0.03 (0.02-0.08)	0.012 (0.01-0.04)	-	-	-
Acenaphthene (Ace)[1]	0.02 (0.01-0.09)	0.03 (0.01-0.09)	0.011 (0.01-0.04)	-	-	-
Fluorene (Flu)[1]	0.02 (0.01-0.25)	0.03 (0.01-0.25)	0.02 (0.01-0.04)	-	-	-
Anthracene (Anth)[1]	0.12 (0.01-0.42)	0.15 (0.05-0.42)	0.09 (0.01-0.21)	0.08 (0.01-0.58)	0.12 (0.01-0.58)	0.05 (0.01-0.36)
Phenanthrene (Phe)[1]	0.03 (0.01-0.09)	0.04 (0.01-0.09)	0.02 (0.01-0.09)	0.02 (0.01-0.08)	0.02 (0.01-0.08)	0.02 (0.01-0.07)
Fluoranthene (Fla)[2]	0.13 (0.01-0.68)	0.22 (0.05-0.68)	0.06 (0.01-0.19)	0.11 (0.01-1.16)	0.22 (0.02-1.16)	0.04 (0.01-0.31)
Pyrene (Pyr)[2]	0.15 (0.01-0.76)	0.24 (0.05-0.76)	0.07 (0.01-0.19)	0.10 (0.01-0.70)	0.19 (0.01-0.69)	0.06 (0.01-0.26)
Benz[a]anthracene (B[a]An)[2]	0.15 (0.01-0.76)	0.25 (0.06-0.76)	0.07 (0.01-0.19)	0.07 (0.01-0.77)	0.16 (0.01-0.77)	0.03 (0.01-1.03)
Chrysene (Chr)[2]	0.28 (0.02-1.17)	0.44 (0.11-1.17)	0.12 (0.02-0.30)	-	-	-
Benzo[b]fluoranthene (B[b]Fl)[3]	0.27 (0.04-1.07)	0.44 (0.12-1.05)	0.10 (0.04-0.22)	0.14 (0.01-1.03)	0.22 (0.03-0.69)	0.08 (0.01-1.03)
Benzo[k]fluoranthene (B[k]Fl)[3]	0.15 (0.01-0.75)	0.27 (0.04-0.75)	0.05 (0.01-0.13)	0.07 (0.01-0.60)	0.13 (0.02-0.60)	0.03 (0.01-0.43)
Benzo[a]pyrene (B[a]P)[3]	0.20 (0.01-1.26)	0.38 (0.06-1.26)	0.05 (0.01-0.20)	0.05 (0.01-0.44)	0.10 (0.02-0.35)	0.02 (0.01-0.44)
Dibenz[a,h]anthracene (DiB[a,h]An)[3]	0.45 (0.01-2.86)	0.89 (0.10-2.86)	0.08 (0.01-0.26)	0.12 (0.01-1.04)	0.22 (0.02-1.04)	0.04 (0.01-0.25)
Benzo[g,h,i]perylene (B[ghi]Pe)[4]	0.07 (0.01-0.40)	0.09 (0.02-0.38)	0.04 (0.01-0.13)	0.13 (0.01-1.22)	0.22 (0.02-1.22)	0.09 (0.01-0.34)
Indeno[1,2,3-c,d]pyrene (InPy)[4]	0.49 (0.03-3.11)	0.85 (0.03-3.11)	0.11 (0.03-0.50)	0.06 (0.01-0.50)	0.10 (0.01-0.50)	0.03 (0.01-0.25)
Total (∑PAHs)	**2.56**	**4.35**	**0.88**	**0.95**	**1.70**	**0.50**
Fatty acids						
Dodecanoic acid (DDA)	5.35 (0.04-17)	7.00 (2.09-17)	3.98 (0.04-12)	3.93 (0.15-15)	4.53 (1.68-10)	3.76 (0.15-14)
Tetradecanoic acid (TDA)	8.05 (0.29-52.19)	7.15 (0.86-52)	8.21 (0.29-18)	18.93 (0.09-94)	30.13 (11-94)	11.07 (0.09-33.05)
Hexadecanoic acid (HDA)	259.47 (2.29-3198)	171.55 (20.3-1201)	423.99 (2.29-3198)	415.19 (1.5-2436)	521.07 (191-1345)	457.11 (4.58-2436)
Octadecanoic acid (ODA)	175.32 (16.6-1508)	221.20 (16.6-730)	189.51 (18.00-1508)	247.14 (3.1-1423)	366.36 (97-894)	229.78 (3.1-1423)
Eicosanoic acid (EA)	8.50 (0.43-34.68)	12.08 (0.43-34.68)	7.07 (0.79-29.12)	6.23 (0.01-37.95)	6.55 (1.59-38)	9.03 (1.2-34.21)
Docosanoic acid (DA)	18.75 (0.10-125)	28.61 (4.96-107)	12.45 (0.10-125)	11.61 (0.1-104)	19.51 (1.27-104)	10.78 (1.44-30)
Tetracosanoic acid (TA)	15.79 (0.69-85)	26.84 (0.98-85)	10.89 (0.80-77)	-	-	-
Oleic acid (OA)	17.07 (0.13-80)	21.34 (3.19-80)	14.81 (0.13-72)	14.61 (0.08-60)	17.06 (5.86-32)	19.00 (2.02-60)

Total (∑FA)	**508.29**	**497.24**	**671.68**	**717.63**	**965.23**	**740.53**
Phthalates						
Diisobutylphthalate (DIBP)	22.19 (2.12-102)	20.92 (3.41-102)	24.17 (2.12-54)	19.72 (0.02-79)	20.42 (5.51-46)	6.50 (0.02-42)
Dibutylphthalate (DnBP)	35.69 (3.86-127)	15.48 (3.86-60)	57.84 (20.09-114)	12.36 (0.05-57)	10.11 (1.80-27)	8.14 (0.05-39)
Bis(2-ethylhexylphthalate) (DEHP)	48.99 (4.93-124)	43.09 (4.93-104)	58.39 (9.13-124)	65.59 (0.66-432)	63.85 (0.66-410)	39.75 (5.21-266)
Total (∑PAE)	**106.88**	**79.49**	**140.40**	**97.68**	**94.38**	**54.39**

Number of rings for PAHs: [1]3 rings; [2]4 rings; [3]5 rings; [4] 6 rings

The contribution of the natural sources as the primary biogenic source can be assumed by calculating the Wax ratio (Wax%). Wax% values were similar for the whole period (13%) at both sites **(Table III-5).** This ratio is in agreement with the value of 16% reported for a Lebanese site under industrial influence, Zakroun in Chekka region and lower than the one observed in a rural site (27%), Kaftoun in Chekka region too (Melki, 2017) due to the absence of primary sources near the site.

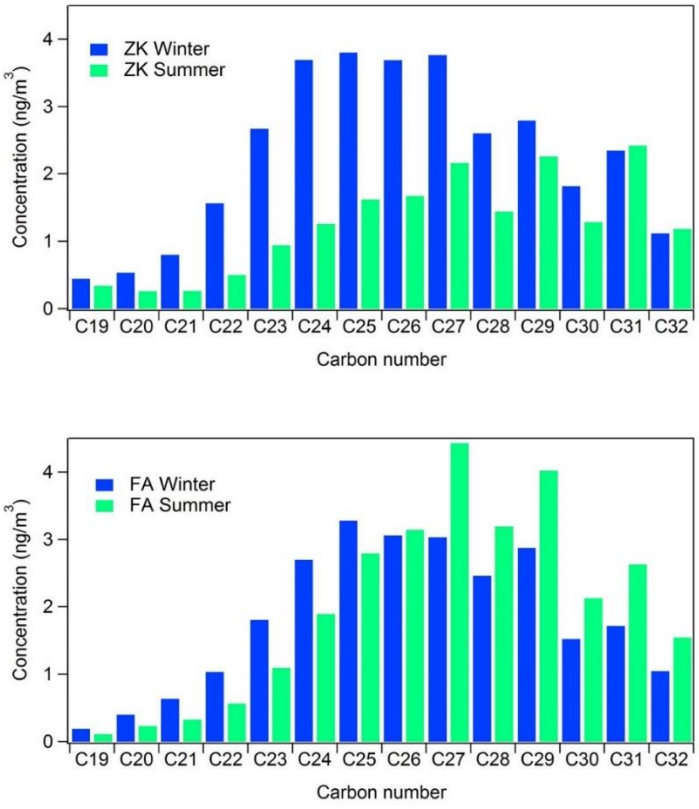

Fig. III-5: n-alkanes profile patterns associated with $PM_{2.5}$ in Zouk (ZK) and Fiaa (FA) in winter and summer periods

The Wax% increased in the summer period, 20% and 14% respectively in ZK and FA (compared to 7% and 9% during winter respectively) emphasizing on the increase of natural source contributions in the summer period. The winter Wax% at ZK and FA are in agreement with the value of 7% obtained in Sin El Fil, an urban site in Lebanon during a winter campaign in 2017 (Badran et al., 2020). The site was characterized by important road traffic, diesel generators, and waste incineration emissions. Additionally, the values appear to be in the range of those measured at an industrial site in Tianjin of 10% in winter and 30% in summer (Li et al., 2010). A good correlation (R^2>0.90) was observed between the Wax% and the Overall CPI at both sites for the whole sampling period which is also noted in other urban areas (Kotianova et al., 2008; Andreou and Rapsomanikis, 2009).

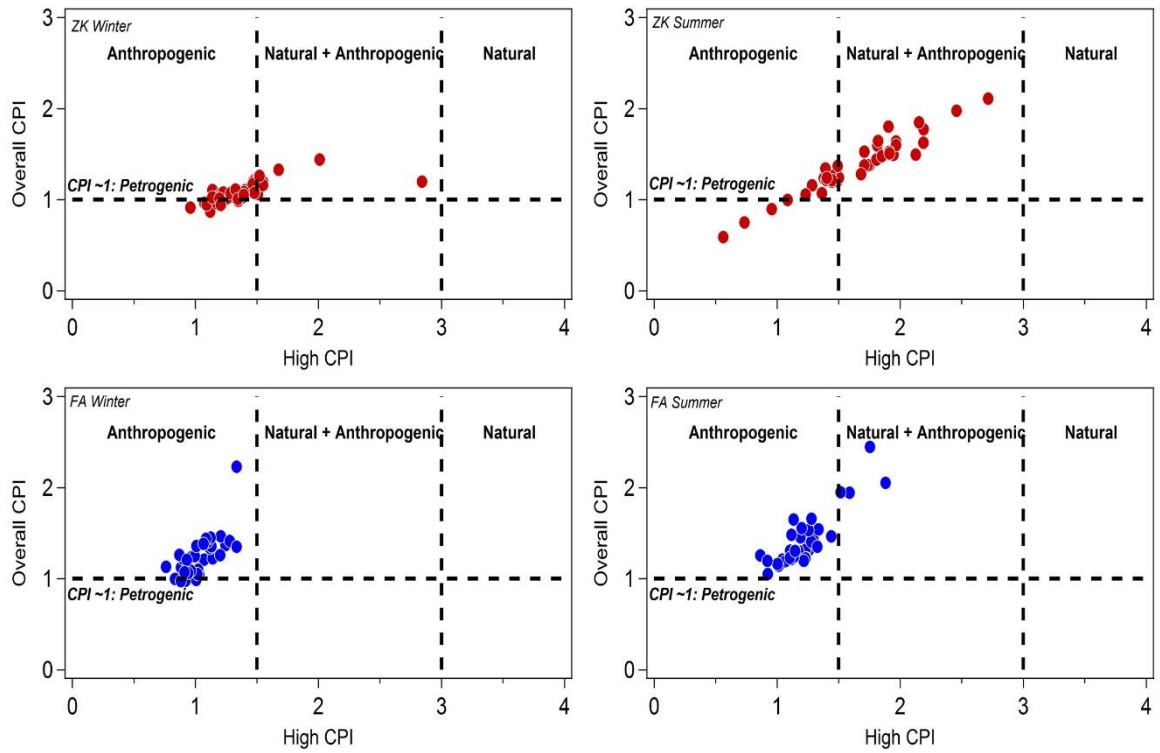

Fig. III-6: Source identification of alkanes using the Carbon Preference index (CPI) during winter and summer period at Zouk (ZK) and Fiaa (FA) sites

Despite the fact that biogenic related alkanes have higher contributions in the hot season at both sites, low wax percentages and CPI values close to unity show that plant waxes are not the major source for these alkanes. Hence, anthropogenic combustion sources related to diesel

generators, road traffic, industrial processes and to residential heating in winter can be assumed to account to the majority of emissions of n-alkanes in the studied areas.

2.1.2 Polycyclic Aromatic Hydrocarbons (PAHs)

The concentration of the 16 priority PAH listed by the United States Environmental Protection Agency (US EPA) in relation with their toxicity, mutagenicity and/or carcinogenic properties has been investigated. The main source of emission of PAHs in the atmosphere is the combustion of fossil and non-fossil fuels (Mastral et al., 2003).

The total PAH concentration was higher in ZK (2.56 ng/m^3) than in FA (0.95 ng/m^3). The concentration of naphthalene was below the detection limit which has been also observed in other studies since the partitioning coefficient favors the gas phase of this compound (Waked et al., 2013; 2014). The total particulate phase PAHs measured values are in agreement with the 1.16 ng/m^3 reported for a background urban site in Lebanon (Borgie et al., 2015) but are lower than those reported in both particulate and gaseous phases by Daher et al. (2013) near Jal el Dib freeway, Lebanon for $PM_{2.5}$ (12.2 ng/m^3) and by Baalbaki et al. (2018) in Zouk Mikael (25.1 and 27.7 ng/m^3 in winter and summer respectively for PM_{10}). Compared to other industrial urban sites, these values are higher than those observed (0.224 ng/m^3) in the Czech Republic (Mikuška et al., 2015) but lower than those in Northern France (7.7 ng/m^3) (Landkocz et al., 2017), and much lower than those measured at an industrial region in China (235 ng/m^3) (Bi et al., 2020).

Table III-5: Alkanes wax ratio for Zouk (ZK) and Fiaa (FA) sites during total, winter, and summer periods

Wax %	**ZK site**			**FA site**		
	Total period	Winter	Summer	Total period	Winter	Summer
Average	13%	7%	20%	13%	9%	14%
Minimum	0%	1%	0%	1%	1%	4%
Maximum	52%	24%	36%	35%	25%	35%

In this study, PAH concentrations tend to be 3 (at FA) to 5 (at ZK) times higher in the winter period (4.35 and 1.70 ng/m^3 at ZK and FA respectively) compared with the summer period (0.88 and 0.50 ng/m^3 respectively). This observation could be due to increasing primary source emissions especially combustion activities alongside the atmospheric stability in winter, partitioning between particulate and gaseous phases, and greater photochemical degradation during summer (Pindado et al., 2009). The ratio of (3+4 rings)/ (5+6 rings) PAHs was calculated

for both seasons and showed the same average of 0.76 at FA while a seasonal difference was evidenced in ZK (0.59 in winter and 1.21 in summer). The lower ratio in winter at ZK could indicate that the contribution of local sources to PAH concentration was higher in this period compared with the summer one (Tan et al., 2011).

Looking at the yearly average concentrations, and comparing the PAH distribution, a specificity appears for the ZK site. While no predominant compound is clearly evidenced at FA site, at ZK site InPy and DiB[a,h]An appear to be the main PAHs. Moreover, a strong correlation during the total sampling period exists for these latter only at ZK (R^2=0.87 at ZK versus R^2=0.40 at FA). This suggests that these compounds are locally emitted and are related to a common source of emission in the ZK study area.

To go further, the contribution of the different sources of PAH was investigated by the study of the PAH diagnostic ratios. Using the Fla/(Fla+Pyr) and the InPy/(InPy+B[ghi]Pe) isomer ratios makes possible the evidencing of the contribution of petrogenic, wood and coal combustion, fuel combustion, and also diesel and gasoline sources. According to the literature, the Fla/(Fla+Pyr) suggests a petrogenic source for a value lower than 0.2, a liquid fossil fuel combustion for 0.4-0.5, and wood or coal combustion for a value higher than 0.5 (Ravindra et al., 2008; Cazier et al., 2016). The InPy/(InPy+B[ghi]Pe) ranging between 0.2 and 0.5 is considered as a marker for gasoline source, 0.35-0.7 for diesel source, and wood and coal combustion for values higher than 0.5 (Riffault et al., 2015; Bi et al., 2020).

At ZK and in both seasons, Fla/(Fla+Pyr) ratio ranges between 0.4 and 0.5 indicating that fuel combustion emissions were predominant **(Fig. III-7).** Moreover, InPy/(InPy+B[ghi]Pe) ratio shows values mainly above 0.8 and only few values in the 0.2-0.7 range. Hence, these observations allow to conclude that at ZK site (i) road traffic is not the predominant source of InPy and B[ghi]Pe since it has a characteristic InPy/(InPy+B[ghi]Pe) value of 0.31 in Lebanon (Daher et al., 2013) in line with Bi et al. (2020) and Riffault et al. (2015) as the traffic in Lebanon is dominated by gasoline (Abdallah et al., 2020), (ii) Diesel private generators are not the main source since the observed ratio values are higher than 0.8, and (iii) this source cannot be associated to biomass burning which has ratio values above 0.6 (Ravindra et al., 2008; Tobiszewski and Namieśnik, 2012) since it contradicts the observed Fla/(Fla+Pyr) values. Therefore, a deepen interpretation of PAH concentrations is needed to identify a potential source with a characteristic ratio above 0.8 specific to liquid fuel combustion.

High values of the InPy/(InPy+B[ghi]Pe) ratio were obtained by Manoli et al. (2004) for oil burning from residential heating appliance chimneys (0.82), cement plants (0.90-0.96) and diesel emissions from taxis and buses (0.96). However, none of these sources are present in the surroundings of the ZK site. Consequently, the thermal power plant located in ZK is a potential source since it uses a third type of liquid fuel; the Heavy Fuel Oil (HFO). To investigate this hypothesis, the samples when the site was predominantly down wind of the power plant encompassing wind speeds above 2m/s were examined. Only two filters met clearly the selection criteria **(Appendix B - Fig. S1)** and showed InPy/(InPy+B[ghi]Pe) ratio values of 0.84 and 0.93 which are in line with our hypothesis. Ratio values varying around 0.9 were encountered in most of the samples which can be explained by the fact that HFO combustion emissions are released at 145 m of height by the 607 MW boilers resulting in an enhanced dispersion affecting a broader area like the surrounding cities ex. Jounieh, but also at around 50 m from the ground by the 396 MW reciprocating engines with consequently less enhanced dispersion impacting a smaller area concentrated on Zouk Mikael entirely and nearest surroundings. This observation results in affected air masses reaching the site from all directions.

Up to our knowledge, the literature is scarce regarding characteristic InPy/(InPy+B[ghi]Pe) ratio value for the heavy fuel oil combustion occurring in power plants. Cecinato et al. (2014) indicates a value of 0.35 based on the emission factors. This value won't vary much for the particulate phase only since partitioning coefficients between particulate and gaseous phases for the two compounds are very close (Kim and Kim, 2015). Values of 0.35 and 0.5 can be also obtained from a study conducted by Yang and co-workers and from the US EPA AP-42 respectively (Yang et al., 1998; USEPA, 2010). However, the representativeness of these values is poor, as several authors in the literature stress on the idea that the PAH emissions strongly depend on the combustion conditions and quality of fuel that might change from a site to another (Masclet et al., 1987; Mastral and Callén, 2000; Ravindra et al., 2008; Tobiszewski and Namieśnik, 2012).

With the idea to better define this new characteristic ratio value, the "Source Profile by Unique Ratio" (SPUR) method was applied (Annegarn et al., 1992; Ledoux et al., 2017). This method consists to plot a ratio involving the characteristic species of the source versus the concentration of the characteristic species.

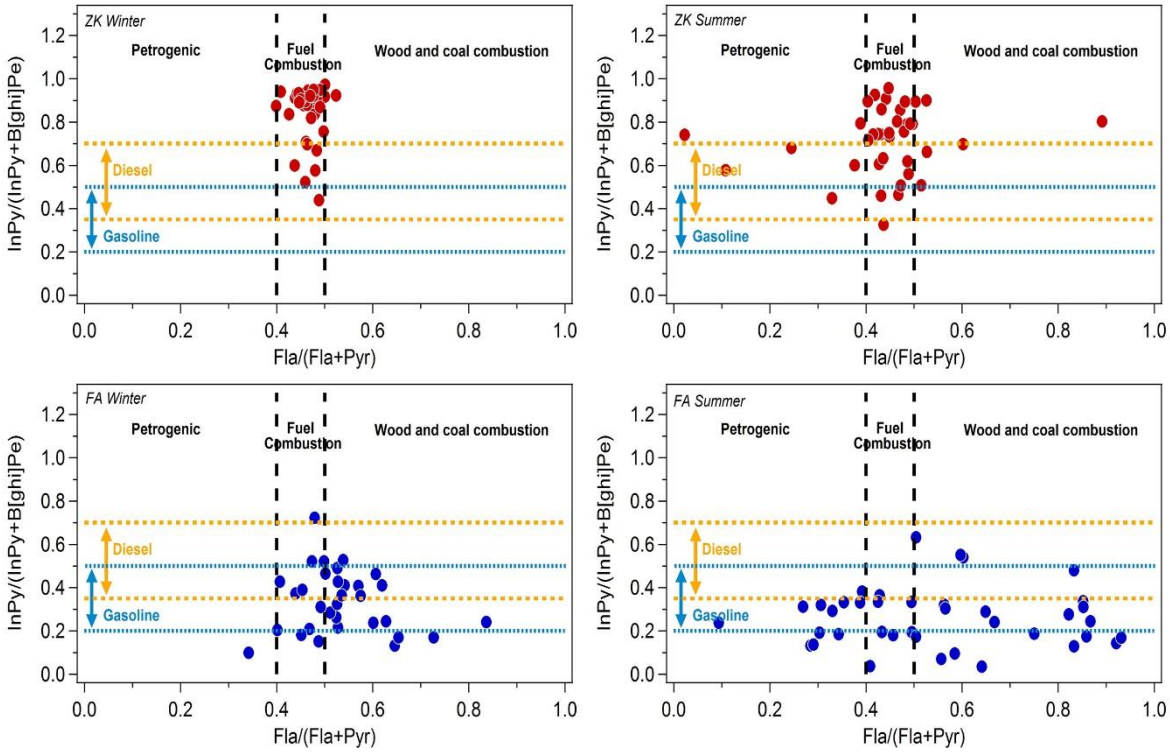

Fig. III-7: Bi-variate plots of InPy/(InPy +B[ghi]Pe) vs. Fla/(Fla+Pyr) ratios at Zouk (ZK) and Fiaa (FA) sites during winter and summer respectively

The limit of the ratio obtained for the highest concentrations of the characteristic species can be assumed as the characteristic ratio of the source. It has been applied to the InPy/(InPy+B[ghi]Pe) ratio versus InPy concentrations **(Fig. III-8)** as InPy shows particularly high concentrations at ZK site. The SPUR method allows to suggest an InPy/(InPy+B[ghi]Pe) characteristic ratio between 0.8 and 1 for the Heavy Fuel Oil combustion occurring in a thermal power plant.

At FA, the InPy/(InPy+B[ghi]Pe) ratio values appear mainly in the 0.2-0.7 range (diesel and gasoline combustion) and no value higher than 0.75. In addition, the Fla/(Fla+Pyr) ratio values indicate a mix of fuel combustion from vehicular emissions and diesel generators along with wood and coal combustion. The cement industries in Chekka use coke as their primary combustion source which explains our results.

Then, the values of B[a]An/(B[a]An+Chr) ratios in ZK were 0.36 and 0.37 for winter and summer respectively with no significant difference between the seasons meaning that these compounds come from a constant activity throughout the sampling period. In addition to that, the B[a]P/(B[a]P+Chr) ratio was 0.46 in winter and 0.28 in summer.

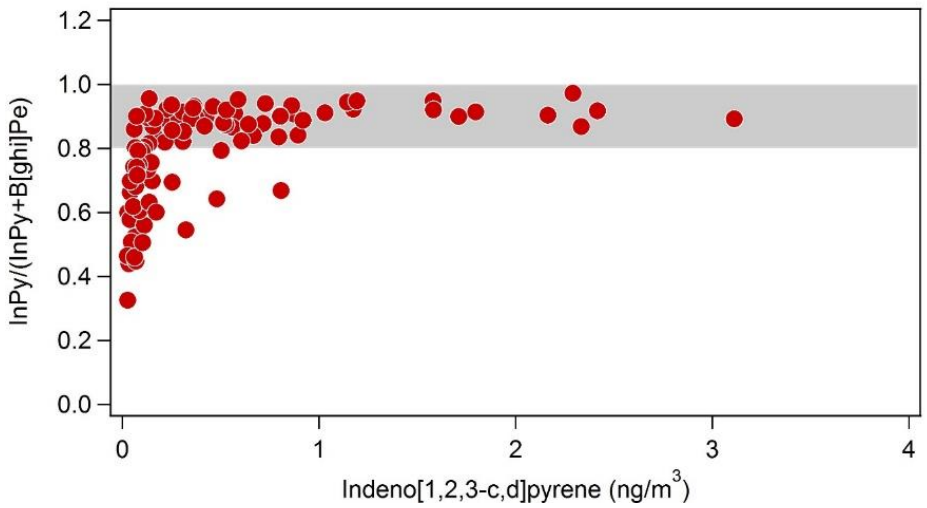

Fig. III-8: The Source profile by unique ratio (SPUR) method applied to the InPy/ (InPy+ B[ghi]Pe) ratio considering ZK site data

According to the literature, the ratio B[a]An/(B[a]An+Chr) refers to a pyrogenic source generated from the combustion of fossil fuel (coal and petroleum) and/or biomass for values higher than 0.35 and a petrogenic one from unburned crude oil and petroleum products for values lower than 0.2 (Boonyatumanond et al., 2007; Wu et al., 2014). On the other hand, the ratio B[a]P/(B[a]P+Chr) is generally used to assess the contribution of vehicular emissions. It was reported as 0.33 at an urban environment (Guo, 2003), 0.49 for gasoline emissions, and 0.73 for diesel emissions (Khalili et al., 1995). In Lebanon, the on-road fleet runs to a high extenton gasoline (Abdallah et al., 2020). Consequently, these two ratios suggest that the road traffic is an important source of B[a]An, B[a]P, and Chr in ZK during both seasons. These ratios were not calculated in FA due to the values of Chr below quantitation limit.

Finally, the combustion PAH (CPAHs) accounted for 71% and 77% during winter and 69% and 72% of the total PAH concentration (TPAH) during summer in ZK and FA, respectively. Despite the difference in the concentrations between the two sites, the combustion source impact is remarkably important and constant during both seasons suggesting that these PAHs are mainly emitted from sources that do not have any seasonal pattern such as diesel private generators, road traffic, and industrial emissions (HFO and coke combustion at ZK and FA, respectively) rather than unburned fossil fuels. These results are in agreement with the dominant anthropogenic origin of the alkanes emissions.

2.1.3 Hopanes

Hopanes are fossil fuel compounds present in unburned lubricating oils and are not found in diesel and gasoline because they belong to the higher boiling fraction of crude petroleum (Henry et al., 1984; Rogge et al., 1993a).

At ZK, the total concentration during the sampling period equals to 4.18 ng/m^3 **(Table III-3**) and is close to that reported in Ostrava, Czech Republic equal to 3.79 ng/m^3 after smog episode (Mikuška et al., 2015). The average concentrations of hopanes were 4.66 and 3.91 ng/m^3 in $PM_{2.5}$ for ZK in the winter and the summer periods respectively. The seasonal difference could be mainly due to the fact that the hopanes are more volatile during the hot season (Ruehl et al., 2011) as well as the lower average road traffic intensity in summer due to the closing of education institutions till September (Waked and Afif, 2012). These values are higher than 1.2 and 1.65 ng/m^3 reported for an urban area in Guangzhou, China for winter and summer, respectively (Wang et al., 2016).

The two most abundant hopanes were 17α(H)-21β(H)-norhopane and 17α(H)-21β(H)-hopane accounting for 50% of the total hopane concentration and exhibit a good correlation (R^2=0.85). The S/(S+R) epimers ratio for 17α(H)-21β(H)-homohopane could indicate that compounds are either emitted from road traffic or from coal combustion with 0.5 as the cutoff value between the two sources (Mikuška et al., 2015). At ZK site, higher concentrations for the S epimer compared with the R epimer were found (S/S+R > 0.5) showing the major influence of road traffic. All these findings were in agreement with El Haddad et al. (2009) who concluded that these compounds were emitted from vehicular emissions.

The observations also show a decrease of 25% on average in hopanes concentration on Sundays (3.27 ng/m^3) compared to weekdays (4.40 ng/m^3) **(Appendix B - Table S1)**. The weekend in general, but specially Sundays exhibit lower traffic related activities.

At the FA site, the $PM_{2.5}$ hopane content was below the detection limit. This is in agreement with the fact that the vehicular emissions in Chekka region are much lower than those in ZK which is also highlighted by the chrysene concentrations which are below the detection limit at FA site.

2.1.4 Fatty acids

In this study, the fatty acids class was the most abundant detected organic compounds with average concentrations over the entire period of 508.29 and 717.63 ng/m^3 at ZK and FA,

respectively. The concentrations are in range of the 644 ng/m^3 reported for the semi urban site in Beirut in summer (Waked et al., 2014) but much higher than the 234 ng/m^3 reported in winter (Waked et al., 2013) for the same site and those reported for 3 urban Indian sites (234-583 ng/m^3) (Gadi et al., 2019). Average concentrations of hexadecanoic acid (HDA) and octadecanoic acid (ODA) were 259.47 and 175.32 ng/m^3 in ZK, and 415.19 and 247.14 ng/m^3 in FA, respectively. Concentrations of these species accounted for 86 and 92% of the total alkanoic acids in ZK and FA, respectively. In addition to that, oleic acid which is an alkenoic acid was analyzed and showed concentrations of 17.07 ng/m^3 at ZK and 14.61 ng/m^3 at FA.

Generally, this class of compounds is the most abundant in the organic fraction (Rogge et al., 1991). The main components are hexadecanoic and octadecanoic acids as saturated fatty acids and oleic acid as unsaturated fatty acid. These compounds have multiple sources but are mostly emitted from cooking activities in urban areas (Rogge et al., 1991) when glycerides present in seed oils are pyrolyzed (Schauer et al., 2002).

HDA and ODA were well correlated in both sites (R^2=0.94 in ZK and R^2=0.96 in FA) but no correlation was found with oleic acid (R^2=0.15 in ZK and R^2=0.20 FA). These results are in agreement with Robinson et al. (2006) who concluded that saturated and unsaturated fatty acids have different cooking dominant sources with the assumption that these compounds are stable in the atmosphere.

The high concentrations observed for fatty acids are mainly due to the residential typology of the sites. The cooking activities are abundant especially with the usage of Canola and Soybean seed oil for frying. The concentrations for the fatty acids are higher in FA than in ZK due to the fact that the sampling site in FA was closer to houses. The seasonal variation in ZK show higher concentrations in summer mainly due to more outdoor cooking activities (i.e., charcoal grilling of meat and chicken) as well as for the restaurants that are more abundant in the area.

2.1.5 Phthalates

Phthalates are a group of man-made chemical compounds with esters of phthalic acid used as plasticizers in industrial final products and building materials (Lu et al., 2018).

To our knowledge, this study is the first dealing with the quantification of phthalates in Lebanon. The average concentration of phthalates was 106.88 and 97.68 ng/m^3 respectively at ZK and FA. These values are lower than those reported in 3 Indian urban sites (211, 159, and

130 ng/m^3) (Gadi et al., 2019) but similar to the 89 ng/m^3 reported in an urban site in Northern Vietnam (Nguyen et al., 2016).

Bis(2-ethylhexylphthalate) (DEHP) has the highest concentration between the compounds during the different seasons at both sites and in all the samples. It is generally found in the particulate phase while other phthalates like diisobutylphthalate (DIBP) and dibutylphthalate (DnBP) are predominant in the gaseous fraction (Pei et al., 2013).

A particular attention was given to DIBP and DnBP at both sites because they show different time series **(Appendix B - Fig. S2)**. At ZK site, similar values and trends were observed between the two species until the 15th of May after which the trend and values became different with higher concentrations of DIBP. While in FA, the contrary occurred with higher concentrations of DIBP than DnBP until the 1st of June 2019 after which concentrations became lower and similar. The comparison of the time series between the sites suggests that the emission sources were not the same and probably mainly related to local influence. Generally, it is known that these compounds are emitted during plastic burning (Simoneit et al., 2005). At FA, the high concentrations of these two phthalates were probably caused by the open waste burning in the North Governorate-which FA is part of- during the whole sampling time in several locations. This phenomenon increased during the March – May period (author field observation).

In order to further investigate this matter, DIBP and DnBP concentrations were plotted versus the sampling date **(Fig. III-9)**. Different correlation trends were observed at both sites. For the FA site, two separate trends with slopes of 1.36 (before June 1st, 2019) and 1.01 (after June 1st, 2019) can be distinguished. The difference might be explained by the different composition of waste that was burned.

A different scenario is shown in ZK between DIBP and DnBP, where the 15th of May 2019 is considered as the cutoff date between two trends for these 2 compounds. Before this date, the compounds are well correlated and show mostly a slope of 1.42 similar to those reported for Chekka region suggesting open waste burning with different waste composition.

This activity might have been reduced in ZK after mid-May because the region is considered as a touristic destination in Lebanon during summer. However, a different slope value and higher DnBP concentrations were reported after this date suggesting higher production rates at the plastic industries located in ZK area and its surroundings in the south-west sector.

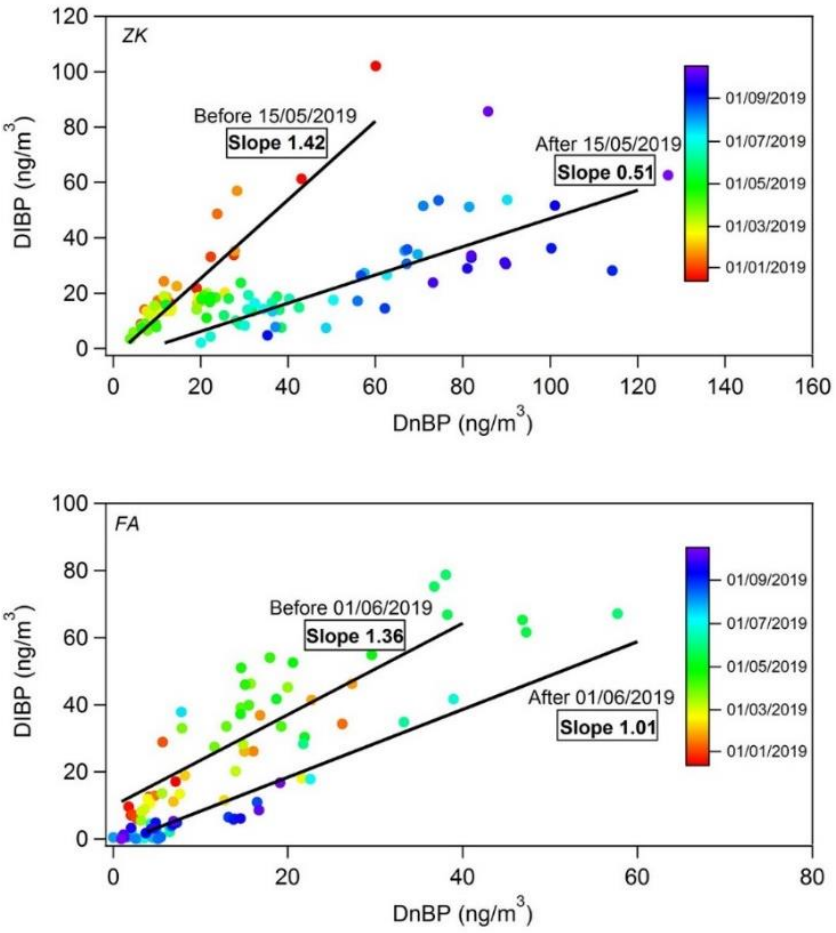

Fig. III-9: Correlations between DIBP and DnBP at Fiaa (FA) and Zouk (ZK) plotted versus the sampling date

Considering the high concentrations of the phthalates in ZK and FA, further investigations should be focused on their emissions in the Lebanon and the middle eastern region. Whether they are emitted from municipal open waste burning or plastic industries, studies have shown that they might cause diverse health effects specially on the endocrine system, (Ji et al., 2014) the reproductive systems and children's intelligence (Lu et al., 2018).

2.2 Secondary Organic Aerosols (SOA)

The secondary organic aerosols (SOA), an important fraction of the particulate matter, encompasses compounds produced from the transformation of organic species in the atmosphere in the gas or condensate phase (Kroll and Seinfeld, 2008). SOA from gas-phase reactions can result from oxidation of Volatile Organic Compounds (VOC) by atmospheric oxidants such as ozone O_3, hydroxyl radicals OH and nitrate radicals NO_3 (Atkinson, 2008).

Isoprene, α-pinene, and β-caryophyllene are mainly emitted from deciduous trees, pine forests, and vegetation respectively as primary emissions. They can be oxidized through photochemical reactions to give Biogenic Secondary Organic Aerosol (BSOA). The formation of these compounds depend largely on temperature variations and photochemical processes of the precursors (Feng et al., 2013). In this part, we will focus on the BSOA as well as dicarboxylic acids which are generally produced by the gas phase photochemical reactions including a variety of anthropogenic and biogenic precursors.

2.2.1 Isoprene oxidation products

Isoprene is mainly emitted by broadleaf vegetation (Guenther et al., 1995) and is considered as a highly reactive compound due to its two double bonds (Carlton et al., 2009). The major SOA tracers identified in the case of isoprene are mainly the 2-methylglyceric acid (2-MGA) and the two diastereoisomers 2-methylthreitol (MT1) and 2-methylerythritol (MT2).

The average concentrations of MT1 and MT2 in summer were respectively 2.64 and 6.53 ng/m^3 at ZK and 3.68 and 10.40 ng/m^3 at FA **(Table III-6).** They were at least 5 times higher than those measured in winter. This phenomenon is mainly due to the fact that the emissions of the precursor depend largely on the temperature variation and solar radiation as it enhances the photochemical reactions in the atmosphere (Feng et al., 2013).

The concentrations of the 2-methyltetrols (MT) were in range of those reported by Feng et al. (2013) for an urban and a suburban sites in Shanghai and lower than those reported for two industrial sites in Ohio for the summer since the authors could not identify these compounds during the cold season (Rutter et al., 2014). In ZK and FA, MT1 and MT2 showed a very good correlation (R^2=0.94 at ZK and R^2=0.96 at FA) along with an MT2/MT1 ratio equal to 2.8 at FA and 2.6 at ZK **(Appendix B - Fig. S3)**. These values are consistent with the value of 2.77 reported by Ion et al. (2005) suggesting that the 2-methyltetrols have the same photochemical reaction scheme, originating from the direct oxidation of isoprene, and their formation rate is relatively constant during the sampling period (Ding et al., 2011; Zhu et al., 2018).

The levels of 2-MGA averaging at 0.47 and 0.86 ng/m^3 at ZK and FA respectively were lower than the 2-methyltetrols **(Table III-6)** at both sites and through the seasons. They are in the range of the concentrations reported for a Mediterranean urban industrial site (0.027-5.9 ng/m^3) in Marseille (El Haddad et al., 2011a) and lower than the 1.29 ng/m^3 observed at an urban site in Shanghai, China (Zhu et al., 2018).

In addition to that, 2-MGA showed a different time series from the two diastereoisomers MT1 and MT2 at both sites **(Appendix B - Fig. S4)** but also higher concentrations during summer and a low correlation with their sum (R^2=0.50 in ZK and 0.57 in FA). Originating from the oxidation of an isoprene first-generation product methacrolein, the formation of 2-MGA in the atmosphere strongly depends among others on humidity, acidity, and NO_x conditions. Oxidation of isoprene under low NOx conditions preferentially lead to the formation of the MT while high NOx conditions favors the 2-MGA formation (Hallquist et al., 2009). Thus, the MT/2-MGA ratio might give an insight on the variation of local conditions. At ZK and FA, the MT/2-MGA ratio increased respectively from 11.9 and 10.9 in winter to 16.7 and 13.5 in summer. The high MT/2-MGA ratio value at both sites let suggest a predominance of the MT formation pathway. The slight increase at both sites in the summer period might be associated to the change of conditions in aerosol acidity or the gas-phase partitioning of the precursors of these compounds (Fu et al., 2014).

2.2.2 α-pinene oxidation products

α-pinene is considered as the main species in the monoterpene class and is emitted from conifers (Guenther et al., 1995). The average total concentration of α-pinene derived SOA were 2.92 and 11.41 ng/m^3 at ZK and 13.68 and 22.88 ng/m^3 at FA during winter and summer periods respectively. These values are higher than those presented for two urban sites in Shanghai (0.8-0.9 ng/m^3 in January and 8.0-10.0 ng/m^3 in July) (Feng et al., 2013). The concentrations in summer at FA are also higher than the 16.8 ng/m^3 found in a study conducted in July in western Germany while those at ZK are lower (Kourtchev et al., 2008). Generally, higher concentrations were recorded at FA at both seasons due a greater coverage of plants and vegetation in the Chekka region.

The oxidation of α-pinene by OH radicals or its ozonolysis leads to pinic acid (PA) and pinonic acid which are considered as lower -or first- generation oxidation products. The concentrations of PA **(Table III-6)** at both sites were found lower than the 16 ng/m^3 reported at a semi-urban site during summer (Waked et al., 2014) and winter (9.87 ng/m^3) in Lebanon (Waked et al., 2013). It is also lower than 4.2 ng/m^3 found in western Germany (Kourtchev et al., 2008).

For A1, A2, A3, and A4, the average concentration in ZK $PM_{2.5}$ were 0.65, 0.62, 0.74, and 0.41 ng/m^3 respectively in winter and about 5 times higher in the summer period. The same observation was highlighted in FA with twice higher concentrations in the hot period **(Table III-6**). Typically, higher temperature and more solar radiations during the summer period

enhance photochemical reactions. In addition to that, A1, A2, A3 and A4 concentrations were highly inter-correlated (R^2= 0.77-0.85 at ZK and 0.78-0.85 at FA) during the total sampling period **(Appendix B - Table S2)** emphasizing their origins as second-generation oxidation products of α-pinene. It is well established that A1 and A4 are generated by further reaction of pinonic acid including OH radical and NO_x (Hallquist et al., 2009). El Haddad et al. (2011a) reported a good correlation between these four compounds suggesting a similar formation process. However, even though belonging to the same class, these compounds did not show any correlation with pinic acid (R^2= 0.10-0.25) probably due to the different formation pathway and the kinetics of the oxidation processes (El Haddad et al., 2011a).

2.2.3 β-caryophyllene oxidation product

The β-caryophyllene (βC) is considered as the most abundant species in the sesquiterpene class emitted from plants. The sesquiterpenes are characterized by their high reactivity and their low vapor pressure (Fu et al., 2010). β-caryophyllinic acid was first identified in smog chambers then in ambient samples (Jaoui et al., 2007). It is considered as the major oxidation product and the molecular marker of β-caryophyllene emitted by terrestrial vegetations.

In this study, the levels of β-caryophyllinic acid were higher in ZK (0.71 ng/m^3) than FA (0.44 ng/m^3). βC did not show any seasonal variations at both sites. The same observation was made during an aircraft campaign over central China (Fu et al., 2014) and in an urban and suburban site in Shanghai, China (Feng et al., 2013).The total average concentrations at both sites are slightly higher than the 0.27 ng/m^3 reported in Marseille, France (El Haddad et al., 2011a) in summer 2008 and comparable with the 0.7 ng/m^3 observed at an urban site in Shanghai (Fu et al., 2014).

However, much higher concentrations were observed at a suburban site in Lebanon with 10.59 ng/m^3 in the summer and 1.21 ng/m^3 in the winter period (Waked et al., 2013; 2014). This difference might be explained by the biomass burning activities in the suburban site leading to higher β-caryophyllinic acid concentrations (Fu et al., 2014).

Table III-6: Atmospheric concentrations (in ng/m^3) of identified secondary organic compounds during the entire sampling period (Total: Dec 2018- Nov 2019), winter (Dec 2018-March 2019), and summer (June 2019-September 2019) periods at Zouk (ZK) and Fiaa (FA) sites

Compounds	Average concentration (min-max) (ng/m^3)					
	ZK site			FA site		
	Total	Winter	Summer	Total	Winter	Summer
Isoprene oxidation products						
2-methylglyceric acid (2-MGA)	0.47 (0.04-5.19)	0.22 (0 .05-0.93)	0.77 (0.04-5.19)	0.86 (0.01-2.64)	0.32 (0.01-1.40)	1.30 (0.17-2.64)
2-methylthreitol (MT1)	1.41 (0.10-5.81)	0.37 (0.10-1.13)	2.64 (0.73-5.81)	2.19 (0.08-13.7)	0.68 (0.08-3.00)	3.68 (0.54-13.7)
2-methylerythritol (MT2)	3.78 (0.53-14.61)	1.43 (0.53-4.69)	6.53 (1.04-15)	6.14 (0.13-39.8)	1.57 (0.13-8.09)	10.40 (0.17-2.64)
Total	**5.67**	**2.01**	**9.93**	**9.19**	**2.56**	**15.38**
α-pinene oxidation products						
Pinic acid (PA)	0.73 (0.09-3.54)	0.50 (0.09-1.75)	0.99 (0.11-3.54)	1.63 (0.10-9.21)	1.24 (0.10-3.96)	1.50 (0.38-3.04)
3-hydroxyglutaric acid (A1)	1.63 (0.01-9.90)	0.65 (0.01-3.28)	2.94 (0.13-9.90)	5.51 (0.02-21.9)	4.31 (0.06-20.02)	7.56 (0.87-21.9)
3-acetylglutaric acid (A2)	1.64 (0.01-8.96)	0.62 (0.01-2.10)	2.74 (0.43-8.96)	3.59 (0.18-13.0)	2.89 (0.18-13.00)	4.65 (0.87-12.2)
3-isopropylglutaric acid (A3)	1.57 (0.05-7.19)	0.74 (0.05-3.03)	2.40 (0.10-7.19)	3.44 (0.09-13.5)	2.79 (0.21-9.62)	4.14 (0.09-13.5)
3-methyl-1,2,3-butanetricarboxylic acid (A4)	1.26 (0.01-8.58)	0.41 (0.01-1.82)	2.34 (0.07-8.58)	3.51 (0.05-15.6)	2.45 (0.07-11.69)	5.03 (0.11-15.6)
Total	**6.82**	**2.92**	**11.41**	**17.68**	**13.68**	**22.88**
β-caryophyllene oxidation product						
β-caryophyllinic acid (βC)	0.71 (0.01-3.29)	0.54 (0.01-1.86)	0.62 (0.03-2.13)	0.44 (0.01-1.66)	0.42 (0.01-1.53)	0.47 (0.02-1.34)
Total	**0.71**	**0.54**	**0.62**	**0.44**	**0.42**	**0.47**
Dicarboxylic acids						
Oxalic acid (diC_2)	1.66 (0.02-6.74)	1.33 (0.02-4.44)	2.05 (0.26-6.74)	3.48 (0.03-70.6)	2.33 (0.19-10.0)	5.34 (0.71-70.6)
Adipic acid (diC_6)	1.67 (0.08-7.48)	1.04 (0.08-4.86)	1.88 (0.17-3.62)	2.89 (0.85-17.8)	4.14 (0.92-17.8)	2.29 (0.85-8.48)
Azelaic acid (diC_9)	10.30 (0.21-47.10)	12.94 (3.63-46.6)	8.03 (0.21-47.1)	5.48 (0.07-47.8)	6.64 (1.10-47.8)	5.36 (1.63-26.8)
Phthalic acid (PhA)	3.41 (0.52-13.73)	4.26 (0.75-7.71)	2.61 (0.52-7.71)	6.65 (0.29-39.1)	13.20 (3.07-39.1)	3.35 (0.50-8.22)
Total	**17.04**	**19.57**	**14.57**	**18.50**	**26.31**	**16.34**

2.2.4 Contribution of biogenic sources to the secondary organic carbon

The apportionment of the Secondary Organic Carbon (SOC) to the different BSOA is based on the SOA tracer method proposed by Kleindienst et al. (2007) in order to determine the highest

contributor to the organic carbon (Waked et al., 2014) among the isoprene, α-pinene, and β-caryophyllene.

Briefly, the measured concentrations of tracer compounds derived from a given hydrocarbon precursor were converted into SOC concentrations by using laboratory generated mass fractions of the same tracers (ratio of the tracers/SOC determined in smog chambers). The considered values for the mass fractions were 0.155 ± 0.039 for isoprene, 0.231 ± 0.111 for α-pinene and 0.023 ± 0.005 for β-caryophyllene (Kleindienst et al., 2007). In addition to that, to assess the SOC contribution of monoterpenes and sesquiterpenes, the SOC estimates of α-pinene and β-caryophyllene were multiplied by 3.2 and 3.6 respectively (Ormeño et al., 2007; Geron and Arnts, 2010; Waked et al., 2014). This method holds high uncertainties due to limiting the complex chemistry behind the SOA formation to a simplified single value for each precursor. This replacement cannot cover neither the whole range of compounds emitted from the precursor nor the meteorological conditions (Kleindienst et al., 2007; Waked et al., 2014). However, the method remains a valuable approach to give insights into apportioning BSOC fractions.

Fig. III-10 shows the contribution of isoprene, monoterpenes, and sesquiterpenes to the SOC at both sites. A clear seasonal pattern is evidenced for the SOC concentrations and could be related to the higher concentrations of the precursors in summer. The total SOC concentrations in FA account for 469 ng/m^3 in the summer period and 255 ng/m^3 in winter. These values are higher than ZK (305 ng/m^3 in summer and 131 ng/m^3 in winter) but lower than those reported for a suburban site in Lebanon (3408 ng/m^3 in summer 2011 and 462 ng/m^3 in winter 2012) (Waked et al., 2013; 2014). In the latter study, the site was located in the suburb of the capital Beirut and was mainly characterized by a high residential density, commercial activities and by forested trees surrounding the sampling site.

As discussed before, the anthropogenic contribution of all the primary species is more important than the biogenic ones in ZK and FA due to the industrial typology of the sites while the Chekka area is more affected by forested pine lands. Monoterpenes are found to be the largest contributors to SOC especially in summer accounting for 47% and 63% in ZK and FA respectively.

2.3 Dicarboxylic acids

Dicarboxylic acids are part of the water-soluble organic compounds. Due to their low vapor pressures, they are mainly present in the particulate phase (Li et al., 2006).

The concentrations of oxalic acid recorded at both sites were 1.33 ng/m^3 and 2.33 ng/m^3 in winter, 2.05 ng/m^3 and 5.34 ng/m^3 in summer at ZK and FA respectively.

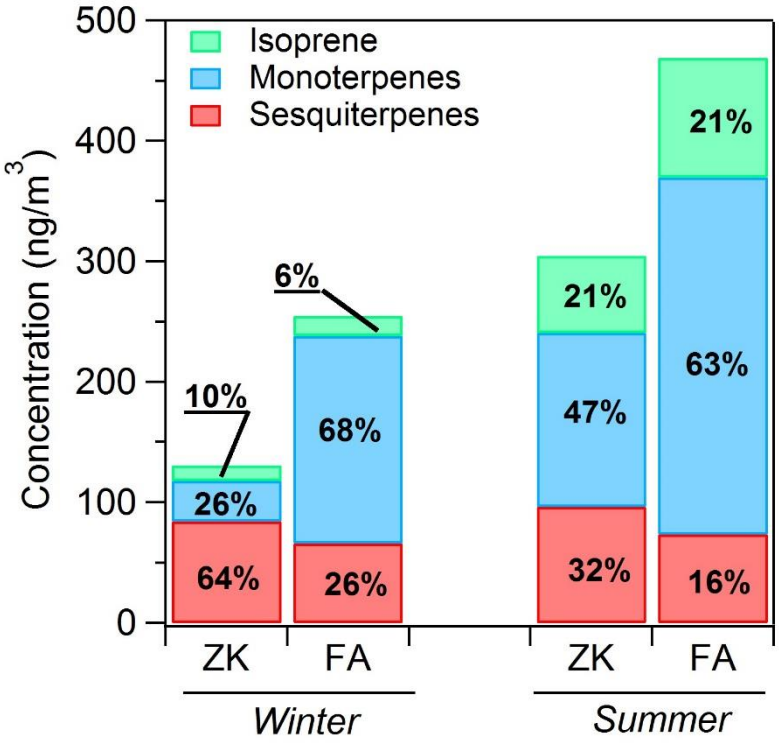

Fig. III-10: The SOC contributions (in ng/m^3) of isoprene, monoterpenes, and sesquiterpenes at Zouk (ZK) and Fiaa (FA) during summer and winter periods

The higher concentrations in summer could be due, as for other SOA, to enhanced photochemical reactions by more intense solar radiations, and favorizing the decomposition of succinic acid to malonic and oxalic acid (Hsieh et al., 2007). Waked et al. (2013); (2014) reported much higher concentrations of this compound in summer (67.8 ng/m^3) and in winter (14.1 ng/m^3) in Mansourieh, Lebanon: a suburban site located in the suburbs of Beirut. Generally, oxalic acid is considered as the dominant species between the dicarboxylic acids because of its stability and its production by atmospheric oxidation of other dicarboxylic acids with higher number of carbons (Yu et al., 2019).

In this study, Azelaic acid (diC_9) is the most abundant dicarboxylic acid at ZK with concentrations of 12.9 and 8.03 ng/m^3 and the second most abundant with 6.64 and 5.36 ng/m^3 at FA in the winter and the summer periods respectively. The summer values are higher than the 4.2 ng/m^3 observed at central Alaska during the hot season (Deshmukh et al., 2018). Azelaic acid is generated by the oxidation process of biogenic unsaturated fatty acids such as oleic acid.

The high concentrations might be explained by the intense cooking activities in ZK and FA as mentioned in Section 2.1.4.

As for the adipic acid (diC_6), higher concentrations **(Table III-6)** were found compared to the value of 2 ng/m^3 reported in the city of Philadelphia (Ray and McDow, 2005) except for 1.04 ng/m^3 observed in ZK during winter. Adipic acid (diC_6) is produced by the photooxidation of cyclohexene via ozone and OH reactions (Kawamura and Yasui, 2005). Cyclohexene can be found in motor exhausts revealing the anthropogenic nature of the compound (Grosjean and Fung, 1984).

Additionally, the average concentrations of phthalic acid (PhA) were 3.41 and 6.65 ng/m^3 at ZK and FA respectively. These values are higher than the 2.4 ng/m^3 reported for a site in southern Sweden (Hyder et al., 2012). PhA is generally produced by secondary photochemical reaction with PAHs, specifically naphthalene, but can also be emitted directly from combustion sources (Nguyen et al., 2016).

As mentioned earlier, PhA and diC_6 are known to be the oxidation products of compounds emitted by anthropogenic sources while diC_9 is mainly from biogenic activities. In order to qualitatively evaluate the evolution of the strength of the anthropogenic versus the biogenic sources of the diacids, the diC_6/diC_9 and the PhA/diC_9 ratios can be used (Meng et al., 2013; Kunwar et al., 2019). Higher ratios will be observed for samples that are more influenced by anthropogenic sources.

The average values of the diC_6/diC_9 and the PhA/diC_9 ratios increased in ZK from 0.09 and 0.38 respectively in winter samples to 0.44 and 0.54 in summer samples. The higher PhA/diC_9 ratio is explained by the lower concentrations of diC_9 in the summer period which might be related to the lower concentrations of one of its precursors such as oleic acid **(Table III-4)** in ZK. This assumption can also stand for the diC_6/diC_9 ratio with also higher diC_6 concentrations that might be caused by an increase in the vehicular emissions during this period.

On the contrary, the ratios decreased in FA from 1.28 and 2.91 in winter to 0.52 and 0.71 in summer for diC_6/diC_9 and PhA/diC_9, respectively. This might be due to a decrease in anthropogenic emissions due to the shutdown of the cement factories in this period (lower PhA and diC_6 concentrations in summer while diC_9 is almost constant).

All of these findings regarding SOA showed firstly the complexity of the atmospheric processes and secondly that the composition of this part of the aerosol strongly depend on local and

seasonal factors affecting the primary emissions and the photooxidation conditions. Thus, trees, plants, and vegetation around the site affect the emissions of the Biogenic Volatile Organic Compounds leading to variations in the concentrations of their oxidation products. In addition to that, meteorological factors, and local atmospheric chemistry (aerosol acidity, NO_x conditions, solar radiation intensity…) influence the formation of the SOA to a high extent.

3 Conclusions

The analysis of the organic fraction in $PM_{2.5}$ collected over a one-year period in Lebanon in the urban-industrial areas of Zouk Mikael and Chekka region, in particular Fiaa, revealed significant variations between the sites on the concentration levels, the potential sources, and the seasonal variations of the organic compounds. The most abundant class of compounds was the fatty acids, that is part of the primary organic aerosols (POA), emitted mainly from cooking activities.

For most of the POA, ZK recorded higher concentrations due to the more urbanized, residential, and industrial influence than FA. The petrogenic source at both sites was highlighted considering the concentrations of the n-alkanes, CPI, Wax% and C_{max} with a low contribution of the primary biogenic emissions especially in winter. The fuel combustion in ZK might be assigned to vehicular emissions, diesel generators and most importantly the HFO combustion from the power plant by observing the PAHs concentrations and their corresponding diagnostic ratios. In addition to the PAH and alkanes, the hopanes identified in ZK underline the importance of the road traffic in the region. On the other hand, the main sources highlighted in Chekka region were a mix of coke and fuel burning. The variation in the concentrations of phthalates at ZK and FA suggests plastic incineration near the study areas alongside a contribution from the plastic production industries in ZK during summer.

For the secondary organic aerosols (SOA), higher concentrations were reported during summer at both sites due to the enhancement of the photochemical reactions and high temperatures. The α-pinene oxidation products were the most abundant class in the secondary biogenic organic aerosols. Even with low concentrations, BSOA compounds can largely contribute to the SOC. Due to higher vegetation and forests in the Chekka region, higher concentrations of the BSOA were noted during both seasons. In addition, industrial activities have an important influence on the SOA formation especially for compounds having their precursors emitted from anthropogenic sources such as phthalic and adipic acids.

Finally, following the high concentrations of the different organic compounds classes of which some are of particular interest to the health field due to their high toxicity, further investigation would be needed specially source apportionment studies and health risk assessment for a better air quality management planning.

Acknowledgments and funding:

The authors would like to acknowledge the National Council for Scientific Research of Lebanon (CNRS-L) for granting a doctoral fellowship to Marc Fadel.

This project was also funded by the Research Council and the Faculty of Sciences of Saint Joseph University of Beirut – Lebanon.

The "Unité de Chimie Environnementale et Interactions sur le Vivant" (UCEIV-UR4492) participates in the CLIMIBIO project, which is financially supported by the Hauts-de-France Region Council, the French Ministry of Higher Education and Research, and the European Regional Development Funds.

References:

Abbas, I., Chaaban, J., Al-Rabaa, A.-R., Shaar, A., Shaar, A., 2019. Solid waste management in Lebanon: challenges and recommendations. Int J Environ Waste Manag

Abdallah, C., Afif, C., Sauvage, S., Borbon, A., Salameh, T., Kfoury, A., Leonardis, T., Karam, C., Formenti, P., Doussin, J.F., Locoge, N., Sartelet, K., 2020. Determination of gaseous and particulate emission factors from road transport in a Middle Eastern capital. Transp Res D Transp Envrion 83, 102361, https://doi.org/10.1016/j.trd.2020.102361.

Afif, C., Chélala, C., Borbon, A., Abboud, M., Gerard, J., Farah, W., Jambert, C., Zaarour, R., Saliba, N., Perros, P., Rizk, T., 2008. SO_2 in Beirut: air quality implication and effects of local emissions and long-range transport. Air Qual Atmos Health 1, 167-178, 10.1007/s11869-008-0022-y.

Anderson, J.O., Thundiyil, J.G., Stolbach, A., 2012. Clearing the air: a review of the effects of particulate matter air pollution on human health. Journal of medical toxicology : official journal of the American College of Medical Toxicology 8, 166-175, 10.1007/s13181-011-0203-1.

Andreou, G., Rapsomanikis, S., 2009. Origins of n-alkanes, carbonyl compounds and molecular biomarkers in atmospheric fine and coarse particles of Athens, Greece. Sci. Total Environ. 407, 5750-5760, https://doi.org/10.1016/j.scitotenv.2009.07.019.

Annegarn, H., Marcazzan, G.M., Cereda, E., Marchionni, M., Zucchiatti, A., 1992. Source profiles by unique ratios (SPUR) analysis: determination of source profiles from receptor-site streaker samples. Atmos Environ 26, 333-343, 10.1016/0960-1686(92)90314-B.

Atkinson, R., 2008. Our present understanding of the gas-phase atmospheric degradation of VOCs. Springer Netherlands, Dordrecht, pp. 1-19.

Baalbaki, R., Nassar, J., Salloum, S., Shihadeh, A.L., Lakkis, I., Saliba, N.A., 2018. Comparison of atmospheric polycyclic aromatic hydrocarbon levels in three urban areas in Lebanon. Atmos Environ 179, 260-267, https://doi.org/10.1016/j.atmosenv.2018.02.028.

Badran, G., Ledoux, F., Verdin, A., Abbas, I., Roumie, M., Genevray, P., Landkocz, Y., Lo Guidice, J.-M., Garçon, G., Courcot, D., 2020. Toxicity of fine and quasi-ultrafine particles: Focus on the effects of organic extractable and non-extractable matter fractions. Chemosphere 243, 125440, https://doi.org/10.1016/j.chemosphere.2019.125440.

Bi, C., Chen, Y., Zhao, Z., Li, Q., Zhou, Q., Ye, Z., Ge, X., 2020. Characteristics, sources and health risks of toxic species (PCDD/Fs, PAHs and heavy metals) in $PM_{2.5}$ during fall and winter in an industrial area. Chemosphere 238, 124620, https://doi.org/10.1016/j.chemosphere.2019.124620.

Boonyatumanond, R., Murakami, M., Wattayakorn, G., Togo, A., Takada, H., 2007. Sources of polycyclic aromatic hydrocarbons (PAHs) in street dust in a tropical Asian mega-city, Bangkok, Thailand. Sci. Total Environ. 384, 420-432, https://doi.org/10.1016/j.scitotenv.2007.06.046.

Borgie, M., Dagher, Z., Ledoux, F., Verdin, A., Cazier, F., Martin, P., Hachimi, A., Shirali, P., Greige-Gerges, H., Courcot, D., 2015. Comparison between ultrafine and fine particulate matter collected in Lebanon: Chemical characterization, in vitro cytotoxic effects and metabolizing enzymes gene expression in human bronchial epithelial cells. Environ. Pollut. 205, 250-260, https://doi.org/10.1016/j.envpol.2015.05.027.

Borgie, M., Ledoux, F., Dagher, Z., Verdin, A., Cazier, F., Courcot, L., Shirali, P., Greige-Gerges, H., Courcot, D., 2016. Chemical characteristics of $PM_{2.5–0.3}$ and $PM_{0.3}$ and consequence of a dust storm episode at an urban site in Lebanon. Atmos Res 180, 274-286, https://doi.org/10.1016/j.atmosres.2016.06.001.

Bray, E.E., Evans, E.D., 1961. Distribution of n-paraffins as a clue to recognition of source beds. Geochim. Cosmochim. Acta 22, 2-15, https://doi.org/10.1016/0016-7037(61)90069-2.

Carlton, A.G., Wiedinmyer, C., Kroll, J.H., 2009. A review of Secondary Organic Aerosol (SOA) formation from isoprene. Atmos. Chem. Phys. 9, 4987-5005, 10.5194/acp-9-4987-2009.

Cazier, F., Genevray, P., Dewaele, D., Nouali, H., Verdin, A., Ledoux, F., Hachimi, A., Courcot, L., Billet, S., Bouhsina, S., Shirali, P., Garçon, G., Courcot, D., 2016. Characterisation and seasonal variations of particles in the atmosphere of rural, urban and industrial areas: Organic compounds. J Environ Sci 44, 45-56, 10.1016/j.jes.2016.01.014.

Cecinato, A., Guerriero, E., Balducci, C., Muto, V., 2014. Use of the PAH fingerprints for identifying pollution sources. Urban Climate 10, 630-643, https://doi.org/10.1016/j.uclim.2014.04.004.

Claeys, M., Graham, B., Vas, G.,Wang,W., Vermeylen, R., Pashynska,, V., C., J., Guyon, P., Andreae, M. O., Artaxo, P., and, Maenhaut, W., 2004. Formation of Secondary Organic Aerosols Through Photooxidation of Isoprene. Sci Mag 303, 1173-1176

Cooper, J.E., Bray, E.E., 1963. A postulated role of fatty acids in petroleum formation. Geochim. Cosmochim. Acta 27, 1113-1127, https://doi.org/10.1016/0016-7037(63)90093-0.

Daher, N., Saliba, N.A., Shihadeh, A.L., Jaafar, M., Baalbaki, R., Sioutas, C., 2013. Chemical composition of size-resolved particulate matter at near-freeway and urban background sites in the greater Beirut area. Atmos Environ 80, 96-106, 10.1016/j.atmosenv.2013.08.004.

De Gouw, J., Jimenez, J.L., 2009. Organic Aerosols in the Earth's Atmosphere. Environ. Sci. Technol. 43, 7614-7618, 10.1021/es9006004.

Deshmukh, D.K., Mozammel Haque, M., Kawamura, K., Kim, Y., 2018. Dicarboxylic acids, oxocarboxylic acids and α-dicarbonyls in fine aerosols over central Alaska: Implications for sources and atmospheric processes. Atmos Res 202, 128-139, https://doi.org/10.1016/j.atmosres.2017.11.003.

Ding, X., Wang, X.-M., Zheng, M., 2011. The influence of temperature and aerosol acidity on biogenic secondary organic aerosol tracers: Observations at a rural site in the central Pearl River Delta region, South China. Atmos Environ 45, 1303-1311, https://doi.org/10.1016/j.atmosenv.2010.11.057.

DRI, 2003. Analysis of Semi-volatile Organic Compound by GC/MS. Desert Research Institute, DRI Standard Operating Procedure., 1–25

Du, Y., Xu, X., Chu, M., Guo, Y., Wang, J., 2016. Air particulate matter and cardiovascular disease: the epidemiological, biomedical and clinical evidence. J Thorac Dis 8, E8-E19, 10.3978/j.issn.2072-1439.2015.11.37.

El Haddad, I., Marchand, N., Dron, J., Temime-Roussel, B., Quivet, E., Wortham, H., Jaffrezo, J.L., Baduel, C., Voisin, D., Besombes, J.L., Gille, G., 2009. Comprehensive primary particulate organic characterization of vehicular exhaust emissions in France. Atmos Environ 43, 6190-6198, https://doi.org/10.1016/j.atmosenv.2009.09.001.

El Haddad, I., Marchand, N., Temime-Roussel, B., Wortham, H., Piot, C., Besombes, J.L., Baduel, C., Voisin, D., Armengaud, A., Jaffrezo, J.L., 2011a. Insights into the secondary fraction of the organic aerosol in a Mediterranean urban area: Marseille. Atmos. Chem. Phys. 11, 2059-2079, 10.5194/acp-11-2059-2011.

El Haddad, I., Marchand, N., Wortham, H., Piot, C., Besombes, J.L., Cozic, J., Chauvel, C., Armengaud, A., Robin, D., Jaffrezo, J.L., 2011b. Primary sources of $PM_{2.5}$ organic aerosol in an industrial Mediterranean city, Marseille. Atmos. Chem. Phys. 11, 2039-2058, 10.5194/acp-11-2039-2011.

Feng, J., Li, M., Zhang, P., Gong, S., Zhong, M., Wu, M., Zheng, M., Chen, C., Wang, H., Lou, S., 2013. Investigation of the sources and seasonal variations of secondary organic aerosols in $PM_{2.5}$ in Shanghai with organic tracers. Atmos Environ 79, 614-622, https://doi.org/10.1016/j.atmosenv.2013.07.022.

Fu, P., Kawamura, K., Kanaya, Y., Wang, Z., 2010. Contributions of biogenic volatile organic compounds to the formation of secondary organic aerosols over Mt. Tai, Central East China. Atmos Environ 44, 4817-4826, https://doi.org/10.1016/j.atmosenv.2010.08.040.

Fu, P.Q., Kawamura, K., Cheng, Y.F., Hatakeyama, S., Takami, A., Li, H., Wang, W., 2014. Aircraft measurements of polar organic tracer compounds in tropospheric particles PM_{10} over central China. Atmos. Chem. Phys. 14, 4185-4199, 10.5194/acp-14-4185-2014.

Gadi, R., Shivani, Sharma, S.K., Mandal, T.K., 2019. Source apportionment and health risk assessment of organic constituents in fine ambient aerosols ($PM_{2.5}$): A complete year study over National Capital Region of India. Chemosphere 221, 583-596, https://doi.org/10.1016/j.chemosphere.2019.01.067.

Geron, C.D., Arnts, R.R., 2010. Seasonal monoterpene and sesquiterpene emissions from Pinus taeda and Pinus virginiana. Atmos Environ 44, 4240-4251, https://doi.org/10.1016/j.atmosenv.2010.06.054.

Grosjean, D., Fung, K., 1984. Hydrocarbons and Carbonyls in Los Angeles Air. Journal of the Air Pollution Control Association 34, 537-543, 10.1080/00022470.1984.10465772.

Guenther, A., Hewitt, C.N., Erickson, D., Fall, R., Geron, C., Graedel, T., Harley, P., Klinger, L., Lerdau, M., Mckay, W.A., Pierce, T., Scholes, B., Steinbrecher, R., Tallamraju, R., Taylor, J., Zimmerman, P., 1995. A global model of natural volatile organic compound emissions. J Geophys Res Atmos 100, 8873-8892, 10.1029/94jd02950.

Guo, H., 2003. Particle-associated polycyclic aromatic hydrocarbons in urban air of Hong Kong. Atmos Environ 37, 5307-5317, 10.1016/j.atmosenv.2003.09.011.

Hallquist, M., Wenger, J.C., Baltensperger, U., Rudich, Y., Simpson, D., Claeys, M., Dommen, J., Donahue, N., George, C., Goldstein, A., Hamilton, J., Herrmann, H., Hoffmann, T., Iinuma, Y., Jang, M., Jenkin, M.E., Jimenez, J., Kiendler-Scharr, A., Maenhaut, W., McFiggans, G., Mentel, T.F., Monod, A., Prévôt, A.S.H., Seinfeld, J.H., Surratt, J.D., Szmigielski, R., Wildt, J., 2009. The formation, properties and impact of secondary organic aerosol: Current and emerging issues. Atmos. Chem. Phys. 9, 5155–5236, 10.5194/acpd-9-3555-2009.

Henry, R.C., Lewis, C.W., Hopke, P.K., Williamson, H.J., 1984. Review of receptor model fundamentals. Atmos Environ 18, 1507-1515, https://doi.org/10.1016/0004-6981(84)90375-5.

Hsieh, L.-Y., Kuo, S.-C., Chen, C.-L., Tsai, Y.I., 2007. Origin of low-molecular-weight dicarboxylic acids and their concentration and size distribution variation in suburban aerosol. Atmos Environ 41, 6648-6661, https://doi.org/10.1016/j.atmosenv.2007.04.014.

Hyder, M., Genberg, J., Sandahl, M., Swietlicki, E., Jönsson, J.Å., 2012. Yearly trend of dicarboxylic acids in organic aerosols from south of Sweden and source attribution. Atmos Environ 57, 197-204, https://doi.org/10.1016/j.atmosenv.2012.04.027.

Ion, A.C., Vermeylen, R., Kourtchev, I., Cafmeyer, J., Chi, X., Gelencsér, A., Maenhaut, W., Claeys, M., 2005. Polar organic compounds in rural $PM_{2.5}$ aerosols from K-puszta, Hungary, during a 2003 summer field campaign: Sources and diel variations. Atmos. Chem. Phys. 5, 1805-1814, 10.5194/acp-5-1805-2005.

Jaafar, M., Baalbaki, R., Mrad, R., Daher, N., Shihadeh, A., Sioutas, C., Saliba, N.A., 2014. Dust episodes in Beirut and their effect on the chemical composition of coarse and fine particulate matter. Sci. Total Environ. 496, 75-83, https://doi.org/10.1016/j.scitotenv.2014.07.018.

Jaoui, M., Lewandowski, M., Kleindienst, T.E., Offenberg, J.H., Edney, E.O., 2007. β-caryophyllinic acid: An atmospheric tracer forβ-caryophyllene secondary organic aerosol. Geophys. Res. Lett. 34, 10.1029/2006gl028827.

Ji, Y., Wang, F., Zhang, L., Shan, C., Bai, Z., Sun, Z., Liu, L., Shen, B., 2014. A comprehensive assessment of human exposure to phthalates from environmental media and food in Tianjin, China. J. Hazard. Mater. 279, 133-140, https://doi.org/10.1016/j.jhazmat.2014.06.055.

Kawamura, K., Yasui, O., 2005. Diurnal changes in the distribution of dicarboxylic acids, ketocarboxylic acids and dicarbonyls in the urban Tokyo atmosphere. Atmos Environ 39, 1945-1960, https://doi.org/10.1016/j.atmosenv.2004.12.014.

Kfoury, A., Ledoux, F., El Khoury, B., Nakat, H., Nouali, H., Cazier, F., Courcot, D., Abi-Aad, E., Aboukaïs, A., 2009. A study of the inorganic chemical composition of atmospheric particulate matter in the region of Chekka, North Lebanon. Lebanese Science Journal 10, 3-16

Khalili, N.R., Scheff, P.A., Holsen, T.M., 1995. PAH source fingerprints for coke ovens, diesel and, gasoline engines, highway tunnels, and wood combustion emissions. Atmos Environ 29, 533-542, https://doi.org/10.1016/1352-2310(94)00275-P.

Kim, Y.-H., Kim, K.-H., 2015. A simple methodological validation of the gas/particle fractionation of polycyclic aromatic hydrocarbons in ambient air. Scientific Reports 5, 11679, 10.1038/srep11679.

Kleindienst, T.E., Jaoui, M., Lewandowski, M., Offenberg, J.H., Lewis, C.W., Bhave, P.V., Edney, E.O., 2007. Estimates of the contributions of biogenic and anthropogenic hydrocarbons to secondary organic aerosol at a southeastern US location. Atmos Environ 41, 8288-8300, https://doi.org/10.1016/j.atmosenv.2007.06.045.

Kotianova, P., Puxbaum, H., Bauer, H., Caseiro, A., Marr, I., Cik, G., 2008. Temporal patterns of n-alkanes at traffic exposed and suburban sites in Vienna. Atmos Environ 42, 2993-3005, 10.1016/j.atmosenv.2007.12.048.

Kourtchev, I., Warnke, J., Maenhaut, W., Hoffmann, T., Claeys, M., 2008. Polar organic marker compounds in $PM_{2.5}$ aerosol from a mixed forest site in western Germany. Chemosphere 73, 1308-1314, https://doi.org/10.1016/j.chemosphere.2008.07.011.

Kroll, J.H., Seinfeld, J.H., 2008. Chemistry of secondary organic aerosol: Formation and evolution of low-volatility organics in the atmosphere. Atmos Environ 42, 3593-3624, https://doi.org/10.1016/j.atmosenv.2008.01.003.

Kunwar, B., Kawamura, K., Fujiwara, S., Fu, P., Miyazaki, Y., Pokhrel, A., 2019. Dicarboxylic acids, oxocarboxylic acids and α-dicarbonyls in atmospheric aerosols from Mt. Fuji, Japan: Implication for primary emission versus secondary formation. Atmos Res 221, 58-71, https://doi.org/10.1016/j.atmosres.2019.01.021.

Landkocz, Y., Ledoux, F., André, V., Cazier, F., Genevray, P., Dewaele, D., Martin, P.J., Lepers, C., Verdin, A., Courcot, L., Boushina, S., Sichel, F., Gualtieri, M., Shirali, P., Courcot, D., Billet, S., 2017. Fine and ultrafine atmospheric particulate matter at a multi-influenced urban site: Physicochemical characterization, mutagenicity and cytotoxicity. Environ. Pollut. 221, 130-140, https://doi.org/10.1016/j.envpol.2016.11.054.

Ledoux, F., Kfoury, A., Delmaire, G., Roussel, G., El Zein, A., Courcot, D., 2017. Contributions of local and regional anthropogenic sources of metals in $PM_{2.5}$ at an urban site in northern France. Chemosphere 181, 713-724, 10.1016/j.chemosphere.2017.04.128.

Lelieveld, J., Pozzer, A., Pöschl, U., Fnais, M., Haines, A., Münzel, T., 2020. Loss of life expectancy from air pollution compared to other risk factors: a worldwide perspective. Cardiovasc. Res., 10.1093/cvr/cvaa025.

Li, M., McDow, S.R., Tollerud, D.J., Mazurek, M.A., 2006. Seasonal abundance of organic molecular markers in urban particulate matter from Philadelphia, PA. Atmos Environ 40, 2260-2273, https://doi.org/10.1016/j.atmosenv.2005.10.025.

Li, W., Peng, Y., Bai, Z., 2010. Distributions and sources of n-alkanes in $PM_{2.5}$ at urban, industrial and coastal sites in Tianjin, China. J Environ Sci 22, 1551-1557, https://doi.org/10.1016/S1001-0742(09)60288-6.

Lu, S., Kang, L., Liao, S., Ma, S., Zhou, L., Chen, D., Yu, Y., 2018. Phthalates in $PM_{2.5}$ from Shenzhen, China and human exposure assessment factored their bioaccessibility in lung. Chemosphere 202, 726-732, https://doi.org/10.1016/j.chemosphere.2018.03.155.

Manoli, E., Kouras, A., Samara, C., 2004. Profile Analysis of Ambient and Source Emitted Particle-Bound Polycyclic Aromatic Hydrocarbons from Three Sites in Northern Greece. Chemosphere 56, 867-878, 10.1016/j.chemosphere.2004.03.013.

Masclet, P., Bresson, M.A., Mouvier, G., 1987. Polycyclic aromatic hydrocarbons emitted by power stations, and influence of combustion conditions. Fuel 66, 556-562, https://doi.org/10.1016/0016-2361(87)90163-3.

Mastral, A., Callén, M., Lopez, J., Murillo, R., Garcia, T., Navarro, M., 2003. Critical review on atmospheric PAH. Assessment of reported data in the Mediterranean basin. Fuel Process. Technol. 80, 183-193, 10.1016/S0378-3820(02)00249-7.

Mastral, A.M., Callén, M.S., 2000. A review on Polycyclic Aromatic Hydrocarbon (PAH) emissions from energy generation. Environ. Sci. Technol. 34, 3051-3057, 10.1021/es001028d.

Melki, P., 2017. Health impact of airborne particulate matter in Northern Lebanon: from a pilot epidemiological study to physico-chemical characterization and toxicological effects assessment.

Melki, P.N., Ledoux, F., Aouad, S., Billet, S., El Khoury, B., Landkocz, Y., Abdel-Massih, R.M., Courcot, D., 2017. Physicochemical characteristics, mutagenicity and genotoxicity of airborne particles under industrial and rural influences in Northern Lebanon. Environ Sci Pollut Res Int 24, 18782-18797, https://doi.org/10.1007/s11356-017-9389-3.

Meng, J., Wang, G., Li, J., Cheng, C., Cao, J., 2013. Atmospheric oxalic acid and related secondary organic aerosols in Qinghai Lake, a continental background site in Tibet Plateau. Atmos Environ 79, 582-589, https://doi.org/10.1016/j.atmosenv.2013.07.024.

Mikuška, P., Křůmal, K., Večeřa, Z., 2015. Characterization of organic compounds in the $PM_{2.5}$ aerosols in winter in an industrial urban area. Atmos Environ 105, 97-108, https://doi.org/10.1016/j.atmosenv.2015.01.028.

Nguyen, L., Kawamura, K., Ono, K., Ram, S., Engling, G., Lee, C.-T., Lin, N.-H., Chang, S.-C., Chuang, M.-T., Hsiao, T.-C., Sheu, G.-R., Ou-Yang, C.-F., Chi, K., Sun, S.-A., 2016. Comprehensive $PM_{2.5}$ organic molecular composition and stable carbon isotope ratios of biomass burning smoke at Sonla, Vietnam: Fingerprint of biomass burning components. Aerosol Air Qual Res 16, 10.4209/aaqr.2015.07.0459.

Ormeño, E., Fernandez, C., Bousquet-Mélou, A., Greff, S., Morin, E., Robles, C., Vila, B., Bonin, G., 2007. Monoterpene and sesquiterpene emissions of three Mediterranean species through calcareous and siliceous soils in natural conditions. Atmos Environ 41, 629-639, https://doi.org/10.1016/j.atmosenv.2006.08.027.

Pei, X.Q., Song, M., Guo, M., Mo, F.F., Shen, X.Y., 2013. Concentration and risk assessment of phthalates present in indoor air from newly decorated apartments. Atmos Environ 68, 17-23, https://doi.org/10.1016/j.atmosenv.2012.11.039.

Pindado, O., Pérez, R.M., García, S., Sánchez, M., Galán, P., Fernández, M., 2009. Characterization and sources assignation of $PM_{2.5}$ organic aerosol in a rural area of Spain. Atmos Environ 43, 2796-2803, https://doi.org/10.1016/j.atmosenv.2009.02.046.

Ravindra, K., Sokhi, R., Vangrieken, R., 2008. Atmospheric polycyclic aromatic hydrocarbons: Source attribution, emission factors and regulation. Atmos Environ 42, 2895-2921, 10.1016/j.atmosenv.2007.12.010.

Ray, J., McDow, S.R., 2005. Dicarboxylic acid concentration trends and sampling artifacts. Atmos Environ 39, 7906-7919, https://doi.org/10.1016/j.atmosenv.2005.09.024.

Riffault, V., Arndt, J., Marris, H., Mbengue, S., Setyan, A., Alleman, L.Y., Deboudt, K., Flament, P., Augustin, P., Delbarre, H., Wenger, J., 2015. Fine and ultrafine particles in the vicinity of industrial activities: A Review. Crit Rev Environ Sci Technol 45, 2305-2356, 10.1080/10643389.2015.1025636.

Robinson, A.L., Subramanian, R., Donahue, N.M., Bernardo-Bricker, A., Rogge, W.F., 2006. Source Apportionment of Molecular Markers and Organic Aerosol. 3. Food Cooking Emissions. Environ. Sci. Technol. 40, 7820-7827, 10.1021/es060781p.

Rogge, W.F., Hildemann, L.M., Mazurek, M.A., Cass, G.R., 1996. Mathematical modeling of atmospheric fine particle-associated primary organic compound concentrations. J Geophys Res 101, 19,379

Rogge, W.F., Hildemann, L.M., Mazurek, M.A., Cass, G.R., Simoneit, B.R.T., 1991. Sources of fine organic aerosol. 1. Charbroilers and meat cooking operations. Environ. Sci. Technol. 25, 1112-1125, 10.1021/es00018a015.

Rogge, W.F., Hildemann, L.M., Mazurek, M.A., Cass, G.R., Simoneit, B.R.T., 1993a. Sources of fine organic aerosol. 2. Noncatalyst and catalyst-equipped automobiles and heavy-duty diesel trucks. Environ. Sci. Technol. 27, 636-651, 10.1021/es00041a007.

Rogge, W.F., Hildemann, L.M., Mazurek, M.A., Cass, G.R., Simoneit, B.R.T., 1993b. Sources of fine organic aerosol. 4. Particulate abrasion products from leaf surfaces of urban plants. Environ. Sci. Technol. 27, 2700-2711, 10.1021/es00049a008.

Ruehl, C.R., Ham, W.A., Kleeman, M.J., 2011. Temperature-induced volatility of molecular markers in ambient airborne particulate matter. Atmos. Chem. Phys. 11, 67-76, 10.5194/acp-11-67-2011.

Rutter, A.P., Snyder, D.C., Stone, E.A., Shelton, B., DeMinter, J., Schauer, J.J., 2014. Preliminary assessment of the anthropogenic and biogenic contributions to secondary organic aerosols at two industrial cities in the upper Midwest. Atmos Environ 84, 307-313, https://doi.org/10.1016/j.atmosenv.2013.11.014.

Salameh, T., Sauvage, S., Afif, C., Borbon, A., Léonardis, T., Brioude, J., Waked, A., Locoge, N., 2015. Exploring the seasonal NMHC distribution in an urban area of the Middle East during ECOCEM campaigns: Very high loadings dominated by local emissions and dynamics. Environ. Chem., 10.1071/EN14154.

Schauer, J.J., Kleeman, M.J., Cass, G.R., Simoneit, B.R.T., 2002. Measurement of Emissions from Air Pollution Sources. 4. C1−C27 Organic Compounds from Cooking with Seed Oils. Environ. Sci. Technol. 36, 567-575, 10.1021/es002053m.

Seinfeld, J.H., Pandis, S.N., 2016. Atmospheric Chemistry and Physics: From Air Pollution to Climate Change, 3r. John Wiley & Sons.

Simoneit, B.R.T., 1989. Organic matter of the troposphere — V: Application of molecular marker analysis to biogenic emissions into the troposphere for source reconciliations. J. Atmos. Chem. 8, 251-275, 10.1007/BF00051497.

Simoneit, B.R.T., 1999. A review of biomarker compounds as source indicators and tracers for air pollution. Environ Sci Pollut Res 6, 159-169, 10.1007/BF02987621.

Simoneit, B.R.T., 2002. Biomass burning — a review of organic tracers for smoke from incomplete combustion. Appl. Geochem. 17, 129-162, https://doi.org/10.1016/S0883-2927(01)00061-0.

Simoneit, B.R.T., Medeiros, P.M., Didyk, B.M., 2005. Combustion products of plastics as indicators for refuse burning in the atmosphere. Environ. Sci. Technol. 39, 6961-6970, 10.1021/es050767x.

Simoneit, B.R.T., Sheng, G., Chen, X., Fu, J., Zhang, J., Xu, Y., 1991. Molecular marker study of extractable organic matter in aerosols from urban areas of China. Atmos Environ 25, 2111-2129, https://doi.org/10.1016/0960-1686(91)90088-O.

Tan, J., Guo, S., Ma, Y., Duan, J., Cheng, Y., He, K., Yang, F., 2011. Characteristics of particulate PAHs during a typical haze episode in Guangzhou, China. Atmos Res 102, 91-98, https://doi.org/10.1016/j.atmosres.2011.06.012.

Tobiszewski, M., Namieśnik, J., 2012. PAH diagnostic ratios for the identification of pollution emission sources. Environ. Pollut. 162, 110-119, https://doi.org/10.1016/j.envpol.2011.10.025.

USEPA, 2010. AP-42: Compilation of air pollutant emission factors; stationary point and area sources, Fifth Edition. US EPA edition.

Waked, A., Afif, C., 2012. Emissions of air pollutants from road transport in Lebanon and other countries in the Middle East region. Atmos Environ 61, 446-452, 10.1016/j.atmosenv.2012.07.064.

Waked, A., Afif, C., Brioude, J., Formenti, P., Chevaillier, S., Haddad, I.E., Doussin, J.-F., Borbon, A., Seigneur, C., 2013. Composition and source apportionment of organic aerosol in Beirut, Lebanon, during winter 2012. Aerosol Sci. Technol. 47, 1258-1266, 10.1080/02786826.2013.831975.

Waked, A., Afif, C., Formenti, P., Chevaillier, S., El-Haddad, I., Doussin, J.-F., Borbon, A., Seigneur, C., 2014. Characterization of organic tracer compounds in $PM_{2.5}$ at a semi-urban site in Beirut, Lebanon. Atmos Res 143, 85-94, 10.1016/j.atmosres.2014.02.006.

Waked, A., Afif, C., Seigneur, C., 2012. An atmospheric emission inventory of anthropogenic and biogenic sources for Lebanon. Atmos Environ 50, 88-96, https://doi.org/10.1016/j.atmosenv.2011.12.058.

Wang, J., Ho, S.S.H., Ma, S., Cao, J., Dai, W., Liu, S., Shen, Z., Huang, R., Wang, G., Han, Y., 2016. Characterization of $PM_{2.5}$ in Guangzhou, China: uses of organic markers for supporting source apportionment. Sci. Total Environ. 550, 961-971, https://doi.org/10.1016/j.scitotenv.2016.01.138.

WHO, 2013. Health effects of particulate matter : policy implications for countries in eastern Europe, Caucasus and central Asia.

Wu, D., Wang, Z., Chen, J., Kong, S., Fu, X., Deng, H., Shao, G., Wu, G., 2014. Polycyclic aromatic hydrocarbons (PAHs) in atmospheric $PM_{2.5}$ and PM_{10} at a coal-based industrial city: Implication for PAH control at industrial agglomeration regions, China. Atmos Res 149, 217-229, 10.1016/j.atmosres.2014.06.012.

Xing, Y.-F., Xu, Y.-H., Shi, M.-H., Lian, Y.-X., 2016. The impact of $PM_{2.5}$ on the human respiratory system. J Thorac Dis 8, E69-E74, 10.3978/j.issn.2072-1439.2016.01.19.

Yammine, P., Kfoury, A., El Beyrouthy, M., Nouali, H., El-Nakat, H., Ledoux, F., Cazier, F., Courcot, D., Aboukaïs, A., 2010. A preliminary evaluation of the inorganic chemical composition of atmospheric TSP in the Selaata region, North Lebanon. Lebanese Science Journal 11, 13-29

Yang, H.-H., Lee, W.-J., Chen, S.-J., Lai, S.-O., 1998. PAH emission from various industrial stacks. J. Hazard. Mater. 60, 159-174, https://doi.org/10.1016/S0304-3894(98)00089-2.

Yu, Q., Chen, J., Qin, W., Cheng, S., Zhang, Y., Ahmad, M., Ouyang, W., 2019. Characteristics and secondary formation of water-soluble organic acids in PM_1, $PM_{2.5}$ and PM_{10} in Beijing during haze episodes. Sci. Total Environ. 669, 175-184, https://doi.org/10.1016/j.scitotenv.2019.03.131.

Zaheer, J., Jeon, J., Lee, S.-B., Kim, J.S., 2018. Effect of Particulate Matter on Human Health, Prevention, and Imaging Using PET or SPECT. 29, 81, 10.14316/pmp.2018.29.3.81.

Zhu, W., Luo, L., Cheng, Z., Yan, N., Lou, S., Ma, Y., 2018. Characteristics and contributions of biogenic secondary organic aerosol tracers to $PM_{2.5}$ in Shanghai, China. Atmos Pollut Res 9, 179-188, https://doi.org/10.1016/j.apr.2017.09.001.

Article 3: $PM_{2.5}$ chemical characterization and sources identification in two sites in the East Mediterranean

Marc Fadel[a,b], *Dominique Courcot*[b], *Marianne Seigneur*[b], *Adib Kfoury*[d], *Konstantina Oikonomou*[c], *Jean Sciare*[c], *Frédéric Ledoux*[b] ,*Charbel Afif* [a,c,*]

[a]Emissions, Measurements, and Modeling of the Atmosphere (EMMA) Laboratory, CAR, Faculty of Sciences, Saint Joseph University, Beirut, Lebanon

[b]Unité de Chimie Environnementale et Interactions sur le Vivant, UCEIV UR4492, FR CNRS 3417, University of Littoral Côte d′Opale (ULCO), Dunkerque, France

[c]Climate and Atmosphere Research Center, The Cyprus Institute, Nicosia, Cyprus

[d]Department of Environmental Sciences, University of Balamand, Al Kourah, Lebanon

*Corresponding author: charbel.afif@usj.edu.lb

Abstract

This study was carried out to identify $PM_{2.5}$ sources and quantify their contribution in two sites in the East Mediterranean. The chemical characteristics of $PM_{2.5}$ were studied during an almost one-year period at two sites in Lebanon: Zouk Mikael (ZK) and Fiaa (FA). $PM_{2.5}$ samples were analyzed for their content in carbonaceous matter (OC and EC), water-soluble ions and major and trace elements. Average $PM_{2.5}$ concentrations were 33.6 µg/m^3 at ZK and 26.0 µg/m^3 at FA. Water-soluble ions contributed to 40% and 47% of $PM_{2.5}$ with SO_4^{2-}, NH_4^+ and NO_3^- as the major contributors at both sites. The 29 analyzed elements contribute to 10% and 8% of $PM_{2.5}$ at ZK and FA, respectively. Different diagnostic tools were used to gain a preliminary picture of the most relevant sources that were further interpreted using Positive Matrix Factorization (PMF). A twelve-factor source profile solution was provided by PMF showing that crustal dust and secondary ammonium sulfate were the major contributors to $PM_{2.5}$ (43.2% and 46.3% at ZK and FA, respectively). Vehicular and industrial emissions contributed more to $PM_{2.5}$ mass at ZK compared to FA (27% at ZK vs 12.6% at FA). Site-specific sources were also identified such as open burning of waste at FA that contributed largely to $PM_{2.5}$ (16%) and diesel generators at ZK (4.5%). Other anthropogenic sources were identified such as cooking and biomass burning at both sites. Cluster analysis of air mass back trajectories emphasized on long range transport of dust from Arabian and African desert, sulfates from Europe, and carbonaceous matter from refineries in Arabian and African countries.

Keywords: $PM_{2.5}$, chemical characterization, PMF, clustering, sources contribution, East Mediterranean

Introduction

Fine particulate matter ($PM_{2.5}$) have been shown to contribute to many environmental problems and might pose serious effects on health especially cardiovascular and respiratory diseases (Anderson et al., 2012). Studies including the Mediterranean region showed that both short and long-term exposures to $PM_{2.5}$ have been linked to an increase in the risk of mortality as well as other diseases (respiratory problems, lung cancer, asthma, etc.) (Samoli et al., 2014; Soheila et al., 2021). $PM_{2.5}$ can originate from various natural and anthropogenic sources such as traffic, industrial activities, fuel burning, open burning of waste, crustal and mineral dust, and secondary inorganic aerosols (Karagulian et al., 2015; Liu et al., 2017).

The East Mediterranean Middle Eastern region (EMME) is considered a hotspot of climate change where model projections showed a typical temperature increase by 5 to 7°C by the end of the century, with very high numbers of heat wave days that will contribute to the increase of photochemical air pollution (Lelieveld et al., 2014). This phenomenon will lead to higher concentrations of pollutants in the atmosphere. Additionally, the premature mortality rate due to outdoor air pollution could double until 2050 in the region (Lelieveld et al., 2015). Beside the different anthropogenic activities, the region is also affected by dust storms which has a significant impact on air quality and human health (De Sario et al., 2013). These sources lead to high levels of PM (Abdo et al., 2016). However, in order to reduce these concentrations and try to meet the new WHO annual guidelines for $PM_{2.5}$ of 5 $\mu g/m^3$ (WHO, 2021), it is essential to identify the sources in the region and quantify their contribution to PM concentrations. Consequently, the emissions of the sources could be mitigated through policy making and law enforcement. To do this, a fundamental step for source identification is constituted by an extensive chemical characterization of $PM_{2.5}$ since its composition varies greatly depending on the sources and types of emissions (Yu and Park, 2021).

Source receptor models have become increasingly important and aim to discriminate the impact of different sources of pollutants on air quality, based on ambient data collected at the sampling sites (Viana et al., 2008; Sun et al., 2020). More specifically, Positive Matrix Factorization (PMF) is considered as the most used receptor model in the last years, followed by Chemical mass balance (CMB) and UNMIX. The number of works using PMF for source apportionment of $PM_{2.5}$ increased by 546% in 2010-2020 compared with the previous years (2000-2010)

(Galvão et al., 2020). This type of model is simple to use and does not require prior knowledge of the source profiles (Hopke, 2008; Belis et al., 2019).

Lebanon, a developing country located on the eastern basin of the Mediterranean sea, is considered one of the most affected countries in the East Mediterranean by outdoor air pollution (MoE, 2017). This is the consequence of several shortcomings, such as a weak infrastructure leading to a constant shortage of electricity and a spread of private backup generators with no law enforcement on stack emissions offering electricity during long interruptions (Bouri and El Assad, 2016; Abi Ghanem, 2018). Additionally, the road transport sector is an important contributor to pollutants emissions in the East Mediterranean countries, especially in Lebanon where the absence of developed public transportation system leads to high traffic especially around the capital Beirut (Waked and Afif, 2012). The national emission inventory of 2010 in Lebanon identifies the industrial sources and power plants as major emitters of PM to the atmosphere (Waked et al., 2012). The country is also affected by long range transport of dust during dust storms coming from Saharan and Arabian deserts (Borgie et al., 2016).

Only few PMF studies were conducted on particulate matter from the East Mediterranean region (Achilleos et al., 2016; Theodosi et al., 2018; Saraga et al., 2019). None of them was performed in Lebanon. Therefore, the major aim of this work is the characterization of the sources of $PM_{2.5}$ including long-range transport through their identification and contribution to $PM_{2.5}$ concentrations. Therefore, $PM_{2.5}$ were collected for almost a year in two urban areas in Lebanon, chemically characterized, and sources apportioned using the US-EPA PMF model. This study will be a first in the East Mediterranean employing an extensive dataset on $PM_{2.5}$ chemical composition with organic and inorganic species in two urban sites and quantifying the contribution of different natural and anthropogenic sources. These findings will be of importance to policymakers in order to improve the air quality in the East Mediterranean and the Middle East region, to the atmospheric science community for model and emissions inventory comparison and evaluation.

1 Materials and methods

1.1 Site description

Sampling sites were described elsewhere (Fadel et al., 2021). Briefly, the sampling took place in two sites in Lebanon: Zouk Mikael (ZK) and Fiaa (FA). The ZK site (33°57’57.07’’N; 35°37’09.46’’E) is located in Mount Lebanon district, on the rooftop of a residential building facing the biggest power plant in Lebanon running on Heavy Fuel Oil (HFO). In addition, the

area is highly populated with a busy highway, a high number of private generators, and small industries **(Fig. III-11)**.

The FA site (34°20'47.8''N; 35°47'14.0''E) is located in Chekka region, Koura district. The site is less populated than ZK **(Fig. III-11)** but is also influenced by private generators, and possibly by the chemical industries in Chekka region (cement industries along with their quarries, power plants, and a sulfuric acid and phosphate fertilizer industry). In addition, the nearest highway is 4 km away from FA with moderate traffic. The distance between the ZK and FA sampling sites is around 50 km **(Fig. III-11).**

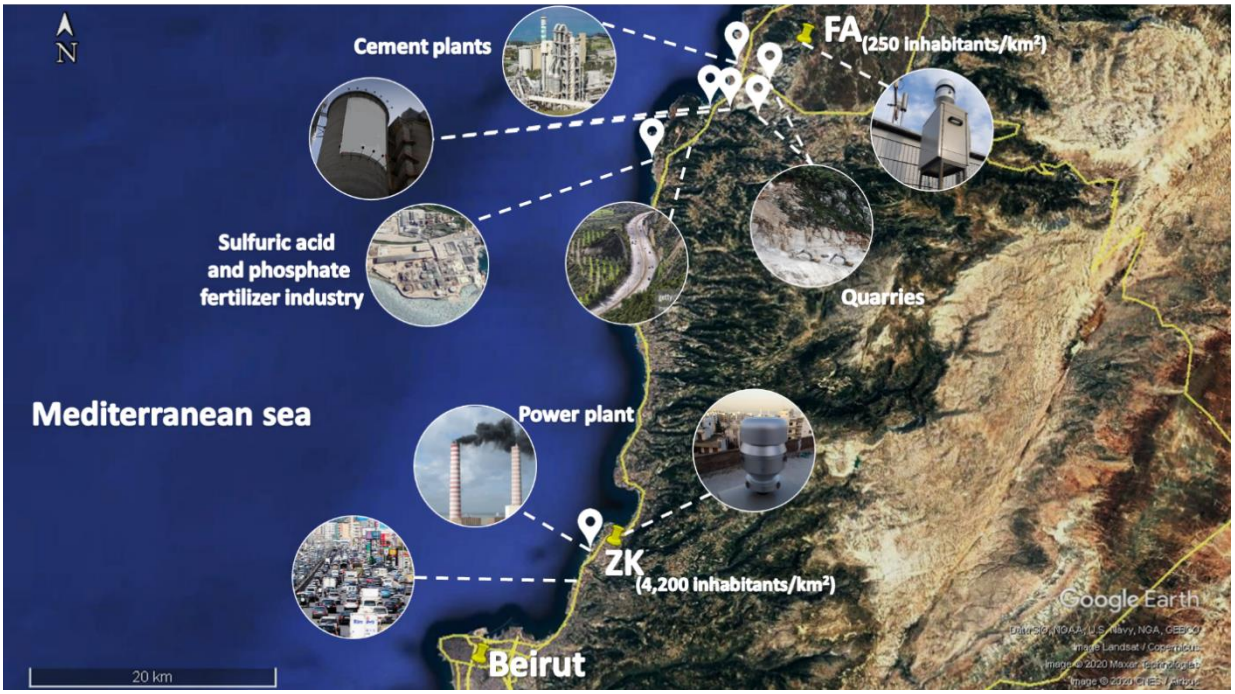

Fig. III-11: Location of the two sampling sites in Lebanon: Zouk Mikael (ZK) and Fiaa (FA) along with different nearby potential pollution sources (modified from Google Earth)

1.2 Sampling strategy

$PM_{2.5}$ were collected on 150 mm pre-heated quartz fiber filters (Fiorini, France) using high volume samplers (CAV-A/mb, MCV S.A., Spain) operating at 30 m^3/h equipped with a $PM_{2.5}$ size selective inlet. The sampling was performed over 24 hours every third day with nominal start time at 6:30 AM (local time) from the 13th of December 2018 to the 15th of October 2019. After sampling, the filters (98 in Zouk and 95 in Fiaa) were sealed in aluminum foil and stored at -20°C until analysis. Field blank filters were also considered at both sites.

1.3 Gravimetric mass analysis

The determination of the $PM_{2.5}$ mass was done following the standard EN 12341:2014. Briefly, $PM_{2.5}$ filters were conditioned and weighted before and after sampling using an electronic balance (Mettler Toledo, AB204, United States of America) with a resolution of 100 µg. The temperature was controlled to 20±0.5°C and the humidity to 50±5% for 48 hours before any weighing of blank and loaded filters. In order to ensure reliable results, additional QA/QC procedures were applied.

1.4 Chemical analysis

The analysis of water-soluble ions, and elements were detailed elsewhere and will be shortly presented here (Ledoux et al., 2006; Kfoury et al., 2016). Cl^-, SO_4^{2-}, NO_3^-, Ca^{2+}, Mg^{2+}, K^+, Na^+, and NH_4^+ were quantified using ion chromatography (Dionex™ ICS-900, Thermo Scientific, United Kingdom). Major and trace elements were analyzed by Inductively Coupled Plasma-Atomic Emission Spectrometry (ICP-AES, iCAP 6000 series, Thermo Scientific, United Kingdom) for Al, Mg, K, Ca, Ba, Fe, Mn, P, Ni, Ti, Sr, Zn, and Pb and ICP-Mass Spectrometry (ICP-MS, Agilent 7900, Varian, United States of America) for As, Cd, Co, Sn, Cu, Cr, Sb, V, La, Ce, Bi, Sc, Rb, Nb, and Tl.

For the carbonaceous matter, a punch of 1.5 cm^2 of the quartz filter was used to quantify organic and elemental carbon by a thermal optical transmission technique using a Sunset Laboratory OC/EC analyzer implementing the EUSAAR2 temperature protocol (Cavalli et al., 2010).

1.5 Data processing

1.5.1 Enrichment factor for elements

The enrichment factor (EF) of an element is considered as the first indication of the relative contribution of crustal and anthropogenic sources. The calculation of the EF was done using Al as a reference element according to the following equation (Chester et al., 1993):

$$EF = \frac{\left(\frac{C_x}{C_{Al}}\right)_{sample}}{\left(\frac{C_x}{C_{Al}}\right)_{crustal}} \quad (Eq.\ 3)$$

Where $\frac{C_x}{C_{Al}}$ is the ratio of the element's concentration to the concentration of Al. The composition data for the upper crust was retrieved from Wedepohl (1995). An enrichment factor close to 1 implies that the metal is of natural origin and is not affected by anthropogenic

emissions while a factor higher than 10 indicates that the origin of the element is derived from anthropogenic sources (Hlavay et al., 1996).

1.5.2 HYSPLIT cluster analysis

In order to study the long-range transport of $PM_{2.5}$, a back-trajectory cluster analysis was performed using the HYSPLIT model (Draxler et al., 2004). Hourly 72h-backward trajectories of air masses ending in ZK site (using GDAS1 meteorological data) were established for the combined sampling days of ZK and FA between December 2018 and October 2019 (4,599 trajectories in total) by HYSPLIT and then clustered by the same program. By this combination of data, we consider that both sites were under the influence of the same air masses since they are relatively close (distant of 50 km).

1.6 $PM_{2.5}$ source apportionment

US EPA PMF 5.0 model was used to identify and quantify the contribution of the sources in the sampling sites (Paatero and Tapper, 1994).

In our database, species having concentrations below the detection limit (D.L.) were replaced by D.L./2 and missing concentration values were replaced by the geometric mean of the measured concentration of the element at the specific sampling site (Polissar et al., 1998). As for uncertainties, they were calculated as s_{ij} + D.L./3, where s_{ij} is the analytical uncertainty, for determined values. The uncertainties of the concentrations that were below the D.L. were replaced by 5/6 D.L., and the uncertainties of the missing values were replaced by 4 times the geometric mean of the measured concentration of the species (Polissar et al., 1998).

After screening the integrity of the input data and evaluating the S/N ratio, 90 samples for each site and 32 species were included in the analysis. The considered species represent a large fraction of the particulate mass such as major ions (Cl^-, SO_4^{2-}, NO_3^-, Na^+ and NH_4^+) and carbonaceous fraction (OC, EC) or are considered as characteristic of certain sources (Belis et al., 2019). Levoglucosan was included as a tracer for biomass burning, V and Ni for HFO combustion, hexadecanoic and octadecanoic acids for cooking activities, isoprene and α-pinene oxidation products as tracers for SOA, 17α(H)-21β(H)-hopane as tracer for vehicular emissions (only detected in ZK samples). This study also considered a set of metals (Mg, Al, Ca, Fe, K, Ni, Ti, Cu, Sb and Sn) and specific n-alkanes (C_{20}, C_{21}, C_{24} and C_{25} for anthropogenic emissions, and C_{27}, C_{29}, and C_{31} for biogenic emissions). The concentrations of the organic species were retrieved from Fadel et al. (2021). The list of all the chosen species along with their corresponding S/N values were reported in **Appendix C -Table S1** and **Table S2**. Even though

NO_3^- showed a S/N value higher than 1 at both sites, it was categorized as "weak" since it was not well modeled (R^2= 0.39 at ZK and 0.6 at FA).

To select the appropriate number of factors, different mathematical diagnostic methods such as maximum individual mean (IM) and maximum individual standard deviation (IS) were investigated and were presented in **Appendix C- Figure S3.** The variability in PMF solutions can be estimated using the bootstrap analysis on F matrix (factor profile matrix) and the displacement analysis method (DISP) on the F matrix (Paatero et al., 2014) and were presented in **Appendix C- Table S3** and **Table S4.**

2 Results and discussions

2.1 $PM_{2.5}$ mass concentration

The average concentrations of $PM_{2.5}$ at ZK and FA were found to be 33.6 ± 22.7 µg/m^3, and 26.0 ± 19.3 µg/m^3, respectively. These average concentrations were approximately six times higher than the new WHO $PM_{2.5}$ annual guideline value of 5 µg/m^3 (WHO, 2021). The average concentrations were close to the mean value of 28.6 µg/m^3 measured in five sites considered as important hotspots and densely populated areas in Lebanon (Abdallah et al., 2018). Comparing with other Mediterranean sites, ZK and FA exhibited higher $PM_{2.5}$ concentrations than an urban site with high traffic in Spain (20 µg/m^3), and an urban site in Turkey (20 µg/m^3) (Escudero et al., 2015; Ozturk and Keles, 2016). Additionally, ZK showed $PM_{2.5}$ concentrations higher than an industrial site in Egypt (27 µg/m^3), and similar concentrations to those found in urban-industrial sites in Algeria (31.6 - 32.8 µg/m^3) (Shaltout et al., 2018; Talbi et al., 2018). However, higher $PM_{2.5}$ concentrations were recorded in other residential, urban, and industrial Egyptian sites (77-100 µg/m^3) (Zakey et al., 2008). The location of these sites in deserted areas increases the dust contribution to the observed concentrations.

2.2 Carbonaceous fraction

EC is mainly emitted from fuel-based combustion activities, and therefore associated with primary emissions, while OC can originate from both primary and secondary sources (Wu and Yu, 2016). In this study, the average concentrations of OC and EC at ZK were consistent with those reported by Waked et al. (2013); (2014) for a suburban site in the suburbs of the capital Beirut (OC: 4.5-5.6 µg/m^3; EC: 1.4-1.8 µg/m^3) **(Table III-7)**, but higher than those measured at FA during the sampling period. The concentrations at both sites are within the range of OC (2.4-4.7 µg/m^3) and EC (0.4-1.9 µg/m^3) concentrations reported for European Mediterranean

sites such as Spain, Greece, and France (El Haddad et al., 2011; Pateraki et al., 2012; Escudero et al., 2015; Liakakou et al., 2020).

EC and OC showed significantly good correlation at both sites ($r=0.7$; $p<0.001$ for ZK and $r=0.8$; $p<0.001$ for FA) indicating that they might be emitted by the same sources. The OC/EC concentration ratio varied between 1.7 and 12.8 at ZK (average: 4.0 ± 1.6) and 1.9 and 18.6 (average: 7.3 ± 3.0) at FA. Ratio values between 0.3 and 1 were reported for light and heavy-duty vehicles both running on diesel, 1.4 to 5 for gasoline catalyst light duty vehicles, while higher ratios were assigned to biomass burning sources (4.1 - 14.5), open burning of waste (7.5), and cooking emissions (33 - 82) (He et al., 2004; Salameh et al., 2015; Wang et al., 2020; Khan et al., 2021). The ratio at ZK site was higher than the range attributed to on-road diesel emissions and was mostly in agreement with gasoline vehicle emissions. This result is compatible with the Lebanese fleet characteristics consisting mainly of gasoline light duty vehicles (Abdallah et al., 2020). A different scenario was observed at FA since the average concentration ratio was in the range of values relative to biomass burning and open burning of waste. It is known that the Chekka region experienced numerous episodes of open burning of municipal solid waste for several years and these episodes were also observed during the sampling period.

2.3 Water-soluble ions (WSI)

The average concentration of WSI contributed to an average of 40% and 47% of $PM_{2.5}$ mass at ZK and FA, respectively **(Table III-7).** The concentrations of the ionic species followed the same order at both sites with the highest concentration for SO_4^{2-}, then NH_4^+, NO_3^-, Ca^{2+}, Na^+, Cl^-, K^+, and the lowest concentration was for Mg^{2+}. SNA (SO_4^{2-}, NH_4^+, and NO_3^-) are considered as the main secondary inorganic aerosols and their abundance mainly depend on the transformation rates and the concentration of their precursor gases (Agarwal et al., 2020). The average concentrations of SNA over the sampling period were 8.9 ± 4.8 µg/m^3 at ZK and 8.7 ± 4.1 µg/m^3 at FA, accounting for 75% at ZK and 84% at FA of total WSI. Additionally, SNA contribute to 31% and 40% of total $PM_{2.5}$ mass at ZK and FA, respectively. On one hand, the concentrations of ammonium are not sufficient to neutralize the concentrations of NO_3^- and SO_4^{2-} at both sites **(Appendix C - Figure S4-a** and **Figure S5-a).** On the other hand, the very good correlation between NH_4^+ and SO_4^{2-} ($r=0.93$; $p<0.001$ at ZK and $r=0.93$; $p<0.001$ at FA) and the absence of correlation between NH_4^+ and NO_3^- indicate mainly the presence of ammonium sulfate ($(NH_4)_2SO_4$) in the atmosphere of ZK and FA (Stockwell et al., 2003; Trebs,

2005). Therefore, NO_3^- could be associated to different cations emitted from sea water such as Na^+, Mg^{2+}, and Ca^{2+} since it is well established that NO_3^- could be associated with sea-salts in the Mediterranean region (Borgie et al., 2016). Hence, when considering the neutralization of SO_4^{2-}, NO_3^-, Cl^- by NH_4^+, Na^+, Mg^{2+}, K^+, Ca^{2+}, we observe a slope of 1.25 and 1.19 at ZK and FA, respectively highlighting an anion deficit. This could be explained by the unmeasured CO_3^{2-} species knowing that Lebanese soils are rich in $CaCO_3$ (Verheye, 1973).

2.4 Elements

The average concentrations of 28 analyzed elements in $PM_{2.5}$ at ZK and FA were summarized in **Table III-7.** The highest concentrations at both sites were for Ca with a share of the total sum of analyzed elements of 55% at ZK and 53% at FA followed by Al (16% at ZK and 19% at FA), and Fe (12% at both sites). In average, the sum of the different elements contributes to 10% and 8% of $PM_{2.5}$ average mass concentrations at ZK and FA, respectively. The total mass concentrations of elements at both sites were lower than the average value reported for a site in Thessaloniki, Greece where it reached 4900 ng/m^3 (Tolis et al., 2015) due to heavy traffic, and different industrial operations, but higher than those of a heavily urbanized site under industrial influence in Antalya, Turkey (2094 ng/m^3) (Tepe and Doğan, 2021).

The enrichment factors (EF) were calculated using Al as reference element in order to distinguish between the anthropogenic or the natural origins of the different elements. The boxplots of the EF values for the different elements **(Fig. III-12)** show a similar classification of elements at both sites: Rb, Nb, Ce, K, Fe, Mn, La, Sr, Ti, Mg and Ba were not enriched with EF values lower than 10, suggesting that these elements originate from crustal sources, mainly soil and desert dust.

The elements Tl, P, Cr, Sc, Ca, and Co were moderately enriched with median values close to 10, indicating a predominance of anthropogenic sources. Finally, high EF values were assigned to Sn, As, V, Cu, Pb, Zn, Ni, Bi, Cd, and Sb, indicating that their concentrations were highly influenced by different anthropogenic activities (Xu et al., 2021).

To better identify the emission sources of the different enriched elements in our study, correlations using the Spearman test **(Appendix C - Figure S2 and Figure S3)** as well as different elemental concentration ratios were investigated. The very good correlation between V and Ni at both sites ($r= 0.92$, $p<0.001$ at ZK and $r= 0.90$, $p<0.001$ at FA) indicate the same emission source.

Table III-7: Average, minimum and maximum (min-max) concentrations of $PM_{2.5}$ and its chemical components (OC, EC, and ions in µg/m^3 and elements in ng/m^3) at Zouk (ZK) and Fiaa (FA) during the sampling period

	Average concentration (min-max)	**Zouk site (ZK)**	**Fiaa site (FA)**
$PM_{2.5}$ (µg/m^3)		**33.6 (4.1-145)**	**26.0 (3.9-96)**
Carbonaceous fraction (µg/m^3)	OC	4.6 (1.3-11.9)	3.0 (0.5-8.9)
	EC	1.3 (0.3-4.4)	0.5 (0.1-1.8)
Total carbon (TC) (µg/m^3)		**5.9 (1.9-16.2)**	**3.5 (0.7-10.3)**
Water-soluble ions (µg/m^3)	Cl^-	0.58 (<D.L.-4.7)	0.22 (<D.L.-3.6)
	NO_3^-	1.6 (0.1-8.0)	1.1 (<D.L.-7.3)
	SO_4^{2-}	5.6 (0.9-15.3)	5.7 (0.9-13.6)
	Na^+	0.72 (0.07-4.7)	0.30 (0.03-2.2)
	NH_4^+	1.8 (0.1-5.4)	1.9 (0.1-5.0)
	K^+	0.15 (0.03-0.45)	0.13 (0.01-0.69)
	Mg^{2+}	0.09 (0.01-0.97)	0.05 (0.01-0.38)
	Ca^{2+}	1.4 (0.04-9.8)	0.94 (<D.L.-4.2)
Total water-soluble ions (µg/m^3)		**11.9 (1.7-28.9)**	**10.3 (1.8-19.9)**
Elements (ng/m^3)	Mn	8 (0.1-66)	6 (0.4-35)
	Mg	231 (1.0-3,102)	179 (12-1,457)
	Ca	2,100 (19-15,560)	1,360 (<D.L-10,030)
	K	264 (34-2,760)	189 (23-1,300)
	Al	593 (<D.L.-8,771)	492 (<D.L.-3,653)
	Ba	14 (<D.L.-75)	9 (<D.L.-26)
	Fe	452 (11-4,634)	300 (10-2,232)
	P	31 (<D.L.-153)	22 (1-93)
	Ti	56 (2-589)	32 (<D.L.-242)
	V	25 (1-150)	13 (1-52)
	Zn	26 (4-95)	17 (<D.L.-74)
	Cu	5 (<D.L.-23)	3 (1-13)
	Ni	12 (11-70)	6 (<D.L.-23)
	Cr	2 (<D.L.-10)	2 (<D.L.-9)
	Pb	13 (<D.L.-171)	17 (<D.L.-220)
	Sr	5 (<D.L.-77)	4 (0.2-35)
	As	0.5 (0.1-1.4)	0.5 (0.1-1.2)
	Sc	0.5 (<D.L.-1.9)	0.5 (<D.L.-1.2)
	Cd	0.1 (0.02-0.9)	0.1 (0.02-0.6)
	Co	1.2 (0.03-12)	0.6 (0.04-6)
	Rb	0.7 (0.1-9)	0.5 (0.04-3)
	Nb	0.3 (<D.L.-2)	0.2 (<D.L.-1)
	Sn	0.8 (0.1-4)	0.6 (<D.L.-5)
	Sb	1.1 (0.1-4)	0.9 (0.1-6)
	La	0.5 (<D.L.-5)	0.3 (<D.L.-2)
	Ce	0.8 (<D.L.-10)	0.6 (<D.L.-4)
	Tl	0.03 (<D.L.-0.1)	0.03 (<D.L.-0.2)
	Bi	0.1 (0.01-1)	0.1 (0.01-1)
Total elements (ng/m^3)		**3,800 (80-35,900)**	**2,580 (66-18,120)**

These elements are considered as typical tracers of fuel oil combustion (Swietlicki and Krejci, 1996). The V/Ni concentration ratio has been reported in the literature between 2.5 and 3.5 for Heavy Fuel Oil combustion from maritime transport (Pandolfi et al., 2011).

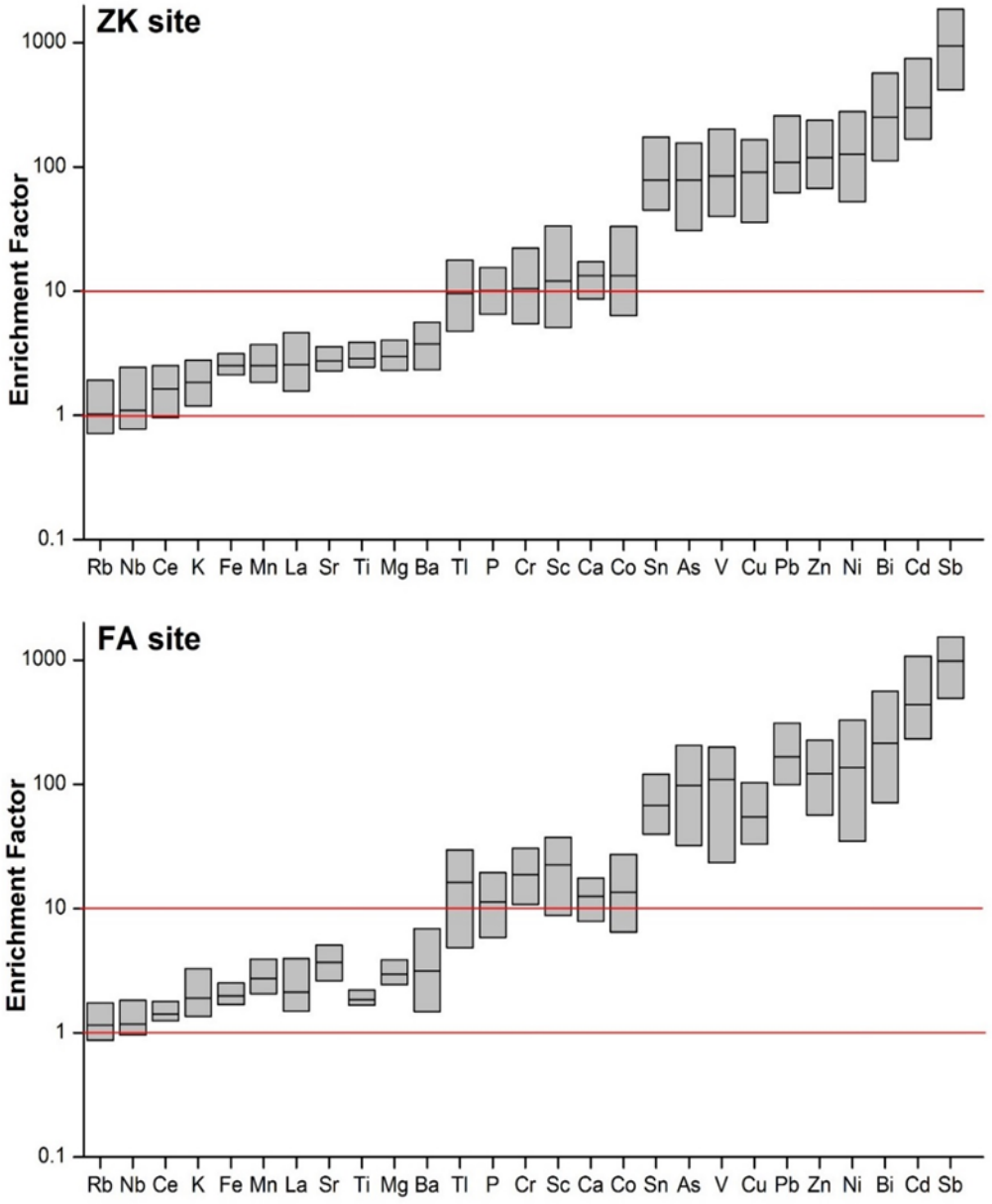

Fig. III-12: Boxplots of enrichment factors (median values, 25th and 75th percentiles) for all analyzed elements in $PM_{2.5}$ collected at ZK and FA sites using Al as reference element.

Lower values (1.9-2.4) were attributed to HFO from domestic heating, values between 1.5 and 1.9 for residual oils in power plants, and the lowest values were reported for diesel and gasoline vehicles (0.02-0.11 for gasoline and 0.15-0.68 for diesel vehicles) and non-road diesel generators (0.21) (Lee et al., 2000; Pandolfi et al., 2011; Zhao et al., 2013; Benetello et al.,

2018; Chifflet et al., 2018; Fadel et al., 2022). The plot of V versus Ni exhibits one trend at FA with a slope of 2.03, while at ZK two trends are observed with different slopes of 2.6 and 1.7 (**Appendix C- Figure S6)**. Since HFO is not used for domestic heating in Lebanon, it can be suggested that V and Ni were mostly emitted from residual oil combustion used in the power plant at ZK and the cement plants and corresponding power plants that are close to the sampling site at FA. The differences in the concentration ratio values might be linked to the fuel quality and its sulfur content since these characteristics can influence the value of this ratio (Ivošević et al., 2016; Ledoux et al., 2017).

Other elements such as Cu, Sn, Sb, Zn, and Cd showed significant correlations at both sites ($r > 0.7$, $p < 0.001$). These elements were mainly attributed to vehicular emissions. Tunnel studies showed that Cu, Cd, Sb, and Sn were mainly emitted from brake wear debris while Zn originated from tailpipe emissions (Lin et al., 2015). To validate these observations, elemental concentration ratios of Cu/Sb was evaluated and presented average ratios of 4.2 and 3.1 at ZK and FA, respectively. Values between 2 and 10 were reported for this ratio in the literature and were attributed to brake wear knowing that this ratio varies greatly depending on the type and the brand of the brakes (Benetello et al., 2018).

2.5 Air-mass back-trajectories cluster analysis

Hourly 72h-backward trajectories of air masses ending in ZK site were established using HYSPLIT and then clustered. Air mass back-trajectories observed during the sampling period can be decomposed into 9 clusters **(Fig. III-13)**. The average concentrations of $PM_{2.5}$ were calculated for the samples of each cluster to evaluate their long-range origin (**Appendix C- Table S5)**. The highest $PM_{2.5}$ concentration levels were attributed to cluster 6 and 4, which air masses originate from the African Sahara and the Arabian desert respectively, with 51.1 $\mu g/m^3$ and 46.5 $\mu g/m^3$, respectively. It is well established that the East Mediterranean region is frequently influenced by dust outbreaks from the African desert areas (Kalivitis et al., 2007) and the Middle East is also impacted by the Arabian desert (Middleton, 1986).

Thus, Lebanon is affected by these two deserts constituting the major source of mineral elements in the environment (Borgie et al., 2016; Fakhri et al., 2021). In our study, these events occurred mainly between December 2018 and April 2019 with the highest concentrations recorded between the episodes during the dust event of 27 January 2019 **(Appendix C - Figure S7).** The observed peaks of $PM_{2.5}$ during dust storms are mainly associated with high levels of Mg, Al, Ti, Ca, Fe, and K (**Appendix C- Table S5)** which are considered as tracers of desert

dust (Querol et al., 2019). The concentrations ratios of Ca/Al and Fe/Al were 5.6 and 1.0 for the samples in cluster 4, and 3.2 and 0.7 for samples in cluster 6. These values were close to those reported for Saharan dust over Mediterranean countries (3.1 for Ca/Al and 0.7 for Fe/Al) and for a mobile site in Saudi Arabia (6.6 for Ca/Al and 0.8 for Fe/Al) which confirms that our sampling sites were mainly influenced by long range transport from both Saharan and Arabian deserts during these periods.

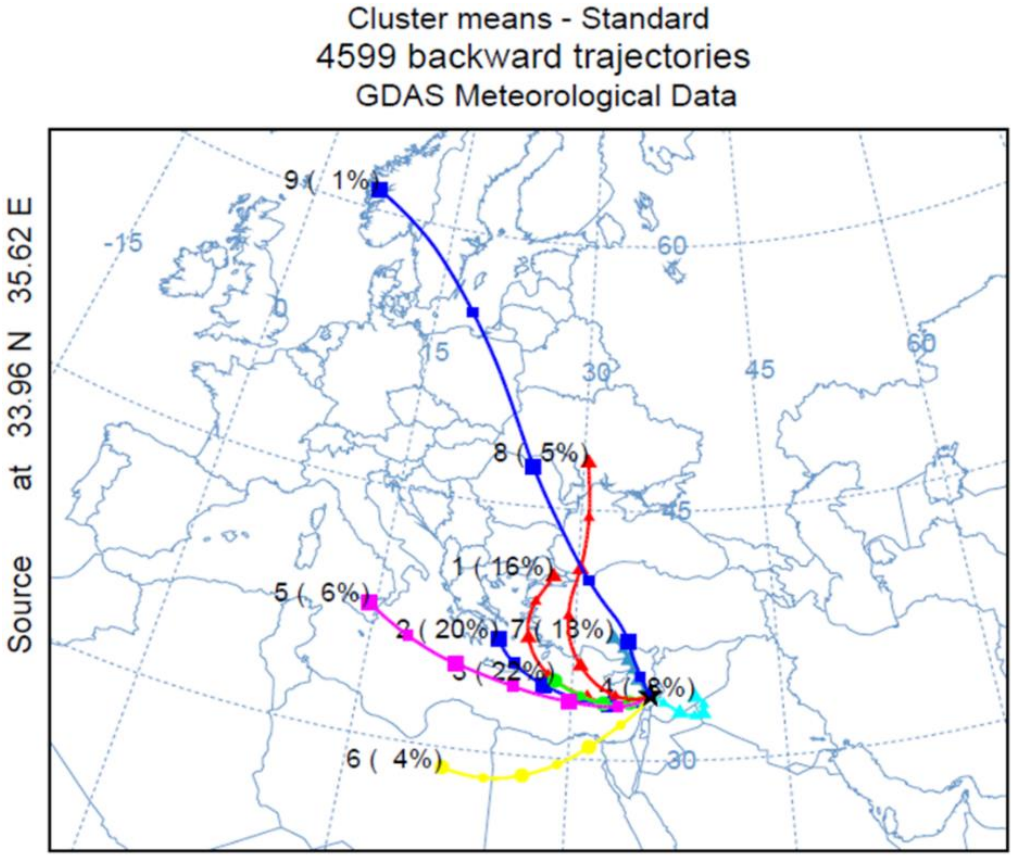

Fig. III-13: HYSPLIT cluster means for the sampling days from December 2018 to October 2019

We also observed that high concentrations of SO_4^{2-} were assigned to clusters 1, 2, 3 and 7 (**Appendix C- Table S5)**. Clusters 1, 2 and 3 encompass air masses originating from Eastern and Central Europe, well-known European industrial areas where air masses can be enriched with SO_2 leading to potential higher SO_4^{2-} concentrations (Afif et al., 2008). On the other hand, cluster 7 represents air masses originating from Turkey. The latter is considered among the top

ten SO_2 emitter countries with coal-based energy production stations as the major source of this pollutant in the country (Dahiya et al., 2020).

As for the carbonaceous matter, considerable concentrations of EC and OC were observed for trajectories in clusters 4 and 6 compared to the other clusters. In order to better understand the origins of the carbonaceous matter, the correlation between desert dust tracers (Mg, Al, Ti, Ca, Fe, and K) and carbonaceous matter (OC+EC) was studied. For clusters 1, 2, 3, 5, 7, 8 and 9, no correlation was observed meaning that the carbonaceous matter for these samples was mainly emitted from local combustion sources. However, dust and carbonaceous matter showed significant correlations in clusters 4 and 6 ($r>0.8$, $p<0.001$) showing that EC and OC, like dust elements, were of long-range origins. Cluster 4 shows air masses passing over Arab countries such as Jordan, Saudi Arabia, Iraq, and Syria. High concentrations of carbonaceous matter were observed in the samples of Cluster 4 possibly due to the abundance of oil fields and refineries in these countries (Qian, 2013). As for cluster 6, air masses originate from Libya and Egypt which are also home to different oil refineries producing a minimum of 120,000 barrels per day.

2.6 PMF results

2.6.1 Optimal number of factors

In order to identify the sources, the resolved source profiles obtained from the PMF analysis were compared to different available $PM_{2.5}$ profiles from the SPECIEUROPE European database and the SPECIATE American Database (Simon et al., 2010; Pernigotti et al., 2016), and to local source profiles (Simon et al., 2010; Pernigotti et al., 2016; Fadel et al., 2022). The optimal number of factors in PMF modeling was determined by examining the model outputs with ascending number of factors.

Graphical representations of the IM and IS statistics showed a constant decrease of their values when increasing the number of factors and a stabilization starting the 12-factor solution for both sites **(Appendix C - Fig. S1).** The latter solution provided physically meaningful source profiles and contributions with scaled residuals normally distributed between -3 and +3, and a Q(true)/Q(robust) ratio close to 1 (0.9 for ZK and 1.1 for FA). Additionally, bootstrap analysis and DISP diagnostics showed a stable solution and indicated a reasonable model fit for the 12-factor solution **(Appendix C - Table S3, Table S4)**. Finally, the 12-factor solution at FPEAK equal to 0 was the best fit with determination coefficients (r^2) higher than 0.83 at ZK and 0.86 at ZK for all the species input in the model **(Appendix C - Table S1, Table S2)**.

2.6.2 Source identification of $PM_{2.5}$ at ZK and FA

The relative contribution of each identified factor to the measured variables and its corresponding $PM_{2.5}$ factor profile were presented in **Fig. III- 14** for ZK site and **Fig. III-15** for FA site. The time series of the different factors are shown in **Appendix C - Figure S8** and **Figure S9**. Twelve factors were identified at each site, some of which were common for both sites, namely biomass burning, HFO combustion, ammonium sulfate, aged sea-salt, biogenic SOA, crustal dust, cooking, plant wax emissions, and road dust. In addition to these common factors, ZK was also characterized by 2 factors for vehicular emissions and one factor for diesel generators, while FA was distinguished with a diesel heavy duty vehicles (HDV), cement plant and open burning of waste factors (**Fig. III- 14** and **Fig. III-15)**.

Biomass burning was identified by high loadings of levoglucosan (74% at ZK and 84% at FA), and an OC/EC ratio of 4.9 and 5.9 at ZK and FA, respectively. Levoglucosan is known to be an organic tracer of biomass burning (Chantara et al., 2019) and the OC/EC ratio is close to the value of 3.4 reported for wood burning in the region (Fadel et al., 2022) and also in the range presented in the literature for the source (4.1-14.5) (Khan et al., 2021). The time series of this factor showed high concentrations during the cold period compared to the warm one. This is mainly due to wood combustion during winter for residential heating at both sites.

HFO combustion factor was recognized by high loadings of V and Ni. ZK site encompasses the biggest power plant in Lebanon which runs on HFO, so this factor was associated with the power plant. On the other hand, cement plants at Chekka use HFO to run their reciprocating engines for electricity production and sometimes as a substitute of petcoke leading to the conclusion that this factor at FA is associated with the cement plants.

Ammonium sulfate factor was characterized by high levels of SO_4^{2-} (45% at ZK and 59% at FA) and NH_4^+ (53% at ZK and 67% at FA) **(Fig. III- 14, Fig. III-15)**. These water-soluble ions are known to be part of the secondary inorganic aerosols. This factor at FA showed the presence of other elements such as V and Ni, tracers of HFO combustion. This difference between the sites can be mainly due to different compositions of HFO especially in their sulfur content. It has been established that sulfate emitted from fuel combustion is function of the fuel sulfur content (Saiyasitpanich et al., 2005) leading to the assumption that the HFO used in the cement plants has higher sulfur content that the one used in the power plant at ZK. According to the time series of this factor at both sites **(Appendix C - Figure S8, Figure S9),** higher

concentrations were observed in the warm period due to higher oxidation rates and solar radiations in summer (Galindo et al., 2008).

Sea-salt factor was identified with high loadings of Na^+, Cl^-, and NO_3^-, as the location of the sampling sites is less than 5 km from the seashore of the Mediterranean Sea. The chloride and sodium detected in this factor correspond to 83% and 82% of Cl^- mass and 68% and 50% of Na^+ mass at ZK and FA, respectively. However, the ratio Cl^-/Na^+ calculated for this factor was 0.89 at ZK and 0.93 at FA , indicative of aged sea-salt since the ratio for fresh sea-salt is known to be 1.8 and a lesser ratio indicate a Cl^- depletion (Seinfeld and Pandis, 2016). This depletion is caused by a reaction between nitric or sulfuric acid in the atmosphere with the sea-salt aerosol (Song and Carmichael, 1999).

Biogenic SOA factor showed high contributions of isoprene and α-pinene oxidation products explaining 81% and 69% of the total mass of each compound at ZK and 72% and 60% of their individual total mass at FA. The integration of these species in the PMF models is not commonly observed but can give an idea on the contribution of biogenic SOA to the $PM_{2.5}$ mass concentration. A clear seasonal variation was observed at both sites with larger concentrations in summer **(Appendix C - Figure S8, Figure S9)** since the emissions of the precursors depend mainly on the variation of temperature and solar radiation as it enhances the photochemical reactions in the atmosphere (Feng et al., 2013).

Crustal dust factor was highly loaded with Al (83% at ZK and 77% at FA), Ca (73% at ZK and 46% at FA), Mg (67% at ZK and 56% at FA), Ti (74% at ZK and FA), and moderately loaded with K (45% at ZK and 38% at FA). These elements were derived from crustal dust (Mason, 1966). The evaluation of the time series of the crustal dust factor at ZK shows that mostly all peaks correspond to dust storm episodes meaning that these crustal elements were transported by air masses from surrounding deserted areas as previously presented **(Appendix C - Figure S8, Figure S9).** However, the crustal dust factor at FA shows also peaks that were not related to dust storms and might be attributed to the quarries works in the region.

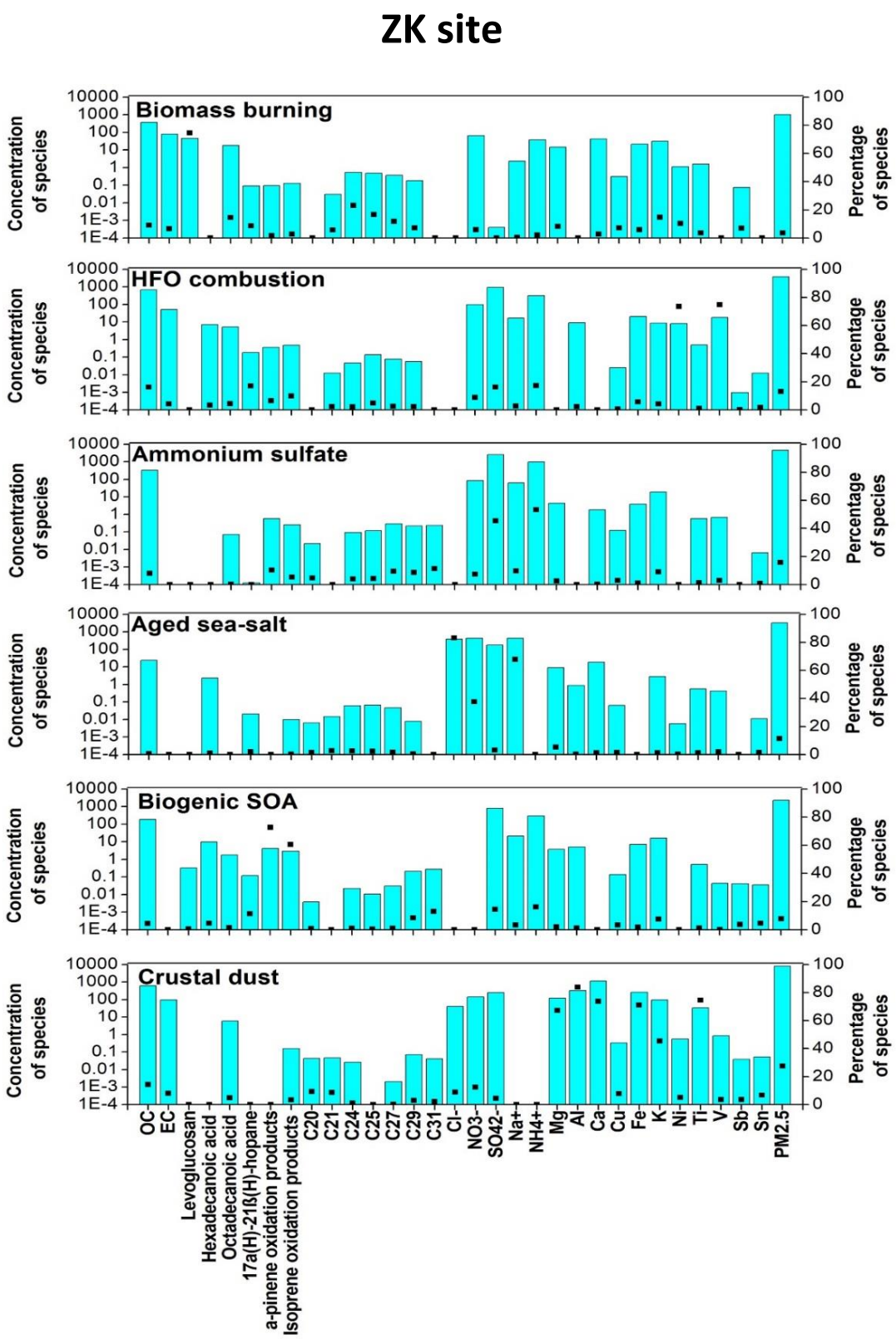
ZK site
Biomass burning
HFO combustion
Ammonium sulfate
Aged sea-salt
Biogenic SOA
Crustal dust
Concentration of species
Percentage of species
10000
1000
100
10
1
0.1
0.01
1E-3
1E-4
100
80
60
40
20
0
OC
EC
Levoglucosan
Hexadecanoic acid
Octadecanoic acid
17a(H)-21ß(H)-hopane
a-pinene oxidation products
Isoprene oxidation products
C20
C21
C24
C25
C27
C29
C31
Cl-
NO3-
SO42-
Na+
NH4+
Mg
Al
Ca
Cu
Fe
K
Ni
Ti
V
Sb
Sn
PM2.5

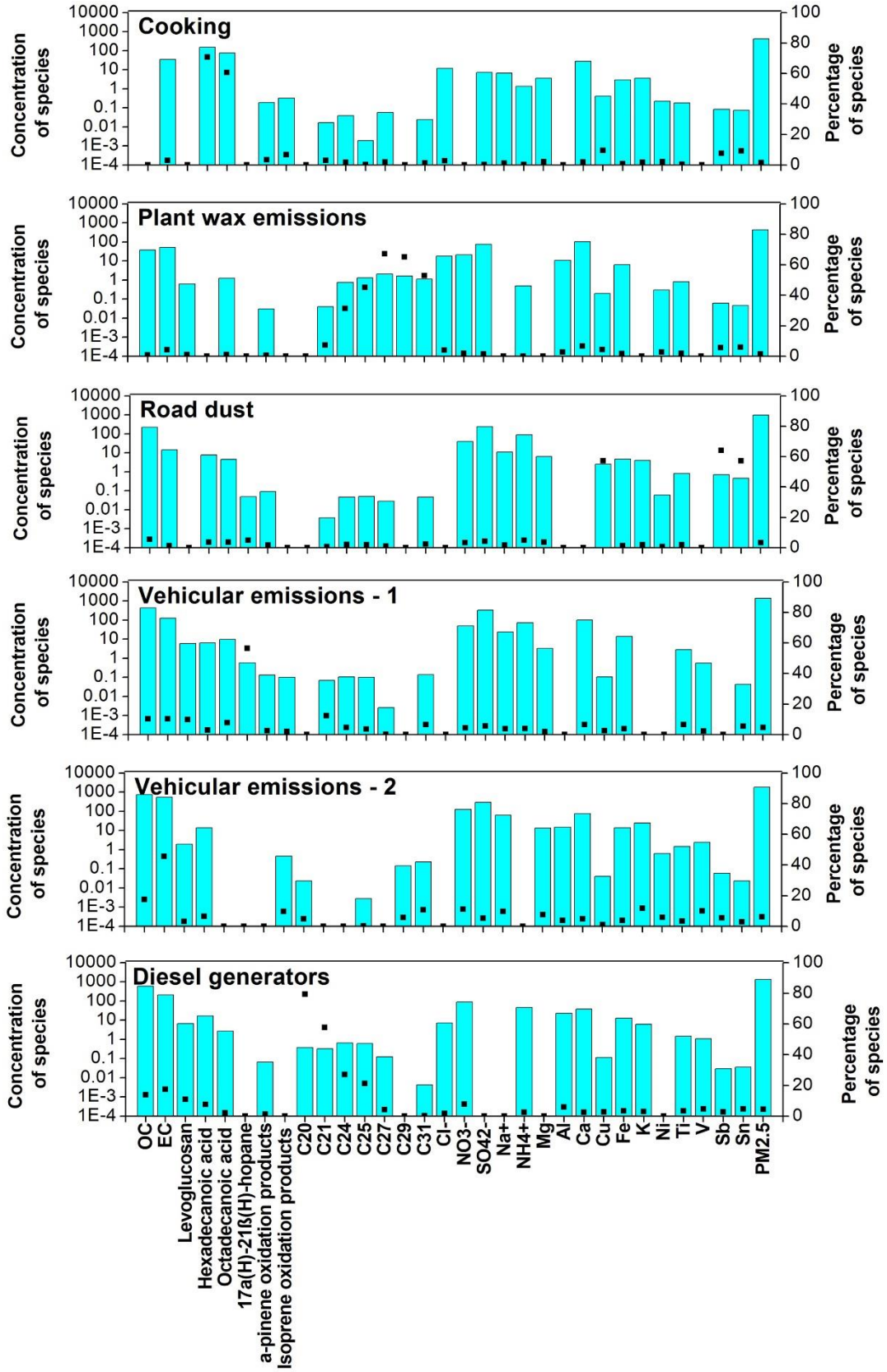

Fig. III- 14: $PM_{2.5}$ profiles of the chemical components of the twelve factors calculated via PMF for the ZK site

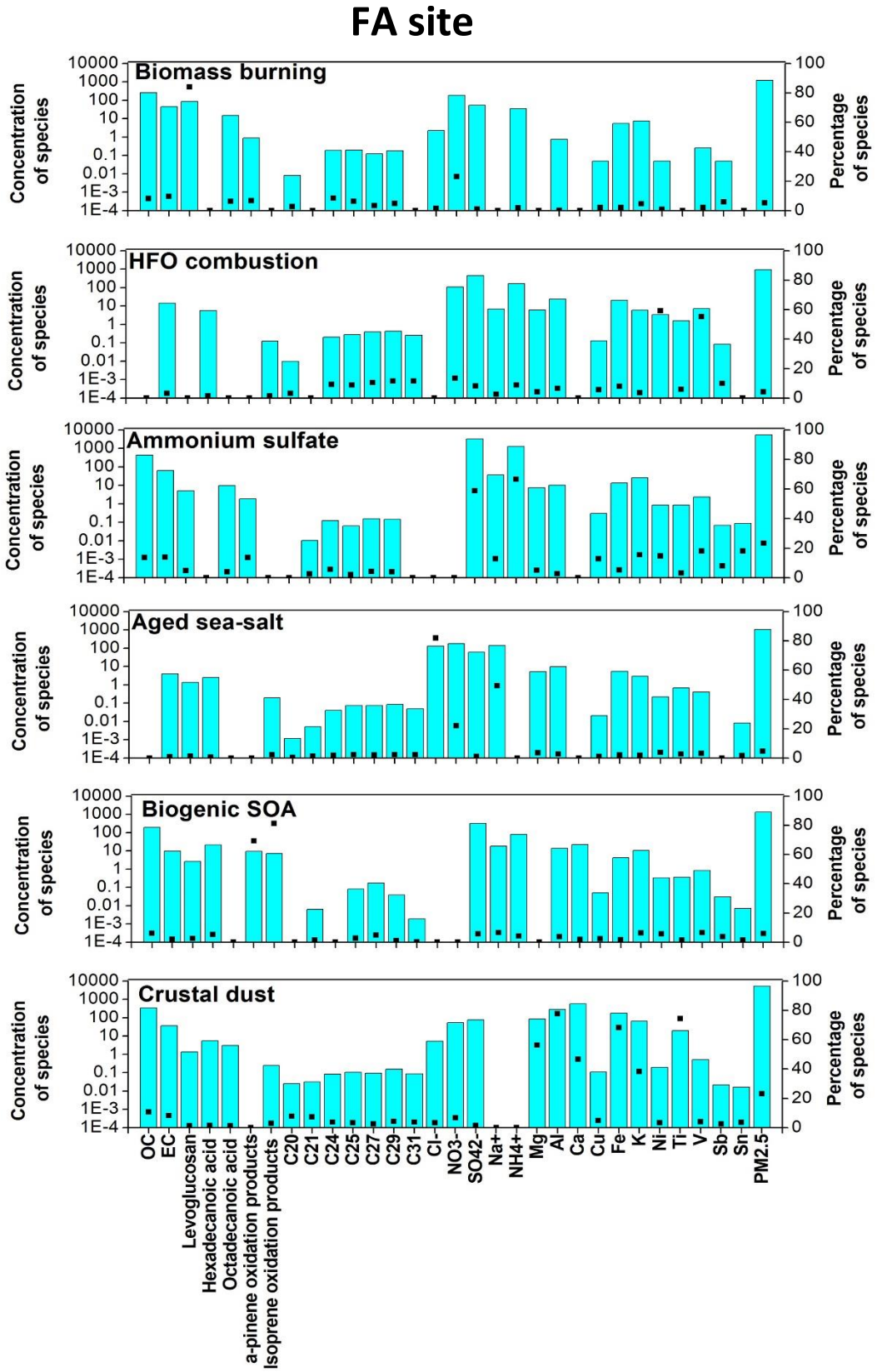
FA site
Biomass burning
HFO combustion
Ammonium sulfate
Aged sea-salt
Biogenic SOA
Crustal dust
Concentration of species
Percentage of species
10000
1000
100
10
1
0.1
0.01
1E-3
1E-4
100
80
60
40
20
0
OC
EC
Levoglucosan
Hexadecanoic acid
Octadecanoic acid
a-pinene oxidation products
Isoprene oxidation products
C20
C21
C24
C25
C27
C29
C31
Cl-
NO3-
SO42-
Na+
NH4+
Mg
Al
Ca
Cu
Fe
K
Ni
Ti
V
Sb
Sn
PM2.5

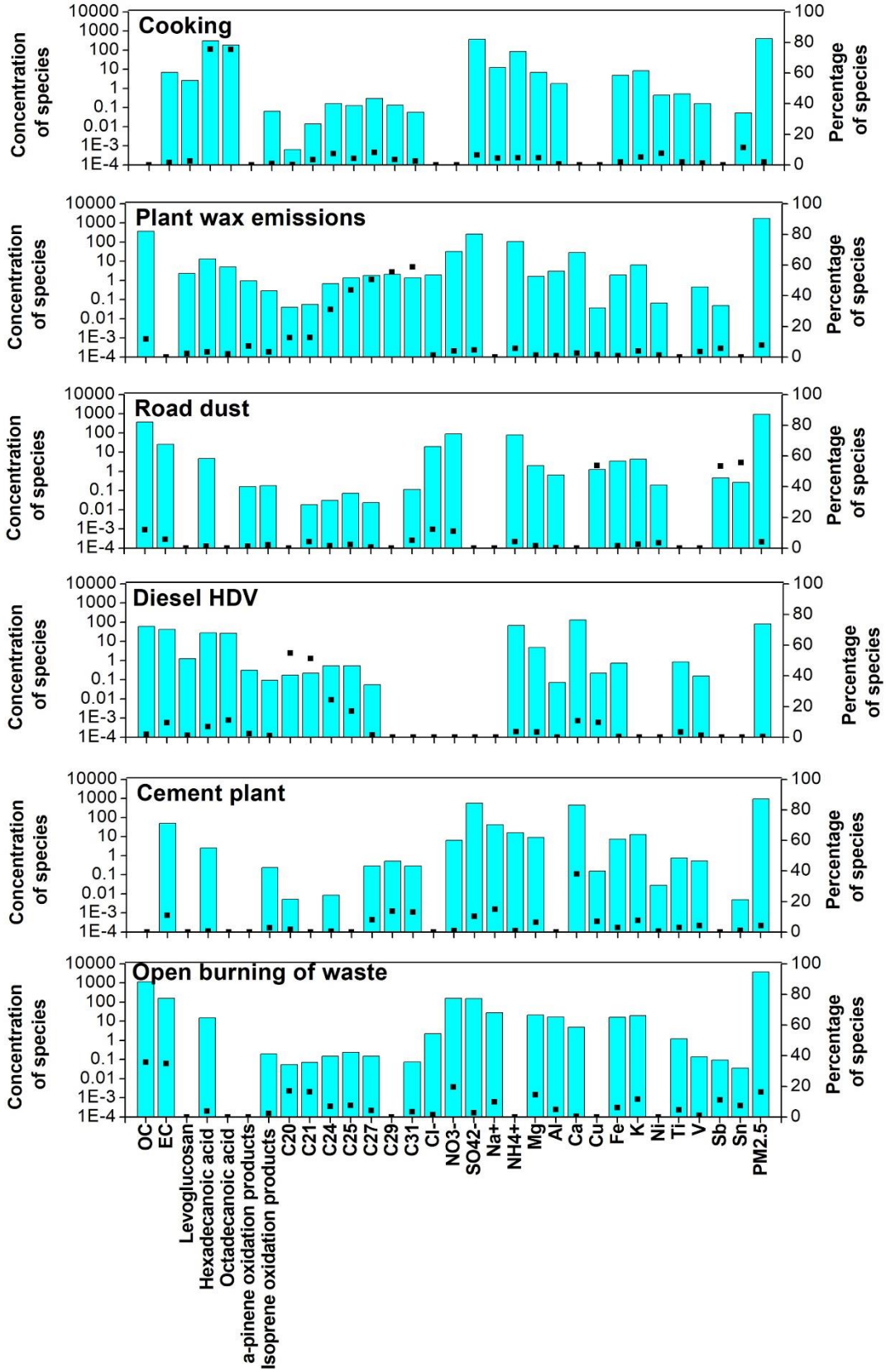

Fig. III-15: $PM_{2.5}$ profiles of the chemical components of the twelve factors calculated via PMF for the FA site

Cooking factor was identified with high contents of hexadecanoic and octadecanoic acids (70% and 60% at ZK, and 75% and 75% at FA, respectively). These compounds are used as organic markers for cooking activities (Abdullahi et al., 2013; Fadel et al., 2022).

Plant wax emissions factor showed more than 50% of the mass of C_{27}, C_{29}, and C_{31} but also showed considerable amounts of C_{24} and C_{25}. Generally, C_{24} and C_{25} were considered as tracers of vehicular emissions (Rogge et al., 1993a) and C_{27},C_{29}, and C_{31} were mainly linked to primary biogenic emissions (Rogge et al., 1993b). However, since very low contributions of OC and EC were recorded for this factor and no tracer elements for vehicular emissions were found, this factor cannot be attributed to vehicular emissions. The good correlation between C_{24} and C_{25} with C_{27}, C_{29}, and C_{31} might indicate that they were all emitted from the same source. This factor was then attributed to plant wax emissions.

Road dust factor was characterized by high loadings of Cu, Sb, and Sn and was mainly linked to vehicular emissions, specifically brake wear debris (Lin et al., 2015). This factor explained 57%, 64%, and 57% of the total mass of each compound at ZK, and 53%, 55%, and 53% at FA for Cu, Sb, and Sn, respectively.

As for the site-specific factors at ZK, Vehicular emissions (1) factor at ZK shows high loadings of 17α(H)-21β(H)-hopane with 60% of its mass in this factor **(Fig. III- 14)**. Hopanes are mainly present in unburned lubricating oils, and thus associated to non-exhaust vehicular emissions. The time series show higher concentrations during the cold period potentially resulting from higher volatilization rate during summer as well as lower traffic intensity (Fadel et al., 2021).

Vehicular emissions (2) factor was identified as a second factor for vehicular emissions with high concentrations of OC and EC with a concentration ratio OC/EC of 1.3 which is in the range of on-road transport vehicles (Salameh et al., 2015). Diesel generators factor at ZK showed high loadings of C_{20} (79% of the mass of the compound), and C_{21} (58%) alkanes in addition to the presence of OC and EC with a ratio OC/EC of 2.7 (**Fig. III- 14)**. C_{20} and C_{21} were mainly associated with diesel fuel combustion and the OC/EC concentration ratio specifies non-road diesel generators (2.9) (Fadel et al., 2022). These generators with no law enforcement are commonly used in Lebanon, especially in populated areas to compensate the shortage of electricity supply.

Regarding the factors specific to FA site, diesel HDV was characterized with C_{20} and C_{21} (50% of the mass of the compound), attributed to diesel fuel but a OC/EC ratio of 1.4 within the range of on-road transport vehicles (Salameh et al., 2015). Diesel HDV are abundant in the region

due to the presence of different industries. Cement plant factor showed high levels of calcium which correspond to 40% of the compound's mass **(Fig. III-15)**. Ca is considered a marker for cement dust (Yubero et al., 2011) since a major part of the clinker composition is calcium and thus the factor is attributed to the emissions of the cement plants in the region. Finally, open burning of waste was characterized by high levels of OC and EC linked to combustion sources **(Fig. III-15)** that cannot be either attributed to vehicular emissions since the concentration ratio OC/EC is high (equal to 7.1) or to biomass burning since no levoglucosan was detected. The OC/EC ratio of 7.1 is close to the value of 7.5 reported for open burning of municipal solid waste (Wang et al., 2020). Other than OC and EC, we can observe some species such as Cl^- that might be associated to incineration profiles (Yang et al., 2016). This phenomenon was recurrently observed in Chekka region.

2.6.3 Source contributions to $PM_{2.5}$

The measured concentration of $PM_{2.5}$ and values reconstructed by PMF were strongly correlated with regression slope of 0.88 and 0.86 and a determination coefficient R^2 of 0.9 and 0.88 at ZK and FA, respectively. Crustal dust and secondary ammonium sulfate provided the greatest contributions between the sources with an average of 8.6 µg/m^3 (27.5%) and 4.9 µg/m^3 (15.7%) at ZK and 5.8 µg/m^3 (23%) and 5.9 µg/m^3 (23.3%) at FA, respectively. The average contribution of ammonium sulfate was at least 4 times higher in summer (8.2 µg/m^3 at ZK and 8.7 µg/m^3 at FA) compared to winter (2 µg/m^3 at ZK and 1.9 µg/m^3 at FA) **(Fig. III- 16).**

$PM_{2.5}$ associated with vehicular emissions showed higher contributions at ZK with three associated factors (vehicular emissions (1) and (2) and road dust) and a contribution of 14% (4.1 µg/m^3) compared to a contribution of 4.4% at FA (road dust and diesel HDV: 1.1 µg/m^3) **(Fig. III- 16)**. This is mainly due to the difference in the characteristics of the sites since ZK is more populated than FA and is closer to a congested highway. Industrial emissions at ZK exhibited a relatively high contribution to $PM_{2.5}$ concentration through HFO combustion from the power plant (13% - 4.1 µg/m^3). While at FA, 8.2% of the $PM_{2.5}$ mass was explained by both the HFO combustion and the production processes at the cement plants (2.1 µg/m^3). Open burning of waste at FA appears an important $PM_{2.5}$ source since it contributes to 16.1% of $PM_{2.5}$. Additionally, primary and secondary biogenic emissions accounted for 1.5% and 7.8% at ZK, and 7.6% and 5.8% at FA, respectively **(Fig. III- 16)**. The contribution of biomass burning was only observed during winter and accounted for 9.3% and 18.8% of average winter $PM_{2.5}$ concentrations (2.4 µg/m^3 at ZK 3.8 µg/m^3 at FA). During the whole sampling period,

the biomass burning source accounted for 3.8% and 5.2% of $PM_{2.5}$. This source was mainly associated with wood burning from residential heating. The aged sea-salt factor contributed to 11.2% of $PM_{2.5}$ at ZK (3.5 µg/m^3) and 4.6% at FA (1.2 µg/m^3). Finally, other anthropogenic sources accounted for 6% at ZK (diesel generators and cooking) and 1.7 % at FA (cooking).

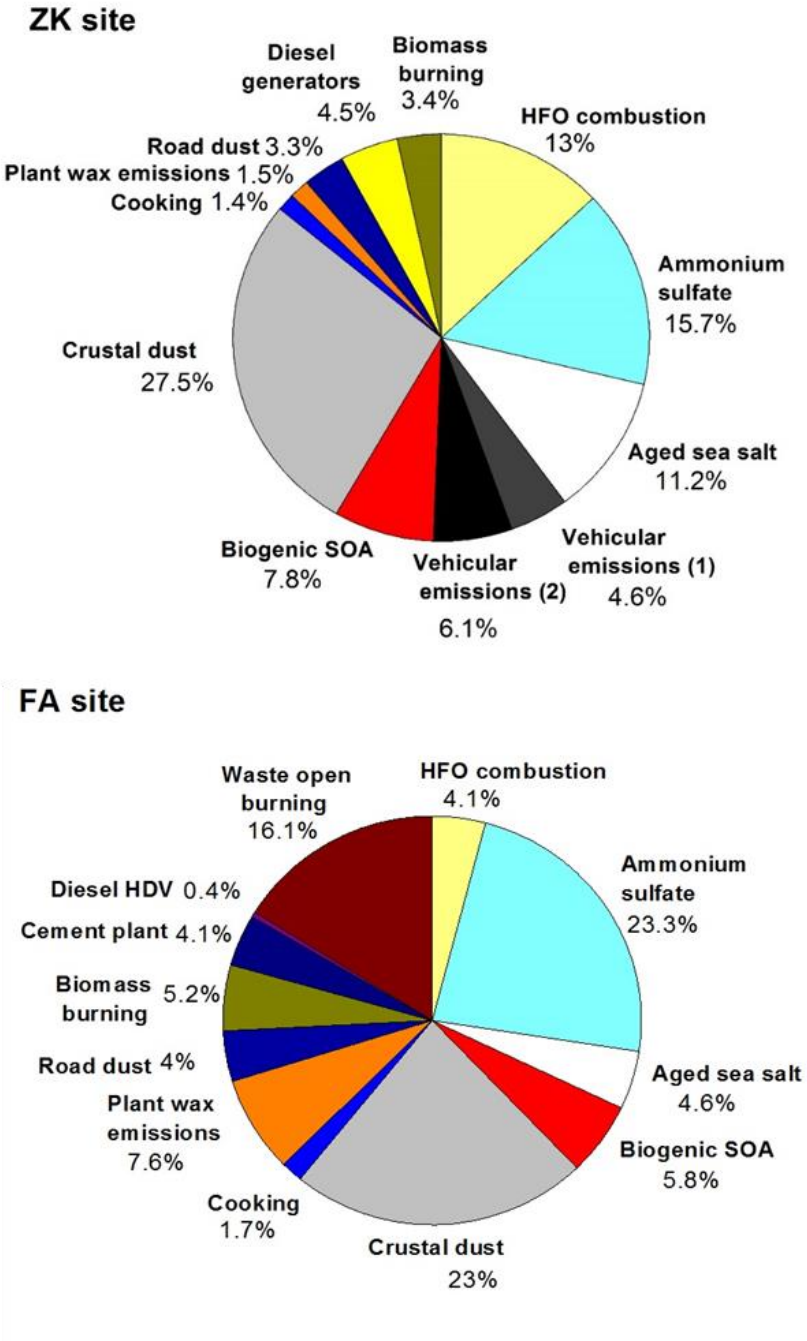

Fig. III- 16: Mean contributions of the twelve identified sources to the total $PM_{2.5}$ mass for Zouk (ZK) and Fiaa (FA) sites

3 Conclusions

The characterization of the composition of urban $PM_{2.5}$ was carried out during an almost one-year study in two sites in the East Mediterranean: Zouk Mikael (ZK) and Fiaa (FA) sites. The chemical composition of $PM_{2.5}$ included the major components such as OC, EC, water-soluble ions, and elements. These species, along with other organic tracers were used to identify the sources of atmospheric aerosols at the sites using a source apportionment model PMF.

The average concentrations of $PM_{2.5}$ were 33.6 µg/m^3 at ZK and 26.0 µg/m^3 at FA. The major chemical species of $PM_{2.5}$ at both sites were OC, SO_4^{2-}, Ca, NH_4^+, and NO_3^-. Several diagnostic tools were used to gain a preliminary picture of the most relevant sources such as concentration ratios and enrichment factors. These tools showed that ZK site was mainly under the influence of vehicular emissions and HFO combustion from the power plant. Whereas at FA, biomass burning and HFO combustion from the cement plants were two important anthropogenic sources. The cluster analysis of air mass back-trajectories showed that the sites were under the influence of long-range transport of dust from Saharan and Arabian deserts which are loaded with carbonaceous matter resulting from the existing refineries in these areas. The sites also experience long range transport of sulfate from Eastern and Central Europe and Turkey.

The PMF model was able to provide quantitative information about the source contributions. Crustal dust and secondary ammonium sulfate contributed to 43.2% of $PM_{2.5}$ mass at ZK. Vehicular and industrial emissions were two important sources at ZK contributing to 14% and 13% of $PM_{2.5}$, respectively. Biogenic emissions including plant wax emissions and secondary organic aerosols contribute to 9.3%. Other anthropogenic sources such as biomass burning, cooking, and diesel generators accounted for 9.8%. While at FA site, crustal dust and secondary ammonium sulfate contributed to 46.3% of $PM_{2.5}$ mass. 8.2% of $PM_{2.5}$ mass concentration was attributed to cement plants, and only 4.4% attributed to vehicular emissions. However, open burning of waste explained 16.1% of $PM_{2.5.}$ Biogenic emissions, biomass burning, and cooking contributed to 13.4%, 5.2%, and 1.7%, respectively.

The results of the characterization and the source apportionment are important to develop effective and efficient air quality management policies. Additionally, the apportionment might serve in health effect models in order to assign PM components to observed health effects. Policymakers should mainly focus on the anthropogenic sources with the highest health impact in order to have better air quality in the region.

Acknowledgments:

The authors would like to acknowledge the National Council for Scientific Research of Lebanon (CNRS-L) and university of Littoral Côte d'Opale for granting a doctoral fellowship to Marc Fadel. This project was also funded by the Research Council and the Faculty of Sciences of Saint Joseph University of Beirut – Lebanon. The "Unité de Chimie Environnementale et Interactions sur le Vivant" (UCEIV-UR4492) participates in the CLIMIBIO project, which is financially supported by the Hauts-de-France Region Council, the French Ministry of Higher Education and Research, and the European Regional Development Funds. This publication has been also produced within the framework of the EMME-CARE project, which has received funding from the European Union's Horizon 2020 Research and Innovation Programme (under grant agreement no. 856612) and the Cyprus Government.

The authors thank Institut Chevreul - Université de Lille for the analysis of elements by ICP-MS. The authors would also like to Dorothée Dewaele (Centre Commun de Mesures, ULCO) for her help in the ICP-AES analysis, and Amaury Kasprowiak for his help in the ionic chromatography analysis.

References:

Abdallah, C., Afif, C., Masri, N., Öztürk, F., Dağkuş Keleş, M., Sartelet, K., 2018. A first annual assessment of air quality modeling over Lebanon using WRF/Polyphemus. Atmos. Pollut. Res. 9, https://doi.org/10.1016/j.apr.2018.01.003.

Abdallah, C., Afif, C., Sauvage, S., Borbon, A., Salameh, T., Kfoury, A., Leonardis, T., Karam, C., Formenti, P., Doussin, J.F., Locoge, N., Sartelet, K., 2020. Determination of gaseous and particulate emission factors from road transport in a Middle Eastern capital. Transp Res D Transp Envrion 83, 102361, https://doi.org/10.1016/j.trd.2020.102361.

Abdo, N., Khader, Y.S., Abdelrahman, M., Graboski-Bauer, A., Malkawi, M., Al-Sharif, M., Elbetieha, A.M., 2016. Respiratory health outcomes and air pollution in the Eastern Mediterranean Region: a systematic review. Rev. Environ. Health 31, 259-280, doi:10.1515/reveh-2015-0076.

Abdullahi, K.L., Delgado-Saborit, J.M., Harrison, R.M., 2013. Emissions and indoor concentrations of particulate matter and its specific chemical components from cooking: A review. Atmos Environ 71, 260-294, https://doi.org/10.1016/j.atmosenv.2013.01.061.

Abi Ghanem, D., 2018. Energy, the city and everyday life: Living with power outages in post-war Lebanon. Energy Research & Social Science 36, 36-43, https://doi.org/10.1016/j.erss.2017.11.012.

Achilleos, S., Wolfson, J.M., Ferguson, S.T., Kang, C.-M., Hadjimitsis, D.G., Hadjicharalambous, M., Achilleos, C., Christodoulou, A., Nisanzti, A., Papoutsa, C., Themistocleous, K., Athanasatos, S., Perdikou, S., Koutrakis, P., 2016. Spatial variability of fine and coarse particle composition and sources in Cyprus. Atmos Res 169, 255-270, https://doi.org/10.1016/j.atmosres.2015.10.005.

Afif, C., Chélala, C., Borbon, A., Abboud, M., Gerard, J., Farah, W., Jambert, C., Zaarour, R., Saliba, N., Perros, P., Rizk, T., 2008. SO_2 in Beirut: air quality implication and effects of local emissions and long-range transport. Air Qual Atmos Health 1, 167-178, 10.1007/s11869-008-0022-y.

Agarwal, A., Satsangi, A., Lakhani, A., Kumari, K.M., 2020. Seasonal and spatial variability of secondary inorganic aerosols in PM2.5 at Agra: Source apportionment through receptor models. Chemosphere 242, 125132, https://doi.org/10.1016/j.chemosphere.2019.125132.

Anderson, J.O., Thundiyil, J.G., Stolbach, A., 2012. Clearing the air: a review of the effects of particulate matter air pollution on human health. Journal of medical toxicology : official journal of the American College of Medical Toxicology 8, 166-175, 10.1007/s13181-011-0203-1.

Belis, C.A., Favez, O., Mircea, M., Diapouli, E., Manousakas, M.I., Vratolis, S., Gilardoni, S., Paglione, M., Decesari, S., Mocnik, G., Mooibroek, D., Salvador, P., Takahama, S., Vecchi, R., Paatero, P., European, C., Joint Research, C., 2019. European guide on air pollution source apportionment with receptor models : revised version 2019.

Benetello, F., Squizzato, S., Masiol, M., Khan, M.B., Visin, F., Formenton, G., Pavoni, B., 2018. A procedure to evaluate the factors determining the elemental composition of $PM_{2.5}$. Case study: the Veneto region (northeastern Italy). Environ Sci Pollut Res Int 25, 3823-3839, 10.1007/s11356-017-0759-7.

Borgie, M., Ledoux, F., Dagher, Z., Verdin, A., Cazier, F., Courcot, L., Shirali, P., Greige-Gerges, H., Courcot, D., 2016. Chemical characteristics of $PM_{2.5–0.3}$ and $PM_{0.3}$ and consequence of a dust storm episode at an urban site in Lebanon. Atmos Res 180, 274-286, https://doi.org/10.1016/j.atmosres.2016.06.001.

Bouri, E., El Assad, J., 2016. The Lebanese Electricity Woes: An Estimation of the Economical Costs of Power Interruptions. Energies 9, 583

Cavalli, F., Viana, M., Yttri, K.E., Genberg, J., Putaud, J.P., 2010. Toward a standardised thermal-optical protocol for measuring atmospheric organic and elemental carbon: the EUSAAR protocol. Atmos. Meas. Tech. 3, 79-89, 10.5194/amt-3-79-2010.

Chantara, S., Thepnuan, D., Wiriya, W., Prawan, S., Tsai, Y.I., 2019. Emissions of pollutant gases, fine particulate matters and their significant tracers from biomass burning in an open-system combustion chamber. Chemosphere 224, 407-416, https://doi.org/10.1016/j.chemosphere.2019.02.153.

Chester, R., Murphy, K.J.T., Lin, F.J., Berry, A.S., Bradshaw, G.A., Corcoran, P.A., 1993. Factors controlling the solubilities of trace metals from non-remote aerosols deposited to the sea surface by the 'dry' deposition mode. Mar. Chem. 42, 107-126, https://doi.org/10.1016/0304-4203(93)90241-F.

Chifflet, S., Amouroux, D., Bérail, S., Barre, J., Van, T.C., Baltrons, O., Brune, J., Dufour, A., Guinot, B., Mari, X., 2018. Origins and discrimination between local and regional atmospheric pollution in Haiphong (Vietnam), based on metal(loid) concentrations and lead isotopic ratios in PM_{10}. Environ Sci Pollut Res Int 25, 26653-26668, 10.1007/s11356-018-2722-7.

Dahiya, S., Anhäuser, A., Farrow, A., Thieriot, H., Kumar, A., L.Myllyvirta, 2020. Global SO2 emission hotspot database. 48 pp

De Sario, M., Katsouyanni, K., Michelozzi, P., 2013. Climate change, extreme weather events, air pollution and respiratory health in Europe. European Respiratory Journal 42, 826-843, 10.1183/09031936.00074712.

Draxler, R., Stunder, B., Rolph, G., Stein, A., Taylor, A., 2004. HYSPLIT4 users's guide.

El Haddad, I., Marchand, N., Wortham, H., Piot, C., Besombes, J.L., Cozic, J., Chauvel, C., Armengaud, A., Robin, D., Jaffrezo, J.L., 2011. Primary sources of $PM_{2.5}$ organic aerosol in an industrial Mediterranean city, Marseille. Atmos. Chem. Phys. 11, 2039-2058, 10.5194/acp-11-2039-2011.

Escudero, M., Viana, M., Querol, X., Alastuey, A., Díez Hernández, P., García Dos Santos, S., Anzano, J., 2015. Industrial sources of primary and secondary organic aerosols in two urban environments in Spain. Environ Sci Pollut Res Int 22, 10413-10424, 10.1007/s11356-015-4228-x.

Fadel, M., Ledoux, F., Farhat, M., Kfoury, A., Courcot, D., Afif, C., 2021. $PM_{2.5}$ characterization of primary and secondary organic aerosols in two urban-industrial areas in the East Mediterranean. J Environ Sci 101, 98-116, https://doi.org/10.1016/j.jes.2020.07.030.

Fadel, M., Ledoux, F., Seigneur, M., Oikonomou, K., Sciare, J., Courcot, D., Afif, C., 2022. Chemical characterization of $PM_{2.5}$ sources from different anthropogenic activities: cooking, wood burning, and diesel generators. Environ.Sci.Technol, under review.

Fakhri, N., Fadel, M., Öztürk, F., Iakovides, M., Pikridas, M., Sciare, J., Hayes, P., Afif, C., 2021. Chemical Characterization of $PM_{2.5}$ in the East Mediterranean during the hot season. Submitted

Feng, J., Li, M., Zhang, P., Gong, S., Zhong, M., Wu, M., Zheng, M., Chen, C., Wang, H., Lou, S., 2013. Investigation of the sources and seasonal variations of secondary organic aerosols in $PM_{2.5}$ in Shanghai with organic tracers. Atmos Environ 79, 614-622, https://doi.org/10.1016/j.atmosenv.2013.07.022.

Galindo, N., Nicolás, J.F., Yubero, E., Caballero, S., Pastor, C., Crespo, J., 2008. Factors affecting levels of aerosol sulfate and nitrate on the Western Mediterranean coast. Atmos Res 88, 305-313, https://doi.org/10.1016/j.atmosres.2007.11.024.

Galvão, E.S., de Cassia Feroni, R., D'Azeredo Orlando, M.T., 2020. A review of the main strategies used in the interpretation of similar chemical profiles yielded by receptor models in the source apportionment of particulate matter. Chemosphere, 128746, https://doi.org/10.1016/j.chemosphere.2020.128746.

He, L.-Y., Hu, M., Huang, X.-F., Yu, B.-D., Zhang, Y.-H., Liu, D.-Q., 2004. Measurement of emissions of fine particulate organic matter from Chinese cooking. Atmos Environ 38, 6557-6564, https://doi.org/10.1016/j.atmosenv.2004.08.034.

Hlavay, J., Polyák, K., Bódog, I., Molnár, Á., Mészáros, E., 1996. Distribution of trace elements in filter-collected aerosol samples. Fresenius. J. Anal. Chem. 354, 227-232, 10.1007/PL00012730.

Hopke, P.K., 2008. The Use of Source Apportionment for Air Quality Management and Health Assessments. J. Toxicol. Environ. Health, Part A 71, 555-563, 10.1080/15287390801997500.

Ivošević, T., Orlić, I., Čargonja, M., 2016. Fine Particulate Matter from Ship Emissions in the Port of Rijeka, Croatia. Croatian Assocation of Maritime Science and Transport.

Kalivitis, N., Gerasopoulos, E., Vrekoussis, M., Kouvarakis, G., Kubilay, N., Hatzianastassiou, N., Vardavas, I., Mihalopoulos, N., 2007. Dust transport over the eastern mediterranean derived from total ozone mapping spectrometer, aerosol robotic network, and surface measurements. Journal of Geophysical Research Atmospheres 112, 10.1029/2006JD007510.

Karagulian, F., Belis, C.A., Dora, C.F.C., Prüss-Ustün, A.M., Bonjour, S., Adair-Rohani, H., Amann, M., 2015. Contributions to cities' ambient particulate matter (PM): A systematic review of local source contributions at global level. Atmos Environ 120, 475-483, https://doi.org/10.1016/j.atmosenv.2015.08.087.

Kfoury, A., Ledoux, F., Roche, C., Delmaire, G., Roussel, G., Courcot, D., 2016. $PM_{2.5}$ source apportionment in a French urban coastal site under steelworks emission influences using constrained non-negative matrix factorization receptor model. J Environ Sci 40, 114-128, https://doi.org/10.1016/j.jes.2015.10.025.

Khan, J.Z., Sun, L., Tian, Y., Shi, G., Feng, Y., 2021. Chemical characterization and source apportionment of PM_1 and $PM_{2.5}$ in Tianjin, China: Impacts of biomass burning and primary biogenic sources. J Environ Sci 99, 196-209, https://doi.org/10.1016/j.jes.2020.06.027.

Ledoux, F., Courcot, L., Courcot, D., Aboukaïs, A., Puskaric, E., 2006. A summer and winter apportionment of particulate matter at urban and rural areas in northern France. Atmos Res 82, 633-642, https://doi.org/10.1016/j.atmosres.2006.02.019.

Ledoux, F., Kfoury, A., Delmaire, G., Roussel, G., El Zein, A., Courcot, D., 2017. Contributions of local and regional anthropogenic sources of metals in $PM_{2.5}$ at an urban site in northern France. Chemosphere 181, 713-724, 10.1016/j.chemosphere.2017.04.128.

Lee, S.W., Pomalis, R., Kan, B., 2000. A new methodology for source characterization of oil combustion particulate matter. Fuel Process. Technol. 65-66, 189-202, https://doi.org/10.1016/S0378-3820(99)00086-7.

Lelieveld, J., Evans, J.S., Fnais, M., Giannadaki, D., Pozzer, A., 2015. The contribution of outdoor air pollution sources to premature mortality on a global scale. Nature 525, 367-371, 10.1038/nature15371.

Lelieveld, J., Hadjinicolaou, P., Kostopoulou, E., Giannakopoulos, C., Pozzer, A., Tanarhte, M., Tyrlis, E., 2014. Model projected heat extremes and air pollution in the eastern

Mediterranean and Middle East in the twenty-first century. Regional Environmental Change 14, 1937-1949, http://dx.doi.org/10.1007/s10113-013-0444-4.

Liakakou, E., Stavroulas, I., Kaskaoutis, D.G., Grivas, G., Paraskevopoulou, D., Dumka, U.C., Tsagkaraki, M., Bougiatioti, A., Oikonomou, K., Sciare, J., Gerasopoulos, E., Mihalopoulos, N., 2020. Long-term variability, source apportionment and spectral properties of black carbon at an urban background site in Athens, Greece. Atmos Environ 222, 117137, https://doi.org/10.1016/j.atmosenv.2019.117137.

Lin, Y.C., Tsai, C.J., Wu, Y.C., Zhang, R., Chi, K.H., Huang, Y.T., Lin, S.H., Hsu, S.C., 2015. Characteristics of trace metals in traffic-derived particles in Hsuehshan Tunnel, Taiwan: size distribution, potential source, and fingerprinting metal ratio. Atmos. Chem. Phys. 15, 4117-4130, 10.5194/acp-15-4117-2015.

Liu, Y., Zhang, W., Bai, Z., Yang, W., Zhao, X., Han, B., Wang, X., 2017. China Source Profile Shared Service (CSPSS): The Chinese $PM_{2.5}$ Database for Source Profiles. Aerosol and Air Quality Research 17, 1501-1514, 10.4209/aaqr.2016.10.0469.

Mason, B., 1966. Principles of geochemistry.

Middleton, N.J., 1986. Dust storms in the Middle East. Journal of Arid Environments 10, 83-96, https://doi.org/10.1016/S0140-1963(18)31249-7.

MoE, 2017. Lebanon's National Strategy for Air Quality Management for 2030. http://www.databank.com.lb/docs/MoE-(2017)-National-Air-Quality-Management-Strategy-EN.pdf.

Ozturk, F., Keles, M., 2016. Wintertime chemical compositions of coarse and fine fractions of particulate matter in Bolu, Turkey. Environ Sci Pollut Res Int 23, 14157-14172, 10.1007/s11356-016-6584-6.

Paatero, P., Eberly, S., Brown, S.G., Norris, G.A., 2014. Methods for estimating uncertainty in factor analytic solutions. Atmos. Meas. Tech. 7, 781-797, 10.5194/amt-7-781-2014.

Paatero, P., Tapper, U., 1994. Positive matrix factorization: A non-negative factor model with optimal utilization of error estimates of data values. Environmetrics 5, 111-126, 10.1002/env.3170050203.

Pandolfi, M., Gonzalez-Castanedo, Y., Alastuey, A., de la Rosa, J.D., Mantilla, E., de la Campa, A.S., Querol, X., Pey, J., Amato, F., Moreno, T., 2011. Source apportionment of PM_{10} and $PM_{2.5}$ at multiple sites in the strait of Gibraltar by PMF: impact of shipping emissions. Environ Sci Pollut Res Int 18, 260-269, 10.1007/s11356-010-0373-4.

Pateraki, S., Assimakopoulos, V.D., Bougiatioti, A., Kouvarakis, G., Mihalopoulos, N., Vasilakos, C., 2012. Carbonaceous and ionic compositional patterns of fine particles over an urban Mediterranean area. Sci. Total Environ. 424, 251-263, 10.1016/j.scitotenv.2012.02.046.

Pernigotti, D., Belis, C.A., Spanò, L., 2016. SPECIEUROPE: The European data base for PM source profiles. Atmos. Pollut. Res. 7, 307-314, 10.1016/j.apr.2015.10.007.

Polissar, A.V., Hopke, P.K., Paatero, P., Malm, W.C., Sisler, J.F., 1998. Atmospheric aerosol over Alaska: 2. Elemental composition and sources. Journal of Geophysical Research: Atmospheres 103, 19045-19057, https://doi.org/10.1029/98JD01212.

Qian, X., 2013. The Development Status and Prospects of Arab Oil and Gas Industry. Journal of Middle Eastern and Islamic Studies (in Asia) 7, 65-92, 10.1080/19370679.2013.12023228.

Querol, X., Tobías, A., Pérez, N., Karanasiou, A., Amato, F., Stafoggia, M., Pérez García-Pando, C., Ginoux, P., Forastiere, F., Gumy, S., Mudu, P., Alastuey, A., 2019. Monitoring the impact of desert dust outbreaks for air quality for health studies. Environ. Int. 130, 104867, https://doi.org/10.1016/j.envint.2019.05.061.

Rogge, W.F., Hildemann, L.M., Mazurek, M.A., Cass, G.R., Simoneit, B.R.T., 1993a. Sources of fine organic aerosol. 2. Noncatalyst and catalyst-equipped automobiles and heavy-duty diesel trucks. Environ. Sci. Technol. 27, 636-651, 10.1021/es00041a007.

Rogge, W.F., Hildemann, L.M., Mazurek, M.A., Cass, G.R., Simoneit, B.R.T., 1993b. Sources of fine organic aerosol. 4. Particulate abrasion products from leaf surfaces of urban plants. Environ. Sci. Technol. 27, 2700-2711, 10.1021/es00049a008.

Saiyasitpanich, P., Lu, M., Keener, T.C., Liang, F., Khang, S.-J., 2005. The Effect of Diesel Fuel Sulfur Content on Particulate Matter Emissions for a Nonroad Diesel Generator. J. Air Waste Manage. Assoc. 55, 993-998, 10.1080/10473289.2005.10464685.

Salameh, D., Detournay, A., Pey, J., Pérez, N., Liguori, F., Saraga, D., Bove, M.C., Brotto, P., Cassola, F., Massabò, D., Latella, A., Pillon, S., Formenton, G., Patti, S., Armengaud, A., Piga, D., Jaffrezo, J.L., Bartzis, J., Tolis, E., Prati, P., Querol, X., Wortham, H., Marchand, N., 2015. PM2.5 chemical composition in five European Mediterranean cities: A 1-year study. Atmos Res 155, 102-117, https://doi.org/10.1016/j.atmosres.2014.12.001.

Samoli, E., Stafoggia, M., Rodopoulou, S., Ostro, B., Alessandrini, E., Basagaña, X., Díaz, J., Faustini, A., Gandini, M., Karanasiou, A., Kelessis, A.G., Le Tertre, A., Linares, C., Ranzi, A., Scarinzi, C., Katsouyanni, K., Forastiere, F., 2014. Which specific causes of death are associated with short term exposure to fine and coarse particles in Southern Europe? Results from the MED-PARTICLES project. Environ. Int. 67, 54-61, https://doi.org/10.1016/j.envint.2014.02.013.

Saraga, D.E., Tolis, E.I., Maggos, T., Vasilakos, C., Bartzis, J.G., 2019. PM2.5 source apportionment for the port city of Thessaloniki, Greece. Sci. Total Environ. 650, 2337-2354, 10.1016/j.scitotenv.2018.09.250.

Seinfeld, J.H., Pandis, S.N., 2016. Atmospheric Chemistry and Physics: From Air Pollution to Climate Change, 3r. John Wiley & Sons.

Shaltout, A.A., Hassan, S.K., Karydas, A.G., Zaki, Z.I., Mostafa, N.Y., Kregsamer, P., Wobrauschek, P., Streli, C., 2018. Comparative elemental analysis of fine particulate matter (PM2.5) from industrial and residential areas in Greater Cairo-Egypt by means of a multi-secondary target energy dispersive X-ray fluorescence spectrometer. Spectrochimica Acta Part B: Atomic Spectroscopy 145, 29-35, https://doi.org/10.1016/j.sab.2018.04.003.

Simon, H., Beck, L., Bhave, P.V., Divita, F., Hsu, Y., Luecken, D., Mobley, J.D., Pouliot, G.A., Reff, A., Sarwar, G., Strum, M., 2010. The development and uses of EPA's SPECIATE database. Atmos. Pollut. Res. 1, 196-206, 10.5094/apr.2010.026.

Soheila, J., Mojgan, K., Mehdi, M., Marzieh, T., Saeid, A., Marjan, M., Nizal, S., 2021. Long-Term Exposure to $PM_{2.5}$ and cardiovascular disease incidence and mortality in an Eastern Mediterranean country: Findings based on a 15-Year Cohort Study. Environmental Health, 10.21203/rs.3.rs-142122/v1.

Song, C.H., Carmichael, G.R., 1999. The aging process of naturally emitted aerosol (sea-salt and mineral aerosol) during long range transport. Atmos Environ 33, 2203-2218, https://doi.org/10.1016/S1352-2310(98)00301-X.

Stockwell, W.R., Kuhns, H., Etyemezian, V., Green, M.C., Chow, J.C., Watson, J.G., 2003. The Treasure Valley secondary aerosol study II: modeling of the formation of inorganic secondary aerosols and precursors for southwestern Idaho. Atmos Environ 37, 525-534, https://doi.org/10.1016/S1352-2310(02)00895-6.

Sun, X., Wang, H., Guo, Z., Lu, P., Song, F., Liu, L., Liu, J., Rose, N.L., Wang, F., 2020. Positive matrix factorization on source apportionment for typical pollutants in different environmental media: a review. Environmental Science: Processes & Impacts 22, 239-255, 10.1039/C9EM00529C.

Swietlicki, E., Krejci, R., 1996. Source characterisation of the Central European atmospheric aerosol using multivariate statistical methods. Nuclear Instruments and Methods in Physics Research Section B: Beam Interactions with Materials and Atoms 109-110, 519-525, https://doi.org/10.1016/0168-583X(95)01220-6.

Talbi, A., Kerchich, Y., Kerbachi, R., Boughedaoui, M., 2018. Assessment of annual air pollution levels with PM_1, $PM_{2.5}$, PM_{10} and associated heavy metals in Algiers, Algeria. Environ. Pollut. 232, 252-263, 10.1016/j.envpol.2017.09.041.

Tepe, A.M., Doğan, G., 2021. Chemical characterization of $PM_{2.5}$ and $PM_{2.5–10}$ samples collected in urban site in Mediterranean coast of Turkey. Atmos. Pollut. Res. 12, 46-59, https://doi.org/10.1016/j.apr.2020.08.012.

Theodosi, C., Tsagkaraki, M., Zarmpas, P., Grivas, G., Liakakou, E., Paraskevopoulou, D., Lianou, M., Gerasopoulos, E., Mihalopoulos, N., 2018. Multi-year chemical composition of the fine-aerosol fraction in Athens, Greece, with emphasis on the contribution of residential heating in wintertime. Atmos. Chem. Phys. 18, 14371-14391, 10.5194/acp-18-14371-2018.

Tolis, E.I., Saraga, D.E., Lytra, M.K., Papathanasiou, A.C., Bougaidis, P.N., Prekas-Patronakis, O.E., Ioannidis, I.I., Bartzis, J.G., 2015. Concentration and chemical composition of PM2.5 for a one-year period at Thessaloniki, Greece: A comparison between city and port area. Atmos. Environ. 113, 197-207, https://doi.org/10.1016/j.atmosenv.2015.05.014.

Trebs, I.M., S.; Meixner, F.X.; Helas, G.N.; Hoffer, A.; Rudich, Y.; Falkovich, A.H.; Moura, M.A.L.; Silva, R.S., da; Artaxo, P.; Slanina, J.; Andreae, M.O., 2005. The NH_4^+-NO_3^--Cl^--SO_4^{2-}-H_2O aerosol system and its gas phase precursors at a pasture site in the Amazon Basin: How relevant are mineral cations and soluble organic acids?

Verheye, W., 1973. Formation, classification and land evaluation of soils in mediterranean areas : with special reference to the southern Lebanon,Gent.

Viana, M., Kuhlbusch, T.A.J., Querol, X., Alastuey, A., Harrison, R.M., Hopke, P.K., Winiwarter, W., Vallius, M., Szidat, S., Prévôt, A.S.H., Hueglin, C., Bloemen, H., Wåhlin, P., Vecchi, R., Miranda, A.I., Kasper-Giebl, A., Maenhaut, W., Hitzenberger, R., 2008. Source apportionment of particulate matter in Europe: A review of methods and results. J. Aerosol Sci. 39, 827-849, 10.1016/j.jaerosci.2008.05.007.

Waked, A., Afif, C., 2012. Emissions of air pollutants from road transport in Lebanon and other countries in the Middle East region. Atmos Environ 61, 446-452, 10.1016/j.atmosenv.2012.07.064.

Waked, A., Afif, C., Brioude, J., Formenti, P., Chevaillier, S., Haddad, I.E., Doussin, J.-F., Borbon, A., Seigneur, C., 2013. Composition and source apportionment of organic aerosol in Beirut, Lebanon, during winter 2012. Aerosol Sci. Technol. 47, 1258-1266, 10.1080/02786826.2013.831975.

Waked, A., Afif, C., Formenti, P., Chevaillier, S., El-Haddad, I., Doussin, J.-F., Borbon, A., Seigneur, C., 2014. Characterization of organic tracer compounds in $PM_{2.5}$ at a semi-urban site in Beirut, Lebanon. Atmos Res 143, 85-94, 10.1016/j.atmosres.2014.02.006.

Waked, A., Afif, C., Seigneur, C., 2012. An atmospheric emission inventory of anthropogenic and biogenic sources for Lebanon. Atmos Environ 50, 88-96, https://doi.org/10.1016/j.atmosenv.2011.12.058.

Wang, J., Niu, X., Sun, J., Zhang, Y., Zhang, T., Shen, Z., Zhang, Q., Xu, H., Li, X., Zhang, R., 2020. Source profiles of $PM_{2.5}$ emitted from four typical open burning sources and its cytotoxicity to vascular smooth muscle cells. Sci. Total Environ. 715, 136949, https://doi.org/10.1016/j.scitotenv.2020.136949.

Wedepohl, K.H., 1995. The composition of the continental crust. Geochim. Cosmochim. Acta 59, 1217-1232, https://doi.org/10.1016/0016-7037(95)00038-2.

WHO, 2021. WHO air quality guidelines. Particulate matter ($PM_{2.5}$ and PM_{10}), ozone, nitrogen dioxide, sulfur dioxide and carbon monoxide. Geneva: World Health Organization Switzerland. Licence: CC BY-NC-SA 3.0 IGO.

Wu, C., Yu, J.Z., 2016. Determination of primary combustion source organic carbon-to-elemental carbon (OC/EC) ratio using ambient OC and EC measurements: secondary OC-EC correlation minimization method. Atmos. Chem. Phys. 16, 5453-5465, 10.5194/acp-16-5453-2016.

Xu, J., Jia, C., Yu, H., Xu, H., Ji, D., Wang, C., Xiao, H., He, J., 2021. Characteristics, sources, and health risks of $PM_{2.5}$-bound trace elements in representative areas of Northern Zhejiang Province, China. Chemosphere 272, 129632, https://doi.org/10.1016/j.chemosphere.2021.129632.

Yang, H.-H., Luo, S.-W., Lee, K.-T., Wu, J.-Y., Chang, C.W., Chu, P.F., 2016. Fine particulate speciation profile and emission factor of municipal solid waste incinerator established by dilution sampling method. J. Air Waste Manage. Assoc. 66, 807-814, 10.1080/10962247.2016.1184195.

Yu, G.H., Park, S., 2021. Chemical characterization and source apportionment of $PM_{2.5}$ at an urban site in Gwangju, Korea. Atmos. Pollut. Res., 101092, https://doi.org/10.1016/j.apr.2021.101092.

Yubero, E., Carratalá, A., Crespo, J., Nicolás, J., Santacatalina, M., Nava, S., Lucarelli, F., Chiari, M., 2011. PM_{10} source apportionment in the surroundings of the San Vicente del Raspeig cement plant complex in southeastern Spain. Environmental science and pollution research international 18, 64-74, 10.1007/s11356-010-0352-9.

Zakey, A.S., Abdel-Wahab, M.M., Pettersson, J.B.C., Gatari, M.J., Hallquist, M., 2008. Seasonal and spatial variation of atmospheric particulate matter in a developing megacity, the Greater Cairo, Egypt. Atmósfera. 21, 171-190

Zhao, M., Zhang, Y., Ma, W., Fu, Q., Yang, X., Li, C., Zhou, B., Yu, Q., Chen, L., 2013. Characteristics and ship traffic source identification of air pollutants in China's largest port. Atmos Environ 64, 277-286, https://doi.org/10.1016/j.atmosenv.2012.10.007.

Conclusion

This chapter presented an exhaustive chemical characterization of $PM_{2.5}$ collected from December 2018 to October 2019 in the two urban industrial areas: Zouk Mikael (ZK) and Fiaa (FA) in Lebanon. The speciation included the analysis of the carbonaceous matter (OC, EC), water-soluble ions, major and trace elements, and organic species. The latter encompasses different families of compounds such as alkanes, PAHs, hopanes, fatty acids, dicarboxylic acids, phthalates, and secondary biogenic species (oxidation products of isoprene, α-pinene, and β-caryophyllene). Some of these species were reported for the first time in Lebanon such as phthalates. A similar characterization was also made for $PM_{2.5}$ samples emitted from different sources commonly observed in the East Mediterranean region. Finally, several species and tracer compounds were gathered in the PMF model in order to assess the contribution of the sources to the $PM_{2.5}$ concentrations. The selection of organic tracers in the PMF model helped identify additional sources and consequently to get a more accurate source apportionment results.

The identification of these sources was based on different organic and inorganic markers found in the literature and in the local sources characterized in order to determine their profile (Article 1) along with different concentration ratios between species. The identified chemical profiles for non-road diesel generators, wood burning and cooking activities including charcoal grilling and general cooking activities showed similarities in the concentration ratios between species with the available profiles of the literature but also differences especially in the abundance of the species and some concentration ratios. The differences were mainly linked to the type of the fuel used, the size of the engine and the operating mode in the case of diesel generators. For biomass burning, it might be due to the type of wood and its moisture content. However, for the cooking profiles, the cooking method, the type of raw materials, the temperature, the ventilation equipment, and the composition of the food could play a major role in the chemical profiles.

During the sampling campaign from December 2018 to October 2019, average $PM_{2.5}$ concentrations were 33.6 $\mu g/m^3$ at ZK and 26.0 $\mu g/m^3$ at FA. The major chemical species of $PM_{2.5}$ at both sites were OC, SO_4^{2-}, Ca, NH_4^+, and NO_3^-. Water-soluble ions contributed to 40% and 47% of $PM_{2.5}$ at ZK and FA, respectively, while elements contribute to 10% of $PM_{2.5}$ at ZK and 8% at FA. The most abundant class of compounds in the organic fraction is the fatty acids.

PMF results showed that ammonium sulfate and crustal dust were the major sources of $PM_{2.5}$ contributing to 43.2% and 46.3% at ZK and FA, respectively. Crustal dust mainly originates from the Saharan and the Arabian deserts through long range transport of air masses. Its corresponding factor is characterized by high loadings of Al, Mg, Ca, Fe, and Ti elements that showed enrichment factors close to 1 (natural origins). On the other hand, high sulfate concentrations were mainly observed in the days where air masses originate from Eastern and Central Europe, and Turkey with higher levels during the warm period compared to the cold one. These hypotheses were validated by the observation of the back trajectories and the cluster analysis.

As for the local anthropogenic sources, ZK site is more influenced by vehicular emissions compared to FA site since ZK encompasses more congested highways. Several compounds such as chrysene and 17α(H)-21β(H)-hopane showed high concentrations at ZK but were not detected at FA. Additionally, the high concentrations of C_{25} linked to gasoline emissions and the different PAHs diagnostic ratios at ZK ((B[a]An/(B[a]An+Chr) and B[a]P/(B[a]P+Chr)) were found to agree with vehicular emissions. This factor contributed to 14% of $PM_{2.5}$ concentrations at ZK compared to 4% at FA. Additionally, since ZK is more populated than FA, higher numbers of diesel generators are installed in the region to compensate for the power shortage with no law enforcement on stack emissions. Non-road diesel generators were found to contribute to 4.5% of $PM_{2.5}$ at ZK.

The industrial influence at ZK was highlighted by the HFO combustion used in the energy industry, and specifically in its local power plant. HFO combustion contributed to 13% of $PM_{2.5}$ mass at ZK. Additionally, high concentrations of indeno[1,2,3-c,d]pyrene were observed at ZK and were linked to the presence of the power plant. A characteristic indeno[1,2,3-c,d]pyrene/(indeno[1,2,3-c,d]pyrene + benzo[g,h,i]perylene) ratio in the range 0.8-1.0 was determined for heavy fuel oil combustion from the power plant. Even though only some samples were down wind of the power plant, the same concentration ratio was encountered due to the fact that HFO combustion emissions are released at around 50 m from the ground by the 396 MW reciprocating engines but also at 145 m of height by the 607 MW boilers leading to an enhanced dispersion of the pollutants in Zouk Mikael region. The industrial influence at FA was highlighted by the contribution of HFO combustion from cement factories and power plants in the Chekka region but also by high levels of Ca associated to the cement manufacturing. These factors contributed to 8.2% of $PM_{2.5}$ mass. Additionally, we did not find a clear contribution of the quarries in the region. Their impact might have been grouped within the

crustal factor at FA since not all the samples that highly contribute to this factor correspond to dust storm episodes. They might be linked to a local source that corresponds to the quarries.

Another important source at FA is the open burning of waste that contributed to 16% of $PM_{2.5}$ mass. Open burning is considered as the consequence of the solid waste crisis and is commonly observed in the North governorate (which FA is part of) where garbage is burned everywhere.

Other anthropogenic sources also contribute to $PM_{2.5}$ at both sites such as cooking emissions identified by two organic markers (hexadecanoic and octadecanoic acids) and biomass burning detected by high levels of levoglucosan especially during the cold period and might be associated with wood burning for residential heating. The contribution of biomass burning is more important at FA compared to ZK since this heating method is mainly used in villages such as FA. The influence of biomass burning at FA was also suggested when evaluating the concentration ratio of Fla/(Fla+Pyr).

As for the natural emissions, primary and secondary biogenic emissions contributed to 9.3% at ZK and 13.4% at FA. The n-alkanes profile pattern showed higher contributions of natural emissions during summer with high levels of C_{27}, C_{29}, and C_{31} markers of plant wax emissions. Secondary biogenic emissions were observed by the oxidation products of α-pinene and isoprene that also showed an important seasonality with higher concentration in the warm period due to higher oxidation rates of the precursors. Finally, the proximity of the sampling sites to the Mediterranean Sea explains the contribution of aged sea-salt to the $PM_{2.5}$ concentration.

The results of the chemical speciation and the sources contribution were of utmost importance to further characterize the atmosphere of these two sites. All of these data will help in future air quality modeling studies in the East Mediterranean and Middle East region which encompasses more than 300 million inhabitants. However, it is also important to evaluate the risks associated with the exposure to these concentrations of pollutants and these sources in order to develop effective and efficient air quality management policies. The evaluation of the health risk associated with the exposure to $PM_{2.5}$ will the subject of the next chapter of this manuscript.

CHAPTER IV

Evaluation of the health risk associated with the exposure to $PM_{2.5}$

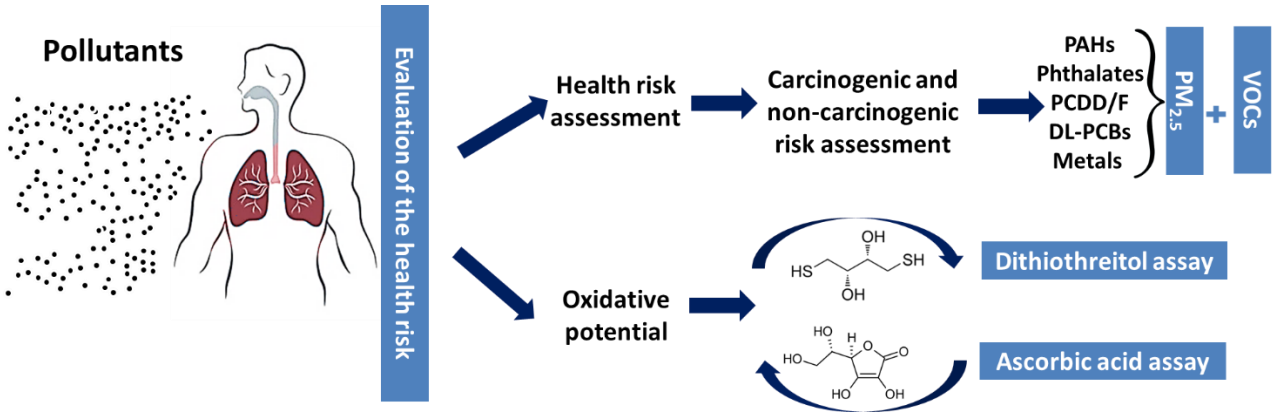

Introduction

Short and long-term exposure to $PM_{2.5}$ has been linked to various health effects such as cardiovascular, pulmonary diseases and lung cancer. The increasing number of excess mortality attributed to the global air pollution is alarming and the projection to the upcoming years does not show any improvement (Lelieveld et al., 2019). Therefore, it is essential to understand which species and sources contributing to $PM_{2.5}$ concentrations are the most implicated in the toxicity to better implement air quality management plans and policies. It has been established that the species that contribute the most to the $PM_{2.5}$ concentrations such as ammonium sulfate, sea-salt species, and crustal dust contribute the least to the toxicity (Borm et al., 2007). However, other species found in low amounts in PM such as PAHs (Bandowe and Meusel, 2017) and elements (Pb, Cr, Mn, etc.) have been shown to largely contribute to toxicity (Chen and Lippmann, 2009; Akhtar et al., 2010; Fortoul et al., 2015). Then when assessing the health risk, it is necessary to focus not only on the PM atmospheric concentration but more importantly on the PM chemical composition. This latter has to be the most complete possible and cover all the chemical families for a better estimation of the health risk associated with $PM_{2.5}$ exposure.

The evaluation of the health risk associated with the exposure to ambient air and specifically $PM_{2.5}$ and their corresponding chemical components will be studied in two approaches: the health risk assessment and the estimation of the oxidative potential. These approaches will help us discover which species and/or sources contribute the most to the toxicity of $PM_{2.5}$ depending on their concentrations and their ability to generate oxidative species in the human body.

The health risk assessment is based on the evaluation of the cancer and the non-cancer health risks associated with different classes of compounds. By definition, the cancer risk represents the incremental probability that an individual might develop cancer over a lifetime as a result of a specific exposure to a carcinogenic chemical. As for the non-cancer risk, it represents the probability to develop health complications other than cancer as a result of exposure to chemical pollutants. This methodology developed by the USEPA takes into account several exposure parameters such as the dose or the intake rate, the characteristics of the exposed individuals, the duration and the frequency of the exposure, and the concentrations of the pollutants. Most of the literature reports the health risks for only one family of compounds and mostly for the inhalation pathway, and by this approach only considers a part of the problem. In this work, we studied the health risks associated with exposure to compounds in the gaseous and particulate phases: the non-methane volatile organic compounds, and more than 70 species bounded to

$PM_{2.5}$ particles including polycyclic aromatic hydrocarbons, phthalates, metals, dioxins, furans and dioxin-like polychlorobiphenyls. Up to our knowledge, this is the first time the risk values for the different class of compounds of $PM_{2.5}$ collected at the same site will be presented together. The health risks were assessed for three exposure pathways (inhalation, ingestion, and dermal contact) and for different age categories (newborns, children, adolescents, and adults). In addition, in order to estimate the total health risk of PAHs in both particulate and gas phase, PAHs concentrations in the gas phase were also estimated based on the calculation of their partitioning coefficients. Finally, a comparison between the health risks associated with the different families of compounds was performed while specifying which compounds contribute the most to the health risk values. All of these results were presented in the first article of this chapter entitled "Human health risk assessment for PAHs, phthalates, elements, PCDD/Fs, and DL-PCBs in $PM_{2.5}$ and for NMVOCs in two East-Mediterranean urban sites under industrial influence" submitted to "Atmospheric Pollution Research" (Impact factor 2021: 4.352).

On the other hand, the oxidation properties of PM components were studied using the oxidative potential. This indicator addresses the intrinsic capacity of PM to generate reactive oxygen species (ROS) able to oxidize different biomolecules such as DNA, proteins and lipids in the lungs (Boukhenouna et al., 2018). In this study, the evaluation of the oxidative potential is based on two acellular methods commonly used in the literature: the ascorbic acid assay (AA) and the dithiothreitol (DTT) assay. These methods have different sensitivities to the classes of compounds of PM and an OP evaluation based on both of them seems therefore appropriate (Moufarrej et al., 2020). This study will be a first in Lebanon and in the East Mediterranean region presenting results for the oxidative potential and their temporal variability. Additionally, in order to further understand which species and sources contribute the most to OP values, different approaches were used. First, Spearman correlations were calculated between OP values and different classes of compounds including carbonaceous matter, water-soluble ions, trace and major elements, and organic compounds among which PAHs, alkanes, hopanes, and levoglucosan. Second, principal component analysis and hierarchical classification were conducted between OP values and the different identified sources by PMF at both sites. These two methods will give a first qualitative insight on the correlation between the OP, the chemical components, and the sources. Finally, a multiple linear regression was employed in order to attribute an intrinsic OP value for the different sources, and to determine the contribution of the different sources to the observed OP values. These results will be the subject of the second article of this chapter entitled "Temporal variations, relationship with chemical composition

and source apportionment of oxidative potential of $PM_{2.5}$ in two East Mediterranean sites" that will be submitted to "Environmental Pollution" (impact factor 2021: 8.071). By the articles of this chapter, we would have shed some light on the sources that contribute the most to the toxicity of $PM_{2.5}$ by the evaluation of the carcinogenic and the non-carcinogenic health risks of the species and which sources contribute to the oxidative potential of $PM_{2.5}$.

References:

Akhtar, U., McWhinney, R., Rastogi, N., Abbatt, J., Evans, G., Scott, J., 2010. Cytotoxic and proinflammatory effects of ambient and source-related particulate matter (PM) in relation to the production of reactive oxygen species (ROS) and cytokine adsorption by particles. Inhalation Toxicol. 22 Suppl 2, 37-47, 10.3109/08958378.2010.518377.

Bandowe, B.A.M., Meusel, H., 2017. Nitrated polycyclic aromatic hydrocarbons (nitro-PAHs) in the environment – A review. Sci. Total Environ. 581-582, 237-257, https://doi.org/10.1016/j.scitotenv.2016.12.115.

Borm, P.J.A., Kelly, F., Künzli, N., Schins, R.P.F., Donaldson, K., 2007. Oxidant generation by particulate matter: from biologically effective dose to a promising, novel metric. Occup. Environ. Med. 64, 73-74, http://dx.doi.org/10.1136/oem.2006.029090.

Boukhenouna, S., Wilson, M.A., Bahmed, K., Kosmider, B., 2018. Reactive oxygen species in chronic obstructive pulmonary disease. Oxidative Medicine and Cellular Longevity 2018, 5730395, 10.1155/2018/5730395.

Chen, L.C., Lippmann, M., 2009. Effects of metals within ambient air particulate matter (PM) on human health. Inhalation Toxicol. 21, 1-31, https://doi.org/10.1080/08958370802105405.

Fortoul, T.I., Rodriguez-Lara, V., Gonzalez-Villalva, A., Rojas-Lemus, M., Colin-Barenque, L., Bizarro-Nevares, P., García-Peláez, I., Cano, M.U.-., López-Zepeda, S., Cervantes-Yépez, S., López-Valdez, N., Meléndez-García, N., Espinosa-Zurutuza, M., Cano-Gutierrez, G., Cano-Rodríguez, M.C., 2015. Health effects of metals in particulate matter.

Lelieveld, J., Klingmüller, K., Pozzer, A., Pöschl, U., Fnais, M., Daiber, A., Münzel, T., 2019. Cardiovascular disease burden from ambient air pollution in Europe reassessed using novel hazard ratio functions. European Heart Journal 40, 1590-1596, 10.1093/eurheartj/ehz135.

Moufarrej, L., Courcot, D., Ledoux, F., 2020. Assessment of the $PM_{2.5}$ oxidative potential in a coastal industrial city in Northern France: Relationships with chemical composition, local emissions and long range sources. Sci. Total Environ. 748, 141448, 10.1016/j.scitotenv.2020.141448.

Article 4: Human health risk assessment for PAHs, phthalates, elements, PCDD/Fs, and DL-PCBs in $PM_{2.5}$ and for NMVOCs in two East-Mediterranean urban sites under industrial influence

Marc Fadel[a,b], *Frédéric Ledoux*[b], *Charbel Afif*[a,c], *Dominique Courcot*[b,*]

[a]Emissions, Measurements, and Modeling of the Atmosphere (EMMA) Laboratory, CAR, Faculty of Sciences, Saint Joseph University, Beirut, Lebanon

[b]Unité de Chimie Environnementale et Interactions sur le Vivant, UCEIV UR4492, FR CNRS 3417, University of Littoral Côte d′Opale (ULCO), Dunkerque, France

[c]Climate and Atmosphere Research Center, The Cyprus Institute, Nicosia, Cyprus

*Corresponding author: dominique.courcot@univ-littoral.fr

Abstract:

This study evaluates the carcinogenic and the non-carcinogenic health risks related to non-methane volatile organic compounds (NMVOCs) and elements, dioxins, furans, dioxin-like polychlorobiphenyls, phthalates and polycyclic aromatic hydrocarbons in $PM_{2.5}$ samples collected during a one-year field campaign in two urban industrial areas in the East Mediterranean region. The concentrations of gas-phase PAHs were also estimated based on the calculation of their partitioning coefficients. The health risk was assessed for the three exposure pathways (ingestion, inhalation, and dermal contact) and for different age categories (newborns, children, adolescents, and adults). The non-carcinogenic risk calculated for the different species showed that benzene, n-heptane, and the sum of elements where Mn, Pb, V, and Ni were the major contributors had values higher than the recommended USEPA limit of 1. The other species under study presented values lower than the limit and their risk was moderate. Benzene, 1,3-butadiene, ethylbenzene, $PM_{2.5}$-bound PAHs, As, Co, Cr (VI), Ni and V concentrations gave cancer risk values higher than the threshold limit of 10^{-6} depending on the age categories while phthalates gave lower values. To our knowledge, this assessment is a first evaluating the health risk of several classes of compounds from both particulate and gas phases.

Keywords: $PM_{2.5}$, NMVOCs, carcinogenic risk, exposure pathways, non-carcinogenic risk.

Introduction

According to the World Health Organization (WHO), air pollution is responsible for about 11% of the worldwide deaths annually, and therefore considered as the biggest environmental threat to human health (WHO, 2016). Outdoor air pollution among which different chemicals can be found in polluted atmosphere such as chromium (VI) compounds, arsenic, cadmium, nickel, benzo[a]pyrene, benzene, 1,3-butadiene, 2,3,4,7,8-pentachlorodibenzofuran, and 2,3,7,8-tetrachlorodibenzo-para-dioxin is classified as Group I "carcinogenic to humans" by the international Agency for Research on Cancer (IARC) (Loomis et al., 2013). Inhalation, oral ingestion, and dermal absorption are the three major routes of both intentional and accidental exposure to atmospheric chemicals. Vapor-phase and fine respirable particulate matter can travel into the respiratory system by adhering to the walls of the respiratory tract or penetrating deep into the lungs (Díaz and Rosa Dominguez, 2009). However, the non-respirable particulates usually enter the human body via the oral ingestion route. The dermal absorption is possible for different physical forms. Particles - especially fine and ultrafine ones (having an aerodynamic diameter less than 2.5 and 0.1 μm, respectively) - exposure to the respiratory tract has been associated with various health problems such as asthma, chronic obstructive pulmonary disease, cardiovascular diseases and lung cancer (Mark Goldberg, 2008; Thurston et al., 2017; Alkoussa et al., 2020; Cochard et al., 2020).

Health risk assessment studies aim at evaluating the potential health effects resulting from human exposure to any source of risk or particular hazard (DoHA, 2012). This approach can be applied in a qualitative or quantitative way. In order to evaluate the severity of the exposure, it takes generally into account several factors such as the dose or intake, the characteristics of the exposed individuals, the duration and the frequency of the exposure, and other parameters related to the harmfulness of the compounds on human health. The evaluation of the health risks associated with exposure to atmospheric pollutants is of utmost importance as it can lead to developing effective risk management policies and strategies for a population (Samet and Krewski, 2007; Chen et al., 2015).

The East Mediterranean is the third region with the highest ambient and household air pollution attributable death rate (age-standardized), scoring an average of 125 per 100,000 population in 2016, after Africa (181) and South East Asia (166), while this number could tend to rise in the future with the increase of the aerosol concentrations due to climate change (Lelieveld et al., 2014). Lebanon, an East Mediterranean country, faces extensive urbanization with heavy traffic, installation of diesel private generators within neighborhoods with no law enforcement,

dust events, open waste burning, along with emissions from different types of industries (Waked et al., 2012). The air quality in the country is considered unsafe as exceedances in $PM_{2.5}$ concentrations above WHO guidelines of 25 µg/m^3 are recorded (MoE, 2017) with more than 170 days in 2014 in Greater Beirut area. In order to evaluate the impact of air quality on human health in Lebanon, different approaches were tackled. Epidemiological studies were carried out to determine the association between outdoor air quality and different diseases such as chronic obstructive pulmonary diseases, chronic bronchitis, cardiovascular diseases and lung cancer (Kobrossi et al., 2002; Salameh et al., 2012; Aoun et al., 2013; Nakhlé et al., 2015; Nasser et al., 2015). These studies were based on questionnaires filled by hospital patients and air quality data. More recently, studies dealing with $PM_{2.5}$ from different areas in Lebanon (Borgie et al., 2015; Melki et al., 2017; Abbas et al., 2019; Badran et al., 2020) evidenced, on pulmonary cells *in vitro,* toxic effects of PM depending on the size and the composition of the particles.

PM atmospheric concentration is a widely used indicator of the air quality level. However, a high share of PM mass consists of compounds with low toxicity such as ammonium, sulfate, nitrate, sea salt, and crustal dust elements (Borm et al., 2007). On the other hand, species that barely contribute to PM mass such as transition metals and organic species can have a major impact on the aerosols' toxicity (Chen and Lippmann, 2009; Bandowe and Meusel, 2017). That's why it is important to evaluate the risk of exposure to PM not as whole but based on its chemical composition. Therefore, most of the studies found in the literature focused on the evaluation of the health risk related to the exposure to a specific family of compounds in PM such as metals, PAHs, and phthalates (Zhang et al., 2019; Bai et al., 2020; Murari et al., 2020) or for Volatile Organic Compounds (VOCs) (Dhaini et al., 2017). To our knowledge, there were no studies comparing the health risk evaluation of different family of compounds present in ambient air.

Therefore, the aims of this work were as follow: (1) evaluate the cancer and non-cancer health risks based on a one-year $PM_{2.5}$ and NMVOCs field campaign in two urban industrial areas, (2) compare the risks associated with the different exposure pathways, and (3) compare the risks associated with the different classes of compounds such as polycyclic aromatic hydrocarbons (PAHs), phthalates, major and trace elements, non-methane volatile organic compounds (NMVOCs), dioxins, furans, and dioxin-like polychlorobiphenyls. This study will be a first evaluating the health impact of the different classes of compounds (organic and inorganic) from particulate and gas phases for the different exposure pathways and for different age categories.

1 Materials and methods

1.1 Site description and sample collection

The description of the sampling sites was detailed elsewhere (Fadel et al., 2021) and will be shortly presented here. $PM_{2.5}$ and NMVOC samples were collected in two urban-industrial sites in Lebanon: Zouk Mikael (33˚57'57.07''N 35˚37'09.46''E) at a rooftop of a 15 m- residential building, and Fiaa in Chekka region (34˚20'47.8''N 35˚47'14.0''E) collocated with the ambient air quality monitoring station of the Lebanese Ministry of Environment. The Zouk Mikael site (ZK) is characterized by a high residential density (4,200 inhabitants/km^2) along with the biggest power plant in Lebanon which runs on Heavy Fuel Oil (HFO), an important number of private generators, and traffic. The Fiaa site (FA) is less populated (250 inhabitants/km^2) with moderate traffic activity and some private generators. The major industrial activities around FA site are related to three cement industries (distant between 5 and 7 km from the sampling site) in the region along with their corresponding quarries and a sulfuric acid and phosphate fertilizer industry (15 km from the sampling site) in Selaata **(Fig. IV-1)**.

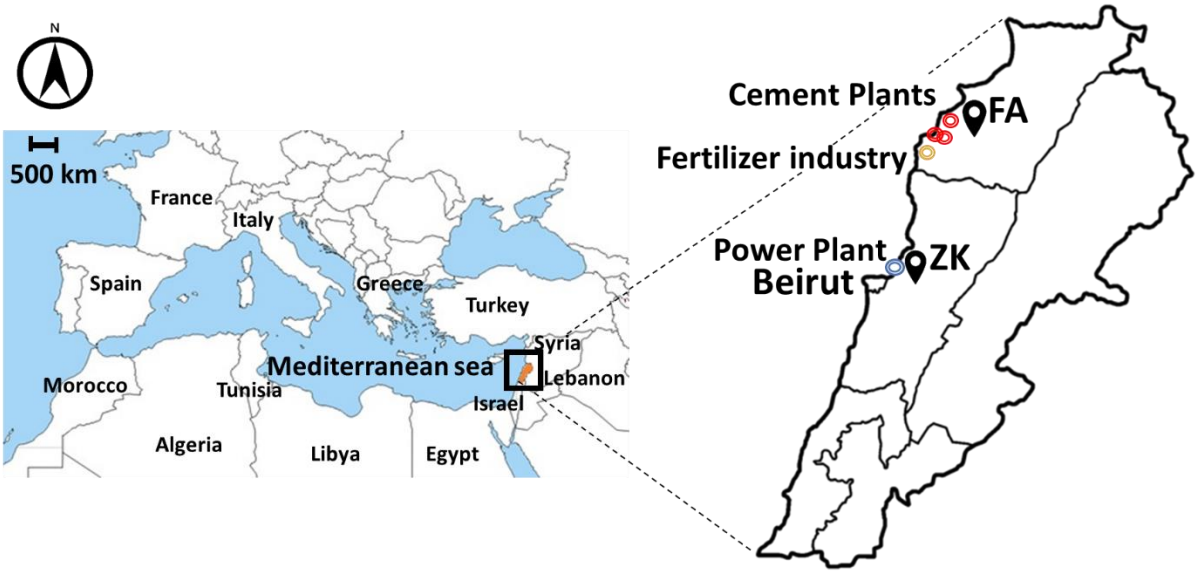

Fig. IV-1: Location of the two sampling sites: Zouk Mikael (ZK) and Fiaa (FA) and the position of the nearby industries

A total of 98 and 95 $PM_{2.5}$ samples were collected at ZK and FA, respectively every third day from the 13th of December 2018 to the 15th of October 2019 on a 24-hour basis. The sampling was carried out using high volume samplers operating at 30 m^3/h, onto 150 mm pure quartz microfibers filters. Prior to sampling, the filters were heated for 12 hours at 550˚C to remove the organic impurities.

In addition, non-methane VOCs (NMVOCs) were collected using passive radial diffuse samplers (Radiello– Code 120) placed for 4 weeks at both sites (11 samples per site). The cartridges were then kept at 4°C away from solvent until the analysis.

As for the 1,3-butadiene, the compound was trapped using Carbopack X diffusion tubes from Gradko International (Winchester, England) also over 4 weeks and a total of 9 samples per site were collected. Once the sampling completed, the tubes were returned to the company for the analysis.

1.2 Analysis of NMVOCs

NMVOCs were chemically extracted from cartridge by adding 2 mL of CS_2 and 100 µL of 2-fluorotoluene as internal standard in the Radiello glass tube without drawing out the cartridge. The solution was stirred from time to time for 30 min before discarding the cartridge, then filtered using PTFE Whatman filter (0.2 µm). 2 µL of the solution was injected in the GC-MS (ISQ 7000, Thermo Scientific, United States of America) operating in the split mode with a split ratio of 25. The GC was equipped with a 100% dimethyl polysiloxane column (50 m x 0.2 mm x 0.5 µm, Supelco, United States of America). The column temperature program consisted of an injection at 35˚C hold for 5 min, a ramp of temperature corresponding to 1˚C/min up to 135˚C followed by another ramp of temperature of 5˚C/min up to 250 ˚C and finally an isothermal hold step at 250 ˚C for 7 min. The GC was interfaced to an ion trap MS with an external electron ionization (EI) source (220 ˚C, 70 eV). The identification of the compounds was made by comparing their retention times and their mass spectrum (full scan mode, range 25-350 m/z) to the authentic standards. The concentrations of the compounds (in ng/m^3) were calculated using the equations provided by the manufacturer of Radiello diffusive passive sampler (Fondazione Salvatore Maugeri- IRCCS, Padova, Italy).

Field blanks and laboratory blanks were analyzed following the the same procedures as the sampling cartridges. The regression coefficient for the calibration curves was in the range of 0.96 - 0.99 for the different compounds.

1,3-butadiene quantification was achieved by the Gradko International company (Winchester, England). The analysis has been carried out in accordance with in-house method GLM 13-6 under UKAS fixed scope accreditation using a thermal desorption-gas chromatography coupled to a mass spectrometer (TD-GC-MS).

1.3 Chemical characterization of $PM_{2.5}$

The methodology used for the $PM_{2.5}$ chemical characterization was detailed elsewhere and will be briefly presented in this paper. PAHs and phthalates were analyzed by GC/MS (ISQ 7000, Thermo Scientific, United States of America) using the method described in Fadel et al. (2021). Major and trace elements were quantified using Inductively Coupled Plasma-Atomic Emission Spectrometry (ICP-AES, iCAP 6000 series, Thermo Scientific, United Kingdom) for Al, Ba, Fe, Mn, Ni, Sr, Zn and Pb, and ICP-Mass Spectrometry (ICP-MS, Agilent 7900, Varian, United States of America) for elements such as As, Cd, Co, Sn, Cu, Cr, Sb, V, La, and Tl. The method is detailed in (Ledoux et al., 2006; Kfoury et al., 2016). The analytical procedure for elements analysis by ICP-AES and ICP-MS was validated considering standard reference materials: urban particulate matter NIST-SRM 1648a (National Institute of Standards and Technology, USA). Recovery rates varied between 89% and 103% with an exception for Cr (76%). Polychlorinated Dibenzo-p-Dioxins (PCDDs), furans (PCDFs), and Dioxin-Like Polychlorinated Biphenyls (DL-PCBs) were analyzed by MicroPolluants Technology SA (Saint Julien Les Metz, France) based on the US Environmental Protection Agency (US EPA) methods 1613 and 1668 (Borgie et al., 2015). The apparatus used is a high-resolution gas chromatography coupled to a high-resolution mass spectrometer (HRGC/HRMS).

1.4 Toxic equivalent concentrations for PAHs and PCDD/Fs and DL-PCBs

1.4.1 2,3,7,8-TCDD equivalents

2,3,7,8-tetrachlorodibenzo-p-dioxin (2,3,7,8-TCDD) is known to be a human carcinogen, highly persistent and widespread environmental contaminant (NTP, 2016). A toxic equivalent factor (TEF) was introduced to assign toxicity values for the different congeners based on the toxicity of 2,3,7,8-TCDD reported as 1 (Van den Berg et al., 2006). The toxic equivalent "TEQ" representing an equivalent concentration of 2,3,7,8-TCDD is calculated following Eq. 1 by summing the product of the congeners' concentration multiplied by its corresponding TEF values (**Appendix D - Table S1**).

$$\mathrm{TEQ} = \sum_{i=1}^{n} C_i \times \mathrm{TEF}_i \quad (\mathrm{Eq.\ 1})$$

1.4.2 Benzo[a]pyrene equivalents

Among the different PAHs, benzo[a]pyrene has been classified as group I "Carcinogenic to humans" by the IARC. Upon that, the B[a]P equivalent concentration ($B[a]P_{eq}$) is often used to characterize the level of toxicity associated with PAHs. It is calculated as follows:

$$B[a]P_{eq} = \sum_{i=1}^{n} C_i \times TEF_i \quad (Eq.\,2)$$

Where C_i is the concentration of the PAHs (ng/m^3) and TEF_i (unitless) is its corresponding Toxic Equivalency Factor compared to B[a]P (TEF for B[a]P is 1) proposed by Nisbet and LaGoy (1992) and listed in **Appendix D - Table S2**.

1.5 Health Risk assessment

The health risk assessment was based on the Human health evaluation guidelines proposed by the United States Environmental Protection Agency (USEPA, 1989, 1991, 2011) and was performed for different age categories: newborns (0 to <1 year), children (1 to <12 years), adolescents (12 to <18 years) and adults (18 to 70 years), and for three exposure pathways: inhalation, ingestion, and dermal absorption on exposed skin when data were available. The average concentrations of the species on the sampling period were considered for the health risk assessment assuming that they represent a typical yearly concentration of the pollutants in the atmosphere of the considered sites.

1.5.1 Non-cancer risk assessment

The assessment of the non-carcinogenic risk resulting from exposure to a chemical was based on the comparison between the exposure estimate such as the average daily dose (ADD_i) to the reference dose (RfD_i) both expressed in mg/kg/day or the comparison of the exposure concentration in air (EC_i) to the reference concentration for inhalation (RfC_i) expressed in mg/m^3. These ratios are known as hazard quotients (HQ_i) and are calculated following one of the formulas of (Eq. 3) depending on the availability of RfD_i or RfCi in the literature:

$$HQ_i = \frac{ADD_i}{RfD_i} \text{ or } HQ_i = \frac{EC_i}{RfC_i} \quad (Eq.\,3)$$

With ADD_i for the different exposure pathways and EC_i for inhalation estimated as follows (Eq. 4 to Eq. 7):

$$ADD_{i-inhalation} = \frac{C_i \times IR_{inh} \times ED \times EF \times 10^{-6}}{BW \times AT} \quad (Eq. 4)$$

$$ADD_{i-ingestion} = \frac{C_i \times IR_{ing} \times ED \times EF \times 10^{-6}}{BW \times AT} \quad (Eq. 5)$$

$$ADD_{i-dermal} = \frac{C_i \times SA \times AF \times ABS \times ED \times EF \times 10^{-6}}{BW \times AT} \quad (Eq. 6)$$

$$EC_i = \frac{C_i \times ET \times EF \times ED \times 10^{-6}}{AT} \quad (Eq. 7)$$

Detailed information of each parameter used in the different formulas is given in **Table IV-1** for newborns, children, adolescents, and adults. Values for RfD_i and RfC_i are presented in **Appendix D - Table S3** for the different exposure pathways.

Total HQ_i is defined as the non-carcinogenic risk for a certain compound in the different exposure pathways assuming additive effects (Eq. 8) and calculated as follows:

$$\text{Total } HQ_i = HQ_{i-inhalation} + HQ_{i-ingestion} + HQ_{i-dermal} \quad (Eq. 8)$$

On the other hand, a receptor may be exposed to a specific family of chemicals associated with non-carcinogenic effects. Accordingly, a hazard index (HI) for a family of chemicals is defined as the total non-carcinogenic hazard for each exposure pathway and calculated as follows (Eq.9):

$$HI_{inhalation/ingestion/dermal} = \sum_i HQ_{i-inhalation\ /\ ingestion/\ dermal} \quad (Eq. 9)$$

Finally, in order to evaluate the total non-carcinogenic risk for a specific family for the combined exposure pathways, the total hazard index (THI) is calculated as follows (Eq. 10):

$$Total\ HI = THI = HI_{inhalation} + HI_{ingestion} + HI_{dermal} \quad (Eq. 10)$$

Generally, the higher the HQ_i, total HQ_i, HI and Total HI values above 1, the greater is the level of concern and the higher the probability of occurrence for hazardous non-carcinogenic effects (USEPA, 2011).

1.5.2 Cancer risk assessment

The risk estimates of carcinogenic chemicals represent the incremental probability that an individual might develop cancer over a lifetime as a result of a specific exposure to a carcinogenic chemical. The risks for inhalation and other pathways are calculated following

(Eq. 11). CSF_i is the cancer slope factor for a chemical in a specific exposure pathway expressed in kg·day/mg. IUR_i is the inhalation unit risk for a chemical expressed in m^3/mg used to calculate the cancer risk associated with the inhalation pathway (USEPA, 1997). CSF_i and IURi values are presented in **Appendix D - Table S3**.

$$CR_{i-inhalation} = EC_i \times IUR_i \quad \text{or} \quad CR_{i-ingestion/dermal} = LADD_i \times CSF_i \quad (Eq.\ 11)$$

When considering carcinogenic species, the exposure period during which the dose is averaged is usually lifetime or 70 years. Accordingly, the lifetime average daily dose ($LADD_i$) calculation equations for the different exposure pathways take the form of (Eq. 4 to 7) with lifetime (25,500 days) replacing the average timing (ED x 365 days) (USEPA, 1989, 2011).

To estimate the carcinogenic risk for a certain compound for the three exposure pathways, total CR_i was calculated as follows (Eq.12):

$$\text{Total } CR_i = CR_{i-inhalation} + CR_{i-ingestion} + CR_{i-dermal} \quad (Eq.\ 12)$$

The total cancer risk for a specific family of chemicals associated with an exposure pathway is estimated as follows (Eq.13):

$$CR_{\text{ inhalation/ingestion/dermal}} = \sum_i CR_{i\text{ inhalation/ingestion/dermal}} \quad (Eq.\ 13)$$

In order to evaluate the cancer risk for a family of chemicals attributed to the combined three exposure pathways, the cumulative cancer risk was calculated according to (Eq.14):

$$C\text{umulative CR} = CCR = CR_{inhalation} + CR_{\text{ ingestion}} + CR_{dermal} \quad (Eq.\ 14)$$

Finally, the estimation of the lifetime cancer risk (LCR) for a species or a group of species, the following equation (Eq.15) was used (OEHHA, 2012) :

$$LCR = \text{Cumulative } CR_{Newborn} \times \frac{1}{70} + \text{Cumulative } CR_{child} \times \frac{11}{70} + \text{Cumulative } CR_{adolescent} \times \frac{6}{70} + \text{Cumumative } CR_{adult} \times \frac{52}{70} \quad (Eq.\ 15)$$

Table IV-1: Exposure parameters for newborns, children, adolescents, and adults through inhalation, ingestion, and dermal contact considered in this study for the health risk assessment

Exposure parameters		Unit	Newborn	Child	Adolescent	Adult	Reference
			0 to <1 year	1 to <12 years	12 to <18 years	18 to 70 years	
Concentration in air	C_i	ng/m^3					
Inhalation intake rate	IR_{inh}	m^3/day	5.4	11.2	15.6	15.5	(USEPA, 2011)
Soil intake rate	IR_{ing}	mg/day	60	100	100	50	(USEPA, 2011)
Body Weight	BW	kg	7.8	25	61	72	(USEPA, 1997, 2011)
Exposure frequency (for residents)	EF	days/year	350	350	350	350	(USEPA, 2004b)
Exposure time	ET	h/day	6	6	8	8	(Dahmardeh Behrooz et al., 2021)
Exposure duration	ED	years	1	11	6	52	(USEPA, 2011)
Average timing	AT	days	AT = ED x 365(days) for non-carcinogens AT = 70 years x 365 for carcinogens				(USEPA, 1989)
Exposed skin surface area	SA	cm^2	1300	3200	4650	5700	(USEPA, 2002)
Dermal adherence factor	AF	mg/cm^2	0.2	0.2	0.2	0.07	(USEPA, 2002)
Dermal adsorption factor	ABS	-	0.13 for PAHs 0.03 for As 0.001 for Cd 0.01 for other elements				(USEPA, 2002)

1.6 Estimating the concentrations of PAHs in the gaseous phase from the particulate phase

The chemical characterization done in this study mainly focuses on the particulate phase but NMVOCs were also quantified in the gas phase. However, the partitioning of semi-volatile organic compounds (SVOCs) between the gas and particulate phases can be deemed as an important parameter to consider for a better assessment of the human exposure. In this study, PAHs were quantified in the particulate phase. It is known that low molecular weight PAHs are rather distributed in the gas phase (Abbas et al., 2018). Therefore, determining the PAHs gas phase concentration appears essential to this study. Among SVOCs, PAHs distribution between

the gas and particulate phases depend on several parameters such as the ambient temperature, the concentration of total suspended particles, along with the saturation vapor pressure of the species (Kim et al., 2016).

The classic approach used to describe the gas/particle partitioning of SVOCs derived from Pankow (1987) and was adapted by Naumova et al. (2003) for the respirable fraction of atmospheric PM. It consists in calculating the partitioning coefficient $Kp_{2.5}$ (expressed in $m^3/\mu g$) between the concentrations (ng/m^3) of the species in the particulate (F) and the gas phase (A), considering atmospheric concentration of $PM_{2.5}$ ($\mu g/m^3$) (Eq. 16).

$$K_{p_{2.5}} = \frac{\frac{F_{2.5}}{PM_{2.5}}}{A} \qquad (Eq.\ 16)$$

When A and F data are not available, different methods have been used to estimate K_p values for SVOCs. One of these is to use the equation (Eq. 17) (Pankow, 1994):

$$K_p = \frac{8.202 \times 10^{-5} \times T}{MW_i \times {p_i}^0 \times 10^6} \qquad (Eq.\ 17)$$

Where T is the temperature (K), MW_i is the molecular weight of the species (g/mol) and ${p_i}^0$ is the saturated vapor pressure (atm). The latter is estimated based on the vapor pressure values for different temperatures determined via the Knudsen Effusion Method for the 16 PAHs (Murray et al., 1974; Oja and Suuberg, 1998; Goldfarb and Suuberg, 2008; Fu and Suuberg, 2011). The vapor pressures reported in the previously mentioned studies were plotted against their corresponding temperatures in order to determine vapor pressure values for the 16 PAHs per sample according to the temperature at the sampling site. Some extrapolation was needed in order to determine these pressures since the literature temperature values were higher than those measured at ZK and FA. Then, K_p values were calculated for all PAHs in each sample using (Eq.17). The percentage of each PAH in the particulate phase was also calculated as the ratio between the $PM_{2.5}$-bound PAH and the sum of the PAH in both phases. These percentages were compared to percentage values derived from PAHs field measurements in both particulate and gas phases in other sites in the Mediterranean region (Akyüz and Çabuk, 2010; Gaga and Ari, 2019; Gurkan Ayyildiz and Esen, 2020) as well as American and Chinese sites (Ma et al., 2018; Pratt et al., 2018) . The average partitioning coefficients, the concentration of the different PAHs in the particulate and gas phases along with the percentage of PAHs in the particulate phase and the literature comparison were reported in **(Appendix D - Table S4)**.

2 Results and discussion

2.1 Atmospheric concentrations of the compounds

The average concentrations of PAHs, phthalates, and elements in $PM_{2.5}$ and NMVOCs are presented in **Table IV-2** for ZK and FA sites. The concentrations of individual PAHs as well as phthalates were presented in details in Fadel et al. (2021). Briefly, the major contributors to the total $PM_{2.5}$-bound PAHs at ZK were chrysene, benzo[b]fluoranthene, benzo[a]pyrene, dibenz[a,h]anthracene, and indeno(1,2,3-c,d)pyrene accounting for 66% of the total PAHs concentration (2.56 ng/m^3). While at FA, fluoranthene, pyrene, benzo[b]fluoranthene, dibenz[a,h]anthracene, and benzo[g,h,i]perylene contribute to 63% of the total PAHs in the particulate phase (0.95 ng/m^3). As for phthalates, the average concentrations of bis(2-ethylhexyl)phthalate (BEHP) and dibutyl phthalate (DBP) over the sampling period were 49 and 37 ng/m^3 at ZK, while at FA, the concentrations were 66 and 12.4 ng/m^3, respectively.

Table IV-3 presents PCDD/Fs, and DL-PCBs congener concentrations observed in ZK and FA sites in the particulate phase. The total average concentrations of PCDDs and PCDFs were 164 and 124 fg/m^3 at ZK and FA, respectively. OCDD and 1,2,3,4,6,7,8-HpCDF were the two dominant congeners among PCDD/Fs contributing to 49% and 46% at ZK and FA, respectively, followed by 1,2,3,4,6,7,8-HpCDD and OCDF. DL-PCB congeners are dominated by PCB 105 and PCB 118 accounting for 86% and 83% of total DL-PCBs at ZK and FA, respectively. Elements' concentrations varied at ZK from 0.03 ng/m^3 for Tl to 593 ng/m^3 for Al, and from 0.03 ng/m^3 for Tl to 492 ng/m^3 for Al at FA **(Table IV-2).** Finally, for NMVOCs, the highest concentrations are observed for benzene, toluene, ethylbenzene, and xylenes. Between these compounds, toluene showed the highest concentrations at both sites and 1,3-butadiene showed the lowest concentrations at ZK and was not detected at FA **(Table IV-2).**

These species have been used for the evaluation of the carcinogenic and the non-carcinogenic risk due to their adverse health effects and the availability of reference values (RfD, RfC, CSF, and IUR) in the literature **(Appendix D - Table S3).**

2.2 Health risk evaluation

The hazard quotient (HQ_i) and the cancer risk (CR_i) associated with each species in the three exposure pathways for the different age categories are reported in **Appendix D - Table S5** and **Table S6** for ZK and FA, respectively. Furthermore, the total hazard index (THI) and the cumulative cancer risk (CCR) for PAHs and TCDD equivalents along with total HQ_i and total

CR_i for phthalates, elements, and NMVOCs were summarized for ZK in **Appendix D- Table S7** and for FA in **Table S8**.

Table IV-2: Atmospheric concentrations of total PAHs, phthalates, and elements in $PM_{2.5}$ along with concentrations of non-methane volatile organic compounds (NMVOCs) during the entire sampling period

Compounds (ng/m^3)	**ZK site**	**FA site**	**Reference**
Total $PM_{2.5}$-bound PAHs	2.56	0.95	(Fadel et al., 2021)
$PM_{2.5}$-bound phthalates			
dibutyl phthalate	37	12.4	(Fadel et al., 2021)
bis(2-ethylhexyl)phthalate	49	66	
Major and trace elements			
As	0.53	0.49	This study
Cd	0.13	0.14	
Co	1.22	0.61	
Cr	1.88	1.97	
Cu	4.63	2.53	
Mn	7.46	5.61	
Ni	11.7	6.29	
Pb	12.8	17.5	
Zn	26.1	16.7	
Ba	14.2	9.1	
Al	593	492	
V	25	13	
Fe	452	298	
Sr	5.4	4.5	
Sn	0.83	0.57	
Sb	1.11	0.95	
La	0.54	0.33	
Tl	0.03	0.03	
NMVOCs			
1,3-butadiene	77.7	<D.L.	This study
hexane	419	150	
tetrachloroethene	291	58	
benzene	4318	1526	
cyclohexane	398	94	
heptane	657	138	
methylcyclohexane	446	88	
toluene	16910	2740	
ethylbenzene	4210	655	
m+p-xylene	5730	743	
o-xylene	4375	605	

Table IV-3: Dioxins (PCDD), furans (PCDF) and dioxin-like polychlorobiphenyls (DL-PCBs) concentrations (fg/m^3) in $PM_{2.5}$ samples at Zouk (ZK) and Fiaa (FA)

Compounds (fg/m^3)	Abbreviations	ZK site	FA site
PCDDs		**81.1**	**52.0**
2,3,7,8-tetrachlorinated dibenzo-p-dioxin	2,3,7,8 TCDD	<D.L.	<D.L.
1,2,3,7,8-pentachlorinated dibenzo-p-dioxin	1,2,3,7,8 PeCDD	0.43	<D.L.
1,2,3,4,7,8-hexachlorinated dibenzo-p-dioxin	1,2,3,4,7,8 HxCDD	0.51	<D.L.
1,2,3,6,7,8-hexachlorinated dibenzo-p-dioxin	1,2,3,6,7,8 HxCDD	1.77	1.69
1,2,3,7,8,9-hexachlorinated dibenzo-p-dioxin	1,2,3,7,8,9 HxCDD	1.26	<D.L.
1,2,3,4,6,7,8-heptachlorinated dibenzo-p-dioxin	1,2,3,4,6,7,8 HpCDD	23.18	16.13
octachlorinated dibenzo-p-dioxin	OCDD	53.98	34.20
	TEQ for PCDD	***1.03***	***0.34***
PCDFs		***82.5***	**71.8**
2,3,7,8 tetrachlorinated dibenzofuran	2,3,7,8 TCDF	1.31	1.57
1,2,3,7,8 pentachlorinated dibenzofuran	1,2,3,7,8 PeCDF	2.43	1.95
2,3,4,7,8 pentachlorinated dibenzofuran	2,3,4,7,8 PeCDF	4.49	7.35
1,2,3,4,7,8 hexachlorinated dibenzofuran	1,2,3,4,7,8 HxCDF	7.76	6.51
1,2,3,6,7,8 hexachlorinated dibenzofuran	1,2,3,6,7,8 HxCDF	6.61	5.37
2,3,4,6,7,8 hexachlorinated dibenzofuran	2,3,4,6,7,8 HxCDF	8.79	8.30
1,2,3,7,8,9 hexachlorinated dibenzofuran	1,2,3,7,8,9 HxCDF	2.79	2.60
1,2,3,4,6,7,8-heptachlorinated dibenzofuran	1,2,3,4,6,7,8 HpCDF	26.43	23.04
1,2,3,4,7,8,9-heptachlorinated dibenzofuran	1,2,3,4,7,8,9 HpCDF	3.16	2.63
octachlorinated dibenzofuran	OCDF	18.75	12.46
	TEQ for PCDF	***4.45***	***4.96***
DL-PCBs		**454.8**	**586.3**
3,4,4',5-tetrachlorobiphenyl	PCB 81	<D.L.	<D.L.
3,3′,4,4′-tetrachlorobiphenyl	PCB 77	21.66	8.39
2,3',4,4',5'-pentachlorobiphenyl	PCB 123	20.20	55.51
2,3',4,4',5-pentachlorobiphenyl	PCB 118	278.17	325.21
2,3,4,4',5-pentachlorobiphenyl	PCB 114	<D.L.	4.59
2,3,3',4,4'-pentachlorobiphenyl	PCB 105	111.37	158.60
3,3',4,4',5-pentachlorobiphenyl	PCB 126	<D.L.	<D.L.
2,3',4,4',5,5'-hexachlorobiphenyl	PCB 167	8.37	<D.L.
2,3,3',4,4',5-hexachlorobiphenyl	PCB 156	15.08	13.40
2,3,3',4,4',5'-hexachlorobiphenyl	PCB 157	<D.L.	<D.L.
3,3',4,4',5,5'-hexachlorobiphenyl	PCB 169	<D.L.	11.66
2,3,3',4,4',5,5'-heptachlorobiphenyl	PCB 189	<D.L.	8.95
	TEQ for PCB	***0.02***	***0.37***
	Total TEQ	***5.49***	***5.67***

2.2.1 Polycyclic Aromatic Hydrocarbons

The $B[a]P_{eq}$ value for the 16 PAHs in the particulate phase was 2.58 and 0.69 ng/m^3 at ZK and FA, respectively. The 7 PAHs classified by the IARC as group 1, 2A or 2B, namely

benz[a]anthracene, chrysene, benzo[b]fluoranthene, benzo[k]fluoranthene, benzo[a]pyrene, dibenz[a,h]anthracene and indeno(1,2,3-c,d)pyrene, accounted for 98% of the $B[a]P_{eq}$ value at ZK and 99% at FA. This indicates that these compounds were the main contributors to $PM_{2.5}$-bound PAHs toxicity. The total estimated concentration of PAHs in the gas phase using the method described in section 1.6 was 32.6 ng/m^3 at ZK (Table S4), 12 times higher than the average PAHs concentrations in the particulate phase (2.56 ng/m^3). As for FA, PAHs concentrations were 1.7 times higher in the gas phase (1.6 ng/m^3 in the gas phase versus 0.95 ng/m^3 in $PM_{2.5}$). Since the particulate phase concentrations of acenaphthylene, acenaphthene and fluorene were below the detection limit of the method at FA, the gas phase concentrations of these three compounds were not determined which could contribute to some extent to the difference in the gas phase concentrations between ZK and FA. The share of PAHs in the particulate phase varied from 0.1% for acenaphthylene to 99.9% for dibenz[a,h]anthracene **(Appendix D - Table S4).** The partitioning of the different PAHs in the gas and the particulate phases were in range of those reported from field measurements in both phases for Mediterranean sites such as in Turkey and Greece (Vasilakos et al., 2007; Akyüz and Çabuk, 2010; Gaga and Ari, 2019) **(Appendix D - Table S4)**.

However, even if the PAHs concentrations are higher in the gas phase at both sites, low $B[a]P_{eq}$ concentrations in the gas phase were found at ZK (0.06 ng/m^3) and FA (0.01 ng/m^3). This can be explained by the high abundance of the 7 above-mentioned PAHs in the particulate phase compared to the gas phase **(Appendix D - Table S4).**

The non-cancer risk for PAHs was evaluated for ingestion and inhalation pathways. Exposure to PAHs via inhalation exhibited the highest risk for the different age categories contributing to more than 80% of the total HI **(Appendix D -Table S5 and S6)**. At both sites, the total HI value related with the exposure to the $PM_{2.5}$-bound PAHs was <1 (acceptable risk), with a higher value for adolescents (0.43 at ZK and 0.11 at FA) then adults (0.42 at ZK and 0.10 at FA), then come the newborns (0.37 at ZK and 0.10 at FA) and the children (0.34 at ZK and 0.09 at FA) **(Appendix D - Table S7, Table S8).** The same behavior was also observed for PAHs in the gas phase but with lower total HI ranging between 1.0×10^{-3} and 1.0×10^{-2}.

The cumulative cancer risk associated with exposure to $PM_{2.5}$-bound PAHs via ingestion, inhalation and dermal contact were evaluated **(Appendix D - Table S7 and S8)**. The results showed that the values exceeded the potential risk value recommended by USEPA (10^{-6}) except for newborns at FA with a trend of children (1.5×10^{-5} at ZK and 4.1×10^{-6} at FA) > adults (1.4×10^{-5} at ZK and 3.9×10^{-6} at FA) > adolescents (3.8×10^{-6} at ZK and 1.0×10^{-6} at FA) >

newborns (2.5 x 10^{-6} at ZK and 7 x 10^{-7} at FA), showing a potential cancer risk at these PAHs concentration exposure levels **(Fig. IV-2).**

The cumulative cancer risk values reported for children and adults at both sites were higher than those reported for a site in Thailand (6.1 x 10^{-9} - 7.7 x 10^{-9} for children and 1.3 x 10^{-8} – 1.4 x 10^{-8} for adults) having lower $B[a]P_{eq}$ concentration (0.06-0.07 ng/m^3) (Pongpiachan, 2015). In terms of exposure pathways, ingestion and dermal contact were the main exposure routes leading to cancer risk (2.0 x 10^{-6} and 3.8 x 10^{-7} at ZK, 5.3 x 10^{-7} and 1.0 x 10^{-7} at FA, respectively), which were at least three times higher than the inhalation pathway (9.4 x 10^{-8} at ZK and 2.5 x 10^{-8} at FA) **(Table IV-4, Table IV-5).**The CR values from inhalation were lower than those reported for a site characterized by high traffic density and industrial activities (4 x 10^{-7} – 8.4 x 10^{-5}), but also an urban Indian site with values in the range of 10^{-6} (Fang et al., 2020; Kumar et al., 2020). These differences are mostly related to $PM_{2.5}$-bound PAHs concentrations (87-608 ng/m^3) that were at least 80 times higher than the ones at our study (2.56 ng/m^3 at ZK and 0.95 ng/m^3 at FA).

For the PAHs in the gas phase, the values for the CR as well as the cumulative cancer risk were reported lower than the acceptable limit indicating that there was no cancer risk from these compounds in the gas phase **(Table IV-4, Table IV-5).**

The lifetime cancer risk values for the exposure to PAHs in both phases were 1.4 x 10^{-5} at ZK and 3.7 x 10^{-6} and FA, exceeding the threshold limit of 10^{-6}. PAHs can be metabolized and can react as electrophilic intermediates capable of forming PAH-DNA adduct, considered as biomarker of DNA damage and that has been linked to cancer (Veglia et al., 2003). Rengarajan et al. (2015) reported that the long-term exposure to mixtures of PAHs can increase the risks of mainly lung and skin, but also bladder and gastrointestinal cancers. The observed concentrations of these species at both sites were mainly attributed to combustion processes such as vehicular emissions, biomass burning, and power plants (Fadel et al., 2021).These results show that exposure to these PAHs emitted from various anthropogenic activities in both gas and particulate phases could be responsible for 14 and 4 additional cancer cases per million habitats at ZK and FA, respectively. Reducing PAHs concentrations, especially from these combustion sources can largely reduce the CCR attributed to PAHs exposure for the inhabitants.

2.2.2 Phthalates

Phthalates (PAEs) are considered as human-made group of chemicals used to increase flexibility in plastics making them harder to break. These species are considered toxic to

humans and animals and were identified as endocrine disruptors and contributing to reproductive toxicity (Tsatsakis et al., 2019; Ma et al., 2020). Hauser et al. (2006) found an association between exposure to phthalates and DNA damage in sperm. Among these compounds, BEHP was classified by the IARC as possibly carcinogenic to humans (group 2B) due to sufficient evidence for carcinogenicity in the liver of animals but little evidence of possible association between BEHP and liver cancer in humans (Rusyn and Corton, 2012). On the other hand, butyl benzyl phthalate (BBP) was classified as non-carcinogenic (group 3), and other phthalate esters such as DBP were not assessed (IARC, 2004). As for the non-carcinogenic effects, asthma and allergies were reported to be linked to exposure to BEHP and BBP, respectively (Jaakkola and Knight, 2008). In this study, the cancer risk of BEHP and the non-cancer risk of DBP and BEHP were studied.

The total HI values, corresponding here to the HI value for ingestion as no RfC_i or RfD_i were found for these phthalates for inhalation or dermal contact, ranged between 10^{-2} and 10^{-3} for the different age categories at both sites resulting in a negligible non-cancer risk (<1).

As for the cancer risk, the only contributor was BEHP. CR values were higher for the ingestion pathway compared to inhalation: 6 times higher for an adult and 18 times higher for a newborn. Conversely, CR for inhalation, ingestion, and cumulative CR (inhalation + ingestion; no value for dermal) presented low cancer risk with values below 10^{-6}. The CR values for inhalation at both sites (3.9×10^{-9} at ZK and 5.2×10^{-9} at FA) **(Table IV-4, Table IV-5)** were in the interval of estimated carcinogenic risk reported by Li et al. (2019) for a regional background site (8.9×10^{-10} - 7.4×10^{-9}). The cumulative CR values for BEHP found in this study were higher than the ones reported by Ma et al. (2020) for a Chinese city (in the range of 10^{-10}). Although the concentration of BEHP (54.8 ng/m^3) in the latter study was close to those reported in ZK and FA, the exposure parameters were different especially for body weight that was reported as 15 kg for a child and 58.6 kg for an adult along with the inhalation rate (7.8 m^3/day for a child and 12.8 m^3/day for an adult). The lifetime cancer risk from exposure to BEHP was 3.8×10^{-7} for ZK and 5.1×10^{-7} for FA.

Phthalates are generally released into the atmosphere during open burning of plastics (Simoneit et al., 2005). Based on the total HI and the cumulative CR values, the risk associated with human exposure to $PM_{2.5}$-bound phthalates were relatively low. However, these compounds should be monitored by reducing open burning of plastics because the exposure to these species even at doses lower than the RfD might be linked to adverse health problems (Chen et al., 2017).

2.2.3 Dioxins, furans and dioxin-like polychlorobiphenyls

PCDD/Fs and DL-PCBs are semi volatile persistent organic pollutants that have attracted research attention due to their potential health impact especially their mutagenic, teratogenic, and carcinogenic effects (Koukoulakis et al., 2020). The exposure to PCDD/Fs might elicit reproductive effects, damage to the immune system, disruption of endocrine, and might also cause cancer (Marquès and Domingo, 2019).

TEQ values were calculated for every class of compounds along with total TEQ (**Table IV-3).** Although contributions in terms of concentrations differ between the two sites, PCDFs were the largest contributors to the total TEQ accounting for 81% (ZK) and 87% (FA) of the total TEQ values. 2,3,4,7,8-PeCDF contributed mostly to total TEQ with a percentage of 23.7% at ZK and 38.9% at FA. These findings were similar to those done in other industrial sites (Chang et al., 2003). DL-PCBs in ZK only contribute to 0.3% of total TEQ while in FA, they contribute to 6.5%. The main difference between the two sites was PCB 169 that was not detected in ZK and highly contributes to the PCB-TEQ at FA.

The total HI value calculated using the total TEQ shows that the non-cancer risk due to exposure to PCDD/Fs and DL-PCBs is negligible at both sites **(Fig. IV-2).** As for the cancer risk, both $CR_{inhalation}$ and $CR_{ingestion}$ have values below 10^{-6} with a higher $CR_{ingestion}$ for adults (7-fold higher) and newborns (100-fold higher).

PCDD/Fs were generally emitted from the incineration of hospital, municipal, and hazardous waste as well as during the manufacturing of chlorinated pesticides (Zubair and Adress, 2019). As for DL-PCBs, they were produced as industrial chemicals or generated unintentionally during incineration of waste (Hogarh et al., 2018). The lifetime cancer risk was found to be 4.0×10^{-7} for both sites. These values can be decreased by reducing waste incineration. LCR values found in our study were lower than the ones reported near different factories in China such as sintering, aluminum and copper plants (Sun et al., 2017; Yang et al., 2017). This might be mainly due to reported values for both particulate and gas phase in the above-mentioned studies and reported equivalent TEQ that were at least 10 times higher compared to our study.

2.2.4 Major and trace elements

The populations living around the study sites are considered the main receptors of airborne elements. It is worth noting that the toxicity of Cr was mainly reported to the hexavalent state Cr(VI). Therefore, the Cr atmospheric concentration was scaled by a factor of 1/7, given the

assumed Cr(VI)/Cr(III) concentration ratio of 1 to 6 (USEPA, 2004a). It was also assumed that the measured arsenic is totally inorganic (Huang et al., 2014). The HQ_i values for all the identified elements (As, Cd, Co, Cr, Cu, Mn, Ni, Pb, Zn, Ba, Al, V, Fe, Sr, Sn, Sb, La and Tl) were calculated for the different exposure pathways and age categories (**Appendix D - Table S5** and **Table S6)**.

As and Zn exhibit higher HQ_i values for dermal contact and ingestion while for Sb, the main health risk is due to ingestion. For this latter route, As, Zn and Sb were more likely to have potential hazard for newborns and children **(Appendix D -Table S6):** these elements can be accumulated in soil and dust and transferred to children through ingestion (Xue et al., 2007). The total HQ_i value for these elements were far less than 1 for the different age categories at both sites; the potential carcinogenic risks were negligible and considered not harmful (**Appendix D - Table S7** and **Table S8**).

Fe, Sr, Sn, La and Tl were only considered via the ingestion pathway and exhibited HQ_i lower than the safe limit value of 1. For Ni, the health risk was mainly explained by dermal contact and inhalation. For the other elements, i.e., Cd, Co, Cr(VI), Cu, Mn, Pb, Ba, Al and V, the main risk was associated with the inhalation route at both sites.

Considering the three routes, i.e., total HQ_i values, the non-carcinogenic risk, from the highest to the lower value, was observed for Mn (highest risk), then Pb, Ni, Co, and V (lowest risk) ; for FA site, the order was as follows: Pb, then Mn, Ni, Co, and V. Even for these elements, Total HQ_i values were less than 1 for the different age categories implying that these elements do not seem to pose any non-carcinogenic health risk.

Mn and Pb contributed to more than 50% of the total HI. This is mainly due to their relatively high concentrations in air. When comparing the three exposure pathways, inhalation contributed the most to the non-cancer risk for the different age categories (77-93%).

However, when considering the total HI for elements, the value is close to 1 for children at ZK and FA and exceeding 1 for newborns while lower values were reported for adolescents and adults **(Fig. IV-2).** This could possibly be explained by the higher rate of exposure and the lower body weight of children and newborns compared to adolescents and adults. The total HI for elements in this study was higher than those presented by Murari et al. (2020) for an urban city in India (10^{-4}- 10^{-3}). The differences are mainly due to the choice made for exposure parameters and the variations in the concentrations of the elements specifically Pb, Mn and Co.

The cancer risk for the different exposure pathways was calculated for As, Cd, Co, Cr(VI), Ni, Pb and V. As shown in **Appendix D - Table S5** and **Table S6**, no values exceeded the average risk acceptance of 10^{-6}/year for dermal contact and ingestion pathways at both sites. However, for the inhalation route, adults were subjected to more carcinogenic risk from As, Co, Cr(VI), Ni and V at ZK since their CR values were 1.2 x 10^{-6}, 1.9 x 10^{-6}, 1.7 x 10^{-6}, 1.5 x 10^{-6} and 5.2 x10^{-5} respectively, exceeding the safe limit of 10^{-6}. Additionally, vanadium showed high cancer risk values of 8.1 x 10^{-6} and 5.9 x 10^{-6} for children and adolescents, respectively. While at FA, values exceeded the limit for As, Cr(VI) and V for adults and also V for children and adolescents. The cancer risks through the inhalation pathway for the elements were either in the same range or higher than the ones reported for a Romanian site (6.5 - 7.2 x 10^{-6}), an urban site in China (7.1 x 10^{-6}), and an urban site in Colombia (3.1 x 10^{-6}) (Liu et al., 2018; Galon-Negru et al., 2019; Ramírez et al., 2020).

The cumulative cancer risk for the three exposure pathways was assessed **(Tables S7 and S8)** and the problematic species were, from highest to lower values, V > Cr(VI) > As > Co > Ni > Pb > Cd for FA and V > As > Cr(VI) > Co > Ni > Pb > Cd for ZK. Hence, V, As, and Cr(VI) were the major carcinogenic toxic elements among these elements. Specifically, V was the top contributor to the cumulative CR with a contribution varying between 40 - 90% according to the different age categories and the sites.

The cancer risk associated to V was higher than 10^{-6} at ZK and FA for all age categories, excepted newborn. The cancer risk values associated with adults were the highest between the different age categories (5.2 x 10^{-5} at ZK and 2.6 x 10^{-5} at FA).
V, along with Ni, were generally considered as important tracers of HFO combustion, Cr and Co were mainly associated with industrial emissions and As was emitted from coal combustion (Becagli et al., 2012; Chen et al., 2021). The exposure to high concentrations of V, Cr(VI), and As can lead to an increased risk of lung cancer according to epidemiological studies (Rondini et al., 2010; Hubaux et al., 2013; Deng et al., 2019).

When considering the cumulative cancer risk for the elements as a whole, it exceeded the average risk acceptance of 10^{-6} per year for all age categories at ZK and the risk is higher for adults, followed by children, adolescents and finally newborns **(Fig. IV-2).** At FA, cumulative CR exceeded the limit of 10^{-6} for all age categories except newborns and the risk occurs on the same order as ZK. This shows that adults were subjected to more carcinogenic risks than the other age categories at both sites.

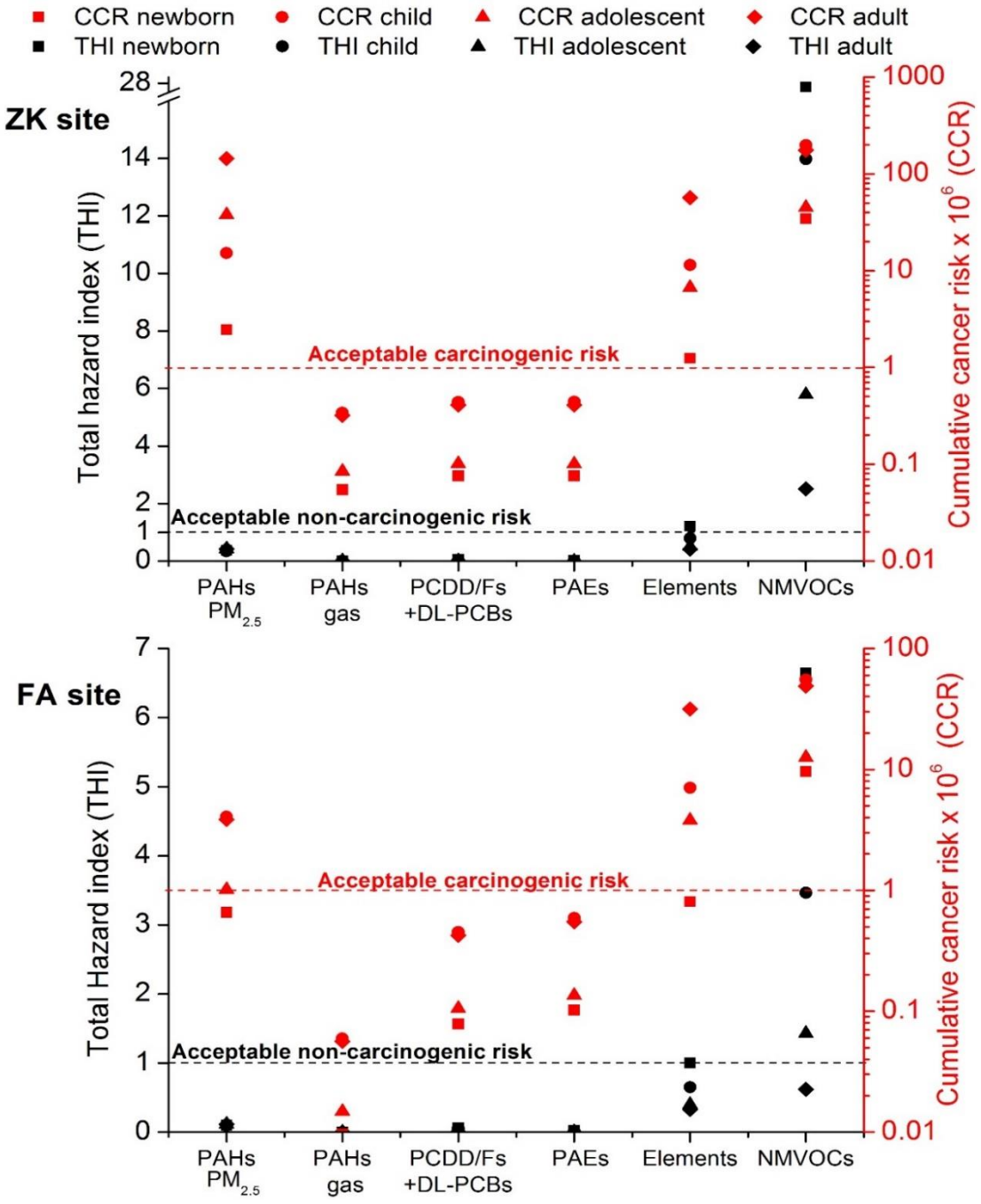

Fig. IV-2: Cumulative Cancer Risk (CCR) and Total hazard index (THI) values for polycyclic aromatic hydrocarbons (PAHs) in gas and particulate phase, total PCDD/Fs and DL-PCBs, phthalates (PAEs), elements, and non-methane volatile organic compounds (NMVOCs) for the different age categories (newborns, children, adolescents, and adults) at Zouk (ZK) and Fiaa (FA) (HI values and Cumulative CR below 1 means acceptable risk).

Table IV-4: Hazard Index (HI) and cancer risk values (CR) for dermal, ingestion and inhalation pathways for the different age categories and family of compounds at Zouk site

Age category	Class of compounds	Hazard Index (HI)			Cancer risk (CR)		
		Dermal	Ingestion	Inhalation	Dermal	Ingestion	Inhalation
Newborns	PAHs – $PM_{2.5}$	-	6.4×10^{-2}	3.1×10^{-1}	3.8×10^{-7}	2.0×10^{-6}	9.4×10^{-8}
	PAHs – gas	-	1.4×10^{-3}	6.9×10^{-3}	8.5×10^{-9}	4.4×10^{-8}	2.1×10^{-9}
	PCDD/Fs + DL-PCBs	-	5.8×10^{-2}	3.3×10^{-5}	-	7.5×10^{-8}	7.1×10^{-10}
	PAEs	-	1.8×10^{-2}	-	-	7.2×10^{-8}	3.9×10^{-9}
	Elements	5.7×10^{-2}	2.2×10^{-1}	9.3×10^{-1}	3.6×10^{-8}	1.1×10^{-7}	1.1×10^{-6}
	NMVOCs	-	2.7×10^{1}	7.2×10^{-2}	-	3.4×10^{-5}	1.6×10^{-7}
Children	PAHs – $PM_{2.5}$	-	3.3×10^{-2}	3.1×10^{-1}	3.2×10^{-6}	1.1×10^{-5}	6.7×10^{-7}
	PAHs – gas	-	7.3×10^{-4}	6.9×10^{-3}	7.2×10^{-8}	2.5×10^{-7}	1.5×10^{-8}
	PCDD/Fs + DL-PCBs	-	3.0×10^{-2}	3.3×10^{-5}	-	4.3×10^{-7}	7.9×10^{-9}
	PAEs	-	9.5×10^{-3}	-	-	4.1×10^{-7}	2.8×10^{-8}
	Elements	4.4×10^{-2}	1.1×10^{-1}	6.3×10^{-1}	3.0×10^{-7}	6.3×10^{-7}	1.1×10^{-5}
	NMVOCs	-	1.4×10^{1}	7.2×10^{-2}	-	2.0×10^{-4}	1.8×10^{-6}
Adolescents	PAHs – $PM_{2.5}$	-	1.4×10^{-2}	4.1×10^{-1}	1.1×10^{-6}	2.5×10^{-6}	2.1×10^{-7}
	PAHs – gas	-	3.0×10^{-4}	9.2×10^{-3}	2.3×10^{-8}	5.6×10^{-8}	4.6×10^{-9}
	PCDD/Fs + DL-PCBs	-	1.2×10^{-2}	4.4×10^{-5}	-	9.6×10^{-8}	5.7×10^{-9}
	PAEs	-	3.9×10^{-3}	-	-	9.2×10^{-8}	8.6×10^{-9}
	Elements	2.6×10^{-2}	4.7×10^{-2}	4.4×10^{-1}	9.9×10^{-8}	1.4×10^{-7}	6.5×10^{-6}
	NMVOCs	-	5.7×10^{0}	9.6×10^{-2}	-	4.4×10^{-5}	1.3×10^{-6}
Adults	PAHs – $PM_{2.5}$	-	5.7×10^{-3}	4.1×10^{-1}	3.4×10^{-6}	9.5×10^{-6}	1.6×10^{-6}
	PAHs – gas	-	1.3×10^{-4}	9.2×10^{-3}	2.3×10^{-8}	2.1×10^{-7}	3.5×10^{-8}
	PCDD/Fs + DL-PCBs	-	5.2×10^{-3}	4.4×10^{-5}	-	3.6×10^{-7}	5.1×10^{-8}
	PAEs	-	1.7×10^{-3}	-	-	3.5×10^{-7}	6.5×10^{-8}
	Elements	9.5×10^{-3}	2.0×10^{-2}	3.9×10^{-1}	3.2×10^{-7}	5.2×10^{-7}	5.6×10^{-5}
	NMVOCs	-	2.4×10^{0}	9.6×10^{-2}	-	1.6×10^{-4}	1.1×10^{-5}

The cumulative cancer risk ($1.3 \times 10^{-6} – 5.9 \times 10^{-5}$ for ZK and 8.0×10^{-7} 3.0×10^{-5} for FA) was mostly found higher than the values presented for a dusty site in Nigeria for children and adults (Sulaymon et al., 2020). These differences were observed due to the higher concentrations of V (highest contributor to cumulative CR) recorded at ZK (25 ng/m^3) and FA (13 ng/m^3) compared to the Nigerian site (5-8 ng/m^3). The lifetime cancer risk for 70 years of exposure exceeded the safe limit of 10^{-6}. Per million habitats, 44 and 25 additional cases of cancer were found based on the LCR calculations at ZK and FA, respectively. In order to decrease these numbers, the concentrations of the major contributor to the CCR, namely Vanadium, should be reduced. This can be done by replacing the energy production based on the combustion of heavy fuel oil used by cleaner energy.

Table IV-5: Hazard Index (HI) and cancer risk values (CR) for dermal, ingestion, and inhalation pathways for the different age categories and family of compounds at Fiaa site

Age category	Class of compounds	Hazard index (HI)			Cancer risk (CR)		
		Dermal	Ingestion	Inhalation	Dermal	Ingestion	Inhalation
Newborns	PAHs – $PM_{2.5}$	-	1.7×10^{-2}	8.3×10^{-2}	1.0×10^{-7}	5.3×10^{-7}	2.5×10^{-8}
	PAHs – gas	-	2.5×10^{-4}	1.2×10^{-3}	1.5×10^{-9}	7.7×10^{-9}	3.7×10^{-10}
	PCDD/Fs + DL-PCBs	-	6.0×10^{-2}	3.4×10^{-5}	-	7.8×10^{-8}	7.4×10^{-10}
	PAEs	-	2.4×10^{-2}	-	-	9.7×10^{-8}	5.2×10^{-9}
	Elements	4.0×10^{-2}	1.7×10^{-1}	7.9×10^{-1}	3.6×10^{-8}	1.1×10^{-7}	6.6×10^{-7}
	NMVOCs	-	6.6×10^{0}	1.6×10^{-2}	-	9.5×10^{-6}	4.7×10^{-8}
Children	PAHs – $PM_{2.5}$	-	8.8×10^{-3}	8.3×10^{-2}	8.6×10^{-7}	3.0×10^{-6}	1.8×10^{-7}
	PAHs – gas	-	1.3×10^{-4}	1.2×10^{-3}	1.3×10^{-8}	4.4×10^{-8}	2.6×10^{-9}
	PCDD/Fs + DL-PCBs	-	3.1×10^{-2}	2.0×10^{-5}	-	4.4×10^{-7}	8.1×10^{-9}
	PAEs	-	1.3×10^{-2}	-	-	5.5×10^{-7}	3.7×10^{-8}
	Elements	3.1×10^{-2}	8.9×10^{-2}	5.3×10^{-1}	3.1×10^{-7}	6.2×10^{-7}	6.1×10^{-6}
	NMVOCs	-	3.4×10^{0}	1.6×10^{-2}	-	5.5×10^{-5}	5.1×10^{-7}
Adolescents	PAHs – $PM_{2.5}$	-	3.6×10^{-3}	1.1×10^{-1}	2.8×10^{-7}	6.8×10^{-7}	5.6×10^{-8}
	PAHs – gas	-	5.3×10^{-5}	1.6×10^{-3}	4.1×10^{-9}	9.9×10^{-9}	8.1×10^{-10}
	PCDD/Fs + DL-PCBs	-	1.3×10^{-2}	4.5×10^{-5}	-	9.9×10^{-8}	5.9×10^{-9}
	PAEs	-	5.2×10^{-3}	-	-	1.2×10^{-7}	1.2×10^{-8}
	Elements	1.8×10^{-2}	3.7×10^{-2}	3.5×10^{-1}	1.0×10^{-7}	1.4×10^{-7}	3.6×10^{-6}
	NMVOCs	-	1.4×10^{0}	2.2×10^{-2}	-	1.2×10^{-5}	3.7×10^{-7}
Adults	PAHs – $PM_{2.5}$	-	1.5×10^{-3}	1.1×10^{-1}	9.0×10^{-7}	2.5×10^{-6}	4.2×10^{-7}
	PAHs – gas	-	2.2×10^{-5}	1.6×10^{-3}	1.3×10^{-8}	3.7×10^{-8}	6.1×10^{-9}
	PCDD/Fs + DL-PCBs	-	5.4×10^{-3}	4.5×10^{-5}	-	3.7×10^{-7}	5.2×10^{-8}
	PAEs	-	2.2×10^{-3}	-	-	4.6×10^{-7}	8.6×10^{-8}
	Elements	6.6×10^{-3}	1.5×10^{-2}	3.1×10^{-1}	3.2×10^{-7}	5.2×10^{-7}	3.1×10^{-5}
	NMVOCs	-	6.0×10^{-1}	2.2×10^{-2}	-	4.6×10^{-5}	3.3×10^{-6}

2.2.5 Non-methane Volatile organic compounds (NMVOCs)

The non-carcinogenic risk related with exposure to the eleven NMVOCs was investigated. Detailed results are shown in **Appendix D - Table S5** and **Table S6**. The species were studied for inhalation and oral ingestion pathways since no RfD_i or CSF_i were found for dermal contact. The ingestion pathway appears as the major exposure route for the different species, contributing to more than 80% of the total HI values at both sites. Heptane and cyclohexane show respectively the highest and the lowest non-carcinogenic risk.

A close examination considering the three routes together, revealed that benzene is the second contributor to total HI. Benzene and heptane explain at least 78 to 94% of the total HI values for NMVOCs at both sites. The total HQ_i value for benzene and n-heptane exceeded the threshold limit of 1 for non-carcinogenic risk for all age categories at ZK and for newborns and

children at FA **(Appendix D - Table S7, Table S8).** Additionally, toluene gave total HQ_i value exceeding the limit at ZK for newborns (1.56). Other species such as tetrachloroethene, ethylbenzene and xylenes recorded total HQ_i values under the threshold limit meaning that these compounds could be associated with acceptable non-carcinogenic effects. The total HI for the NMVOCs class of compounds showed values higher than 1 for all the age categories at ZK and for newborns, children, and adolescents at FA. It ranged between 26.8 (newborns) and 2.9 (adults) at ZK, and between 6.6 (newborns) and 0.8 (adults) at FA **(Fig. IV-2).**

Up to our knowledge, most of the studies focused mainly on BTEX and there have been no studies reporting hazard index values for both ingestion and inhalation pathways despite the higher contribution of the ingestion compared to the inhalation pathway as shown in this study. Considering NMVOCs measured as a whole, the HI values presented in this study for the inhalation pathway ($2 \times 10^{-2} – 8 \times 10^{-2}$) were similar to the ones reported in Tehran, a Middle Eastern city (in the order of 10^{-2} - 10^{-3}) with a population of approximately 9 million (Miri et al., 2016).

5 NMVOCs (1,3-butadiene, n-hexane, tetrachloroethene, benzene and ethylbenzene) were considered for evaluating the cancer risk through two exposure pathways: inhalation and oral ingestion **(values in Appendix D - Table S5, Table S6)**. Among these compounds, 1,3-butadiene and benzene were classified as carcinogenic to humans according to the IARC causing leukemia. While tetrachloroethene was also classified by IARC as potential human carcinogen based on limited evidence and might cause bladder cancer. The carcinogenic risk values from the ingestion pathway were at least ten times higher than the inhalation route. Additionally, benzene was associated with the highest total CR_i with values in the order of 10^{-5} - 10^{-4} at ZK and 10^{-6} - 10^{-5} at FA. These cancer risk values exceeded the acceptable USEPA threshold limit for both sites and for the different age categories. Furthermore, 1,3-butadiene and ethylbenzene also exhibited values higher than 10^{-6} at ZK site with total CR_i values for the different age categories in the following order: child (2.8×10^{-5} for 1,3-butadiene and 2.6×10^{-5} for ethylbenzene)> adult (2.4×10^{-5} for 1,3-butadiene and 2.4×10^{-5} for ethylbenzene)> adolescent (6.3×10^{-6} for 1,3-butadiene and 6.0×10^{-6} for ethylbenzene)> newborn (4.9×10^{-6} for 1,3-butadiene and 4.5×10^{-6} for ethylbenzene). Ethylbenzene gave values higher than the threshold limit at FA for children and adults only (~4×10^{-6}). The lifetime cancer risk values at ZK for benzene (1.2×10^{-4}), 1,3-butadiene (2.3×10^{-5}) and ethylbenzene(2.2×10^{-5}) reported in this study were higher than the values reported for a suburban site in Lebanon during winter (1.3×10^{-5}, 1.2×10^{-5}, 6×10^{-6}, for the same compounds respectively) and summer (1.6×10^{-5},

8×10^{-6}, 3×10^{-6})(Dhaini et al., 2017). However, n-hexane and tetrachloroethene showed values lower than the acceptable threshold implying a moderate cancer risk for these species. The cumulative cancer risk for all NMVOCs measured exceeded the permissible risk level at both sites and for the different age categories and varied from 3.5×10^{-5} for newborns to 1.8×10^{-4} for adults and from 1×10^{-5} for newborns to 6×10^{-5} for children at ZK and FA, respectively. The lifetime cancer risk was 170 (1.7×10^{-4}) and 46 (4.6×10^{-5}) times higher than the USEPA limit at ZK and FA, respectively. This is mainly due to high concentrations of benzene and ethylbenzene at both sites, and additionally 1,3-butadiene at ZK. Benzene and 1,3-butadiene were known to be mainly generated from combustion sources leading to the assumption that fuel combustion emissions were considered as significant contributors to the cumulative cancer risk calculated for NMVOCs (Salameh et al., 2015; 2016). At least 70% of the additional cancer cases (120 at ZK and 42 at FA per million habitats based on LCR calculations) were caused by the exposure to high concentrations of benzene at both sites, might be highly emitted from traffic gasoline combustion. These numbers can be reduced by implementing strict vehicle emission control measures.

2.3 Health risk comparison between the classes of compounds and limitations of the study

As observed in **Fig. IV-2,** total HI values related to the non-cancer risk were significantly higher than the acceptable limit of 1 for NMVOCs for the different age categories at both sites (except for adults at FA), and for elements for newborns. These compounds might pose non-carcinogenic health problems to humans like neurological effects, liver and kidney toxicities, lymphocyte count decrease, etc. (Dhaini et al., 2017). The major compounds contributing to the non-carcinogenic risk were mainly n-heptane, benzene, and toluene for NMVOCs. While in the particulate phase, $B[a]P_{eq}$, Mn, Pb, V and Ni were the major contributors despite their values of total HQ_i less than 1. Conversely, PAHs in both phases, dioxins, furans, dioxin-like polychlorobiphenyls, and phthalates have an acceptable non-cancer risk since their total HI values were lower than the USEPA limit. When comparing the different families of compounds, NMVOCs exhibited the highest values of total HI for the different age categories, followed by elements, $PM_{2.5}$-bound PAHs, gas-phase PAHs, phthalates, and finally PCDD/Fs and DL-PCBs **(Fig. IV-2).**

For the cancer risk assessment, cumulative CR values for PAHs in the particulate phase, elements and NMVOCs exhibited values higher than the threshold limit of 10^{-6} proposed by the USEPA. The major contributors to cancer risk were benzene, ethylbenzene, and 1,3-butadiene

(at ZK site) in the gas phase, while PAHs, Ni, Cr(VI), Co, and As were the main components in the particulate phase. Additionally, a similar order to the total hazard index was observed for the cumulative cancer risk of the different families of compounds except for $PM_{2.5}$-bound PAHs that showed CCR values higher than elements **(Fig. IV-2).**

Species that have CCR values higher than the threshold limit were mainly associated to combustion sources such as vehicular emissions, biomass burning, and HFO combustion leading to additional cancer cases for the different families of species. This emphasizes on the relevance of reducing the concentrations of the species by adopting an effective air quality management plan, implementing a national transportation system in urban areas to reduce traffic emissions (Abdallah et al., 2018) and shifting to cleaner energy instead of traditional biomass and fuel combustion. This study used a comprehensive and well-defined calculation method for the carcinogenic and non-carcinogenic risk assessment due to exposure to different classes of compounds considered individually. However, the cancer and non-cancer risks for the classes of compounds were not summed since there were no available methods for the calculation of health risk hazards due to exposure to total air contaminants. These were considered as limitations of the health assessment studies which assume an independence between toxic actions within and across compounds. Actually, the interactions between the different contaminants on health, defined as cocktail effect reflecting synergism or antagonism action is not well defined as it still remains unsolved. Additionally, uncertainties accompany risk assessment studies especially in the choice of exposure parameters and reference values.

3 Conclusions

This study provided for the first time an extensive health risk assessment considering different classes of compounds such as phthalates, dioxins, furans, dioxin-like polychlorobiphenyls, and elements in $PM_{2.5}$, NMVOCs, and PAHs in both particulate and gas phases, according to age categories and different exposure pathways.

The non-carcinogenic risk estimated for the different components showed a risk from benzene and n-heptane exposure. Additionally, this was also observed for the sum of elements where Mn, Pb, V and Ni were the major contributors to the total hazard index. PAHs in both particulate and gas phases, phthalates, PCDD/Fs, and DL-PCBs exhibited lower values and present acceptable non-carcinogenic health risks. As for the carcinogenic risk, CR for different species such as benzene, 1,3-butadiene (at Zouk site), ethylbenzene, $PM_{2.5}$-B[a]P_{eq}, As, Co, Cr(VI), Ni, and V showed values higher than the threshold limit of 10^{-6} meaning that these compounds

present a carcinogenic risk to different age categories. These compounds were mainly associated to different combustion sources such as vehicular emissions, biomass burning and HFO combustion. The results from this study are of major importance to assess the impact of the different contaminants on the human health. Additionally, health risk assessment results should be combined to source apportionment studies in order to better relate health impact of the different sources of pollutants released in the atmosphere.

Acknowledgments:

The authors would like to acknowledge the National Council for Scientific Research of Lebanon (CNRS-L) and University of Littoral Côte d'Opale (ULCO) for granting a doctoral fellowship to Marc Fadel. This project was also funded by the Research Council and the Faculty of Sciences of Saint Joseph University of Beirut – Lebanon. The "Unité de Chimie Environnementale et Interactions sur le Vivant" (UCEIV-UR4492) participates in the CLIMIBIO project, which is financially supported by the Hauts-de-France Region Council, the French Ministry of Higher Education and Research, and the European Regional Development Funds. This publication has been also produced within the framework of the EMME-CARE project, which has received funding from the European Union's Horizon 2020 Research and Innovation Programme (under grant agreement no. 856612) and the Cyprus Government.

The authors thank MicroPolluants Technologie S.A. (Saint Julien Les Metz, France) for dioxins, furans, and DL-PCBs analysis and Institut Chevreul - Université de Lille for the analysis of elements by ICP-MS. The authors would also like to thank Adib Kfoury for his help in the field campaign, Dorothée Dewaele (Centre Commun de Mesures, ULCO) for her contribution in the ICP-AES analysis, and Mariana Farhat for her help in the organic species analysis.

References:

Abbas, I., Badran, G., Verdin, A., Ledoux, F., Roumié, M., Courcot, D., Garçon, G., 2018. Polycyclic aromatic hydrocarbon derivatives in airborne particulate matter: sources, analysis and toxicity. Environ. Chem. Lett. 16, 439-475, https://doi.org/10.1007/s10311-017-0697-0.

Abbas, I., Badran, G., Verdin, A., Ledoux, F., Roumie, M., Lo Guidice, J.-M., Courcot, D., Garçon, G., 2019. In vitro evaluation of organic extractable matter from ambient $PM_{2.5}$ using human bronchial epithelial BEAS-2B cells: Cytotoxicity, oxidative stress, pro-

inflammatory response, genotoxicity, and cell cycle deregulation. Environ. Res. 171, 510-522, https://doi.org/10.1016/j.envres.2019.01.052.

Abdallah, C., Afif, C., Masri, N., Öztürk, F., Dağkuş Keleş, M., Sartelet, K., 2018. A first annual assessment of air quality modeling over Lebanon using WRF/Polyphemus. Atmos. Pollut. Res. 9, https://doi.org/10.1016/j.apr.2018.01.003.

Akyüz, M., Çabuk, H., 2010. Gas–particle partitioning and seasonal variation of polycyclic aromatic hydrocarbons in the atmosphere of Zonguldak, Turkey. Sci. Total Environ. 408, 5550-5558, https://doi.org/10.1016/j.scitotenv.2010.07.063.

Alkoussa, S., Hulo, S., Courcot, D., Billet, S., Martin, P., 2020. Extracellular vesicles as actors in the air pollution related cardiopulmonary diseases. Crit. Rev. Toxicol. 50., https://doi.org/10.1080/10408444.2020.1763252.

Aoun, J., Saleh, N., Waked, M., Salamé, J., Salameh, P., 2013. Lung cancer correlates in Lebanese adults: a pilot case-control study. J Epidemiol Glob Health 3, 235-244, https://doi.org/10.1016/j.jegh.2013.06.005.

Badran, G., Ledoux, F., Verdin, A., Abbas, I., Roumie, M., Genevray, P., Landkocz, Y., Lo Guidice, J.-M., Garçon, G., Courcot, D., 2020. Toxicity of fine and quasi-ultrafine particles: Focus on the effects of organic extractable and non-extractable matter fractions. Chemosphere 243, 125440, https://doi.org/10.1016/j.chemosphere.2019.125440.

Bai, L., Chen, W., He, Z., Sun, S., Qin, J., 2020. Pollution characteristics, sources and health risk assessment of polycyclic aromatic hydrocarbons in $PM_{2.5}$ in an office building in northern areas, China. Sustainable Cities Soc. 53, 101891, https://doi.org/10.1016/j.scs.2019.101891.

Bandowe, B.A.M., Meusel, H., 2017. Nitrated polycyclic aromatic hydrocarbons (nitro-PAHs) in the environment – A review. Sci. Total Environ. 581-582, 237-257, https://doi.org/10.1016/j.scitotenv.2016.12.115.

Becagli, S., Sferlazzo, D.M., Pace, G., di Sarra, A., Bommarito, C., Calzolai, G., Ghedini, C., Lucarelli, F., Meloni, D., Monteleone, F., Severi, M., Traversi, R., Udisti, R., 2012. Evidence for heavy fuel oil combustion aerosols from chemical analyses at the island of Lampedusa: a possible large role of ships emissions in the Mediterranean. Atmos. Chem. Phys. 12, 3479-3492, https://doi.org/10.5194/acp-12-3479-2012.

Borgie, M., Dagher, Z., Ledoux, F., Verdin, A., Cazier, F., Martin, P., Hachimi, A., Shirali, P., Greige-Gerges, H., Courcot, D., 2015. Comparison between ultrafine and fine particulate matter collected in Lebanon: Chemical characterization, in vitro cytotoxic effects and metabolizing enzymes gene expression in human bronchial epithelial cells. Environ. Pollut. 205, 250-260, https://doi.org/10.1016/j.envpol.2015.05.027.

Borm, P.J.A., Kelly, F., Künzli, N., Schins, R.P.F., Donaldson, K., 2007. Oxidant generation by particulate matter: from biologically effective dose to a promising, novel metric. Occup. Environ. Med. 64, 73-74, http://dx.doi.org/10.1136/oem.2006.029090.

Chang, M.B., Weng, Y.M., Lee, T.Y., Chen, Y.W., Chang, S.H., Chi, K.H., 2003. Sampling and analysis of ambient dioxins in northern Taiwan. Chemosphere 51, 1103-1110, https://doi.org/10.1016/S0045-6535(02)00711-7.

Chen, L.C., Lippmann, M., 2009. Effects of metals within ambient air particulate matter (PM) on human health. Inhalation Toxicol. 21, 1-31, https://doi.org/10.1080/08958370802105405.

Chen, P., Bi, X., Zhang, J., Wu, J., Feng, Y., 2015. Assessment of heavy metal pollution characteristics and human health risk of exposure to ambient $PM_{2.5}$ in Tianjin, China. Particuology 20, 104-109, https://doi.org/10.1016/j.partic.2014.04.020.

Chen, Q., Yang, H., Zhou, N., Sun, L., Bao, H., Tan, L., Chen, H., Ling, X., Zhang, G., Huang, L., Li, L., Ma, M., Yang, H., Wang, X., Zou, P., Peng, K., Liu, T., Shi, X., Feng, D., Zhou, Z., Ao, L., Cui, Z., Cao, J., 2017. Phthalate exposure, even below US EPA reference doses, was associated with semen quality and reproductive hormones: Prospective MARHCS study in general population. Environ. Int. 104, 58-68, https://doi.org/10.1016/j.envint.2017.04.005.

Chen, R., Jia, B., Tian, Y., Feng, Y., 2021. Source-specific health risk assessment of PM2.5-bound heavy metals based on high time-resolved measurement in a Chinese megacity: insights into seasonal and diurnal variations. Ecotoxicol. Environ. Saf. 216, 112167, https://doi.org/10.1016/j.ecoenv.2021.112167.

Cochard, M., Ledoux, F., Landkocz, Y., 2020. Atmospheric fine particulate matter and epithelial mesenchymal transition in pulmonary cells: state of the art and critical review of the in vitro studies. Journal of Toxicology and Environmental Health, Part B, Critical reviews 23, 293-318, https://doi.org/10.1080/10937404.2020.1816238.

Dahmardeh Behrooz, R., Kaskaoutis, D.G., Grivas, G., Mihalopoulos, N., 2021. Human health risk assessment for toxic elements in the extreme ambient dust conditions observed in Sistan, Iran. Chemosphere 262, 127835, https://doi.org/10.1016/j.chemosphere.2020.127835.

Deng, Y., Wang, M., Tian, T., Lin, S., Xu, P., Zhou, L., Dai, C., Hao, Q., Wu, Y., Zhai, Z., Zhu, Y., Zhuang, G., Dai, Z., 2019. The Effect of hexavalent chromium on the incidence and mortality of human cancers: A meta-analysis based on published epidemiological cohort studies. Front Oncol 9, 24-24, https://doi.org/10.3389/fonc.2019.00024.

Dhaini, H.R., Salameh, T., Waked, A., Sauvage, S., Borbon, A., Formenti, P., Doussin, J.-F., Locoge, N., Afif, C., 2017. Quantitative cancer risk assessment and local mortality burden for ambient air pollution in an eastern Mediterranean City. Environ Sci Pollut Res Int 24, 14151-14162, https://doi.org/10.1007/s11356-017-9000-y.

Díaz, R.V., Rosa Dominguez, E., 2009. Health risk by inhalation of $PM_{2.5}$ in the metropolitan zone of the City of Mexico. Ecotoxicol. Environ. Saf. 72, 866-871, https://doi.org/10.1016/j.ecoenv.2008.09.014.

DoHA, 2012. Environmental health risk assessment : guidelines for assessing human health risks from environmental hazards. Department of Health and Ageing and enHealth Council. https://www1.health.gov.au/internet/main/publishing.nsf/content/A12B57E41EC9F326CA257BF0001F9E7D/$File/Environmental-health-Risk-Assessment.pdf.

Fadel, M., Ledoux, F., Farhat, M., Kfoury, A., Courcot, D., Afif, C., 2021. $PM_{2.5}$ characterization of primary and secondary organic aerosols in two urban-industrial areas in the East Mediterranean. J Environ Sci 101, 98-116, https://doi.org/10.1016/j.jes.2020.07.030.

Fang, B., Zhang, L., Zeng, H., Liu, J., Yang, Z., Wang, H., Wang, Q., Wang, M., 2020. $PM_{2.5}$-bound polycyclic aromatic hydrocarbons: sources and health risk during non-heating and heating periods (Tangshan, China). Int. J. Environ. Res. Public Health 17, https://doi.org/10.3390/ijerph17020483.

Fu, J., Suuberg, E.M., 2011. Solid vapor pressure for five heavy PAHs via the Knudsen effusion method. J. Chem. Thermodyn. 43, 1660-1665, https://doi.org/10.1016/j.jct.2011.05.030.

Gaga, E.O., Ari, A., 2019. Gas-particle partitioning and health risk estimation of polycyclic aromatic hydrocarbons (PAHs) at urban, suburban and tunnel atmospheres: Use of measured EC and OC in model calculations. Atmospheric Pollution Research 10, 1-11, https://doi.org/10.1016/j.apr.2018.05.004.

Galon-Negru, A.G., Olariu, R.I., Arsene, C., 2019. Size-resolved measurements of $PM_{2.5}$ water-soluble elements in Iasi, north-eastern Romania: Seasonality, source apportionment and potential implications for human health. Sci. Total Environ. 695, 133839, https://doi.org/10.1016/j.scitotenv.2019.133839.

Goldfarb, J.L., Suuberg, E.M., 2008. Vapor pressures and enthalpies of sublimation of ten polycyclic aromatic hydrocarbons determined via the Knudsen effusion method. J. Chem. Eng. Data 53, 670-676, https://doi.org/10.1021/je7005133.

Gurkan Ayyildiz, E., Esen, F., 2020. Atmospheric polycyclic aromatic hydrocarbons (PAHs) at two sites, in Bursa, Turkey: Determination of concentrations, gas-particle partitioning, sources, and health risk. Arch. Environ. Contam. Toxicol. Archives of Environmental Contamination and Toxicology 78, 350-366, https://doi.org/10.1007/s00244-019-00698-7.

Hauser, R., Meeker, J.D., Singh, N.P., Silva, M.J., Ryan, L., Duty, S., Calafat, A.M., 2006. DNA damage in human sperm is related to urinary levels of phthalate monoester and oxidative metabolites. Hum. Reprod. 22, 688-695, https://doi.org/10.1093/humrep/del428.

Hogarh, J.N., Seike, N., Kobara, Y., Carboo, D., Fobil, J.N., Masunaga, S., 2018. Source characterization and risk of exposure to atmospheric polychlorinated biphenyls (PCBs) in Ghana. Environ Sci Pollut Res Int 25, 16316-16324, 10.1007/s11356-018-2090-3.

Huang, M., Chen, X., Zhao, Y., Yu Chan, C., Wang, W., Wang, X., Wong, M.H., 2014. Arsenic speciation in total contents and bioaccessible fractions in atmospheric particles related to human intakes. Environ. Pollut. 188, 37-44, https://doi.org/10.1016/j.envpol.2014.01.001.

Hubaux, R., Becker-Santos, D.D., Enfield, K.S.S., Rowbotham, D., Lam, S., Lam, W.L., Martinez, V.D., 2013. Molecular features in arsenic-induced lung tumors. Molecular Cancer 12, 20, https://doi.org/10.1186/1476-4598-12-20.

IARC, 2004. IARC monographs on the evaluation of carcinogenic risks to humans.

Jaakkola, J.J., Knight, T.L., 2008. The role of exposure to phthalates from polyvinyl chloride products in the development of asthma and allergies: a systematic review and meta-analysis. Environ. Health Perspect. 116, 845-853, https://doi.org/10.1289/ehp.10846.

Kfoury, A., Ledoux, F., Roche, C., Delmaire, G., Roussel, G., Courcot, D., 2016. $PM_{2.5}$ source apportionment in a French urban coastal site under steelworks emission influences using

constrained non-negative matrix factorization receptor model. J Environ Sci 40, 114-128, https://doi.org/10.1016/j.jes.2015.10.025.

Kim, Y., Sartelet, K., Seigneur, C., Charron, A., Besombes, J.-L., Jaffrezo, J.-L., Marchand, N., Polo, L., 2016. Effect of measurement protocol on organic aerosol measurements of exhaust emissions from gasoline and diesel vehicles. Atmos Environ 140, 176-187, https://doi.org/10.1016/j.atmosenv.2016.05.045.

Kobrossi, R., Nuwayhid, I., Sibai, A.M., El-Fadel, M., Khogali, M., 2002. Respiratory health effects of industrial air pollution on children in North Lebanon. Int J Environ Health Res 12, 205-220, https://doi.org/10.1080/09603/202/000000970.

Koukoulakis, K.G., Kanellopoulos, P.G., Chrysochou, E., Costopoulou, D., Vassiliadou, I., Leondiadis, L., Bakeas, E., 2020. Atmospheric concentrations and health implications of PAHs, PCBs and PCDD/Fs in the vicinity of a heavily industrialized site in Greece. Applied Sciences 10, 9023, https://doi.org/10.3390/app10249023.

Kumar, A., Ambade, B., Sankar, T.K., Sethi, S.S., Kurwadkar, S., 2020. Source identification and health risk assessment of atmospheric $PM_{2.5}$-bound polycyclic aromatic hydrocarbons in Jamshedpur, India. Sustainable Cities Soc. 52, 101801, https://doi.org/10.1016/j.scs.2019.101801.

Ledoux, F., Laversin, H., Courcot, D., Courcot, L., Zhilinskaya, E.A., Puskaric, E., Aboukaïs, A., 2006. Characterization of iron and manganese species in atmospheric aerosols from anthropogenic sources. Atmos Res 82, 622-632, https://doi.org/10.1016/j.atmosres.2006.02.018.

Lelieveld, J., Hadjinicolaou, P., Kostopoulou, E., Giannakopoulos, C., Pozzer, A., Tanarhte, M., Tyrlis, E., 2014. Model projected heat extremes and air pollution in the eastern Mediterranean and Middle East in the twenty-first century. Regional Environmental Change 14, 1937-1949, http://dx.doi.org/10.1007/s10113-013-0444-4.

Li, P.-h., Jia, H.-y., Wang, Y., Li, T., Wang, L., Li, Q.-q., Yang, M.-m., Yue, J.-j., Yi, X.-l., Guo, L.-q., 2019. Characterization of $PM_{2.5}$-bound phthalic acid esters (PAEs) at regional background site in northern China: Long-range transport and risk assessment. Sci. Total Environ. 659, 140-149, https://doi.org/10.1016/j.scitotenv.2018.12.246.

Liu, J., Chen, Y., Chao, S., Cao, H., Zhang, A., Yang, Y., 2018. Emission control priority of $PM_{2.5}$-bound heavy metals in different seasons: A comprehensive analysis from health risk perspective. Sci. Total Environ. 644, 20-30, https://doi.org/10.1016/j.scitotenv.2018.06.226.

Loomis, D., Grosse, Y., Lauby-Secretan, B., Ghissassi, F.E., Bouvard, V., Benbrahim-Tallaa, L., Guha, N., Baan, R., Mattock, H., Straif, K., 2013. The carcinogenicity of outdoor air pollution. Lancet Oncol. 14, 1262-1263, https://doi.org/10.1016/S1470-2045(13)70487-X.

Ma, B., Wang, L., Tao, W., Liu, M., Zhang, P., Zhang, S., Li, X., Lu, X., 2020. Phthalate esters in atmospheric $PM_{2.5}$ and PM_{10} in the semi-arid city of Xi'an, Northwest China: Pollution characteristics, sources, health risks, and relationships with meteorological factors. Chemosphere 242, 125226, https://doi.org/10.1016/j.chemosphere.2019.125226.

Ma, W.-L., Liu, L.-Y., Jia, H.-L., Yang, M., Li, Y.-F., 2018. PAHs in Chinese atmosphere Part I: Concentration, source and temperature dependence. Atmos Environ 173, 330-337, https://doi.org/10.1016/j.atmosenv.2017.11.029.

Mark Goldberg, 2008. A systematic review of the relation between long-term exposure to ambient air pollution and chronic diseases. Rev. Environ. Health 23, 243-298, https://doi.org/10.1515/REVEH.2008.23.4.243.

Marquès, M., Domingo, J.L., 2019. Concentrations of PCDD/Fs in Human Blood: A Review of Data from the Current Decade. Int. J. Environ. Res. Public Health 16, 3566, https://doi.org/10.3390/ijerph16193566.

Melki, P.N., Ledoux, F., Aouad, S., Billet, S., El Khoury, B., Landkocz, Y., Abdel-Massih, R.M., Courcot, D., 2017. Physicochemical characteristics, mutagenicity and genotoxicity of airborne particles under industrial and rural influences in Northern Lebanon. Environ Sci Pollut Res Int 24, 18782-18797, https://doi.org/10.1007/s11356-017-9389-3.

Miri, M., Rostami Aghdam Shendi, M., Ghaffari, H.R., Ebrahimi Aval, H., Ahmadi, E., Taban, E., Gholizadeh, A., Yazdani Aval, M., Mohammadi, A., Azari, A., 2016. Investigation of outdoor BTEX: Concentration, variations, sources, spatial distribution, and risk assessment. Chemosphere 163, 601-609, https://doi.org/10.1016/j.chemosphere.2016.07.088.

MoE, 2017. Lebanon's National Strategy for Air Quality Management for 2030. http://www.databank.com.lb/docs/MoE-(2017)-National-Air-Quality-Management-Strategy-EN.pdf.

Murari, V., Singh, N., Ranjan, R., Singh, R.S., Banerjee, T., 2020. Source apportionment and health risk assessment of airborne particulates over central Indo-Gangetic Plain. Chemosphere 257, 127145, https://doi.org/10.1016/j.chemosphere.2020.127145.

Murray, J.J., Pottie, R.F., Pupp, C., 1974. The vapor pressures and enthalpies of sublimation of five polycyclic aromatic hydrocarbons. Can. J. Chem. 52, 557-563, https://doi.org/10.1139/v74-087.

Nakhlé, M.M., Farah, W., Ziadé, N., Abboud, M., Salameh, D., Annesi-Maesano, I., 2015. Short-term relationships between emergency hospital admissions for respiratory and cardiovascular diseases and fine particulate air pollution in Beirut, Lebanon. Environ. Monit. Assess. 187, 196, https://doi.org/10.1007/s10661-015-4409-6.

Nasser, Z., Salameh, P., Dakik, H., Elias, E., Abou Abbas, L., Levêque, A., 2015. Outdoor air pollution and cardiovascular diseases in Lebanon: a case-control study. J Environ Public Health 2015, 810846, https://doi.org/10.1155/2015/810846.

Naumova, Y.Y., Offenberg, J.H., Eisenreich, S.J., Meng, Q., Polidori, A., Turpin, B.J., Weisel, C.P., Morandi, M.T., Colome, S.D., Stock, T.H., Winer, A.M., Alimokhtari, S., Kwon, J., Maberti, S., Shendell, D., Jones, J., Farrar, C., 2003. Gas/particle distribution of polycyclic aromatic hydrocarbons in coupled outdoor/indoor atmospheres. Atmos Environ 37, 703-719, https://doi.org/10.1016/S1352-2310(02)00820-8.

Nisbet, I.C., LaGoy, P.K., 1992. Toxic equivalency factors (TEFs) for polycyclic aromatic hydrocarbons (PAHs). Regulatory toxicology and pharmacology : RTP 16, 290-300, https://doi.org/10.1016/0273-2300(92)90009-X.

NTP, 2016. National Toxicology program, Report on carcinogens, fourteenth edition, Research Triangle Park, NC: U.S. Department of Health and Human Services, Public Health Service. https://ntp.niehs.nih.gov/go/roc14.

OEHHA, 2012. Technical Support Document for Exposure Assessment and Stochastic Analysis. Office of Environmental Health Hazard Assessment, California Environmental Protection Agency, Sacramento, [Sacramento, Calif.].

Oja, V., Suuberg, E.M., 1998. Vapor pressures and enthalpies of sublimation of Polycyclic Aromatic Hydrocarbons and their derivatives. J. Chem. Eng. Data 43, 486-492, https://doi.org/10.1021/je970222l.

Pankow, J.F., 1987. Review and comparative analysis of the theories on partitioning between the gas and aerosol particulate phases in the atmosphere. Atmos Environ 21, 2275-2283, https://doi.org/10.1016/0004-6981(87)90363-5.

Pankow, J.F., 1994. An absorption model of gas/particle partitioning of organic compounds in the atmosphere. Atmos Environ 28, 185-188, https://doi.org/10.1016/1352-2310(94)90093-0.

Pongpiachan, S., 2015. Incremental lifetime cancer risk of $PM_{2.5}$ bound polycyclic aromatic hydrocarbons (PAHs) before and after the wildland fire episode. Aerosol and Air Quality Research x, 1-13, https://doi.org/10.4209/aaqr.2015.01.0011.

Pratt, G.C., Herbrandson, C., Krause, M.J., Schmitt, C., Lippert, C.J., McMahon, C.R., Ellickson, K.M., 2018. Measurements of gas and particle polycyclic aromatic hydrocarbons (PAHs) in air at urban, rural and near-roadway sites. Atmos Environ 179, 268-278, https://doi.org/10.1016/j.atmosenv.2018.02.035.

Ramírez, O., Sánchez de la Campa, A.M., Sánchez-Rodas, D., de la Rosa, J.D., 2020. Hazardous trace elements in thoracic fraction of airborne particulate matter: Assessment of temporal variations, sources, and health risks in a megacity. Sci. Total Environ. 710, 136344, https://doi.org/10.1016/j.scitotenv.2019.136344.

Rengarajan, T., Rajendran, P., Nandakumar, N., Lokeshkumar, B., Rajendran, P., Nishigaki, I., 2015. Exposure to polycyclic aromatic hydrocarbons with special focus on cancer. Asian Pacific Journal of Tropical Biomedicine 5, 182-189, https://doi.org/10.1016/S2221-1691(15)30003-4.

Rondini, E.A., Walters, D.M., Bauer, A.K., 2010. Vanadium pentoxide induces pulmonary inflammation and tumor promotion in a strain-dependent manner. Part Fibre Toxicol 7, 9-9, https://doi.org/10.1186/1743-8977-7-9.

Rusyn, I., Corton, J.C., 2012. Mechanistic considerations for human relevance of cancer hazard of di(2-ethylhexyl) phthalate. Mutat. Res. 750, 141-158, https://doi.org/10.1016/j.mrrev.2011.12.004.

Salameh, P., Salame, J., Khayat, G., Akhdar, A., Ziadeh, C., Azizi, S., Khoury, F., Akiki, Z., Nasser, Z., Abou Abbass, L., Saadeh, D., Waked, M., 2012. Exposure to outdoor air pollution and chronic bronchitis in adults: a case-control study. Int J Occup Environ Med 3, 165-177

Salameh, T., Sauvage, S., Afif, C., Borbon, A., Léonardis, T., Brioude, J., Waked, A., Locoge, N., 2015. Exploring the seasonal NMHC distribution in an urban area of the Middle East during ECOCEM campaigns: Very high loadings dominated by local emissions and dynamics. Environ. Chem., 10.1071/EN14154.

Salameh, T., Sauvage, S., Afif, C., Borbon, A., Locoge, N., 2016. Source apportionment vs. emission inventories of non-methane hydrocarbons (NMHC) in an urban area of the Middle East: local and global perspectives. Atmospheric Chemistry and Physics Discussions 15, https://doi.org/10.5194/acp-16-3595-2016.

Samet, J., Krewski, D., 2007. Health Effects Associated With Exposure to Ambient Air Pollution. J. Toxicol. Environ. Health, Part A 70, 227-242, https://doi.org/10.1080/15287390600884644.

Simoneit, B.R.T., Medeiros, P.M., Didyk, B.M., 2005. Combustion products of plastics as indicators for refuse burning in the atmosphere. Environ. Sci. Technol. 39, 6961-6970, 10.1021/es050767x.

Sulaymon, I.D., Mei, X., Yang, S., Chen, S., Zhang, Y., Hopke, P.K., Schauer, J.J., Zhang, Y., 2020. $PM_{2.5}$ in Abuja, Nigeria: Chemical characterization, source apportionment, temporal variations, transport pathways and the health risks assessment. Atmos Res 237, 104833, https://doi.org/10.1016/j.atmosres.2019.104833.

Sun, J., Tang, J., Chen, Z., Nie, J., Zhang, S., Li, J., 2017. PCDD/Fs profile in ambient air of different types factories and human health risk assessment in Suzhou of Jiangsu province, China. Atmos. Pollut. Res. 8, 74-79, https://doi.org/10.1016/j.apr.2016.07.010.

Thurston, G.D., Kipen, H., Annesi-Maesano, I., Balmes, J., Brook, R.D., Cromar, K., De Matteis, S., Forastiere, F., Forsberg, B., Frampton, M.W., Grigg, J., Heederik, D., Kelly, F.J., Kuenzli, N., Laumbach, R., Peters, A., Rajagopalan, S.T., Rich, D., Ritz, B., Samet, J.M., Sandstrom, T., Sigsgaard, T., Sunyer, J., Brunekreef, B., 2017. A joint ERS/ATS policy statement: what constitutes an adverse health effect of air pollution? An analytical framework. European Respiratory Journal 49, 1600419, 10.1183/13993003.00419-2016.

Tsatsakis, A.M., Katsikantami, I., Kalantzi, O.-I., Sevim, Ç., Tsarouhas, K., Sarigiannis, D., Tzatzarakis, M.N., Rizos, A.K., 2019. Phthalates: exposure and health effects. in: Nriagu, J. (Ed.). Encyclopedia of Environmental Health (Second Edition). Elsevier, Oxford, pp. 163-173.

USEPA, 1989. General quantitative risk assessment guidelines for noncancer health effects. External review draft. Risk assessment forum technical panel on risk assessment guidelines for noncancer health effects, U.S. Environmental Protection Agency, Washington, DC.

USEPA, 1991. Risk Assessment Guidance for Superfund: Volume I - Human Health Evaluation Manual (Part B, Development of Risk-based Preliminary Remediation Goals) Publication 9285.7-01B. Office of Emergency and Remedial Response, Washington, DC. NTIS PB92-963333.

USEPA, 1997. Exposure factors handbook. Washington DC: Office of research and development, national center for environmental assessment.

USEPA, 2002. Supplemental guidance for developing soil screening levels for Superfund sites.U.S. Environmental Protection Agency, Washington, DC.

USEPA, 2004a. Region 9, Preliminary remediation goals, air–water calculations. U.S. Environmental Protection Agency, Washington, DC.

USEPA, 2004b. Risk assessment guidance for superfund volume I. Human Health Evaluation Manual (Part E, Supplemental Guidance for Dermal Risk Assessment), Final. EPA/540/R/99/005. Office of Solid Waste and Emergency Response, Washington, DC. PB99-963312.

USEPA, 2011. Exposure factors handbook : 2011 edition (Final Report). U.S. Environmental Protection Agency, Washington, DC (EPA/600/R-09/052F).

Van den Berg, M., Birnbaum, L.S., Denison, M., De Vito, M., Farland, W., Feeley, M., Fiedler, H., Hakansson, H., Hanberg, A., Haws, L., Rose, M., Safe, S., Schrenk, D., Tohyama, C., Tritscher, A., Tuomisto, J., Tysklind, M., Walker, N., Peterson, R.E., 2006. The 2005 World Health Organization reevaluation of human and Mammalian toxic equivalency factors for dioxins and dioxin-like compounds. Toxicol. Sci. 93, 223-241, https://doi.org/10.1093/toxsci/kfl055.

Vasilakos, C., Levi, N., Maggos, T., Hatzianestis, J., Michopoulos, J., Helmis, C., 2007. Gas-particle concentration and characterization of sources of PAHs in the atmosphere of a suburban area in Athens, Greece. J. Hazard. Mater. 140, 45-51, https://doi.org/10.1016/j.jhazmat.2006.06.047.

Veglia, F., Matullo, G., Vineis, P., 2003. Bulky DNA adducts and risk of cancer: a meta-analysis. Cancer epidemiology, biomarkers & prevention : a publication of the American Association for Cancer Research, cosponsored by the American Society of Preventive Oncology 12, 157-160

Waked, A., Afif, C., Seigneur, C., 2012. An atmospheric emission inventory of anthropogenic and biogenic sources for Lebanon. Atmos Environ 50, 88-96, https://doi.org/10.1016/j.atmosenv.2011.12.058.

WHO, 2016. Ambient air pollution : a global assessment of exposure and burden of disease. Switzerland, Geneva.https://apps.who.int/iris/bitstream/10665/250141/1/9789241511353-eng.pdf.

Xue, J., Zartarian, V., Moya, J., Freeman, N., Beamer, P., Black, K., Tulve, N., Shalat, S., 2007. A meta-analysis of children's hand-to-mouth frequency data for estimating Nondietary ingestion Exposure. Risk Anal. 27, 411-420, https://doi.org/10.1111/j.1539-6924.2007.00893.x.

Yang, L., Liu, G., Zheng, M., Jin, R., Zhu, Q., Zhao, Y., Zhang, X., Xu, Y., 2017. Atmospheric occurrence and health risks of PCDD/Fs, polychlorinated biphenyls, and polychlorinated naphthalenes by air inhalation in metallurgical plants. Sci. Total Environ. 580, 1146-1154, https://doi.org/10.1016/j.scitotenv.2016.12.071.

Zhang, X., Wang, Q., Qiu, T., Tang, S., Li, J., Giesy, J.P., Zhu, Y., Hu, X., Xu, D., 2019. $PM_{2.5}$ bound phthalates in four metropolitan cities of China: Concentration, seasonal pattern and health risk via inhalation. Sci. Total Environ. 696, 133982, https://doi.org/10.1016/j.scitotenv.2019.133982.

Zubair, M., Adress, A., 2019. Dioxins and Furans: emerging contaminants of air. in: Olvera, J.D.R. (Ed.). Air Pollution - Monitoring, Quantification and Removal of Gases and Particles. IntechOpen.

Article 5: Temporal variations, relationship with chemical composition and source apportionment of oxidative potential of $PM_{2.5}$ in two East Mediterranean sites

Marc Fadel[a,b], *Dominique Courcot*[b], *Gilles Delmaire*[c], *Gilles Roussel*[c], *Charbel Afif* [a,d], *Frédéric Ledoux*[b,*]

[a]Emissions, Measurements, and Modeling of the Atmosphere (EMMA) Laboratory, CAR, Faculty of Sciences, Saint Joseph University, Beirut, Lebanon

[b]Unité de Chimie Environnementale et Interactions sur le Vivant, UCEIV UR4492, FR CNRS 3417, University of Littoral Côte d′Opale (ULCO), Dunkerque, France

[c]Laboratoire d'Informatique Signal et Image de la Côte d'Opale (LISIC), University of Littoral Côte d'Opale, Calais, France

[d]Climate and Atmosphere Research Center, The Cyprus Institute, Nicosia, Cyprus

*Corresponding author: frederic.ledoux@univ-littoral.fr

Abstract:

Oxidative potential (OP) of $PM_{2.5}$ collected between December 2018 and October 2019 in two urban sites in the East Mediterranean was evaluated using dithiothreitol (DTT) and ascorbic acid (AA) assays. The mean volume normalized OP-AA value was 0.67 ± 0.29 $nmol.min^{-1}.m^{-3}$ at ZK and 0.46 ± 0.33 $nmol.min^{-1}.m^{-3}$ at FA. On the other hand, the mean $OP\text{-}DTT_v$ was 0.52 ± 0.32 $nmol.min^{-1}.m^{-3}$ at ZK and 0.29 ± 0.16 $nmol.min^{-1}.m^{-3}$. Different approaches were used to study the relationship between the species under study (carbonaceous matter, ions, major and trace elements, and organic compounds) or the sources contribution and OP values. Spearman correlations and hierarchical classification after principal components analysis showed that both $OP\text{-}DTT_v$ and $OP\text{-}AA_v$ at ZK were correlated with HFO combustion, diesel generators, crustal dust, road dust and vehicular emissions, while OP-AA is additionally correlated with biomass burning and plant wax emissions. OP-AA at FA showed a correlation with biomass burning, road dust, and heavy-duty vehicles diesel emissions while OP-DTT was more linked to HFO combustion, open burning of waste, and cement plant sources. The multiple linear regression applied to the contribution of the sources and the OP values at ZK site showed that biomass burning (32.8% of $OP\text{-}AA_v$ and 8.8% of $OP\text{-}DTT_v$), vehicular emissions (19.7% and 22.6%), and HFO combustion (31.4% and 46.0%) contribute the most to the $OP\text{-}AA_v$ and $OP\text{-}DTT_v$, respectively.

Introduction

Air pollution is considered as one of the major environmental challenges and poses a major threat to health and climate. According the World Health Organization (WHO), 99% of people worldwide were living in areas where air quality exceeded the WHO air quality guidelines in 2019 (WHO, 2021). It is estimated that the attributable excess mortality rate from ambient air pollution is about 8.8 million per year (Lelieveld et al., 2019). Among the different air pollutants, particulate matter with an aerodynamic diameter less than 2.5 μm ($PM_{2.5}$) can be easily inhaled into the lungs and might cause diverse health effects especially cardiovascular and respiratory diseases (Anderson et al., 2012; Xing et al., 2016; Lelieveld and Münzel, 2020). The exact mechanisms of toxicity induced by exposure to PM are still poorly understood. Toxicological studies have shown that the exposure to PM could induce oxidative stress by stimulating cells to produce reactive oxygen species (ROS) in excess of the antioxidant capacity of the body (Ayres et al., 2008; Bates et al., 2015). This imbalance triggers a cascade of effects such as inflammation, DNA damage and cell death (Becker et al., 2005; Wang et al., 2019). Additionally, the toxicological effects due to the induction of oxidative stress by PM are related to their physico-chemical characteristics such as surface properties and chemical composition (Crobeddu et al., 2017). Borm et al. (2007) stressed on the idea that the major PM components (ammonium sulfate, sodium chloride, crustal dust, etc.) contribute the least to the toxicity. However, organic compounds and metals have been shown to catalyze redox reactions in the body (Ghio et al., 2012). Hence, the oxidative potential (OP) of PM has been found to be a practical indicator for the evaluation of the oxidative capacity of PM components as a whole (Crobeddu et al., 2017). According to Daellenbach et al. (2020), if the OP could be linked to the major health impacts, it may be more effective to control sources of particulate matter rather than overall particulate mass concentration.

Recently, different acellular assays were developed for measuring OP. The most common include electron spin (OP-ESR), dithiothreitol (OP-DTT), ascorbic acid (OP-AA) and glutathione (OP-GSH) assays (Guo et al., 2020). Among those, OP-AA and OP-DTT are widely used and are based on spectrophotometric kinetic methods (Bates et al., 2019). They are less time-consuming assays and less resource intensive than cellular assays. The OP-DTT assay measures the depletion rate of dithiothreitol, a chemical proxy used as a substitute of cellular reductants owing to its sulfhydryl groups, evaluating by that the generation of superoxide radicals in vivo (Cho et al., 2005). The OP-AA assay measures the ability of PM to deplete antioxidants (ascorbic acid in this case) in the respiratory tract lining fluid (RTLF) (Mudway et

al., 2004). The depletion rates are proportional to the generation rate of ROS and the ability of PM to contribute to ROS overproduction. Up until today, there is no standard methodology to measure oxidative potential (Janssen et al., 2014). The methodology should include different tests due to their different sensitivities to PM components (Ayres et al., 2008). The current state of knowledge regarding the correlation between species and the different OP assays is not enough to reach a conclusion about the specificity of the tests to classes of compounds. However, an OP assessment based on the OP-AA and OP-DTT assays seems appropriate when considering different families of PM components due to the complementarity between these assays (Guo et al., 2020). However, the study of the relationship between OP values and PM sources is sometimes limited since PM species and elements contributing to OP values can be emitted by several sources. Additionally, few studies tried to determine OP values produced by specific sources such as biomass burning and urban traffic (Saffari et al., 2014; Bates et al., 2015). Therefore, assuming that OP is a predictive metric of the PM toxicity, it has become increasingly important to link the OP values with PM sources in order to identify the sources with the greatest possible impact. Bates et al. (2015) and Weber et al. (2018) developed methodologies for the evaluation of the contributions of the sources using a multiple linear regression approach in order to assign OP-AA and OP-DTT values for different sources obtained by source apportionment application.

In this context, the objectives of this research were to examine the temporal variations of oxidative potential of $PM_{2.5}$ measured using AA and DTT assays, to study the relationship between the $PM_{2.5}$ chemical components and OP results (Spearman correlations and principal component analysis), and to assign intrinsic OP values to the different sources identified by source-receptor modeling using Positive Matrix Factorization (PMF) in two East Mediterranean sites. The two sites under study are located in Lebanon in urban areas under industrial influence with on-road traffic, industrial, and residential emissions as major anthropogenic sources (Waked et al., 2012). Additionally, the region is under the influence of long range transport of dust from Saharan and Arabian deserts, and pollutant particles from urban and industrial areas of North and East Europe (Pietrogrande et al., 2018). $PM_{2.5}$ samples were collected between December 2018 and October 2019. This study will be a first in Lebanon and in the East Mediterranean and the Middle East region presenting results of oxidative potential (OP-AA and OP-DTT), studying the correlation between the OP values and different classes of compounds (carbonaceous, ionic, elemental, and organic) and attributing OP values to the $PM_{2.5}$ identified

sources at the sites. The findings of this study will be of utmost importance to policymakers in order to implement policies to protect health and improve the air quality in the region.

1 Materials and methods

1.1 $PM_{2.5}$ sampling

$PM_{2.5}$ were sampled in Lebanon at Zouk Mikael site (ZK) and Fiaa site (FA). Detailed information about the sampling sites and the sample collection were presented in Fadel et al. (2021). Briefly, the ZK site (33°57'57.07''N; 35°37'09.46''E) is highly urbanized with a residential density of 4,200 inhabitants/km^2, located at 1.2 km of a congested highway linking the capital Beirut to the North of Lebanon. This site encompasses the biggest power plant which runs on Heavy Fuel Oil (HFO). On the other hand, the FA site (34°20'47.8''N; 35°47'14.0''E) might be under the influence of different chemical industries such as cement plants and a sulfuric acid and phosphate fertilizer industry. This site, located in the Chekka region, is less populated (250 inhabitants/km^2) than ZK with moderate traffic activity in the region.

PM2.5 samples were collected on pre-cleaned Quartz microfibres filters (150 mm, Fiorini, France) over a 24 h period every third day from 13th of December 2018 to 15th of October 2019, using a high-volume sampler (CAV-A/mb, MCV S.A., Spain) operating at 30 m^3/h.

1.2 $PM_{2.5}$ chemical characterization

The $PM_{2.5}$ atmospheric mass concentration determination was based on the standard EN 12341:2014. An electronic balance (Mettler Toledo, AB204, United States of America) with a resolution of 100 µg was used for weighing filters before and after sampling in a temperature (20 ± 0.5°C) and humidity (50 ± 5%) controlled room. Various analytical methods were used to analyze the different chemical fractions of $PM_{2.5}$. Organic compounds such as Polycyclic Aromatic Hydrocarbons (PAHs), alkanes, hopanes and levoglucosan were analyzed by gas chromatography coupled to a mass spectrometer GC/MS (ISQ 7000, Thermo Scientific, United States of America) using the method described in Fadel et al. (2021). The analysis of major and trace elements was performed using an Inductively Coupled Plasma-Atomic Emission Spectrometry (ICP-AES, iCAP 6000 series, Thermo Scientific, United Kingdom), and an ICP-Mass Spectrometry (ICP-MS, Agilent 7900, Varian, United States of America), respectively using the method described in Ledoux et al. (2006). Water-soluble ions were analyzed by ion chromatography (Dionex™ ICS-900, Thermo Scientific, United Kingdom) following the method presented by Kfoury et al. (2016). Finally, a punch of the filter was used to quantify

OC and EC by a thermal optical transmission technique using a Sunset Laboratory analyzer implementing the EUSAAR2 temperature protocol (Cavalli et al., 2010).

1.3 Oxidative potential measurements

The method used for the assessment of the oxidative potential using AA and DTT assays was detailed in Moufarrej et al. (2020) and will be briefly presented here. A punch of the filter (19 mm diameter) was extracted by 5 mL of a Gamble solution (pH = 7.4) daily prepared according to the specifications presented by Colombo et al. (2008). The extraction tubes were placed in a heated orbital shaker for 24 h at 37°C, at a speed of 250 oscillations per min. The extracted solutions were then filtered on 0.45 µm nylon filters, placed in flasks, and stored at -20°C until OP analysis.

The measurement of DTT depletion was carried out in 96 well black plates with clear flat bottom (Costar® 3631, Corning Incorporated Life Sciences, USA). In each well, 120 µL of phosphate buffer solution (pH = 7.4) and 40 µL of the PM leachate (or blank or 1,4-naphtoquinone used as positive control) were added. Then the plate was placed at 37°C for 10 min under shaking. The oxidation reaction was initiated by adding 25 µL of DTT (0.4 mM) and the estimation of the remaining DTT was done by adding 15 µL of 5,5-dithio-bis-(2-nitrobenzoic acid) (DTNB) in the wells after 0, 5, 10, 20, 30, 45 and 60 min of reaction between the PM leachate and DTT at 37°C. The remaining DTT reacts with DTNB and is converted to 2-nitro-5-thiobenzoic acid (TNB). The absorbance of TNB was measured 10 min after the last DTNB addition at 37°C at 412 nm (spectrophotometer Multiskan Go, Thermo Fischer Scientific, Finland). The DTT depletion rate was then calculated using the slope of the linear regression of the remaining DTT versus time, then converted to OP-DTT_v expressed in $nmol.min^{-1}.m^{-3}$ and OP-DTT_m expressed in $nmol.min^{-1}.\mu g^{-1}$ after blank corrections. Extracts were analyzed in triplicates and the relative standard deviation was below 10%.

The OP-AA assay was done in 96 well plates with UV-transparent flat bottom (UV-Star® 655801, Greiner bio-one, Austria). In each well, 160 µL of PM extracts were added and then the plate was incubated at 37°C for 10 min under shaking. Then, 40 µL of the AA solution (1mM) was added to the extract and incubated for 1 min before placing it in the spectrophotometer (Multiskan Go, Thermo Fischer Scientific, Finland). The absorbance of the remaining AA was measured at 265 nm every 2 min for 2 hours after 30 s shaking. The AA depletion rate was concluded by considering the slope of the linear part of the curve representing remaining AA versus time. OP-AA values were normalized to the mass and to the volume (OP-

AA_v and OP-AA_m) after blank corrections. Extracts were also analyzed in triplicates and the relative standard deviation was below 7%.

1.4 Data processing

1.4.1 Study of correlations

In order to assess correlations between OP data and $PM_{2.5}$ components, statistical tests were used after the study of the normality of the data. The Shapiro-Wilk test was performed to evaluate the normality of the distributions. Most of the variables were not showing data normally distributed ($p<0.001$). Therefore, we chose the Spearman correlation coefficient, a non-parametric test to study the correlations. Three levels of significance were generally applied, $p<0.05$ for 95% confidence, $p<0.001$ for 99% confidence, and $p<0.001$ for 99.9% confidence. The seasonal variability of the OP values was analyzed using the Mann-Whitney statistical test. Additionally, principal component analysis was also conducted after data normalization.

1.4.2 Apportionment method for OP

Since OP is considered as a reactivity value, it cannot be directly integrated into a mass-balance model such as the Positive Matrix Factorization (PMF). Therefore, a multiple linear regression method is essential in order to estimate the contributions of PM sources to OP. This method was developed by Weber et al. (2018) using an inversion method and assuming that the OP values are linearly related to the contributions of the sources using the following equation (Eq.1):

$$OP_{obs} = \sum_{i=1}^{n} m_{i-PM} \times \beta_i + \varepsilon \qquad (Eq.1)$$

Where OP_{obs} is the observed OP_v value matrix expressed in $nmol.min^{-1}.m^{-3}$, $m_{i\text{-}PM}$ is the mass of PM attributed to the source i in the source contribution matrix expressed in $\mu g.m^{-3}$, β_i represents the intrinsic OP of the source ($nmol.min^{-1}.m^{-3}$), ε is the OP uncertainty expressed in $nmol.min^{-1}.m^{-3}$. An intercept representing a constant unit term expressed in $nmol.min^{-1}.m^{-3}$ was also added into the algorithm and used as a check for the method. If the obtained intercept value is close to zero, it means that the system is well constrained with no missing sources.

Solving this multiple linear regression (MLR) system required a weighted least square approach and by ruling out negative solutions since negative values of OP cannot be considered. Therefore, the following algorithm was adopted by Weber et al. (2018):

- Solve the weighted least square algorithm and estimate the values of intrinsic OP
- If an intrinsic OP value is negative, set the value to zero and resolve the algorithm
- Repeat until all the intrinsic OP values for the sources are either positive or zero.

The input data for this model are the contributions of the sources resulting from the PMF, the values of OP-AA_v and OP-DTT_v along with corresponding uncertainties. The latter were calculated at 2σ based on the RSD of the triplicates, the uncertainty related with the sampling instrumentation, and the uncertainties associated with the experimental procedures.

Once the initial run is done and values of intrinsic OP are calculated, a bootstrap analysis on the MLR model is applied to evaluate the variability of the obtained intrinsic OP results. This method creates sets of bootstrap data constructed by randomly selecting blocks of observations from the initial dataset. The size of the blocks is generally calculated according to Politis and White (2004) and was taken in this case as 5 samples per block. Additionally, 100 bootstrap runs were randomly performed to ensure the robustness of the statistics. The results of the different runs were presented in a boxplot presenting the median and the percentile (5, 25, 75 and 90) of the runs.

2 Results and discussions

2.1 $PM_{2.5}$ composition and sources contribution

The concentrations of the different $PM_{2.5}$ components at ZK and FA sites were detailed elsewhere (Fadel et al., 2021; 2022) and will be briefly presented here. Additionally, the chemical markers of the sources identified using PMF along with the sources average contributions are presented in **Table IV-6**.

$PM_{2.5}$ average concentrations were 33.6 µg.m^{-3} and 26.0 µg.m^{-3} at ZK and FA, respectively. The major chemical components at both sites were OC, SO_4^{2-}, Ca, NH_4^+ and NO_3^- contributing to approximately 50% of the $PM_{2.5}$ mass. These species, along with other organic and inorganic markers were used for the estimation of the sources contribution by applying PMF (Fadel et al., 2022). In brief, different mathematical diagnostic methods such as maximum individual mean (IM) and maximum individual standard deviation (IS) were investigated to choose the most suitable number of factors. Moreover, the variability in PMF solutions using the bootstrap

analysis and the displacement analysis method (DISP) was performed. PMF-Bootstrap analysis conducted on the F matrix showed the highest mapping rates for the 12- factors solution at both sites (mapping over 90%). Additionally, the PMF-DISP diagnostic at ZK and FA showed good results and the absence of rotational ambiguity in the solution. The different sources were identified at both sites along with the contributions that are given in **Table IV-6**.

The ZK site was more influenced by vehicular emissions than the FA site (14% of $PM_{2.5}$ mass at ZK compared to 4.5% at FA), since ZK site is close to a congested highway. Additionally, the industrial influence was highlighted by a relatively high contribution of HFO combustion from the power plant at ZK (13% of $PM_{2.5}$ mass) and the HFO combustion from cement and power plants in the Chekka region (4.1%). Additionally, high levels of calcium were associated to the cement manufacturing (4.1% of $PM_{2.5}$ at FA). OC, EC, C_{20} and C_{21} were used as markers for diesel combustion and were associated with diesel generators at ZK and to diesel Heavy Duty Vehicles (HDV) emissions at FA due to the difference in the OC/EC concentration ratio between the two profiles (Fadel et al., 2022). Biomass burning source was mainly identified by the presence of levoglucosan in the profile and contributed to 3.4% of $PM_{2.5}$ at ZK and 5.2% at FA while open burning of waste was only identified at FA where it highly contributed to $PM_{2.5}$ (16.1%). Primary (plant wax emissions) and secondary (isoprene and α-pinene oxidation products) biogenic aerosols contributed to 9.3% and 13.4% of $PM_{2.5}$ at ZK and FA, respectively **(Table IV-6).**

2.2 Oxidative potential of $PM_{2.5}$

The average volume and mass-normalized OP-AA and OP-DTT values at ZK and FA are presented in **Table IV-7** for the whole studied period along with the values for winter and summer periods. Additionally, time series for the different variables ($OP\text{-}AA_v$, $OP\text{-}AA_m$, $OP\text{-}DTT_v$, $OP\text{-}DTT_m$) for both sites are presented in **Figure IV-3** and **Figure IV-4**. The mass-normalized OP corresponds to the intrinsic OP value related to the oxidative properties of PM per unit mass while volume-normalized OP takes into account the dilution of PM in the atmosphere and was considered to have a closer relationship with human exposure (Hakimzadeh et al., 2020).

The mean $OP\text{-}AA_v$ value was 0.67 ± 0.29 $nmol.min^{-1}.m^{-3}$ (0.15-1.49 $nmol.min^{-1}.m^{-3}$) at ZK and 0.46 ± 0.33 $nmol.min^{-1}.m^{-3}$ (0.01-1.49 $nmol.min^{-1}.m^{-3}$) at FA. On the other hand, the mean $OP\text{-}DTT_v$ value was 0.52 ± 0.32 $nmol.min^{-1}.m^{-3}$ (0.11-1.93 $nmol.min^{-1}.m^{-3}$) at ZK and

0.29 ± 0.16 nmol.min^{-1}.m^{-3} (0.05-0.75 nmol.min^{-1}.m^{-3}) at FA. OP-AA_v and OP-DTT_v values were higher at ZK compared to FA.

Table IV-6: Markers of the identified sources at Zouk (ZK) and Fiaa (FA) sites along with their average contribution in ng.m^{-3} and percentages to the composition of $PM_{2.5}$ (Fadel et al., 2022)

Source	Markers	Contrib. at ZK (ng.m^{-3})	Contrib. at ZK to $PM_{2.5}$ (%)	Contrib. at FA (ng.m^{-3})	Contrib. at FA to $PM_{2.5}$ (%)
Biomass burning	OC, EC, levoglucosan	1,003	3.4%	1,204	5.2%
HFO combustion	V, Ni	3,817	13%	951	4.1%
Ammonium sulfate	SO_4^{2-}, NH_4^+	4,610	15.7%	5,370	23.3%
Aged sea salt	Na^+, Cl^-, NO_3^-	3,290	11.2%	1,060	4.6%
Biogenic SOA	isoprene and α-pinene oxidation products	2,275	7.8%	1,334	5.8%
Crustal dust	Al, Ca, Mg, Ti, K	8,068	27.5%	5,309	23%
Cooking	hexadecanoic and octadecanoic acids	408	1.4%	402	1.7%
Plant wax emissions	C_{27}, C_{29}, C_{31}	436	1.5%	1,761	7.6%
Road dust	Cu, Sb, Sn	971	3.3%	925	4%
Diesel generators	OC, EC, C_{20}, C_{21}	1,309	4.5%	-	-
Vehicular emissions (1)	17α(H)-21β(H)-hopane	1,360	4.6%	-	-
Vehicular emissions (2)	OC, EC	1,783	6.1%	-	-
Diesel HDV	OC, EC, C_{20}, C_{21}	-	-	81	0.4%
Cement plant	Ca, EC	-	-	937	4.1%
Open burning of waste	OC, EC, NO_3^-, Na^+, Mg, K, and Cl^-	-	-	3,721	16.1%

The values in our study for OP-AA_v were in the range of those reported for different urban and industrial sites in France such as Grenoble, Nice, Talence, and Dunkirk (0.2-1.6 nmol.min^{-1}.m^{-3}) (Calas et al., 2019; Moufarrej et al., 2020). However, our values were higher than the ones reported for a Central Mediterranean suburban site of the flat Salento's peninsula where OP-AA_v average reported value was 0.29 nmol.min^{-1}.m^{-3} (Pietrogrande et al., 2018).

As for OP-DTT_v **(Table IV-7)**, the found values were in the range of values observed over the southern United States (0.1-1.5 nmol.min^{-1}.m^{-3}), for French sites (0.36-4.12 nmol.min^{-1}.m^{-3}), and for Chinese sites (0.19-1.1 nmol.min^{-1}.m^{-3}) (Verma et al., 2014; Calas et al., 2019; Wang et al., 2020).

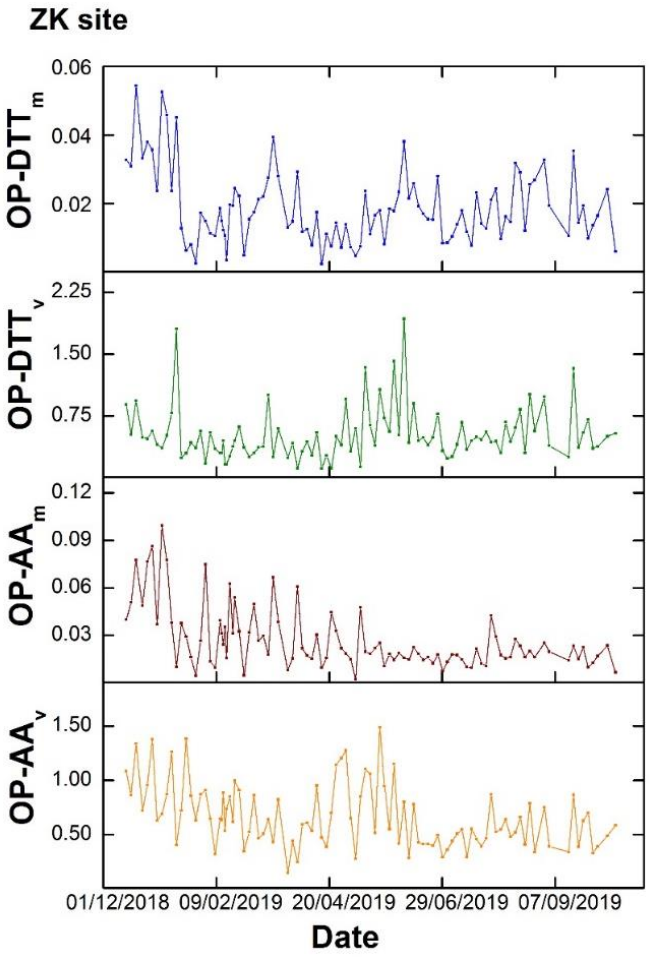

Figure IV-3: Time series of volume (nmol.min^{-1}.m^{-3}) (OP-AA$_v$ and OP-DDT$_v$) and mass (nmol.min^{-1}.µg^{-1}) (OP-AA$_m$ and OP-DTT$_m$) normalized oxidative potential (OP) at Zouk (ZK) site

The average OP-AA$_m$ and OP-DTT$_m$ were 0.03 ± 0.02 and 0.02 ± 0.01 nmol.min^{-1}.µg^{-1} for ZK, and 0.02 ± 0.02 and 0.01 ± 0.01 nmol.min^{-1}.µg^{-1} for FA, respectively and were also comparable to the values reported in the above-mentioned studies. Despite the closeness in the average values of OP-AA$_v$ and OP-DTT$_v$, a different temporal evolution is observed for OP-AA$_v$ and OP-DTT$_v$ (**Figure IV-3** and **Figure IV-4).** This might be due to the specificity of the assay towards certain $PM_{2.5}$ components.

When comparing winter and summer periods, OP-DTT$_v$ did not show any significant variability ($p>0.05$) at both sites. This mainly means that the major sources that contribute to the value of OP-DTT were not seasonal and were present during the whole sampling period. However, a different scenario was observed for OP-AA$_v$. This variable did not show a significant variability at FA ($p>0.05$), but at ZK, the OP-AA$_v$ values were significantly higher ($p<0.001$) during winter period compared to summer at ZK.

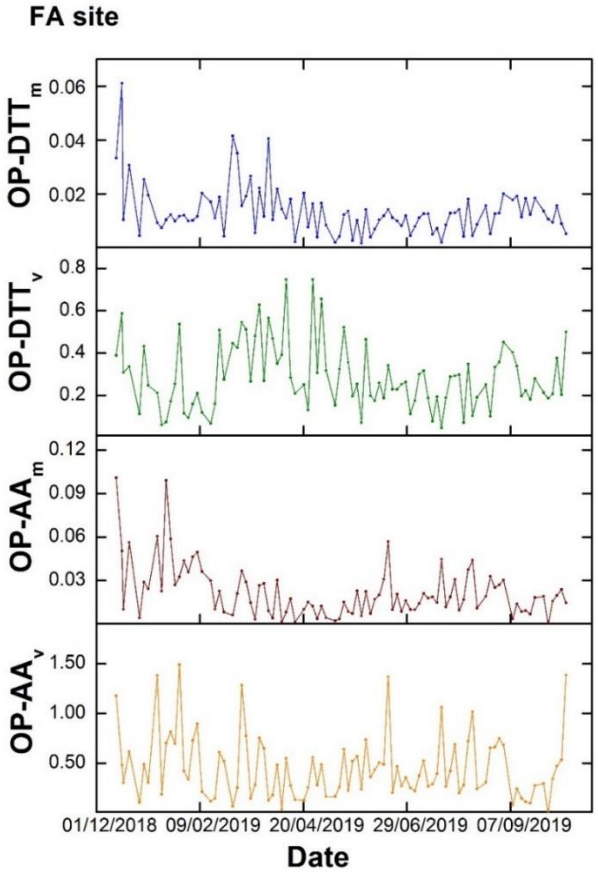

Figure IV-4: Time series of volume (nmol.min^{-1}.m^{-3}) (OP-AA$_v$ and OP-DDT$_v$) and mass (nmol.min^{-1}.µg^{-1}) (OP-AA$_m$ and OP-DTT$_m$) normalized oxidative potential (OP) at Fiaa (FA) site

This observation indicates that the AA-active components changed according to the period. A similar seasonal trend was observed by Calas et al. (2018) for Chamonix site.

2.3 Correlation between OP-AA$_v$ OP-DTT$_v$ and $PM_{2.5}$ chemical components

To investigate the relationships between OP values and species concentrations, Spearman correlation coefficients between volume-normalized OP-AA or OP-DTT and $PM_{2.5}$ components were calculated **(Table IV-8)**. The species include the carbonaceous matter (OC, EC), water-soluble ions, elements, and different classes of organic compounds among which alkanes, polycyclic aromatic hydrocarbons (PAHs), hopanes, and levoglucosan. This approach allows us to give insights into the species and the sources that might contribute to oxidative properties of PM. However, these assumptions should be used with attention since even a good correlation may not reflect any causality (Weber et al., 2021).

Table IV-7: Average volume (nmol.min^{-1}.m^{-3})(OP-AA_v and OP-DTT_v) and mass (nmol.min^{-1}.µg^{-1}) (OP-AA_m and OP-DTT_m) normalized OP-AA and OP-DTT measured for $PM_{2.5}$ with their standard deviations for the total period (Dec 2018-Nov 2019), winter (Dec 2018-March 2019), and summer (June 2019-September 2019) for Zouk (ZK) and Fiaa (FA) sites

	ZK site			**FA site**		
	Total	**Winter**	**Summer**	**Total**	**Winter**	**Summer**
OP-AA_v	0.67 ± 0.29	0.74 ± 0.30	0.51 ± 0.17	0.46 ± 0.33	0.54 ± 0.39	0.44 ± 0.29
OP-AA_m	0.03 ± 0.02	0.04 ± 0.02	0.02 ± 0.01	0.02 ± 0.02	0.03 ± 0.02	0.02 ± 0.01
OP-DTT_v	0.52 ± 0.32	0.47 ± 0.30	0.57 ± 0.33	0.29 ± 0.16	0.31 ± 0.18	0.24 ± 0.10
OP-DTT_m	0.02 ± 0.01	0.02 ± 0.01	0.02 ± 0.01	0.01 ± 0.01	0.02 ± 0.01	0.01 ± 0.01

At both sites, both assays appeared sensitive to metals but organic compounds including hopanes, levoglucosan, alkanes, and PAHs were not found to correlate with OP-DTT_v at ZK and weak to no correlations at FA **(Table IV-8)**.The same observations were done by Liu et al. (2020) in different areas in China. On the other hand, these compounds showed significant correlations with OP-AA_v showing that the AA assay is more sensitive to organic compounds compared to the DTT one. Additionally, weak correlations were found for elements associated with crustal dust such as Al, Mg, K, and Ti for both assays. OP-DTT_v values for samples collected during dust storm episodes (0.6 nmol.min^{-1}.m^{-3} at ZK and 0.3 nmol.min^{-1}.m^{-3} at FA) are not different from the average of DTT_v of PM observed in the sampling period at both sites **(Table IV-7).** Similar conclusions were presented by Chirizzi et al. (2017) who studied the influence of Saharan dust outbreaks on OP-DTT_v values.

A remarkable difference was observed when examining OP-AA_v values for samples under the influence of long-range transport from Saharan and Arabian deserts. Samples under the influence of Saharan dust showed values (0.47 nmol.min^{-1}.m^{-3} at ZK and 0.28 nmol.min^{-1}.m^{-3} at FA) lower than the average OP-AA_v, while samples influenced by dust outbreaks from Arabian deserts presented values (0.92 nmol.min^{-1}.m^{-3} at ZK and 0.82 nmol.min^{-1}.m^{-3} at FA) that were 1.4 and 1.8 times higher than the average OP-AA_v at ZK, and FA, respectively. This might be explained by the higher concentrations of carbonaceous matter in $PM_{2.5}$ for samples collected were under the influence of Arabian deserts and that were transported with the dust from the numerous refineries (Fadel et al., 2022).

OP-AA_v and OP-DTTv were shown to be more correlated at ZK compared to FA meaning that some sources at ZK might be responsible of the oxidation of both DTT and AA while at FA, sources were either associated to OP-AA_v or OP-DTT_v. OP-AA_v did not show a significant

correlation with $PM_{2.5}$ at ZK and very weak correlation at FA, while OP-DTT_v showed stronger correlations with $PM_{2.5}$ at both sites. Similar observations were done by Calas et al. (2019) and Yang et al. (2014) stressing on the idea that the OP values correlate more with specific species rather than $PM_{2.5}$ mass as a whole.

At ZK site, a strong correlation was found between OP-DTT_v and elements originating from different anthropogenic sources namely V, Ni, Zn, Cu, Sn and Sb **(Table IV-8)**. Elements such as Cu, V and Ni are known to be involved in the production of radicals via the Fenton reaction involving the reduction of H_2O_2 by a transition metal (Visentin et al., 2016) and control the DTT oxidation. Additionally, good, and moderate correlations were found between OP-DTT_v and OC and EC, respectively. OC and EC were mainly attributed to vehicular emissions at the sampling site while Cu, Sb and Sn mainly originate from resuspension of road dust (non-exhaust vehicular emissions) and V and Ni from HFO combustion. Similar correlations were observed between OP-DTT_v and elements in Moufarrej et al. (2020) in Dunkirk, a coastal industrial city in Northern France. Additionally, OP-DTT_v did not show any significant correlation with PAHs that might be linked to vehicular emissions, in agreement with Vreeland et al. (2017).

On the other hand, OC, EC, many PAHs and levoglucosan showed good correlations with OP-AA_v. These results are in agreement with previous studies that showed a high sensitivity of OP-AA_v assay to biomass burning and also to road traffic chemical markers (OC, EC, fluoranthene, pyrene, chrysene, benzo[a]pyrene) (Janssen et al., 2014; Calas et al., 2018; Weber et al., 2021). Additionally, a strong correlation was observed between OP-AA_v and indeno[1,2,3-c,d]pyrene that was linked with the HFO combustion from the power plant at ZK in our previous study (Fadel et al., 2021).

As for FA site, no strong correlation was observed between OP-DTT_v and species. The highest correlation coefficients were observed for Zn, Cd and Sb that were linked mainly to non-exhaust vehicular emissions. OP-DTT_v did not exhibit a strong correlation with V and Ni, showing that HFO combustion from cement and power plants in the region do not highly contribute to the observed values. It is worth noting that the PM extracts used in the assays do not only contain the components that were analyzed and identified, but also unanalyzed species. These unidentified species might further explain the values of OP at the sites especially at FA since the correlations between the identified species and OP values are weak, unlike the ZK site. OP-DTT_v at FA might be associated for example to water soluble organic carbon (WSOC) that was not characterized in this study. Indeed, it has already been established that WSOC have very

strong correlation with OP-DTT_v, notably water-soluble organic matter such as quinones and humic-like substances (Wang et al., 2020) OP-AA_v shows significant but not strong correlation with levoglucosan meaning that biomass burning contributes to the value of OP-AA_v. OP-AA_v was more correlated to OC, EC, and some PAHs linked to other combustion sources.

Table IV-8: Spearman correlation coefficient (r) between Oxidative Potential derived from AA and DTT depletion measurements (OP-AA_v and OP-DTT_v), $PM_{2.5}$ concentrations, and $PM_{2.5}$ components (carbonaceous fraction, water-soluble ions, elements, and organic species) – Correlation coefficients for which p-value <0.05 are reported (*p<0.001; bold r>0.5) at both sites

	ZK site		**FA site**	
Species	**OP-AA_v**	**OP-DTT_v**	**OP-AA_v**	**OP-DTTv**
OP-AA_v		0.41*		0.25
$PM_{2.5}$		0.42*	0.24	0.35*
OC	**0.53***	**0.51***	0.40*	0.30
EC	**0.53***	0.43*	**0.53***	0.34*
Cl^-				0.23
NO_3^-	0.28	0.21	0.38*	0.42*
SO_4^{2-}		0.46*		
Na^+				
NH_4^+		0.38*		
K^+	0.31	**0.53***	0.22	0.22
Mg^{2+}				
Ca^{2+}	0.21	0.26	0.21	
Mg		0.23	0.24	
Mn	0.42*	0.31	0.29	0.21
Al				
Ba	0.35*	0.24		
Ca	0.22	0.23	0.25	
Fe	0.22	0.29	0.28	
K	0.26	0.39*	0.30	0.22
Ni	0.47	**0.76***		0.38
P	0.30	**0.52***	0.32	0.25
V	0.29	**0.69***	0.24	0.37
Pb	**0.52***	0.47*	0.25	0.30
Sr		0.23	0.26	
Ti		0.23	0.22	
Zn	0.46	**0.67***	0.26	0.45*
Sc				
Cr				
Co	0.42*	0.46*	0.24	0.38*
Cu	0.38*	**0.50***	0.38*	0.31*
As		0.47*		0.25
Rb		0.31	0.27	0.18
Nb				
Cd	0.31	0.41*	0.37*	0.39*

Sn	0.27	**0.50***	0.27	0.36*
Sb	0.48*	**0.65***	0.40*	0.44*
La			0.23	0.23
Ce				
Tl		0.48*	0.24	
Bi		**0.50***	0.23	
C_{19} – nonadecane	0.28		0.44*	0.14
C_{20} – eicosane	0.29		0.39*	0.09
C_{21}- heneicosane	0.41*		0.37*	0.06
C_{22} - docosane	0.41*		0.35*	
C_{23} - tricosane	0.43*		0.36*	0.07
C_{24} - tetracosane	0.43*		0.31	
C_{25} - pentacosane	0.39*		0.32	
C_{26} – hexacosane	0.39*		0.27	
C_{27} - heptacosane	0.33*		0.28	0.10
C_{28} – octacosane	0.34*		0.27	
C_{29} – nonacosane	0.25		0.30	0.11
C_{30} - triacontane	0.32		0.28	
C_{31} - hentriacontane		0.21	0.31	0.14
C_{32} - dotriacontane	0.25	0.29	0.30	
acenaphthylene	0.40*		-	-
acenaphthene	0.35*		-	-
fluorene	0.25		-	-
anthracene	0.46*		0.34*	0.23
phenanthrene	**0.51***		0.29	0.22
fluoranthene	**0.50***		0.39*	0.29
pyrene	**0.51***		0.34	0.32
benz[a]anthracene	**0.52***		0.39*	
chrysene	**0.56***		-	-
benzo[b]fluoranthene	**0.50***		0.35*	0.23
benzo[k]fluoranthene	0.43*		0.34*	0.22
benzo[a]pyrene	**0.52***		0.32	
dibenz[a,h]anthracene	**0.52***		**0.50***	0.29
benzo[g,h,i]perylene	0.45*		**0.52***	0.25
indeno[1,2,3-c,d]pyrene	**0.57***		**0.50***	0.24
levoglucosan	**0.50***		0.30	0.30
trisnorneohopane	0.23		-	-
17α(H)-trisnorhopane	0.32		-	-
17α(H)-21β(H)-norhopane	0.32	0.26	-	-
17α(H)-21β(H)-hopane	0.36*	0.25	-	-
17α(H)-21β(H)-22S-homohopane	0.26	0.24	-	-
17α(H)-21β(H)-22R-homohopane		0.28	-	-

2.4 Hierarchical clustering on principal components

To further understand the correlations between the OP values and the identified PMF sources, principal component analysis was conducted, for each site separately, on the source contributions and considering OP-AA_v and OP-DTT_v as supplementary variables. The results of the PCA are presented in **Appendix E, Figure S1 and Figure S3.** The focus will only be on the two first principal components at ZK since they show significant correlations with OP.

These axes represent together 38% of the total variance of the data. Axis 1 (22.8% of the variance) was shown to be correlated with OP-AA_v and diesel generators, biomass burning, vehicular emissions (1), and wax emissions **(Appendix E, Table S1)**. Axis 2 (16% of the variance) was shown to be correlated with OP-AA_v and OP-DTT_v and HFO combustion, vehicular emissions (2), aged sea-salt, and crustal dust. As for FA, the only significant correlation with OP was found in the axis 2 (16% of the variance) between OP-DTT_v and open burning of waste, cement plant, road dust, and HFO combustion **(Appendix E, Table S2).**

However, these results were insufficient to reveal clear trends between OP values and sources especially at FA and that therefore hierarchical clustering was adopted to evidence subgroups of $PM_{2.5}$ samples with similar characteristics (Chanana et al., 2020) **(Appendix E, Figure S2 and Figure S3)**. The results of the clustering are presented in **Table IV-9** for ZK site and **Table IV-10** for FA site. In this paragraph, we will focus on the clusters that show significant test values with OP-AAv and OP-DTTv at both sites.

Subgroup 1 at ZK counts 40% of the $PM_{2.5}$ samples which are characterized by relatively low OP-AA_v values compared to other $PM_{2.5}$ samples and also low contributions of vehicular emissions (1) and plant wax emissions, and especially diesel generators and biomass burning. This could indicate that the latter sources contribute highly to the OP-AA_v value. As well, it shows that ammonium sulfate and biogenic SOA do not contribute to OP. These findings were also similar to the subgroup 4 corresponding to 15% of the samples showing high test-values for OP-AA_v with significant contributions of biomass burning, diesel generators, vehicular emissions (1), and plant wax emissions **(Table IV-9).** These results appear in agreement with the correlations found between with OP-AA_v values and organic compounds such as PAHs, alkanes and levoglucosan which are typically emitted by the above-cited sources.

Additionally, the results at ZK indicate that a subgroup of the data (cluster 3) showed samples with significantly high contributions of OP-AA_v and OP-DTT_v with crustal dust, diesel generators, HFO combustion and vehicular emissions (2).

Even though the number of samples in this subgroup is limited (6 samples), this still means that these mentioned sources could contribute to the values of both OP-AA_v and OP-DTT_v. As mentioned before, the OP values do not correlate with the elements from the crustal dust factor (Al, Ti, Fe, Mg, etc.) but with the carbonaceous matter that comes from long range transport.

Table IV-9: Test values obtained for OP-AA_v, OP-DTT_v and PMF sources in the different clusters obtained by hierarchical clustering on principal components at ZK. Only significant values were reported (*p-value<0.05; **p-value<0.01; *** p-value<0.001).

ZK site	Cluster 1	Cluster 2	Cluster 3	Cluster 4
Number of samples	35	33	6	13
OP-AA_v	**-4.29*****		**4.23*****	**2.83*****
OP-DTT_v			**5.57*****	
Ammonium sulfate	6.05***	-3.97***		
Biogenic SOA	5.59***	-3.67***		-2.26*
Biomass burning	-5.21***			6.03***
Cooking	3.13**	-3.73***		
Crustal dust	-2.45*		3.56***	
Diesel generators	-4.79***		2.06*	4.46***
HFO combustion			7.07***	-2.32*
Vehicular emissions (1)	-2.97**			6.31***
Vehicular emissions (2)		-2.89**	4.15***	
Plant wax emissions	-2.91**			3.93***

Relation with OP-AA_v		Relationship with both OP-AAv and OP-DTT_v	

At FA, cluster 3 and cluster 4 are respectively characterized by relatively high value of OP-DTT_V and OP-AA_V. No subgroup of samples showing both relatively high values of OP-AAv and OP-DTTv was observed. The subgroup 3 shows high loading of OP-DTT_v with high contribution of HFO combustion, open burning of waste, road dust cement plant. As for the subgroup 4, it is characterized by relatively high OP-AA_v values and also high contributions of biomass burning, road dust, and HDV diesel **(Table IV-10)**. Additionally, for both sites, no relationship was found between OP-AA_v and OP-DTT_v, with aged sea-salt and cooking emissions. Furthermore, secondary sources such as ammonium sulfate and biogenic SOA that highly contribute to the subgroup 1 at each site **(Table IV-9; Table IV-10)** did not show any relationship with OP values.

2.5 Apportionment of OP sources

2.5.1 Accuracy of the model

The multiple linear regression method presented by Weber et al. (2018) was used to estimate the contribution of PM sources to the OP values. It was applied to the database of ZK and FA separately and for OP-AA_v and OP-DTT_v. The accuracy of the model was verified by the values of the intercept, the evaluation of the residuals and the reconstruction of OP values.

Table IV-10: Test-values obtained for $OP\text{-}AA_v$, $OP\text{-}DTT_v$ and PMF sources in the different clusters obtained by hierarchical clustering on principal components at FA. Only significant values were reported (*p-value<0.05; **p-value<0.01; *** p-value<0.001)

FA site	Cluster 1	Cluster 2	Cluster 3	Cluster 4
Number of samples	**40**	**33**	**4**	**8**
$OP\text{-}AA_v$				**4.76*** **
$OP\text{-}DTT_v$			**3.19****	
Ammonium sulfate	6.46***	-4.57***		-2.37*
Biogenic SOA	5.93***	-4.63***		-2.03*
Biomass burning	-5.27***			7.16***
Cooking				
Crustal dust	-2.69**	2.22*		
HFO combustion		-3.14**	4.03***	
Wax emissions		-2.43*		
Open burning of waste		-2.11*	4.42***	
Road dust	-1.97*		5.49***	2.37*
Aged sea-salt	-2.22*	2.65**		
Cement plant		-3.16**	4.81***	
HDV diesel	-2.37*			6.29***

Relation with $OP\text{-}AA_v$		Relationship with $OP\text{-}DTT_v$	

The values of the intercept were 0.12 and 0.08 $nmol.min^{-1}.m^{-3}$ for $OP\text{-}AA_v$ and $OP\text{-}DTT_v$ at ZK, respectively. Intercept values are quite low showing that the identified sources are sufficient to explain the observed values of $OP\text{-}AA_v$ and $OP\text{-}DTT_v$. Considering the ZK data, the residuals between the observed and the modeled OP values were close to zero for low OP values and slightly higher values were recorded for higher OP values **(Figure IV-5)**. Additionally, the distribution of the residuals is normal (Shapiro Wilk test $p<0.05$) for both OP-AA and OP-DTT with a slight tendency towards the underestimation. A very good correlation was observed between OP reconstructed and observed ($R^2>0.7$) with a regression line close to 0.8. All of these findings show that the model is valid (Weber et al., 2021), and the results of intrinsic OP can be presented.

However, at FA site, even though the intercept values for both tests were at zero, showing that the system is well constrained, the residuals did not show satisfactory results **(Figure IV-5).** The residuals distribution shows that the model was not able to reconstruct even the low values of OP. Additionally, the residuals distribution is not normal (Shapiro Wilk test $p>0.05$) with a strong asymmetry towards the underestimation of the values **(Figure IV-5)**. Additionally, the reconstruction rate between observed and modeled OP values was 26% for OP-AA and 36%

for OP-DTT. Hence, the results cannot be analyzed since the modeled OP calculated by the MLR method were not sufficient to explain the observed OP values. This might be linked to the different limitations of the application of this method. First of all, according to Weber et al. (2018), the model is strongly constrained by the contributions of the sources to $PM_{2.5}$ since no uncertainty values is attributed to the sources by the PMF.

Additionally, the MLR regression presented here assumes that a linear link exists between OP values and source contributions. However, it has been shown that OP is not always proportional to the mass and this relationship varies depending on local parameters and non-linear effects between species such as synergetic and/or antagonistic effects between $PM_{2.5}$ components (Borlaza et al., 2021). The latter study also showed that the efficiency of linear regressions varies depending on the characteristics of the sampling sites. Calas et al. (2018) and references therein stated that the oxidative potential from the different components of PM are not always additive. Additionally, the bad reconstruction of OP values at FA and the moderate to weak correlations between the species and observed OP values might also be linked to a $PM_{2.5}$ source that might have not been identified by the PMF model. This source could have a very low contribution to the mass but also highly contribute to the OP values. For these reasons, we present in this paper the intrinsic OP values only for ZK site.

2.5.2 Intrinsic source OP values for ZK site

The values of intrinsic OP obtained from the initial run as well as the median values of OP and associated 5^{th}, 25^{th}, 75^{th} and 95^{th} percentile obtained from the bootstrap analysis were presented in **Figure IV-6**. The use of a boxplot representation allows to quickly evaluate the stability of the results: a certain confidence could be set on the intrinsic OP values showing low variability during the bootstrap procedure (25^{th} and 75^{th} percentile close to the median value). On the other hand, when 25^{th} and 75^{th} percentile values are far away from the median values (high interquartile range), conclusion should be carefully drawn regarding the obtained intrinsic OP value for the considered source.

For OP-AA_v, crustal dust did not show any contribution. This result was in agreement with Weber et al. (2018). The bootstrap procedure evidenced few variabilities for the intrinsic source OP values obtained for diesel generators, biomass burning, HFO combustion and vehicular emissions (1) and (2), but also ammonium sulfate, aged sea salts and crustal dust which showed intrinsic source OP values close to zero.

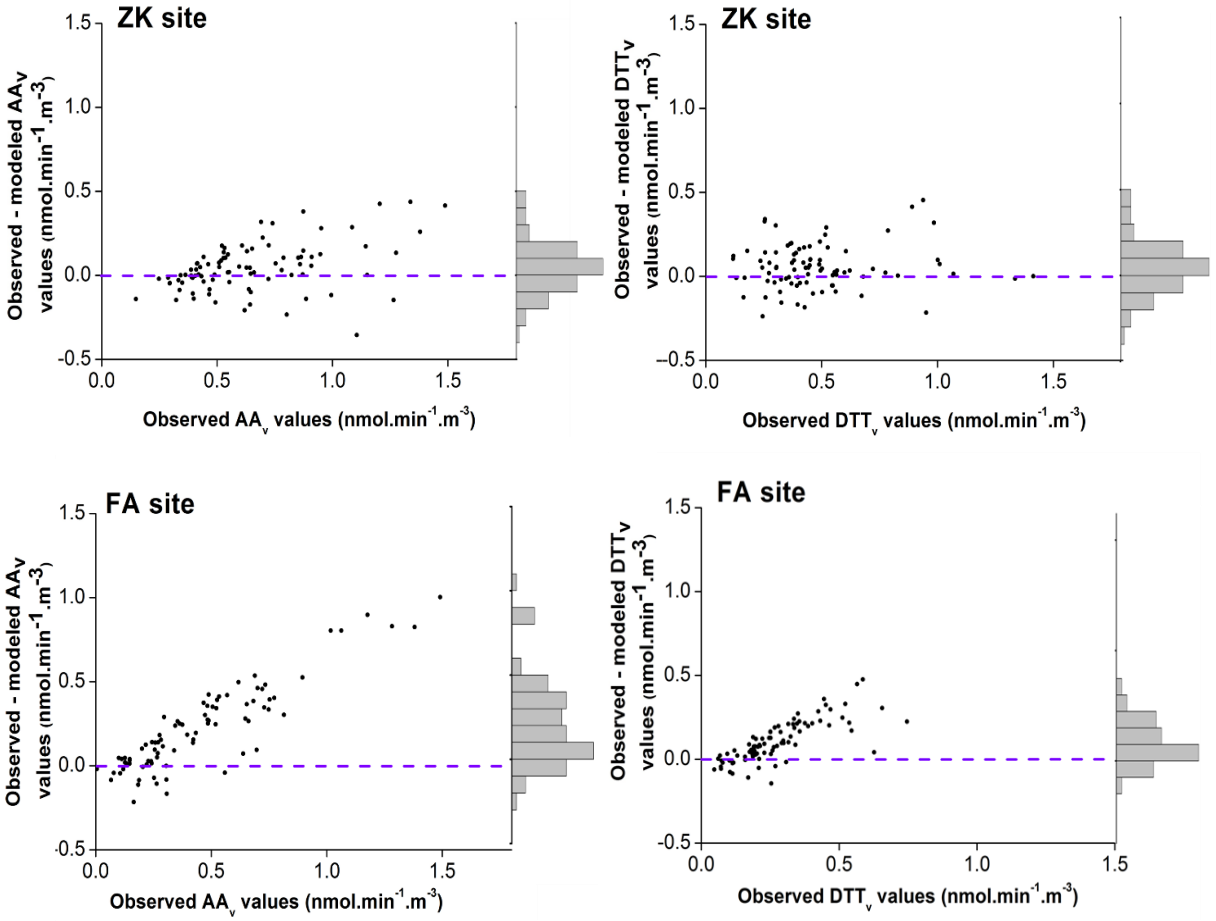

Figure IV-5: Residual distribution for the regression of AA and DTT assays (88 samples at ZK and 85 samples at FA). The histogram is the distribution of the residuals.

Additionally, we also observe that the intrinsic OP values from the initial run and median values from the bootstrap analysis were close. On the other hand, a strong variability was observed for the cooking, wax emissions and road dust sources. For these three sources, both null and high intrinsic OP values were obtained discarding the possibility to discuss and compare the values with confidence. From the calculation, the biomass burning source showed the highest intrinsic OP with a value of 0.147 nmol.min^{-1}.µg^{-1}, followed by HFO combustion (0.037 nmol.min^{-1}.µg^{-1},) vehicular emission (2) (0.030 nmol.min^{-1}.µg^{-1}), vehicular emissions (1) (0.027 nmol.min^{-1}.µg^{-1}), diesel generators (0.017 nmol.min^{-1}.µg^{-1}) ,biogenic SOA (0.011 nmol.min^{-1}.µg^{-1}) and aged sea-salt (0.003 nmol.min^{-1}.µg^{-1}).

For OP-DTT$_v$, diesel generators and aged sea-salt did not show any contribution. The bootstrap method applied to the MLR results showed few variabilities for intrinsic OP values for biomass burning, HFO combustion, ammonium sulfate, vehicular emissions (1) and (2), biogenic SOA,

and crustal dust. These sources also show close values between the obtained OP values from the initial run and median values from the bootstrap analysis. On the other hand, a strong variability was observed for the wax emissions, road dust and cooking. A high uncertainty is attributed to the intrinsic OP values of these sources due to their strong variability and will not be used for the calculation of the contribution of the sources to OP. From the calculation, HFO combustion source showed the highest intrinsic OP-DTT_v value (0.04 $nmol.min^{-1}.\mu g^{-1}$), followed by vehicular emissions (2) (0.035 $nmol.min^{-1}.\mu g^{-1}$), biomass burning (0.029 $nmol.min^{-1}.\mu g^{-1}$), ammonium sulfate (0.012 $nmol.min^{-1}.\mu g^{-1}$), vehicular emissions (1) (0.011 $nmol.min^{-1}.\mu g^{-1}$), biogenic SOA (0.004 $nmol.min^{-1}.\mu g^{-1}$) and crustal dust (0.001 $nmol.min^{-1}.\mu g^{-1}$).

The sources either present different intrinsic OP values for the AA and DTT tests or only show a reactivity towards one of the assays. Sources like HFO combustion and vehicular emissions (2) showed a similar reactivity to both tests. OP-AA results show to be mostly linked to biomass burning with an intrinsic value at least 4 times higher than the value of HFO combustion and vehicular emission sources **(Appendix E – Table S3)**. OP-DTT response seems to be multi-source influenced with close intrinsic values for biomass burning, HFO combustion, and vehicular emissions. Similar observations were done by Weber et al. (2018) when applying the method to the Chamonix site in France. Additionally, similar to our observations before, sources where organic compounds show high contributions in their chemical profiles, show higher intrinsic values for AA test compared to DTT such as biomass burning, biogenic SOA, diesel generators and vehicular emissions (1) (having high loading of 17α(H)-21β(H)-hopane). As for sources characterized by elements such as HFO combustion, intrinsic OP values were similar for both tests since AA and DTT are sensitive to elements (Bates et al., 2019). On the other hand, road dust source characterized by high content of Cu, Sb and Sn showed a strong variability in the MLR bootstrap results and no certain OP intrinsic value can be attributed to this source. Although these metals, such as Cu, are known to stimulate the production of radicals (Visentin et al., 2016), no intrinsic OP value was then attributed neither for AA nor for DTT.

Weber et al. (2018); (2021) presented intrinsic OP for these elements, but they were either combined to sea-salts or to carbonaceous matter related to exhaust vehicular emissions that largely contribute to the values of OP. The same observation was made in this study for the vehicular emissions (2) source showing a considerable intrinsic OP value for both assays. The ammonium sulfate source showed high intrinsic OP-DTT_v value as previously showed by Weber et al. (2018).

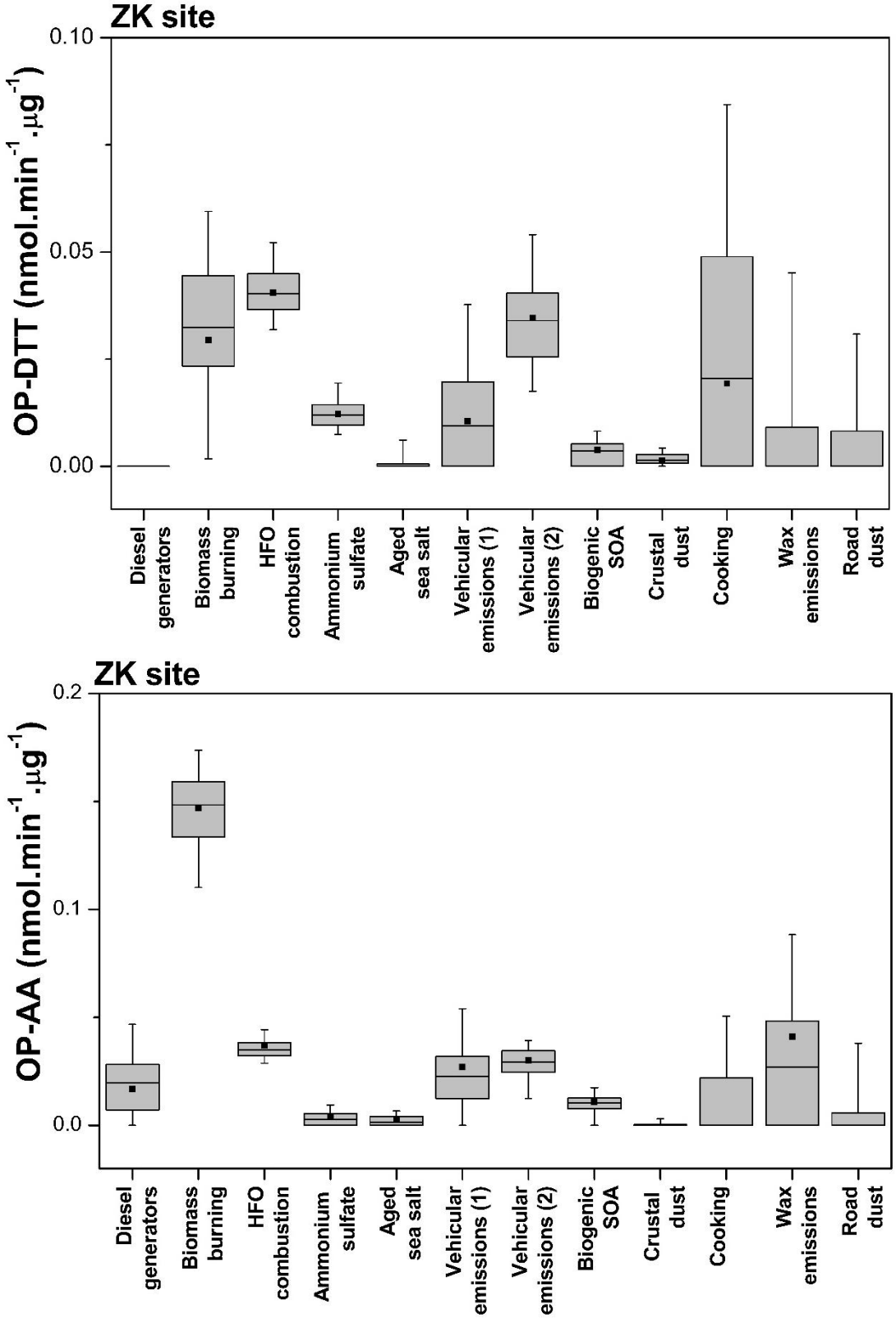

Figure IV-6: Boxplots of intrinsic OP values obtained from the bootstrap analysis for both AA and DTT values expressed in $nmol.min^{-1}.\mu g^{-1}$ (5^{th}, 25^{th}, 50^{th}, 75^{th}, and 95^{th} percentiles) and the OP value obtained from the initial run for the identified sources by PMF at ZK

2.5.3 Contribution of the sources to the OP values

The relative average contribution of the sources to the $PM_{2.5}$ concentration, OP-AA_v, and OP-DTT_v were presented in **Figure IV-7**. In this calculation, only the sources that showed few variability in the intrinsic OP values were considered for the calculation of the contribution of the sources (biomass burning, HFO combustion, ammonium sulfate, vehicular emissions (1) and (2), biogenic SOA, diesel generators, ammonium sulfate, aged sea-salt and crustal dust). It can be directly observed that the sources that contribute largely to $PM_{2.5}$ are not the ones contributing the most to the OP values. Crustal dust and ammonium sulfate that globally explained 43.2% of the $PM_{2.5}$ mass, contributed to only 3.6% of OP-AA_v and 19.5% of OP-DTT_v values combined.

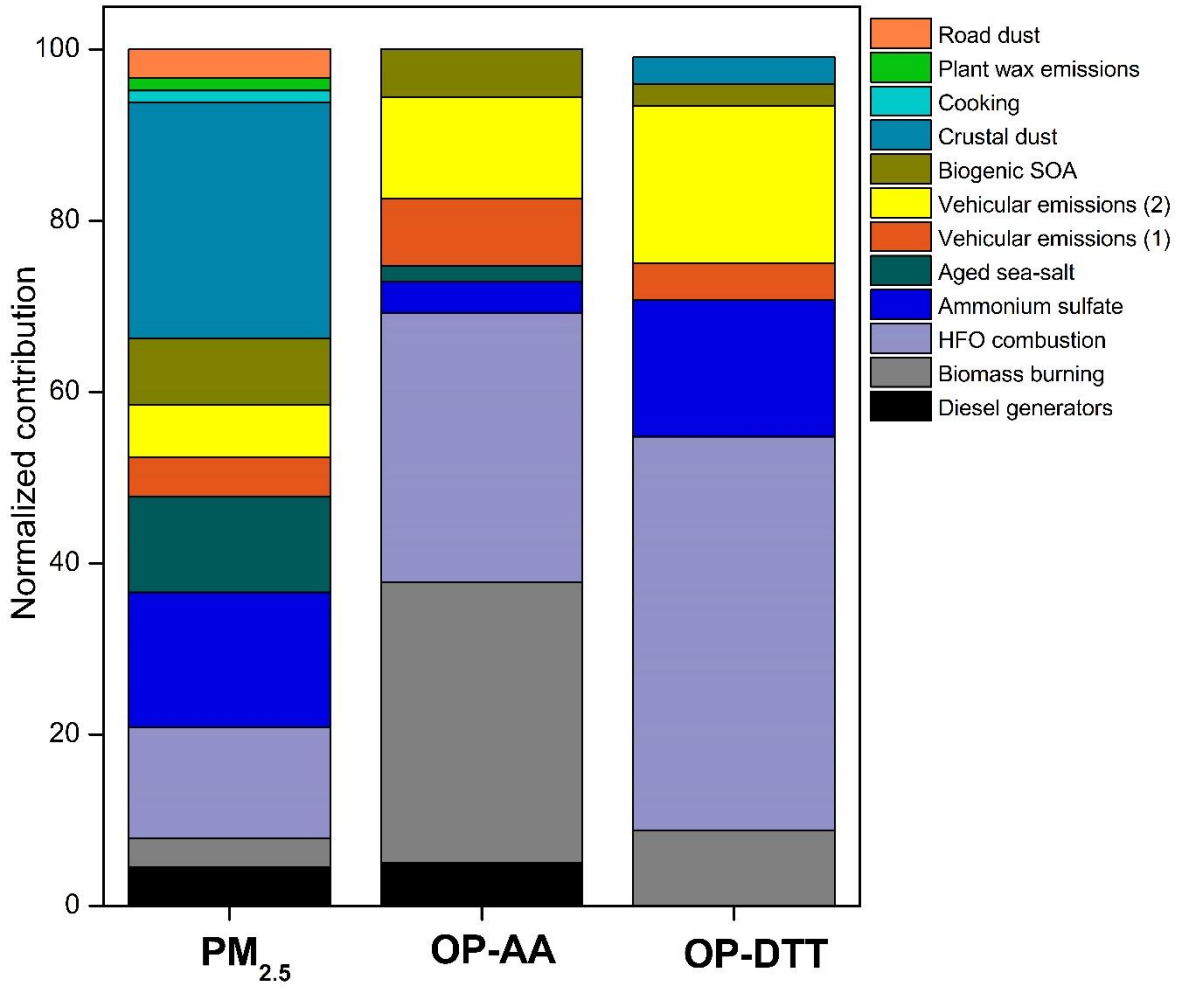

Figure IV-7: Normalized contribution of the sources to $PM_{2.5}$ concentration, OP-AA_v, and OP-DTT_v.

Biomass burning that was only responsible for 3.4% of $PM_{2.5}$, also showed a low contribution to OP-DTT_v (8.8%), but the highest share of OP-AA_v between the sources (32.8%). Vehicular emissions sources contributed to both OP-AA_v and OP-DTT_v with a share of 19.7% and 22.7%, respectively. As related to the industrial typology of the site, HFO combustion attributed to the power plant showed high shares to both assays with a contribution of 31.4% for OP-AA_v and 46.0% for OP-DTT_v. We can by that conclude that common sources contribute the most to the values of OP, namely biomass burning, vehicular emissions, and HFO combustion explaining 84% of OP-AA_v value and 78% of OP-DTT_v. These results were consistent with several literature studies that report dominant contribution to biomass combustion (Verma et al., 2014; Fang et al., 2016; Perrone et al., 2019), exhaust and non-exhaust vehicular emissions as well as fuel oil combustion to OP-DTT_v and OP-AA_v values (Crobeddu et al., 2017; Moreno et al., 2017) (Yang et al., 2014). Secondary biogenic emissions account for 5.6% of OP-AA_v value and 2.6% of OP-DTT_v. Diesel generator source did not contribute to OP-DTT_v but contributed to 5% of OP-AA_v. Since the OP values are proportional to the ROS production, these different sources contributing to the OP could possibly have the highest impact on human health even though they do not largely contribute to the $PM_{2.5}$ atmospheric concentration.

3 Conclusions

In this work, the oxidative potential of $PM_{2.5}$ collected in two urban sites under industrial influence, ZK and FA, in the East Mediterranean in 2018-2019 was evaluated using the AA and DTT assays. The mean OP-AA_v value was 0.67 ± 0.29 $nmol.min^{-1}.m^{-3}$ at ZK and 0.46 ± 0.33 $nmol.min^{-1}.m^{-3}$ at FA. On the other hand, the mean OP-DTT_v was 0.52 ± 0.32 $nmol.min^{-1}.m^{-3}$ at ZK and 0.29 ± 0.16 $nmol.min^{-1}.m^{-3}$. Different approaches for the evaluation of the relationship between OP values, chemical species in $PM_{2.5}$, and sources identified by PMF were used. Spearman correlations and hierarchical classification of principal components showed that both OP-AA_v and OP-DTT_v at ZK were mainly correlated with HFO combustion source (V and Ni elements), diesel generators, crustal dust, road dust, and carbonaceous matter emitted from vehicular emissions. Additionally, OP-AA_v at ZK was also correlated with organic compounds from biomass burning (levoglucosan) and vehicular emissions (PAHs and hopanes), and plant wax emissions. On the other hand, low to moderate correlations at FA showed that the OP-DTTv was mainly linked to road dust and OP-AA_v was correlated with carbonaceous matter emitted from open burning of waste. The hierarchical classification revealed that OP-AA_v might also be linked to biomass burning, road dust, and HDV diesel, and

$OP\text{-}DTT_v$ might be also correlated to HFO combustion, open burning of waste, and cement plant sources.

A multiple linear regression method was applied to both databases in order to estimate contributions of the PM sources to the OP values. Due to the inaccuracy of the model for the data at FA, only results concerning the ZK site were presented. The results showed that the sources that highly contribute to the $PM_{2.5}$ mass (crustal dust and ammonium sulfate) were not the major sources contributing to the values of OP. For the ascorbic acid assay, biomass burning (32.8%) and HFO combustion (31.4%) contributed the most to the $OP\text{-}AA_v$ followed by vehicular emissions (19.7%), biogenic SOA (5.6%), diesel generators (5.0%) and ammonium sulfate (3.7%). For the dithiothreitol assay, HFO combustion contributed the most (46.0%), followed by vehicular emissions (22.6%), ammonium sulfate (16.8%), biomass burning (8.8%), crustal dust (3.1%) and biogenic SOA (2.1%). Since the OP values are proportional to the ROS production, HFO combustion, biomass burning, and vehicular emissions that have the highest contribution to OP might have the highest impact on human health.

Overall, this study has provided insight into the relationship between PM sources and oxidative potential in two urban sites in the East Mediterranean. It is clear that more studies are required to further explain the association between the two acellular methods. Additionally, it is also essential to combine the contribution of the identified sources at the sites and the values of OP with non-linear multiple regression models in order to take into account the synergetic and antagonistic effects. These results in the region are essential in designing new approaches for air quality management and emission control technologies focusing more on specific toxic components and sources.

Acknowledgments:

The authors would like to acknowledge the National Council for Scientific Research of Lebanon (CNRS-L) and University of Littoral Côte d'Opale (ULCO) for granting a doctoral fellowship to Marc Fadel. This project was also funded by the Research Council and the Faculty of Sciences of Saint Joseph University of Beirut – Lebanon. The "Unité de Chimie Environnementale et Interactions sur le Vivant" (UCEIV-UR4492) participates in the CLIMIBIO project, which is financially supported by the Hauts-de-France Region Council, the French Ministry of Higher Education and Research, and the European Regional Development Funds. This publication has been also produced within the framework of the EMME-CARE

project, which has received funding from the European Union's Horizon 2020 Research and Innovation Programme (under grant agreement no. 856612) and the Cyprus Government.

The authors thank Institut Chevreul - Université de Lille for the analysis of elements by ICP-MS and The Cyprus Institute for the OC/EC analysis. The authors would also like to thank Dorothée Dewaele (Centre Commun de Mesures, ULCO) for her help in the ICP-AES analysis, Amaury Kasprowiak and Marianne Seigneur for their help in the ionic chromatography analysis, and Mariana Farhat for her help in the organic fraction analysis.

References:

Anderson, J.O., Thundiyil, J.G., Stolbach, A., 2012. Clearing the air: a review of the effects of particulate matter air pollution on human health. J Med Toxicol 8, 166-175, 10.1007/s13181-011-0203-1.

Ayres, J.G., Borm, P., Cassee, F.R., Castranova, V., Donaldson, K., Ghio, A., Harrison, R.M., Hider, R., Kelly, F., Kooter, I.M., Marano, F., Maynard, R.L., Mudway, I., Nel, A., Sioutas, C., Smith, S., Baeza-Squiban, A., Cho, A., Duggan, S., Froines, J., 2008. Evaluating the toxicity of airborne particulate matter and nanoparticles by measuring oxidative stress potential—A Workshop Report and Consensus Statement. Inhalation Toxicol. 20, 75-99, 10.1080/08958370701665517.

Bates, J.T., Fang, T., Verma, V., Zeng, L., Weber, R.J., Tolbert, P.E., Abrams, J.Y., Sarnat, S.E., Klein, M., Mulholland, J.A., Russell, A.G., 2019. Review of acellular assays of ambient particulate matter oxidative potential: methods and relationships with composition, Sources, and Health Effects. Environ. Sci. Technol. 53, 4003-4019, 10.1021/acs.est.8b03430.

Bates, J.T., Weber, R.J., Abrams, J., Verma, V., Fang, T., Klein, M., Strickland, M.J., Sarnat, S.E., Chang, H.H., Mulholland, J.A., Tolbert, P.E., Russell, A.G., 2015. Reactive Oxygen Species generation linked to sources of atmospheric particulate matter and cardiorespiratory effects. Environ. Sci. Technol. 49, 13605-13612, 10.1021/acs.est.5b02967.

Becker, S., Dailey, L.A., Soukup, J.M., Grambow, S.C., Devlin, R.B., Huang, Y.-C.T., 2005. Seasonal variations in air pollution particle-induced inflammatory mediator release and oxidative stress. Environ. Health Perspect. 113, 1032-1038, 10.1289/ehp.7996.

Borlaza, L.J.S., Weber, S., Jaffrezo, J.L., Houdier, S., Slama, R., Rieux, C., Albinet, A., Micallef, S., Trébluchon, C., Uzu, G., 2021. Disparities in particulate matter (PM_{10}) origins and oxidative potential at a city scale (Grenoble, France) – Part 2: Sources of PM_{10} oxidative potential using multiple linear regression analysis and the predictive applicability of multilayer perceptron neural network analysis. Atmos. Chem. Phys. 21, 9719-9739, 10.5194/acp-21-9719-2021.

Borm, P.J.A., Kelly, F., Künzli, N., Schins, R.P.F., Donaldson, K., 2007. Oxidant generation by particulate matter: from biologically effective dose to a promising, novel metric. Occup. Environ. Med. 64, 73-74, http://dx.doi.org/10.1136/oem.2006.029090.

Calas, A., Uzu, G., Besombes, J.-L., Martins, J.M.F., Redaelli, M., Weber, S., Charron, A., Albinet, A., Chevrier, F., Brulfert, G., Mesbah, B., Favez, O., Jaffrezo, J.-L., 2019. Seasonal Variations and Chemical Predictors of Oxidative Potential (OP) of Particulate Matter (PM), for Seven Urban French Sites. Atmosphere 10, 698

Calas, A., Uzu, G., Kelly, F.J., Houdier, S., Martins, J.M.F., Thomas, F., Molton, F., Charron, A., Dunster, C., Oliete, A., Jacob, V., Besombes, J.L., Chevrier, F., Jaffrezo, J.L., 2018. Comparison between five acellular oxidative potential measurement assays performed with detailed chemistry on PM10 samples from the city of Chamonix (France). Atmos. Chem. Phys. 18, 7863-7875, 10.5194/acp-18-7863-2018.

Cavalli, F., Viana, M., Yttri, K.E., Genberg, J., Putaud, J.P., 2010. Toward a standardised thermal-optical protocol for measuring atmospheric organic and elemental carbon: the EUSAAR protocol. Atmos. Meas. Tech. 3, 79-89, 10.5194/amt-3-79-2010.

Chanana, S., Thomas, C.S., Zhang, F., Rajski, S.R., Bugni, T.S., 2020. hcapca: Automated Hierarchical Clustering and Principal Component Analysis of Large Metabolomic Datasets in R. Metabolites 10, 297, 10.3390/metabo10070297.

Chirizzi, D., Cesari, D., Guascito, M.R., Dinoi, A., Giotta, L., Donateo, A., Contini, D., 2017. Influence of Saharan dust outbreaks and carbon content on oxidative potential of water-soluble fractions of $PM_{2.5}$ and PM_{10}. Atmos Environ 163, 1-8, https://doi.org/10.1016/j.atmosenv.2017.05.021.

Cho, A.K., Sioutas, C., Miguel, A.H., Kumagai, Y., Schmitz, D.A., Singh, M., Eiguren-Fernandez, A., Froines, J.R., 2005. Redox activity of airborne particulate matter at different sites in the Los Angeles Basin. Environ. Res. 99, 40-47, 10.1016/j.envres.2005.01.003.

Colombo, C., Monhemius, A.J., Plant, J.A., 2008. Platinum, palladium and rhodium release from vehicle exhaust catalysts and road dust exposed to simulated lung fluids. Ecotoxicol. Environ. Saf. 71, 722-730, https://doi.org/10.1016/j.ecoenv.2007.11.011.

Crobeddu, B., Aragao-Santiago, L., Bui, L.-C., Boland, S., Baeza Squiban, A., 2017. Oxidative potential of particulate matter 2.5 as predictive indicator of cellular stress. Environ. Pollut. 230, 125-133, https://doi.org/10.1016/j.envpol.2017.06.051.

Daellenbach, K.R., Uzu, G., Jiang, J., Cassagnes, L.-E., Leni, Z., Vlachou, A., Stefenelli, G., Canonaco, F., Weber, S., Segers, A., Kuenen, J.J.P., Schaap, M., Favez, O., Albinet, A., Aksoyoglu, S., Dommen, J., Baltensperger, U., Geiser, M., El Haddad, I., Jaffrezo, J.-L., Prévôt, A.S.H., 2020. Sources of particulate-matter air pollution and its oxidative potential in Europe. Nature 587, 414-419, 10.1038/s41586-020-2902-8.

Fadel, M., Afif, C., Seigneur, M., Kfoury, A., Oikonomou, K., Sciare, J., Ledoux, F., Courcot, D., 2022. $PM_{2.5}$ chemical characterization and sources identification in two sites in the East Mediterranean.

Fadel, M., Ledoux, F., Farhat, M., Kfoury, A., Courcot, D., Afif, C., 2021. $PM_{2.5}$ characterization of primary and secondary organic aerosols in two urban-industrial areas in the East Mediterranean. J Environ Sci 101, 98-116, https://doi.org/10.1016/j.jes.2020.07.030.

Fang, T., Verma, V., Bates, J.T., Abrams, J., Klein, M., Strickland, M.J., Sarnat, S.E., Chang, H.H., Mulholland, J.A., Tolbert, P.E., Russell, A.G., Weber, R.J., 2016. Oxidative

potential of ambient water-soluble PM2.5 in the southeastern United States: contrasts in sources and health associations between ascorbic acid (AA) and dithiothreitol (DTT) assays. Atmos. Chem. Phys. 16, 3865-3879, 10.5194/acp-16-3865-2016.

Ghio, A.J., Carraway, M.S., Madden, M.C., 2012. Composition of air pollution particles and oxidative stress in cells, tissues, and living systems. Journal of toxicology and environmental health. Part B, Critical reviews 15, 1-21, 10.1080/10937404.2012.632359.

Guo, H., Jin, L., Huang, S., 2020. Effect of PM characterization on PM oxidative potential by acellular assays: a review. Rev. Environ. Health 35, 461-470, doi:10.1515/reveh-2020-0003.

Hakimzadeh, M., Soleimanian, E., Mousavi, A., Borgini, A., De Marco, C., Ruprecht, A.A., Sioutas, C., 2020. The impact of biomass burning on the oxidative potential of PM2.5 in the metropolitan area of Milan. Atmos Environ 224, 117328, https://doi.org/10.1016/j.atmosenv.2020.117328.

Janssen, N.A.H., Yang, A., Strak, M., Steenhof, M., Hellack, B., Gerlofs-Nijland, M.E., Kuhlbusch, T., Kelly, F., Harrison, R., Brunekreef, B., Hoek, G., Cassee, F., 2014. Oxidative potential of particulate matter collected at sites with different source characteristics. Sci. Total Environ. 472, 572-581, https://doi.org/10.1016/j.scitotenv.2013.11.099.

Kfoury, A., Ledoux, F., Roche, C., Delmaire, G., Roussel, G., Courcot, D., 2016. $PM_{2.5}$ source apportionment in a French urban coastal site under steelworks emission influences using constrained non-negative matrix factorization receptor model. J Environ Sci 40, 114-128, https://doi.org/10.1016/j.jes.2015.10.025.

Ledoux, F., Courcot, L., Courcot, D., Aboukaïs, A., Puskaric, E., 2006. A summer and winter apportionment of particulate matter at urban and rural areas in northern France. Atmos Res 82, 633-642, https://doi.org/10.1016/j.atmosres.2006.02.019.

Lelieveld, J., Klingmüller, K., Pozzer, A., Pöschl, U., Fnais, M., Daiber, A., Münzel, T., 2019. Cardiovascular disease burden from ambient air pollution in Europe reassessed using novel hazard ratio functions. European Heart Journal 40, 1590-1596, 10.1093/eurheartj/ehz135.

Lelieveld, J., Münzel, T., 2020. Air pollution, the underestimated cardiovascular risk factor: European Heart Journal 41, 904-905, 10.1093/eurheartj/ehaa063.

Liu, Q., Lu, Z., Xiong, Y., Huang, F., Zhou, J., Schauer, J.J., 2020. Oxidative potential of ambient PM2.5 in Wuhan and its comparisons with eight areas of China. Sci. Total Environ. 701, 134844, https://doi.org/10.1016/j.scitotenv.2019.134844.

Moreno, T., Kelly, F.J., Dunster, C., Oliete, A., Martins, V., Reche, C., Minguillón, M.C., Amato, F., Capdevila, M., de Miguel, E., Querol, X., 2017. Oxidative potential of subway PM2.5. Atmos Environ 148, 230-238, https://doi.org/10.1016/j.atmosenv.2016.10.045.

Moufarrej, L., Courcot, D., Ledoux, F., 2020. Assessment of the $PM_{2.5}$ oxidative potential in a coastal industrial city in Northern France: Relationships with chemical composition, local emissions and long range sources. Sci. Total Environ. 748, 141448, 10.1016/j.scitotenv.2020.141448.

Mudway, I.S., Stenfors, N., Duggan, S.T., Roxborough, H., Zielinski, H., Marklund, S.L., Blomberg, A., Frew, A.J., Sandström, T., Kelly, F.J., 2004. An in vitro and in vivo

investigation of the effects of diesel exhaust on human airway lining fluid antioxidants. Arch. Biochem. Biophys. 423, 200-212, 10.1016/j.abb.2003.12.018.

Perrone, M., Bertoli, I., Romano, S., Russo, M., Rispoli, G., Pietrogrande, M., 2019. $PM_{2.5}$ and PM_{10} oxidative potential at a Central Mediterranean Site: Contrasts between dithiothreitol- and ascorbic acid-measured values in relation with particle size and chemical composition. Atmos Environ 210, 10.1016/j.atmosenv.2019.04.047.

Pietrogrande, M.C., Perrone, M.R., Manarini, F., Romano, S., Udisti, R., Becagli, S., 2018. PM_{10} oxidative potential at a Central Mediterranean Site: Association with chemical composition and meteorological parameters. Atmos Environ 188, 97-111, https://doi.org/10.1016/j.atmosenv.2018.06.013.

Politis, D.N., White, H., 2004. Automatic Block-Length Selection for the Dependent Bootstrap. Econometric Reviews 23, 53-70, 10.1081/ETC-120028836.

Saffari, A., Daher, N., Shafer, M.M., Schauer, J.J., Sioutas, C., 2014. Seasonal and spatial variation in dithiothreitol (DTT) activity of quasi-ultrafine particles in the Los Angeles Basin and its association with chemical species. Journal of environmental science and health. Part A, Toxic/hazardous substances & environmental engineering 49, 441-451, 10.1080/10934529.2014.854677.

Verma, V., Fang, T., Guo, H., King, L., Bates, J.T., Peltier, R.E., Edgerton, E., Russell, A.G., Weber, R.J., 2014. Reactive oxygen species associated with water-soluble $PM_{2.5}$ in the southeastern United States: spatiotemporal trends and source apportionment. Atmos. Chem. Phys. 14, 12915-12930, 10.5194/acp-14-12915-2014.

Visentin, M., Pagnoni, A., Sarti, E., Pietrogrande, M.C., 2016. Urban $PM_{2.5}$ oxidative potential: Importance of chemical species and comparison of two spectrophotometric cell-free assays. Environ. Pollut. 219, 72-79, https://doi.org/10.1016/j.envpol.2016.09.047.

Vreeland, H., Weber, R., Bergin, M., Greenwald, R., Golan, R., Russell, A.G., Verma, V., Sarnat, J.A., 2017. Oxidative potential of $PM_{2.5}$ during Atlanta rush hour: Measurements of in-vehicle dithiothreitol (DTT) activity. Atmos Environ 165, 169-178, https://doi.org/10.1016/j.atmosenv.2017.06.044.

Waked, A., Afif, C., Seigneur, C., 2012. An atmospheric emission inventory of anthropogenic and biogenic sources for Lebanon. Atmos Environ 50, 88-96, https://doi.org/10.1016/j.atmosenv.2011.12.058.

Wang, J., Lin, X., Lu, L., Wu, Y., Zhang, H., Lv, Q., Liu, W., Zhang, Y., Zhuang, S., 2019. Temporal variation of oxidative potential of water soluble components of ambient PM2.5 measured by dithiothreitol (DTT) assay. Sci. Total Environ. 649, 969-978, https://doi.org/10.1016/j.scitotenv.2018.08.375.

Wang, Y., Wang, M., Li, S., Sun, H., Mu, Z., Zhang, L., Li, Y., Chen, Q., 2020. Study on the oxidation potential of the water-soluble components of ambient PM2.5 over Xi'an, China: Pollution levels, source apportionment and transport pathways. Environ. Int. 136, 105515, https://doi.org/10.1016/j.envint.2020.105515.

Weber, S., Uzu, G., Calas, A., Chevrier, F., Besombes, J.L., Charron, A., Salameh, D., Ježek, I., Močnik, G., Jaffrezo, J.L., 2018. An apportionment method for the oxidative potential

of atmospheric particulate matter sources: application to a one-year study in Chamonix, France. Atmos. Chem. Phys. 18, 9617-9629, 10.5194/acp-18-9617-2018.

Weber, S., Uzu, G., Favez, O., Borlaza, L.J.S., Calas, A., Salameh, D., Chevrier, F., Allard, J., Besombes, J.-L., Albinet, A., Pontet, S., Mesbah, B., Gille, G., Zhang, S., Pallares, C., Leoz-Garziandia, E., Jaffrezo, J.-L., 2021. Source apportionment of atmospheric PM_{10} oxidative potential: synthesis of 15 year-round urban datasets in France. Atmos. Chem. Phys. 21, 11353-11378, 10.5194/acp-21-11353-2021.

WHO, 2021. WHO air quality guidelines. Particulate matter ($PM_{2.5}$ and PM_{10}), ozone, nitrogen dioxide, sulfur dioxide and carbon monoxide. Geneva: World Health Organization Switzerland. Licence: CC BY-NC-SA 3.0 IGO.

Xing, Y.-F., Xu, Y.-H., Shi, M.-H., Lian, Y.-X., 2016. The impact of $PM_{2.5}$ on the human respiratory system. J Thorac Dis 8, E69-E74, 10.3978/j.issn.2072-1439.2016.01.19.

Yang, A., Jedynska, A., Hellack, B., Kooter, I., Hoek, G., Brunekreef, B., Kuhlbusch, T.A.J., Cassee, F.R., Janssen, N.A.H., 2014. Measurement of the oxidative potential of PM2.5 and its constituents: The effect of extraction solvent and filter type. Atmos Environ 83, 35-42, https://doi.org/10.1016/j.atmosenv.2013.10.049.

Conclusion

This chapter presented the evaluation of the health risks associated with the exposure to $PM_{2.5}$ in ambient air in two urban sites in the East Mediterranean between December 2018 and October 2019: Zouk Mikael (ZK) and Fiaa (FA). This evaluation was done using two different approaches. The assessment of carcinogenic and non-carcinogenic risks is based on the concentration of the species at the sites and different exposure parameters and was achieved for the three exposure pathways (inhalation, ingestion and dermal contact) and for different age categories (newborns, children, adolescents and adults). As for the oxidative potential, it was measured using two acellular methods based on the kinetics of oxidation of AA and DTT for evaluating the oxidative capacity of the different $PM_{2.5}$ components. These two methods were applied for the first time on $PM_{2.5}$ from two sites in the East Mediterranean, and in Lebanon in particular. The obtained results would underline the major sources and species contributing to the toxicity of $PM_{2.5}$ at our sites.

In particular, the health risk assessment applied to different classes of compounds in $PM_{2.5}$ and to NMVOCs was essential to evidence classes of compounds mostly responsible for the carcinogenic and non-carcinogenic risk value. This study evaluated the total hazard index and the cumulative cancer risk for phthalates, dioxins, furans, dioxin-like polychlorobiphenyls, major and trace elements in $PM_{2.5}$, NMVOCs and PAHs in both particulate and gas phases. Among NMVOCs, benzene and n-heptane showed values higher than the threshold limit of one for non-carcinogenic risk at both sites with the highest values recorded for newborns and the lowest for adults. As for the particulate phase, the sum of elements showed for some age categories values exceeding the threshold limit where Mn, Pb, V, and Ni were the major contributors to the total hazard index. On the other hand, PAHs at both sites, phthalates, PCDD/Fs, and DL-PCBs exhibited values lower than one and by that they present acceptable non-carcinogenic risk.

As for the carcinogenic risk, cancer risk for NMVOCs showed values higher than the threshold limit of 10^{-6} for benzene and ethylbenzene at both sites and 1,3-butadiene at ZK. The lifetime cancer risk due only to the exposure to NMVOCs was 170 and 46 times higher than the threshold limit at ZK and FA, respectively. These compounds are mainly known to be emitted from fuel combustion sources especially traffic gasoline combustion. As for the particulate phase, $PM_{2.5}$-B[a]P_{eq} showed cancer risk higher than 10^{-6} with a trend of children, adults, adolescents, and newborns at both sites. These compounds were mainly emitted from various

anthropogenic activities at the sites such as biomass burning, vehicular emissions, and power plants.

As for elements, the lifetime cancer risk for 70 years of exposure exceeded the threshold limit with 44 and 25 additional cancer cases of cancer per million habitats at ZK and FA, respectively. Among these elements, As, Co, Cr, Ni, and V were the major contributors and presented alone values higher than the limit. These elements were mainly linked to anthropogenic sources in urban areas. The highest recorded cumulative cancer risk in the particulate phase was attributed to vanadium that is mainly linked to HFO combustion showing the influence of the power plant at ZK and the cement and power plants at FA. As for phthalates, PCDD/Fs, DL-PCBs, and PAHs in the gaseous phase showed values in the range of acceptable cancer risk.

When comparing the classes of compounds for their carcinogenic and non-carcinogenic risks, NMVOCs exhibited the higher risk followed by elements, PAHs, phthalates, and finally PCDD/Fs, and DL-PCBs. It is worth noting that the risks between the classes of compounds were not summed to have a global impact since there were no available methods for the calculation of the cumulative health risks due to the exposure to total air contaminants. This idea was an important limitation of the study since we assume an independence between toxic effects within and across compounds due to the lack of knowledge on the cocktail effect showing synergism or antagonism actions.

The second approach in this chapter differs from the first since the oxidative potential assays (AA and DTT in our case) respond to the oxidative species solubilized in the Gamble solution (simulated lung fluid) after leaching of the collected PM. The extracts contain then not only the identified and analyzed compounds but also unidentified species that might contribute to the values of OP. This means that this approach is more global. Different methods were used in this study in order to link the observed values of OP to the different identified species and sources at both sites such as spearman correlations, principal components, and hierarchical classification. Additionally, a multiple linear regression was adopted in order to assign intrinsic OP values to the sources and discover the contribution of the sources to the values of OP-AA and OP-DTT. The mean $OP\text{-}AA_v$ value was 0.67 ± 0.29 $nmol.min^{-1}.m^{-3}$ at ZK and 0.46 ± 0.33 $nmol.min^{-1}.m^{-3}$ at FA. On the other hand, the mean $OP\text{-}DTT_{v\ was}$ 0.52 ± 0.32 $nmol.min^{-1}.m^{-3}$ at ZK and 0.29 ± 0.16 $nmol.min^{-1}.m^{-3}$. These values were in range of different studies across the world. The temporal series showed strong variations from day to another for the same test and also a difference between $OP\text{-}AA_v$ and $OP\text{-}DTT_v$ values. Both assays at FA and $OP\text{-}DTT_v$ at

ZK did not show a significant seasonality. However, OP-AA_v at ZK showed significant variations with higher values during winter period compared to summer. This might be linked to a seasonal source that contribute largely to the value of OP-AA_v at ZK which is biomass burning for residential heating. The spearman correlations and hierarchical classification showed a predominance of anthropogenic sources influencing the values of OP. Organic compounds were more correlated to OP-AA_v while elements showed sensitivity to both assays. At ZK site, a significant correlation was observed between the assays, meaning that common sources contribute to the OP at the site (HFO combustion, diesel generators, crustal dust, road dust, and vehicular emissions). Also, OP-AA_v at ZK showed significant correlations with biomass burning, vehicular emissions, and plant wax emissions. This exercice was more complicated at FA since there were no species that show good correlation with OP-AA_v and OP-DTT_v. The hierarchical classification for small subgroups of the data highlighted that there were no common sources between the assays. OP-AA_v is mainly linked to biomass burning, road dust, and HDV diesel and OP-DTT_v was correlated with HFO combustion, open burning of waste, and cement plant sources.

The multiple linear regression method was applied to both databases in order to find intrinsic OP values for the different sources identified by PMF. Due to the inaccuracy of the obtained results for the FA site, the results were only presented for ZK site where the distribution of the residuals is quite normal, and the model is accurate. An intrinsic OP value was attributed to the different sources for OP-AA_v and OP-DTT_v while some of these sources were excluded during the inversion process. The results show that the crustal dust and ammonium sulfate sources that largely contribute to the $PM_{2.5}$ concentration are not the major contributors to the OP values. According to our study, OP-AA_v and OP-DTT_v were both majorly influenced by the same sources but with different shares. The identified sources that contributed the most to the $PM_{2.5}$ concentrations were not the most toxic, highlighting the importance of an extensive chemical characterization in order to find the species responsible for $PM_{2.5}$ toxicity. Biomass burning and HFO combustion are the major sources influencing the values of OP-AA_v contributing to more than 64% of its value. As for OP-DTT_v, HFO combustion contribute to 46% of the OP value and biomass burning contribute only to 8.8%. Vehicular emissions sources contribute equally to both assays with a relative contribution of 19.7% and 22.6% for OP-AA_v, and OP-DTT_v, respectively. This method presented also some limitations since the mathematical model is based on the assumption of linearity between OP values and PM source contributions, which

is not always the case. That is why, nonlinear regression models should be tested in order to take into account the synergistic and antagonistic effects between the pollutants.

Even if the two approaches presented in this chapter were different, they lead to similar conclusions. At ZK site, the elements that contribute the most to the cumulative cancer risk (V and Ni) show good correlations with OP values and their emission source (HFO combustion) contribute to both OP-AAv and OP-DTT_v. Other elements and PAHs show also values higher than the threshold limit of cancer and might be linked to vehicular emissions that also contributes to the values of OP. As for biomass burning, this source shows high contribution to OP-AA_v. On the other hand, the conclusions for FA seem more complicated due to the inaccuracy of the MLR model. However, V and Ni that show high cancer risk values were linked to the HFO combustion from the power and cement plants. This source also showed contribution to OP-DTT_v by the hierarchical classifications. Since vehicular emissions is not a source contributing significantly at the site, PAHs that show carcinogenic risks might be linked to other combustion sources such as biomass burning and open burning of waste. Biomass burning also showed correlations with OP-AA_v while open burning of waste correlated with OP-DTT_v.

The chemical characterization was essential for both approaches used in this chapter that gave us a better image of the close relationships between chemical composition of $PM_{2.5}$, sources contribution and impact on health. Oxidative potential values that are proportional to the ROS production are mainly affected by anthropogenic sources that do not largely contribute to the $PM_{2.5}$ atmospheric concentration but have the highest impact on human health. These results should be taken into account while presenting recommendations for policymakers (presented in the last chapter of this manuscript) in order to design new approaches for air quality management focusing more on toxic components and sources rather than only working on emissions limits for PM.

General Conclusions, recommendations and perspectives

General Conclusion

The aim of this work was to characterize the $PM_{2.5}$ in two urban-industrial sites in the East Mediterranean through the identification of the sources and quantification of their contribution to $PM_{2.5}$, and the evaluation of the associated health risk. This was achieved by: i) studying the chemical composition of the collected $PM_{2.5}$ collected for their carbonaceous matter, water soluble ions, elements, and organic species; ii) identifying the sources and quantifying their contribution by source-receptor modeling achieved by the Positive Matrix Factorization after having chosen organic and inorganic markers, iii) evaluating the health risk due to the exposure to different classes of compounds in $PM_{2.5}$ and VOCs, iv) measuring the oxidative potential of $PM_{2.5}$ and linking it to the sources.

For this purpose, $PM_{2.5}$ and VOC samples were collected in two sites in Lebanon (Zouk Mikael and Fiaa) between December 2018 and October 2019. Zouk Mikael site (ZK) encompasses the biggest power plant of the country which runs on heavy fuel oil while Fiaa site (FA) in Chekka region, is under the influence of the emissions from cement plants and their corresponding quarries. $PM_{2.5}$ samples were extensively studied for their chemical composition including the analysis of carbonaceous matter (OC, EC), water-soluble ions, major and trace elements, and organic compounds. The organic speciation includes different families of compounds such as alkanes, polycyclic aromatic hydrocarbons, phthalates, fatty acids, dioxins, furans, dioxin-like polychlorobiphenyls, dicarboxylic acids, and secondary biogenic species (oxidation products of isoprene, α-pinene, and β-caryophyllene). Among these species, several compounds considered as source markers were gathered along with their uncertainties as input data for the PMF model at both sites in order to identify and quantify the contribution of the sources to $PM_{2.5}$. The identification of the sources was based on literature PM source profiles but also on chemical profiles of $PM_{2.5}$ samples collected nearby typical sources associated with typical practices encountered in the East Mediterranean region: non-road diesel generators, wood burning, charcoal grilling, and general cooking activities. These profiles showed similarities with the profiles found in the literature but also differences in the abundance of the species and some concentration ratios At both site, 12 natural and anthropogenic sources were identified, some of which were common for both sites such as crustal dust, ammonium sulfate, HFO combustion, cooking, biomass burning, etc. and others were site-specific such as vehicular emissions and diesel generators emissions at ZK and open burning of waste and heavy duty diesel vehicles at FA. On the other hand, the health risk evaluation was based at first on the carcinogenic and non-carcinogenic risks due to the exposure to different families of compounds

in $PM_{2.5}$ and VOCs. Secondly, the measurement of the oxidative potential that is considered as a predictive indicator for Reactive Oxygen Species (ROS) generation due to the exposure of $PM_{2.5}$, will help us also evaluate the human health risk. Finally, the combination between source contribution by PMF and oxidative potential values was performed by multiple linear regression analysis in order to assign intrinsic OP values to the sources and then assess the contribution of the sources to the observed OP.

Average $PM_{2.5}$ were reported as 33.6 µg/m^3 at ZK and 26.0 µg/m^3 at FA, at least five times higher than the 2021 WHO $PM_{2.5}$ annual guideline value of 5 µg/m^3. The major chemical species in $PM_{2.5}$ at both sites were OC, Ca, and secondary inorganic ions (SO_4^{2-}, NO_3^-, and NH_4^+) **(Table III-7)**. Water-soluble ions contributed to 40% and 47% of $PM_{2.5}$ at ZK and FA, respectively, while major and trace elements contribute to 10% of $PM_{2.5}$ at ZK and 8% at FA. As for the carbonaceous matter (OC+EC), they explain 17.6% at ZK and 13.5% at FA of $PM_{2.5}$ mass **(Table III-7)**. Additionally, all the identified primary and secondary organic compounds contribute only to 16.7% of OC mass at ZK and 34.8% at FA with levoglucosan and fatty acids as the major contributors.

The health risk assessment at ZK showed that V and Ni, considered as tracers for HFO combustion, recorded the highest cumulative cancer risk values between $PM_{2.5}$ components for all age categories, exceeding the cancer risk threshold limit and adding by that 40 additional cancer cases per million habitants. Concerning VOCs, high concentrations of benzene, ethylbenzene, and 1,3-butadiene were detected in the region and are mainly linked to combustion processes. The cancer risk values due to the exposure to these species exceeded 166 times the threshold limit.

As previously mentioned, ZK site is under the influence of the power plant that is still operating on HFO, although the plant is close to residential areas. The main tracers that were assigned to this source were indeno[1,2,3-c,d]pyrene, V and Ni. A characteristic ratio of indeno[1,2,3-c,d]pyrene/(indeno[1,2,3-c,d]pyrene + benzo[g,h,i] perylene) in the range of 0.80-1.0 was assigned to the HFO combustion from the power plant. This source ranked third in contribution to $PM_{2.5}$ (13%) after crustal dust (27.5%) and secondary ammonium sulfate (15.7%), and first in contribution regarding primary anthropogenic emissions **(Fig. III- 16)**. HFO combustion source showed significant correlations with both assays of oxidative potential (OP-AA and OP-DTT), contributing to 31.4% of the average value of $OP\text{-}AA_v$ and 46.0% of $OP\text{-}DTT_v$ average value **(Figure IV-7)**. All of these results show that HFO combustion in particular and the power

plant in general not only show a major impact on the air quality in the region, but also might lead to health problems. Another anthropogenic source that has a high impact on the air quality in the ZK region is the vehicular emissions. In fact, due to the absence of public transportation systems, the air quality in Lebanon in general is affected by road transport emissions. Particularly, exhaust and non-exhaust vehicular emissions contribute to 14% of $PM_{2.5}$ at ZK. It was mainly identified by different tracers such as carbonaceous matter, hopanes, PAHs, and elements (Cu, Sb, and Sn attributed to road dust). The proximity of the site to a congested highway linking the capital Beirut to the North of Lebanon might explain this high contribution. Additionally, exhaust and non-exhaust (from lubricating oil emissions) vehicular emissions contribute to both OP-AA (18.9%) and OP-DTT (22.1%). However, we did not find any contribution of road dust to OP-AA and OP-DTT while applying the multiple linear regression, although Cu, Sb, and Sn were highly correlated to OP-DTT. More investigation should be made in order to further understand the reason behind this finding. Even though the biomass burning source from residential heating did not highly contribute to $PM_{2.5}$ (3.4%), we have found that it largely contributes to the value of OP-AA (31.5%) and less to OP-DTT (8.6%) **(Figure IV-7)**. This source is characterized by a strong seasonality with high concentrations of its organic tracer, levoglucosan, in the winter period compared to the summer one. Finally, diesel generators emissions did not highly contribute to the $PM_{2.5}$ atmospheric concentration (4.5%) and only show a contribution to OP evaluated by the DDT assay (4.8% for OP-DTT and no contribution for OP-AA). The low contribution of diesel generators to the $PM_{2.5}$ concentration might be linked to the presence of these generators between residential buildings that does not allow an important dispersion of the pollutants and it varies depending on the numbers of generators installed in the region.

Concerning FA site, the concentrations of V and Ni have led to high carcinogenic levels, exceeding the threshold limit of 10^{-6} and adding at least 20 additional cancer cases per million habitats at the site. Additionally, PAHs in $PM_{2.5}$, benzene, and ethylbenzene attributed to combustion activities showed cancer risk values exceeding the threshold limit for several age categories.

The industrial influence at FA was materialized by a factor attributed to the HFO combustion from cement factories and power plants in the Chekka region (4.1%) and another factor showing high levels of Ca and that was attributed to the cement manufacturing process (4.1%). It is worth noting that during the sampling period, the Lebanese government stopped the activity of

the cement plants for specific periods and suspended access to the quarries. That might explain the relatively low contribution of industrial emissions to $PM_{2.5}$ at FA. Nevertheless, HFO combustion and the cement plants emission show an important relationship with OP-DTT_v as observed by the hierarchical classification **(Table IV-10)**. We did not find a contribution of the quarries to the $PM_{2.5}$ concentrations but their impact might have been combined with the crustal factor since not all the samples that highly contribute to this factor were attributed to dust storm episodes. Another important anthropogenic source at FA is the open burning of waste (16.1%). It was mainly identified with high loadings of carbonaceous matter (OC and EC) and an OC/EC ratio of 7.1 that is generally attributed to municipal waste burning. This phenomenon is commonly observed in the North governorate of Lebanon where waste with different compositions is burned in different locations in the surroundings of the sampling site. This source also showed a relationship with OP-DTT_v. Finally, biomass burning source showed a relationship with OP-AA_v when evaluating the hierarchical classification. This source contributed to 5.2% of $PM_{2.5}$ mass and was identified with high loadings of levoglucosan as well as different concentration ratios of PAHs in the range of biomass burning.

For natural sources at both sites, primary and secondary biogenic emissions contributed to 9.3% at ZK and 13.4% at ZK site **(Fig. III- 16)**. These sources did not show an important contribution to the OP values at ZK and no relationship was detected between these sources and OP at FA. This could mean that these sources do not pose an important risk on human health. Furthermore, another natural source that highly contributes to the $PM_{2.5}$ concentrations at both sites is the crustal dust (27.5% at ZK and 23% at FA). Crustal dust mainly originates from the Saharan and Arabian deserts through long range transport of air masses with high loadings of Al, Mg, Ca, Fe, and Ti. Another influence of long-range transport is observed by high sulfate concentrations when air masses originate from Eastern and Central Europe, and Turkey with higher concentrations during summer period compared to winter. The ammonium sulfate factor contributes to 15.7% of $PM_{2.5}$ at ZK and 23.3% at FA. It also shows a considerable contribution with OP-DTT_v with 16.4% and a lower contribution for OP-AA_v (3.6%).

ZK site was influenced by anthropogenic emissions mainly HFO combustion from the power plant, vehicular emissions and biomass burning that showed an important contribution the OP measurements presented in this work. As for FA, the site was influenced by industrial emissions from cement factories and power plants and by open burning of waste. Biomass burning was also considered as an important anthropogenic source. These sources are deteriorating the air

quality at the considered sites and are emitting toxics for human health. That is why, different actions should be undertaken to reduce the impact of air pollution.

Recommendations

As already discussed, natural sources do not largely contribute to the toxicity of the air that we breathe. This toxicity was mainly linked to local anthropogenic sources and their effects could be mitigated via different actions and policies.

First of all, heavy fuel oil combustion has been shown to significantly contribute to $PM_{2.5}$ and has serious impact on human health. As it is definitely not possible to quickly stop such a power plant, it is essential to update the regulations regarding the quality of the fuel oil imported including its sulfur content and to update regulations regarding the emission limits for stack emissions from existing industrial establishments. Additionally, it is also recommended to replace HFO by a cleaner energy such as natural gas especially in big facilities such as the power plant at ZK and the cement factories at FA. This energy source is considered more friendly to the environment with greater efficiency and cost effectiveness. The usage of natural gas might be also a consistent solution to replace biomass burning for heating during winter periods. Additionally, even though the non-road diesel generators emissions did not highly contribute to $PM_{2.5}$ emissions, it is necessary to implement policies presenting limits for their stack emissions.

As for vehicular emissions, first of all, it is important to implement a national transportation system to reduce traffic emissions especially in urban areas and around the capital Beirut. Second of all, it is essential to update the current laws and regulations regarding on-road transport sector, and to implement cleaner fuel and Euro emission standards on vehicles.

One of the major sources identified at FA at the time of sampling was the open burning of waste that have severe consequences on human health. It is essential then to enforce the ban of open burning of garbage and to implement a national solid waste management plan in order to mitigate the health effects of this source. One of the proposed solutions might be the controlled incineration of waste in order to produce energy.

Finally, all of these recommendations will not give the desired results unless the law was enforced on the current regulations and legislations. Additionally, the Lebanese population should participate in this change. More accurate and scientific information on the health and

the environmental effects of these sources of atmospheric pollutants can be an efficient measure to reduce air pollution by raising awareness.

Perspectives

Thanks to the work done during this thesis, we have a better knowledge about the sources impacting two East-Mediterranean sites and the health risks associated to these sources by evaluating the health risk associated with exposure to different classes of compounds and by measuring the oxidative potential. As a result of this research, future studies should be mainly focused on several points that will presented hereafter.

The determination of intrinsic oxidative potential values in the study was made using multiple linear regression model that showed accurate results at one of the two sites. It is by that important to evaluate the intrinsic oxidative potential values using other mathematical approaches such as non-linear regression, non-negative least squares, and Anova models in order to better reconstruct OP values at FA and to compare the accuracy of the results at ZK between the models. Additionally, it is also important to apply the multiple linear regression model to the databases of the sites using tracer species and species correlating the most with OP values instead of sources.

On the other hand, the health risk assessment method was applied in this study on different classes of compounds considering species or a family of species. Many efforts should be done on the development of a model assessing the global health risk related to the combined exposure to different classes of pollutants. Therefore, it is convenient to try to integrate the health risk assessment in the PMF model in order to attribute carcinogenic and non-carcinogenic risks to different sources instead of attributing them to species.

Finally, a further characterization of fine particulate matter can be done by analyzing the concentrations of water-soluble organic compounds (WSOC) that might give us a further insight on the correlations with OP.

Appendices

Appendix A: Supplementary information 1

Chemical profiles of $PM_{2.5}$ emitted from various anthropogenic sources of the Eastern Mediterranean: cooking, wood burning, and diesel generators

Marc Fadel[1,2], Frédéric Ledoux[2], Marianne Seigneur[2], Konstantina Oikonomou[3], Jean Sciare[3], Dominique Courcot[2], Charbel Afif [1,3,].*

[1]Emissions, Measurements, and Modeling of the Atmosphere (EMMA) Laboratory, CAR, Faculty of Sciences, Saint Joseph University, Beirut, Lebanon

[2]Unité de Chimie Environnementale et Interactions sur le Vivant, UCEIV UR4492, FR CNRS 3417, University of Littoral Côte d′Opale (ULCO), Dunkerque, France

[3]Climate and Atmosphere Research Center, The Cyprus Institute, Nicosia, Cyprus

*Corresponding author: charbel.afif@usj.edu.lb

Table S1: Carbonaceous fractions, water-soluble ions and elements in $PM_{2.5}$ emitted by the different sources – (mg/g of sum of species)

	Species	**Wood burning** (WB)	**Diesel generator** (DG)	**Cooking**		
				Beef charcoal grilling (BG)	Chicken charcoal grilling (CG)	General cooking activities (GCA)
Number of samples		**3**	**4**	**1**	**1**	**5**
Carbonaceous fraction	OC	537 ± 109	633 ± 50	817	967	605 ± 121
	EC	181 ± 95	226 ± 51	18	1.55	34 ± 8
Total carbon (TC)		**718 ± 168**	**859 ± 40**	**835**	**969**	**639 ± 121**
Water-soluble ions	Cl^-	65.2 ± 45.6	<D.L	15.2	1.31	<D.L
	NO_3^-	3.01 ± 2.02	16.9 ± 5.0	6.51	1.34	28.5 ± 1.4
	SO_4^{2-}	16.5 ± 5.9	19.5 ± 4.8	11.4	3.61	121 ± 67
	Na^+	2.31 ± 1.38	3.25 ± 1.74	2.83	0.48	3.56 ± 1.62
	NH_4^+	8.15 ± 6.07	6.51 ± 1.61	0.90	0.30	41.0 ± 24.5
	K^+	65.8 ± 45.7	1.98 ± 1.21	23.7	5.61	4.05 ± 1.29
	Mg^{2+}	1.32 ± 0.36	0.67 ± 0.28	1.62	0.57	1.11 ± 0.28
	Ca^{2+}	16.6 ± 6.7	22.5 ± 9.2	8.43	1.69	23.8 ± 13.4
Total water-soluble ions		**179 ± 112**	**71 ± 21**	**71**	**15**	**223 ± 58**
Elements	Mg	2.16 ± 0.74	2.04 ± 0.55	3.14	0.76	4.30 ± 1.13
	Mn	0.15 ± 0.04	<D.L	0.08	0.01	0.13 ± 0.06
	Al	7.83 ± 1.73	8.49 ± 3.37	6.99	0.99	18.6 ± 2.9
	Na	5.25 ± 1.11	<D.L	4.75	1.24	16.1 ± 5.0
	Ca	22.3 ± 12.8	39.0 ± 11.4	46.8	5.02	34.73± 12.6
	Fe	4.37 ± 2.22	3.52 ± 0.81	3.44	0.39	7.63 ± 2.41
	K	51.8 ± 36.8	2.16 ± 0.75	21.4	4.89	4.49 ± 1.15
	P	0.63 ± 0.28	0.78 ± 0.15	1.01	0.30	1.01 ± 0.14
	S	7.22 ± 2.25	11.0 ± 3.0	5.53	2.47	47.6 ± 22.4
	Ti	0.61 ± 0.32	0.71 ± 0.2	0.53	0.05	1.06 ± 0.38
	V	0.02 ± 0.01	0.03 ± 0.01	0.02	0.004	0.28 ± 0.23
	Zn	0.51 ± 0.27	1.5 ± 0.09	0.25	0.03	1.06 ± 0.28
	Cu	0.03 ± 0.02	0.08 ± 0.02	0.03	0.01	0.10 ± 0.07

Ni	0.04 ± 0.02	0.14 ± 0.06	<D.L	<D.L	0.37 ± 0.20
Ba	<D.L	<D.L	<D.L	<D.L	<D.L
Cr	0.05 ± 0.02	<D.L	0.05	0.026	<D.L
Pb	0.41 ± 0.49	0.06 ± 0.01	0.05	<D.L	0.58 ± 0.14
Sr	0.04 ± 0.02	0.05 ± 0.01	0.17	0.035	0.10 ± 0.03
As	0.004 ± 0.001	0.0005 ± 0.0004	0.002	0.001	0.007 ± 0.001
Cd	0.013 ± 0.004	0.0005 ± 0.0003	0.031	0.001	0.003 ± 0.001
Co	0.002 ± 0.001	0.004 ± 0.001	0.004	0.000	0.009 ± 0.006
Rb	0.04 ± 0.02	<D.L	0.029	0.008	0.007 ± 0.003
Nb	0.004 ± 0.001	<D.L	0.021	0.002	0.009 ± 0.004
Ag	0.07 ± 0.05	0.24 ± 0.16	0.088	0.022	0.25 ± 0.16
Sn	0.002 ± 0.001	<D.L	0.002	<D.L	<D.L
Sb	0.003 ± 0.002	0.006 ± 0.001	0.002	0.001	0.03 ± 0.02
La	0.005 ± 0.003	<D.L	0.006	0.001	0.021 ± 0.014
Ce	0.009 ± 0.001	0.005 ± 0.002	0.010	0.002	0.010 ± 0.005
Bi	0.0007 ± 0.0002	0.0010 ± 0.0003	0.0005	0.0001	0.002 ± 0.001
Total elements	**104 ± 57**	**70.0 ± 19.8**	**94.4**	**16.3**	**139 ± 31**

Table S2: Chemical mass fraction to OC of n-alkanes, PAHs, carboxylic acids, and levoglucosan in $PM_{2.5}$ for the different sources (mg/g of OC)

	Species		**Wood burning** (WB)	**Diesel generator** (DG)	**Cooking**		
					Beef grilling (BG)	Chicken grilling (CG)	General cooking activities (GCA)
Alkanes	Tridecane	C13	<D.L	<D.L	0.02	0.01	<D.L
	Tetradecane	C14	<D.L	0.04 ± 0.01	0.03	0.01	<D.L
	Pentadecane	C15	<D.L	0.21 ± 0.18	0.04	0.03	<D.L
	Hexadecane	C16	<D.L	0.79 ± 0.60	0.04	0.02	0.07 ± 0.04
	Heptadecane	C17	<D.L	2.06 ± 1.23	0.05	0.04	0.06 ± 0.02
	Octadecane	C18	<D.L	6.16 ± 1.88	0.05	0.02	0.03 ± 0.01
	Nonadecane	C19	0.10 ± 0.08	14.2 ± 4.3	0.98	0.55	0.1 ± 0.04
	Eicosane	C20	0.07 ± 0.02	26.0 ± 5.8	0.40	0.38	0.14 ± 0.04
	Heneicosane	C21	0.13 ± 0.07	26.8 ± 6.9	0.19	0.16	0.25 ± 0.06
	Docosane	C22	0.16 ± 0.07	23.5 ± 6.6	0.34	0.19	0.54 ± 0.2
	Tricosane	C23	0.40 ± 0.13	17.5 ± 4.9	1.24	0.49	1.07 ± 0.6
	Tetracosane	C24	0.23 ± 0.10	13.0 ± 3.7	0.83	0.42	1.13 ± 0.2
	Pentacosane	C25	0.61 ± 0.36	7.27 ± 2.46	5.02	1.43	0.93 ± 0.39
	Hexacosane	C26	0.31 ± 0.10	4.20 ± 1.51	0.06	0.04	0.64 ± 0.1
	Heptacosane	C27	1.61 ± 1.15	1.73 ± 0.73	0.05	0.03	0.82 ± 0.19
	Octacosane	C28	0.32 ± 0.15	0.68 ± 0.38	0.04	0.05	0.61 ± 0.1
	Nonacosane	C29	3.39 ± 2.76	0.50 ± 0.28	0.40	0.11	1.44 ± 0.58
	Triacontane	C30	0.45 ± 0.30	0.24 ± 0.01	0.04	0.02	0.43 ± 0.12
	Hentriacontane	C31	1.68 ± 1.30	0.12 ± 0.08	0.16	0.10	0.94 ± 0.43
	Dotriacontane	C32	0.29 ± 0.19	0.08 ± 0.04	0.06	0.03	0.72 ± 0.4
	Total	**∑A**	**9.75 ± 6.50**	**145 ± 39**	**10.0**	**4.14**	**9.92 ± 2.25**
	Acenaphthylene	Acy	0.02 ± 0.01	<D.L	0.002	0.05	<D.L
	Acenaphthene	Ace	0.007 ± 0.004	0.005 ± 0.002	0.001	0.001	0.008 ± 0.006
	Fluorene	Flu	0.019 ± 0.005	0.005 ± 0.002	0.001	0.001	<D.L
	Anthracene	Anth	0.08 ± 0.06	0.04 ± 0.02	0.04	0.02	<D.L
	Phenanthrene	Phe	0.03 ± 0.01	0.008 ± 0.006	0.01	0.01	0.004 ± 0.001
	Fluoranthene	Fla	0.58 ± 0.31	0.09 ± 0.02	0.13	0.13	0.03 ± 0.01

Polycyclic Aromatic Hydrocarbons (PAHs)	Pyrene	Pyr	0.58 ± 0.29	0.27 ± 0.07	0.12	0.10	0.03 ± 0.02
	Benzo[a]anthracene	B[a]An	0.60 ± 0.08	0.02 ± 0.01	0.08	0.04	0.03 ± 0.02
	Chrysene	Chr	0.46 ± 0.07	0.02 ± 0.01	0.09	0.05	0.03 ± 0.01
	Benzo[b]fluoranthene	B[b]Fl	0.32 ± 0.14	0.02 ± 0.01	0.06	0.03	0.04 ± 0.03
	Benzo[k]fluoranthene	B[k]Fl	0.39 ± 0.04	0.013 ± 0.005	0.04	0.01	0.03 ± 0.02
	Benzo[a]pyrene	B[a]P	0.40 ± 0.13	0.006 ± 0.003	0.03	0.01	0.014 ± 0.008
	Dibenzo[a,h]anthracene	DiB[a,h]An	0.57 ± 0.26	<D.L	0.06	0.02	<D.L
	Benzo[g,h,i]perylene	B[ghi]Pe	0.26 ±0.07	0.019 ± 0.002	0.03	0.01	<D.L
	Indeno[1,2,3-c,d]pyrene	InPy	0.22 ± 0.09	0.004 ± 0.002	0.04	0.01	<D.L
	Total	**∑PAHs**	**4.55** ± 1.05	**0.53 ± 0.14**	**0.72**	**0.47**	**0.21 ± 0.15**
Carboxylic Acids	Dodecanoic acid	DDA	0.74 ± 0.26	8.85 ± 3.11	0.69	0.40	4.35 ± 2.16
	Tetradecanoic acid	TDA	1.34 ± 0.2	8.50 ± 3.02	13.2	2.62	6.04 ± 2.48
	Hexadecanoic acid	HDA	30.5 ± 14.5	23.7 ± 7.4	133	85.6	139 ± 52
	Octadecanoic acid	ODA	16.0 ± 7.0	35.9 ± 11.1	87.3	36.1	162 ± 87
	Eicosanoic acid	EA	6.16 ± 3.2	14.8 ± 5.5	3.23	3.50	11.2 ± 4.3
	Docosanoic acid	DA	26.7 ± 10.2	5.74 ± 2.75	5.87	12.8	35.8 ± 17.1
	Tetracosanoic acid	TA	8.57 ± 5.85	0.2 ± 0.1	0.54	1.26	6.07 ± 3.9
	Total	**∑FA**	**90.1 ± 31.8**	**97.3 ± 32.3**	**244**	**142**	**363 ± 138**
Sugars	Levoglucosan	Lev	302 ± 103	1.30 ± 0.49	2.43	0.53	24.5 ± 31.7

Table S3: PCDD/F and DL-PCBs contribution to OC (pg/g of OC) for the different sources

Compounds		TEF	Wood burning	Diesel generator	Cooking	
					Beef and chicken charcoal grilling	General cooking activities
PCDD						
2,3,7,8-tetrachlorinated dibenzo-p-dioxin	2,3,7,8 TCDD	1	<D.L	<D.L	< D.L	< D.L
1,2,3,7,8-pentachlorinated dibenzo-p-dioxin	1,2,3,7,8 PeCDD	1	<D.L	<D.L	60	< D.L
1,2,3,4,7,8-hexachlorinated dibenzo-p-dioxin	1,2,3,4,7,8 HxCDD	0.1	<D.L	<D.L	< D.L	< D.L
1,2,3,6,7,8-hexachlorinated dibenzo-p-dioxin	1,2,3,6,7,8 HxCDD	0.1	<D.L	<D.L	110	< D.L
1,2,3,7,8,9-hexachlorinated dibenzo-p-dioxin	1,2,3,7,8,9 HxCDD	0.1	<D.L	<D.L	< D.L	< D.L
1,2,3,4,6,7,8-heptachlorinated dibenzo-p-dioxin	1,2,3,4,6,7,8 HpCDD	0.01	1880	2370	800	2600
octachlorinated dibenzo-p-dioxin	OCDD	0.0003	5160	7750	2240	< D.L
		Total PCDD	***7040***	***10120***	***3210***	***2600***
		TEQ for PCDD	**20**	**26**	**78**	**26**
PCDF						
2,3,7,8 tetrachlorinated dibenzofuran	2,3,7,8 TCDF	0.1	< D.L	< D.L	< D.L	< D.L
1,2,3,7,8 pentachlorinated dibenzofuran	1,2,3,7,8 PeCDF	0.03	< D.L	< D.L	< D.L	< D.L
2,3,4,7,8 pentachlorinated dibenzofuran	2,3,4,7,8 PeCDF	0.3	< D.L	< D.L	170	< D.L
1,2,3,4,7,8 hexachlorinated dibenzofuran	1,2,3,4,7,8 HxCDF	0.1	< D.L	< D.L	110	< D.L
1,2,3,6,7,8 hexachlorinated dibenzofuran	1,2,3,6,7,8 HxCDF	0.1	< D.L	< D.L	100	< D.L
2,3,4,6,7,8 hexachlorinated dibenzofuran	2,3,4,6,7,8 HxCDF	0.1	< D.L	1195	180	< D.L
1,2,3,7,8,9 hexachlorinated dibenzofuran	1,2,3,7,8,9 HxCDF	0.1	< D.L	< D.L	< D.L	< D.L
1,2,3,4,6,7,8-heptachlorinated dibenzofuran	1,2,3,4,6,7,8 HpCDF	0.01	725	3307	450	1070
1,2,3,4,7,8,9-heptachlorinated dibenzofuran	1,2,3,4,7,8,9 HpCDF	0.01	< D.L	< D.L	< D.L	< D.L
octachlorinated dibenzofuran	OCDF	0.0003	1430	4195	640	< D.L
		Total PCDF	***2156***	***8698***	***1650***	***1070***
		TEQ for PCDF	**8**	**154**	**93**	**11**
PCB						
3,4,4',5-Tetrachlorobiphenyl	PCB 81	0.0003	< D.L	< D.L	< D.L	< D.L
3,3′,4,4′-Tetrachlorobiphenyl	PCB 77	0.0001	< D.L	< D.L	< D.L	< D.L
2,3',4,4',5'-Pentachlorobiphenyl	PCB 123	0.00003	8930	5580	3510	< D.L
2,3',4,4',5-Pentachlorobiphenyl	PCB 118	0.00003	52130	90630	18010	192700

2,3,4,4',5-Pentachlorobiphenyl	PCB 114	0.00003	3330	< D.L	< D.L	9700
2,3,3',4,4'-Pentachlorobiphenyl	PCB 105	0.00003	27710	59940	10120	118670
3,3',4,4',5-Pentachlorobiphenyl	PCB 126	0.1	< D.L	< D.L	< D.L	< D.L
2,3',4,4',5,5'-Hexachlorobiphenyl	PCB 167	0.00003	< D.L	< D.L	< D.L	12830
2,3,3',4,4',5-Hexachlorobiphenyl	PCB 156	0.00003	< D.L	< D.L	2310	35330
2,3,3',4,4',5'-Hexachlorobiphenyl	PCB 157	0.00003	< D.L	< D.L	< D.L	< D.L
3,3',4,4',5,5'-Hexachlorobiphenyl	PCB 169	0.03	< D.L	< D.L	< D.L	< D.L
2,3,3',4,4',5,5'-Heptachlorobiphenyl	PCB 189	0.00003	< D.L	< D.L	< D.L	< D.L
		Total PCB	***92100***	***156150***	***33950***	***369230***
		TEQ for PCB	**3**	**5**	**1**	**11**
		Total TEQ	**31**	**185**	**172**	**48**

Figure S1: Contents (in µg/g) of the different species in the carbonaceous, ionic, and elemental fractions for the different sources

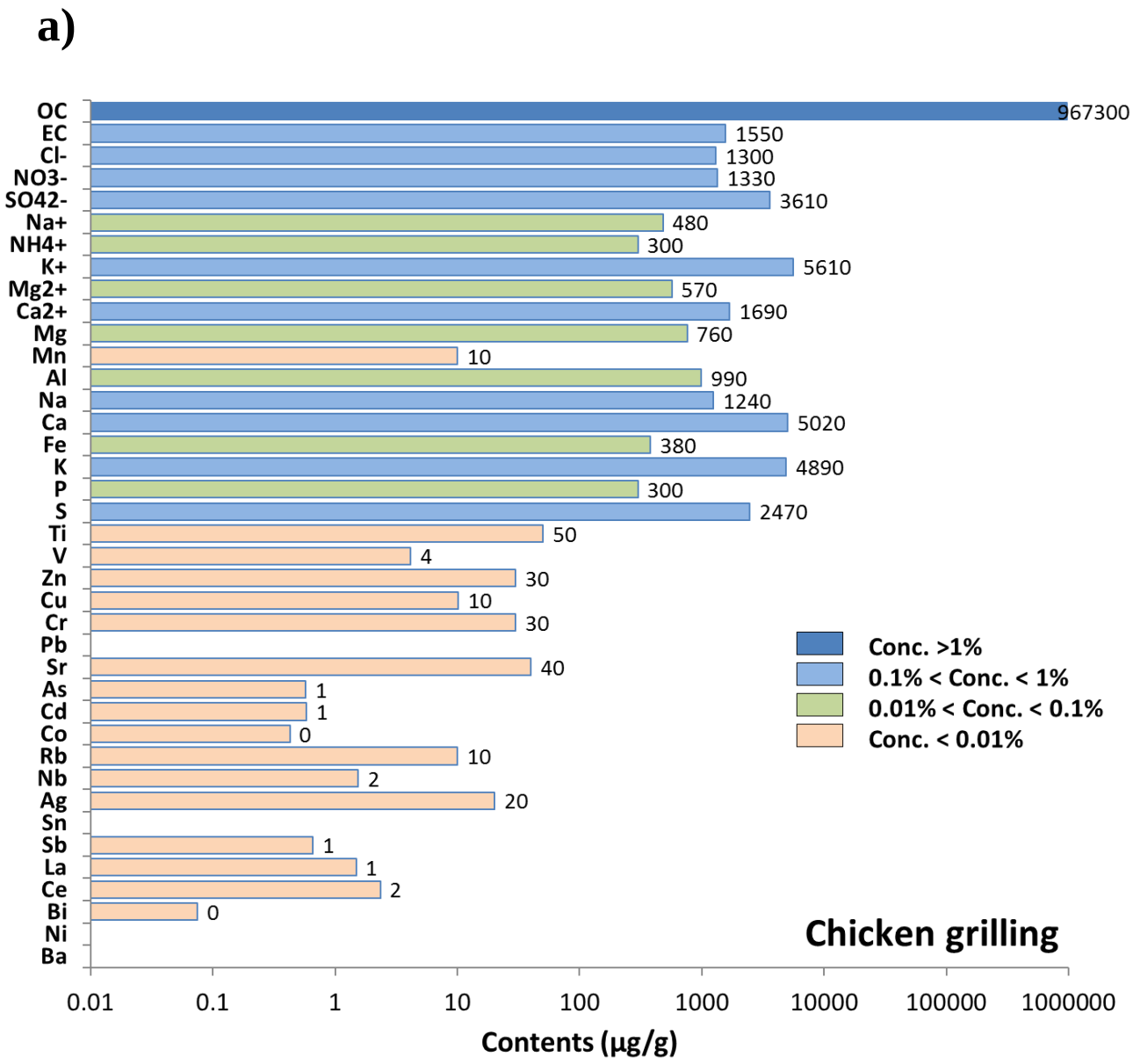

b)

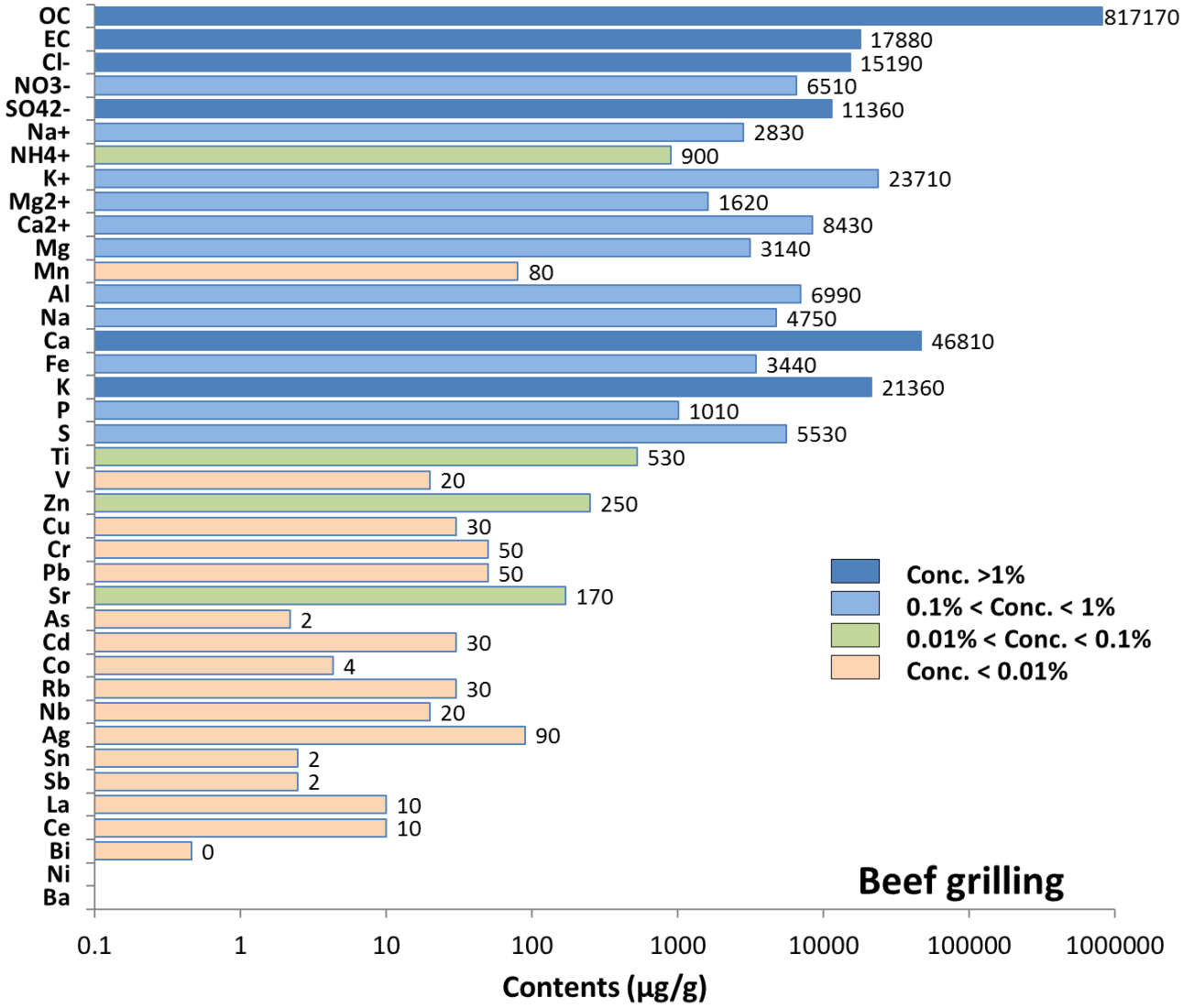
OC
EC
Cl-
NO3-
SO42-
Na+
NH4+
K+
Mg2+
Ca2+
Mg
Mn
Al
Na
Ca
Fe
K
P
S
Ti
V
Zn
Cu
Cr
Pb
Sr
As
Cd
Co
Rb
Nb
Ag
Sn
Sb
La
Ce
Bi
Ni
Ba
817170
17880
15190
6510
11360
2830
900
23710
1620
8430
3140
80
6990
4750
46810
3440
21360
1010
5530
530
20
250
30
50
50
170
2
30
4
30
20
90
2
2
10
10
0
Conc. >1%
0.1% < Conc. < 1%
0.01% < Conc. < 0.1%
Conc. < 0.01%
Beef grilling
0.1
1
10
100
1000
10000
100000
1000000
Contents (µg/g)

c)

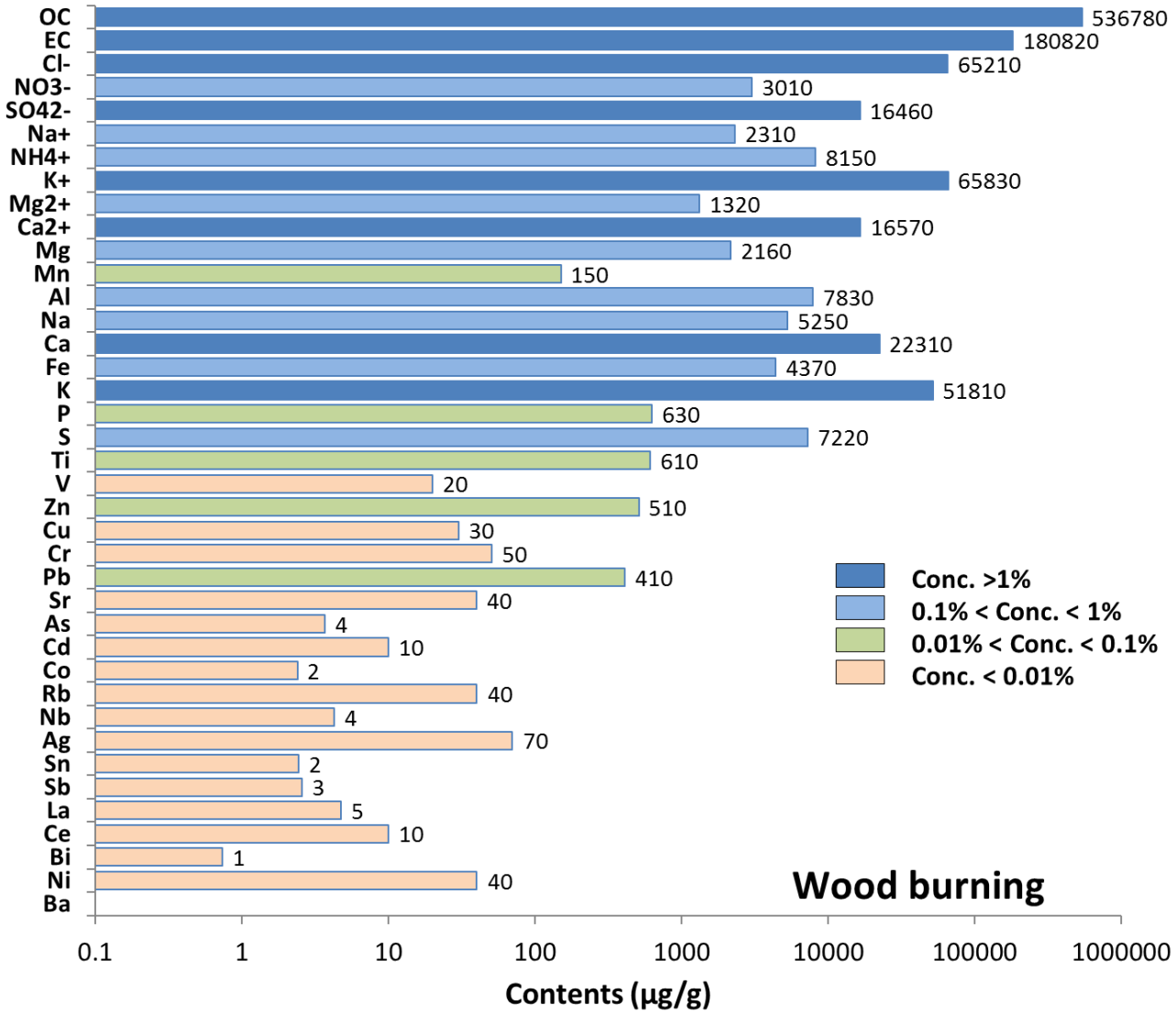
OC 536780
EC 180820
Cl- 65210
NO3- 3010
SO42- 16460
Na+ 2310
NH4+ 8150
K+ 65830
Mg2+ 1320
Ca2+ 16570
Mg 2160
Mn 150
Al 7830
Na 5250
Ca 22310
Fe 4370
K 51810
P 630
S 7220
Ti 610
V 20
Zn 510
Cu 30
Cr 50
Pb 410
Sr 40
As 4
Cd 10
Co 2
Rb 40
Nb 4
Ag 70
Sn 2
Sb 3
La 5
Ce 10
Bi 1
Ni 40
Ba
Conc. >1%
0.1% < Conc. < 1%
0.01% < Conc. < 0.1%
Conc. < 0.01%
Wood burning
0.1
1
10
100
1000
10000
100000
1000000
Contents (µg/g)

d)

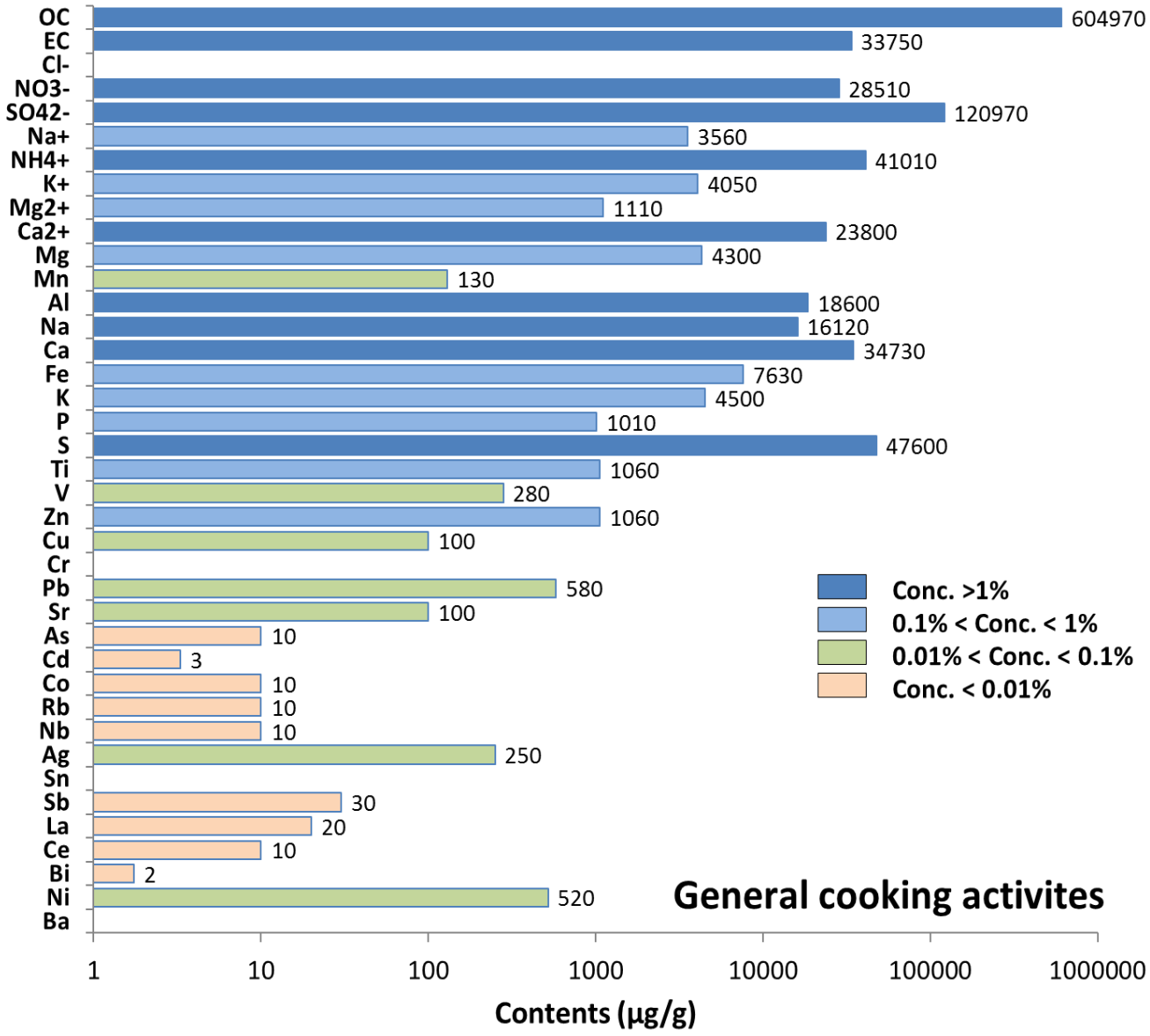
OC
EC
Cl-
NO3-
SO42-
Na+
NH4+
K+
Mg2+
Ca2+
Mg
Mn
Al
Na
Ca
Fe
K
P
S
Ti
V
Zn
Cu
Cr
Pb
Sr
As
Cd
Co
Rb
Nb
Ag
Sn
Sb
La
Ce
Bi
Ni
Ba
604970
33750
28510
120970
3560
41010
4050
1110
23800
4300
130
18600
16120
34730
7630
4500
1010
47600
1060
280
1060
100
580
100
10
3
10
10
10
250
30
20
10
2
520
Conc. >1%
0.1% < Conc. < 1%
0.01% < Conc. < 0.1%
Conc. < 0.01%
General cooking activites
1
10
100
1000
10000
100000
1000000
Contents (µg/g)

e)

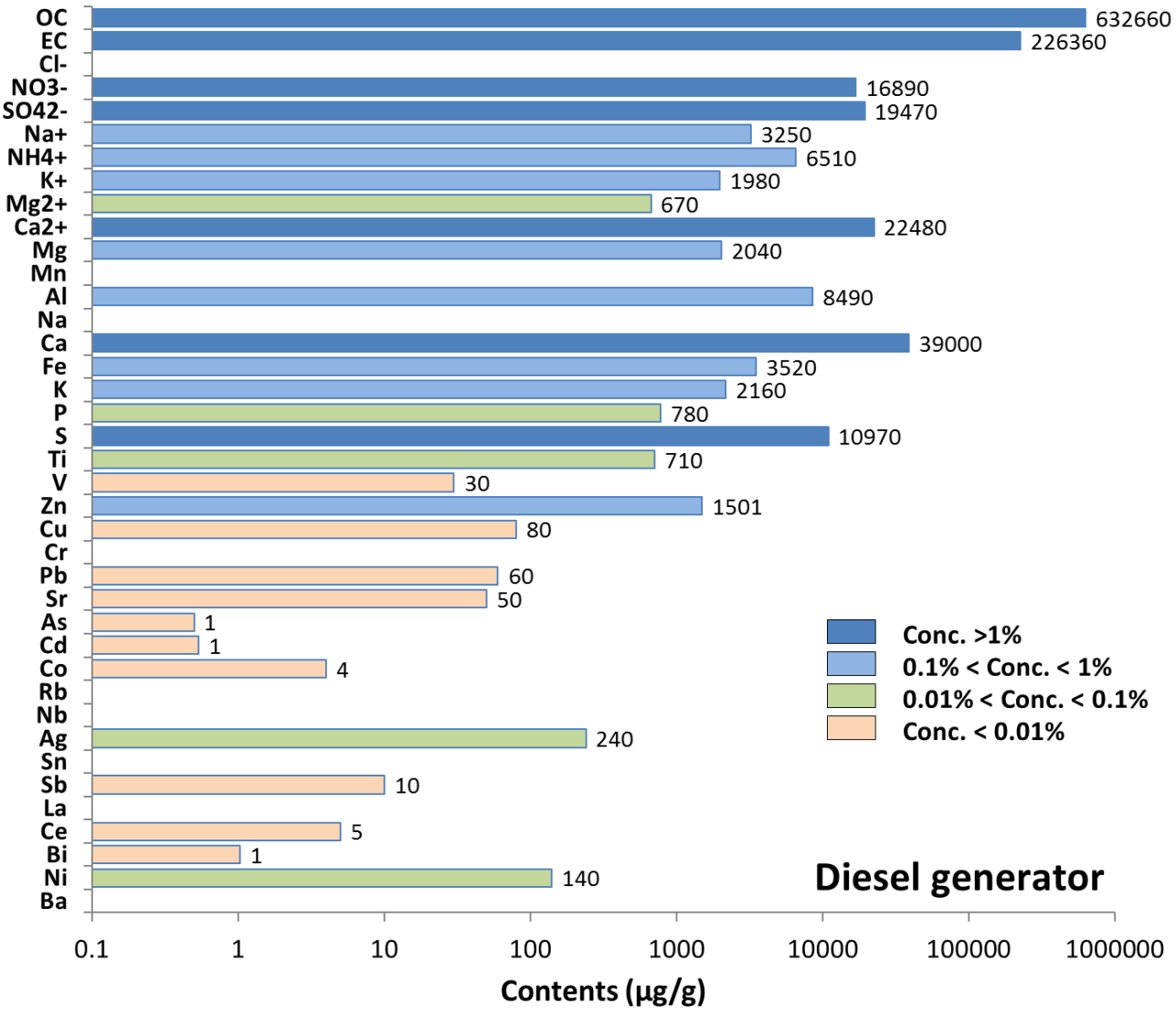
OC
EC
Cl-
NO3-
SO42-
Na+
NH4+
K+
Mg2+
Ca2+
Mg
Mn
Al
Na
Ca
Fe
K
P
S
Ti
V
Zn
Cu
Cr
Pb
Sr
As
Cd
Co
Rb
Nb
Ag
Sn
Sb
La
Ce
Bi
Ni
Ba
632660
226360
16890
19470
3250
6510
1980
670
22480
2040
8490
39000
3520
2160
780
10970
710
30
1501
80
60
50
1
1
4
240
10
5
1
140
Conc. >1%
0.1% < Conc. < 1%
0.01% < Conc. < 0.1%
Conc. < 0.01%
Diesel generator
0.1
1
10
100
1000
10000
100000
1000000
Contents (µg/g)

Appendix B: Supplementary information 2

$PM_{2.5}$ characterization of primary and secondary organic aerosols in two urban-industrial areas in the East Mediterranean

Marc Fadel[1,2], Frédéric Ledoux[2], Mariana Farhat[1], Adib Kfoury[3], Dominique Courcot[2], Charbel Afif[1,4,]*

5. Emissions, Measurements, and Modeling of the Atmosphere (EMMA) Laboratory, CAR, Faculty of Sciences, Saint Joseph University, Beirut, Lebanon
6. Unité de Chimie Environnementale et Interactions sur le Vivant, UCEIV UR4492, FR CNRS 3417, University of Littoral Côte d′Opale (ULCO), Dunkerque, France
7. Department of Environmental Sciences, University of Balamand, Al Kourah, Lebanon
8. Climate and Atmosphere Research Center, The Cyprus Institute, Nicosia, Cyprus

---

*Corresponding author. charbel.afif@usj.edu.lb (Charbel Afif)

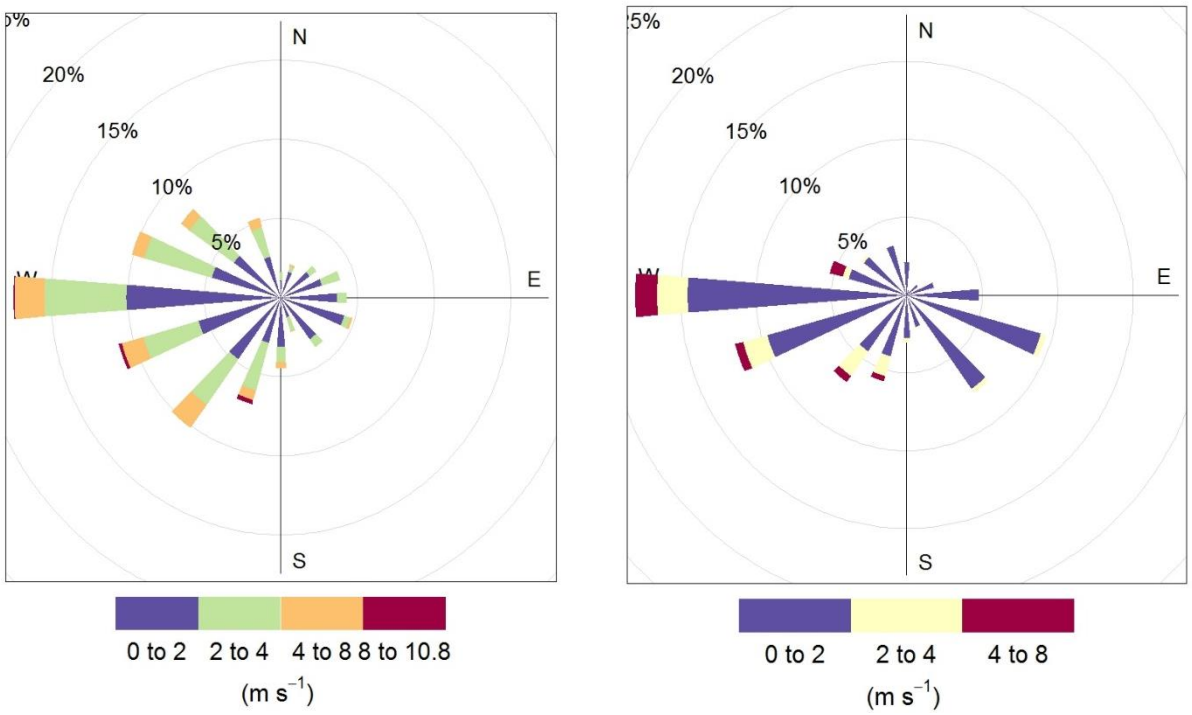

Fig. S1: Windrose of the two selected filters in Zouk (ZK) that are predominately down wind of the power plant (to the west of the sampling site) encompassing wind speeds higher than 2 m/s

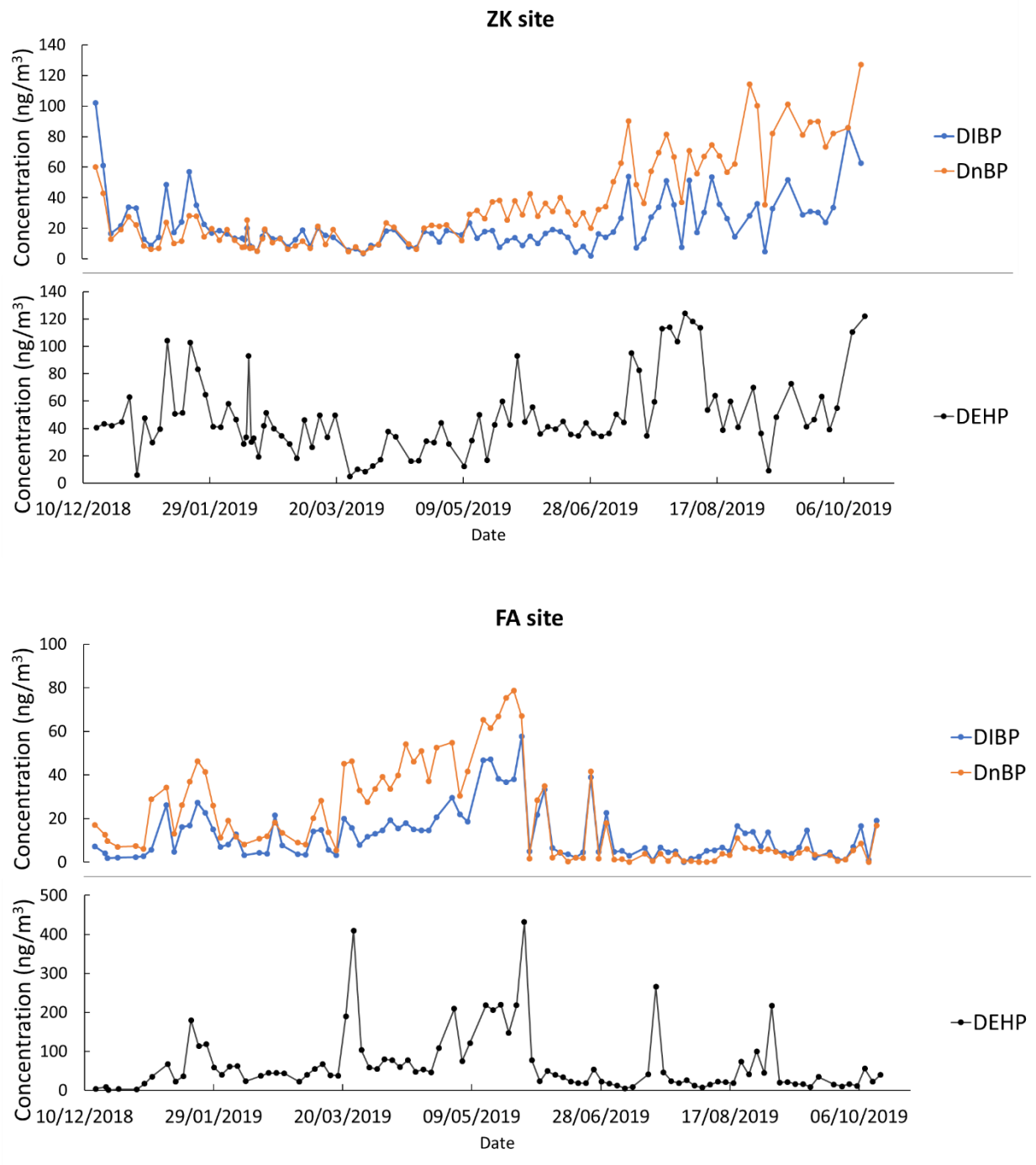

Fig. S2: Time Series of diisobutylphthalate (DIBP), dibutylphthalate (DnBP) Bis(2-ethylhexylphthalate) (DEHP) at Zouk (ZK) and Fiaa (FA) for the total period

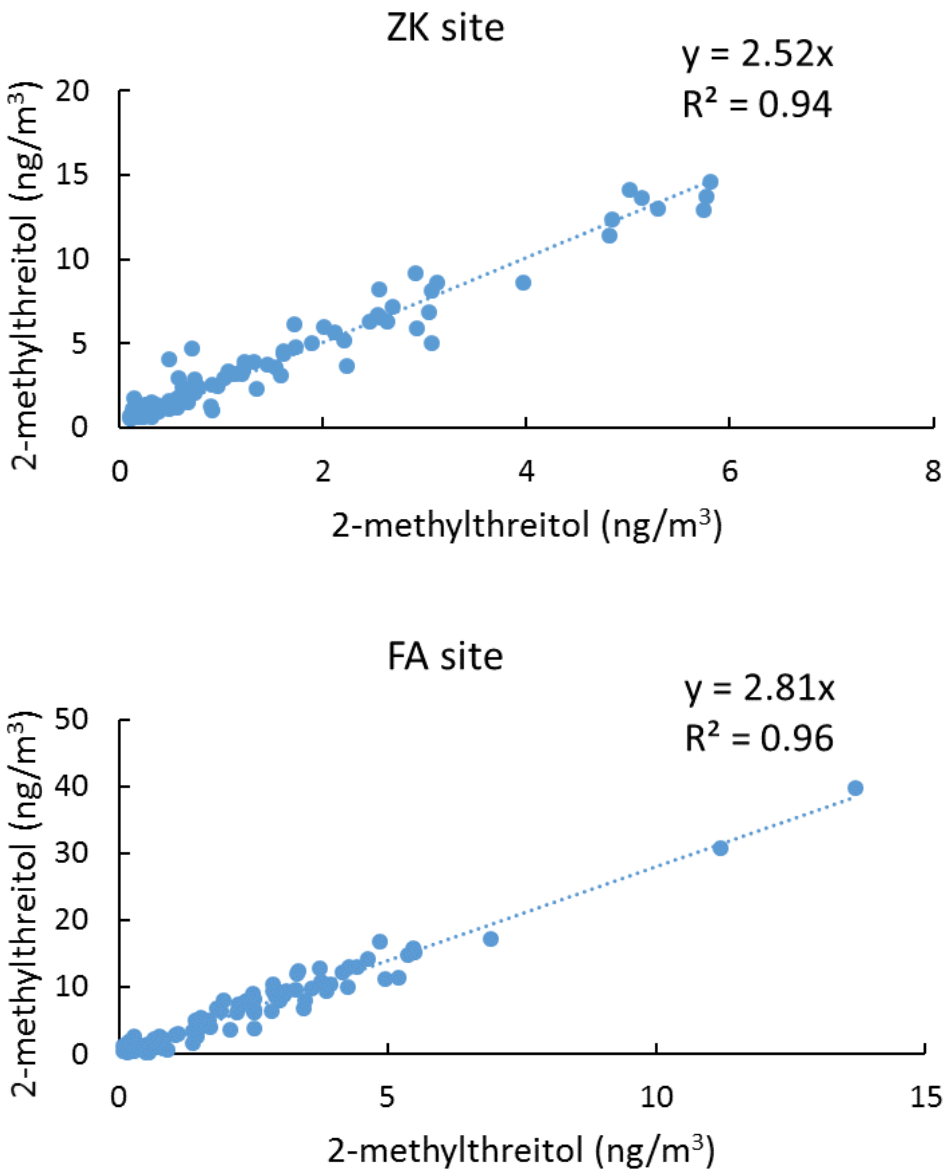

Fig. S3: Scatter plot between 2-methylthreitol (MT1) vs 2 methylerythritol (MT2) at Zouk (ZK) and Fiaa (FA) for the total period

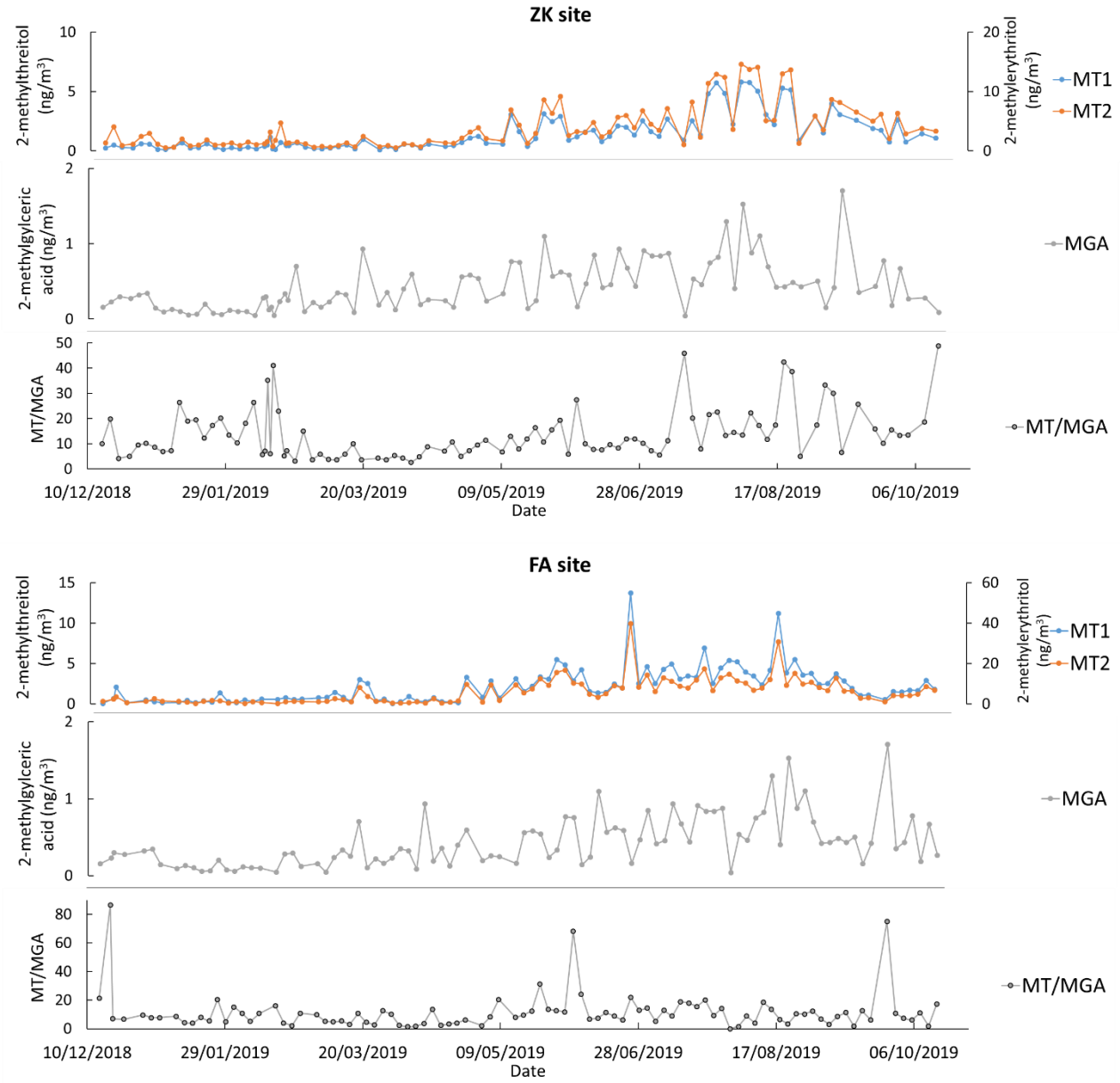

Fig. S4: Time Series of 2-methylthreitol (MT1), 2-methylerythritol (MT2) 2-methylglyceric acid (2-MGA), and the ratio of (MT1+MT2)/(2-MGA) at Zouk (ZK) and Fiaa (FA) for the total period

Table S1: Atmospheric concentrations (in ng/m^3) of identified hopanes during weekdays (Mondays to Saturdays) and on Sundays for the total period at Zouk (ZK)

Average concentration (ng/m^3)			
Hopanes		Weekdays	Sundays
trisnorneohopane	H1	0.29	0.21
17α(H)-trisnorhopane	H2	0.38	0.32
17α(H)-21β(H)-norhopane	H3	1.11	0.83
17α(H)-21β(H)-hopane	H4	1.12	0.85
17α(H)-21β(H)-22S-homohopane	H5	0.79	0.54
17α(H)-21β(H)-22R-homohopane	H6	0.71	0.52
Total Hopanes	**∑Hop**	**4.40**	**3.27**

Table S2: Determination coefficient (R^2) for the correlation between 3-hydroxyglutaric acid (A1), 3-acetylglutaric acid (A2), 3-isopropylglutaric acid (A3), and 3-methyl-1,2,3-butanetricarboxylic acid (A4) at Zouk (ZK) and Fiaa (FA)

ZK	A1	A2	A3	A4
A1				
A2	0.83			
A3	0.80	0.82		
A4	0.85	0.84	0.77	

FA	A1	A2	A3	A4
A1				
A2	0.84			
A3	0.78	0.80		
A4	0.85	0.82	0.75	

Appendix C: Supplementary information 3

$PM_{2.5}$ chemical characterization and sources identification in two sites in the East Mediterranean

Marc Fadel[a,b], Dominique Courcot[b], Marianne Seigneur[b], Adib Kfoury[d], Konstantina Oikonomou[c], Jean Sciare[c], Frédéric Ledoux[b] ,Charbel Afif [a,c,„]*

[a] Emissions, Measurements, and Modeling of the Atmosphere (EMMA) Laboratory, CAR, Faculty of Sciences, Saint Joseph University, Beirut, Lebanon

[b] Unité de Chimie Environnementale et Interactions sur le Vivant, UCEIV UR4492, FR CNRS 3417, University of Littoral Côte d′Opale (ULCO), Dunkerque, France

[c] Climate and Atmosphere Research Center, The Cyprus Institute, Nicosia, Cyprus

[d] Department of Environmental Sciences, University of Balamand, Al Kourah, Lebanon

*Corresponding author: charbel.afif@usj.edu.lb

Table S1: Input data statistics for PMF model at ZK site

Species	**Category**	**S/N**	**R^2**
$PM_{2.5}$	Total Variable (Defaults to Weak)	7.3	0.90
OC	Strong	3.6	0.85
EC	Strong	5.3	0.98
SO_4^{2-}	Strong	6.8	0.98
NO_3^-	Weak	2.8	0.39
NH_4^+	Strong	7.6	0.99
Cl^-	Strong	1.4	0.95
Na^+	Strong	2.5	0.86
Al	Strong	2.9	0.97
Ca	Strong	2.2	0.92
Cu	Strong	4.2	0.98
Fe	Strong	7.3	0.99
K	Strong	3.7	0.95
Mg	Strong	3.7	0.96
Ni	Strong	4.7	0.99
Sb	Strong	4.2	0.94
Sn	Strong	4.4	0.96
Ti	Strong	7.7	0.99
V	Strong	5.6	0.98
C_{20}	Strong	2.9	0.94
C_{21}	Strong	3.7	0.94
C_{24}	Strong	2.2	0.80
C_{25}	Strong	5.6	0.97
C_{27}	Strong	5.2	0.97
C_{29}	Strong	4.4	0.95
C_{31}	Strong	4.2	0.94
Levoglucosan	Strong	1.0	0.83
17α(H)-21β(H)-hopane	Strong	3.6	0.98
Hexadecanoic acid	Strong	2.8	0.96
Octadecanoic acid	Strong	2.2	0.94
Isoprene oxidation products	Strong	3.1	0.94
α-pinene oxidation products	Strong	2.4	0.93

Table S2: Input data statistics for PMF model at FA site

Species	**Category**	**S/N**	**R^2**
$PM_{2.5}$	Total Variable (Defaults to Weak)	7.3	0.88
OC	Strong	5.9	0.96
EC	Strong	4.3	0.89
SO_4^{2-}	Strong	9.8	0.99
NO_3^-	Weak	3.4	0.6
NH_4^+	Strong	9.5	0.99
Cl^-	Strong	2.1	0.98
Na^+	Strong	3.4	0.94
Al	Strong	2.1	0.94
Ca	Strong	5.0	0.95
Cu	Strong	7.7	0.99
Fe	Strong	4.1	0.98
K	Strong	3.8	0.96
Mg	Strong	3.6	0.91
Ni	Strong	3.2	0.97
Sb	Strong	4.3	0.98
Sn	Strong	5.2	0.98
Ti	Strong	5.3	0.97
V	Strong	4.3	0.99
C_{20}	Strong	3.5	0.95
C_{21}	Strong	3.4	0.93
C_{24}	Strong	2.3	0.92
C_{25}	Strong	4.8	0.93
C_{27}	Strong	4.0	0.97
C_{29}	Strong	4.0	0.97
C_{31}	Strong	2.7	0.96
Levoglucosan	Strong	2.3	0.98
17α(H)-21β(H)-hopane	-	-	-
Hexadecanoic acid	Strong	3.5	0.94
Octadecanoic acid	Strong	2.8	0.97
Isoprene oxidation products	Strong	2.8	0.98
α-pinene oxidation products	Strong	2.9	0.97

Table S3: Base error estimation summary for PMF results at ZK site

DISP diagnostics													
Error code	0												
Largest Decrease	-0.025												
%dQ	-0.002302535												
Swaps by Factors	1	2	3	4	5	6	7	8	9	10	11	12	
	0	0	0	0	0	0	0	0	0	0	0	0	
Bootstrap Mapping													
	1	2	3	4	5	6	7	8	9	10	11	12	Unmapped
Boot Factor 1	99	0	0	0	0	0	1	0	0	0	0	0	0
Boot Factor 2	0	92	2	0	0	1	3	0	0	0	1	0	1
Boot Factor 3	0	0	100	0	0	0	0	0	0	0	0	0	0
Boot Factor 4	0	0	0	100	0	0	0	0	0	0	0	0	0
Boot Factor 5	0	0	0	0	100	0	0	0	0	0	0	0	0
Boot Factor 6	0	0	1	0	0	98	1	0	0	0	0	0	0
Boot Factor 7	0	0	1	0	0	0	98	1	0	0	0	0	0
Boot Factor 8	0	0	0	0	0	1	1	96	2	0	0	0	0
Boot Factor 9	0	0	0	0	0	0	0	0	100	0	0	0	0
Boot Factor 10	0	0	0	0	0	0	0	0	0	100	0	0	0
Boot Factor 11	0	0	0	0	0	0	0	0	0	0	100	0	0
Boot Factor 12	0	0	0	0	0	0	0	0	0	0	0	100	0

Table S4: Base error estimation summary for PMF results at FA site

DISP diagnostics													
Error code	0												
Largest Decrease	0												
%dQ	0												
Swaps by Factors	1	2	3	4	5	6	7	8	9	10	11	12	
	0	0	0	0	0	0	0	0	0	0	0	0	
Bootstrap Mapping													
	1	2	3	4	5	6	7	8	9	10	11	12	Unmapped
Boot Factor 1	100	0	0	0	0	0	1	0	0	0	0	0	0
Boot Factor 2	0	98	0	0	0	0	0	0	1	1	0	0	0
Boot Factor 3	0	0	100	0	0	0	0	0	0	0	0	0	0
Boot Factor 4	0	1	0	98	1	0	0	0	0	0	0	0	0
Boot Factor 5	0	0	0	0	99	0	0	1	0	0	0	0	0
Boot Factor 6	0	0	0	0	0	100	0	0	0	0	0	0	0
Boot Factor 7	0	0	0	0	0	0	100	0	0	0	0	0	0
Boot Factor 8	0	0	0	0	0	0	0	100	0	0	0	0	0
Boot Factor 9	0	0	0	0	0	0	0	0	100	0	0	0	0
Boot Factor 10	0	0	0	0	0	2	0	1	0	97	0	0	0
Boot Factor 11	0	0	0	0	0	0	0	0	0	0	100	0	0
Boot Factor 12	1	0	1	0	0	0	0	1	0	1	0	96	0

Table S5: Average concentrations in µg.m^{-3} of $PM_{2.5}$, SO_4^{2-}, OC, EC, and the sum of elements (Mg, Al, Ti, Ca, Fe and K) for samples attributed to the different clusters (values in bold are indicative of long-range transport)

Cluster	**$PM_{2.5}$**	**SO_4^{2-}**	**NH_4^+**	**NO_3^-**	**OC**	**EC**	**Sum of elements (Mg, Al, Ti, Ca, Fe and K)**
1	23.7	**8.2**	2.7	0.7	2.9	0.6	1.3
2	22.1	**6.7**	2.2	1.1	2.9	0.6	1.5
3	32.9	**6.6**	2.3	1.5	4.1	0.9	2.8
4	**46.5**	3.6	1.2	1.7	**6.2**	**1.6**	**6.5**
5	22.0	3.0	0.9	1.4	3.2	0.7	2.1
6	**51.1**	3.1	0.5	2.1	**3.6**	**0.8**	**6.3**
7	35.3	**5.6**	1.8	1.6	4.8	1.0	3.4
8	12.0	2.3	0.7	0.5	1.9	0.5	0.7
9	17.1	2.0	0.5	0.9	3.3	0.6	0.4

Diagnostic factors of PMF models

For every number of factors chosen by PMF, two parameters can be calculated based on the scaled residuals matrix : the maximum individual mean (IM) and the maximum individual standard deviation (IS) where (Lee et al., 1999):

$$IM = \max_{j=1\ldots m}\left(\frac{1}{n}\times\sum_{i=1}^{n} r_{ij}\right) \; and \; IS = \max_{j=1\ldots m}\left(\sqrt{\frac{1}{n-1}\times\sum_{i=1}^{n}\left(r_{ij}-\bar{r_j}\right)^2}\right)$$

$$r_{ij} = \frac{e_{ij}}{s_{ij}}$$

When the number of factors increases to a critical value, IM and IS will show a drastic drop.

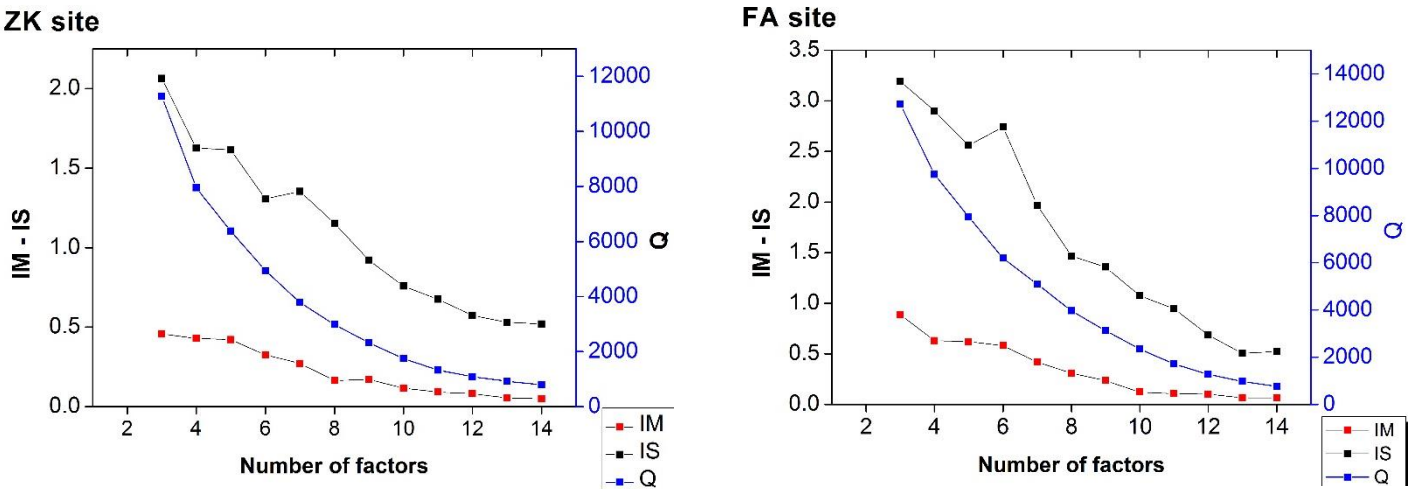

Figure S1: The diagnostic factor of PMF model showing IM, IS and Q-value for the different factor solutions for Zouk (ZK) and Fiaa (FA) sites

	Mg	Mn	Al	Ba	Ca	Fe	K	Ni	P	Pb	Sr	Ti	Zn	Sc	Cr	Co	Cu	As	Rb	Nb	Cd	Sn	Sb	La	Ce	Tl	Bi	V	Cl^-	NO_3^-	SO_4^{2-}	Na^+	NH_4^+	K^+	Mg^{2+}	Ca^{2+}	OC	EC	$PM_{2.5}$
Mg																																							
Mn	0.78																																						
Al	0.88	0.81																																					
Ba	0.69	0.82	0.63																																				
Ca	0.90	0.87	0.85	0.78																																			
Fe	0.93	0.89	0.92	0.76	0.94																																		
K	0.81	0.79	0.75	0.71	0.75	0.81																																	
Ni	0.26	0.28	0.29	0.22	0.27	0.34	0.32																																
P	0.75	0.67	0.71	0.59	0.75	0.80	0.68	0.66																															
Pb	0.40	0.49	0.43	0.45	0.43	0.47	0.41	0.58	0.64																														
Sr	0.95	0.84	0.90	0.77	0.95	0.97	0.82	0.27	0.78	0.45																													
Ti	0.93	0.87	0.92	0.77	0.93	0.97	0.78	0.27	0.73	0.44	0.96																												
Zn	0.57	0.61	0.50	0.59	0.60	0.67	0.67	0.75	0.79	0.65	0.61	0.59																											
Sc	0.08	0.11	0.14	-0.01	0.08	0.12	-0.01	-0.08	0.09	0.00	0.05	0.10	-0.12																										
Cr	0.36	0.24	0.28	0.09	0.28	0.34	0.28	0.06	0.34	0.15	0.34	0.31	0.17	0.45																									
Co	0.52	0.45	0.53	0.45	0.52	0.57	0.38	0.75	0.81	0.69	0.51	0.52	0.66	0.14	0.21																								
Cu	0.71	0.71	0.65	0.64	0.75	0.75	0.66	0.58	0.76	0.62	0.72	0.73	0.76	-0.16	0.11	0.64																							
As	0.48	0.38	0.41	0.29	0.46	0.50	0.59	0.49	0.55	0.28	0.48	0.46	0.66	-0.12	0.07	0.36	0.61																						
Rb	0.86	0.74	0.85	0.63	0.80	0.87	0.85	0.36	0.76	0.44	0.88	0.85	0.64	-0.06	0.30	0.54	0.68	0.64																					
Nb	0.48	0.32	0.35	0.21	0.35	0.44	0.45	0.16	0.39	0.13	0.44	0.42	0.33	0.35	0.82	0.28	0.18	0.19	0.43																				
Cd	0.41	0.40	0.34	0.40	0.43	0.42	0.50	0.52	0.52	0.66	0.41	0.38	0.65	-0.14	0.00	0.47	0.64	0.62	0.57	-0.01																			
Sn	0.68	0.60	0.63	0.52	0.70	0.73	0.65	0.63	0.80	0.62	0.71	0.68	0.79	-0.11	0.18	0.66	0.87	0.76	0.74	0.21	0.73																		
Sb	0.56	0.60	0.51	0.54	0.60	0.60	0.62	0.67	0.75	0.75	0.57	0.53	0.81	-0.15	0.05	0.60	0.76	0.57	0.57	0.13	0.72	0.80																	
La	0.54	0.34	0.43	0.27	0.44	0.49	0.43	0.19	0.48	0.31	0.51	0.49	0.32	0.31	0.82	0.40	0.29	0.29	0.50	0.71	0.17	0.40	0.25																
Ce	0.51	0.32	0.43	0.22	0.40	0.45	0.37	0.13	0.41	0.22	0.47	0.46	0.22	0.42	0.79	0.34	0.16	0.19	0.44	0.78	0.01	0.25	0.13	0.89															
Tl	0.47	0.37	0.47	0.24	0.34	0.44	0.61	0.37	0.46	0.37	0.45	0.42	0.47	-0.02	0.23	0.33	0.47	0.61	0.59	0.43	0.39	0.50	0.42	0.45	0.37														
Bi	0.30	0.19	0.29	0.18	0.29	0.31	0.43	0.59	0.45	0.25	0.33	0.28	0.51	-0.24	0.11	0.41	0.58	0.66	0.45	0.14	0.48	0.65	0.45	0.27	0.14	0.52													
V	0.25	0.17	0.26	0.12	0.24	0.32	0.30	0.92	0.65	0.47	0.26	0.24	0.70	-0.18	0.00	0.70	0.51	0.57	0.41	0.06	0.54	0.65	0.62	0.19	0.07	0.38	0.65												
Cl^-	0.45	0.24	0.32	0.20	0.39	0.31	0.23	0.17	0.34	0.23	0.36	0.32	0.10	0.06	0.06	0.35	0.31	0.09	0.32	-0.01	0.30	0.33	0.29	0.11	0.14	0.04	0.13	0.17											
NO_3^-	0.55	0.43	0.44	0.52	0.55	0.50	0.41	0.35	0.53	0.40	0.50	0.48	0.46	0.04	0.00	0.55	0.50	0.26	0.50	0.00	0.52	0.54	0.57	0.13	0.13	0.13	0.19	0.33	0.68										
SO_4^{2-}	0.01	-0.13	0.00	-0.19	-0.02	0.04	0.16	0.46	0.26	0.05	0.01	-0.01	0.41	-0.25	-0.05	0.19	0.23	0.65	0.24	0.02	0.43	0.43	0.33	0.13	-0.02	0.40	0.63	0.65	-0.12	0.05									
Na^+	0.48	0.11	0.28	0.09	0.31	0.28	0.26	0.20	0.34	0.10	0.33	0.29	0.15	-0.11	0.07	0.36	0.32	0.26	0.38	0.06	0.29	0.37	0.27	0.18	0.17	0.17	0.28	0.28	0.85	0.60	0.18								
NH_4^+	-0.25	-0.33	-0.23	-0.33	-0.25	-0.20	-0.06	0.35	0.03	-0.06	-0.24	-0.26	0.25	-0.24	-0.15	0.05	0.02	0.48	0.02	-0.11	0.32	0.21	0.16	-0.01	-0.14	0.22	0.49	0.55	-0.27	-0.06	0.93	0.02							
K^+	0.43	0.39	0.33	0.35	0.38	0.39	0.63	0.51	0.55	0.45	0.41	0.34	0.61	-0.17	0.11	0.42	0.56	0.62	0.57	0.21	0.67	0.60	0.68	0.26	0.16	0.53	0.51	0.52	0.30	0.51	0.49	0.40	0.34						
Mg^{2+}	0.77	0.43	0.61	0.36	0.59	0.61	0.57	0.30	0.62	0.33	0.66	0.62	0.42	-0.03	0.27	0.52	0.53	0.44	0.68	0.30	0.42	0.57	0.48	0.42	0.40	0.43	0.34	0.33	0.72	0.67	0.17	0.81	-0.08	0.57					
Ca^{2+}	0.88	0.82	0.83	0.73	0.96	0.92	0.74	0.33	0.77	0.44	0.92	0.90	0.63	0.04	0.32	0.56	0.75	0.51	0.82	0.38	0.48	0.73	0.62	0.47	0.42	0.41	0.34	0.30	0.44	0.62	0.09	0.42	-0.16	0.48	0.71				
OC	0.48	0.59	0.43	0.56	0.57	0.55	0.55	0.54	0.58	0.62	0.49	0.48	0.71	-0.11	0.02	0.54	0.72	0.55	0.57	0.07	0.71	0.70	0.78	0.23	0.11	0.38	0.37	0.45	0.18	0.54	0.21	0.15	0.10	0.63	0.38	0.60			
EC	0.56	0.70	0.52	0.67	0.68	0.63	0.61	0.41	0.58	0.49	0.61	0.60	0.64	-0.14	0.04	0.40	0.75	0.47	0.51	0.01	0.51	0.66	0.68	0.14	0.06	0.32	0.36	0.33	0.27	0.46	0.03	0.17	-0.13	0.49	0.37	0.66	0.70		
$PM_{2.5}$	0.76	0.60	0.74	0.53	0.72	0.75	0.74	0.54	0.82	0.49	0.76	0.71	0.72	-0.05	0.21	0.65	0.74	0.73	0.86	0.24	0.67	0.85	0.71	0.43	0.34	0.57	0.58	0.61	0.46	0.63	0.45	0.53	0.22	0.67	0.74	0.78	0.64	0.55	

Figure S2: Spearman correlation coefficients between the different compounds at ZK with yellow-colored values for coefficients higher than 0.8 and blue colored values for coefficients between 0.6 and 0.8

	Mg	Mn	Al	Ba	Ca	Fe	K	Ni	P	Pb	Sr	Ti	Zn	Sc	Cr	Co	Cu	As	Rb	Nb	Cd	Sn	Sb	La	Ce	Tl	Bi	V	Cl^-	NO_3^-	SO_4^{2-}	Na^+	NH_4^+	K^+	Mg^{2+}	Ca^{2+}	OC	EC	$PM_{2.5}$
Mg																																						
Mn	0.88																																					
Al	0.89	0.90																																				
Ba	0.35	0.35	0.41																																			
Ca	0.88	0.87	0.85	0.28																																		
Fe	0.92	0.96	0.95	0.33	0.89																																	
K	0.81	0.93	0.85	0.37	0.84	0.89																																
Ni	-0.01	0.18	-0.01	-0.18	0.09	0.14	0.20																															
P	0.73	0.84	0.71	0.25	0.82	0.82	0.85	0.38																														
Pb	0.41	0.48	0.42	0.27	0.44	0.43	0.47	0.06	0.49																													
Sr	0.94	0.91	0.88	0.37	0.94	0.94	0.87	0.14	0.82	0.40																												
Ti	0.92	0.92	0.94	0.33	0.88	0.97	0.84	0.03	0.76	0.36	0.91																											
Zn	0.44	0.61	0.29	0.22	0.41	0.48	0.61	0.46	0.58	0.43	0.48	0.36																										
Sc	0.54	0.50	0.53	0.19	0.61	0.50	0.47	0.11	0.46	0.21	0.58	0.54	0.01																									
Cr	0.66	0.74	0.68	0.25	0.69	0.71	0.79	0.21	0.73	0.42	0.71	0.65	0.45	0.65																								
Co	0.51	0.55	0.43	0.16	0.52	0.53	0.50	0.56	0.71	0.39	0.57	0.43	0.52	0.32	0.51																							
Cu	0.46	0.60	0.46	0.17	0.51	0.52	0.65	0.13	0.66	0.58	0.50	0.42	0.53	0.33	0.60	0.55																						
As	0.21	0.41	0.19	0.16	0.29	0.32	0.45	0.55	0.56	0.18	0.34	0.23	0.45	0.38	0.49	0.58	0.54																					
Rb	0.86	0.95	0.91	0.36	0.85	0.95	0.94	0.15	0.84	0.40	0.91	0.91	0.54	0.52	0.76	0.52	0.58	0.42																				
Nb	0.77	0.81	0.83	0.39	0.77	0.83	0.80	0.05	0.74	0.32	0.82	0.84	0.37	0.50	0.73	0.44	0.54	0.32	0.84																			
Cd	0.37	0.55	0.35	0.19	0.42	0.45	0.63	0.24	0.63	0.65	0.42	0.35	0.63	0.21	0.53	0.39	0.75	0.51	0.54	0.39																		
Sn	0.41	0.59	0.40	0.19	0.47	0.50	0.64	0.28	0.65	0.70	0.45	0.39	0.63	0.31	0.62	0.51	0.81	0.53	0.53	0.45	0.86																	
Sb	0.36	0.48	0.34	0.08	0.42	0.42	0.55	0.27	0.60	0.73	0.40	0.34	0.58	0.24	0.50	0.46	0.72	0.44	0.44	0.38	0.86	0.85																
La	0.69	0.72	0.74	0.27	0.75	0.74	0.69	0.28	0.76	0.40	0.77	0.72	0.43	0.49	0.67	0.72	0.57	0.48	0.75	0.70	0.40	0.45	0.46															
Ce	0.82	0.83	0.88	0.38	0.79	0.87	0.79	0.04	0.71	0.43	0.84	0.88	0.36	0.52	0.72	0.47	0.49	0.32	0.87	0.85	0.40	0.43	0.41	0.84														
Tl	0.25	0.39	0.27	-0.05	0.30	0.37	0.41	0.56	0.42	0.04	0.36	0.31	0.27	0.41	0.47	0.36	0.35	0.54	0.42	0.33	0.33	0.28	0.21	0.36	0.36													
Bi	0.14	0.31	0.02	-0.01	0.26	0.22	0.42	0.57	0.47	0.15	0.28	0.13	0.47	0.20	0.40	0.44	0.44	0.63	0.32	0.17	0.44	0.42	0.44	0.37	0.13	0.46												
V	0.12	0.30	0.07	-0.13	0.24	0.23	0.35	0.90	0.52	0.07	0.29	0.13	0.49	0.22	0.36	0.57	0.31	0.64	0.31	0.20	0.42	0.40	0.39	0.42	0.14	0.64	0.66											
Cl^-	0.32	0.23	0.34	0.27	0.27	0.24	0.21	-0.03	0.18	0.23	0.24	0.33	0.26	0.21	0.14	0.24	0.14	0.08	0.22	0.27	0.03	0.19	0.16	0.28	0.33	0.05	-0.06	-0.06										
NO_3^-	0.45	0.43	0.41	0.23	0.41	0.38	0.38	-0.06	0.40	0.61	0.37	0.38	0.40	0.12	0.30	0.37	0.50	0.05	0.34	0.32	0.46	0.51	0.54	0.38	0.40	-0.01	0.06	0.00	0.43									
SO_4^{2-}	-0.10	0.12	-0.10	-0.25	0.05	0.05	0.21	0.59	0.25	-0.15	0.06	0.00	0.21	0.10	0.29	0.18	0.19	0.62	0.18	0.08	0.34	0.26	0.24	0.21	0.06	0.54	0.64	0.70	-0.17	-0.26								
Na^+	0.42	0.24	0.27	-0.07	0.38	0.27	0.30	0.16	0.27	0.05	0.35	0.30	0.14	0.26	0.31	0.29	0.14	0.21	0.22	0.23	0.04	0.11	0.08	0.29	0.23	0.28	0.32	0.21	0.52	0.24	0.17							
NH_4^+	-0.29	-0.04	-0.31	-0.37	-0.19	-0.14	0.06	0.54	0.11	-0.10	-0.15	-0.25	0.20	-0.07	0.12	0.10	0.18	0.54	0.01	-0.12	0.39	0.29	0.30	0.00	-0.16	0.38	0.56	0.62	-0.34	-0.29	0.88	-0.09						
K^+	0.38	0.55	0.38	0.12	0.51	0.48	0.70	0.32	0.59	0.32	0.47	0.42	0.44	0.26	0.54	0.35	0.52	0.48	0.57	0.46	0.57	0.53	0.49	0.46	0.47	0.44	0.59	0.46	0.27	0.26	0.49	0.47	0.33					
Mg^{2+}	0.79	0.64	0.68	0.26	0.71	0.66	0.63	0.10	0.55	0.23	0.72	0.69	0.35	0.38	0.56	0.46	0.32	0.24	0.62	0.59	0.18	0.26	0.19	0.60	0.65	0.37	0.24	0.21	0.48	0.44	0.05	0.77	-0.25	0.47				
Ca^{2+}	0.78	0.79	0.83	0.27	0.95	0.81	0.77	0.08	0.74	0.38	0.83	0.85	0.31	0.51	0.63	0.41	0.44	0.28	0.78	0.73	0.36	0.40	0.36	0.70	0.76	0.32	0.22	0.21	0.36	0.43	0.08	0.43	-0.21	0.58	0.74			
OC	0.56	0.67	0.54	0.22	0.66	0.61	0.73	0.17	0.74	0.71	0.60	0.53	0.52	0.43	0.65	0.59	0.82	0.47	0.61	0.51	0.80	0.81	0.81	0.62	0.58	0.26	0.44	0.31	0.17	0.60	0.14	0.21	0.11	0.59	0.39	0.58		
EC	0.64	0.74	0.59	0.12	0.69	0.69	0.76	0.16	0.78	0.67	0.66	0.62	0.57	0.34	0.60	0.48	0.70	0.30	0.70	0.58	0.69	0.68	0.71	0.56	0.65	0.29	0.36	0.28	0.17	0.63	0.03	0.22	-0.01	0.55	0.45	0.62	0.80	
$PM_{2.5}$	0.58	0.69	0.63	0.23	0.66	0.64	0.73	0.24	0.73	0.56	0.62	0.59	0.48	0.46	0.69	0.58	0.73	0.58	0.68	0.58	0.71	0.76	0.70	0.70	0.67	0.39	0.42	0.42	0.30	0.59	0.35	0.32	0.23	0.66	0.56	0.67	0.81	0.65

Figure S3: Spearman correlation coefficients between the different compounds at FA with yellow-colored values for coefficients higher than 0.8 and blue colored values for coefficients between 0.6 and 0.8

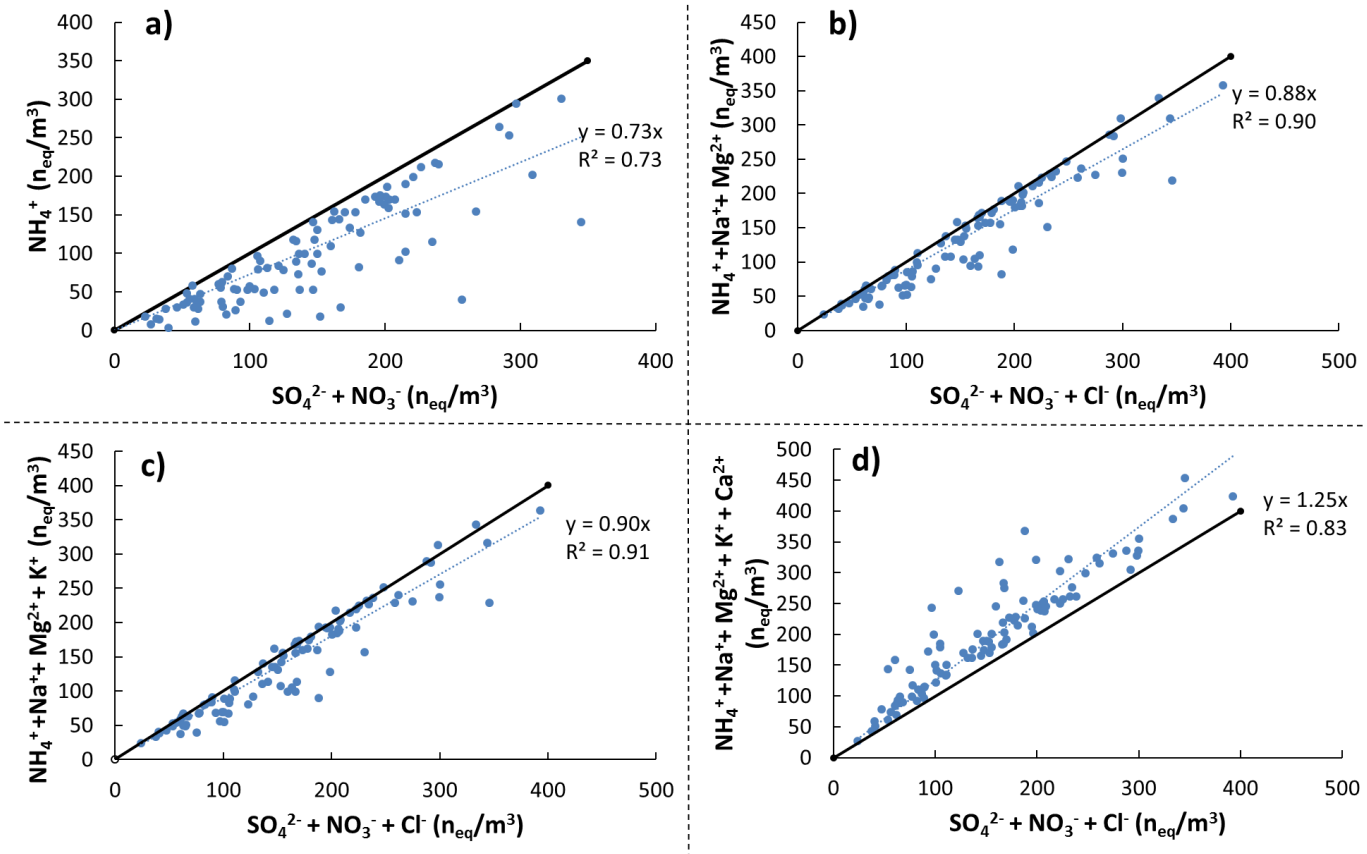

Figure S4: Ion balance evaluation between water soluble ions in $PM_{2.5}$ at ZK considering a) SO_4^{2-}, NO_3^-, and NH_4^+, b) SO_4^{2-}, NO_3^-, Cl^- and NH_4^+, Na^+, Mg^{2+}, c) SO_4^{2-}, NO_3^-, Cl^- and NH_4^+, Na^+, Mg^{2+}, K^+, (d) all analyzed cations and anions

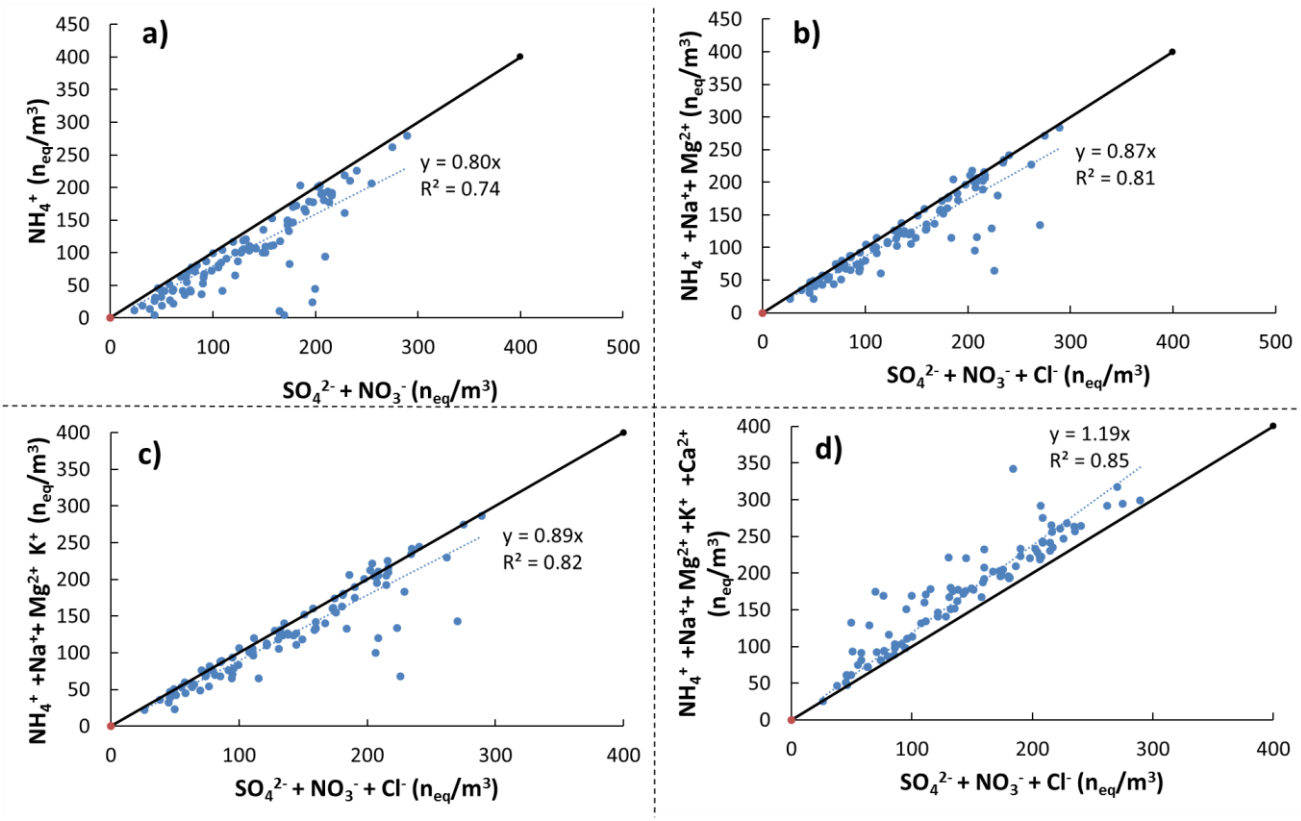

Figure S5: Ion balance evaluation between water soluble ions in $PM_{2.5}$ at FA considering a) SO_4^{2-},NO_3^-, and NH_4^+, b) SO_4^{2-}, NO_3^-, Cl^- and NH_4^+, Na^+, Mg^{2+}, c) SO_4^{2-}, NO_3^-, Cl^- and NH_4^+, Na^+, Mg^{2+}, K^+, (d) all analyzed cations and anions

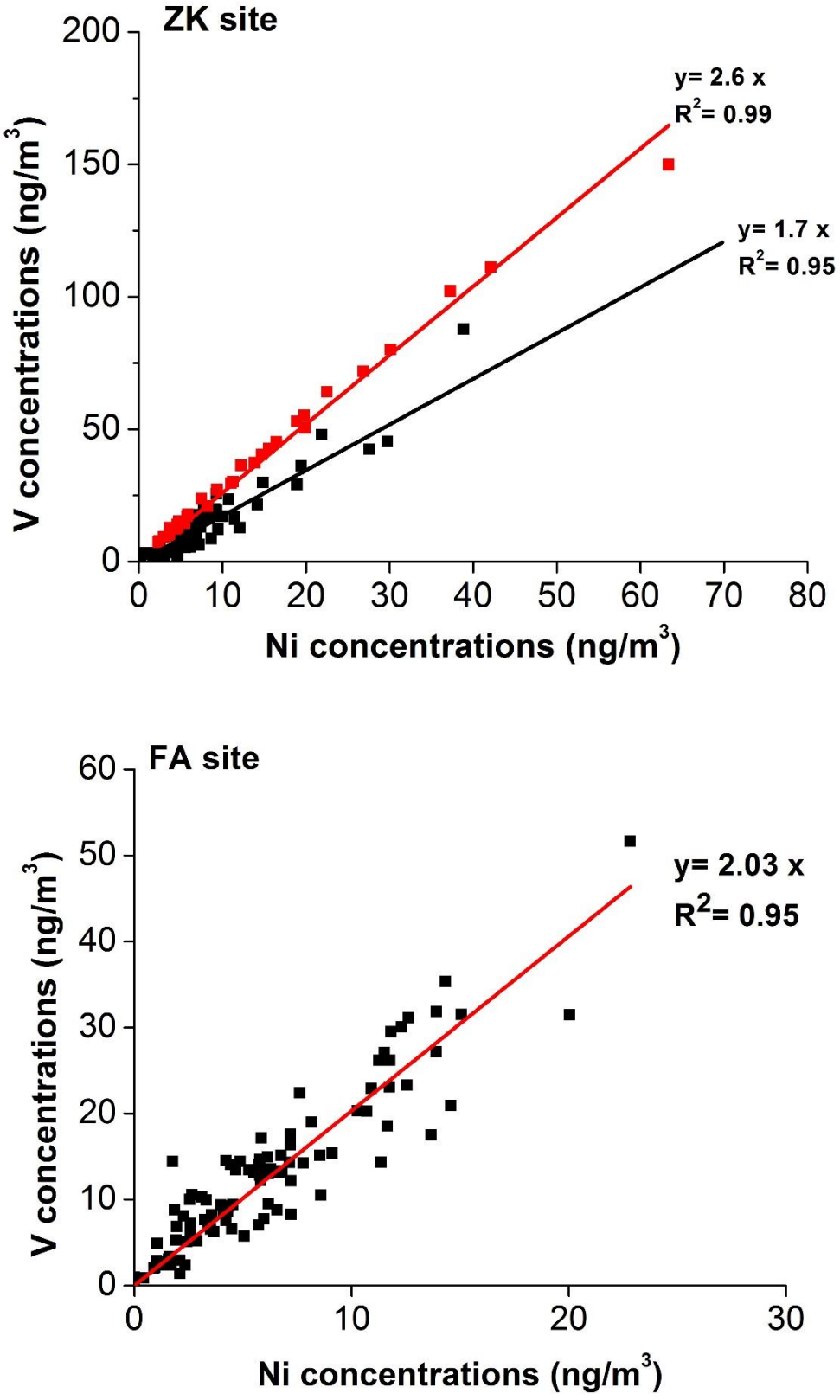

Figure S6: Scatter plot between V and Ni at Zouk (ZK) and Fiaa (FA) for the total period

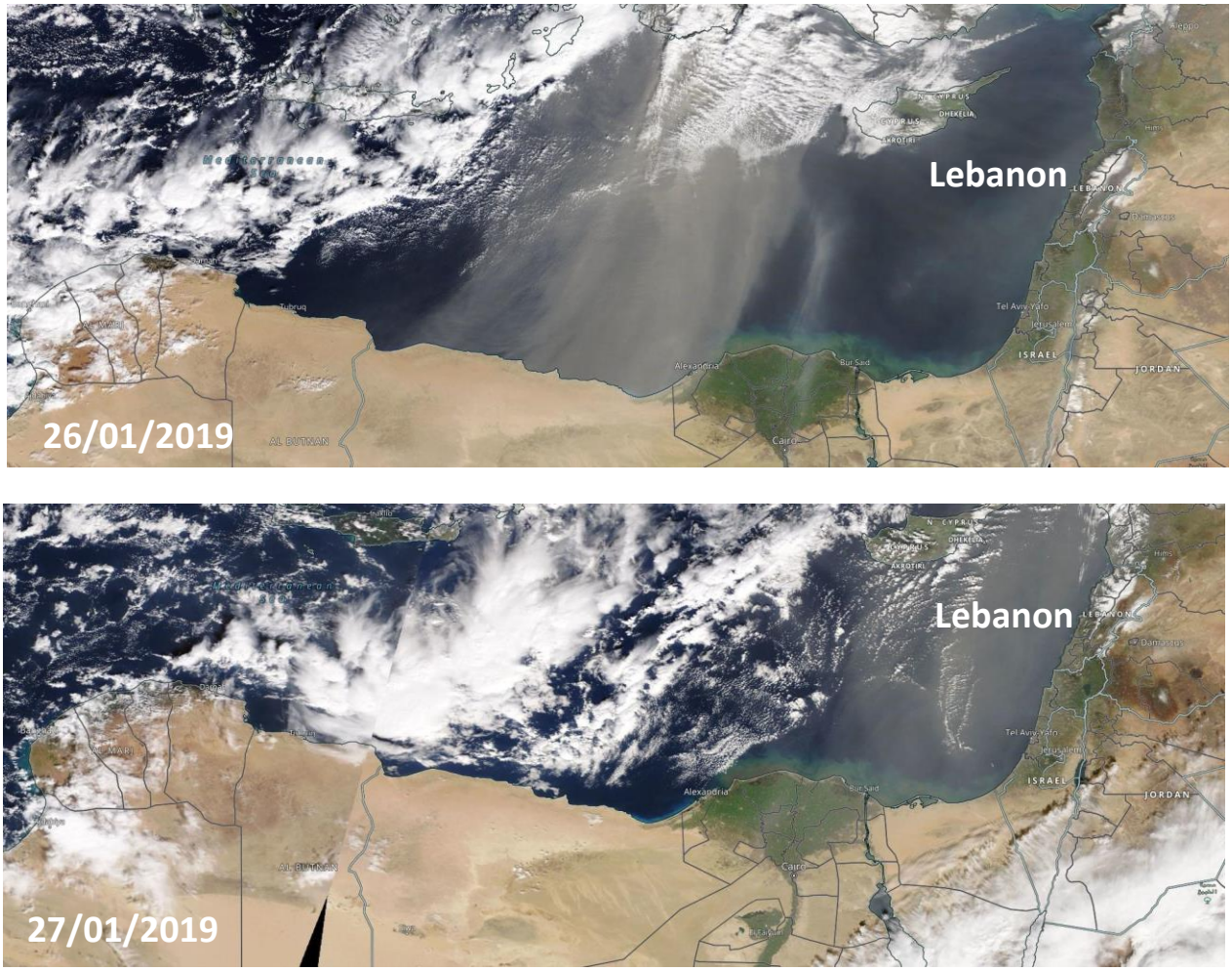

Figure S7: Saharan dust event during the field campaign (https://earthdata.nasa.gov/labs/worldview/)

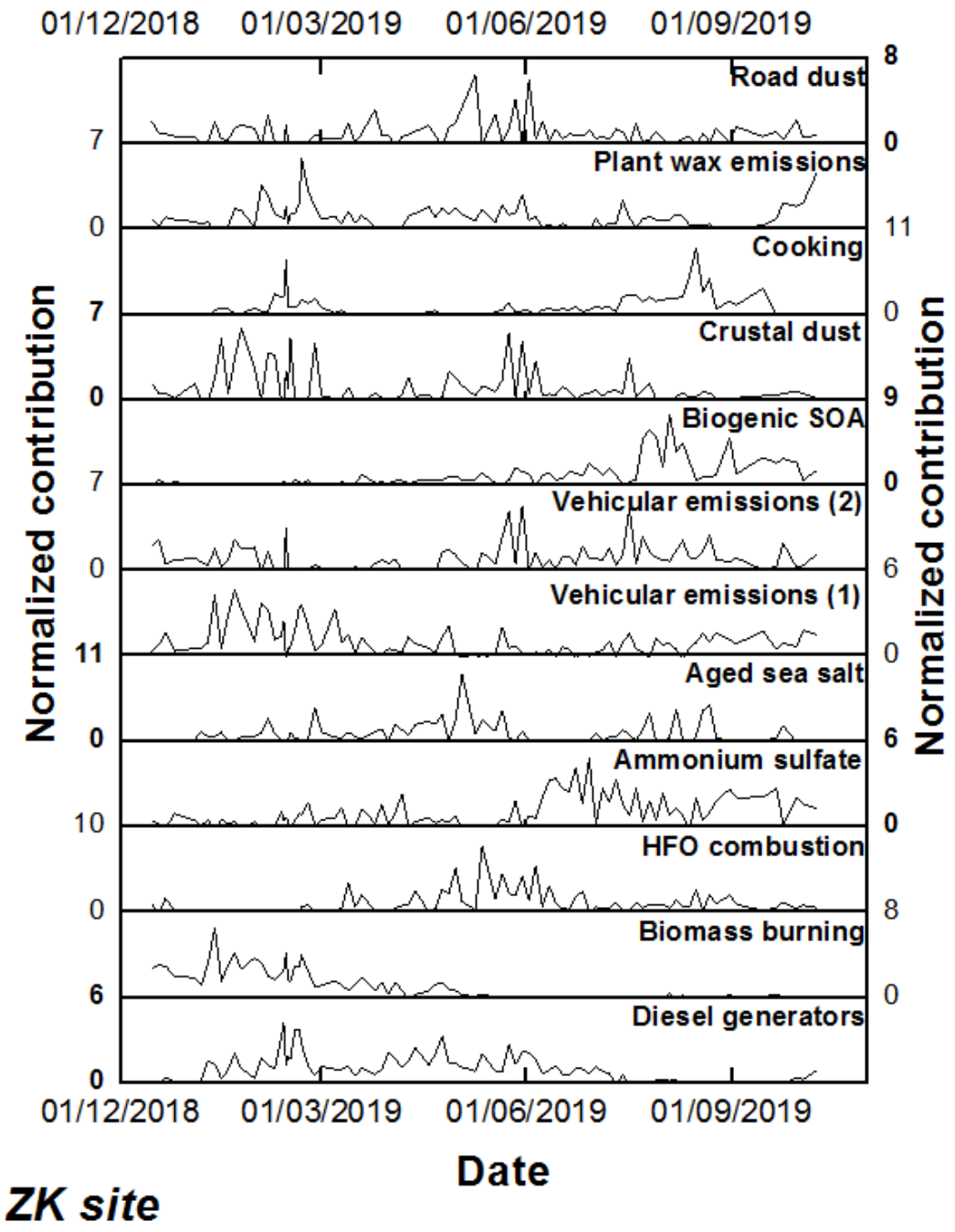

Figure S8: Time series of PMF source factor contributions in $PM_{2.5}$ mass at ZK site

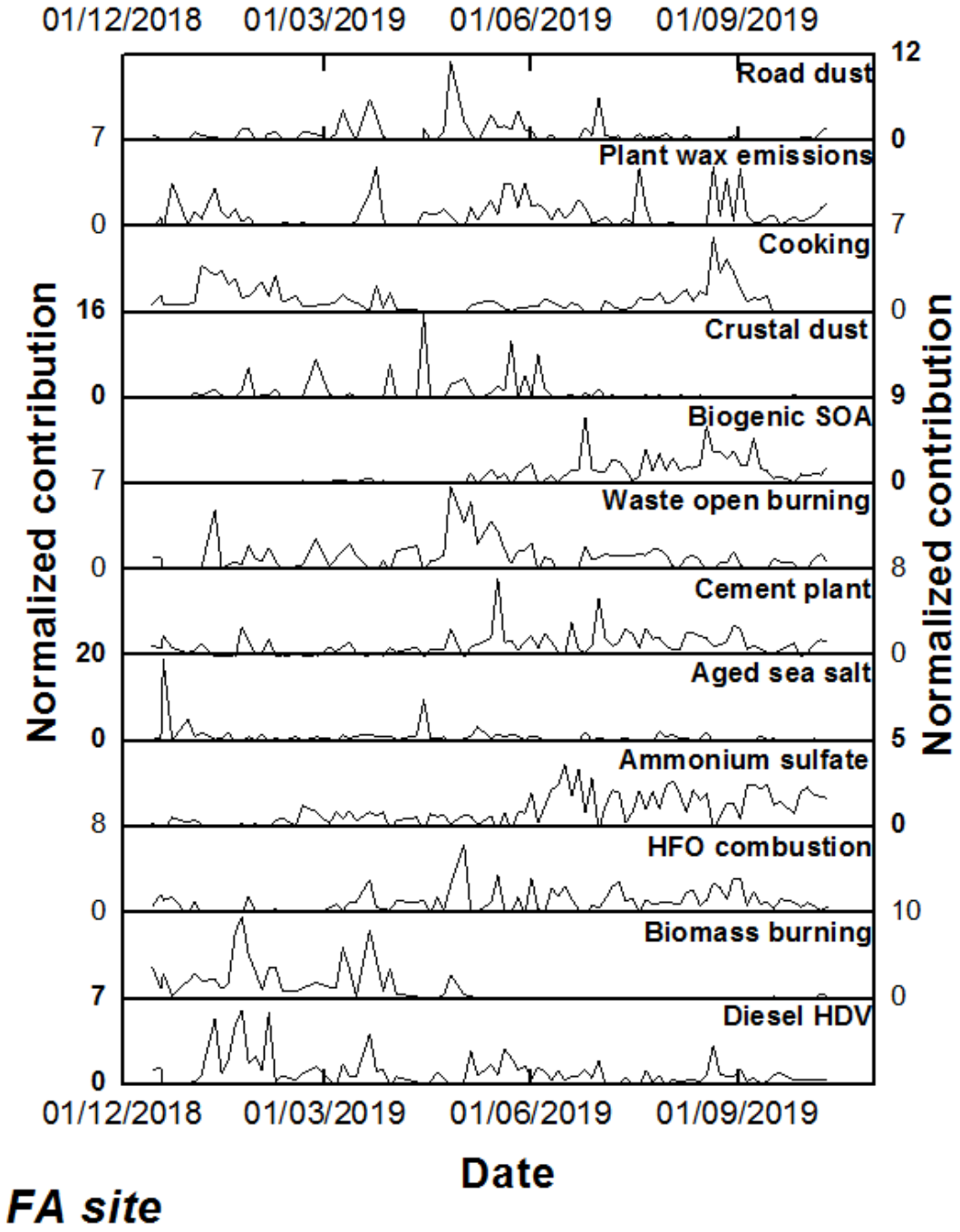

Figure S9: Time series of PMF source factor contributions in $PM_{2.5}$ mass at FA site

Appendix D: Supplementary information 4

Human health risk assessment for PAHs, phthalates, elements, PCDD/Fs, and DL-PCBs in $PM_{2.5}$ and for NMVOCs in two East-Mediterranean urban sites under industrial influence

Marc Fadel[a,b], *Frédéric Ledoux*[b], *Charbel Afif*[a,c], *Dominique Courcot*[b,*]

[a]Emissions, Measurements, and Modeling of the Atmosphere (EMMA) Laboratory, CAR, Faculty of Sciences, Saint Joseph University, Beirut, Lebanon

[b]Unité de Chimie Environnementale et Interactions sur le Vivant, UCEIV UR4492, FR CNRS 3417, University of Littoral Côte d′Opale (ULCO), Dunkerque, France

[c]Climate and Atmosphere Research Center, The Cyprus Institute, Nicosia, Cyprus

*Corresponding author: dominique.courcot@univ-littoral.fr

Table S1 **:** List of PCDD/F and DL-PCBs with their corresponding TEF values re-evaluated by Van den Berg et al. (2006)

Values of TEF	**WHO 2005**
PCDD	
2,3,7,8-tetrachlorinated dibenzo-p-dioxin	1
1,2,3,7,8-pentachlorinated dibenzo-p-dioxin	1
1,2,3,4,7,8-hexachlorinated dibenzo-p-dioxin	0.1
1,2,3,6,7,8-hexachlorinated dibenzo-p-dioxin	0.1
1,2,3,7,8,9-hexachlorinated dibenzo-p-dioxin	0.1
1,2,3,4,6,7,8-heptachlorinated dibenzo-p-dioxin	0.01
octachlorinated dibenzo-p-dioxin	0.0003
PCDF	
2,3,7,8 tetrachlorinated dibenzofuran	0.1
1,2,3,7,8 pentachlorinated dibenzofuran	0.03
2,3,4,7,8 pentachlorinated dibenzofuran	0.3
1,2,3,4,7,8 hexachlorinated dibenzofuran	0.1
1,2,3,6,7,8 hexachlorinated dibenzofuran	0.1
2,3,4,6,7,8 hexachlorinated dibenzofuran	0.1
1,2,3,7,8,9 hexachlorinated dibenzofuran	0.1
1,2,3,4,6,7,8-heptachlorinated dibenzofuran	0.01
1,2,3,4,7,8,9-heptachlorinated dibenzofuran	0.01
octachlorinated dibenzofuran	0.0003
PCB	
3,4,4',5-tetrachlorobiphenyl	0.0003
3,3′,4,4′-tetrachlorobiphenyl	0.0001
2,3',4,4',5'-pentachlorobiphenyl	0.00003
2,3',4,4',5-pentachlorobiphenyl	0.00003
2,3,4,4',5-pentachlorobiphenyl	0.00003
2,3,3',4,4'-pentachlorobiphenyl	0.00003
3,3',4,4',5-pentachlorobiphenyl	0.1
2,3',4,4',5,5'-hexachlorobiphenyl	0.00003
2,3,3',4,4',5-hexachlorobiphenyl	0.00003
2,3,3',4,4',5'-hexachlorobiphenyl	0.00003
3,3',4,4',5,5'-hexachlorobiphenyl	0.03
2,3,3',4,4',5,5'-heptachlorobiphenyl	0.00003

Table S2 : Toxic equivalent factors (TEF) for the different PAHs proposed by Nisbet and LaGoy (1992)

Compound name	TEF value
acenaphthylene	0.001
acenaphthene	0.001
fluorene	0.001
anthracene	0.01
phenanthrene	0.001
fluoranthene	0.001
pyrene	0.001
benz[a]anthracene	0.1
chrysene/triphenylene	0.01
benzo[b]fluoranthene	0.1
benzo[k]fluoranthene	0.1
benzo[a]pyrene	1
dibenz[a,h]anthracene	5
benzo[g,h,i]perylene	0.01
indeno(1,2,3-C,D)pyrene	0.1

Table S3: Values of RfD, RfC, CSF, and IUR reported in the literature for the different species

Compound	**Reference dose (RfD) (mg/kg/day)**			**Reference concentration (RfC) (mg/m^3)**	**Cancer slope factor (CSF) (kg·day/mg)**			**Inhalation unit risk (IUR) m^3/mg**
	Dermal	**Ingestion**	**Inhalation**		**Dermal**	**Ingestion**	**Inhalation**	
Polycyclic Aromatic Hydrocarbons								
benzo[a]pyrene		3×10^{-4} [c]		2×10^{-6} [c]	25 [a]	7.3 [a]	3.85 [a]	6×10^{-1} [c]
PCDD/F and PCB								
2,3,7,8-TCDD		7×10^{-10} [c] 7×10^{-8} (WHO TEF)		4×10^{-8} [c]		1.3×10^{5} [c]		3.8×10^{4} [c]
Phthalates								
bis(2-ethylhexyl)phthalate		2×10^{-2} [c]				1.4×10^{-2} [c]	8.4×10^{-3} [b]	2.4×10^{-3} [c]
dibutylphthalate		1×10^{-1} [c]			***Not carcinogenic to humans***			
diisobutylphthalate	***Not assessed***							
Elements								
arsenic, inorganic	1.23×10^{-4} [d]	3×10^{-4} [c,d]	3.01×10^{-4} [d]	1.5×10^{-5} [c]	1.5 [e,g]	1.5 [c]	15.1 [c,d]	4.3 [c]
cadmium	1×10^{-5} [d]	1×10^{-2} [d] 1×10^{-3} [c] 3×10^{-4} [i]	1×10^{-5} [d]	1×10^{-5} [c]			6.3 [e]	1.8 [c]
cobalt	1.6×10^{-2} [d]	2×10^{-2} [d] 3×10^{-3} [c]	5.71×10^{-6} [d]	6×10^{-6} [c]			9.8 [e]	9 [c]
chromium (VI)	6×10^{-5} [d]	$3x\ 10^{-3}$ [c,d]	2.86×10^{-5} [d]	1×10^{-4} [c]	20 [g]	5×10^{-1} [c]	41 [c]	84 [c]
copper	1.2×10^{-2} [d]	4×10^{-2} [c,d]	6.9×10^{-4} [d]					
manganese	1.84×10^{-3} [d]	4.6×10^{-2} [d] 1.4×10^{-1} [c]	1.43×10^{-5} [d]	5×10^{-5} [c]				
nickel	9×10^{-5} [d]	2×10^{-2} [c,d]	9×10^{-5} [d]	9×10^{-5} [c]			0.84 [d]	0.26 [c]
lead	5.2×10^{-4} [d]	3.52×10^{-3} [d]	3.5×10^{-5} [d]		8.5×10^{-3} [g]	8.5×10^{-3} [e]	4.2×10^{-2} [e]	1.2×10^{-5} [h]
zinc	6×10^{-2} [d]	3×10^{-1} [c,d]	3×10^{-1} [d]					
mercury	3×10^{-4} [c]	3×10^{-4} [c]	3×10^{-4} [c]	3×10^{-4} [c]				
barium		2×10^{-1} [c]		5×10^{-4} [c]				

aluminum		1 [c]		5×10^{-3} [c]				
vanadium		5×10^{-3} [c]		1×10^{-4} [c]				8.3 [i]
iron		7×10^{-1} [c]						
strontium		6×10^{-1} [c]						
tin		6×10^{-1} [c]						
antimony metallic		4×10^{-4} [c]		3×10^{-4} [c]				
lanthanum		5×10^{-5} [c]						
thallium (soluble salts)		1×10^{-5} [c]						
NMVOCs								
commercial hexane n-hexane		1.1×10^{1} [i] 6×10^{-2} [j]		6×10^{-1} [c] 7×10^{-1}				2×10^{-4} [c]
benzene		4×10^{-3} [c]		3×10^{-2} [c]		5.5×10^{-2} [c]	2.7×10^{-2} [c]	7.8×10^{-3} [c]
cyclohexane				6 [c]				
n-heptane		3×10^{-4} [c]		4×10^{-1} [c]				
Methylcyclohexane				3 [f,j]				
toluene		8×10^{-2} [c]		5 [c]				
tetrachloroethylene		6×10^{-3} [c]		4×10^{-2} [c]		2.1×10^{-3} [c]		2.6×10^{-4} [c]
ethylbenzene		1×10^{-1} [c]		1 [c]		1.1×10^{-2} [c]		2.5×10^{-3} [c]
xylenes (m+p, o)		2×10^{-1} [c]		1×10^{-1} [c]				
naphthalene		2×10^{-2} [c]		3×10^{-3} [c]		1.2×10^{-1} [c]		3.4×10^{-2} [c]
1,3-butadiene				2×10^{-3} [c]		6×10^{-1} [c]		3×10^{-2} [c]

a (Peng et al., 2011)
b (OEHHA, 2011)
c USEPA IRIS https://cfpub.epa.gov/ncea/iris_drafts/AtoZ.cf
d (Hao et al., 2020)
e (Bello et al., 2017)
f (USEPA, 2009)
g calculated using the formula : $CSF_{dermal} = \frac{CSF_o}{GIABS}$
h Cal EPA: California Environmental Protection Agency; https://oehha.ca.gov/
i Provisional Peer-Reviewed Toxicity Values archive
j Health effect assessment summary tables- Archive https://www.epa.gov/radiation/heast
k RAIS toxicity values https://rais.ornl.gov/cgi-bin/tools/TOX_search?select=chemtox

Table S4 : PAHs concentrations in $PM_{2.5}$ (Fadel et al., 2021), calculated concentrations in the gaseous phase at Zouk (ZK) and Fiaa (FA) sites, fraction of the species in the particulate phase and compared to the range of percentages found in the literature for other sites

	ZK site				FA site				Literature	References
	K_p ($m^3/\mu g$)	$PM_{2.5}$ (ng/m^3)	Gas (ng/m^3)	% of compound in $PM_{2.5}$	K_p ($m^3/\mu g$)	$PM_{2.5}$ (ng/m^3)	Gas (ng/m^3)	% of compound in $PM_{2.5}$	Range of % of compound in $PM_{2.5}$	
acenaphthylene	4.7×10^{-5}	0.02	18.7	0.1%	5.4×10^{-5}	-*	-*	-*	0.0% - 10.5%	(Gurkan Ayyildiz and Esen, 2020) (Gaga and Ari, 2019) (Akyüz and Çabuk, 2010) (Vasilakos et al., 2007) (Pratt et al., 2018) (Ma et al., 2018)
acenaphthene	8.5×10^{-5}	0.02	9.4	0.3%	1×10^{-4}	-*	-*	-*	0.0% - 5.3%	
fluorene	4.4×10^{-4}	0.02	2.1	1.2%	5.3×10^{-4}	-*	-*	-*	0.0% - 20.6%	
anthracene	1.9×10^{-2}	0.12	0.3	31.5%	2.2×10^{-2}	0.08	0.173	34.7%	0.6%- 50.0%	
phenanthrene	1.2×10^{-3}	0.03	1.1	3.1%	1.4×10^{-3}	0.02	0.615	3.9%	0.8% - 33.5%	
fluoranthene	7.9×10^{-3}	0.13	0.6	17.3%	9.3×10^{-3}	0.11	0.528	19.6%	6.8% - 77.5%	
pyrene	1.7×10^{-2}	0.15	0.3	30.4%	2×10^{-2}	0.10	0.25	33.3%	7.6%- 81.7%	
benz[a]anthracene	4.2×10^{-1}	0.15	0.01	89.2%	5×10^{-1}	0.07	0.007	90.4%	53.1%- 98.8%	
chrysene	1.9×10^{-1}	0.28	0.1	81.1%	2.2×10^{-2}	-*	-*	-*	38.5% - 96.4%	
benzo[b]fluoranthene	1.9	0.27	0.005	97.4%	2.2	0.14	0.003	97.7%	80.8% - 99.4%	
benzo[k]fluoranthene	1.8	0.15	0.003	97.4%	2.1	0.07	0.002	97.7%	53.8% - 100.0%	
benzo[a]pyrene	3.9×10^{-1}	0.20	0.02	89.7%	4.5×10^{-1}	0.05	0.005	90.5%	91.1% - 100.0%	
dibenz[a,h]anthracene	38	0.45	0.0004	99.9%	44	0.12	0.0001	99.9%	64.4% - 100.0%	
benzo[g,h,i]perylene	14	0.07	0.0002	99.7%	16	0.13	0.0004	99.7%	75.0% - 100.0%	
indeno[1,2,3-c,d]pyrene	8.9	0.5	0.002	99.5%	10	0.06	0.0003	93.0%	86.7% - 100.0%	
	Total	**2.56**	**32.6**			**0.95**	**1.6**			

**The compound was not detected in the particulate phase and therefore cannot be estimated in the gaseous phase*

Table S5 : Hazard quotient (HQ_i) and cancer risk (CR_i) for dermal, ingestion, and inhalation for the different age categories at Zouk site

		Hazard quotient				Cancer risk			
	Pathway	Newborn	Child	Adolescent	Adult	Newborn	Child	Adolescent	Adult
$PM_{2.5}$-bound $B[a]P_{eq}$	Dermal	-	-	-	-	3.8E-07	3.2E-06	1.1E-06	3.4E-06
	Ingestion	0.06	0.03	0.01	0.01	2.0E-06	1.1E-05	2.5E-06	9.5E-06
	Inhalation	0.31	0.31	0.41	0.41	9.4E-08	6.7E-07	2.1E-07	1.6E-06
gas phase $B[a]P_{eq}$	Dermal	-	-	-	-	8.5E-09	7.2E-08	2.3E-08	7.5E-08
	Ingestion	0.001	0.001	0.0003	0.0001	4.4E-08	2.5E-07	5.6E-08	2.1E-07
	Inhalation	0.007	0.007	0.009	0.009	2.1E-09	1.5E-08	4.6E-09	3.5E-08
TCDD equivalents (TEQ)	Dermal	-	-	-	-	-	-	-	-
	Ingestion	0.06	0.03	0.01	0.005	7.5E-08	4.3E-07	9.6E-08	3.6E-07
	Inhalation	0.00003	0.00003	0.00004	0.00004	7.2E-10	7.9E-09	5.7E-09	5.1E-08
dibutylphthalate (DBP)	Dermal	-	-	-	-	-	-	-	-
	Ingestion	0.0002	0.0002	0.0001	0.0001	-	-	-	-
	Inhalation	-	-	-	-	-	-	-	-
bis(2ethylhexyl)phthalate (BEHP)	Dermal	-	-	-	-	-	-	-	-
	Ingestion	0.018	0.009	0.004	0.002	7.2E-08	4.1E-07	9.2E-08	3.5E-07
	Inhalation	-	-	-	-	3.9E-09	2.8E-08	8.6E-09	6.5E-08
arsenic (As)	Dermal	0.0040	0.0031	0.0018	0.0007	1.1E-08	8.9E-08	2.9E-08	9.3E-08
	Ingestion	0.0126	0.0065	0.0027	0.0011	8.1E-08	4.6E-07	1.0E-07	3.9E-07
	Inhalation	0.0011	0.0007	0.0004	0.0004	7.3E-08	5.2E-07	1.6E-07	1.2E-06
cadmium (Cd)	Dermal	0.0004	0.0003	0.0002	0.0001	-	-	-	-
	Ingestion	0.0009	0.0005	0.0002	0.0001	-	-	-	-
	Inhalation	0.0082	0.0053	0.0030	0.0026	7.4E-09	5.3E-08	1.6E-08	1.2E-07
cobalt (Co)	Dermal	0.00002	0.00002	0.00001	0.000004	-	-	-	-
	Ingestion	0.0030	0.0015	0.0006	0.0003	-	-	-	-
	Inhalation	0.1401	0.0903	0.0517	0.0437	1.1E-07	7.9E-07	2.5E-07	1.9E-06
chromium Cr(VI)	Dermal	0.0014	0.0011	0.0007	0.0002	2.4E-08	2.1E-07	6.7E-08	2.2E-07
	Ingestion	0.0007	0.0003	0.0001	0.0001	1.4E-08	8.1E-08	1.8E-08	6.7E-08
	Inhalation	0.0062	0.0040	0.0023	0.0019	1.0E-07	7.4E-07	2.3E-07	1.7E-06
copper (Cu)	Dermal	0.0001	0.0001	0.0001	0.00002	-	-	-	-
	Ingestion	0.0008	0.0004	0.0002	0.0001	-	-	-	-
	Inhalation	0.0044	0.0028	0.0016	0.0014	-	-	-	-
manganese (Mn)	Dermal	0.0013	0.0010	0.0006	0.0002	-	-	-	-
	Ingestion	0.0004	0.0002	0.0001	0.0000	-	-	-	-
	Inhalation	0.3462	0.2230	0.1276	0.1080	-	-	-	-

		Hazard quotient				Cancer risk			
		Newborn	Child	Adolescent	Adult	Newborn	Child	Adolescent	Adult
nickel (Ni)	Dermal	0.042	0.032	0.019	0.007	-	-	-	-
	Ingestion	0.004	0.002	0.001	0.000	-	-	-	-
	Inhalation	0.086	0.056	0.032	0.027	9.3E-08	6.6E-07	2.1E-07	1.5E-06
lead (Pb)	Dermal	0.008	0.006	0.004	0.001	5.0E-10	4.2E-09	1.4E-09	4.4E-09
	Ingestion	0.027	0.014	0.006	0.002	1.1E-08	6.5E-08	1.5E-08	5.5E-08
	Inhalation	0.242	0.156	0.089	0.076	5.1E-09	3.6E-08	1.1E-08	8.4E-08
zinc (Zn)	Dermal	0.00014	0.00011	0.00006	0.00002	-	-	-	-
	Ingestion	0.00064	0.00033	0.00014	0.00006	-	-	-	-
	Inhalation	0.00006	0.00004	0.00002	0.00002	-	-	-	-
barium (Ba)	Dermal	-	-	-	-	-	-	-	-
	Ingestion	0.00052	0.00027	0.00011	0.00005	-	-	-	-
	Inhalation	0.00681	0.00681	0.00909	0.00909	-	-	-	-
aluminum (Al)	Dermal	-	-	-	-	-	-	-	-
	Ingestion	0.0044	0.0023	0.0009	0.0004	-	-	-	-
	Inhalation	0.0285	0.0285	0.0379	0.0379	-	-	-	-
vanadium (V)	Dermal	-	-	-	-	-	-	-	-
	Ingestion	0.038	0.020	0.008	0.003	-	-	-	-
	Inhalation	0.062	0.062	0.083	0.083	7.4E-07	8.1E-06	5.9E-06	5.2E-05
iron (Fe)	Dermal	-	-	-	-	-	-	-	-
	Ingestion	0.0048	0.0025	0.0010	0.0004	-	-	-	-
	Inhalation	-	-	-	-	-	-	-	-
strontium (Sr)	Dermal	-	-	-	-	-	-	-	-
	Ingestion	0.00007	0.00003	0.00001	0.00001	-	-	-	-
	Inhalation	-	-	-	-	-	-	-	-
tin (Sn)	Dermal	-	-	-	-	-	-	-	-
	Ingestion	0.000010	0.000005	0.000002	0.000001	-	-	-	-
	Inhalation	-	-	-	-	-	-	-	-
antimony (Sb)	Dermal	-	-	-	-	-	-	-	-
	Ingestion	0.001	0.001	0.001	0.001	-	-	-	-
	Inhalation	0.020	0.010	0.004	0.002	-	-	-	-
lanthanum (La)	Dermal	-	-	-	-	-	-	-	-
	Ingestion	0.08	0.04	0.02	0.01	-	-	-	-
	Inhalation	-	-	-	-	-	-	-	-
thallium (Tl)	Dermal	-	-	-	-	-	-	-	-
	Ingestion	0.021	0.011	0.004	0.002	-	-	-	-
	Inhalation	-	-	-	-	-	-	-	-

		Hazard quotient				Cancer risk			
		Newborn	Child	Adolescent	Adult	Newborn	Child	Adolescent	Adult
1,3-butadiene	Dermal	-	-	-	-	-	-	-	-
	Ingestion	-	-	-	-	4.9E-06	2.8E-05	6.3E-06	2.4E-05
	Inhalation	0.01	0.01	0.01	0.01	8.0E-09	8.8E-08	6.4E-08	5.6E-07
hexane	Dermal	-	-	-	-	-	-	-	-
	Ingestion	0.00028	0.00015	0.00006	0.00003	-	-	-	-
	Inhalation	0.00017	0.00017	0.00022	0.00022	2.9E-10	3.2E-09	2.3E-09	2.0E-08
tetrachloroethene	Dermal	-	-	-	-	-	-	-	-
	Ingestion	0.36	0.19	0.08	0.03	6.4E-08	3.7E-07	8.2E-08	3.1E-07
	Inhalation	0.002	0.002	0.002	0.002	2.6E-10	2.9E-09	2.1E-09	1.8E-08
benzene	Dermal	-	-	-	-	-	-	-	-
	Ingestion	7.96	4.14	1.70	0.72	2.5E-05	1.4E-04	3.2E-05	1.2E-04
	Inhalation	0.03	0.03	0.03	0.05	1.2E-07	1.3E-06	9.2E-07	8.2E-06
cyclohexane	Dermal	-	-	-	-	-	-	-	-
	Ingestion	-	-	-	-	-	-	-	-
	Inhalation	0.00002	0.00002	0.00002	0.00002	-	-	-	-
heptane	Dermal	-	-	-	-	-	-	-	-
	Ingestion	16.15	8.40	3.44	1.46	-	-	-	-
	Inhalation	0.0004	0.0004	0.0005	0.0005	-	-	-	-
methylcyclohexane	Dermal	-	-	-	-	-	-	-	-
	Ingestion	-	-	-	-	-	-	-	-
	Inhalation	0.00004	0.00004	0.00005	0.00005	-	-	-	-
toluene	Dermal	-	-	-	-	-	-	-	-
	Ingestion	1.56	0.81	0.33	0.14	-	-	-	-
	Inhalation	0.001	0.001	0.001	0.001	-	-	-	-
ethylbenzene	Dermal	-	-	-	-	-	-	-	-
	Ingestion	0.31	0.16	0.07	0.03	4.4E-06	2.5E-05	5.7E-06	2.1E-05
	Inhalation	0.001	0.001	0.001	0.001	3.6E-08	4.0E-07	2.9E-07	2.6E-06
m+p-xylene	Dermal	-	-	-	-	-	-	-	-
	Ingestion	0.21	0.11	0.05	0.02	-	-	-	-
	Inhalation	0.01	0.01	0.02	0.02	-	-	-	-
o-xylene	Dermal	-	-	-	-	-	-	-	-
	Ingestion	0.16	0.08	0.03	0.01	-	-	-	-
	Inhalation	0.01	0.01	0.01	0.01	-	-	-	-

Table S6: Hazard quotient (HQ_i) and cancer risk (CR_i) for dermal, ingestion, and inhalation for the different age categories at Fiaa site

		Hazard quotient				Cancer risk			
	Pathway	Newborn	Child	Adolescent	Adult	Newborn	Child	Adolescent	Adult
$PM_{2.5}$-bound $B[a]P_{eq}$	Dermal	-	-	-	-	1.0E-07	8.6E-07	2.8E-07	9.0E-07
	Ingestion	0.017	0.009	0.004	0.002	5.3E-07	3.0E-06	6.8E-07	2.5E-06
	Inhalation	0.083	0.083	0.110	0.110	2.5E-08	1.8E-07	5.6E-08	4.2E-07
gas phase $B[a]P_{eq}$	Dermal	-	-	-	-	1.5E-09	1.3E-08	4.1E-09	1.3E-08
	Ingestion	0.00025	0.00013	0.00005	0.00002	7.7E-09	4.4E-08	9.9E-09	3.7E-08
	Inhalation	0.001	0.001	0.002	0.002	3.7E-10	2.6E-09	8.1E-10	6.1E-09
TCDD equivalents (TEQ)	Dermal	-	-	-	-	-	-	-	-
	Ingestion	0.06	0.03	0.01	0.01	7.8E-08	4.4E-07	9.9E-08	3.7E-07
	Inhalation	0.00003	0.01957	0.00005	0.00005	7.4E-10	8.1E-09	5.9E-09	5.2E-08
dibutylphthalate (DBP)	Dermal	-	-	-	-	-	-	-	-
	Ingestion	0.00008	0.00005	0.00003	0.00003	-	-	-	-
	Inhalation	-	-	-	-	-	-	-	-
bis(2ethylhexyl)phthalate (BEHP)	Dermal	-	-	-	-	-	-	-	-
	Ingestion	0.024	0.013	0.005	0.002	9.7E-08	5.5E-07	1.2E-07	4.6E-07
	Inhalation	-	-	-	-	5.2E-09	3.7E-08	1.2E-08	8.6E-08
arsenic (As)	Dermal	0.0038	0.0029	0.0017	0.0006	1.0E-08	8.5E-08	2.8E-08	8.8E-08
	Ingestion	0.0120	0.0062	0.0026	0.0011	7.7E-08	4.4E-07	9.9E-08	3.7E-07
	Inhalation	0.0011	0.0007	0.0004	0.0003	7.0E-08	5.0E-07	1.5E-07	1.2E-06
cadmium (Cd)	Dermal	0.0004	0.0003	0.0002	0.0001	-	-	-	-
	Ingestion	0.0010	0.0005	0.0002	0.0001	-	-	-	-
	Inhalation	0.0091	0.0059	0.0034	0.0028	8.2E-09	5.8E-08	1.8E-08	1.4E-07
cobalt (Co)	Dermal	0.00001	0.00001	0.00001	0.00000	-	-	-	-
	Ingestion	0.002	0.001	0.000	0.000	-	-	-	-
	Inhalation	0.071	0.046	0.026	0.022	5.7E-08	4.0E-07	1.3E-07	9.4E-07
chromium Cr(VI)	Dermal	0.0015	0.0012	0.0007	0.0002	2.6E-08	2.2E-07	7.1E-08	2.3E-07
	Ingestion	0.0007	0.0004	0.0001	0.0001	1.5E-08	8.5E-08	1.9E-08	7.1E-08
	Inhalation	0.0065	0.0042	0.0024	0.0020	1.1E-07	7.8E-07	2.4E-07	1.8E-06
copper (Cu)	Dermal	0.00007	0.00005	0.00003	0.00001	-	-	-	-
	Ingestion	0.00047	0.00024	0.00010	0.00004	-	-	-	-
	Inhalation	0.00243	0.00157	0.00090	0.00076	-	-	-	-

		Hazard quotient				Cancer risk			
		Newborn	Child	Adolescent	Adult	Newborn	Child	Adolescent	Adult
manganese (Mn)	Dermal	0.0010	0.0007	0.0004	0.0002	-	-	-	-
	Ingestion	0.0003	0.0002	0.0001	0.0000	-	-	-	-
	Inhalation	0.2604	0.1677	0.0960	0.0812	-	-	-	-
nickel (Ni)	Dermal	0.022	0.017	0.010	0.004	-	-	-	-
	Ingestion	0.002	0.001	0.000	0.000	-	-	-	-
	Inhalation	0.046	0.030	0.017	0.014	5.0E-08	3.6E-07	1.1E-07	8.3E-07
lead (Pb)	Dermal	0.011	0.008	0.005	0.002	6.8E-10	5.7E-09	1.9E-09	6.0E-09
	Ingestion	0.037	0.019	0.008	0.003	1.6E-08	9.0E-08	2.0E-08	7.5E-08
	Inhalation	0.332	0.214	0.123	0.104	1.4E-09	1.0E-08	3.1E-09	2.3E-08
zinc (Zn)	Dermal	0.00009	0.00007	0.00004	0.00001	-	-	-	-
	Ingestion	0.00041	0.00021	0.00009	0.00004	-	-	-	-
	Inhalation	0.00004	0.00002	0.00001	0.00001	-	-	-	-
barium (Ba)	Dermal	-	-	-	-	-	-	-	-
	Ingestion	0.00033	0.00017	0.00007	0.00003	-	-	-	-
	Inhalation	0.00434	0.00434	0.00579	0.00579	-	-	-	-
aluminum (Al)	Dermal	-	-	-	-	-	-	-	-
	Ingestion	0.0036	0.0019	0.0008	0.0003	-	-	-	-
	Inhalation	0.0236	0.0236	0.0314	0.0314	-	-	-	-
vanadium (V)	Dermal	-	-	-	-	-	-	-	-
	Ingestion	0.019	0.010	0.004	0.002	-	-	-	-
	Inhalation	0.031	0.031	0.041	0.041	3.7E-07	4.0E-06	2.9E-06	2.6E-05
iron (Fe)	Dermal	-	-	-	-	-	-	-	-
	Ingestion	0.0031	0.0016	0.0007	0.0003	-	-	-	-
	Inhalation	-	-	-	-	-	-	-	-
strontium (Sr)	Dermal	-	-	-	-	-	-	-	-
	Ingestion	0.000055	0.000028	0.000012	0.000005	-	-	-	-
	Inhalation	-	-	-	-	-	-	-	-
tin (Sn)	Dermal	-	-	-	-	-	-	-	-
	Ingestion	0.000007	0.000004	0.000001	0.000001	-	-	-	-
	Inhalation	-	-	-	-	-	-	-	-
antimony (Sb)	Dermal	-	-	-	-	-	-	-	-
	Ingestion	0.017	0.009	0.004	0.002	-	-	-	-
	Inhalation	0.001	0.001	0.001	0.001	-	-	-	-
lanthanum (La)	Dermal	-	-	-	-	-	-	-	-
	Ingestion	0.049	0.026	0.011	0.004	-	-	-	-
	Inhalation	-	-	-	-	-	-	-	-

thallium (Tl)	Dermal	-	-	-	-	-	-	-	-
	Ingestion	0.023	0.012	0.005	0.002	-	-	-	-
	Inhalation	-	-	-	-	-	-	-	-
		Hazard quotient				Cancer risk			
		Newborn	Child	Adolescent	Adult	Newborn	Child	Adolescent	Adult
1,3-butadiene	Dermal	-	-	-	-	-	-	-	-
	Ingestion	-	-	-	-	-	-	-	-
	Inhalation	-	-	-	-	-	-	-	-
hexane	Dermal	-	-	-	-	-	-	-	-
	Ingestion	0.00010	0.00005	0.00002	0.00001	-	-	-	-
	Inhalation	0.00006	0.00006	0.00008	0.00008	1.0E-10	1.1E-09	8.2E-10	7.3E-09
tetrachloroethene	Dermal	-	-	-	-	-	-	-	-
	Ingestion	0.0713	0.0371	0.0152	0.0064	1.3E-08	7.3E-08	1.6E-08	6.1E-08
	Inhalation	0.0003	0.0003	0.0005	0.0005	5.2E-11	5.7E-10	4.1E-10	3.6E-09
benzene	Dermal	-	-	-	-	-	-	-	-
	Ingestion	2.81	1.46	0.60	0.25	8.8E-06	5.1E-05	1.1E-05	4.2E-05
	Inhalation	0.01	0.01	0.01	0.02	4.1E-08	4.5E-07	3.3E-07	2.9E-06
cyclohexane	Dermal	-	-	-	-	-	-	-	-
	Ingestion	-	-	-	-	-	-	-	-
	Inhalation	0.000004	0.000004	0.000005	0.000005	-	-	-	-
heptane	Dermal	-	-	-	-	-	-	-	-
	Ingestion	3.39	1.76	0.72	0.31	-	-	-	-
	Inhalation	0.0001	0.0001	0.0001	0.0001	-	-	-	-
methylcyclohexane	Dermal	-	-	-	-	-	-	-	-
	Ingestion	-	-	-	-	-	-	-	-
	Inhalation	0.00001	0.00001	0.00001	0.00001	-	-	-	-
toluene	Dermal	-	-	-	-	-	-	-	-
	Ingestion	0.25	0.13	0.05	0.02	-	-	-	-
	Inhalation	0.0001	0.0001	0.0002	0.0002	-	-	-	-
ethylbenzene	Dermal	-	-	-	-	-	-	-	-
	Ingestion	0.048	0.025	0.010	0.004	6.9E-07	4.0E-06	8.8E-07	3.3E-06
	Inhalation	0.0002	0.0002	0.0002	0.0002	5.6E-09	6.2E-08	4.5E-08	4.0E-07
m+p-xylene	Dermal	-	-	-	-	-	-	-	-
	Ingestion	0.027	0.014	0.006	0.002	-	-	-	-
	Inhalation	0.002	0.002	0.002	0.002	-	-	-	-
o-xylene	Dermal	-	-	-	-	-	-	-	-
	Ingestion	0.022	0.012	0.005	0.002	-	-	-	-
	Inhalation	0.001	0.001	0.002	0.002	-	-	-	-

Table S7 : The total HI and cumulative cancer risk for PAHs and TCDD equivalents, and Total HQ_i and Total CR_i for phthalates, metals, and NMVOCs (for dermal, ingestion, and inhalation) for the different age categories at Zouk site

	Total HI/ Total HQ_i				Cumulative CR / Total CR_i			
	Newborn	Child	Adolescent	Adult	Newborn	Child	Adolescent	Adult
$PM_{2.5}$-bound $B[a]P_{eq}$	0.37	0.34	0.43	0.42	2.5E-06	1.5E-05	3.8E-06	1.4E-05
gas phase $B[a]P_{eq}$	0.01	0.01	0.01	0.01	5.5E-08	3.4E-07	8.4E-08	3.2E-07
TCDD equivalents	0.06	0.03	0.01	0.01	7.6E-08	4.4E-07	1.0E-07	4.1E-07
dibutylphthalate	0.0002	0.0002	0.0001	0.0001	-	-	-	-
bis(2ethylhexyl)phthalate	0.018	0.009	0.004	0.002	7.6E-08	4.4E-07	1.0E-07	4.1E-07
arsenic (As)	0.018	0.010	0.005	0.002	1.6E-07	1.1E-06	3.0E-07	1.7E-06
cadmium (Cd)	0.010	0.006	0.003	0.003	7.4E-09	5.3E-08	1.6E-08	1.2E-07
cobalt (Co)	0.143	0.092	0.052	0.044	1.1E-07	7.9E-07	2.5E-07	1.9E-06
chromium Cr(VI)*	0.008	0.005	0.003	0.002	1.4E-07	1.0E-06	3.2E-07	2.0E-06
copper (Cu)	0.005	0.003	0.002	0.001	-	-	-	-
manganese (Mn)	0.348	0.224	0.128	0.108	-	-	-	-
nickel (Ni)	0.132	0.090	0.052	0.034	9.3E-08	6.6E-07	2.1E-07	1.5E-06
lead (Pb)	0.277	0.176	0.099	0.079	1.7E-08	1.1E-07	2.7E-08	1.4E-07
zinc (Zn)	0.0008	0.0005	0.0002	0.0001	-	-	-	-
barium (Ba)	0.01	0.01	0.01	0.01	-	-	-	-
aluminum (Al)	0.03	0.03	0.04	0.04	-	-	-	-
vanadium (V)	0.10	0.08	0.09	0.09	7.4E-07	8.1E-06	5.9E-06	5.2E-05
iron (Fe)	0.0048	0.0025	0.0010	0.0004	-	-	-	-
strontium (Sr)	0.00007	0.00003	0.00001	0.00001	-	-	-	-
tin (Sn)	0.000010	0.000005	0.000002	0.000001	-	-	-	-
antimony (Sb)	0.021	0.011	0.005	0.003	-	-	-	-
lanthanum (La)	0.08	0.04	0.02	0.01	-	-	-	-
thallium (Tl)	0.021	0.011	0.004	0.002	-	-	-	-
1,3-butadiene	0.01	0.01	0.01	0.01	4.9E-06	2.8E-05	6.3E-06	2.4E-05
hexane	0.0004	0.0003	0.0003	0.0002	2.9E-10	3.2E-09	2.3E-09	2.0E-08
tetrachloroethene	0.36	0.19	0.08	0.03	6.5E-08	3.7E-07	8.4E-08	3.3E-07
benzene	8.0	4.18	1.72	0.77	2.5E-05	1.4E-04	3.3E-05	1.3E-04
cyclohexane	0.00002	0.00002	0.00002	0.00002	-	-	-	-
heptane	16.15	8.40	3.44	1.46	-	-	-	-
methylcyclohexane	0.00004	0.00004	0.00005	0.00005	-	-	-	-
toluene	1.56	0.81	0.33	0.14	-	-	-	-

ethylbenzene	0.31	0.16	0.07	0.03	4.5E-06	2.6E-05	6.0E-06	2.4E-05
m+p-xylene	0.22	0.12	0.07	0.04	-	-	-	-
o-xylene	0.17	0.09	0.04	0.02	-	-	-	-

*Cr(VI) = 1/7 * Cr (USEPA, 2004)

Table S8: The total HI and cumulative cancer risk for PAHs and TCDD equivalents, and Total HQ_i and Total CR_i for phthalates, metals, and NMVOCs (for dermal, ingestion, and inhalation) for the different age categories at Fiaa site

	Total HI/ Total HQ_i				Cumulative CR / Total CR_i			
	Newborn	Child	Adolescent	Adult	Newborn	Child	Adolescent	Adult
$PM_{2.5}$-bound $B[a]P_{eq}$	0.10	0.09	0.11	0.10	6.6E-07	4.1E-06	1.0E-06	3.9E-06
gas phase $B[a]P_{eq}$	0.001	0.001	0.002	0.002	9.6E-09	5.9E-08	1.5E-08	5.6E-08
TCDD equivalents	0.06	0.05	0.01	0.01	7.8E-08	4.5E-07	1.1E-07	4.2E-07
dibutylphthalate	0.00008	0.00005	0.00003	0.00003	-	-	-	-
bis(2ethylhexyl)phthalate	0.018	0.009	0.004	0.002	1.0E-07	5.9E-07	1.4E-07	5.5E-07
arsenic (As)	0.017	0.010	0.005	0.002	1.6E-07	1.0E-06	2.8E-07	1.6E-06
cadmium (Cd)	0.011	0.007	0.004	0.003	8.2E-09	5.8E-08	1.8E-08	1.4E-07
cobalt (Co)	0.072	0.047	0.026	0.022	5.7E-08	4.0E-07	1.3E-07	9.4E-07
chromium Cr(VI)*	0.009	0.006	0.003	0.002	1.5E-07	1.1E-06	3.3E-07	2.1E-06
copper (Cu)	0.003	0.002	0.001	0.001	-	-	-	-
manganese (Mn)	0.262	0.169	0.096	0.081	-	-	-	-
nickel (Ni)	0.071	0.048	0.028	0.018	5.0E-08	3.6E-07	1.1E-07	8.3E-07
lead (Pb)	0.380	0.241	0.135	0.109	1.8E-08	1.1E-07	2.5E-08	1.0E-07
zinc (Zn)	0.0005	0.0003	0.0001	0.0001	-	-	-	-
barium (Ba)	0.005	0.005	0.006	0.006	-	-	-	-
aluminum (Al)	0.03	0.03	0.03	0.03	-	-	-	-
vanadium (V)	0.10	0.08	0.09	0.09	3.7E-07	4.0E-06	2.9E-06	2.6E-05
iron (Fe)	0.0031	0.0016	0.0007	0.0003	-	-	-	-
strontium (Sr)	0.000055	0.000028	0.000012	0.000005	-	-	-	-
tin (Sn)	0.000007	0.000004	0.000001	0.000001	-	-	-	-
antimony (Sb)	0.018	0.010	0.005	0.003	-	-	-	-
lanthanum (La)	0.049	0.026	0.011	0.004	-	-	-	-
thallium (Tl)	0.023	0.012	0.005	0.002	-	-	-	-

1,3-butadiene	-	-	-	-	-	-	-	-
hexane	0.0002	0.0001	0.0001	0.0001	1.0E-10	1.1E-09	8.2E-10	7.3E-09
tetrachloroethene	0.07	0.04	0.02	0.01	1.3E-08	7.4E-08	1.7E-08	6.5E-08
benzene	2.83	1.48	0.61	0.27	8.9E-06	5.1E-05	1.2E-05	4.5E-05
cyclohexane	0.000004	0.000004	0.000005	0.000005	-	-	-	-
heptane	3.39	1.76	0.72	0.31	-	-	-	-
methylcyclohexane	0.00001	0.00001	0.00001	0.00001	-	-	-	-
toluene	0.25	0.13	0.05	0.02	-	-	-	-
ethylbenzene	0.048	0.025	0.011	0.005	7.0E-07	4.0E-06	9.3E-07	3.7E-06
m+p-xylene	0.029	0.016	0.008	0.005	-	-	-	-
o-xylene	0.02	0.01	0.01	0.00	-	-	-	-

*Cr(VI) = 1/7 * Cr (USEPA, 2004)

References :

Akyüz, M., Çabuk, H., Gas–particle partitioning and seasonal variation of polycyclic aromatic hydrocarbons in the atmosphere of Zonguldak, Turkey, *Sci. Total Environ.* **408**(2010), pp. 5550-5558. https://doi.org/10.1016/j.scitotenv.2010.07.063

Bello, S., Muhammad, B.G., Bature, B., Total Excess Lifetime Cancer risk estimation from enhanced heavy metals concentrations resulting from tailings in Katsina steel rolling mill, Nigeria, *Journal of Material Sciences and engineering* **6**(2017), p. 338. 10.4172/2169-0022.1000338

Fadel, M., Ledoux, F., Farhat, M., Kfoury, A., Courcot, D., Afif, C., $PM_{2.5}$ characterization of primary and secondary organic aerosols in two urban-industrial areas in the East Mediterranean, *J Environ Sci* **101**(2021), pp. 98-116. https://doi.org/10.1016/j.jes.2020.07.030

Gaga, E.O., Ari, A., Gas-particle partitioning and health risk estimation of polycyclic aromatic hydrocarbons (PAHs) at urban, suburban and tunnel atmospheres: Use of measured EC and OC in model calculations, *Atmospheric Pollution Research* **10**(2019), pp. 1-11. https://doi.org/10.1016/j.apr.2018.05.004

Gurkan Ayyildiz, E., Esen, F., Atmospheric Polycyclic Aromatic Hydrocarbons (PAHs) at two sites, in Bursa, Turkey: determination of concentrations, gas-particle partitioning, sources, and health risk, *Arch. Environ. Contam. Toxicol. Archives of Environmental Contamination and Toxicology* **78**(2020), pp. 350-366. https://doi.org/10.1007/s00244-019-00698-7

Hao, Y., Luo, B., Simayi, M., Zhang, W., Jiang, Y., He, J., Xie, S., Spatiotemporal patterns of $PM_{2.5}$ elemental composition over China and associated health risks, *Environ. Pollut.* **265**(2020), p. 114910. https://doi.org/10.1016/j.envpol.2020.114910

Ma, W.-L., Liu, L.-Y., Jia, H.-L., Yang, M., Li, Y.-F., PAHs in Chinese atmosphere Part I: Concentration, source and temperature dependence, *Atmos Environ* **173**(2018), pp. 330-337. https://doi.org/10.1016/j.atmosenv.2017.11.029

Nisbet, I.C., LaGoy, P.K., Toxic equivalency factors (TEFs) for polycyclic aromatic hydrocarbons (PAHs), *Regul Toxicol Pharmacol* **16**(1992), pp. 290-300. https://doi.org/10.1016/0273-2300(92)90009-X

OEHHA, Chemical-specific summaries of the information used to derive unit risk and cancer potency values, (2011).

Peng, C., Chen, W., Liao, X., Wang, M., Ouyang, Z., Jiao, W., Bai, Y., Polycyclic aromatic hydrocarbons in urban soils of Beijing: Status, sources, distribution and potential risk, *Environmental Pollution* **159**(2011), pp. 802-808. https://doi.org/10.1016/j.envpol.2010.11.003

Pratt, G.C., Herbrandson, C., Krause, M.J., Schmitt, C., Lippert, C.J., McMahon, C.R., Ellickson, K.M., Measurements of gas and particle polycyclic aromatic hydrocarbons (PAHs) in air at urban, rural and near-roadway sites, *Atmos Environ* **179**(2018), pp. 268-278. https://doi.org/10.1016/j.atmosenv.2018.02.035

USEPA, 2004. Region 9, Preliminary remediation goals, air–water calculations. U.S. Environmental Protection Agency, Washington, DC.

USEPA, Provisional peer-reviewed toxicity values for complex mixtures of aliphatic and aromatic hydrocarbons (2009).

Van den Berg, M., Birnbaum, L.S., Denison, M., De Vito, M., Farland, W., Feeley, M., Fiedler, H., Hakansson, H., Hanberg, A., Haws, L., Rose, M., Safe, S., Schrenk, D., Tohyama, C., Tritscher, A., Tuomisto, J., Tysklind, M., Walker, N., Peterson, R.E., The 2005 World Health Organization reevaluation of human and Mammalian toxic equivalency factors for dioxins and dioxin-like compounds, *Toxicol. Sci.* **93**(2006), pp. 223-241. https://doi.org/10.1093/toxsci/kfl055

Vasilakos, C., Levi, N., Maggos, T., Hatzianestis, J., Michopoulos, J., Helmis, C., Gas-particle concentration and characterization of sources of PAHs in the atmosphere of a suburban area in Athens, Greece, *J. Hazard. Mater.* **140**(2007), pp. 45-51. https://doi.org/10.1016/j.jhazmat.2006.06.047

Appendix E: Supplementary information 5

Temporal variations, relationship with chemical composition and source apportionment of oxidative potential of $PM_{2.5}$ in two East Mediterranean sites

Marc Fadel[a,b], Dominique Courcot[b], Gilles Delmaire[c], Gilles Roussel[c], Charbel Afif [a,d], Frédéric Ledoux[b,]*

[a]Emissions, Measurements, and Modeling of the Atmosphere (EMMA) Laboratory, CAR, Faculty of Sciences, Saint Joseph University, Beirut, Lebanon

[b]Unité de Chimie Environnementale et Interactions sur le Vivant, UCEIV UR4492, FR CNRS 3417, University of Littoral Côte d′Opale (ULCO), Dunkerque, France

[c] Laboratoire d'Informatique Signal et Image de la Côte d'Opale (LISIC), University of Littoral Côte d'Opale, Calais, France

[d]Climate and Atmosphere Research Center, The Cyprus Institute, Nicosia, Cyprus

*Corresponding author: frederic.ledoux@univ-littoral.fr

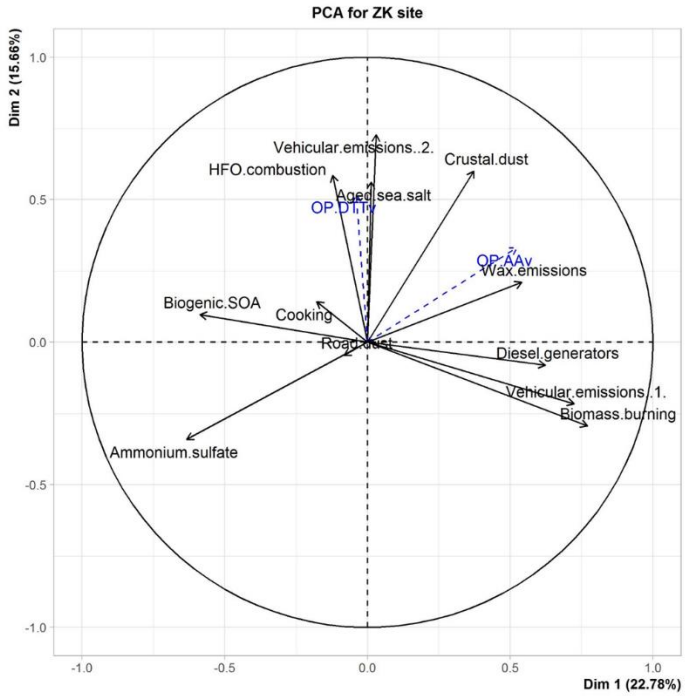

Figure S1: Principal component analysis related to the samples at ZK (variables factor map showing Axis 1 and Axis 2 with supplementary variables in blue)

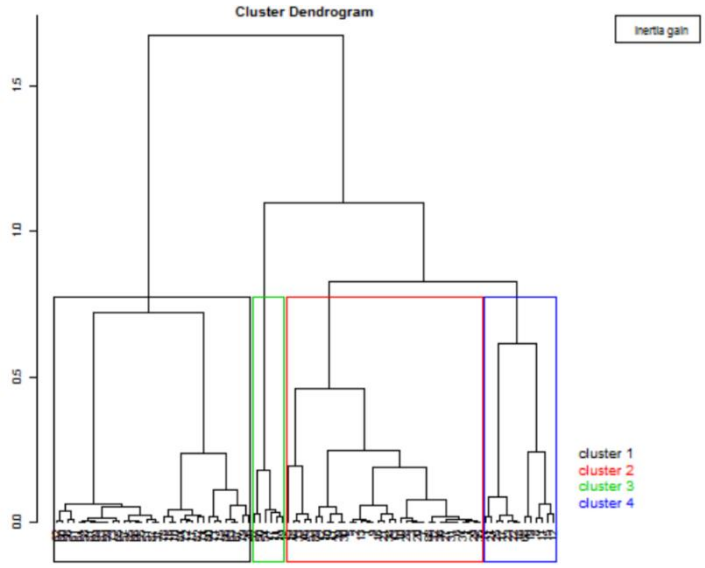

Figure S2: Hierarchical clustering for the samples at ZK

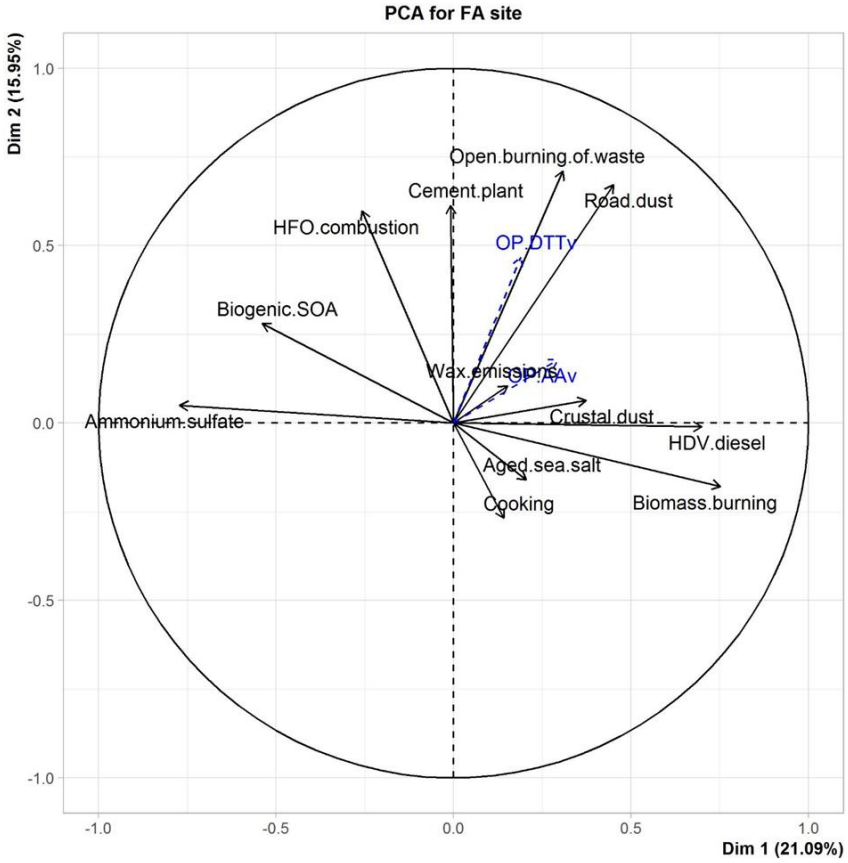

Figure S3: Principal component analysis related to the samples at FA (variables factor map showing Axis 1 and Axis 2 with supplementary variables in blue)

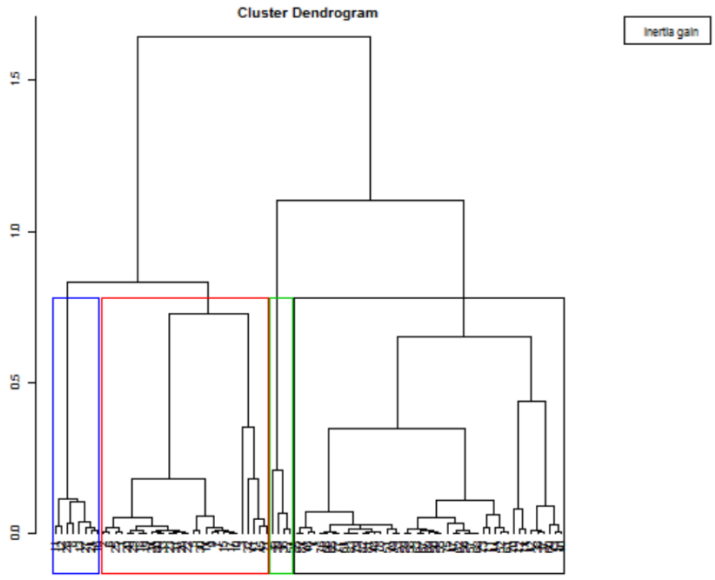

Figure S4: Hierarchical clustering for the samples at FA

Table S1: Principal component analysis for OP-AA_v, OP-DTT_v and identified sources by PMF at ZK (showing only axis 1 and 2 that showed significant correlations with OP)- Values in bold represent r>0.5

	Axis 1 (22.8%)	Axis 2 (15.7%)
OP-AA_v	**0.52**	**0.33**
OP-DTT_v	-0.04	**0.52**
Biomass burning	**0.77**	-0.29
HFO combustion	-0.12	**0.59**
Ammonium sulfate	-0.63	-0.34
Aged sea salt	0.01	**0.56**
Biogenic SOA	-0.59	0.10
Crustal dust	0.37	**0.60**
Cooking	-0.18	0.14
Plant wax emissions	**0.54**	0.21
Road dust	-0.08	-0.05
Diesel generators	**0.62**	-0.08
Vehicular emissions (1)	**0.72**	-0.22
Vehicular emissions (2)	0.03	**0.73**

Table S2: Principal component analysis for OP-AA_v, OP-DTT_v and identified sources by PMF at FA (showing only axis 1 and 2 that showed significant correlations with OP)- Values in bold represent r>0.5

	Axis 1 (21.1%)	Axis 2 (16.0%)
OP-AA_v	0.29	0.18
OP-DTT_v	0.19	**0.50**
Biomass burning	**0.75**	-0.18
HFO combustion	-0.26	**0.60**
Ammonium sulfate	-0.77	0.05
Aged sea-salt	0.21	-0.16
Biogenic SOA	-0.54	0.28
Crustal dust	0.37	0.06
Cooking	0.14	-0.27
Plant wax emissions	0.15	0.10
Road dust	0.45	**0.67**
Diesel HDV	**0.70**	-0.01
Cement plant	-0.01	**0.61**
Open burning of waste	0.31	**0.71**

Table S3: Intrinsic OP values expressed in $nmol.min^{-1}.\ \mu g^{-1}$ at ZK for the AA and DTT assays. Sources with no values mean that they were excluded during the inversion process according to Weber et al. (2018)

Sources	**Intrinsic OP – AA test**	**Intrinsic OP – DTT test**
Biomass burning	0.147	0.029
HFO combustion	0.037	0.040
Ammonium sulfate	0.004	0.012
Aged sea salt	0.003	-
Biogenic SOA	0.011	0.004
Crustal dust	-	0.001
Cooking	-	-
Plant wax emissions	-	-
Road dust	-	-
Diesel generators	0.017	-
Vehicular emissions (1)	0.027	0.011
Vehicular emissions (2)	0.030	0.035

Résumé substantiel en français

1. Sujet de recherche et contexte scientifique

La région méditerranéenne est une région où les conditions météorologiques peu dispersives, conjuguées à un ensoleillement intense, sont particulièrement propices à la formation et à l'accumulation de particules en suspension dans l'air et de composés atmosphériques secondaires tels que l'ozone et/ou des aérosols organiques secondaires (AOS). La région Est de la Méditerranée est considérée comme un hotspot du changement climatique. Les projections indiquent un réchauffement de 3,5 à 7°C jusqu'à la fin du siècle avec une augmentation des jours de canicule et une pollution photochimique plus forte entrainant une concentration plus élevée des polluants dans l'atmosphère. Dans cette région et dans le Moyen Orient, bien que les émissions de CO et NO_x soient principalement dues au transport routier (Waked and Afif, 2012), les activités industrielles en expliquent également une part non négligeable. Au Liban, le secteur industriel et celui de l'énergie sont les principaux émetteurs de particules et de dioxyde de soufre (Waked et al., 2012), et contribuent à dégrader la qualité de l'air (Waked et al., 2013; Abdallah et al., 2018). A ce jour, les études menées au Liban se sont intéressées essentiellement aux zones urbaines, notamment Beyrouth (Afif et al., 2008; Waked et al., 2014; Salameh et al., 2015; Borgie et al., 2016; Salameh et al., 2016; Badran et al., 2020). Quelques études ponctuelles ont porté sur la pollution de l'air dans les zones industrielles : Kfoury et al. (2009) ont analysé les particules totales dans la région de Chekka où sont installées les plus grandes cimenteries sans trouver une empreinte claire des industries tandis que Melki et al. (2017) ont montré que les concentrations de $PM_{2.5}$ dépassaient les valeurs recommandées par l'Organisation Mondiale de la Santé. Yammine et al. (2010), quant à eux, ont montré une influence des émissions d'une industrie de production d'engrais à Selaata sur la qualité de l'air à proximité du site. Les études menées par Waked et al. (2013) et Abdallah et al., (2018) montrent une forte pollution de l'air dans cette région. Finalement, Baalbaki et al., (2018) ont montré que les concentrations des Hydrocarbures Aromatiques Polycycliques (HAP) étaient plus élevées dans la région industrielle de Zouk Mikael où est implantée la plus grande centrale thermique du Liban que dans d'autres sites urbains du pays. Actuellement, il y a cependant un manque de données pour caractériser finement les émissions dans les zones industrielles au Liban et évaluer leur impact sur la qualité de l'air.

2. Objectifs de la thèse

Cette thèse est axée sur l'impact des émissions industrielles sur les niveaux de concentration et la composition de $PM_{2.5}$ et des hydrocarbures non méthaniques (HCNM) dans deux régions au

Liban : celle de Chekka où essentiellement des cimenteries sont installées et celle de Zouk Mikaël où la plus grande centrale thermique du Liban est implantée. De manière plus détaillée, les principaux objectifs sont les suivants :

1. Analyser la composition et de la variabilité temporelle de l'atmosphère urbaine des deux sites sous influence industrielle.
2. Identifier les sources qui contribuent aux concentrations des $PM_{2.5}$ et l'estimation de leurs contributions.
3. Evaluer le risque sanitaire dû à l'exposition aux $PM_{2.5}$ et HCNM.

Les données et les résultats de cette étude vont constituer une base de données qui pourrait être utilisée entre autres dans le futur pour la modélisation de la qualité de l'air dans ces régions, aider dans la mise en place d'un plan de gestion de la qualité de l'air, suivre l'évolution temporelles des concentrations en différents polluants, évaluer l'efficacité de la mise en place d'actions de réduction de la pollution atmosphérique dans ces régions, etc.

Une liste de questions scientifiques sont alors posés pour atteindre ces objectifs :

- Quelle est la concentration et la composition chimique des $PM_{2.5}$ dans les sites ? (Chapitre III)
- Quelles sont les principales sources de $PM_{2.5}$ naturelles et anthropiques qui affectent les sites de mesure ? (Chapitre III)
- Comment peut-on évaluer l'impact sanitaire des $PM_{2.5}$ et des COV dans la région et quelles espèces sont les plus toxiques à l'homme ? (Chapitre IV)

3. Démarche scientifique

Pour atteindre les objectifs, il a été retenu en premier lieu, de réaliser une campagne d'échantillonnage des $PM_{2.5}$ et des HCNM dans les régions de Chekka et de Zouk Mikael. Cette première phase de la thèse a été suivie de l'analyse chimique de la composition des $PM_{2.5}$ (fraction carbonée, organique, éléments majeurs et traces , ions hydrosolubles majeurs…) et des HCNM.

Afin d'identifier les sources de pollution et de quantifier leurs contributions à la concentration des $PM_{2.5}$, le modèle source-récepteur, basé sur la factorisation matricielle positive (PMF) a été utilisé . Ce modèle constitue une approche mathématique basée sur l'hypothèse de la conservation de masse entre la source d'émission et le site récepteur. Les données d'entrée de ce modèle sont les concentrations des espèces présentes dans l'atmosphère (fraction organique,

ions hydrosolubles majeurs, éléments et carbone élémentaire) ainsi que les incertitudes correspondantes. Il est en effet important d'inclure dans l'analyse une sélection d'éléments et de marqueurs moléculaires qui faciliteront l'identification des sources. Les différentes méthodes de diagnostic ont également été utilisées en plus de ces modèles pour retirer une information sur les sources : Carbon Preference Index (CPI), indice Wax et C_{max} pour les alcanes, les ratios caractéristiques surtout pour les HAP, ratios OC/EC, ou encore le calcul du facteur d'enrichissement pour les éléments.

En complément, l'évaluation de l'impact sanitaire lié à une exposition aux polluants atmosphériques a été abordée par deux approches différentes :

- La méthode d'évaluation du risque sanitaire (Health Risk assessment), appliquée en considérant différentes familles d'espèces pour estimer les risques sanitaires cancérogènes et non-cancérogènes associés aux HCNM, éléments, phthalates, HAPs, dioxines et furanes.
- La mesure du potentiel oxydant (PO) des échantillons de particules fines prélevées sur les 2 sites sous influence industrielle (Zouk et Fiaa) et l'étude de la contribution des sources aux valeurs de PO

4. Travail expérimental

a) Echantillonnage

Les campagnes d'échantillonnage des $PM_{2.5}$ et des HCNM ont été lancées en décembre 2018 sur les sites de Zouk Mikael et Chekka. Le site de Zouk est situé en centre-ville en haut d'un immeuble. L'autoroute de Zouk Mikael et le site d'échantillonnage sont séparés d'une distance de 1,2 km. Cette région est caractérisée par une forte densité de population (4200 habitants/km^2) ainsi que des activités commerciales et industrielles diverses (petites industries travaillant le plastique, le bois, l'extrusion d'aluminium, et d'autres spécialisées dans la production de marbre et de granit). Zouk renferme la plus grande centrale thermique au Liban de 1GW de capacité et qui utilise le fioul lourd (HFO) comme carburant. Cette dernière est située à 1,2 km du site de prélèvements. Au sein de la ville, un grand nombre de groupes électrogènes privés sont aussi utilisés pour l'approvisionnement en électricité.

Le village de Fiaa est moins peuplé que Zouk (250 habitants/km^2). Il est aussi influencé par des émissions des groupes électrogènes mais aussi par les industries chimiques présentes dans la région de Chekka : 3 cimenteries ainsi que leurs carrières distantes de 5 à 7 km du site de mesure. Le site d'échantillonnage choisi est colocalisé avec la station de la qualité de l'air du

ministère de l'environnement**.** L'autoroute la plus proche se situe à 4 km du site d'échantillonnage et connait un trafic modéré.

Les informations sur les conditions d'échantillonnage sur les deux sites sont présentées dans le

Tableau *1*. Les particules fines ($PM_{2.5}$) ont été collectées sur des filtres en fibres de quartz sans liant de 150 mm de diamètre (Fiorini, France), préalablement traités à 550 °C pendant 12 heures pour éliminer toute trace de composés organiques. Au moins une fois par mois, un blanc de terrain a été réalisé sur chacun des sites (mise en place du filtre dans le préleveur sans aspiration pour 24 heures). Ces filtres ont été conditionnés à 20 ± 0,5 °C et à une humidité relative de 50 ± 5% pendant au moins 48 hures, puis pesés avant et après l'échantillonnage pour déterminer la masse des $PM_{2.5}$. Des procédures de contrôle qualité ont été mises en place afin de s'assurer de la fiabilité des mesures (utilisation de masses étalons de 1 mg à 5 g avant chaque pesée, pesée systématique d'un même lot de filtres de contrôle à chaque session de conditionnement).

Tableau 1: Informations sur les conditions d'échantillonnage dans les sites de Zouk Mikael et Fiaa

	Site 1 : Zouk Mikael	**Site 2 : Fiaa, Chekka**
Date de début de la campagne	15 décembre 2018	13 décembre 2018
Date de fin de la campagne	15 octobre 2019	16 octobre 2019
Instruments présents sur le site	Préleveur haut débit (CAV-A/mb, MCV S.A., Spain) fonctionnant à 30 m^3/h avec une tête de prélèvement pour les $PM_{2.5.}$	
	Durée d'échantillonnage : 24 heures Fréquence : 1 jour sur 3	
	Tubes passifs Radiello (Code 120) pour mesurer les HCNM (1 échantillon collecté chaque 4 semaines) Tubes passifs de mesure de 1,3-butadiène (Carbopack X diffusion tubes) (1 échantillon collecté chaque 4 semaines)	
Fréquence de visite sur les des sites	2 jours sur 3	2 jours sur 3
Nombre de filtres échantillonnés	98 filtres 6 blancs de terrain	95 filtres 8 blancs de terrain
Nombre de tubes Radiello	11	11
Nombre de tubes pour piégeage du 1,3-butadiène	9	9

De plus, des tubes passifs Radiello (Code 120) ont été installés sur les sites pour mesurer les HCNM ainsi que des tubes Carbopack X pour la mesure de la concentration du 1,3-butadiène (Carbopack X). Ces derniers ont été analysés par Gradko environmental – Royaume Uni.

Etant donné le manque de connaissances sur les profils de certaines sources, il est apparu judicieux d'obtenir des informations sur des profils de source qui soient les plus représentatifs que possible d'émissions locales (sources locales ou émissions liées à des pratiques ou des habitudes culinaires locales) en vue d'aider à l'interprétation des résultats obtenus par PMF. Il a donc été proposé de procéder à des prélèvements à la source, pour différents types d'émission :

- 3 échantillons pour les émissions de combustion de bois ;
- 4 échantillons pour les émissions d'un générateur privé fonctionnant au diesel ;
- 5 échantillons pour les émissions associées aux opérations de cuisson dans une cuisine (cafétéria universitaire) ;
- 2 échantillons pour les émissions liées à la cuisson de viandes (poulet et bœuf) au grill à charbon de bois

Les échantillons collectés ont été analysés pour toutes les fractions en suivant les mêmes protocoles analytiques que ceux suivis pour les échantillons de $PM_{2.5}$ recueillis sur filtres au niveau des sites de Zouk Mikael et Fiaa.

Les 230 filtres collectés sur les deux sites ont été analysés pour la fraction organique, carbonée, les dioxines, les furanes ainsi que les éléments et les ions hydrosolubles. Ils ont été alors divisés en 1/4 et 1/8 de filtre selon les besoins de chaque analyse.

b) Analyses chimiques

- Analyse de la fraction carbonée

Les analyses du carbone organique (OC), carbone élémentaire (EC) et du carbone total ont été réalisées au Cyprus Institute (Nicosie, Chypre) en considérant un poinçon de 1,5 cm^2, par une technique de transmission thermo-optique. Le protocol EUSAAR 2 a été appliqué (European Supersites for Atmospheric Aerosol Research) (Cavalli et al., 2010).

- Analyse de la fraction organique

Un quart de chaque filtre a été utilisé pour analyser les composés organiques primaires et secondaires par chromatographie en phase gazeuse couplée à un spectromètre de masse (GC/MS). L'acide cis-ketopinic pour les composés polaires et le bornylacétate pour les

composés apolaires ont été utilisés comme étalons internes. Le protocole de préparation est résumé sur le schéma de la **Fig. 1.**et est détaillé dans Fadel et al. (2020).

- Analyse des hydrocarbures non-méthaniques

22 tubes passifs au total ont été collectés sur les 2 sites. Les composés ont été extraits des cartouches en utilisant du CS_2 et en ajoutant le 2-fluorotoluène comme étalon interne avant d'être analysés par GC/MS.

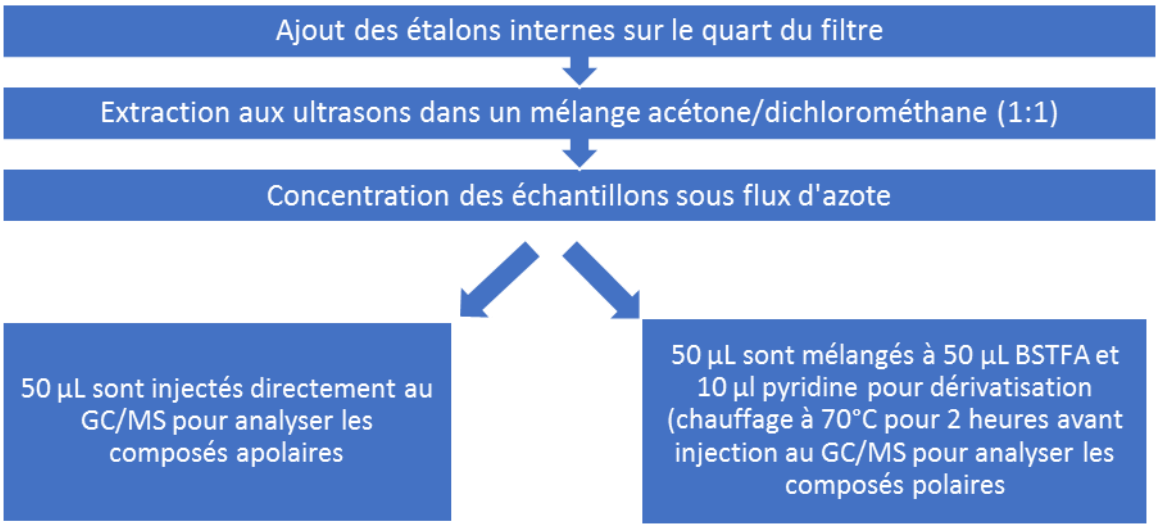

Fig. 1 : Démarche expérimentale de l'analyse de la fraction organique

- Analyse des ions hydrosolubles majeurs par chromatographie ionique

Trois poinçons de filtre de 19 mm de diamètre ont été utilisés pour analyser les ions hydrosolubles. L'extraction se fait en plaçant le filtre dans de l'eau ultrapure et en traitant aux ultrasons pendant 20 minutes, 3 fois successivement. Les extraits sont ensuite groupés, puis filtrés sur membrane en Nylon de porosité 0,2 µm et stockés à -20°C jusqu'à l'analyse. Les échantillons ont été analysés en chromatographie ionique pour l'identification de Cl^-, SO_4^{2-}, NO_3^-, F^-, PO_4^{3-}, Ca^{2+}, Mg^{2+}, K^+, Na^+ et NH_4^+.

- Analyse des éléments majeurs et traces

Les analyses des éléments ont été réalisées pour les échantillons des 2 sites ainsi que ceux des profils de source. La méthode d'extraction comprend une minéralisation totale des particules d'un poinçon de 47 mm de diamètre de chaque filtre en milieu acide et une filtration sur

membrane en acétate de cellulose de porosité 0,45 µm avant le stockage dans des flacons de scintillation en polyéthylène à -20°C jusqu'à l'analyse. Les échantillons ont été analysés par spectrométrie à plasma induit (ICP-OES) et spectrométrie de masse à plasma induit (ICP-MS). L'absence de dérive de l'appareillage a été vérifiée par analyse d'un échantillon de concentration connue tous les 10 échantillons ; de plus la préparation ainsi que l'analyse d'un échantillon certifié (Urban Particulate Matter – 1648a) a permis de valider l'ensemble de la procédure analytique.

- Analyse des dioxines , furanes, et polychlorobiphényls dioxin-like

Les dioxines, furanes et polychlorobiphényls dioxin-like sont des composés présents à l'état de traces dans les $PM_{2.5}$ et il est nécessaire de travailler avec une masse minimale de 15 mg de $PM_{2.5}$ pour espérer pouvoir les détecter . Pour cela, un regroupement de filtres a été réalisé. Ainsi, 3 échantillons représentatifs des périodes hivernale, estivale et intermédiaire pour chacun des 2 sites ainsi que 4 échantillons représentatifs de sources ont été considérés. Ces échantillons ont été analysés par Micropolluants Technology SA en se basant sur les méthodes d'analyse 1613 et 1668 proposés par l'Agence Américaine de Protection de l'Environnement (USEPA). Les composés ont été analysés par chromatographie gazeuse haute résolution couplée à un spectromètre de masse haute résolution (HRGC/HRMS).

- Mesure du potentiel oxydant des échantillons

Dans le cadre de la thèse, les tests utilisant l'acide ascorbique (AA) et le dithiothreitol (DTT) ont été choisis. La mesure du potentiel oxydant a été réalisée sur les échantillons de Zouk Mikael, Fiaa (sites industriels et résidentiels), ainsi que des échantillons des profils de source. Le protocole expérimental est résumé sur la **Fig 2**. Les échantillons sont tout d'abord extrait dans un fluide pulmonaire synthétique (Solution de Gamble) pendant 24h à 37°C. Brièvement, dans le test de l'acide ascorbique, on suit la cinétique de disparition de l'AA (un réducteur présent dans le fluide épithélial pulmonaire) pendant 2 heures, par mesure de. l'absorbance à 265 nm(utilisation d'un spectrophotomètre lecteur de plaque). Pour le test au DTT, de la même manière, on suit la consommation de DTT à différents instants. L'absorbance mesurée à 412 nm correspond au TNB- acide 2-nitro-5-sulfanylbenzoïque- (produit de la réaction entre DTT restant et DNTB - dithiobis(2-acide nitrobenzoïque)-) et qui est proportionnelle à la quantité restante de DTT. Dans les deux cas, le potentiel oxydant correspond à la vitesse de consommation de l'AA ou du DTT en présence de l'extrait de $PM_{2.5}$.

a) Application du modèle source-récepteur : PMF

La PMF est un outil statistique qui permet d'identifier et de déterminer la contribution des principales sources à la concentration de polluants dans l'air ambiant à partir d'un jeu de données incluant les concentrations des espèces et les incertitudes associées. Des traitements préliminaires des séries de données ont été réalisées avant de lancer l'analyse PMF, afin de considérer les données manquantes, les valeurs inférieures à la limite de détection et les valeurs extrêmes liées à des évènements ponctuels. De plus, la sélection des données d'entrée est une étape importante surtout quand il y a un grand nombre d'espèces. Le choix des données d'entrée se concentre prioritairement sur les espèces considérées comme marqueurs de sources. La robustesse du résultat obtenu a été validée par la méthode de "Bootstrap" et de "Displacement" disponible dans le modèle EPA PMF 5.0.

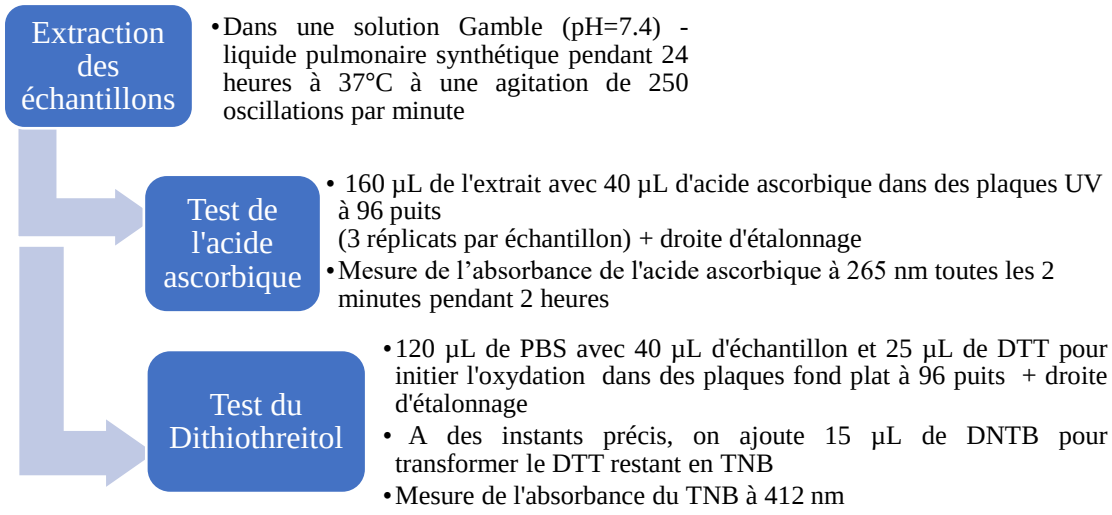

Fig 2 : Résumé du protocole expérimental pour la détermination du potentiel oxydant des $PM_{2.5}$ en utilisant l'Acide Ascorbique (AA) et le Dithiothreitol (DTT) (Moufarrej et al., 2020)

b) Attribution du potentiel oxydant aux sources d'émissions des $PM_{2.5}$

Du fait que le potentiel oxydant est considéré comme une donnée de réactivité et non comme une donnée représentant une partie de la masse de $PM_{2.5}$, il est difficile d'intégrer le potentiel oxydant dans les méthodes sources-récepteurs comme la PMF. Afin d'estimer dans quelle mesure une source contribue au potentiel oxydant, il a été retenu d'utiliser un modèle d'inversion entre les contributions de sources identifiées par PMF et les valeurs de potentiel oxydant des particules. Pour y parvenir, l'approche proposée par Weber et al., (2018) a été

utilisée. Il s'agit d'une méthode de régression linéaire multiple qui se base sur une relation linéaire entre les valeurs du potentiel oxydant et les contributions de source.

5. Synthèse générale et discussions

a) Etablissement des profils chimiques de $PM_{2.5}$

Des profils de composition chimiques des $PM_{2.5}$ émises par les groupes électrogènes, par la combustion de bois, par les activités de cuisson à l'huile et les activités de grillade au charbon de bois ont été déterminés. Ces sources sont communément rencontrées dans la région Méditerranéenne et n'ont été que peu étudiées jusqu'à présent. Cette caractérisation chimique regroupe la fraction carbonée (OC/EC), les ions hydrosolubles, les éléments majeurs et traces et la fraction organique. Cette dernière fraction renferme différentes familles de composés comme les alcanes aliphatiques, les hydrocarbures aromatiques polycycliques, les acides carboxyliques, le lévoglucosan, les dioxines, les furanes et les polychlorobiphényls dioxin-like.

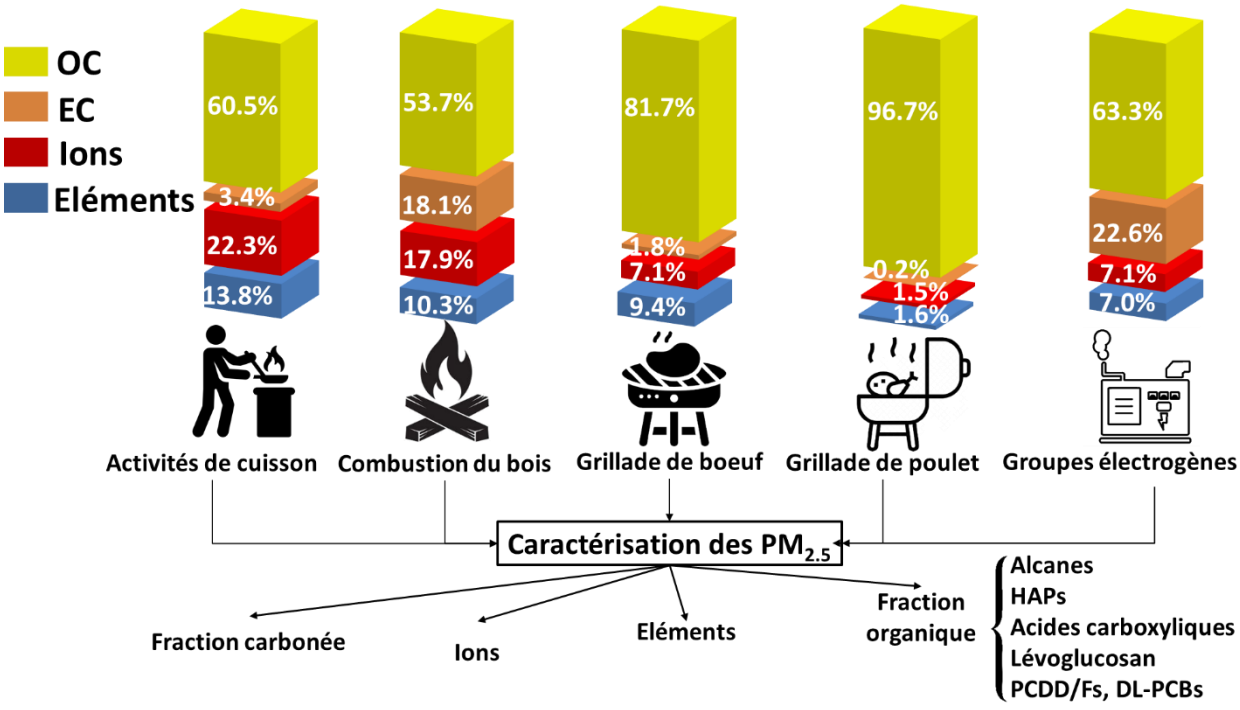

Fig. 3 : Contribution de chaque famille de composés (OC, EC, ions hydrosolubles et éléments) par rapport à la somme totale des espèces analysées pour les différentes sources de $PM_{2.5}$ (activités de cuisson, combustion de bois, grillade de bœuf, grillade de poulet et les groupes électrogènes)

La fraction carbonée (OC+EC) contribue le plus à la masse de $PM_{2.5}$ émis par les différentes sources : elle représente 64% pour les activités de cuisson, 72% pour la combustion du bois, 84% pour la grillade de bœuf, 86% pour les groupements électrogènes et 97% pour la grillade de poulet avec différents rapports OC/EC **(Fig. 3)**. D'autre part, l'abondance des ions hydrosolubles dans les $PM_{2.5}$ varie entre 1.5% pour la grillade de poulet et 22% pour les activités de cuisson. De plus, les éléments contribuent le plus à la masse de $PM_{2.5}$ émis par les activités de cuisson (14%) et le moins au profil de grillade de poulet (1.6%).

L'étude de la composition de la fraction organique ainsi que l'utilisation de différents ratios comme le CPI, l'indice Wax et les ratios entre les HAP ont permis de caractériser les profils de ces sources.

Les marqueurs de la combustion du bois sont OC, EC (avec un ratio OC/EC de 3,4), de même que K et Cl^- qui contribuent dans l'ensemble à 90% de la masse toutes les espèces quantifiées. En complément, le profil de cette source est caractérisé par le lévoglucosan, des alcanes C_{27}, C_{29} et C_{31} et des HAPs comme le fluoranthène, le pyrène et le benzo[a]anthracène. Les rapports de concentration des HAP sont de 0,49 pour le rapport fluoranthène/(fluoranthène + pyrène) et 0,57 pour le rapport benzo[a]anthracène/(benz[a]anthracène + chrysène). En outre, les valeurs des rapports de concentration K^+/EC et K^+/OC qui permettent de différencier la combustion de biomasse et la combustion des combustibles fossiles, étaient de 0,36 et 0,12 respectivement pour ce profil.

Pour le profil des émissions des groupes électrogènes, OC et EC contribuent le plus à la masse de $PM_{2.5}$ suivis de SO_4^{2-}, NO_3^-, Ca, Ca^{2+}. Pour la fraction organique, les alcanes montrent une contribution importante à l'OC avec un maximum pour C_{20}-C_{21}, un CPI proche de l'unité et une valeur faible de l'indice Wax (1.4%). De plus, les ratios de concentration des HAP pour la combustion du diesel étaient de 0,24 pour le rapport fluoranthène/(fluoranthène + pyrène), 0,41 pour le rapport benzo[a]anthracène/(benzo[a]anthracène + chrysène) et 0,18 pour le rapport indeno[1,2,3-c,d]pyrène /(indeno[1,2,3-c,d]pyrène + benzo[g,h,i]pérylène). Les ratios de concentration K^+/EC et K^+/OC étaient de 0,01 et 0,003 respectivement.

Les 3 profils de cuisson (grillade de bœuf, grillade de poulet et activités de cuisson à l'huile) présentent des similarités : une contribution importante des acides carboxyliques à l'OC surtout l'acide hexadécanoïque et l'acide octadécanoique, une contribution élevée de l'OC mais une contribution faible pour l'EC par rapport à la somme des espèces. Cependant, la quantité de graisses présente dans les aliments contribue également à la quantité d'OC émise par les sources

de cuisson. OC contribue à 96% de la masse des espèces dans le profil de grillade de poulet avec un ratio OC/EC de 622, suivi par EC et Cl^- qui contribue chacun à presque 0.2%. D'autre part, les marqueurs de la grillade de bœuf sont OC, EC (avec un ratio OC/EC de 45), Cl^-, K, NO_3^- et SO_4^{2-}. Pour la fraction organique, plusieurs indices montrent l'influence de la combustion du charbon dans les profils de grillade de bœuf et de poulet : concentration élevée en C_{25} dans les deux profils, abondance des HAP à 4 cycles aromatiques et rapports de concentration de fluoranthène/(fluoranthène + pyrène) , benz[a]anthracène/(benz[a]anthracène + chrysène) et indeno[1,2,3-c,d]pyrène /(indeno[1,2,3-c,d]pyrène + benzo[g,h,i]pérylène) proche de 0,5. Un profil différent a été observé pour les activités de cuisson à l'huile avec un rapport OC/EC de 18, et une contribution importante des ions SO_4^{2-}, NO_3^- et NH_4^+.

Ces résultats ont permis de disposer de connaissances nouvelles sur les caractéristiques de différentes sources de $PM_{2.5}$ dans la région dans laquelle a été conduite notre étude. Ces connaissances pourront désormais être utilisées dans différentes études futures faisant appel à l'utilisation de modèles sources-récepteurs.

b) Caractérisation chimique des $PM_{2.5}$ et estimation des contributions des sources

Durant la période d'étude proche d'une année (décembre 2018-octobre 2019), la concentration moyenne de $PM_{2.5}$ était de 33,6 µg/m^3 à ZK et 26,0 µg/m^3 at FA. Ces concentrations dépassent les nouvelles concentrations limites fixées par l'Organisation Mondiale de la Santé (5 µg/m^3 en moyenne annuelle et 15 µg/m^3 en moyenne journalière). Les concentrations les plus élevées en $PM_{2.5}$ sur les deux sites ont été principalement attribuées à des tempêtes de poussières provenant du Sahara et du désert d'Arabie.

Les concentrations en OC et EC étaient respectivement de 4,6 µg/m^3 et 1,3 µg/m^3 à ZK et de 3 µg/m^3 et 0,5 µg/m^3 à FA. De plus, une bonne corrélation a été observée entre ces deux espèces sur les deux sites. Le ratio OC/EC a été utilisé pour essayer d'identifier les sources de matière carbonée. La valeur de ce ratio était de 4 à ZK et de 7,3 à FA . Il a pu être montré que le ratio obtenu à ZK était révélateur des émissions de véhicules fonctionnant à l'essence, sachant que la plupart des voitures au Liban utilisent ce type de carburant. En revanche, la valeur du ratio OC/EC obtenue à FA a pu être expliquée par une combinaison de l'influence des émissions de combustion de la biomasse et de celles issues de la combustion non contrôlée des déchets.

Les ions hydrosolubles ont contribué largement aux $PM_{2.5}$ en expliquant environ 40% de la masse à ZK et 47% à FA. Les espèces majeures de cette fraction sont NO_3^-, SO_4^{2-} et NH_4^+ qui font partie de l'aérosol inorganique secondaire et qui contribuent au moins à 75% de la masse

totale des ions. Un examen de la balance ionique a permis de montrer un déficit d'anions. Cette observation peut être due à des composés qui n'ont pas été analysés en chromatographie ionique comme les carbonates. En effet, il faut savoir que les sols libanais sont riches en $CaCO_3$ et cela pourrait expliquer le déficit en anions.

Les 29 éléments majeurs et traces analysés contribuent à 10% de la masse des $PM_{2.5}$ à ZK et à 8% à FA. Les éléments majeurs étaient Ca, Fe et Al qui contribuent à plus que 80% de la masse des éléments. Les facteurs d'enrichissement (EF) ont été calculés pour mieux comprendre l'origine naturelle ou anthropique de ces éléments en utilisant Al comme élément de référence. Les résultats étaient similaires sur les deux sites avec : une valeur de facteur d'enrichissement EF<10 pour les éléments Rb, Nb, Ce, K, Fe, Mn, La, Sr, Ti, Mg et Ba qui ne sont pas enrichis, présentent donc principalement une origine naturelle. Avec des valeurs d'EF proche de 10, les éléments Tl, P, Cr, Sc, Ca, Co et Sn se sont avérés être moyennement enrichis . Enfin, As, V, Cu, Pb, Zn, Ni, Bi, Cd et Sb apparaissent comme les éléments les plus enrichis (EF>10) et présentaient, en conclusion, des origines anthropiques. De plus, l'évaluation des coefficients de corrélation ainsi que l'étude des ratios entre les éléments ont montré que V et Ni étaient principalement reliés à la combustion de fioul lourd dans la centrale thermique à ZK et dans les cimenteries à FA. D'autres éléments comme Cu, Sn et Sb ont été principalement reliés aux émissions véhiculaires hors échappement, notamment l'usure des freins.

Les résultats PMF ont permis de montrer que les sources correspondant au sulfate d'ammonium et aux poussières crustales contribuaient le plus à la masse de $PM_{2.5}$ avec 43,2% à ZK et 46,3% à FA **(Fig. 4)**. Les poussières proviennent principalement du transport sur de longues distances de masses d'air issues du Sahara et du désert d'Arabie. La source correspondant aux "poussières crustales" est caractérisée par une abondance en éléments Al , Mg, Ca, Fe et Ti. D'autre part, les concentrations élevées en sulfate, ont été attribuées au transport long distance de l'Est de l'Europe, l'Europe centrale et la Turquie. Cette hypothèse d'un impact d'un transport de particules sur de longues distances a été validée par l'étude des rétro trajectoires des masses d'air et les résultats obtenus par l'application de la méthode du clustering des trajectoires.

Concernant les sources anthropiques locales, le site de ZK est plus influencé par les émissions véhiculaires que le site de FA du fait de la proximité du site de ZK avec un grand axe autoroutier très fréquenté. Différents composés comme le chrysène et le 17α(H)-21β(H)-hopane ont montré des concentrations élevées à ZK mais n'ont pas été détectés à FA. De plus, les concentrations élevées en C_{25} et les valeurs des ratios ((B[a]An/(B[a]An+Chr) et B[a]P/(B[a]P+Chr)) valident l'impact des émissions véhiculaires. Cette source contribue à 14% de la masse de $PM_{2.5}$ à ZK

et seulement 4% à FA. En outre, la forte densité de population à ZK coïncide avec l'utilisation d'un nombre plus élevé de groupes électrogènes qui sont installés dans ces régions pour compenser les longues coupures d'électricité. Cette source "groupes électrogènes" contribue à 4,5% de la masse de $PM_{2.5}$ à ZK.

L'influence industrielle à ZK est représentée la combustion du fioul lourd provenant de la centrale thermique à la masse des $PM_{2.5}$ (contribution de 13%). De plus, des concentrations élevées ont été observées pour l'indeno[1,2,3-c,d]pyrène et une attention particulière a été portée pour le ratio Indeno[1,2,3-c,d]pyrène /(Indeno[1,2,3-c,d]pyrène + Benzo[g,h,i]pérylène) à Zouk, où les valeurs obtenues se trouvent entre 0,8 et 1 pour la plupart. Une exploitation approfondie de nos résultats nous a permis de proposer cet intervalle pour ce ratio qui semble caractéristique des émissions reliées à la combustion des fiouls lourds au niveau de la centrale thermique.

L'influence industrielle à Fiaa est représentée par la source "combustion du fioul lourd" attribué aux cimenteries et aux centrales thermiques de la région Nord du Liban et aussi une autre source dans laquelle on retrouve une abondance élevée pour le calcium qui a pu être attribué au procédé de fabrication du ciment. Ces facteurs contribuent à 8,2% de la masse de $PM_{2.5}$ à FA **(Fig. 4)**. Nous ne sommes pas parvenus à identifier clairement et évaluer l'impact de l'activité industrielle des carrières (roches riches en $CaCO_3$) qui se trouvent dans la région. Leur impact pourrait être combiné avec la source "poussières crustales" du fait que les échantillons qui contribuent le plus à ce facteur ne correspondent pas tous à des épisodes de tempête de sable. Les échantillons correspondants pourraient alors être associés à une source plus locale et notamment l'activité des carrières.

Une autre source importante de particules identifiées à FA correspondait aux émissions liées à l'incinération non contrôlée des déchets : sa contribution à la masse des $PM_{2.5}$ y atteint 16% . Ce phénomène apparait comme une conséquence de la crise des déchets solides au Liban et cette combustion est communément observée au Liban, notamment au Nord, où les déchets sont brûlés dans différents emplacements.

De même, d'autres sources anthropiques contribuent à la masse des $PM_{2.5}$ comme les émissions liées à la cuisson des aliments. Cette dernière a pu être identifiée par la présence des acides hexadécanoïques et octadécanoique tandis que l'impact de la combustion de biomasse a pu être révélée par le lévoglucosan (traceur spécifique) surtout durant la période hivernale et qui peut

être associée au chauffage résidentiel. L'influence de la combustion de la biomasse a été détectée aussi en évaluant le ratio fluoranthène/(fluoranthène + pyrène).

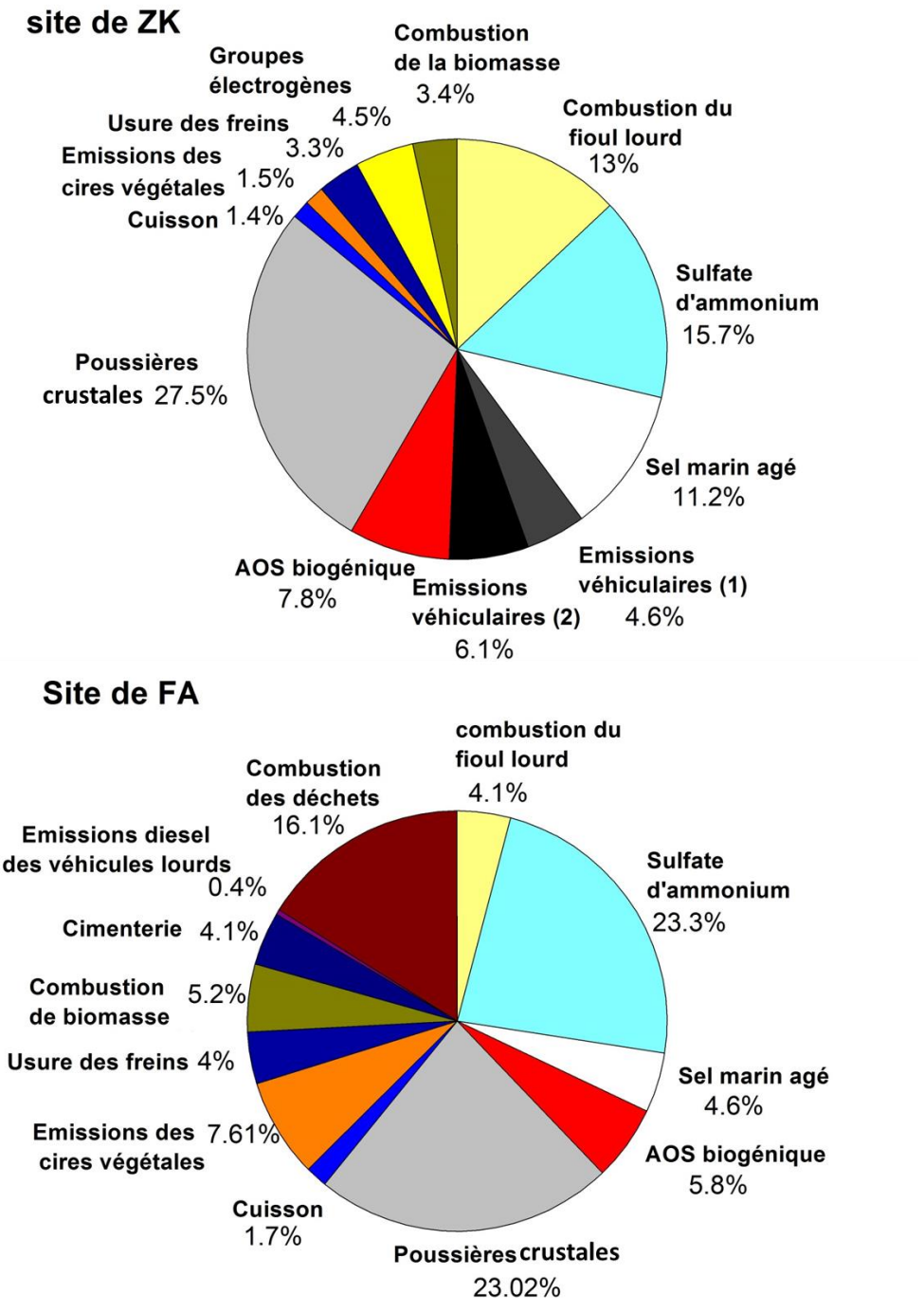

Fig. 4: Contribution moyenne des 12 sources identifiées par PMF pour les sites de Zouk et Fiaa

Pour les émissions naturelles, les émissions biogéniques primaires et secondaires ont contribué à 9.3% de la masse des $PM_{2.5}$ à ZK et à 13.4% à FA. Il a pu être observé que les profils des alcanes étaient décalés vers les alcanes les plus lourds durant l'été (C_{27}-C_{31}). Cette observation a pu être attribuée aux émissions des cires des plantes, qui sont plus abondantes à cette saison. Les émissions biogéniques secondaires ont été détectées par les produits d'oxydation de l'isoprène et de l'α-pinène qui montrent aussi une variation saisonnière importante avec des concentrations plus élevées durant l'été. Finalement, la proximité des sites avec la Mer Méditerranée explique des contributions significatives de sels marins à la masse des $PM_{2.5}$ **(Fig. 4)**.

c) L'évaluation du risque sanitaire

L'évaluation du risque sanitaire dans ces travaux a été réalisée suivant deux approches : le « Health Risk Assessment » qui se base sur le calcul du risque sanitaire cancérogène et non-cancérogène des différentes classes de composés (approche de l'Agence de protection de l'environnement des États-Unis, U.S. EPA) et la mesure du potentiel oxydant qui est lié à la surproduction d'espèces réactives de l'oxygène (ERO).

La méthode du « Health Risk assessment » a été appliquée pour le calcul du risque sanitaire cancérogène et non-cancérogène associé à l'exposition aux éléments, hydrocarbures aromatiques polycycliques (HAPs), phthalates, dioxines, furanes et polychlorobiphényls dioxin-like dans les $PM_{2.5}$ mais aussi aux HCNM. Dans notre étude, les 3 voies d'exposition (inhalation, ingestion et contact dermique) ainsi que différentes catégories d'âge de la personne exposée ont été considérées (nouveau-né entre 0 et 1 an, enfant entre 1 et 12 ans, adolescent entre 12 et 18 ans et adulte entre 18 et 70 ans). Ce calcul prend en compte les concentrations moyennes des espèces dans l'atmosphère ainsi que des paramètres d'exposition comme les taux d'inhalation et d'ingestion journaliers, le poids de l'individu, la fréquence et le taux d'exposition. Le risque non-cancérogène est évalué à partir du rapport entre la concentration moyenne journalière calculée à partir des paramètres précédemment présentés et une dose journalière tolérable pour chaque composé. Le risque cancérogène est déterminé en multipliant la concentration moyenne journalière par le coefficient de cancérogénicité. Les termes et les abréviations utilisés dans cette partie sont présentés dans le

Tableau *2*. Plus la valeur de HQ_i, total HQ_i, HI ou total HI est supérieure à 1, plus la probabilité d'occurrence d'effets non cancérogènes est importante. De même les valeurs de CRi, total CR_i, CR et CCR sont comparées à la valeur seuil de 10^{-6} recommandée par l'U.S. EPA. Cette étude

est la première dans la région Est de la Méditerranée à présenter l'évaluation du risque d'effets sanitaires pour plusieurs familles de composés dans les fractions gazeuse et particulaire de prélèvements réalisés sur période de quasiment une année.

Les résultats de cette étude montrent que le benzène et l'heptane ont des valeurs de total HQ_i supérieures à 1 (valeur limite pour les risques non-cancérogènes) parmi les HCNM. Un même constat est observé pour l'ensemble des éléments chez les nouveau-nés pour les deux sites. Les principaux éléments qui contribuent à la valeur élevée de Total HI sont Mn, Pb, V et Ni. En revanche, les HAPs dans les phases gazeuse et particulaire, les phthalates, les PCDD/F et DL-PCBs présentent des valeurs plus petites que la limite et par la suite leur impact peut être qualifié de négligeable, selon cette approche.

Pour le risque cancérogène, différents HCNM comme le benzène, l'éthylbenzène et le 1,3-butadiène (sur le site de ZK) et des composants des $PM_{2.5}$ comme les HAPs, As, Co, Cr(VI), Ni et V présentent un risque d'effets cancérogènes pour les différentes catégories d'âge en se basant sur les valeurs de risque de cancer qui apparaissent supérieures à la limite de 10^{-6}.

Cette méthode présente aussi des limites dans le sens où elle est basée sur une absence d'interdépendance des effets toxiques des composés de différentes familles. De ce fait, le risque cancérogène ne peut pas être additionnés pour les différentes familles de composés puisque les interactions entre les familles ne sont pas bien encore établies. Ceci s'applique aussi au risque non-cancérogène. De plus, des incertitudes existent surtout dans le choix des paramètres d'exposition et des valeurs de référence.

La deuxième approche pour l'évaluation du risque sanitaire diffère de la première. Elle est basée sur la mesure du potentiel oxydant (PO-AA et PO-DTT dans notre cas) des composés des $PM_{2.5}$ capables de se solubiliser dans une solution de Gamble (solution qui simule la composition du fluide pulmonaire). Les extraits contiennent alors non seulement les composés identifiés et analysés mais aussi des espèces non identifiées qui pourraient contribuer aux valeurs du PO. Cela signifie que cette approche est plus globale en tenant compte de l'ensemble des espèces oxydantes, quelque soient leurs formes chimiques ou les familles de composés auxquelles elles appartiennent. Différentes méthodes ont été utilisées dans cette étude afin de relier les valeurs observées de PO aux différentes espèces et sources identifiées sur les deux sites, telles que les corrélations de Spearman, l'analyse en composantes principales et la classification ascendante hiérarchique. En outre, la méthode de régression linéaire multiple a été adoptée afin d'attribuer

des valeurs intrinsèques de PO aux sources et de découvrir la contribution des sources aux valeurs de PO-AA_v et de PO-DTT_v.

La valeur moyenne du PO-AA_v (PO normalisé par rapport au volume) était de 0,67 ± 0,29 nmol.min^{-1}.m^{-3} à ZK et de 0,46 ± 0,33 nmol.min^{-1}.m^{-3} à FA. D'autre part, la valeur moyenne de PO-DTT_v était de 0,52 ± 0,32 nmol.min^{-1}.m^{-3} à ZK et de 0,29 ± 0,16 nmol.min^{-1}.m^{-3}à FA.

Tableau 2 : Liste des termes, abréviations et définitions des termes employés dans le Health risk assessment

Terme	Abréviation	Définition
Hazard quotient	HQ_i	risque non cancérogène d'un composé pour une voie d'exposition spécifique
Total Hazard quotient	Total HQ_i	risque non cancérogène pour un composé pour toutes les voies d'exposition
Hazard index	HI	risque non cancérogène pour une famille de composés pour une voie d'exposition
Total Hazard index	Total HI	risque non cancérogène pour une famille de composés pour toutes les voies d'exposition
Cancer risk	CR_i	risque cancérogène d'un composé pour une voie d'exposition spécifique
Total cancer risk	Total CR_i	risque cancérogène d'un composé pour toutes les voies d'exposition
Cancer risk	CR	risque cancérogène pour une famille de composés pour une voie d'exposition
Cumulative cancer risk	CCR	risque cancérogène pour une famille de composés pour toutes les voies d'exposition

Ces valeurs se situent dans l'intervalle des valeurs observées dans différentes études réalisées dans le monde. Les évolutions temporelles ont montré de fortes variations de PO d'un jour à l'autre pour le même test et également des différences entre les valeurs de PO-AA_v et PO-DTT_v pour un même échantillon. Le PO déterminé selon les deux méthodes à FA et PO-DTT_v à ZK n'ont pas montré de variation saisonnière significative, à la différence de PO-AA_v à ZK qui a montré des valeurs significativement plus élevées pendant la période hivernale. Cela pourrait être lié à une source saisonnière qui contribue largement à la valeur du PO-AA_v et qui pourrait être le chauffage résidentiel.

Les corrélations de Spearman et la classification ascendante hiérarchique ont montré que les sources anthropiques influencent le plus les valeurs du PO. Les composés organiques étaient plus corrélés au PO-AA_v tandis que les deux tests ont montré une sensibilité égale aux deux tests. PO-AA_v a montré une corrélation significative avec les sources de combustion de

biomasse et l'usure des freins sur les deux sites. De plus, PO-AA_v corrélait avec la source des groupes électrogènes, émissions véhiculaires, combustion du fioul lourd et l'usure des freins à ZK et ave les émissions diesel des véhicules lourds à FA. Concernant PO-DTT_v, il corrélait avec la combustion du fioul lourd sur ZK et FA. De plus, il était lié aux sources d'émissions véhiculaires et groupes électrogènes à ZK , et à l'incinération non contrôlée des déchets à FA.

La méthode de régression linéaire multiple a été appliquée aux deux bases de données afin de trouver les valeurs intrinsèques des PO pour les différentes sources identifiées par PMF. En raison de la grande variabilité des résultats obtenus pour le site FA et la difficulté de reconstruire les valeurs de OP par le modèle, seuls les résultats pour le site ZK ont pu être exploités. Pour ce site, le modèle a permis une bonne reconstruction des données de PO tout en obtenant une distribution normale de la part non expliquée. Les résultats montrent que les poussières crustales et la source de sulfate d'ammonium qui contribuent largement à la masse de $PM_{2.5}$ ne sont pas les principales sources contribuant aux valeurs de PO. Selon l'étude, le PO-AA_v et le PO-DTT_v ont été influencés par les mêmes sources mais avec des contributions différentes. La combustion de biomasse et la combustion du fioul lourd sont les principales sources influençant les valeurs du PO-AA_v et contribuent ensemble à plus de 64% de la valeur moyenne du PO-AA_v. Quant au PO-DTT_v, la combustion du fioul lourd contribue à 46 % et la combustion de biomasse contribue seulement à 8,8 %. Les sources d'émissions véhiculaires influent également sur les valeurs obtenues par les deux tests avec une contribution relative de 19.7 % pour PO-AA_v et 22,6 % pour PO-DTT_v. Cette méthode présente également certaines limites puisque le modèle mathématique est basé sur l'hypothèse de la linéarité entre les valeurs PO de la masse des PM, ce qui n'est pas toujours le cas. C'est pourquoi, des modèles de régression non linéaires pourraient être appliqués à l'avenir afin de prendre en compte l'effet cocktail d'un mélange de polluants.

d) Contribution des sources et risque sanitaire

En guise de conclusion, ce travail de thèse de doctorat a permis d'identifier et d'évaluer les contributions des différentes sources à la concentration de $PM_{2.5}$ sur les deux sites, les risques sanitaires associés aux différentes classes de composés et les contributions des sources aux valeurs de PO-AA_v et PO-DTT_v. Pour le site de ZK, les sources qui contribuent le plus à la masse (poussières crustales et sulfate d'ammonium contribuant à 43.2% de la masse de $PM_{2.5}$) ne sont pas celles qui apparaissent les plus problématiques en termes d'effet sur la santé humaine. Les sources qui sont les plus problématiques sont la combustion du fioul lourd, les émissions véhiculaires et la combustion de la biomasse. Le site FA était influencé par la

combustion non contrôlée des déchets, les cimenteries, la combustion du fioul lourd et la combustion de la biomasse.

e) Recommandations

Les conséquences potentielles sur la santé humaine d'une exposition aux $PM_{2.5}$ et aux HCNM sont principalement liées à des sources anthropiques locales et cette exposition pourrait être atténuée par le suivi de différentes recommandations comme par exemple :

- Remplacer le fioul lourd par une autre source d'énergie comme le gaz naturel surtout dans les grandes installations telles que la centrale thermique à ZK et les cimenteries à FA. Cette même source d'énergie pourrait également constituer une solution pour réduire la combustion de la biomasse à laquelle la population a aujourd'hui largement recours pour le chauffage résidentiel.
- Mettre en place un réseau de transport national pour réduire les émissions dues au trafic surtout dans les zones urbaines. En complément, il pourrait être recommandé de mettre en place des valeurs limites d'émissions pour les véhicules, et aussi de les faire respecter scrupuleusement.
- Interdire l'incinération non contrôlée des déchets et mettre en œuvre un plan national de gestion des déchets solides.
- Sensibiliser la population sur les effets néfastes de ces sources de polluants atmosphériques sur l'environnement et sur la santé humaine.

Résumé :

Les objectifs principaux de ce travail étaient d'étudier la composition et la variabilité temporelle de l'atmosphère urbaine de deux sites sous influence industrielle dans l'Est de la Méditerranée. Cette étude est axée sur la caractérisation des $PM_{2.5}$ et des composés organiques volatils (COV), l'identification des sources de $PM_{2.5}$ et l'évaluation de l'impact sanitaire dû à l'exposition à ces polluants. Les particules fines et les COV ont été collectés dans deux sites au Liban entre décembre 2018 et octobre 2019. Le site de Zouk Mikael abrite la plus grande centrale thermique au Liban qui utilise comme combustible du fioul lourd et le site de Fiaa dans la région de Chekka est sous l'influence des émissions des cimenteries et leurs carrières. La composition des $PM_{2.5}$ a été déterminée suite à la quantification des fractions carbonée et organique, des ions hydrosolubles ainsi que celle des éléments majeurs et traces. La caractérisation de la fraction organique inclut l'étude de composés primaires (alcanes, phtalates, hydrocarbures aromatiques polycycliques, hopanes et acides gras) et secondaires (produits d'oxydation de l'isoprène, α-pinène et β-caryophyllène et les acides dicarboxyliques). De plus, différentes méthodes ont été utilisées pour avoir une idée sur les sources dans les deux régions. Afin d'identifier les sources de particules fines et quantifier leurs contributions à la concentration des $PM_{2.5}$, le modèle source-récepteur basé sur la factorisation matricielle positive (Positive Matrix Factorization) a été utilisé. L'identification des sources a été soutenue grâce aux connaissances sur des profils chimiques de sources disponibles dans la littérature mais aussi grâce à des données de profils de $PM_{2.5}$ déterminés dans le cadre de cette étude pour des sources de PM dont les caractéristiques physico-chimiques sont spécifiques au Bassin Est-Méditerranéen. Enfin, l'évaluation de l'impact sanitaire dû à l'exposition aux $PM_{2.5}$ a été abordée par deux approches différentes : l'évaluation du risque sanitaire pour différentes familles d'espèces de $PM_{2.5}$ et COV et la mesure du potentiel oxydant par deux méthodes acellulaires (test à l'acide ascorbique et celui utilisant le dithiothréitol). Enfin, des valeurs de potentiel oxydant intrinsèque à chaque source ont été évaluées par une méthode de régression linéaire afin de relier la contribution des sources de $PM_{2.5}$ aux valeurs de potentiel oxydant observées.

Mots-clés : $PM_{2.5}$, Est de la Méditerranée, contribution des sources, potentiel oxydant, évaluation du risque sanitaire, milieux urbano-industriels.

Abstract:

The main objectives of this work were to study the chemical composition and the temporal variability in the urban atmosphere of two East Mediterranean sites under industrial influence. This study was focused on the chemical characterization of $PM_{2.5}$ and volatile organic compounds (VOCs), the identification of $PM_{2.5}$ sources and the evaluation of the health risk associated with the exposure to these pollutants. Fine particulate matter and VOCs were collected between December 2018 and October 2019 in two sites in Lebanon. The Zouk Mikael site encompasses the biggest power plant in the region which runs on heavy fuel oil and the Fiaa site, in Chekka region, is under the influence of the cement plants and their corresponding quarries. The chemical composition of the collected $PM_{2.5}$ was determined through the quantification of the carbonaceous and organic fractions, water-soluble ions, and major and trace elements. The organic characterization included primary (alkanes, polycyclic aromatic hydrocarbons, phthalates, hopanes, and fatty acids) and secondary organic aerosols (oxidation products of α-pinene, isoprene, and β-caryophyllene and dicarboxylic acids). Additionally, different tools were employed in order to have a preliminary idea of the most relevant sources. In order to identify the $PM_{2.5}$ sources and quantify their contributions to $PM_{2.5}$ concentrations, the source-receptor model Positive Matrix Factorization (PMF) was used. The identification of the sources was based on the available chemical profiles in the literature but also from the chemical characterization of $PM_{2.5}$ samples collected at near field for local sources with physico-chemical characteristics specific to the Eastern Mediterranean Basin. Finally, the health risk evaluation due to the exposure to $PM_{2.5}$ was presented by two different approaches: the evaluation of the health risk for different classes of compounds of $PM_{2.5}$ and VOCs and the measure of the oxidative potential using two acellular assays (ascorbic acid and dithiothreitol assays). Finally, the attribution of intrinsic oxidative potential values for the sources was evaluated by multiple linear regression in order to link the contribution of the sources to the observed values of the oxidative potential.

Keywords: $PM_{2.5}$, East-Mediterranean, source apportionment, oxidative potential, health risk assessment, urban-industrial sites.